HEAVY METAL TOXICITY IN PLANTS: RECENT INSIGHTS ON PHYSIOLOGICAL AND MOLECULAR ASPECTS

EDITED BY: Rafaqat Ali Gill, Mukesh Kumar Kanwar, Andre Rodrigues dos Reis and Basharat Ali

PUBLISHED IN: Frontiers in Plant Science

frontiers Research Topics

ISSN 1664-8714
ISBN 978-2-88974-172-4
DOI 10.3389/978-2-88974-172-4

About Frontiers

Frontiers is more than just an open-access publisher of scholarly articles: it is a pioneering approach to the world of academia, radically improving the way scholarly research is managed. The grand vision of Frontiers is a world where all people have an equal opportunity to seek, share and generate knowledge. Frontiers provides immediate and permanent online open access to all its publications, but this alone is not enough to realize our grand goals.

Frontiers Journal Series

The Frontiers Journal Series is a multi-tier and interdisciplinary set of open-access, online journals, promising a paradigm shift from the current review, selection and dissemination processes in academic publishing. All Frontiers journals are driven by researchers for researchers; therefore, they constitute a service to the scholarly community. At the same time, the Frontiers Journal Series operates on a revolutionary invention, the tiered publishing system, initially addressing specific communities of scholars, and gradually climbing up to broader public understanding, thus serving the interests of the lay society, too.

Dedication to Quality

Each Frontiers article is a landmark of the highest quality, thanks to genuinely collaborative interactions between authors and review editors, who include some of the world's best academicians. Research must be certified by peers before entering a stream of knowledge that may eventually reach the public - and shape society; therefore, Frontiers only applies the most rigorous and unbiased reviews.
Frontiers revolutionizes research publishing by freely delivering the most outstanding research, evaluated with no bias from both the academic and social point of view. By applying the most advanced information technologies, Frontiers is catapulting scholarly publishing into a new generation.

What are Frontiers Research Topics?

Frontiers Research Topics are very popular trademarks of the Frontiers Journals Series: they are collections of at least ten articles, all centered on a particular subject. With their unique mix of varied contributions from Original Research to Review Articles, Frontiers Research Topics unify the most influential researchers, the latest key findings and historical advances in a hot research area! Find out more on how to host your own Frontiers Research Topic or contribute to one as an author by contacting the Frontiers Editorial Office: frontiersin.org/about/contact

HEAVY METAL TOXICITY IN PLANTS: RECENT INSIGHTS ON PHYSIOLOGICAL AND MOLECULAR ASPECTS

Topic Editors:
Rafaqat Ali Gill, Chinese Academy of Agricultural Sciences, China
Mukesh Kumar Kanwar, Zhejiang University, China
Andre Rodrigues dos Reis, São Paulo State University, Brazil
Basharat Ali, University of Agriculture, Pakistan

Citation: Gill, R. A., Kanwar, M. K., Reis, A. R. d., Ali, B., eds. (2022). Heavy Metal Toxicity in Plants: Recent Insights on Physiological and Molecular Aspects. Lausanne: Frontiers Media SA. doi: 10.3389/978-2-88974-172-4

Table of Contents

05 ***Editorial: Heavy Metal Toxicity in Plants: Recent Insights on Physiological and Molecular Aspects***
Rafaqat Ali Gill, Mukesh Kumar Kanwar, Andre Rodrigues dos Reis and Basharat Ali

10 ***Reduced Glutathione Protects Subcellular Compartments From Pb-Induced ROS Injury in Leaves and Roots of Upland Cotton* (Gossypium hirsutum L.)**
Mumtaz Khan, Samrana Samrana, Yi Zhang, Zaffar Malik, Muhammad Daud Khan and Shuijin Zhu

22 ***Transcription Factor GmWRKY142 Confers Cadmium Resistance by Up-Regulating the Cadmium Tolerance 1-Like Genes***
Zhandong Cai, Peiqi Xian, Huan Wang, Rongbin Lin, Tengxiang Lian, Yanbo Cheng, Qibin Ma and Hai Nian

39 ***K Fertilizers Reduce the Accumulation of Cd in* Panax notoginseng *(Burk.) F.H. by Improving the Quality of the Microbial Community***
Yue Shi, Lisha Qiu, Lanping Guo, Jinhui Man, Bingpeng Shang, Rongfeng Pu, Xiaohong Ou, Chunyan Dai, Pengfei Liu, Ye Yang and Xiuming Cui

52 ***A Maize* ZmAT6 *Gene Confers Aluminum Tolerance* via *Reactive Oxygen Species Scavenging***
Hanmei Du, Ying Huang, Min Qu, Yihong Li, Xiaoqi Hu, Wei Yang, Hongjie Li, Wenzhu He, Jianzhou Ding, Chan Liu, Shibin Gao, Moju Cao, Yanli Lu and Suzhi Zhang

64 ***Seed Priming Improved Antioxidant Defense System and Alleviated Ni-Induced Adversities in Rice Seedlings Under N, P, or K Deprivation***
Fahad Khan, Saddam Hussain, Sehrish Khan and Mingjian Geng

76 ***Novel Insights Into the Hyperaccumulation Syndrome in* Pycnandra *(Sapotaceae)***
Sandrine Isnard, Laurent L'Huillier, Adrian L. D. Paul, Jérôme Munzinger, Bruno Fogliani, Guillaume Echevarria, Peter D. Erskine, Vidiro Gei, Tanguy Jaffré and Antony van der Ent

90 ***Glutamic Acid-Assisted Phytomanagement of Chromium Contaminated Soil by Sunflower (Helianthus annuus L.): Morphophysiological and Biochemical Alterations***
Mujahid Farid, Sheharyaar Farid, Muhammad Zubair, Muhammad Awais Ghani, Muhammad Rizwan, Hafiz Khuzama Ishaq, Saad Alkahtani, Mohamed M. Abdel-Daim and Shafaqat Ali

104 ***Photosynthesis Performance and Antioxidative Enzymes Response of* Melia azedarach *and* Ligustrum lucidum *Plants Under Pb–Zn Mine Tailing Conditions***
XinHao Huang, Fan Zhu, ZhiXiang He, XiaoYong Chen, GuangJun Wang, MengShan Liu and HongYang Xu

121 ***Indigenous Tocopherol Improves Tolerance of Oilseed Rape to Cadmium Stress***
Essa Ali, Zeshan Hassan, Muhammad Irfan, Shabir Hussain, Haseeb-ur-Rehman, Jawad Munawar Shah, Ahmad Naeem Shahzad, Murtaza Ali, Saad Alkahtani, Mohamed M. Abdel-Daim, Syed Asad Hussain Bukhari and Shafaqat Ali

133 ***Plant Cadmium Resistance 2 (SaPCR2) Facilitates Cadmium Efflux in the Roots of Hyperaccumulator Sedum* alfredii *Hance***
Jiayu Lin, Xiaoyu Gao, Jianqi Zhao, Jie Zhang, Shaoning Chen and Lingli Lu

144 ***Role of Exogenous and Endogenous Hydrogen Sulfide (H_2S) on Functional Traits of Plants Under Heavy Metal Stresses: A Recent Perspective***
Muhammad Saleem Arif, Tahira Yasmeen, Zohaib Abbas, Shafaqat Ali, Muhammad Rizwan, Nada H. Aljarba, Saad Alkahtani and Mohamed M. Abdel-Daim

158 ***Lead Toxicity in Cereals: Mechanistic Insight Into Toxicity, Mode of Action, and Management***
Muhammad Aslam, Ayesha Aslam, Muhammad Sheraz, Basharat Ali, Zaid Ulhassan, Ullah Najeeb, Weijun Zhou and Rafaqat Ali Gill

178 ***Effect of Engineered Nickel Oxide Nanoparticle on Reactive Oxygen Species–Nitric Oxide Interplay in the Roots of* Allium cepa *L.***
Indrani Manna, Saikat Sahoo and Maumita Bandyopadhyay

frontiers in Plant Science

EDITORIAL
published: 18 February 2022
doi: 10.3389/fpls.2021.830682

Editorial: Heavy Metal Toxicity in Plants: Recent Insights on Physiological and Molecular Aspects

Rafaqat Ali Gill[1]*, *Mukesh Kumar Kanwar*[2], *Andre Rodrigues dos Reis*[3] and *Basharat Ali*[4]*

[1] Key Laboratory of Biology and Genetic Improvement of Oil Crops, The Ministry of Agriculture and Rural Affairs, Oil Crops Research Institute of Chinese Academy of Agricultural Sciences, Wuhan, China, [2] Department of Horticulture, College of Agriculture and Biotechnology, Zhejiang University, Hangzhou, China, [3] São Paulo State University "Júlio de Mesquita Filho" (UNESP), Tupã, Brazil, [4] Department of Agronomy, University of Agriculture, Faisalabad, Pakistan

Keywords: heavy metals stress, plant genome, phytoremediation, nutrient deprivation, management, cell morphology

OPEN ACCESS

Edited by:
Carla S. Santos, Catholic University of Portugal, Portugal

Reviewed by:
Zygmunt Mariusz Gusiatin, University of Warmia and Mazury in Olsztyn, Poland
Boris Bokor, Comenius University, Slovakia

***Correspondence:**
Rafaqat Ali Gill
drragill@caas.cn
Basharat Ali
basharat2018@yahoo.com

Specialty section:
This article was submitted to Plant Nutrition, a section of the journal Frontiers in Plant Science

Received: *07 December 2021*
Accepted: *29 December 2021*
Published: *18 February 2022*

Citation:
Gill RA, Kanwar MK, Rodrigues dos Reis A and Ali B (2022) Editorial: Heavy Metal Toxicity in Plants: Recent Insights on Physiological and Molecular Aspects. Front. Plant Sci. 12:830682. doi: 10.3389/fpls.2021.830682

Editorial on the Research Topic

Heavy Metal Toxicity in Plants: Recent Insights on Physiological and Molecular Aspects

The topmost soil (i.e., surface O and A) is of great importance for plants as it contains the majority of the mineral elements required for normal plant growth and development (PG&D). However, the same soil also serves as a sink for hazardous pollutants including heavy metals (HMs) such as cadmium (Cd), lead (Pb), chromium (Cr), arsenic (As), and mercury (Hg) concentrated due to anthropogenic activities (industrialization and urbanization) that severely impact on PG&D. These toxic metal ions after entering into plant body disturbed cell wall, cell membrane, the activity of mitochondria (root) and cytoplasm (leaf) induced MDA and ROS content, and negatively impact the antioxidative machinery, fatty acids (i.e., linoleic acid and linolenic acid), and some other enzymes such as NADPH oxidase, etc. Further, HM toxicity caused the disturbance of water and nutrient supply from soil to upper parts of plants and deterioration in the activities of leaf pigment such as chlorophyll content and PS II impact on the sugar production and then transportation system from upper to lower parts of plants. These above drastic changes altogether caused the alterations in the various physiological and biochemical processes resulted in the reduction of the fresh biomass (root and shoot), overall PG&D, and finally decreased the grain quantity and quality. To tackle this, the researchers explored various perspectives while studying plants grown under HMs stressed environments. First, they explored plant response mechanisms as they activate its enzymatic (SOD, POD, CAT, APX, and GR) and non-enzymatic (GSH and ASA) antioxidant machinery. Secondly, plants modify their cell wall and root exudates. The third strategy is the utilization of plants (phytoremediation-hyperaccumulation) to absorb more content of HMs from the soil. Fourth, overexpression of metal responsive genes such as *PCR2*, *AT6*, *CDT1*, and *WRKY* creates the protective shield against metal toxicity. Lastly, exogenous applications of growth regulators such as GA, H_2S, and GSH provide relief to plant species coping hazardous behavior of HMs. In a nutshell, an integrated strategy based on above all alternatives can strengthen the plant defense system and increase the seed yield of the crop plants growing in the toxic environment.

This Research Topic primarily focuses on HM induced abnormalities in plants, like nutrient imbalance, alteration in PG&D, microflora degradation, and enzymes dis-functioning. The present "Research Topic" succeeded in collecting 11 original research papers, one review and one perspective on diverse HMs like Cd, Pb, zinc (Zn), Cr, nickel (Ni), aluminum (Al), and a signaling molecule hydrogen sulfide (H_2S).

CD TOXICITY IN PLANTS: HAZARDOUS IMPACTS AND ITS ALLEVIATION THROUGH VARIOUS STRATEGIES

Cadmium (Cd) becomes a part of the soil–plant environment as plants absorbs water and nutrients from the soil. In this context, Shi et al. explore the alleviating role of potassium (K) fertilizers to reduce the Cd content in *Panax notoginseng* by enhancing activities of soil micro-organism as they influenced by soil pH, total organic matter (TOM), and cation exchange capacity (CEC). Their pot experiment's results probed the impact of exogenously applied K on the biologically available of amount of Cd content (bio-Cd), soil pH, TOM, CEC, and endogenous Cd content in *Panax notoginseng*. Moreover, they considered that K_2SO_4 (0.6 $g{\cdot}kg^{-1}$) was optimal treatment to reduce the Cd uptake. However, in the field condition their results showed the positive impact of K_2SO_4 on the soil microbial community (i.e., Acidobacteria, Mortierellomycota, Proteobacteria, and Bacteroidetes) and the consequences on the soil pH, TOM, and CEC. Potassium application enhances the activities of Mortierellomycota, Proteobacteria, and Bacteroidetes and decreased the activity of Acidobacteria. Moreover, they explored the correlation of above-mentioned microbe species with soil pH, TOM, CEC, and bio-Cd. In a nutshell, K fertilizers decreased the accumulation of Acidobacteria, as they involved in the acidification of the soil pH and CEC, and enhanced the activities of Mortierellomycota, Proteobacteria, and Bacteroidetes, which were found to be responsible for increased pH, TOM, and CEC and reduced the bio-Cd content in the soil.

Oilseed rape (*B. napus*) contains soluble lipids including tocopherols, also known as vitamin E, is an essential nutrient for animals and human beings. The finding by Ali et al. suggested that tocopherols act as an antioxidant in tackling the reactive oxygen species (ROS) induced by Cd stress in two contrasting genotypes (Jiu-Er-13XI and Zheyou-50, differing in seed oil content) of *B. napus*. Their results showed that Cd significantly caused more damages in low seed oil content containing cultivar (Jiu-Er-13XI) compared to high seed oil content cultivar (Zheyou-50). They probed that level of ROS was significantly high in low seed oil content cultivar and physiological damages was appeared in terms of destroyed chloroplast and photosynthetic structures. Further, total fatty acids such as linoleic acid (18:2) and linolenic acid (18:3), were deteriorated due to increase in malondialdehyde (MDA) and tocopherols content, and Cd accumulation were more prominent in the roots of low seed oil content cultivar compared to high-seed oil content cultivar. They also showed that in resistant cultivar (Zheyou-50), the accumulation of α-Tocopherol and transcript levels of genes involved in the biosynthesis of tocopherol were much higher. As a whole, tocopherol not only restricts the uptake of Cd in roots and then translocation to the shoots but also scavenging ROS, lowering the MDA content, and play a role in polyunsaturated fatty acids remained intact with chloroplast membrane.

As an adaptive strategy, plants have evolved a diverse set of mechanisms to cope with Cd stress. Their strategy involved a combination of enzymatic, non-enzymatic antioxidants, extrusion of Cd across the plasma membrane, restriction of Cd movement toward roots and finally sequestration of Cd to the metabolically inactive plant parts such as root cell wall and leaf vacuoles. Recent progress on the role of WRKY transcription factors (TFs) (pronounced "worky" are the proteins that contain WRKY conserved domain and are involved in the regulation of several biotic and abiotic stress responses) in conferring the Cd tolerance in various plant species evidenced its role. Cai et al. have identified 29 Cd-responsive WRKY-TFs in Soybean. Among, 26 genes were upregulated and three were downregulated under Cd treatment. They identified a novel Cd-responsive GmWRKY142 gene and cloned to investigate its detailed tolerance mechanism in Cd stress. Their result showed that the above TF was localized in the nucleus and exhibit higher transcriptional activity in root when plants subjected to Cd stress. Moreover, in the overexpressed (*GmWRKY142*) lines (both in Arabidopsis and Soybean), expression levels of other Cd-responsive genes such as *ATCDT1*, *GmCDT1-2* encoding cadmium tolerance 1, and *GmCDT1-1* were enhanced compared to wild type (WT), which indicated that the upregulation of *GmCDT1-1* and *GmCDT1-2* resulted in the deterioration of Cd uptake and improves tolerance. Thus, GmWRKY142-GmCDT1-1/2 cascade opened up a new avenue/strategy to potentially cope Cd accumulation in Soyabean.

Another adaptive strategy to cope with Cd toxicity is by growing hyperaccumulators to the affected soils as they contained a sophisticated metal detoxification system. For example, in China *Sedum alfredii* Hance is a potential Cd hyperaccumulator plant as reported by Lin et al. They explored Cd-detoxification mechanism in hyperaccumulating ecotype (HE) of *Sedum alfredii* and discovered a gene named SaPCR2 that belongs to a plant Cd resistance (PCR) family. In the over-expressed lines, *SaPCR2* was highly expressed in root and its expression level not changed significantly under Cd exposure. Moreover, subcellular localization results in tobacco leaves and yeast showed that *SaPCR2* is a plasma membrane localized gene and its expression level (its protein in a Zn/Cd-sensitive yeast Δ*zrc1*) enhanced significantly resulted in the increased tolerance to Cd stress by deteriorating Cd content in cells. These findings suggested that overexpression of *SaPCR2* protects the root cells from Cd phytotoxicity by Cd leak out from the root cells. As a whole, these above findings suggested alternative routes to cope Cd tolerance and provides the basis for producing the metal tolerance commercial cultivars.

PB TOXICITY IN PLANTS: NEGATIVE INFLUENCE, AND ANTIOXIDANT AND GENOMIC RESPONSES

Lead is considered as non-essential element and negatively affect the plant growth, when taken by plants. Huang et al. reveals the differences of tolerance between *M. azedarach* and *L. lucidum* under Pb–Zn polluted mine-tailings. Their results suggested that Pb-Zn pollutant significantly deteriorated the net

photosynthetic rates and leaf photosynthetic pigment content by biochemical limitation (BL). Moreover, they explored that Pb-Zn tailing particularly affected on the PSII activity as evidenced the changes in the values of reaction center (RC) in the forms of electron movement, maximum quantum yield for primary photochemistry, the density of PSII RC per excited cross-section, and the absorption of antenna chlorophylls per PSII RC. Besides, they noted that Pb–Zn toxicity also affected the oxidation and reduction state of PSI resulted in an enhancement of ROS contents and lipid peroxidation. Further, their antioxidant activities related data showed that at lower level of Pb-Zn tailing catalase (CAT), superoxide dismutase (SOD), and peroxidase (POD) activities were increased but under higher level of Pb-Zn tailing were started declining. Both species showed the diversity in response to the above pollutants as *L. lucidum* exhibits more tolerance in terms of better net photosynthesis efficiency and higher enzymatic antioxidant activities. Another possible strategy to cope the Pb toxicity is the exogenous application of growth regulators. For instance, Khan M. et al. studied the negative impact of Pb stress and alleviating role of reduced glutathione (GSH) in cotton crop. Their controlled experiment suggested that Pb exposure (10 days) increased the MDA content and ROS level such as hydrogen peroxide (H_2O_2) and hydroxyl radical (OH•) and deteriorated the activities of CAT and ascorbate peroxidase (APX) in terminal and radial leaves. In contrast, CAT activity was enhanced and APX was decreased in the primary and secondary root. Similarly, activities of SOD and POD were increased in the median leaves and declining trend was recorded in the terminal leaves, primary and secondary roots. Moreover, glutathione reductase activity, ascorbic acid (ASA) and GSH contents were increased in all plant parts; except ASA content was deteriorated in the median leaves. Their electron microscopic observations from terminal and median leaves further evidenced the negative influence of Pb toxicity in the forms of damaged cell wall, cell membrane, chloroplast, and mitochondria. Similarly, in the root's micrographs, Pb induced damages were noticed in nucleus, cell membrane, and mitochondria. Interestingly, exogenously GSH application had significant impact on plants in terms of stabilized leaf and root cell ultra-structures by modulating the cell membranes, formation of multivesicular body vesicles and maintaining the structural integrity of other organelles. In a nutshell, GSH is involved in the alleviation of Pb-induced negative impacts in the cotton. Lastly, the review by Aslam et al. highlights the mechanism(s) involved in Pb uptake and translocation in cereals, critically reviews the possible management strategies to menace Pb toxicity in cereals. In detail, they have discussed that high Pb-stress caused the negative impacts on biochemical and physiological processes that are responsible for grain quality in cereals. Pb effect not only impact on the cell organelles integrity including membrane stability index but also several metabolic processes involved in the electron transport chain, PSII connectivity, mineral transportation, oxygen evolving complex and antioxidant system. Further, they argued on the role of plant growth-promoting rhizobacteria as potential and less expensive Pb-remediators in the soil. Lastly, they insight on the molecular and other cellular changes occurred by the utilization of TFs such as bZIP, ERF and GARP, and other proteins including MTP and NRAMP to cope the Pb induced toxicity.

CR TOXICITY IN PLANTS: CHELATE-ASSISTED PHYTOREMEDIATION

After Cd and Pb, Cr is considered the most harmful HM in the soil as it is present in the topsoil where plants struggle for the macro- and micro-nutrients to continue their normal life processing. To extract HMs from soil, utilization of chelators (chelator-assisted phytoremediation) is one of the most suitable strategy in terms of sustainability and economics as it enhance the bio-availability of HMs, which then increased the process of phytoextraction. Farid et al. study the role of organic chelator, glutamic acid (GA) in improving the phytoextraction of Cr by utilizing the sunflower (*H. annuus*). Their result first stated the negative role of Cr stress (with increasing concentration in the top soil) as it significantly reduced the plant growth and development resulted in deterioration in biomass, leaf areas antioxidant activities, and photosynthetic machinery related attributes. Secondly, their results showed that exogenously applied GA statistically improved the Cr-induced hazardous impacts. Interestingly, GA application increased the Cr uptake in the plants by enhancing availability and mobilization of Cr toward roots of sunflower plants that later on translocated to the upper plant's parts. As a whole, these finding suggested the dual role of GA as its application not only protects the plants form Cr-induced toxicity but also enhanced Cr accumulation (phytoextraction) by sunflower plants.

NI-INDUCED TOXICITY IN PLANTS: IMPACT ON THE MACRO-MOLECULES, AND ITS ALLEVIATION THROUGH HYPER-ACCUMULATION AND BIO-ACCUMULATION

Ni is an essential micro-element for higher plant species but required at very low concentrations. However, excess Ni in soil medium can be toxic and may disturb the normal PG&D. Growing evidence stated that like other HMs, extreme Ni stress also caused the production of ROS that severely damage the cell ultrastructure. For example, Khan F. et al. investigated negative impact of Ni induced toxicity alone and with deprivation of macro-nutrients i.e., nitrogen (N), phosphorus (P), and potassium (K) on nutrient uptake, plant growth, oxidative metabolism in rice seedlings. Their results stated that both Ni and nutrient deprivation induced stress severely negative impact on the establishment of rice seedlings, reduction in shoot length and fresh biomass. Among all combinations of Ni with N, P, and K, more severe results were recorded in Ni with N deprivation medium except the root length. Interestingly, Ni with P and K deprivation mediums had similar impact on root fresh biomass compared with plants grown on normal N, P, and K medium. Further, they probed that Ni alone in combination with N, P,

and K deprivation induced stresses caused the generation of ROS, lipid peroxidation and reduction in antioxidant machinery except GR and vitamin E. Also, they recorded that Ni stress caused the reduction of N in shoot and in reverse N deprivation plants stored more Ni content in shoot. However, seedlings with K deprivation stored more Ni in root. Lastly, they also noted the positive impact of seed priming with selenium (Se) and salicylic acid (SA) under Ni stress or nutrient deprivation condition. As expected, their findings showed that Se and SA primed seedlings expressed more tolerance to Ni and no nutrient environment and better seedling growth and fresh biomass, which may be due to lower ROS level, greater membrane stability, improved antioxidant machinery and nutrient homeostasis.

The term "hyper accumulator" was first time used by Isnard et al. in their report published in 1976. According to their finding and later on observations of other researchers, hyper-accumulator are those plants that accumulate specific metal or metalloids in their tissues (living) 100 or 1,000 times more than normal uptake for most of plant species. In line with above, Isnard et al. conduct a comprehensive study hydroponically to explore the genetic mechanism in Ni hyperaccumulation and then its translocation in genus *Pycnandra*. Their data (after foliar application of Ni) stated that the genus *Pycnandra*, species acuminata can resist up to 3,000 μM. Moreover, the Ni portioning was spread throughout the plant body, but was more obvious in latex (124,000 μg g−1). Further, their phylogenetic analysis revealed that phenomenon of "hyperaccumulation" evolved independently in two subgenera and five species of the above-mentioned genus. Later on, extreme resistance to Ni stress becomes the unique property of lacticifers. As a whole, these findings suggested further investigation to explore the genetic makeup of latex producing cells to explore their Ni storing mechanism/s.

Now a days researchers are more anxious about probing the consequences of HMs starts from the external environment *via* their uptake or bioaccumulation into different parts of plant's body. There is such example of engineered nanoparticles of Ni oxide (NiO-NP) investigated by Manna et al. in the roots of *Allium cepa*. Their results showed that before entering into cell organelles, NiO-NP first damage the cell membrane and then disturb the cellular homeostasis and finally minimize the survival chances. In result, a boom in the generation of ROS and nitric oxide (NO) were occurred resulted in the alteration of several important biochemicals. Meanwhile, in response to external stress, transcription rate and activities of antioxidants such as CAT, POD, SOD were enhanced (on an average up to 50–250%). Moreover, their results showed that the transcript levels of two subunits of Rubisco activase were also increased. Besides, they noticed that increased in the NO content was dose dependent and also may due to increase in the accumulation of other enzymes such as NADPH oxidase, NO synthase and nitrate reductase. Moreover, they also highlighted the general cellular response (changes in ROS-NO nexus) to external stress, for instance, modifications in K/Na ratio, enhancement in proline, and GABA content. Overall, above findings not only explored the detailed negative consequences of NiO-NP but also highlighted the response of general stress indicators.

AL-INDUCED TOXICITY IN PLANTS: IMPACT ON PG&D, ROS AND ANTIOXIDANT MACHINERY, AND ITS ALLEVIATION THROUGH OVER-EXPRESSION OF RELATED GENE/S

Soils having pH lower than ≤5.5 considered as acid soils. In total, acid soils comprise of 30% of arable and 50% of potential cultivated land. Al is the third most abundant element present in the earth crust that can be converted to soluble and lethal form (Al^{+3}), which is the promising limiting factor of PG&D in acid soils that ultimately impact on seed yield. Du et al. explored the genes participate in Al tolerance mechanism by taking maize crop plant as an example. His results showed that *aluminum tolerance 6* (*ZmAT6*) gene that expressed in almost all tissue/organs but upregulated more in shoot and then root under Al stress. Further, investigation in the over-expressed maize and Arabidopsis plants confirmed the role of *ZmAT6 in* Al tolerance as in the transgenic plants better root growth, lower Evans blue absorption, lower accumulation of Al, reduction in the generation of ROS, increment in the proline content and several antioxidants such as SOD (including its transcript level, *ZmSOD*), POD, CAT, and APX were recorded compared to WT.

THE ALLEVIATING ROLE OF H_2S IN PLANTS UNDER HM STRESS

Lastly, Arif et al. presented the perspective on the role of H_2S in alleviating the negative impacts of HMs in plants. They discuss the detailed role of H_2S as a signaling molecule counter the HMs induced ROS and then improves plant tolerance. In detail, the alleviating role of H_2S in terms of eliminating the negative impacts of metal-element induced toxicity, improving several key physiological and biochemical processes. Lastly, they argued on the cross-talk of H_2S with other endogenous hormones improves plant growth and development and mitigated the metal induced phytotoxicity under hazardous environmental conditions.

AUTHOR CONTRIBUTIONS

RG and BA wrote the first draft of the article. MK and AR made a substantial, intellectual contribution to the work, and approved it for publication. All authors contributed to the article and approved the submitted version.

ACKNOWLEDGMENTS

We thank all the contributors to this Research Topic.

Conflict of Interest: The authors declare that the research was conducted in the absence of any commercial or financial relationships that could be construed as a potential conflict of interest.

Publisher's Note: All claims expressed in this article are solely those of the authors and do not necessarily represent those of their affiliated organizations, or those of the publisher, the editors and the reviewers. Any product that may be evaluated in this article, or claim that may be made by its manufacturer, is not guaranteed or endorsed by the publisher.

frontiers in Plant Science

ORIGINAL RESEARCH
published: 15 April 2020
doi: 10.3389/fpls.2020.00412

Reduced Glutathione Protects Subcellular Compartments From Pb-Induced ROS Injury in Leaves and Roots of Upland Cotton (*Gossypium hirsutum* L.)

Mumtaz Khan[1,2,3], Samrana Samrana[1], Yi Zhang[1], Zaffar Malik[4], Muhammad Daud Khan[3] and Shuijin Zhu[1]**

[1] Department of Agronomy, Institute of Crop Sciences, College of Agriculture and Biotechnology, Zhejiang University, Hangzhou, China, [2] Department of Environmental Sciences, Faculty of Engineering, Gomal University, Dera Ismail Khan, Pakistan, [3] Department of Biotechnology and Genetic Engineering, Kohat University of Science and Technology, Kohat, Pakistan, [4] Department of Soil Sciences, University College of Agriculture & Environmental Sciences, The Islamia University of Bahawalpur, Bahawalpur, Pakistan

OPEN ACCESS

Edited by:
Basharat Ali,
University of Agriculture, Pakistan

Reviewed by:
Muhammad Rizwan,
Government College University Faisalabad, Pakistan
Najeeb Ullah,
The University of Sydney, Australia
Muhammad Ahsan Farooq,
Zhejiang University, China

***Correspondence:**
Mumtaz Khan
mkhan@gu.edu.pk
Shuijin Zhu
shjzhu@zju.edu.cn

Specialty section:
This article was submitted to Plant Nutrition, a section of the journal Frontiers in Plant Science

Received: *16 January 2020*
Accepted: *23 March 2020*
Published: *15 April 2020*

Citation:
Khan M, Samrana S, Zhang Y, Malik Z, Khan MD and Zhu S (2020) Reduced Glutathione Protects Subcellular Compartments From Pb-Induced ROS Injury in Leaves and Roots of Upland Cotton (Gossypium hirsutum L.). Front. Plant Sci. 11:412. doi: 10.3389/fpls.2020.00412

Heavy metals-based changes in the plants and their alleviation through eco-friendly agents including reduced glutathione (GSH) have been widely studied. In the present experiment, we tested the alleviatory role of reduced glutathione (GSH) in seedlings of upland cotton cultivar, TM-1 under lead (Pb) toxicity. Plants were grown in the Hoagland solution containing Pb (0 μM), Pb (500 μM), GSH (50 μM), and GSH + Pb (50 μM + 500 μM). Lead exposure exacerbated hydrogen peroxide (H_2O_2) and hydroxyl radical ($OH^•$) levels, induced lipid peroxidation (MDA), and decreased the activities of catalase (CAT) and ascorbate peroxidase (APX) in the terminal and median leaves of 28-days old cotton seedlings stressed for 10 days. However, in the primary and secondary roots, CAT activity was increased but APX decreased. Similarly, peroxidase (POD) and superoxide dismutase (SOD) activities were enhanced in the median leaves but a declining trend was observed in the terminal leaves, primary roots and secondary roots. Glutathione reductase (GR) activity, ascorbic acid (AsA) contents and GSH concentrations were increased in all parts except AsA in the median leaves. Transmission electron micrographs of Pb-treated plants exhibited deformed cell wall and cell membrane, disfigured chloroplasts and irregularly shaped mitochondria in the terminal and median leaves. Further, cell membrane, mitochondria, nucleus and other cell organelles in root cells were severely affected by the Pb. Thus their identification was little bit difficult through ultramicroscopy. External GSH stabilized leaf and root ultramorphology by stabilizing cell membranes, stimulating formation of multivesicular body vesicles, and by maintaining structural integrity of other organelles. Evidently, GSH played major alleviatory role against Pb toxicity in upland cotton.

Keywords: heavy metals stress, cell morphology, reactive oxygen species, antioxidant enzymes, chloroplast, mitochondria

INTRODUCTION

Environmental lead (Pb) has increased 1000 fold in the past three centuries, mainly due to huge industrial demands and less recycling, causing its accumulation in the plants and animals (ATSDR, 2007; Rahman and Singh, 2019). Its uptake causes physiological and morphological changes in plant's organs including roots and leaves (Jiang et al., 2014b; Khan et al., 2016). Moreover, biomolecules such as proteins, nucleic acids, lipids and hormones are also affected by the Pb (Pourrut et al., 2011; Lanier et al., 2019). During metal stress, excess reactive oxygen species (ROS) such as superoxide anion ($^{\bullet}O^{-}$), hydrogen peroxide (H_2O_2), hydroxyl ion ($OH^{\bullet}$) and malondialdehyde (MDA) are produced which cause oxidative damage to cell membranes and biomolecules (Das and Roychoudhury, 2014; Berni et al., 2019). Plants respond to excess ROS by inducing enzymatic and non-enzymatic antioxidants like superoxide dismutase (SOD), catalase (CAT), ascorbate peroxidase (APX), peroxidase (POD), glutathione reductase (GR), ascorbic acid (AsA) and reduced glutathione (GSH) that work synergistically to cope with metal toxicity (Ali et al., 2014a; Berni et al., 2019).

Among antioxidants, SODs constitute cell's first line defense against ROS (Mishra and Sharma, 2019). Based on metal cofactor and protein folding, SODs have been grouped into Fe-SOD, Mn-SOD and Cu-Zn-SOD (Szőllősi, 2014). They dismutate highly reactive $^{\bullet}O^{-}$, produced at the sites of electron transport chain, to form less toxic H_2O_2 and O_2. Both, CAT and APX neutralize H_2O_2, however; former is more effective scavenger due its higher affinity for H_2O_2 (Cuypers et al., 2016). Peroxidases are abundantly present in the plant cells and use H_2O_2 as a substrate to produce H_2O and O_2. Glutathione reductase reduces oxidized glutathione (GSSG) back into GSH to maintain balanced levels of the later in cells (Lu, 2013). Ascorbic acid scavenges ROS through glutathione-ascorbate pathway and serves as a cofactor for various enzymes (Hasanuzzaman et al., 2019).

Reduced glutathione, found in the most life forms, is bestowed with myriad of cell functions (Hausladen and Alscher, 2017). It is biosynthesized as a tripeptide of glutamate, cysteine and glycine in two ATP-dependent steps by glutamate cysteine ligase ("GSH1") and glutathione synthetase ("GSH2") enzymes. In addition to its role as precursor for phytochelatins (PCs), GSH plays roles in redox signaling, ion homeostasis and sulfur assimilations. Moreover, it maintains catalytic and regulatory thiol groups in the reduced state (Zechmann, 2014). In earlier research work, GSH has alleviated oxidative stress, induced by range of pollutants, in several plant species (Sobrino-Plata et al., 2014; Daud et al., 2016; Adams et al., 2020). Besides this, GSH promotes PCs synthesis in a transpeptidation reaction catalyzed by phytochelatin synthase (Grill et al., 1987). Being functionally analogous to metallothioneins, PCs bind to heavy metals (HMs) through thiol group (Cobbett, 2000). Further, in GSH redox cycle, it reduces H_2O_2 and lipid peroxides via reactions catalyzed by GSH peroxidase. During this process, GSH is oxidized to GSSG, which can be reversed to GSH by GR, depending on NADPH, thereby keeping optimum GSH pools for proper cell functioning. However, HMs adversely affect GSH concentrations in the plants (Eroglu et al., 2015), and that external feeding of GSH may help alleviate oxidative stress in upland cotton.

In previous experiment, we have studied the alleviatory effect of exogenous GSH on photosynthesis and chloroplast morphology in Pb-stressed cotton seedlings (Khan et al., 2016). However, how GSH alleviates Pb stress in different leaves and roots of cotton needs a detailed study. Keeping in view of this fact, we designed current experiment to observe Pb-triggered biochemical and morphological changes in terminal and median leaves, and primary and secondary roots of upland cotton, and subsequent recovery through reduced glutathione application.

MATERIALS AND METHODS

Growth Conditions and Plant Sectioning

Upland cotton variety TM-1 was selected for this study which is a standard genetic line and comparatively a heavy metal tolerant variety. Its seeds were obtained from Cotton Germplasm Lab, Zhejiang University, Hangzhou, China, and grown hydroponically according to Khan et al. (2016). Briefly, sterilized upland cotton seeds were grown in growth chamber adjusted to 16/8 h day/night, 60/80% humidity, 45 $\mu E\ m^{-2}\ s^{-1}$ irradiance, and 350 $\mu M\ M^{-1}\ CO_2$ concentrations. Uniformly selected 28-days old seedlings were categorized into four groups; (1) control (0 μM Pb), (2) 500 μM Pb as Pb $(NO_3)_2$, (3) 50 μM GSH, and (4) 50 μM GSH + 500 μM Pb. These treatment levels were selected based on earlier findings from screening tests done in our lab and cotton's seedling threshold level. After 10 days of stress period, harvested plants were separated into terminal leaves (fully expanded upper pair of terminal leaves excluding apical region), median leaves (excluding cotyledonary leaves), primary roots and secondary roots. Seedling stage is the best time to study biochemical and morphological changes in leaves and roots of plants. Plant samples were either freshly used for biochemical assays or stored at −80°C till further analyses.

Sample Extraction for Biochemical Assays

Enzyme extracts (EE) were obtained from plant samples to determine ROS, antioxidant enzymes and AsA content. Briefly, samples were treated with 10 M Na-EDTA to remove unbound Pb, and thoroughly washed with distilled water. Then 8 mL of pre-cooled phosphate buffer solution (PBS, 16.385 g $Na_2HPO_4.12H_2O\ L^{-1}$ and 0.663 $NaH_2PO_4.2H_2O\ L^{-1}$), adjusted to pH 6.5, was added to 0.5 g plant sample in a pre-cooled mortar and pestle. Thoroughly homogenized samples were centrifuged at 12000 × *g* for 20 min at 4°C and supernatants were collected in 10 mL tubes, and kept at −30°C till further use.

Assays for Reactive Oxygen Species

Reactive oxygen species such as H_2O_2, $OH^{\bullet}$ and MDA were determined according to Kaur et al. (2015) with slight modifications. Briefly, H_2O_2 was determined based on KI oxidation by H_2O_2. To 1 mL PBS, 2 mL potassium iodide (KI, 1 M) and 1 mL EE were added and absorbance was recorded

at 390 nm. Molar extinction coefficient (ε) of 0.028 μM cm^{-1} was used to calculate H_2O_2 contents and expressed as μM g^{-1} fresh weight. For MDA, 1.5 mL EE and 2.5 mL mixture of 5% trichloroacetic acid (TCA) + 5% thiobarbituric acid (TBA) was incubated at 95°C for 15 min and then immediately cooled on ice. After short centrifugation at 4800 × *g*, the absorbance of MDA-TBA adduct was measured at 532 nm and 600 nm. The MDA content was determined using ε = 155 mM cm^{-1} and expressed as μM g^{-1} fresh weight. For $OH^{\bullet}$ determination, the reaction mixture comprised of 0.7 mL EE, 3 mL 0.5% TBA and 1 mL glacial acetic acid. After incubation at 100°C for 30 min, the reaction mixture was immediately cooled at 4°C and absorbance was measured at 532 nm. The $OH^{\bullet}$ concentration in the sample was calculated using extinction coefficient, ε = 155 mM cm^{-1} and values were expressed as μM g^{-1} fresh weight.

Antioxidant Assays

The activities of CAT and APX were determined according to Ali et al. (2014b). For CAT, the reaction solution contained 0.1 mL of 300 mM H_2O_2, 0.1 mL EE and 2.8 mL PBS. The reaction mixture was shaken gently before taking reading at 240 nm. One unit of CAT activity was considered equal to the amount of enzyme required to catalyze one micro mole of H_2O_2 per min. For APX, the reaction mixture contained 0.1 mL H_2O_2 (300 mM), 0.1 mL EE, 0.1 mL AsA (7.5 mM) and 2.7 mL PBS. The absorbance was measured at 290 nm. One unit of APX activity was defined as the amount of enzyme needed to oxidize one micro mole of ascorbate per minute. The POD and SOD activities were determined according to Mei et al. (2015). For POD, the reaction mixture was comprised of 0.1 mL each of EE, guaiacol (1.5%) and H_2O_2 (300 mM), and 2.7 mL PBS. The absorbance was measured at 470 nm. For SOD activity, a reaction solution of 75 μM nitroblue tetrazolium (NBT), 20 μM riboflavin, 100 μM Na-EDTA and 130 mM methionine was prepared. Then, 2.725 mL reaction solution, 0.25 mL ddH_2O and 0.025 mL EE were mixed and kept under light (4000 Lux) for 20 min, followed by recording absorbance at 560 nm. One unit of SOD activity was equal to the amount of enzyme required to inhibit 50% of NBT reduction. The GR activity was determined as decline in NADPH levels at 390 nm absorbance using extinction coefficient of 6.2 mM cm^{-1} (Jiang and Zhang, 2001).

Pb and GSH Quantification

Lead contents in leaves and roots of upland cotton were determined according to Khan et al. (2016). Briefly, plant materials were weighed, ashed in muffle furnace and acid digested. Then homogenate was filtered several times to get clear extract for Pb quantification by ICP-MS. Pb contents were expressed as μg g^{-1} fresh weight. For GSH determination, plant samples (0.4 g) were grinded with 4 mL trichloroacetic acid (5% v/v) and the homogenate was centrifuged at 4000 × *g* for 10 min at 4°C to get supernatant. To 2.6 mL NaH_2PO_4 (150 mM, pH 7.8), 0.25 mL supernatant was added and shaked. Then, 0.18 mL DNTP, dissolved in phosphate buffer, was added and mixture was kept at 300°C for 5 min. Absorbance was measured at 412 nm and GSH was quantified against standard curve.

Root Scanning and Transmission Electron Microscopy

Cotton roots were scanned by MIN MAC, STD 1600^{+} root scanner (Regent Instruments) using WinRhizo software for image acquisition. Transmission electron microscopy of terminal and median leaves and primary roots and secondary roots was done according to Khan et al. (2016). Briefly, small leaf and root sections (2–3 mm) were excised by a sharp blade and kept overnight in 3% glutaraldehyde (prepared in 1 M PBS, pH 7.2), and vacuumed several times before fixing in 1% OsO_4 for 1.5 h. Then graded series of ethanol i.e., 50–100% and absolute acetone

TABLE 1 | Lead (Pb) and reduced glutathione (GSH) mediated hydrogen peroxide (H_2O_2), hydroxyl ion ($OH^{\bullet}$) and malondialdehyde (MDA) contents in upland cotton leaves and roots.

Treatments	Terminal leaves	Median leaves	Primary roots	Secondary roots
H_2O_2 (μM g^{-1} FW)				
Control	75 ± 3.6b	65.37 ± 1.7c	45.26 ± 2.4b	9.98 ± 0.6c
500 μM Pb	113 ± 4.4a	95.33 ± 3.3a	64.00 ± 2.3a	15.24 ± 1.8a
50 μM GSH	79 ± 4.8b	78.58 ± 8.4b	37.87 ± 1.2c	9.83 ± 0.8c
50 μM GSH + 500 μM Pb	63 ± 8.5c	56.89 ± 8.9c	32.99 ± 1.8d	12.57 ± 1.1b
$OH^{\bullet}$ (μM g^{-1} FW)				
Control	0.02 ± 0.001c	0.02 ± 0.001c	0.03 ± 0.002c	0.02 ± 0.004c
500 μM Pb	0.06 ± 0.002a	0.05 ± 0.001a	0.12 ± 0.004a	0.10 ± 0.007a
50 μM GSH	0.03 ± 0.001b	0.02 ± 0.002c	0.02 ± 0.002c	0.02 ± 0.001c
50 μM GSH + 500 μM Pb	0.03 ± 0.001b	0.03 ± 0.003b	0.06 ± 0.002b	0.07 ± 0.011b
MDA (μM g^{-1} FW)				
Control	92 ± 3.9b	76 ± 6.5bc	7 ± 0.9b	9 ± 0.9b
500 μM Pb	172 ± 6.3a	129 ± 5.6a	14 ± 1.6a	11 ± 0.9a
50 μM GSH	72 ± 4.5d	64 ± 9.9c	7 ± 0.9b	7 ± 0.9c
50 μM GSH + 500 μM Pb	82 ± 5.3c	87 ± 7.1b	6 ± 0.1b	7 ± 0.9c

Data presented here was obtained from three independent biological replications. Means possessing same alphabets are not significant at 5% probability as determined by Duncan's multiple range test. The values are means ± standard deviation (SD).

were used to dehydrate samples. Samples were then put in 1:1 and 3:1 mixture of absolute acetone and final spur resin for 1 and 3 h, respectively. After, keeping the samples overnight in final spur resin, 100 nm thin samples, cut on a ultramicrotome (Reichert Ultracut E, Germany), were stained with 6% aqueous uranyl acetate and Renold's lead citrate, and mounted on copper grids.

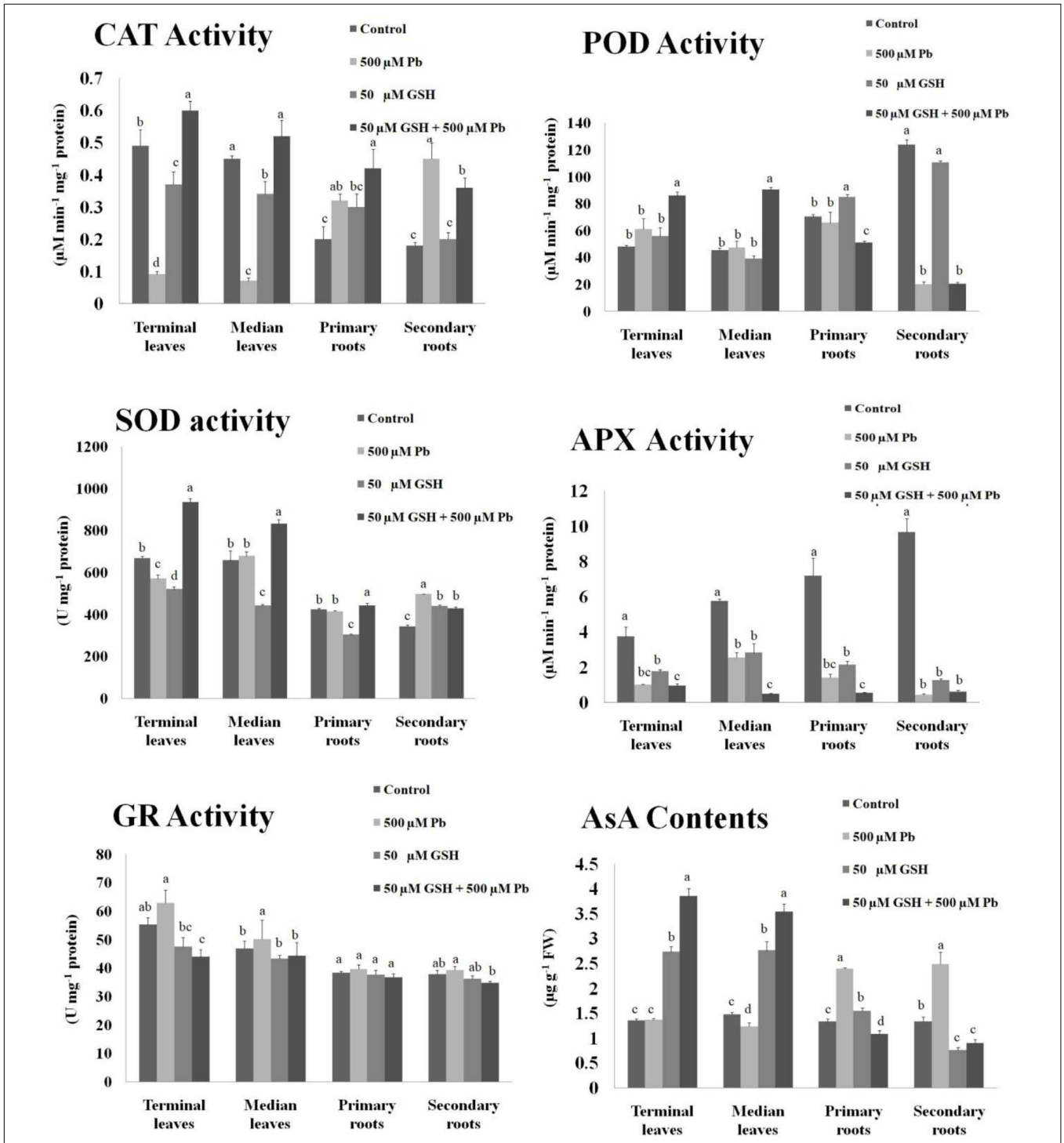

FIGURE 1 | Antioxidant activities in upland cotton under Pb and GSH applications. Response of catalase (CAT), peroxidase (POD), superoxide dismutase (SOD), ascorbate peroxidase (APX), glutathione reductase (GR) and ascorbic acid (AsA) in cotton leaves and roots exposed for 10 days to Pb and GSH in Hoagland solution. Same alphabets on bars represent no significance at 5% probability according to Duncan's multiple range test. Values are mean ± standard deviation (SD) obtained from three independent biological replicates.

Micrographs were taken on transmission electron microscope model-7650, Hitachi Japan operating at 80 kv.

Data Analysis

Data obtained from three replications were subjected to ANOVA, using statistical software package, SPSS 16.0 (SPSS Inc., United States). Significant differences among various treatment means were determined at 5% probability by Duncan's multiple range test. The data were presented as mean ± SD (standard deviation) of three independent biological replicates.

RESULTS

Generation of Stress Biomarkers

Data revealed that ROS levels in leaves and roots of upland cotton were elevated upon Pb exposure, followed by reduction through GSH application (**Table 1**). In control group, leaves generated more H_2O_2 than roots. Pb caused a significant percent increase of 52, 46, 41 and 53 in H_2O_2 in terminal leaves, median leaves, primary roots and secondary roots respectively as compared with control. GSH alone treatment increased H_2O_2 levels in all studied plant parts except secondary roots. GSH + Pb treatment maximally reduced H_2O_2 in primary roots than terminal and median leaves, while less reduction was found in secondary roots. Similarly, highest increase (vs. respective controls) in the $OH^{\bullet}$ due to Pb was found in primary roots (98%) and secondary roots (80%) as compared to terminal (67%) and median leaves (60%). The highest decline in $OH^{\bullet}$ was caused by GSH in terminal leaves in the presence of Pb. Although, GSH reduced $OH^{\bullet}$ levels in the terminal and median leaves, its levels were still higher than primary and secondary roots. Notably, after Pb exposure, primary roots faced more lipid peroxidation (MDA) than terminal and median leaves, and secondary roots. GSH effectively controlled lipid peroxidation in all plant sections except median leaves.

Impact of Pb and GSH on Antioxidants

Results demonstrated changes in the activities of antioxidant enzymes upon Pb, and Pb + GSH exposures (**Figure 1**). The CAT activity in Pb alone treatment was declined in the terminal (0.09 μM/min/mg protein) and median leaves (0.07 μM/min/mg protein), but was elevated in plants subjected to GSH + Pb treatment. The POD activity was boosted in the Pb + GSH treatment in the terminal (85.86 μM/min/mg protein) and median leaves (90.56 μM/min/mg protein), but a declining trend was observed in the primary (51.01 μM/min/mg protein) and secondary roots (20.34 μM/min/mg protein). The highest POD activity was observed in the control group. A differential response was observed for the SOD activity in various treatments. The SOD activity was declined in the terminal leaves (570 U/mg protein) and primary roots (415 U/mg protein) but secondary roots (497 U/mg protein) demonstrated an increase in the Pb group as compared with respective control. However, all parts showed increase in the SOD activity in GSH + Pb group, with highest seen in the terminal leaves. The APX activity was declined in the Pb and GSH + Pb groups in all plant sections as compared with control. However, maximum APX activity (9.65 μM/min/mg protein) was recorded in the secondary roots of control group and lowest (0.48 μM/min/mg protein) in the median leaves of GSH + Pb group. Pb stress caused increase in GR activity in the cotton seedlings with peak levels reported in the terminal leaves (62.84 U/mg protein) and least in the secondary roots (36.23 U/mg protein). The highest GR activity in the GSH + Pb treated plants was observed in the median leaves (44.28 U/mg protein) and lowest in the secondary roots (34.79 U/mg protein). The AsA contents were declined in the terminal and median leaves but increased in both primary and secondary roots under Pb stress. GSH alone increased AsA contents in all parts except secondary roots (0.76 μg/g FW). However, GSH with Pb combination significantly increased AsA contents in the terminal and median

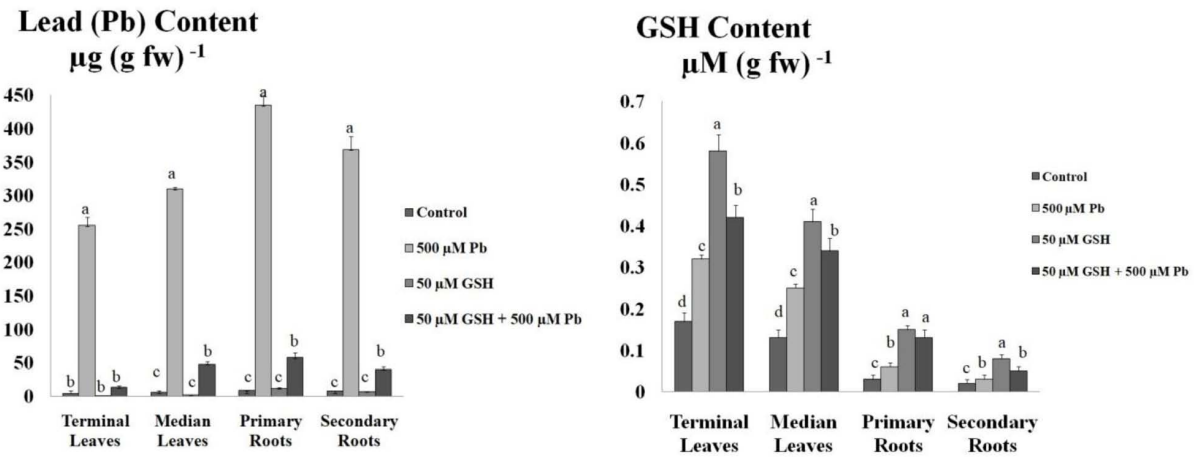

FIGURE 2 | Lead (Pb) and GSH concentration in upland cotton leaves and roots. Upland cotton seedlings exposed to Pb (500 μM) and GSH (50 μM) alone and in combination showing Pb uptake and GSH concentration in terminal leaves and median leaves, and primary roots and secondary roots. Error bars on columns show standard deviation among the values. Chart data are means of three independent biological replications, analyzed through one way analysis of variance (ANOVA) and significant difference determined by Duncan's multiple range test at 0.05% probability level.

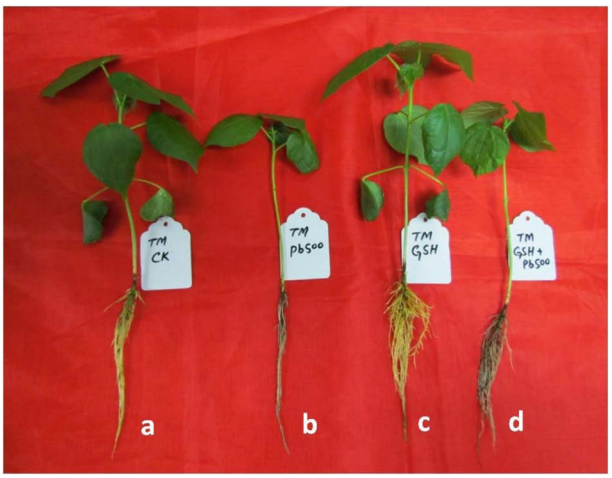

FIGURE 3 | Visual impact of Pb and GSH on upland cotton seedlings. Photographs of upland cotton seedlings (variety TM-1) representing control **(a)**, and those treated with 500 μM Pb **(b)**, 50 μM GSH **(c)** and 500 μM Pb + 50 μM GSH **(d)**.

leaves but the response was meager in the primary and secondary roots.

Pb Accumulation and GSH Content

Results revealed that maximum Pb uptake was observed in the primary roots followed by secondary roots (**Figure 2**). Further, Pb was significantly translocated to the upper foliation but its levels in the median leaves were higher than terminal leaves. GSH application significantly reduced Pb uptake in the leaves and root system of upland cotton. After GSH exposure, least Pb accumulation was found in the terminal leaves while highest in the primary roots.

Leaf Morphology and Microscopy Under Pb and GSH Treatments

Representative photographs clearly showed the adverse effects of Pb and the alleviating impact of GSH on the Pb-treated cotton seedlings (**Figure 3**). As a whole, there were few small leaves on the Pb-treated cotton seedlings having black roots while larger leaves and denser roots were observed in the GSH treatments. Distinct differences were also observed in the transmission

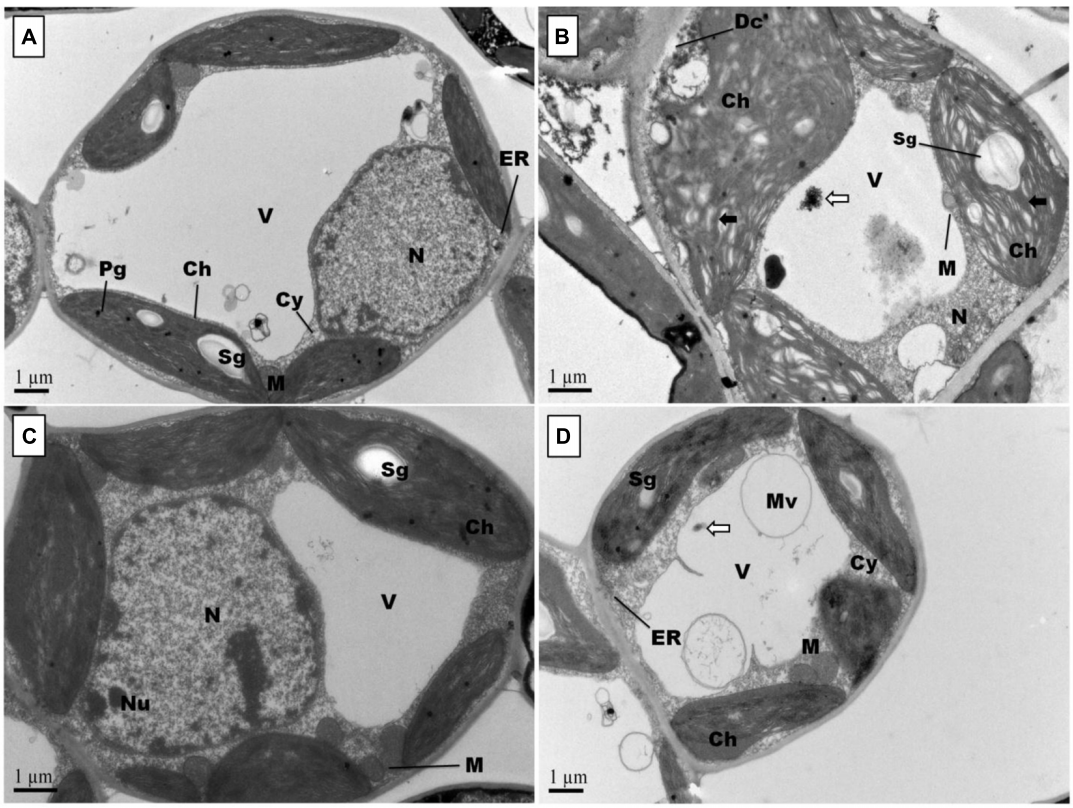

FIGURE 4 | Effects of Pb and GSH on ultrastructure of upland cotton terminal leaves. Transmission electron micrographs represent leaf cell morphology of control **(A)**, 500 μM Pb **(B)**, 50 μM GSH **(C)** and 500 μM Pb + 50 μM GSH **(D)** in cotton seedlings. In control cells **(A)**, cytoplasm (Cy) contained large central vacuole (V), nucleus (N) and well developed chloroplasts (Ch) with starch grains (Sg) and plastoglobuli (Pg). Rounded mitochondria (M) and endoplasmic reticulum (ER) can also be detected. After Pb exposure **(B)**, chloroplasts were highly dilated and granal stacks, represented by black arrow (→), were broken. Similarly, electron dense particles and cell debris, represented by white arrow (⟸), was accumulated in the vacuole. GSH-treated leaf cells **(C)** possessed large chloroplasts, nucleus, nucleolus (Nu), and number of mitochondria were located in between chloroplasts. In GSH + Pb group **(D)**, chloroplasts were dilated but still intact. Moreover, large vacuole with multivesicular structure (Mv), endoplasmic reticulum and nucleus with nucleoli (Nu) were present also.

electron micrographs (TEMs) of Pb- and GSH-treated cotton terminal and median leaves (**Figures 4**, **5**). In control plants, mesophyll cells in both types of leaves were occupied by a bulky central vacuole which pressed plasma membrane against the cell wall. Cytoplasm possessed several adjoining chloroplasts, mitochondria, a large nucleus with scattered chromatin network, endoplasmic reticulum (ER) and ribosomes. Well-developed chloroplasts with elliptical starch grains were observed near cell wall which contained integrated granal stacks and lamellae. Spherical mitochondria, found at chloroplast junctions, were enriched with cristae and electron dense granules. However, clear nucleoli were invisible in the median leaves. In the Pb group, swollen chloroplasts were displaced from the peripheral cell wall boundary. The granal stacking and intergranal lamellae were disfigured. Similarly, mitochondria lost round shape and thread-like structures, probably cell debris and electron dense molecules, were accumulated in bulky vacuoles. The adverse effects of Pb were more pronounced in the median leaves as compared with terminal leaves. In GSH-treated plants, terminal and median leaves contained large well-developed chloroplasts, crowded with grana stacks and lamellae. Nucleus possessed highly condensed chromatin network and visible nucleolus. However, contrary to the control and Pb treatments, bulky vacuole was squeezed due to the presence of "mega" size chloroplasts and dilation of the nucleus in terminal leaves. Moreover, several mitochondria were assembled in the terminal leaves at chloroplast intersections, recognizable by their typical round shape. In the GSH + Pb group, dilated chloroplasts were filled with several starch grains in both terminal and median leaves. In the central vacuole, multivesicular structures were seen instead of dense electron particles or thread-like structures. Moreover, mitochondria were swollen and created gaps between two chloroplasts. But these gaps were larger in the median leaves as compared with terminal leaves.

Root Morphology and Microscopy Under Pb and GSH Treatments

Root scanning revealed that Pb stress reduced density of cotton roots; however, GSH increased root density in primary and secondary roots (**Figure 6**). Like leaves, Pb changed the orientation of subcellular organelles in primary and secondary roots of cotton (**Figures 7**, **8**). Under control conditions, TEMs displayed plasma membrane pressed to thick cell walls. Moreover, the cytoplasm contained multiple cell organelles like mitochondria, Golgi vesicles, vacuole and centrally located large nucleus with nucleoli in primary roots. TEMs of Pb-treated roots exhibited a devastating ultramorphology, with

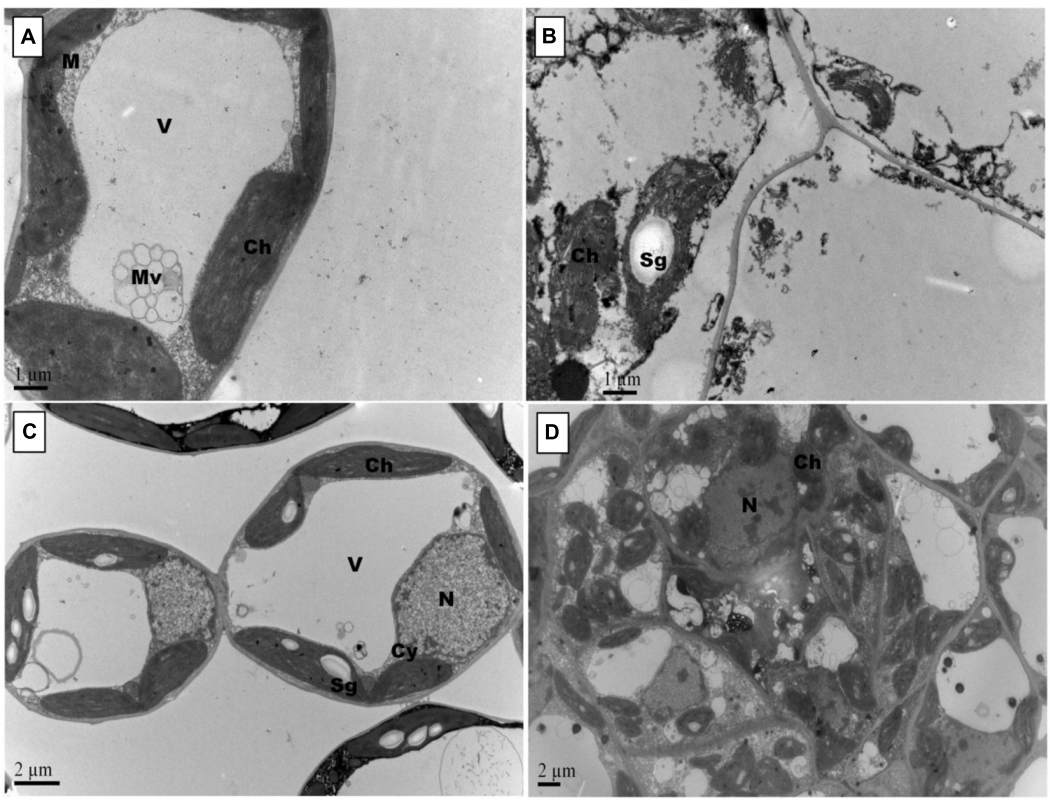

FIGURE 5 | Effects of Pb and GSH on ultrastructure of upland cotton median leaves Transmission electron micrographs represent leaf cell morphology of control **(A)**, 500 μM Pb **(B)**, 50 μM GSH **(C)** and 500 μM Pb + 50 μM GSH **(D)** in cotton seedlings. Control cells **(A)**, contained large central vacuole (V), well developed chloroplasts and rounded mitochondria (M). After Pb exposure **(B)**, chloroplasts were highly dilated and plasma membrane detached from cell walls. GSH-treated leaf cells **(C)** demonstrated large chloroplasts and clearly located nucleus. In GSH + Pb group **(D)**, chloroplasts were dilated but increased in number.

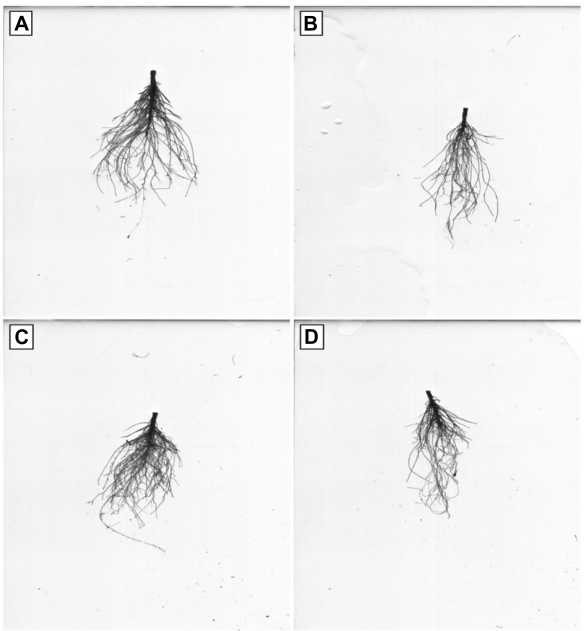

FIGURE 6 | Effects of Pb and GSH on growth and length of primary and secondary roots. Scanned roots represent control **(A)**, cotton roots treated with 500 μM Pb **(B)**, cotton roots treated with 50 μM GSH **(C)** and root of plant treated with combined application of 500 μM Pb and 50 μM GSH **(D)**.

collapsed membrane-bound compartments in both primary and secondary roots. The plasma membrane was ruptured and seen scattered between cytoplasm and cell wall. The cytoplasm itself was highly dilated, probably due to increased permeability of cell wall and plasma membrane, and covered almost entire cell lumen. The cytoplasm contained electron-dense particles, presumably disintegrated cell organelles and Pb particles. Only few endoplasmic reticulum and multivesicular body vesicles were noticed in the root micrographs. No mitochondria or nucleus were clearly located inside the cell. The adverse effects were more pronounced in the secondary roots as compared to primary roots. In the GSH-treated group, primary root cell micrographs showed cell organelles embedded in the cell lumen (**Figure 5C**). But plasma membrane was discontinues due to expansion caused by multivesicular body vesicles and vacuoles. Multivesicular body vesicles were mainly located longitudinally at opposite poles and possessed dense particles. Contrary to leaf micrographs, multiple small vacuoles were found, which contained cell debris. Centrally located nucleus was marked with dense chromatin material and less mitochondria. In the GSH + Pb group, plasma membrane appeared intact and pressed to the thick cell wall in both primary and secondary roots. Moreover, cytoplasm had large numbers of clear and denser multivesicular body vesicles. The central vacuole was filled with cell debris and, probably, with Pb particles. Multiple mitochondria were located near cell wall and nucleus in primary roots but unclear in secondary roots. Nucleus was stretched across whole cell length, with nucleoli being located in the center. Endoplasmic reticulum and dictyosomes were seen distributed near cell wall. Further, spherical amyloplasts contained thylakoids, and abundant microtubules were found in the cells of primary roots. However, there was less growth recovery in secondary roots, and clear identification of cell organelles was difficult.

DISCUSSION

Previous research has shown that cotton can accumulate significant amounts of heavy metals including Pb in seeds, leaves and roots, thereby bringing physiological, metabolic and ultrastructural changes (Daud et al., 2009; Khan et al., 2016). However, study about the role of GSH in modulating antioxidant enzymes and alleviating the ultrastructural-based alterations under Pb-toxicity in terminal and median leaves, and primary and secondary roots of upland cotton seedlings is scarce in the available literature. Leaves are the primary organs of photosynthesis and transpiration in plants while roots absorb essential elements and water from the soil. So, alterations in their ultramorphology and biochemistry may cause growth retardation in plants.

ROS such as H_2O_2, $OH^{\bullet}$ and MDA are stress indicators (Cuypers et al., 2016). They affect enzymes, proteins, nucleic acids and intracellular organelles; however, intensity and pathway of ROS generation is dependent on the cell organelles and stress conditions (Thyrring et al., 2015). Mostly, ROS are produced at active sites in the cells such as cell membranes, mitochondria, endoplasmic reticulum and peroxisomes; however, they migrate through plasma membrane and can be found anywhere in the cell. In current study, higher H_2O_2 generation and lipid peroxidation (MDA) was observed in the cotton's terminal and median leaves as compared with primary and secondary roots (**Table 1**). This is because of more active sites of ROS generation in leaves than roots. Moreover, GSH neutralized ROS levels in cotton median and terminal leaves and primary and secondary roots. Basically, GSH neutralizes ROS by donating H^+ and keeps protein cysteine in active reduced form by offering e^- (Lu, 2013). The ability of GSH as reducing agent is dependent on the GSH/GSSG ratio and total glutathione concentration, which are negatively affected by stress conditions. Moreover, higher GSH-mediated ROS control was observed in leaves as compared to roots in this study. It may be due to GSH-mediated restricted translocation of Pb to the foliar regions (Nakamura et al., 2013) and enhanced GSH synthesis in the leaves (Frendo et al., 1999). Further, two most important steps of glutathione-mediated xenobiotics detoxification identified in the plants are chemical/toxicant transformation and compartmentation (Coleman et al., 1997; Singh et al., 2016). In the first instance, electrophilic xenobiotics, which have high affinity toward making covalent bonds with nucleophilic sites, are transformed into less toxic forms by conjugating with glutathione in cytosol, thereby increasing their hydrophilicity and decreasing biological half life. In the second step, conjugates are transported to the vacuoles or across plasma membrane by ATP-dependent transporters, like one present in the tonoplast. Plants have the ability to produce two types of Cys-containing metal binding legends i.e., metallothioneins and phytochelatins, which are

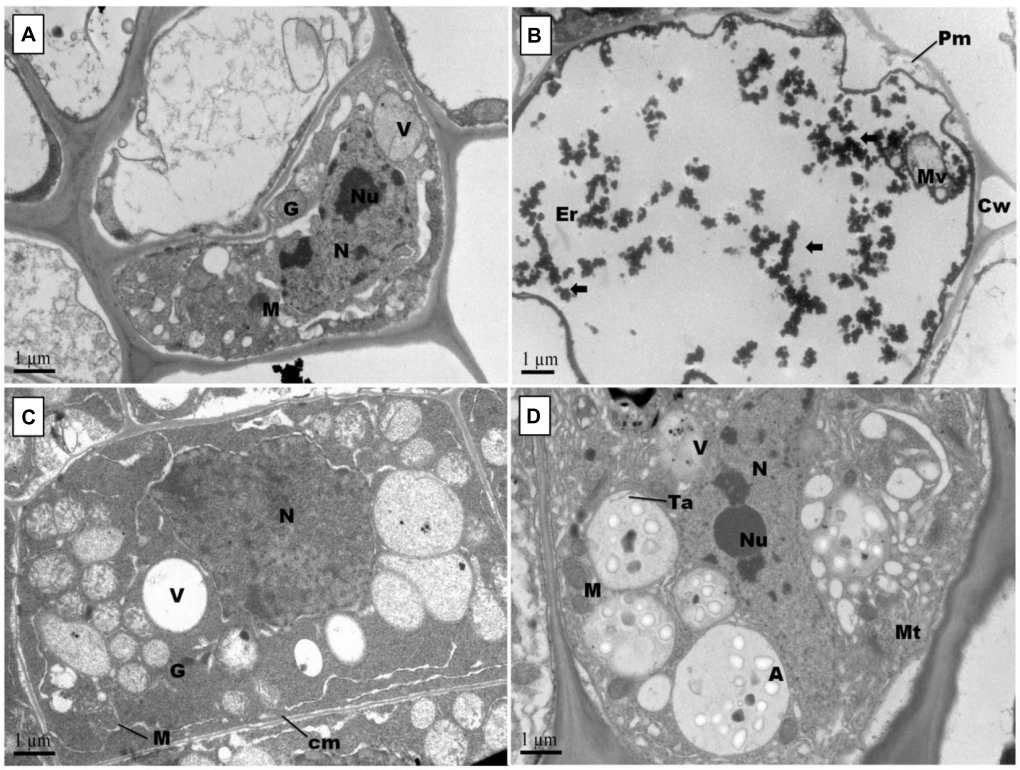

FIGURE 7 | Effect of Pb and GSH on primary root ultrastructure in upland cotton Transmission electron micrographs represent root tips cell morphology of control **(A)**, 500 µM Pb **(B)**, 50 µM GSH **(C)** and 500 µM Pb + 50 µM GSH **(D)** in cotton seedlings. Control cells **(A)** posses cytoplasm embedded with nucleus (N) containing nucleoli (Ne), vacuole (V), Golgi vesicles (G) and several mitochondria (M). In Pb-treated cells **(B)**, plasma membrane (Pm) was broken and cytoplasm severely damaged. Electron dense particles (⟸) were scattered throughout the cell. GSH **(C)** induced formation of vacuoles, mitochondria and multivesicular structures. In GSH + Pb **(D)**, large multivesicular structures contained amyloplasts (A), thylakoids (Ta) and microtubules (Mt).

functionally analogous (Shukla et al., 2016). Role of glutathione in phytochelatin synthesis is well documented as it serves as its precursor and increase plant tolerance to metal stress (Vezza et al., 2019). Under heavy metal stress, phytochelatin synthase, a key enzyme in phytochelatin synthesis, is activated which causes increased formation of phytochelatins. Phytochelatins make complexes with heavy metals including Pb and subsequently sequestered in vacuoles where more complex aggregation occurs (Sharma et al., 2016).

In earlier work, changes in CAT, POD, SOD, APX, and GR under Pb have been reported in plants (Pourrut et al., 2011; Ali et al., 2014a). However, variation in enzyme activities is dependent on Pb concentrations, time of exposure, plant species examined, etc. In heavy metal stress, GSH plays dual role; as an antioxidant metabolite and as a precursor for PCs (Hausladen and Alscher, 2017). The antioxidant property of GSH is dependent on its reduced cysteine moiety, which is oxidized when GSH reduces target molecules (Pompella et al., 2003). Results showed modulation of CAT, POD, SOD, and APX activities in both terminal and median leaves, and primary and secondary roots of upland cotton (**Figure 1**). Previously, GSH has alleviated cadmium stress in upland cotton (Daud et al., 2016), chromium stress in rice (Cao et al., 2013) and cesium stress in Arabidopsis (Adams et al., 2020); mainly by regulating antioxidants. Furthermore, GR activity was enhanced in the terminal and median leaves, but remained nearly unchanged in the groups treated with Pb alone and in combination with GSH. Previously, it was also observed that GSH levels were increased during stress conditions, but GR activity remained unchanged, pointing to the GSH *de novo* synthesis (Liu et al., 2015). In current study, Pb contents and GSH concentrations in terminal and median leaves and primary and secondary roots were also measured (**Figure 2**). Results revealed that GSH significantly reduced Pb uptake in both leaves and roots. This may be due to increase in the internal GSH concentrations caused by the external application as previously reported by Adams et al. (2020). Membrane stability, phytochelatin synthesis and compartmentalization of Pb, mediated by GSH may be contributing factors for Pb detoxification and restricted upward translocation to the aerial parts (Adams et al., 2020).

Changes in cell wall ultrastructure of terminal and median leaves (**Figures 4**, **5**) and primary and secondary roots (**Figures 7**, **8**) under Pb stress and some re-establishment of intact structures by GSH were observed in the current study. Pb alters cell wall morphology by increasing K^+ influx from the cell, and turnover of cell wall-bound Ca^{2+} and Mg^{2+}, creating nutrient deficiency and altering other cell structures and functions that depend on the intactness of these elements

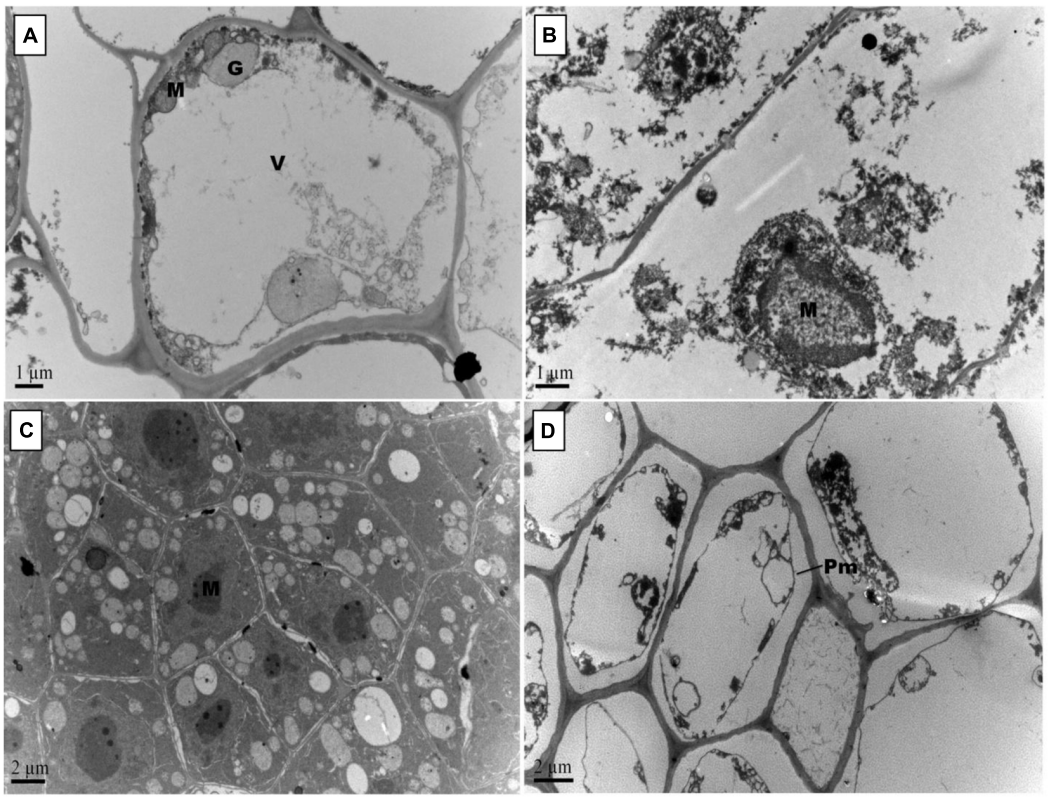

FIGURE 8 | Effect of Pb and GSH on secondary root ultrastructure in upland cotton. Transmission electron micrographs show secondary roots cell morphology of control **(A)**, 500 μM Pb **(B)**, 50 μM GSH **(C)** and 500 μM Pb + 50 μM GSH **(D)** in cotton seedlings. Control cells **(A)** possessed large central vacuole (V), Golgi vesicles (G) and mitochondria (M). In Pb-treated cells **(B)**, cell morphology was severely altered. GSH-treated roots **(C)** had developed cell organelles and formation of several multivesicular vesicles. In GSH + Pb **(D)**, plasma membrane (Pm) was detached from cell wall in almost every cell.

(Sharma and Dubey, 2005; Ali et al., 2014c). Moreover, Pb-inspired-ROS generation may accelerate lipid peroxidation by converting unsaturated fatty acids into saturated ones, causing damage to the plasma membrane (Thyrring et al., 2015). In earlier research work, GSH has played role in stabilizing plasma membrane under stress conditions (Zechmann, 2014). Conformational changes in chloroplasts upon Pb exposure were observed in terminal and median leaves of upland cotton. It is well established that chloroplasts have the inbuilt capacity to generate ROS; however, it is fortified under stress conditions (Khan et al., 2019). In addition, chloroplast proteome possesses reactive cysteines which are required for the catalytic functions of proteins and work under the control of glutaredoxin and thioredoxin systems (Zaffagnini et al., 2012; Couturier et al., 2013). These reactive cysteines are sensitive to ROS-triggered oxidation. Further, heavy metals replace Mg^{2+} ions in the chlorophyll and form heavy metal-chlorophyll complex (HM-*Chl*), for example cadmium (Cd)-*chl* complex (Küpper et al., 2006). Chlorophylls with heavy metal-complex face conformational changes due to light exposure and acidic nature of thylakoids. Moreover, it is suggested that chlorophyll degradation is not only caused by Pb-*Chl* complex but by generation of $O^{\bullet-}$ also, which is triggered by this complex. Further, Pb^{2+} being analogous to Mg^{2+} may replace the later in chlorophylls, causing further deterioration in the chloroplast ultrastructure. A recent study, conducted on *Lemna trisulca* L. has reported rearrangement of chloroplast as an avoidance strategy to Pb stress (Samardakiewicz et al., 2015) which is at par with our findings. Moreover, GSH promotes glutathionylation, a process of protein posttranslational modifications via disulphide bond, using H_2O_2 as stimulant in chloroplasts (Zaffagnini et al., 2012), thus playing role in stabilizing chloroplast ultrastructure.

In this study, mitochondria were seen deformed both in terminal and median leaves, and primary and secondary roots of upland cotton under Pb exposure. These changes may be attributed to excess ROS generation, as mitochondria release free electrons in electron transport chain to form $O^{\bullet-}$ and other ROSs (Dourmap et al., 2019). As a first line defense, SODs neutralize $O^{\bullet-}$ in mitochondria, that's why SOD activity was increased in GSH + Pb group. Moreover, $O^{\bullet-}$ may cause H_2O_2 production, which can be neutralized by CAT, but the later is present in peroxisomes only, providing strong evidence for H_2O_2 neutralization through GSH redox system (Lu, 2013), and alleviating Pb stress. In GSH redox system, H_2O_2 is reduced to H_2O by GPX mainly using GSH as a substrate (Ribas et al., 2014). Further, NADPH-dependent GR reduces GSSG, mainly found in the mitochondria, to GSH and may be the second important enzyme to regulate the function and structure of mitochondria.

Pb also altered cell nuclear matrix in the terminal and median leaves, and primary and secondary roots of upland cotton in current study. Previous research has shown some release of nuclear proteins such as nucleophosmin, nucleolin and fibrillarin from nucleolus to the cytoplasm in *Allium cepa* L. root tips cells upon exposure to Pb (Jiang et al., 2014a). These nuclear proteins play important roles in protein formation and ribosomal biogenesis. Moreover, Pb inhibits DNA synthesis, which may lead to reduced and impaired mitosis and cell division (Patra et al., 2004). We observed nuclear stabilization due to GSH application, both in leaves and roots. Importantly, nucleus contains GSH levels twice than cytosol, which are closely paralleled by DNA synthesis in early stages of cell proliferation (Noctor et al., 2012). Even under stress conditions, GSH supply to the nucleus remains uninterrupted (Zechmann, 2014). Thus, it is suggested that a continuous supply of GSH to the nucleus from cytoplasm might have maintained the nuclear stability in leaves and roots of upland cotton under Pb stress.

CONCLUSION

Lead is an unavoidable toxic heavy metal in the agro-ecosystems. In this multi-organ study, Pb increased ROS generation and decreased the activities of CAT, POD, SOD, APX, and SOD but increased GR activity in the terminal and median leaves, and primary and secondary roots of upland cotton. External GSH neutralized excess ROS levels, optimized activities of antioxidant enzymes and reduced Pb uptake in leaves and roots. However, maximum decline in the Pb uptake and peak GSH contents were observed in the terminal leaves. Moreover, Pb deteriorated ultrastructural configuration in both type of leaves and root system by affecting cell wall, plasma membrane, chloroplasts, mitochondria, and nucleus. GSH application maintained better cell morphology in the terminal leaves and primary roots as compared to other parts, mainly by regulating antioxidant machinery and restricted uptake of Pb. However, how DNA is regulated under external GSH supply in cotton leaves and roots in the presence of Pb needs further investigation.

DATA AVAILABILITY STATEMENT

The datasets generated for this study are available on request to the corresponding author.

AUTHOR CONTRIBUTIONS

MK, SS, and YZ equally contributed to the lab work. ZM and MDK prepared figures, tables and conducted transmission electron microscopy. SZ acquired funding, supervised this research work and critically revised the manuscript.

FUNDING

The authors of this manuscript greatly acknowledge The National Key Technology R&D program of China (2016YFD0101404), Agriculture Research System of China (CARS-18-25), Jiangsu Collaborative Innovation Center for Modern Crop Production, and Higher Education Commission of Pakistan for funding this research work.

REFERENCES

Adams, E., Miyazaki, T., Watanabe, S., Ohkama-Ohtsu, N., Seo, M., and Shin, R. (2020). Glutathione and its biosynthetic intermediates alleviate cesium stress in Arabidopsis. *Front. Plant Sci.* 10:1711. doi: 10.3389/fpls.2019.01711

Ali, B., Mwamba, T. M., Gill, R. A., Yang, C., Ali, S., Daud, M. K., et al. (2014a). Improvement of element uptake and antioxidative defense in *Brassica napus* under lead stress by application of hydrogen sulfide. *Plant Growth Regul.* 74, 261–273. doi: 10.1007/s10725-014-9917-9

Ali, B., Qian, P., Jin, R., Ali, S., Khan, M., Aziz, R., et al. (2014b). Physiological and ultra-structural changes in *Brassica napus* seedlings induced by cadmium stress. *Biol. Plant.* 58, 131–138. doi: 10.1007/s10535-013-0358-5

Ali, B., Song, W., Hu, W., Luo, X., Gill, R., Wang, J., et al. (2014c). Hydrogen sulfide alleviates lead-induced photosynthetic and ultrastructural changes in oilseed rape. *Ecotoxicol. Environ. Saf.* 102, 25–33. doi: 10.1016/j.ecoenv.2014.01.013

ATSDR (2007). *Toxicological profile for lead. Agency for Toxic Substances and Disease Registry*. Atlanta, GA: US Department of Health and Human Services.

Berni, R., Luyckx, M., Xu, X., Legay, S., Sergeant, K., Hausman, J.-F., et al. (2019). Reactive oxygen species and heavy metal stress in plants: impact on the cell wall and secondary metabolism. *Environ. Exp. Bot.* 161, 98–106. doi: 10.1016/j.envexpbot.2018.10.017

Cao, F., Wang, N., Zhang, M., Dai, H., Dawood, M., Zhang, G., et al. (2013). Comparative study of alleviating effects of GSH, Se and Zn under combined contamination of cadmium and chromium in rice (*Oryza sativa*). *BioMetals* 26, 297–308. doi: 10.1007/s10534-013-9611-9

Cobbett, C. S. (2000). Phytochelatins and their roles in heavy metal detoxification. *Plant Physiol.* 123, 825–832. doi: 10.1104/pp.123.3.825

Coleman, J., Blake-Kalff, M., and Davies, E. (1997). Detoxification of xenobiotics by plants: chemical modification and vacuolar compartmentation. *Trends Plant Sci.* 2, 144–151. doi: 10.1016/s1360-1385(97)01019-4

Couturier, J., Chibani, K., Jacquot, J.-P., and Rouhier, N. (2013). Cysteine–based redox regulation and signaling in plants. *Front. Plant Sci.* 4:105. doi: 10.3389/fpls.2013.00105

Cuypers, A., Hendrix, S., Amaral Dos Reis, R., De Smet, S., Deckers, J., Gielen, H., et al. (2016). Hydrogen peroxide, signaling in disguise during metal phytotoxicity. *Front. Plant Sci.* 7:470. doi: 10.3389/fpls.2016.00470

Das, K., and Roychoudhury, A. (2014). Reactive oxygen species (ROS) and response of antioxidants as ROS-scavengers during environmental stress in plants. *Front. Environ. Sci.* 2:53.

Daud, M., Sun, Y., Dawood, M., Hayat, Y., Variath, M., Wu, Y.-X., et al. (2009). Cadmium-induced functional and ultrastructural alterations in roots of two transgenic cotton cultivars. *J. Hazard. Mater.* 161, 463–473. doi: 10.1016/j.jhazmat.2008.03.128

Daud, M. K., Mei, L., Azizullah, A., Dawood, M., Ali, I., Mahmood, Q., et al. (2016). Leaf-based physiological, metabolic, and ultrastructural changes in cultivated cotton cultivars under cadmium stress mediated by glutathione. *Environ. Sci. Pollut. Res.* 23, 15551–15564. doi: 10.1007/s11356-016-6739-5

Dourmap, C., Roque, S., Morin, A., Caubrière, D., Kerdiles, M., Béguin, K., et al. (2019). Stress signalling dynamics of the mitochondrial electron transport chain and oxidative phosphorylation system in higher plants. *Ann. Bot.* mcz184. doi: 10.1093/aob/mcz184

Eroglu, A., Dogan, Z., Kanak, E. G., Atli, G., and Canli, M. (2015). Effects of heavy metals (Cd, Cu, Cr, Pb, Zn) on fish glutathione metabolism. *Environ. Sci. Pollut. Res.* 22, 3229–3237. doi: 10.1007/s11356-014-2972-y

Frendo, P., Gallesi, D., Turnbull, R., Van De Sype, G., Hérouart, D., and Puppo, A. (1999). Localisation of glutathione and homoglutathione in *Medicago truncatulais* correlated to a differential expression of genes involved in their synthesis. *Plant J.* 17, 215–219. doi: 10.1046/j.1365-313x.1999.00367.x

Grill, E., Winnacker, E.-L., and Zenk, M. H. (1987). Phytochelatins, a class of heavy-metal-binding peptides from plants, are functionally analogous to metallothioneins. *Proc. Natl. Acad. Sci. U.S.A.* 84, 439–443. doi: 10.1073/pnas.84.2.439

Hasanuzzaman, M., Bhuyan, M., Anee, T. I., Parvin, K., Nahar, K., Mahmud, J. A., et al. (2019). Regulation of ascorbate-glutathione pathway in mitigating oxidative damage in plants under abiotic stress. *Antioxidants* 8:384. doi: 10.3390/antiox8090384

Hausladen, A., and Alscher, R. G. (2017). "Glutathione," in *Antioxidants in Higher Plants*, eds R. G. Alscher and J. L. Hess (Boca Raton, FL: CRC Press), 1–30.

Jiang, M., and Zhang, J. (2001). Effect of abscisic acid on active oxygen species, antioxidative defence system and oxidative damage in leaves of maize seedlings. *Plant Cell Physiol.* 42, 1265–1273. doi: 10.1093/pcp/pce162

Jiang, Z., Qin, R., Zhang, H., Zou, J., Shi, Q., Wang, J., et al. (2014a). Determination of Pb genotoxic effects in *Allium cepa* root cells by fluorescent probe, microtubular immunofluorescence and comet assay. *Plant Soil* 383, 357–372. doi: 10.1007/s11104-014-2183-9

Jiang, Z., Zhang, H., Qin, R., Zou, J., Wang, J., Shi, Q., et al. (2014b). Effects of lead on the morphology and structure of the nucleolus in the root tip meristematic cells of *Allium cepa* L. *Int. J. Mol. Sci.* 15, 13406–13423. doi: 10.3390/ijms150813406

Kaur, G., Singh, H. P., Batish, D. R., Mahajan, P., Kohli, R. K., and Rishi, V. (2015). Exogenous nitric oxide (NO) interferes with lead (Pb)-induced toxicity by detoxifying reactive oxygen species in hydroponically grown wheat (*Triticum aestivum*) roots. *PLoS One* 10:e0138713. doi: 10.1371/journal.pone.0138713

Khan, M., Daud, M. K., Basharat, A., Khan, M. J., Azizullah, A., Muhammad, N., et al. (2016). Alleviation of lead-induced physiological, metabolic, and ultramorphological changes in leaves of upland cotton through glutathione. *Environ. Sci. Pollut. Res.* 23, 8431–8440. doi: 10.1007/s11356-015-5959-4

Khan, M., Nawaz, N., Ali, I., Azam, M., Rizwan, M., Ahmad, P., et al. (2019). "Regulation of photosynthesis under metal stress," in *Photosynthesis, Productivity and Environmental Stress* (Hoboken, NJ: John Wiley & Sons, Ltd,), 95–105. doi: 10.1002/9781119501800.ch6

Küpper, H., Küpper, F. C., and Spiller, M. (2006). "[Heavy metal]-chlorophylls formed in vivo during heavy metal stress and degradation products formed during digestion, extraction and storage of plant material," in *Chlorophylls and Bacteriochlorophylls: Biochemistry, Biophysics, Functions and Applications*, eds B. Grimm, R. J. Porra, W. Rüdiger, and H. Scheer (Dordrecht: Springer), 67–77. doi: 10.1007/1-4020-4516-6_5

Lanier, C., Bernard, F., Dumez, S., Leclercq-Dransart, J., Lemière, S., Vandenbulcke, F., et al. (2019). Combined toxic effects and DNA damage to two plant species exposed to binary metal mixtures (Cd/Pb). *Ecotoxicol. Environ. Saf.* 167, 278–287. doi: 10.1016/j.ecoenv.2018.10.010

Liu, X., Zhang, S., Whitworth, R. J., Stuart, J. J., and Chen, M.-S. (2015). Unbalanced activation of glutathione metabolic pathways suggests potential involvement in plant defense against the gall midge mayetiola destructor in wheat. *Sci. Rep.* 5:8092. doi: 10.1038/srep08092

Lu, S. C. (2013). Glutathione synthesis. *Biochim. Biophys. Acta* 1830, 3143–3153.

Mei, L., Daud, M. K., Ullah, N., Ali, S., Khan, M., Malik, Z., et al. (2015). Pretreatment with salicylic acid and ascorbic acid significantly mitigate oxidative stress induced by copper in cotton genotypes. *Environ. Sci. Pollut. Res.* 22, 9922–9931. doi: 10.1007/s11356-015-4075-9

Mishra, P., and Sharma, P. (2019). "Superoxide Dismutases (SODs) and their role in regulating abiotic stress induced oxidative stress in plants," in *Reactive Oxygen, Nitrogen and Sulfur Species in Plants: Production, Metabolism, Signaling and Defense Mechanisms*, eds M. Hasanuzzaman, V. Fotopoulos, K. Nahar, and M. Fujita (Hoboken, NJ: Wiley), 53–88. doi: 10.1002/9781119468677.ch3

Nakamura, S.-I., Suzui, N., Nagasaka, T., Komatsu, F., Ishioka, N. S., Ito-Tanabata, S., et al. (2013). Application of glutathione to roots selectively inhibits cadmium transport from roots to shoots in oilseed rape. *J. Exp. Bot.* 64, 1073–1081. doi: 10.1093/jxb/ers388

Noctor, G., Mhamdi, A., Chaouch, S., Han, Y., Neukermans, J., Marquez-Garcia, B., et al. (2012). Glutathione in plants: an integrated overview. *Plant Cell Environ.* 35, 454–484. doi: 10.1111/j.1365-3040.2011.02400.x

Patra, M., Bhowmik, N., Bandopadhyay, B., and Sharma, A. (2004). Comparison of mercury, lead and arsenic with respect to genotoxic effects on plant systems and the development of genetic tolerance. *Environ. Exp. Bot.* 52, 199–223. doi: 10.1016/j.envexpbot.2004.02.009

Pompella, A., Visvikis, A., Paolicchi, A., Tata, V. D., and Casini, A. F. (2003). The changing faces of glutathione, a cellular protagonist. *Biochem. Pharmacol.* 66, 1499–1503. doi: 10.1016/s0006-2952(03)00504-5

Pourrut, B., Shahid, M., Dumat, C., Winterton, P., and Pinelli, E. (2011). "Lead uptake, toxicity, and detoxification in plants," in *Reviews of Environmental Contamination and Toxicology*, Vol. 213, ed. M. D. Whitacre (New York, NY: Springer), 113–136. doi: 10.1007/978-1-4419-9860-6_4

Rahman, Z., and Singh, V. P. (2019). The relative impact of toxic heavy metals (THMs)(arsenic (As), cadmium (Cd), chromium (Cr)(VI), mercury (Hg), and lead (Pb)) on the total environment: an overview. *Environ. Monit. Assess.* 191:419. doi: 10.1007/s10661-019-7528-7

Ribas, V., García-Ruiz, C., and Fernández-Checa, J. C. (2014). Glutathione and mitochondria. *Front. Pharmacol.* 5:151. doi: 10.3389/fphar.2014.00151

Samardakiewicz, S., Krzeszowiec-Jeleń, W., Bednarski, W., Jankowski, A., Suski, S., Gabryś, H., et al. (2015). Pb-induced avoidance-like chloroplast movements in fronds of *Lemna trisulca* L. *PLoS One* 10:e0116757. doi: 10.1371/journal.pone.0116757

Sharma, P., and Dubey, R. S. (2005). Lead toxicity in plants. *Braz. J. Plant Physiol.* 17, 35–52. doi: 10.1590/s1677-04202005000100004

Sharma, S. S., Dietz, K. J., and Mimura, T. (2016). Vacuolar compartmentalization as indispensable component of heavy metal detoxification in plants. *Plant Cell Environ.* 39, 1112–1126. doi: 10.1111/pce.12706

Shukla, D., Trivedi, P. K., Nath, P., and Tuteja, N. (2016). "Metallothioneins and phytochelatins: role and perspectives in heavy metal (loid) s stress tolerance in crop plants," in *Abiotic Stress Response in Plants*, eds N. Tuteja and S. S. Gill (Weinheim: Wiley-VCH Verlag GmbH and Co. KGaA).

Singh, A., Prasad, S. M., and Singh, R. P. (2016). *Plant Responses to Xenobiotics*. Berlin: Springer.

Sobrino-Plata, J., Meyssen, D., Cuypers, A., Escobar, C., and Hernández, L. E. (2014). Glutathione is a key antioxidant metabolite to cope with mercury and cadmium stress. *Plant Soil* 377, 369–381. doi: 10.1007/s11104-013-2006-4

Szőllősi, R. (2014). "Chapter 3 - Superoxide Dismutase (SOD) and Abiotic Stress Tolerance in Plants: An Overview- Ahmad, Parvaiz," in *Oxidative Damage to Plants*, ed. P. Ahmad (San Diego, CA: Academic Press), 89–129. doi: 10.1016/b978-0-12-799963-0.00003-4

Thyrring, J., Juhl, B. K., Holmstrup, M., Blicher, M. E., and Sejr, M. K. (2015). Does acute lead (Pb) contamination influence membrane fatty acid composition and freeze tolerance in intertidal blue mussels in arctic Greenland? *Ecotoxicology* 24, 2036–2042. doi: 10.1007/s10646-015-1539-0

Vezza, M. E., Luna, D. F., Agostini, E., and Talano, M. A. (2019). Glutathione, a key compound for as accumulation and tolerance in soybean plants treated with AsV and AsIII. *Environ. Exp. Bot.* 162, 272–282. doi: 10.1016/j.envexpbot.2019.03.002

Zaffagnini, M., Bedhomme, M., Lemaire, S. D., and Trost, P. (2012). The emerging roles of protein glutathionylation in chloroplasts. *Plant Sci.* 185–186, 86–96. doi: 10.1016/j.plantsci.2012.01.005

Zechmann, B. (2014). Compartment-specific importance of glutathione during abiotic and biotic stress. *Front. Plant Sci.* 5:566. doi: 10.3389/fpls.2014.00566

Conflict of Interest: The authors declare that the research was conducted in the absence of any commercial or financial relationships that could be construed as a potential conflict of interest.

The reviewer MF declared a shared affiliation, with no collaboration, with several of the authors ZM, SS, YZ, and SZ to the handling Editor at the time of review.

frontiers in Plant Science

ORIGINAL RESEARCH
published: 03 June 2020
doi: 10.3389/fpls.2020.00724

Transcription Factor GmWRKY142 Confers Cadmium Resistance by Up-Regulating the Cadmium Tolerance 1-Like Genes

*Zhandong Cai[1,2,3,4†], Peiqi Xian[1,2,3,4†], Huan Wang[1,2,3,4], Rongbin Lin[1,2,3,4], Tengxiang Lian[1,2,3,4], Yanbo Cheng[1,2,3,4], Qibin Ma[1,2,3,4] and Hai Nian[1,2,3,4]**

[1] The State Key Laboratory for Conservation and Utilization of Subtropical Agro-bioresources, South China Agricultural University, Guangzhou, China, [2] The Key Laboratory of Plant Molecular Breeding of Guangdong Province, College of Agriculture, South China Agricultural University, Guangzhou, China, [3] Guangdong Laboratory for Lingnan Modern Agriculture, Guangzhou, China, [4] The Guangdong Subcenter of the National Center for Soybean Improvement, College of Agriculture, South China Agricultural University, Guangzhou, China

Cadmium (Cd) is a widespread pollutant that is toxic to living organisms. Previous studies have identified certain WRKY transcription factors, which confer Cd tolerance in different plant species. In the present study, we have identified 29 Cd-responsive *WRKY* genes in Soybean [*Glycine max* (L.) Merr.], and confirmed that 26 of those *GmWRKY* genes were up-regulated, while 3 were down-regulated. We have also cloned the novel, positively regulated *GmWRKY142* gene from soybean and investigated its regulatory mechanism in Cd tolerance. GmWRKY142 was highly expressed in the root, drastically up-regulated by Cd, localized in the nucleus, and displayed transcriptional activity. The overexpression of *GmWRKY142* in *Arabidopsis thaliana* and soybean hairy roots significantly enhanced Cd tolerance and lead to extensive transcriptional reprogramming of stress-responsive genes. *ATCDT1*, *GmCDT1-1*, and *GmCDT1-2* encoding cadmium tolerance 1 were induced in overexpression lines. Further analysis showed that *GmWRKY142* activated the transcription of *ATCDT1*, *GmCDT1-1*, and *GmCDT1-2* by directly binding to the W-box element in their promoters. In addition, the functions of *GmCDT1-1* and *GmCDT1-2*, responsible for decreasing Cd uptake, were validated by heterologous expression in *A. thaliana*. Our combined results have determined GmWRKYs to be newly discovered participants in response to Cd stress, and have confirmed that *GmWRKY142* directly targets *ATCDT1*, *GmCDT1-1*, and *GmCDT1-2* to decrease Cd uptake and positively regulate Cd tolerance. The GmWRKY142-GmCDT1-1/2 cascade module provides a potential strategy to lower Cd accumulation in soybean.

Keywords: transcription factor, WRKY, cadmium stress, CDT1-likes, soybean

OPEN ACCESS

Edited by:
Basharat Ali,
University of Agriculture Faisalabad, Pakistan

Reviewed by:
Matthew John Milner,
National Institute of Agricultural Botany (NIAB), United Kingdom
Jian Li Yang,
Zhejiang University, China

***Correspondence:**
Hai Nian
hnian@scau.edu.cn

† These authors have contributed equally to this work

Specialty section:
This article was submitted to Plant Nutrition, a section of the journal Frontiers in Plant Science

Received: *26 February 2020*
Accepted: *06 May 2020*
Published: *03 June 2020*

Citation:
Cai Z, Xian P, Wang H, Lin R, Lian T, Cheng Y, Ma Q and Nian H (2020) Transcription Factor GmWRKY142 Confers Cadmium Resistance by Up-Regulating the Cadmium Tolerance 1-Like Genes. Front. Plant Sci. 11:724. doi: 10.3389/fpls.2020.00724

INTRODUCTION

Cadmium (Cd) is a non-essential metallic trace element that is toxic to both plants and animals. Recently, global climate change and rapid industrialization have contributed to an increase in Cd deposition in soil, leading to a major global threat to crop productivity and human health (Das et al., 1997; Moulis and Thévenod, 2010; Clemens et al., 2013; Okereafor et al., 2020;

Zheng et al., 2020). The cultivation of cadmium tolerant crops and reduction of cadmium concentration in the edible parts of plants are solutions that could potentially alleviate the risks to human health (Grant et al., 1998; Gill and Tuteja, 2011; Tang et al., 2017; Zhao and Huang, 2018). To this effect, it is necessary to understand the mechanisms of Cd tolerance in plants and to investigate important genes encoding Cd tolerance.

Plants have evolved a set of versatile adaptive mechanisms to cope with Cd stress. These mainly involve the use of enzymatic and non-enzymatic antioxidants, the extrusion of Cd across the plasma membrane, the restriction of Cd movement to roots by mycorrhizas, and finally, the sequestration of metals in metabolically inactive parts such as root cell walls and leaf vacuoles (Dong et al., 2007; Hasan et al., 2009; Nagajyoti et al., 2010; Gallego et al., 2012; Rizwan et al., 2017; Shanying et al., 2017; Kumar et al., 2019; Sheng et al., 2019; Zhang Z. H. et al., 2019). Considerable progress has recently been made in understanding the molecular mechanisms of Cd accumulation in plants. Several key genes encoding metal transporters, chelator proteins, antioxidant enzymes, defensin genes and transcription factors have been reported to participate in Cd detoxification and tolerance in plants (Zhu et al., 1999a,b; Wu et al., 2012; Sasaki et al., 2014; Chen et al., 2016; Yang et al., 2016; Cai et al., 2017; Luo et al., 2019a,b; Mekawy et al., 2020). Of these functional proteins, Cysteine (Cys) -rich proteins are considered the most important Cd chelator proteins and generally have relatively low molecular weights (4–14 kDa) with a high ratio of cysteine residues (Song et al., 2004; Kuramata et al., 2009). Since the characterization of the first Cd-binding Cys-rich membrane protein from horse kidneys in 1957 (Margoshes and Vallee, 1957), a number of Cd-binding Cys-rich genes have been identified in plants, including *AtPcr1* (Song et al., 2004), *ThMT3* (Yang et al., 2011), *OsDEP1* (Kunihiro et al., 2013), *CnMT1* and *CnMT2* (Palacios et al., 2014), and *OsMT-3a* (Mekawy et al., 2020). Particularly, DcCDT1 (*Digitaria ciliaris* cadmium tolerance 1) and its homologues (AtCDT1 and OsCDT1) are specific to higher plants; they are unique and distinctive in both their peptide lengths (49–60 amino acids) and in their arrangement of Cys residues in the consensus sequence of CL-(Y/F)-A-(C/T)-X5-CC-(F/C)-CCYE-(T/K)-C-(E/K)-C-(CLDCL or delete)-CCCC (Kuramata et al., 2009; Matsuda et al., 2009). Transgenic *A. thaliana* plants or yeast cells overexpressing *DcCDT1*, *OsCDT1*, or *AtCDT1* consistently displayed a Cd tolerant phenotype and accumulated lower amounts of Cd. Moreover, 5 *DcCDT1* homologs in rice (OsCDT1 – 5) were up-regulated to varying degrees by Cd treatment (Kuramata et al., 2009). However, the mechanism of CDT1 regulation by Cd stress remains to be elucidated.

Transcription factors (TFs) are potentially the core components in the regulatory networks of Cd detoxification and tolerance owing to their functions as key regulators of the Cd stress response via their control on downstream gene expression. Most types of transcription factors regulating Cd detoxification and tolerance have been identified in plants, including metal response element transcription factors (MTF) (Smirnova et al., 2000; Solis et al., 2002; Lin et al., 2017), basic helix-loop-helix (bHLH) transcription factors (Wu et al., 2012; Yao et al., 2018), myeloblastosis (MYB) transcription factors (Hu et al., 2017; Xu et al., 2018; Zhang P. et al., 2019), ethylene responsive factors (ERF) (Yi et al., 2004; Tang et al., 2005; Lin et al., 2017), SQUAMOSA PROMOTER-BINDING PROTEIN-LIKE (SPL) transcription factors (Chen et al., 2018), Zn-regulated (Zip) transporters (Liu et al., 2019; Wu et al., 2019), and WRKY transcription factors (Yang et al., 2016; Hong et al., 2017; Han et al., 2019; Sheng et al., 2019). The WRKY proteins are a superfamily of transcription factors with up to 100, 90, and 170 representatives in Arabidopsis, Rice (*Oryza sativa* L.) and Soybean (*Glycine max*. L), respectively (Eulgem et al., 2000; Song et al., 2016; Xu et al., 2016; Yang et al., 2017). The first gene encoding WRKY transcription factor in plants was identified more than 20 years ago (Ishiguro and Nakamura, 1994; Rushton et al., 1995, 1996), and substantial progress in this area of research has since been achieved. Generally, WRKY proteins, composed of a WRKY domain (WRKYGQK) and a novel zinc-finger-like motif (Cx4–5Cx22–23HxH or Cx7Cx23HxC) at the N-terminal, can specifically recognize and bind the cis-acting W-box elements (TTGACC/T) of downstream genes (Eulgem et al., 2000; Eulgem and Somssich, 2007; Rushton et al., 2010). Several studies have found that WRKY TFs participate in the response to Cd stress by regulating the expression of downstream target genes such as *AtWRKY12* (Han et al., 2019), *AtWRKY13* (Sheng et al., 2019), *ThWRKY7* (Yang et al., 2016), and *CaWRKY41* (Dang et al., 2019). However, little is known about the role of the soybean WRKY TFs in Cd tolerance.

Soybean is important oil crops and the plant proteins resources widely grown around the world. Heavy metal contamination is an important factor that seriously inhibits soybean growth and threatens the human health. A better understanding of how soybean responds to heavy metal contamination would lay the foundations for developing effective countermeasures. Using the comprehensive mRNA transcriptome of soybean under Cd stress, 29 Cd-responsive WRKY genes were identified and confirmed by qRT-PCR analyses. Of these, *GmWRKY142* was selected to verify the function of Cd tolerance, due to its higher expression in root under normal conditions, as well as its strong up-regulation under Cd stress. We demonstrated that *GmWRKY142* overexpression in *A. thaliana* and soybean hair roots resulted in increased Cd tolerance and decreased Cd accumulation. Further analysis indicated that *GmWRKY142* directly activated *ATCDT1*, *GmCDT1-1*, and *GmCDT1-2* expression to enhance Cd tolerance. In summary, the GmWRKY142-GmCDT1-1/2 cascade module is potentially useful for the production of soybean with tolerance to Cd stress along with decreased Cd accumulation in their edible parts.

MATERIALS AND METHODS

Plant Materials and Growth Conditions

The soybean cultivar "Huaxia 7" was used to perform RNA sequencing (RNA-seq) analyses, mRNA expression and phenotype profiling. Plump seeds of a similar size were surface sterilized in 75% alcohol followed by germination for 3 days in sterile vermiculite. Seedlings of a similar size were transplanted

to modified 1/2 Hoagland solution (pH 5.8) containing the following macronutrients KNO_3 (2.5 mM), $Ca(NO_3)_2{\cdot}4H_2O$ (2.5 mM), $MgSO_4{\cdot}7H_2O$ (3.5 mM), and KH_2PO_4 (0.5 mM), and the micronutrients Fe-EDTA (50 μM), H_3BO_3 (7.5 μM), $(NH_4)_6Mo_7O_{24}$ (2.5 μM), $MnCl_2$ (1.25 μM), $ZnSO_4$ (1 μM), and $CuSO_4$ (0.5 μM) (Hoagland and Arnon, 1950; Dang et al., 2019) with or without Cd, in an illuminated growth incubator (Model GXZ-300D; Ningbo, China) under a 16 h light/8 h dark photoperiod, for subsequent RNA-seq, gene cloning, and transcriptional expression experiments. For the Cd dose-response experiment, seedlings were subjected to modified 1/2 Hoagland solution containing 0, 5, 10, 15, 25, or 50 μM of $CdCl_2$ for 2 h. During the time-course experiment, seedlings were subjected to modified 1/2 Hoagland solution with 25 μM $CdCl_2$ for 0, 1, 2, 4, 6, 8, 12, or 24 h. Seedlings cultured in modified 1/2 Hoagland solution with 0 or 25 μM of $CdCl_2$ for 4 h were sampled and subjected to RNA-seq analysis (LC-Bio, Hangzhou, China), according to the vendor's protocol. All the experiments were performed with three independent biological replicates.

All *A. thaliana* seeds including the wild-type (WT) ecotype Col-0, and transgenic plants were surface-sterilized and transferred to sterilized matrix soil (Jiffy, Oslo, Norway). Following vernalization in the dark at 4°C for 3 days, the seeds were cultivated in an illuminated growth incubator (Model GXZ-300D, Ningbo, China) under a 16 h light / 8 h dark photoperiod at 24°C.

RNA-Seq and Bioinformatics Analysis

RNA-seq analysis was performed by LC-Bio company (Hangzhou, China). For the transcriptomic analysis of Cd stress in soybean, 3-day old seedlings were cultured in modified 1/2 Hoagland solution with 0 or 25 μM of $CdCl_2$ for 4 h were sampled and subjected to RNA-seq analysis. For the *Arabidopsis thaliana*, 2-week old seedlings of both the WT (Col-0) and the GmWRKY142-OX line (Line 6) under non-stress conditions were used for transcriptomic analysis. Following the manufacturer's procedure, total RNA was extracted from the samples using the Spectrum Plant Total RNA Kit (Sigma-Aldrich, St. Louis, MO, United States, STRN10-1KT) and mRNA was enriched and fragmented into shorter fragments by mixed with fragmentation buffer. First-strand cDNA was synthesized from fragmented mRNA using random hexamer primer. End repair of the double-stranded cDNAs was performed using T4 polynucleotide kinase, T4 DNA polymerase and DNA polymerase I Klenow fragment. Then, T4 DNA ligase was used to ligate the fragments to adapters. The available fragments were selected and then enriched by PCR amplification. The constructed libraries were qualified and quantified using an Agilent 2100 Bioanaylzer and the ABI StepOnePlus Real-Time PCR System and then sequenced via Illumina Novaseq™ 6000. The obtained raw reads were then cleaned by removing the low-quality reads and/or adaptor sequences. The clean reads were mapped to reference sequences using SOAPaligner/SOAP2 (Li et al., 2009). The reference genomes and genes set of Soybean and Arabidopsis thaliana were downloaded from the NCBI (National Center for Biotechnology Information) site[1], [2]. The gene expression levels were calculated using the reads per kilobase per million reads method according to (Mortazavi et al., 2008). Subsequently, based on sequence homology, the differentially expressed genes by gene ontology terms[3] were imported into Blast2GO, a software package that retrieves GO terms, allowing gene functions to be determined and compared. To further understand the biological pathways in which the differentially expressed genes are involved, the differentially expressed genes were compared against the KEGG database[4]. Based on reports of the soybean WRKY gene family from previous studies and differentially expressed genes annotation in this study, probable WRKY transcription factors in soybean were identified and named according to (Yu et al., 2016) (**Supplementary Table S3**). The sequences for both the soybean and *Arabidopsis thaliana* used in the present study can be downloaded from the Phytozome database (Version 12)[5] according the gene numbers.

RNA Isolation and qRT-PCR Analysis

Total RNA was isolated from samples using the Plant Total RNA Purification Kit (TR02-150, GeneMarkbio, Taiwan, China). The first-strand cDNA was reverse transcribed by PrimeScript™ RT reagent Kit with a gDNA Eraser kit (RR047, Takara Bio, Shiga, Japan). qRT-PCR analysis was carried out using TB Green™ Premix Ex Taq™ II (RR820, Takara Bio) and CFX96 Real-Time PCR Detection System (Bio-Rad, Hercules, CA, United States). In all experiments, qRT-PCR analyses were performed as triplicates on three different RNA samples isolated independently from each tested condition. Relative gene expression levels were detected using the $2^{-\Delta\ \Delta\ Ct}$ algorithm (Livak and Schmittgen, 2001) normalized to the expression of the Actin genes *GmACT3* (GenBank: AK285830.1) or *AtActin2* (GenBank: AT3g18780). Three independent biological replicates were tested in each experiment for the qRT-PCR analysis. Primers used are listed in **Supplementary Table S1**.

DNA and cDNA Clones, Vector Construction, and Plant Transformation

The cDNA sequences of *GmWRKY142*, *GmCDT1-1* and *GmCDT1-2* genes were isolated using specific primers (**Supplementary Table S1**) and inserted into the *Xba* I and *Sac* I sites of the pTF101.1 vector, using the ClonExpress® II One Step Cloning Kit (C112, Vazyme, Nanjing, China). The resulting plasmid was mobilized into *Agrobacterium* strains GV3101 and K599 by heat shock, and subsequently used to transform Arabidopsis and soybean hairy roots according to the *Agrobacterium*-mediated floral dip (Clough and Bent, 1998) and *Agrobacterium rhizogenes*-based transformation (Matthews and Youssef, 2016) methods, respectively. The complete coding

[1] ftp://ftp.ncbi.nlm.nih.gov/genomes/all/GCF/000/004/515/GCF_000004515.5_Glycine_max_v2.1

[2] ftp://ftp.arabidopsis.org/home/tair/Sequences/whole_chromosomes/

[3] http://www.geneontology.org

[4] http://www.kegg.jp/kegg

[5] https://phytozome.jgi.doe.gov/pz/portal.html#

sequence of *GmWRKY142* was cloned into the pCambia 1302, pGBKT7, pGADT7, and pGreenII 62-SK binary vectors using the ClonExpress® II One Step Cloning Kit (C112, Vazyme) for the determination of subcellular localization, transcriptional activation activity assay, Yeast one-hybrid assay and Dual LUC assay, respectively. The genomic DNA of Huaxia 7 and WT plants were extracted using the Plant Genomic DNA Kit (DP305, TIANGEN, Beijing, China). Upstream sequences spanning 2,000 bp from the start codons of the *ATCDT1*, *GmCDT1-1*, and *GmCDT1-2* genes were analyzed to determine the W-box elements. The original *ATCDT1*, *GmCDT1-1,* and *GmCDT1-2* promoter fragments containing a genuine W-box element were amplified by PCR, while mutated W-box elements were identified by a change in the W-box sequence into "TAAAAT." Either original or mutated fragments were cloned into the pAbAi vector using the ClonExpress® II One Step Cloning Kit (C112, Vazyme) and used as baits in yeast one-hybrid assays. Details of primers used in vector construction are listed in **Supplementary Table S1**.

Subcellular Localization

Subcellular localization was investigated by transiently overexpressing *35S:GmWRKY142-GFP* in tobacco (*Nicotiana tabacum*) leaves via *Agrobacterium*-mediated transformation (Sparkes et al., 2006). Nuclear dye (DAPI) and GFP fluorescence signals were observed using confocal scanning microscopy (Model LSM780, Zeiss, Jena, Germany).

Yeast One-Hybrid Assay

This assay was performed using the MATCHMAKER® Gold Yeast One-Hybrid Library Screening System (Clontech) and the YEASTMAKER^{TM} Yeast Transformation System 2 (Clontech). The full-length coding sequence of *GmWRKY142* was cloned from cDNA and inserted into the effector construct pGADT7. A DNA fragments that consisted of two W-box motifs (TATGCTTTA GCTGGAATTGACTTCACCAGGTTTGACCTTACAGGTAGG TAGTTGAGT) or their mutants (ATATGCTTTAGCTGGAA TAAAATTCACCAGGTTAAAACTTACAGGTAGGTAGTTGA GT) were synthesized and introduced into the upstream region of the mini-promoter of AurR (pAbAi), which were termed pAbAi-Wbox and pAbAi-mWbox, respectively. The promoter sequences of *GmCDT1-1*, *GmCDT1-2*, and *AtCDT1* were amplified and introduced into the upstream region of the mini-promoter of AurR, respectively. Prey and reporter vectors were co-transformed into the yeast strain Y1H Gold. Cells were grown in SD/-Leu liquid media to an OD_{600} of 0.1 and diluted 10-fold with normal saline. For each dilution, a volume of 7 μL was spotted on SD/-Leu media plates containing either 0 or 150 ng mL^{-1} AbA in order to test the strength of the interaction. Plates were incubated for 3–4 days at 30°C.

Cd Tolerance Assay

Twenty-five-day-old plants grown in pots (length × width × height = 7.0 × 7.0 × 7.6 cm) were placed in trays and saturated either with 1/10 Hoagland solution (as control) or with 1/10 Hoagland solution containing 500 μM of $CdCl_2$ solution for 10 days. Pots were then transferred to trays containing normal culture medium to promote plant recovery for 12–15 days, after which the plants' fresh weight and height were measured. Cd content was also measured using an atomic absorption spectrometer (Model AA-6800, Shimadzu Corporation, Japan). The experiment was performed with three independent biological replicates.

Statistical Analysis

All data were analyzed using GraphPad Prism® 5 (Version 5.01, GraphPad Software, Inc., United States) for calculating mean and standard deviation. At least three biological replicates were included in the data, and all data were analyzed using ANOVA or Duncan's test for the determination of the significant differences with SPSS 21 (IBM Corp, 2012).

RESULTS

The GmWRKY Family of Genes Responds to Cd Stress in Soybean

To identify Cd-responsive WRKY family members in soybean, genome wide transcriptomic analysis was conducted with Huaxia 7 roots exposed to Cd stress. By comparing the transcriptome expression patterns between control and Cd treated groups, a total of 5,285 differentially expressed genes (DEGs) were identified in soybean plants under Cd stress (**Supplementary Table S2**). Based on reports from previous studies, the soybean genome contains at least 170 WRKY family members (Song et al., 2016; Yang et al., 2017). However, genome wide transcriptomic analysis revealed that only 29 genes were up- or down-regulated more than 1.5-fold in roots in response to Cd stress (**Table 1**). Of these, 26 GmWRKY genes in the roots were up-regulated, while 3 were down-regulated. Furthermore, qRT-PCR analyses of all 29 Cd-responsive WRKY genes confirmed their differential expression in response to Cd stress (**Table 1**). It should be noted that *GmWRKY142* registered a higher fragments per kilobase of transcript per million mapped reads (FPKM) under normal conditions, as well as being strongly up-regulated by Cd stress, which prompted our interest in further research.

Expression Patterns of *GmWRKY142*

To further characterize *GmWRKY142*, qRT-PCR was employed to analyze tissue samples and determine Cd-induced expression patterns. As shown in **Figure 1A**, *GmWRKY142* expression was detected in all examined tissues, with higher expression levels in roots, pods, seeds and leaves than stems, apex and flowers. To examine the expression patterns of *GmWRKY142* following Cd stress, 5-day-old soybean roots were exposed to different Cd concentrations for varying periods of time. After 2 h of treatment, *GmWRKY142* expression was significantly up-regulated by 10–50 μM Cd, whereby the fold change increased with increasing concentration (**Figure 1B**). Cd-induced *GmWRKY142* expression was also observed in a time-dependent manner, whereby treatment with 25 μM Cd resulted in the

TABLE 1 | GmWRKY family genes respond to Cd stress.

Gene ID of NCBI	Gene numbers	Gene name	Fragments Per kilobase per million (FPKM)						Fold change (FC)	Log2(FC)	qRT-PCR
			CK_1	CK_2	CK_3	Cd_1	Cd_2	Cd_3			
100781603	*Glyma.15G186300*	*GmWRKY146*	3.89	3.23	2.47	1.13	0.68	0.69	0.26	−1.94	-4.33 ± 0.23
100788213	*Glyma.09G129100*	*GmWRKY95*	1.27	1.29	0.91	0.61	0.10	0.22	0.27	−1.90	-4.89 ± 0.52
100783661	*Glyma.19G221700*	*GmWRKY184*	10.66	6.40	10.14	3.12	2.35	3.11	0.32	−1.66	-3.52 ± 0.34
100127370	*Glyma.01G224800*	*GmWRKY7*	2.42	0.97	0.90	3.14	5.27	4.05	2.90	1.54	2.35 ± 0.84
100127423	*Glyma.03G220100*	*GmWRKY25*	2.65	1.32	3.06	8.96	7.07	4.43	2.91	1.54	2.58 ± 0.09
100802124	*Glyma.15G110300*	*GmWRKY142*	33.19	30.90	27.40	76.42	104.34	92.06	2.98	1.58	4.02 ± 0.52
100127367	*Glyma.01G128100*	*GmWRKY4*	2.18	2.36	0.82	5.55	6.03	4.63	3.02	1.60	2.36 ± 0.07
100127421	*Glyma.11G163300*	*GmWRKY114*	11.68	10.37	13.61	31.62	46.88	34.56	3.17	1.66	3.67 ± 0.10
100170682	*Glyma.18G213200*	*GmWRKY172*	0.12	0.48	1.41	2.66	1.44	2.53	3.30	1.72	2.48 ± 0.12
100797998	*Glyma.12G097100*	*GmWRKY115*	0.93	0.67	0.12	1.93	2.32	1.74	3.48	1.80	3.47 ± 0.25
100127387	*Glyma.03G256700*	*GmWRKY28*	1.32	0.41	0.61	2.45	3.76	2.27	3.61	1.85	3.41 ± 0.33
100807966	*Glyma.07G023300*	*GmWRKY68*	3.93	2.48	5.31	12.84	13.75	15.90	3.62	1.86	4.08 ± 0.41
732588	*Glyma.15G003300*	*GmWRKY141*	3.02	3.59	4.41	11.78	16.75	15.86	4.03	2.01	3.59 ± 0.53
100795177	*Glyma.06G307700*	*GmWRKY66*	1.85	2.13	1.23	7.68	8.35	7.12	4.44	2.15	4.13 ± 0.22
102666898	*Glyma.03G042700*	*GmWRKY21*	2.34	2.68	1.48	8.34	11.75	11.64	4.88	2.29	4.53 ± 0.84
100127375	*Glyma.08G021900*	*GmWRKY78*	0.58	0.85	0.58	2.10	4.09	4.09	5.13	2.36	5.55 ± 1.19
100787050	*Glyma.05G127600*	*GmWRKY44*	0.29	0.36	0.26	1.82	1.36	1.82	5.47	2.45	5.58 ± 0.98
100170747	*Glyma.16G026400*	*GmWRKY147*	0.87	0.77	0.70	5.04	7.62	4.47	7.31	2.87	8.22 ± 1.14
100798500	*Glyma.04G061400*	*GmWRKY31*	0.12	0.20	0.15	1.74	1.39	1.01	8.89	3.15	8.47 ± 1.21
100790050	*Glyma.19G254800*	*GmWRKY185*	0.17	0.45	0.74	4.05	4.74	4.00	9.41	3.23	10.77 ± 1.49
100779533	*Glyma.18G092200*	*GmWRKY168*	0.27	0.77	0.38	4.28	5.13	4.97	10.13	3.34	12.36 ± 1.37
100816891	*Glyma.08G082400*	*GmWRKY81*	0.32	0.65	0.28	4.53	5.10	5.47	12.11	3.60	14.56 ± 2.56
100812027	*Glyma.06G125600*	*GmWRKY56*	0.21	0.48	0.09	3.03	3.24	3.82	12.94	3.69	15.21 ± 1.74
100127378	*Glyma.08G011300*	*GmWRKY76*	0.06	0.27	0	0.31	2.27	1.73	13.30	3.73	13.97 ± 1.55
100127373	*Glyma.06G061900*	*GmWRKY53*	0.02	0.21	0.22	2.05	2.66	1.68	13.97	3.80	15.20 ± 2.48
100776906	*Glyma.04G238300*	*GmWRKY39*	0.05	0.06	0.03	0.31	0.67	1.38	18.34	4.20	20.24 ± 3.0
102667019	*Glyma.01G222300*	*GmWRKY6*	0.05	0.11	0	0.36	2.24	1.54	26.11	4.71	27.55 ± 2.76
100798375	*Glyma.13G370100*	*GmWRKY126*	0.03	0.07	0.28	2.26	4.43	4.22	28.21	4.82	28.42 ± 2.45
732586	*Glyma.19G094100*	*GmWRKY180*	1.04	0.48	0.64	20.04	30.36	28.53	36.42	5.19	44.87 ± 5.64

highest 5.6-fold expression to be reached at the 4th hour, followed by a decrease at the 6th hour (**Figure 1C**).

Cloning and Characterization of *GmWRKY142*

The *GmWRKY142* open reading frame (ORF) was isolated from the soybean variety Huaxia 7, based on putative sequence information available from the Phytozome database. The complete *GmWRKY142* ORF (Accession number: MN639600) spanned 1,677 bp and encoded a 558 amino acid protein with an estimated molecular mass of 59.851 kDa and an isoelectric point of 6.81. Protein sequence alignment showed that GmWRKY142 shared homology with the corresponding genes of AtWRKY6 (51.7%), AtWRKY31 (51.0%), AtWRKY42 (55.8%), OsWRKY1 (48.8%), and OsWRKY43 (44.5%). In addition, GmWRKY142 and its homologous proteins contain a typical WRKY domain that includes the highly conserved amino acid sequence "WRKYGQK," as well as a C_2H_2 zinc-finger motif (**Figure 2A**), indicating that GmWRKY142 is a member of the WRKY transcription factor family. Further analyses were performed to confirm the status of GmWRKY142 as a typical transcription factor. The subcellular localization of GmWRKY142 was investigated, whereby the full-length *GmWRKY142* ORF without the stop codon was fused in-frame to the 5′ end of the green fluorescent protein (GFP), under the control of the cauliflower mosaic virus (CaMV) 35S promoter. The GmWRKY142-GFP fusion protein was exclusively observed in the nucleus using confocal microscopy (**Figure 2B**). WRKY transcription factors are characterized by their common binding activity to the cis-element W-box (TTGACC/T) in promoters of downstream genes. A tandem DNA fragment consisting of two W-box motifs (TTGACT and TTGACC) was synthesized and used to determine the transcriptional activity of GmWRKY142. In the yeast one-hybrid (Y1H) assay, cotransformants carrying pGADT7-GmWRKY142 and the pAbAi-Wbox vectors could grow on SD/-Leu plates containing 150 ng/mL AbA. However, when the W-box sequences were mutated to TAAAAT or TAAAAT, the yeast cells could not grow, which is similar to the results of the blank vector (**Figure 2C**). Furthermore, a dual luciferase (LUC) assay involving *N. benthamiana* leaves was performed using the constructs shown in **Figure 2D**. Finally, the co-expression of Effecter-GmWRKY142 with Reporter-Wbox led to a higher LUC/REN ratio than that observed in the control and mutated

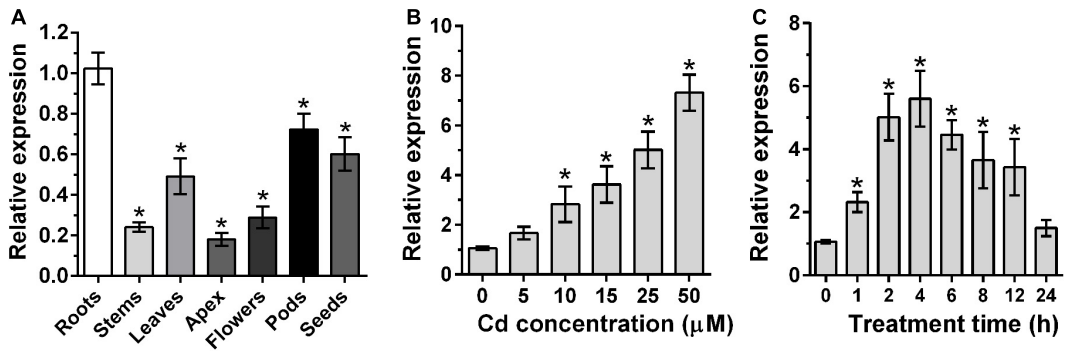

FIGURE 1 | Analysis of expression patterns of GmWRKY142. **(A)** qRT-PCR analysis of the GmWRKY142 transcript in different tissues of the soybean variety Huaxia 7. mRNAs were isolated from roots, stems, leaves, apex, flowers, pods, and seeds. **(B)** Dose-dependent GmWRKY142 expression in roots. Roots were exposed to different Cd concentrations (0, 5, 10, 15, 25, and 50 μM) for 6 h. **(C)** For the time-course experiment, seedlings were exposed to 25 μM $CdCl_2$ for 0, 1, 2, 4, 6, 8, 12, or 24 h. Samples were separately harvested for qRT-PCR analysis. Values are expressed as the means ± SD ($n = 3$). The experiment was performed with at least three independent biological replicates. Significant differences according to the one-way analysis of variance are denoted as follows: $^*p < 0.01$.

reporter (Reporter-mWbox), indicating that GmWRKY142 may transcriptionally activate downstream target genes.

Overexpression of *GmWRKY142* in Transgenic *A. thaliana* and Soybean Hair Roots Confers Cd Tolerance

In order to determine the role of GmWRKY142 in Cd resistance, ectopic expression of *GmWRKY142* was carried out in Arabidopsis. The seeds of three independent homozygous T3 transgenic lines exhibiting a higher gene expression, as well as WT plants were collected for functional gene analyses (**Supplementary Figure S1**). No differences in growth and development were observed between WT and GmWRKY142-OE plants under normal growth conditions. However, under Cd stress, GmWRKY142-OE plants displayed enhanced Cd tolerance compared with WT plants (**Figure 3A**). Leaf chlorosis of leaves and growth inhibition are two typical symptoms of Cd stress in plants (DalCorso et al., 2008). As shown in **Figure 3A**, the degree of chlorosis in leaves at 10 days of exposure to Cd stress was higher in WT than in GmWRKY142-OE plants. Further evaluations revealed that the plant height and fresh weights of the GmWRKY142-OE plants were significantly higher than those of WT (**Figures 3B,C**), and that Cd content was higher in WT compared to GmWRKY142-OE plants (**Figures 3D,E**).

To assess the effect of *GmWRKY142* overexpression on Cd tolerance in soybean, transgenic hairy roots were produced using the *A. rhizogenes*-mediated transformation system. Analysis revealed that the transcripts for GmWRKY142 were up-regulated in GmWRKY142-OX hairy roots at an average fold of 5.63 (**Supplementary Figure S2**). WT and transgenic soybean hairy roots, each 2 cm long, were subsequently treated with 0 or 15 μM Cd for 5 days. As shown in **Figure 4**, no apparent difference was found between the GmWRKY142 transgenic and WT hairy roots in the absence of Cd. However, obvious differences were observed between transgenic and control hairy roots treated with 15 μM Cd. Relative root elongation was 45.18% in the WT, compared to 75.15% in transgenic GmWRKY142 hairy roots (**Figure 4B**). Moreover, Cd content in the transgenic GmWRKY142 hairy roots was significantly lower than in WT roots after Cd treatment, consistent with the phenotypes of the transgenic *A. thaliana* assay (**Figure 3**). These combined results suggest that *GmWRKY142* overexpression in Arabidopsis and soybean hairy roots can enhance Cd tolerance.

GmWRKY142 Overexpression Leads to Extensive Transcriptional Reprogramming of Stress-Responsive Genes

RNA-seq was performed on an OX line (Line 6) and WT plants to determine how Cd resistance in Arabidopsis was mediated by *GmWRKY142* and also to identify potential target genes that it may regulate. The difference in expression levels between two samples was determined as log2 Fold change >1.0 and false discovery rate <0.05. A total of 746 genes showed altered transcript levels (385 up-regulated and 239 down-regulated) in the transgenic line, compared with the WT (**Figure 5A** and **Supplementary Table S4**). Data obtained from RNA-seq were confirmed by analysis, using qRT-PCR, of the transcription of eight upregulated genes which were classified into either detoxification of Cd ion (GO:0071585) or response to Cd ion (GO:0046686) genes. As shown in **Figure 5B**, qRT-PCR analyses on expression patterns for all of the tested genes were highly consistent with the RNA-Seq, suggesting that DEG screening based on RNA-seq is reliable.

Analysis through the Kyoto Encyclopedia of Genes and Genomes (KEGG) suggested that 68 pathways were identified in DEGs (**Supplementary Table S5**). The top 11 most enriched pathways with $p < 0.05$ were plant hormone signal transduction, tryptophan metabolism, fatty acid elongation, limonene and pinene degradation, stilbenoid, diarylheptanoid and gingerol biosynthesis, flavone and flavonol biosynthesis, cutin, suberin, and wax biosynthesis, phenylalanine metabolism, plant-pathogen interaction, diterpenoid biosynthesis, and, finally, phenylpropanoid biosynthesis (**Figure 5C**). Gene ontology

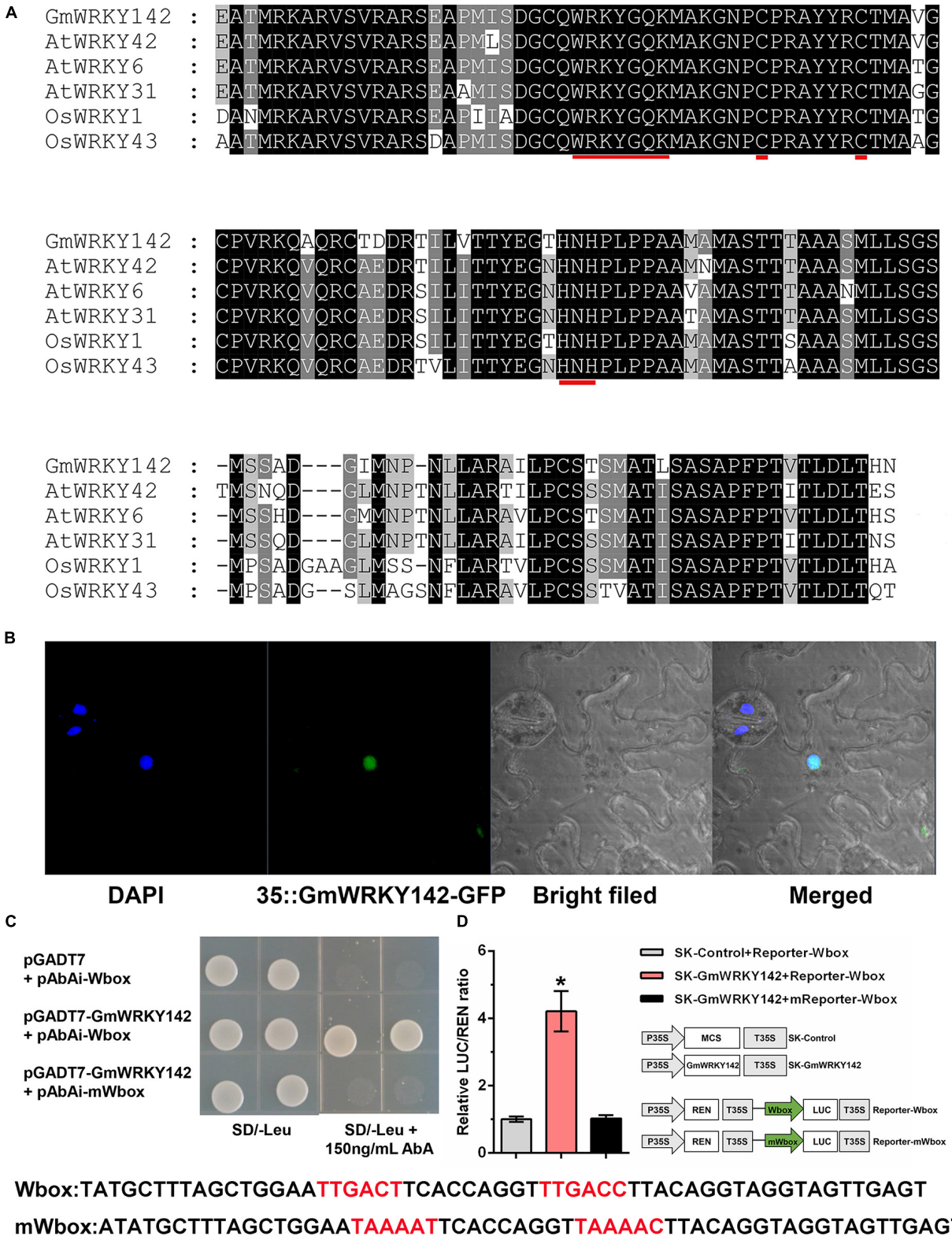

FIGURE 2 | Sequence analysis, subcellular localization, and transcriptional activity assays of the GmWRKY142 protein. **(A)** Multiple alignments of the conserved WRKY domains between the WRKYs of soybean, rice and Arabidopsis. Identical amino acids are shown with a black background and analogous amino acids are shaded in gray. The WRKY motif and zinc-finger structures are denoted by red lines. **(B)** Subcellular localization of GmWRKY142 in *Nicotiana benthamiana*. DAPI

(Continued)

FIGURE 2 | Continued
was used to stain the nucleus. The overlapped images are shown on the right. **(C)** The growth phenotype of the cotransformant that harbored pGADT7-GmWRKY142 and bait vectors on a selective DO medium plate (SD/-Leu) with or without 150 ng mL^{-1} Aureobasidin A (AbA). **(D)** Schematic diagrams of the effector and reporter constructs used for transient luciferase (LUC) assays. Full-length CDS of GmWRKY142 was inserted into pGreen II 62-SK to produce an effector, while the original or mutated W-box elements were inserted into pGreen II 0800-LUC to generate reporters. MCS, multiple cloning site. P35S and T35S, the promoter and terminator of CaMV 35S, respectively. REN (Renilla luciferase) was used as an internal control for activity normalization. Transient expression assay of the promoter activity, shown as LUC/REN ratio, using tobacco leaves co-transformed with the effector and the reporters. LUC/REN ratio of the control co-transformed with the reporters and the empty effector vector (pGreen II 62-SK) was set as 1. Values are expressed as the means ± SD (n = 3). Significant differences according to the one-way analysis of variance are denoted as follows: $^{*}p < 0.01$.

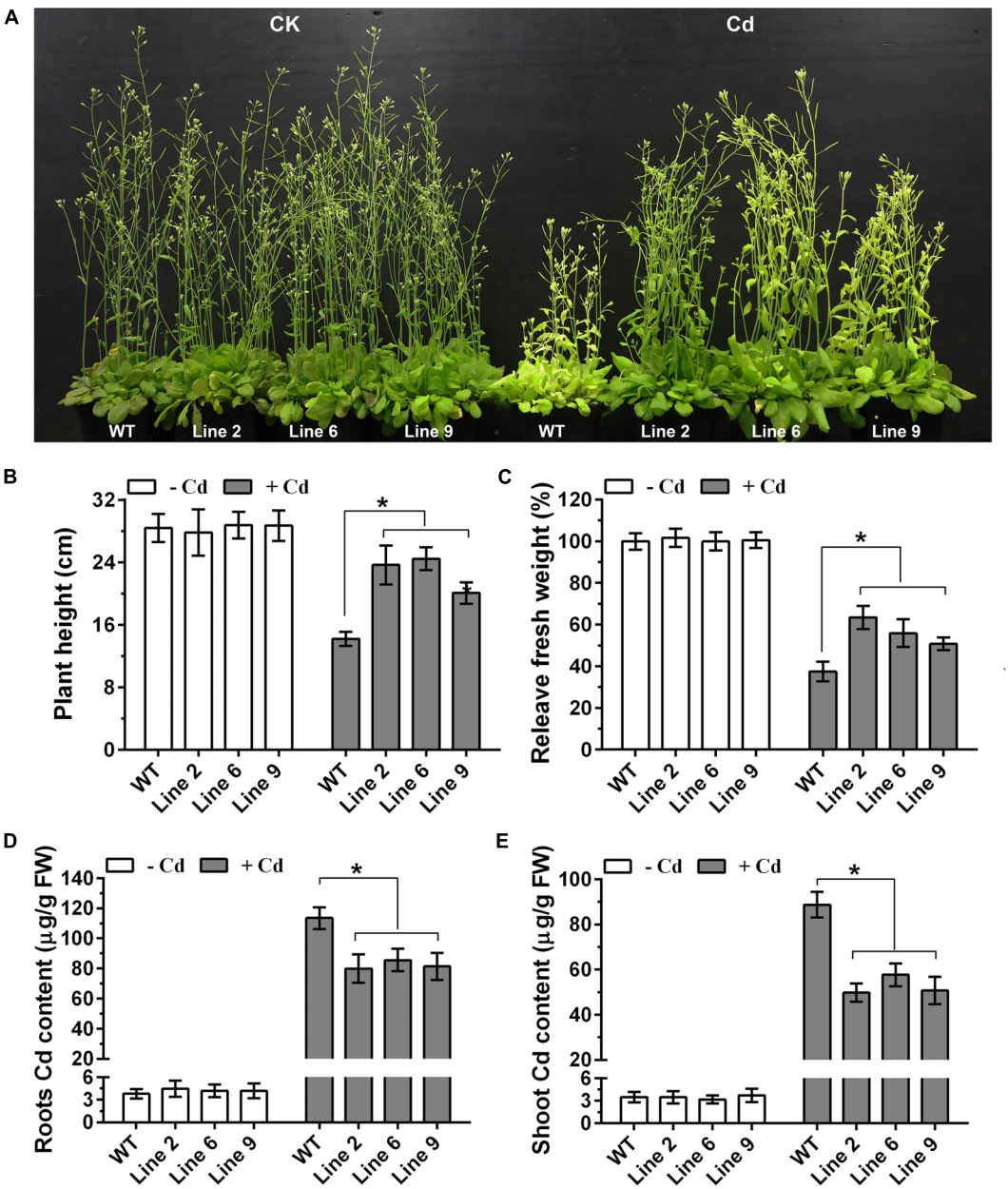

FIGURE 3 | Overexpression of GmWRKY142 conferred enhanced Cd tolerance in transgenic Arabidopsis thaliana. **(A)** Phenotypes of *A. thaliana* transgenic lines (2, 6, and 9) and wild type (WT) under normal conditions or under Cd treatment conditions. **(B–E)** Plant height **(B)**, relative fresh weight **(C)**, root **(D)**, and shoot **(E)** Cd content of the WT and transgenic lines. The experiment was performed with three independent biological replicates. Significant differences according to the one-way analysis of variance are denoted as follows: $^{*}p < 0.01$.

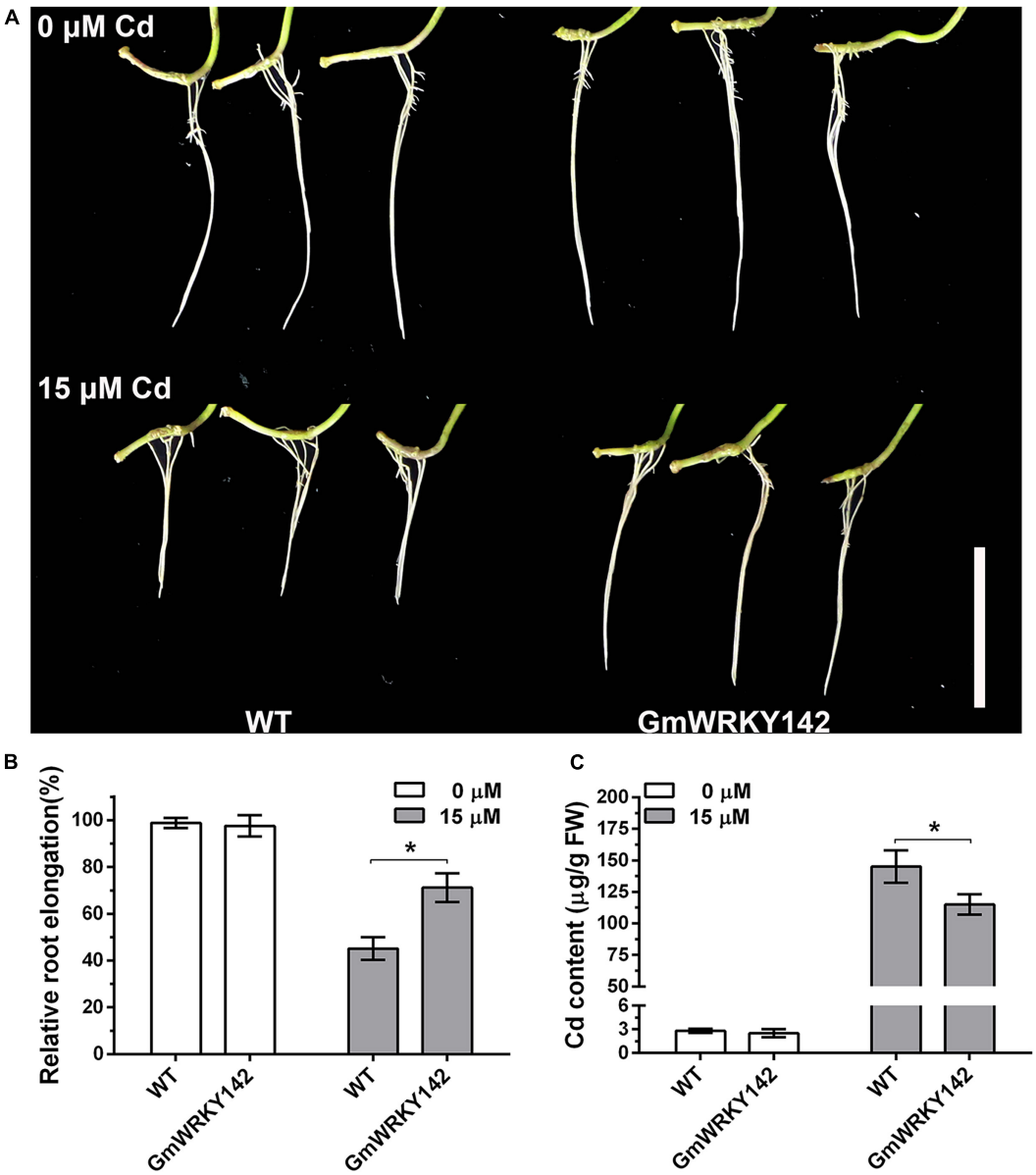

FIGURE 4 | Overexpression of GmWRKY142 conferred enhanced Cd tolerance in transgenic soybean hairy roots. **(A)** Phenotypes of GmWRKY142 transgenic lines and wild type (WT) under normal conditions or under Cd treatment conditions. Relative root elongation **(B)** and Cd content **(C)** of the WT and transgenic lines were measured after 15 μM Cd treatment for 5 days. The experiment was performed with three independent biological replicates. Significant differences according to the one-way analysis of variance are denoted as follows: $^{*}p < 0.01$.

(GO) analysis showed that 237 GO were significantly enriched in the DEGs (**Supplementary Table S6**) with the top 20 most enriched GO shown in **Figure 5D**. Further analyses identified 255 up-regulated DEGs containing W-box in their promoters (**Supplementary Table S7**), which may be direct downstream genes. We noticed that a group of downstream genes that have been shown to play direct roles in stress tolerance were up-regulated in the transgenic line, including mental stress induced proteins, auxin-responsive proteins, cell wall structural proteins and an array of transcription factors that are known as positive regulators of stress response. It should be noted that 13 genes belonging to GO:0071585 (detoxification of Cd ion) and GO:0046686 (response to Cadmium ion) were identified, with *AT1G52827* (Cadmium Tolerance 1, ATCDT1) being the only gene belonging to GO:0071585 (**Supplementary Table S8**). By homology search in the PANTHER (Protein Analysis Through Evolutionary Relationships) classification system[6] using the PTHR35470 (PANTHER ID) of plant Cadmium Tolerance 1, two homologous genes in the soybean genome were identified on chromosomes 13 (*Glyma.13G361300*) and

[6]http://www.pantherdb.org/

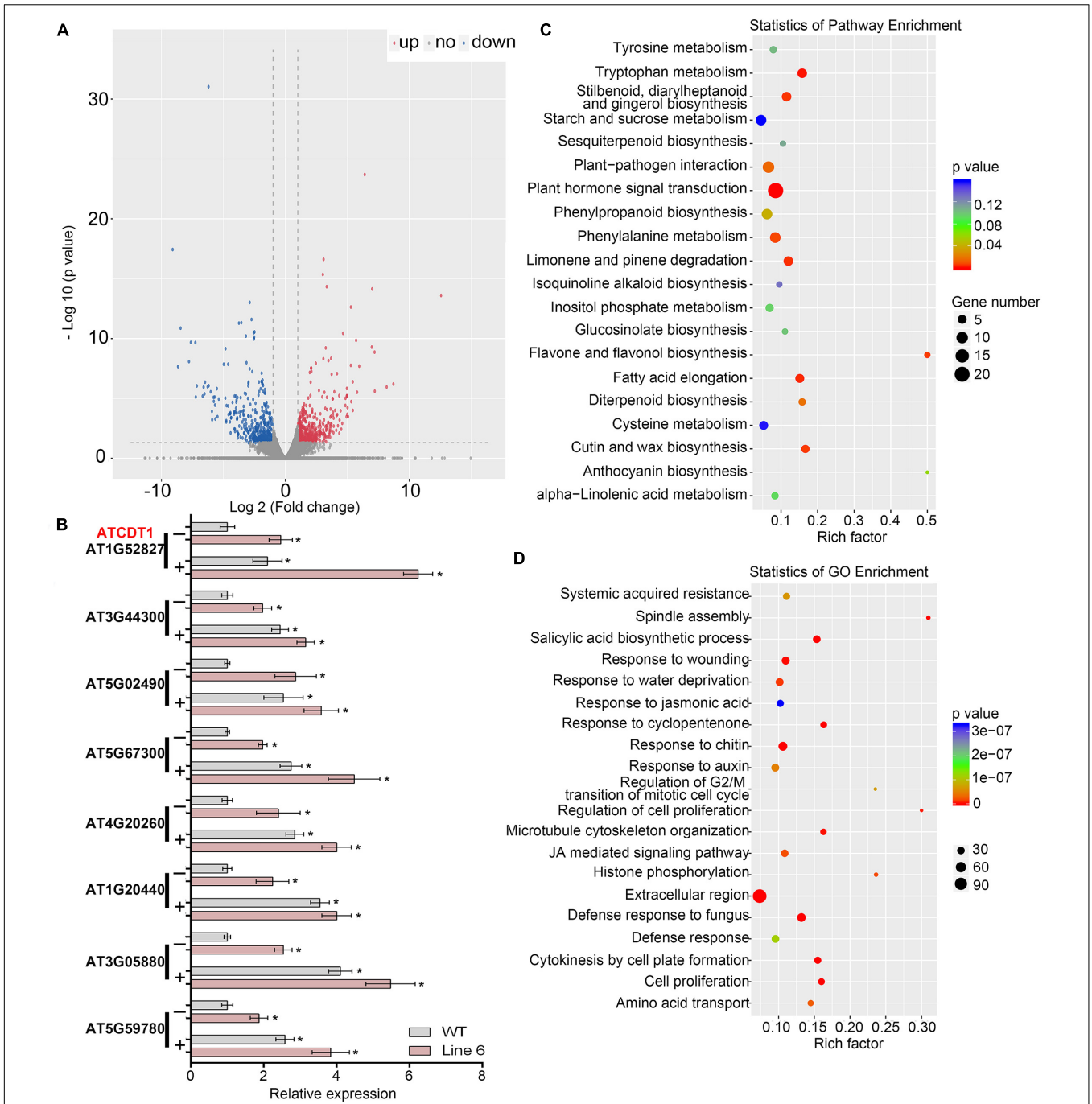

FIGURE 5 | Overexpression of GmWRKY142 caused global transcriptional reprogramming in transgenic Arabidopsis thaliana. **(A)** Scatterplots of gene expression patterns in the transgenic line compared with the WT. Red represents up-regulated genes, while blue represents down-regulated ones. **(B)** Validation of the expression of eight selected Cd tolerance related genes by qRT-PCR. **(C)** KEGG pathways enriched among differentially expressed genes (DEGs). **(D)** GO analysis of DEGs. Three independent biological replicates were tested in qRT-PCR assay. Significant differences according to the one-way analysis of variance are denoted as follows: $^{*}p < 0.01$.

15 (*Glyma.15G012600*), hereafter denoted as *GmCDT1-1* and *GmCDT1-2*. Compared with expression levels in control hairy root (CK), the transcription levels of both GmCDT1-1 and GmCDT1-2 were significantly increased in the *GmWRKY142*-overexpressed hairy roots (**Supplementary Figure S3**). These results suggest that *GmWKY142* activates *ATCDT1*, *GmCDT1-1*, and *GmCDT1-2* expression in *A. thaliana* or soybean. Further work investigated whether *ATCDT1* and its homologous genes *GmCDT1-1* and *GmCDT1-2* were direct target genes of *GmWRKY142*.

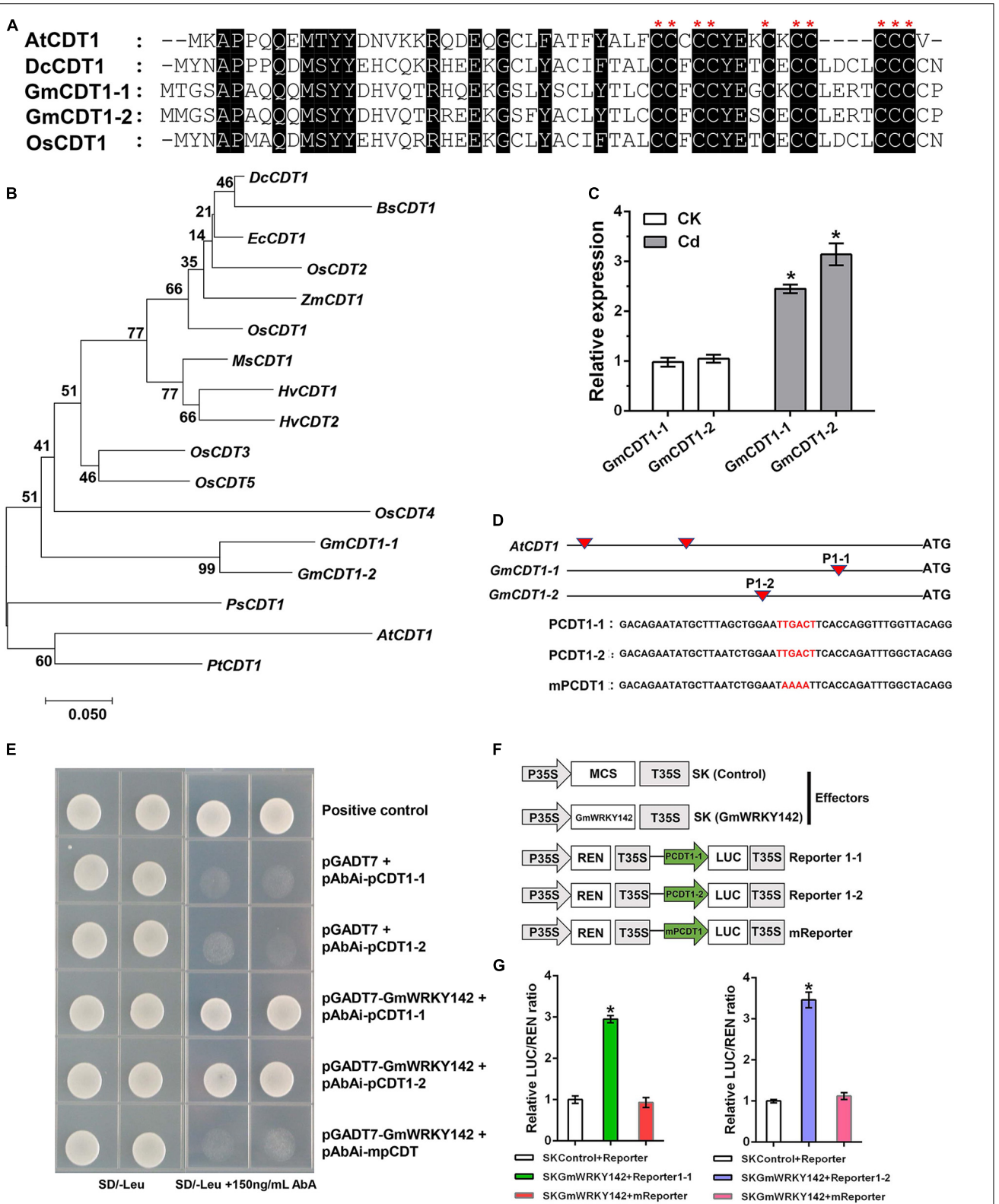

FIGURE 6 | GmWRKY142 was bound to and activated the promoters of the GmCDT1-like genes. **(A)** Multiple alignments of the conserved CDT domains. Identical amino acids are shown with a black background. **(B)** Phylogenetic relationships between GmCDT1s and related proteins. Accession numbers are: AtCDT1, NM_202281; BsCDT1, ABL85053; EcCDT1, AB426477; HvCDT1, AK251605; HvCDT2, AK249080; MsCDT1, AB426478; OsCDT1, AK121052; OsCDT2,

(Continued)

FIGURE 6 | Continued
AK061597; OsCDT3, AK062450; OsCDT4, AK059641; OsCDT5, AK099514; PsCDT1, EF081525; PtCDT1, CU225257; ZmCDT1, AY103859. **(C)** GmCDT1-1 and GmCDT1-2 were induced by Cd. The Huaxia 7 roots cultured in 0 or 25 μM of CdCl2 for 6 h were sampled and qRT-PCR assay was performed. **(D)** Schematic diagrams of ATCDT1, GmCDT1-1, and GmCDT1-2 promoters and partial sequences containing W-box used in yeast one-hybrid assays. **(E)** Culture of yeast cells co-transformed with the prey and bait, as well as the positive control (pGADT7-Rec-p53+p53-AbAi) on selective medium with or without 150 ng mL^{-1} Aureobasidin A (AbA). **(F)** Schematic diagrams of the effector and reporter constructs used for transient luciferase (LUC) assays. Full-length CDS of GmWRKY142 was inserted into pGreen II 62-SK to produce an effector, while the original or mutated W-box elements were inserted into pGreen II 0800-LUC to generate reporters. MCS, multiple cloning site. P35S and T35S, the promoter and terminator of CaMV 35S, respectively. REN (Renilla luciferase) was used as an internal control for activity normalization. **(G)** Transient expression assay of the promoter activity, shown as LUC/REN ratio, using tobacco leaves co-transformed with the effector and the reporters. LUC/REN ratio of the control co-transformed with the reporters and the empty effector vector (pGreen II 62-SK) was set as 1. Values are expressed as the means ± SD ($n = 3$). The experiment was performed with at least three independent biological replicates. Significant differences according to the one-way analysis of variance are denoted as follows: $^*p < 0.01$.

GmWRKY142 Directly Binds to and Activates the Promoter of *ATCDT1*, *GmCDT1-1* and *GmCDT1-2*

Previous studies have demonstrated that *ATCDT1* and its homologous genes (*DcCDT1* and *OsCDT1*) confer Cd tolerance to yeast or *A. thaliana* (Song et al., 2004; Kuramata et al., 2009; Matsuda et al., 2009). The amino acid sequences of GmCDT1-1 and GmCDT1-2 peptides share a high level of identity with ATCDT1, DcCDT1, and OsCDT1, and all contain 10 conserved Cys residues clustered in their carboxy-distal regions (**Figure 6A**). Protein sequence alignment showed that GmCDT1-1 and GmCDT1-2 shared a high amino acid sequence similarity of up to 94.6%. Two soybean CDT1 genes shared homology with the corresponding genes of AtCDT1 (58%), DcCDT1 (64%), and OsCDT1 (67%). A phylogenetic tree constructed based on the GmCDT1-1 and GmCDT1-2 and using a total of 17 CDT1 genes from different plant species shows that they could be classified into two major groups (**Figure 6B**). From phylogenetic analysis, GmCDT1-1 and GmCDT1-2 are found to be closest to DcCDT1, BsCDT1, ZmCDT1, OsCDTs, HvCDTs, and MsCDT1, whereas AtCDT1 forms another clade with PsCDT1 and PtCDT1 (**Figure 6B**). In addition, *GmCDT1-1* and *GmCDT1-2* expression levels were induced by Cd (**Figure 6C**), suggesting that these two genes may play a role in Cd tolerance.

Most WRKY transcription factors regulate their target stress-related genes via binding to the W-box of promoters (Ülker and Somssich, 2004; Jiang et al., 2014; Sheng et al., 2019). Isolation of the promoter sequence spanning 2,000 bp upstream of the first ATG of *ATCDT1*, *GmCDT1-1*, and *GmCDT1-2* identified 2, 1 and 1 W-boxes, respectively (**Figure 6D**). To test whether *GmWRKY142* can directly bind to the identified W-box, yeast one-hybrid (Y1H) was performed using *GmWRKY142* as prey, and promoter sequence fragments containing either original or mutated W-box elements as baits (**Figure 6C** and **Supplementary Figure S4**). Results showed that *GmWRKY142* could interact with selected promoter sequence fragments that contained the original W-box. However, yeast cells co-transformed with the prey and mutated W-box bait or pGADT7 and original W-box elements did not exhibit normal growth (**Figure 6E** and **Supplementary Figure S4**), suggesting the ability of *GmWRKY142* to bind to the W-box element in the *ATCDT1*, *GmCDT1-1* and *GmCDT1-2* promoters. To determine whether the GmWRKY142 transcription factor could activate GmCDT1-1 and GmCDT1-2 transcription, a dual luciferase (LUC) assay was performed in *N. benthamiana* leaves (**Figure 6F**). As shown in **Figures 6G**, the co-expression of Effecter-GmWRKY142 with Reporter1-1 and Reporter1-2 led to a higher LUC/REN ratio than that observed in the control and mutated reporter (mReporter), indicating that GmWRKY142 is a transcriptional activator of *GmCDT1-1* and *GmCDT1-2*.

Overexpression of *GmCDT1-1* and *GmCDT1-2* in Transgenic *A. thaliana* Confer Cd Tolerance

The results described above strongly support that *GmCDT1-1* and *GmCDT1-2* are direct targets of *GmWRKY142* and that they play a functional role in Cd tolerance. To explore the function of *GmCDT1-1* and *GmCDT1-2* during Cd stress, transgenic Arabidopsis and WT plants were subjected to treatment with $CdCl_2$. The results showed that both *GmCDT1-1* OX lines (OX 2 and 5) and *GmCDT1-2* OX lines (OX D and H) exhibited a higher biomass accumulation than the WT (**Figures 7A,B**). The average fresh weight and plant height of OX lines were higher than those of the WT (**Figures 7C,D**). Analysis of the Cd content in the WT and OX plants under Cd stress revealed that higher Cd levels were detected in the root and shoot of WT plants compared to OX plants (**Figures 7E,F**). These results suggest that *GmCDT1-1* and *GmCDT1-2* overexpression in Arabidopsis can enhance Cd tolerance by limiting Cd uptake.

DISCUSSION

Heavy metal stresses such as high concentration of Cd, Cu and As are among the major environmental factors which not only limit the productivity and growth potential of plants, but also cause serious problems for human health (Gallego et al., 1996; der Maur et al., 1999; Matsuda et al., 2009). Fortunately, a number of strategies have been employed in plants to resist heavy metal stress, including uptake, accumulation, translocation, and detoxification of the metal. Various transcription factor-mediated metal stress sensing and coping strategies have been reported in plants (Liu et al., 2017; Zhu et al., 2018). The WRKY transcription factor family is one of the most important regulator families reported to be involved in a variety of heavy metal stresses. For example, several studies have revealed the differential transcript

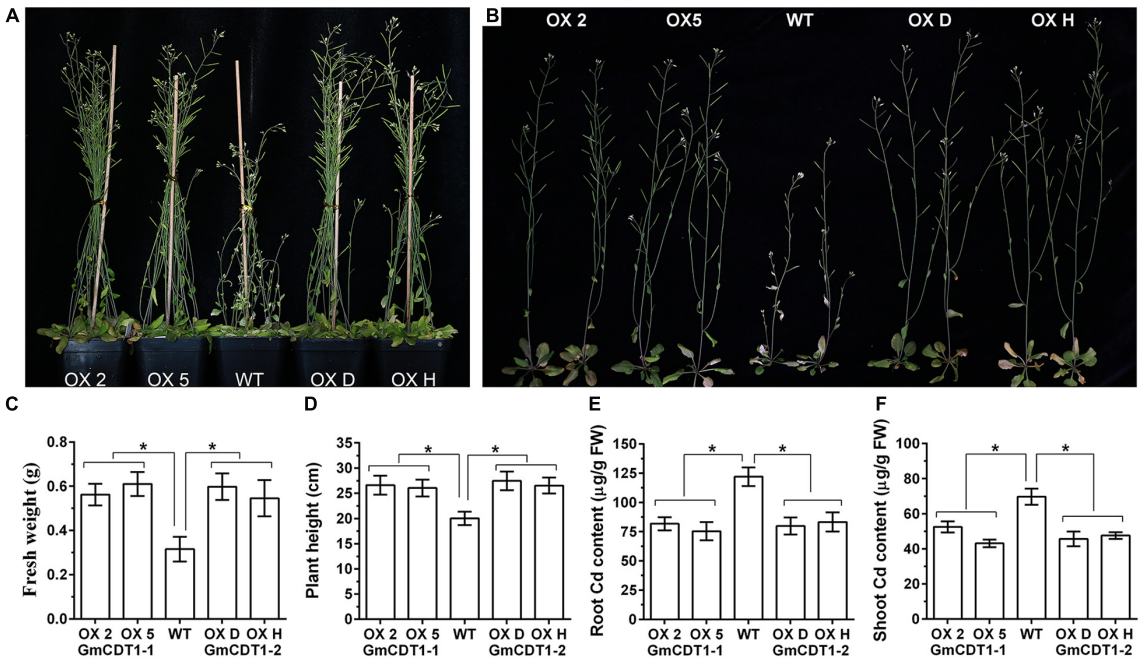

FIGURE 7 | The overexpression *Arabidopsis thaliana* lines of GmCDT1-1 or GmCDT1-2 showed tolerance to Cd stress. **(A,B)** Phenotypes of A. thaliana transgenic lines and wild type (WT) after Cd treatment. **(C–F)** Fresh weight **(C)**, plant height **(D)**, root **(E)**, and shoot **(F)** Cd content of the WT and transgenic lines. The experiment was performed with at least three independent biological replicates. Significant differences according to the one-way analysis of variance are denoted as follows: $^{*}p < 0.01$.

expression of WRKY transcription factors under Cd stress in different plant species (Yang et al., 2016; Hong et al., 2017; Cheng et al., 2018; Han et al., 2019; Sheng et al., 2019). An increasing number of WRKYs that were identified to confer Cd tolerance in plants also exemplify the importance of heavy metal tolerance in plants. To date, no report on the role of soybean WRKYs in Cd detoxification and tolerance has been published. In the present study, 29 GmWRKYs were detected as Cd-responsive DEGs using genome wide transcriptomic analysis in roots (**Table 1**). Of these, 26 GmWRKYs were up-regulated and 3 were down-regulated, suggesting that functional differentiation may exist. We further demonstrated that *GmWRKY142* is involved in Cd resistance and provided several lines of evidence supporting this observation. Firstly, GmWRKY142 is a nucleic protein with transcriptional activation activity and its expression was rapidly induced by Cd in a dose-dependent manner (**Figures 1**, **2**). Secondly, *GmWRKY142* overexpression in Arabidopsis and soybean hair roots resulted in improved Cd resistance, indicating that *GmWRKY142* is a positive regulator of Cd tolerance (**Figures 3**, **4**). Thirdly, *GmWRKY142* overexpression lead to the extensive transcriptional reprogramming of stress-responsive genes. We noticed that several downstream genes that have been shown to play direct roles in stress tolerance were prominently influenced by *GmWRKY142* overexpression including crucial metabolic regulators, mental stress induced proteins, auxin-responsive proteins, cell wall structural proteins and an array of transcription factors. One of them, the salicylic acid biosynthetic process (GO:0009697), which included 22 up-regulated and 9 down-regulated genes, had previously been found to be

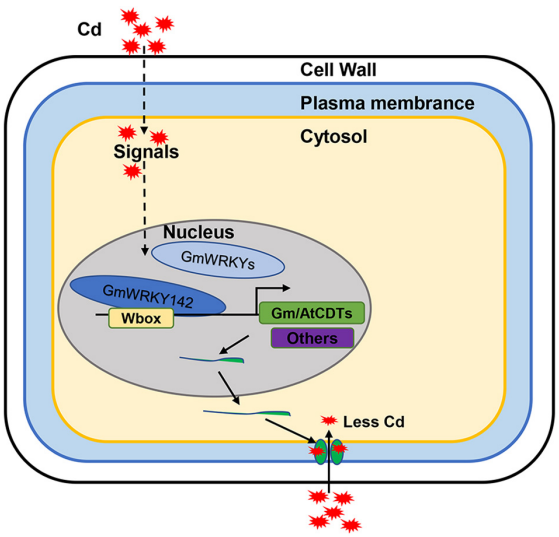

FIGURE 8 | A working model for the role of GmWRKY142 in regulating Cd tolerance. Cd stress promotes GmWRKY142 expression and thereby directly activates the transcript of the GmCDT1-1 and GmCDT1-2 genes encoding Cys-rich peptides, which results in chelating Cd at the cellular surface and prevent further entry of Cd into the cells, and thus, conferring enhanced tolerance.

significantly associated with Cd tolerance in plants (Belkhadi et al., 2010; Chao et al., 2010; Szalai et al., 2013), and was enriched in the transgenic line (**Figure 4** and **Supplementary Table S9**).

Finally, the present study demonstrated that the GmWRKY142-AT/GmCDT1 cascade module confers Cd tolerance (**Figures 5**, **6**). These findings suggest that GmWRKYs act as novel participants in the response of soybean to Cd stress, although further studies will be required to support this conclusion.

WRKYs can activate or repress the transcription of stress-related and co-regulated genes by directly recognizing and binding to the W-box element within the promoters of target genes (Eulgem et al., 2000; Ülker and Somssich, 2004; Han et al., 2019). In the present study, we demonstrated that overexpression of *GmWRKY142* in transgenic *A. thaliana* or soybean hairy roots lead to enhanced tolerance to Cd and activated the expression of the *ATCDT1* or *GmCDT1*-like genes (*GmCDT1-1* and *GmCDT1-2*) encoding Cd-binding Cys-rich proteins (**Figures 3**, **5** and **Supplementary Figure S3**). The *ATCDT1*, *GmCDT1-1*, and *GmCDT1-2* promoters were found to contain 2, 1, and 1 W-box elements, respectively (**Figure 6C**). We further demonstrated that *GmWRKY142* activated the *ATCDT1*, *GmCDT1-1*, and *GmCDT1-2* promoters through interactions with the W-box element using the yeast one-hybrid or dual luciferase (LUC) assays (**Figures 6D,E** and **Supplementary Figure S4**). So far, a plethora of target genes have been characterized for various WRKY members. However, only a limited number of WRKY TFs and their target genes were identified to regulate Cd tolerance in plants. *AtWRKY13* is induced by Cd stress and directly activates the expression of the Cd^{2+} extrusion pump gene *AtPDR8*; therefore, *AtWRKY13* overexpression in transgenic *A. thaliana* leads to an enhanced tolerance to Cd (Sheng et al., 2019). *AtWRKY12* as a negative regulator directly targets *GSH1* and indirectly represses PC synthesis-related genes expression to negatively regulate Cd accumulation and tolerance in Arabidopsis (Han et al., 2019). These two studies show that WRKY proteins can act as transcriptional activators or repressors to regulate Cd accumulation and tolerance. Herein, the characterization of *ATCDT1* and *GmCDT1*-like genes as direct targets of *GmWRKY142* provides valuable clues to better understand the WRKY regulatory mechanisms associated with Cd stress. However, RNA-seq results indicated that *ATCDT1* and *GmCDT1*-like genes were not the only identified target genes (**Figure 5**), thereby highlighting the importance of confirming the identity of the other target genes to better understand the molecular mechanism of *GmWRKY142* in Cd tolerance.

In the previous studies, three members of the CDT1 family, namely, DcCDT1, OsCDT1 and ATCDT1, from *Digitaria ciliaris*, *Oryza sativa* and *A. thaliana* were isolated and characterized for Cd tolerance (Song et al., 2004; Kuramata et al., 2009; Matsuda et al., 2009). In contrast to other Cys-rich peptides, CDT1 peptides are only present in angiosperms and gymnosperms, and are relatively small in size with 49 to 60 amino acid residues (Song et al., 2004). In the present study, two homologous CDT1s were identified in soybean and their expression induced by Cd stress (**Figure 6B**). Consistent with *DcCDT1*, *OsCDT1*, and *ATCDT1*, overexpression of *GmCDT1-1* or *GmCDT1-2* conferred Cd-tolerance to transgenic *A. thaliana* plants by lowering Cd accumulation in plants (**Figure 7**). A conserved sequence with 10 Cys-rich peptides, CC-(C/F)-CCYE-X-C-(K/E)-CC-(LDCL/LERT/delete)-CCC-(V/C), in their C-termini was identified in this study. Plants have evolved a set of versatile adaptive mechanisms to cope with Cd stress. One such means is by reducing the cellular accumulation of Cd by either enhancing Cd efflux or suppressing its uptake. The Cys-rich membrane proteins in different plant species have been found to play an important role in plant Cd resistance by chelating Cd at the cellular surface and limiting further entry of Cd into the cells (Song et al., 2004; Kuramata et al., 2009; Matsuda et al., 2009; Pirzadeh and Shahpiri, 2016; Niederwanger et al., 2017). Here, we have demonstrated that expression of GmCDT1-1 or GmCDT1-2 conferred Cd tolerance to Arabidopsis plants by reducing their cellular Cd contents. GmCDT1-1 and GmCDT1-2 are Cys-rich peptides, so it is highly likely that they can directly bind Cd. Based on our current findings, therefore, the most plausible mechanism we envisage for GmCDT1s and AtCDT1 function is that these proteins chelate Cd at the cellular surface and prevent further entry of Cd into the cells. These findings suggest that CDT1s play an important role in Cd tolerance.

In summary, 29 Cd-responsive WRKY genes were identified and confirmed in soybean roots, of which 26 were up-regulated and 3 were down-regulated. Among these GmWRKYs, the up-regulated *GmWRKY142*, in particular, directly activated expression of the *ATCDT1* and *GmCDT1*-like genes, which resulted in reduced Cd accumulation, thereby conferring Cd tolerance (**Figure 8**). The identification of 29 Cd-responsive GmWRKYs as well as the GmWRKY142-CDT1 cascade module provides the first step in determining that GmWRKYs may be critical factors in Cd tolerance. More GmWRKYs-targeted cascade modules conferring Cd tolerance need to be further studied.

DATA AVAILABILITY STATEMENT

The data sets supporting the results of this study are included in the article. The RNA-seq data have been deposited into the NCBI Short Read Archive (SRA, https://www.ncbi.nlm.nih.gov/sra/) under accession number PRJNA605520.

AUTHOR CONTRIBUTIONS

ZC, PX, HW, and RL performed the experiments and data analyses. ZC and HN prepared the manuscript. HN planned, supervised, and financed this work. YC, TL, and QM reviewed and edited the manuscript. All authors have read and approved the final version of the manuscript to be published.

FUNDING

This work was supported by the National Key R&D Program of China (2018YFD0201006), the National Natural Science Foundation of China (31771816 and 31971965), and the Research Project of the State Key Laboratory for Conservation and Utilization of Subtropical Agro-bioresources (SKLCUSA-b201804).

ACKNOWLEDGMENTS

We thank the members of the Guangdong Subcenter of the National Center for Soybean Improvement for their daily help.

SUPPLEMENTARY MATERIAL

The Supplementary Material for this article can be found online at: https://www.frontiersin.org/articles/10.3389/fpls.2020.00724/full#supplementary-material

REFERENCES

Belkhadi, A., Hediji, H., Abbes, Z., Nouairi, I., Barhoumi, Z., Zarrouk, M., et al. (2010). Effects of exogenous salicylic acid pre-treatment on cadmium toxicity and leaf lipid content in *Linum usitatissimum* L. *Ecotoxicol. Environ. Saf.* 73, 1004–1011. doi: 10.1016/j.ecoenv.2010.03.009

Cai, S. Y., Zhang, Y., Xu, Y. P., Qi, Z. Y., Li, M. Q., Ahammed, G. J., et al. (2017). HsfA1a upregulates melatonin biosynthesis to confer cadmium tolerance in tomato plants. *J. Pineal Res.* 62:e12387. doi: 10.1111/jpi.12387

Chao, Y.-Y., Chen, C.-Y., Huang, W.-D., and Kao, C. H. (2010). Salicylic acid-mediated hydrogen peroxide accumulation and protection against Cd toxicity in rice leaves. *Plant Soil* 329, 327–337.

Chen, J., Yang, L., Yan, X., Liu, Y., Wang, R., Fan, T., et al. (2016). Zinc-finger transcription factor ZAT6 positively regulates cadmium tolerance through the glutathione-dependent pathway in Arabidopsis. *Plant Physiol.* 171, 707–719. doi: 10.1104/pp.15.01882

Chen, W. W., Jin, J. F., Lou, H. Q., Liu, L., Kochian, L. V., and Yang, J. L. (2018). LeSPL-CNR negatively regulates Cd acquisition through repressing nitrate reductase-mediated nitric oxide production in tomato. *Planta* 248, 893–907. doi: 10.1007/s00425-018-2949-z

Cheng, D., Tan, M., Yu, H., Li, L., Zhu, D., Chen, Y., et al. (2018). Comparative analysis of Cd-responsive maize and rice transcriptomes highlights Cd co-modulated orthologs. *BMC Genomics* 19:709. doi: 10.1186/s12864-018-5109-8

Clemens, S., Aarts, M. G., Thomine, S., and Verbruggen, N. (2013). Plant science: the key to preventing slow cadmium poisoning. *Trends Plant Sci.* 18, 92–99. doi: 10.1016/j.tplants.2012.08.003

Clough, S. J., and Bent, A. F. (1998). Floral dip: a simplified method for *Agrobacterium*-mediated transformation of *Arabidopsis thaliana*. *Plant J.* 16, 735–743. doi: 10.1046/j.1365-313x.1998.00343.x

DalCorso, G., Farinati, S., Maistri, S., and Furini, A. (2008). How plants cope with cadmium: staking all on metabolism and gene expression. *J. Integr. Plant Biol.* 50, 1268–1280. doi: 10.1111/j.1744-7909.2008.00737.x

Dang, F., Lin, J., Chen, Y., Li, G. X., Guan, D., Zheng, S. J., et al. (2019). A feedback loop between CaWRKY41 and H2O2 coordinates the response to *Ralstonia solanacearum* and excess cadmium in pepper. *J. Exp. Bot.* 70, 1581–1595. doi: 10.1093/jxb/erz006

Das, P., Samantaray, S., and Rout, G. (1997). Studies on cadmium toxicity in plants: a review. *Environ. Pollut.* 98, 29–36. doi: 10.1016/s0269-7491(97)00110-3

der Maur, A. A., Belser, T., Elgar, G., Georgiev, O., and Schaffner, W. (1999). Characterization of the transcription factor MTF-1 from the Japanese pufferfish (*Fugu rubripes*) reveals evolutionary conservation of heavy metal stress response. *Biol. Chem.* 380, 175–185. doi: 10.1515/BC.1999.026

Dong, J., Mao, W., Zhang, G., Wu, F., and Cai, Y. (2007). Root excretion and plant tolerance to cadmium toxicity-a review. *Plant Soil Environ.* 53, 193–200.

Eulgem, T., Rushton, P. J., Robatzek, S., and Somssich, I. E. (2000). The WRKY superfamily of plant transcription factors. *Trends Plant Sci.* 5, 199–206. doi: 10.1016/s1360-1385(00)01600-9

Eulgem, T., and Somssich, I. E. (2007). Networks of WRKY transcription factors in defense signaling. *Curr. Opin. Plant Biol.* 10, 366–371. doi: 10.1016/j.pbi.2007.04.020

Gallego, S. M., Benavides, M. P., and Tomaro, M. L. (1996). Effect of heavy metal ion excess on sunflower leaves: evidence for involvement of oxidative stress. *Plant Sci.* 121, 151–159.

Gallego, S. M., Pena, L. B., Barcia, R. A., Azpilicueta, C. E., Iannone, M. F., Rosales, E. P., et al. (2012). Unravelling cadmium toxicity and tolerance in plants: insight into regulatory mechanisms. *Environ. Exp. Bot.* 83, 33–46. doi: 10.1016/j.jhazmat.2017.04.058

Gill, S. S., and Tuteja, N. (2011). Cadmium stress tolerance in crop plants: probing the role of sulfur. *Plant Signal. Behav.* 6, 215–222. doi: 10.4161/psb.6.2.14880

Grant, C., Buckley, W., Bailey, L., and Selles, F. (1998). Cadmium accumulation in crops. *Can. J. Plant Sci.* 78, 1–17.

Han, Y., Fan, T., Zhu, X., Wu, X., Ouyang, J., Jiang, L., et al. (2019). WRKY12 represses *GSH1* expression to negatively regulate cadmium tolerance in *Arabidopsis*. *Plant Mol. Biol.* 99, 149–159. doi: 10.1007/s11103-018-0809-7

Hasan, S. A., Fariduddin, Q., Ali, B., Hayat, S., and Ahmad, A. (2009). Cadmium: toxicity and tolerance in plants. *J. Environ. Biol.* 30, 165–174.

Hoagland, D. R., and Arnon, D. I. (1950). The water-culture method for growing plants without soil. *Circular* 347:32.

Hong, C., Cheng, D., Zhang, G., Zhu, D., Chen, Y., and Tan, M. (2017). The role of ZmWRKY4 in regulating maize antioxidant defense under cadmium stress. *Biochem. Biophys. Res. Commun.* 482, 1504–1510. doi: 10.1016/j.bbrc.2016.12.064

Hu, S., Yu, Y., Chen, Q., Mu, G., Shen, Z., and Zheng, L. (2017). *OsMYB45* plays an important role in rice resistance to cadmium stress. *Plant Sci.* 264, 1–8. doi: 10.1016/j.plantsci.2017.08.002

IBM Corp (2012). *IBM SPSS Statistics for Windows, Version 21.0*. Armonk, NY: IBM Corp.

Ishiguro, S., and Nakamura, K. (1994). Characterization of a cDNA encoding a novel DNA-binding protein, SPF1, that recognizes SP8 sequences in the 5′ upstream regions of genes coding for sporamin and ß-amylase from sweet potato. *Mol. Gen. Genet.* 244, 563–571. doi: 10.1007/BF00282746

Jiang, Y., Liang, G., Yang, S., and Yu, D. (2014). *Arabidopsis* WRKY57 functions as a node of convergence for jasmonic acid–and auxin-mediated signaling in jasmonic acid–induced leaf senescence. *Plant Cell* 26, 230–245. doi: 10.1105/tpc.113.117838

Kumar, A., Pandey, R., and Siddiqi, N. (2019). Oxidative stress biomarkers of cadmium toxicity in mammalian systems and their distinct ameliorative strategy. *J. Appl. Biotechnol. Bioeng.* 6, 126–135.

Kunihiro, S., Saito, T., Matsuda, T., Inoue, M., Kuramata, M., Taguchi-Shiobara, F., et al. (2013). Rice DEP1, encoding a highly cysteine-rich G protein γ subunit, confers cadmium tolerance on yeast cells and plants. *J. Exp. Bot.* 64, 4517–4527. doi: 10.1093/jxb/ert267

Kuramata, M., Masuya, S., Takahashi, Y., Kitagawa, E., Inoue, C., Ishikawa, S., et al. (2009). Novel cysteine-rich peptides from *Digitaria ciliaris* and *Oryza sativa* enhance tolerance to cadmium by limiting its cellular accumulation. *Plant Cell Physiol.* 50, 106–117. doi: 10.1093/pcp/pcn175

Li, R., Yu, C., Li, Y., Lam, T. W., Yiu, S. M., Kristiansen, K., et al. (2009). SOAP2: an improved ultrafast tool for short read alignment. *Bioinformatics* 25, 1966–1967. doi: 10.1093/bioinformatics/btp336

Lin, T., Yang, W., Lu, W., Wang, Y., and Qi, X. (2017). Transcription factors PvERF15 and PvMTF-1 form a cadmium stress transcriptional pathway. *Plant Physiol.* 173, 1565–1573. doi: 10.1104/pp.16.01729

Liu, X. S., Feng, S. J., Zhang, B. Q., Wang, M. Q., Cao, H. W., Rono, J. K., et al. (2019). OsZIP1 functions as a metal efflux transporter limiting excess zinc, copper and cadmium accumulation in rice. *BMC Plant Biol.* 19:283. doi: 10.1186/s12870-019-1899-3

Liu, Y., Yu, X., Feng, Y., Zhang, C., Wang, C., Zeng, J., et al. (2017). Physiological and transcriptome response to cadmium in cosmos (*Cosmos bipinnatus* Cav.) seedlings. *Sci. Rep.* 7:14691. doi: 10.1038/s41598-017-14407-8

Livak, K. J., and Schmittgen, T. D. (2001). Analysis of relative gene expression data using real-time quantitative PCR and the 2- ΔΔCT method. *Methods* 25, 402–408.

Luo, J.-S., Gu, T., Yang, Y., and Zhang, Z. (2019a). A non-secreted plant defensin AtPDF2.6 conferred cadmium tolerance via its chelation in *Arabidopsis*. *Plant Mol. Biol.* 100, 561–569. doi: 10.1007/s11103-019-00878-y

Luo, J.-S., Yang, Y., Gu, T., Wu, Z., and Zhang, Z. (2019b). The Arabidopsis defensin gene *AtPDF2.5* mediates cadmium tolerance and accumulation. *Plant Cell Environ.* 42, 2681–2695. doi: 10.1111/pce.13592

Margoshes, M., and Vallee, B. L. (1957). A cadmium protein from equine kidney cortex. *J. Am. Chem. Soc.* 79, 4813–4814.

Matsuda, T., Kuramata, M., Takahashi, Y., Kitagawa, E., Youssefian, S., and Kusano, T. (2009). A novel plant cysteine-rich peptide family conferring cadmium tolerance to yeast and plants. *Plant Signal. Behav.* 4, 419–421. doi: 10.4161/psb.4.5.8272

Matthews, B. F., and Youssef, R. M. (2016). *Agrobacterium rhizogenes*-based transformation of soybean roots to form composite plants. *Bio Protoc.* 6:e1708.

Mekawy, A. M. M., Assaha, D. V. M., and Ueda, A. (2020). Constitutive overexpression of rice metallothionein-like gene *OsMT-3a* enhances growth and tolerance of Arabidopsis plants to a combination of various abiotic stresses. *J. Plant Res.* 133, 429–440. doi: 10.1007/s10265-020-01187-y

Mortazavi, A., Williams, B. A., McCue, K., Schaeffer, L., and Wold, B. (2008). Mapping and quantifying mammalian transcriptomes by RNA-Seq. *Nat. Methods* 5, 621–628. doi: 10.1038/nmeth.1226

Moulis, J.-M., and Thévenod, F. (2010). *New Perspectives in Cadmium Toxicity: an Introduction*. Berlin: Springer.

Nagajyoti, P. C., Lee, K. D., and Sreekanth, T. (2010). Heavy metals, occurrence and toxicity for plants: a review. *Environ. Chem. Lett.* 8, 199–216.

Niederwanger, M., Dvorak, M., Schnegg, R., Pedrini-Martha, V., Bacher, K., Bidoli, M., et al. (2017). Challenging the *Metallothionein* (*MT*) gene of *Biomphalaria glabrata*: unexpected response patterns due to cadmium exposure and temperature stress. *Int. J. Mol. Sci.* 18:1747. doi: 10.3390/ijms18081747

Okereafor, U., Makhatha, M., Mekuto, L., Uche-Okereafor, N., Sebola, T., and Mavumengwana, V. (2020). Toxic metal implications on agricultural soils, plants, animals, aquatic life and human health. *Int. J. Environ. Res. Public Health* 17:2204. doi: 10.3390/ijerph17072204

Palacios, Ò., Espart, A., Espín, J., Ding, C., Thiele, D. J., Atrian, S., et al. (2014). Full characterization of the Cu-, Zn-, and Cd-binding properties of CnMT1 and CnMT2, two metallothioneins of the pathogenic fungus *Cryptococcus neoformans* acting as virulence factors. *Metallomics* 6, 279–291. doi: 10.1039/c3mt00266g

Pirzadeh, S., and Shahpiri, A. (2016). Functional characterization of a type 2 metallothionein isoform (OsMTI-2b) from rice. *Int. J. Biol. Macromol.* 88, 491–496. doi: 10.1016/j.ijbiomac.2016.04.021

Rizwan, M., Ali, S., Adrees, M., Ibrahim, M., Tsang, D. C., Zia-ur-Rehman, M., et al. (2017). A critical review on effects, tolerance mechanisms and management of cadmium in vegetables. *Chemosphere* 182, 90–105. doi: 10.1016/j.chemosphere.2017.05.013

Rushton, P. J., Macdonald, H., Huttly, A. K., Lazarus, C. M., and Hooley, R. (1995). Members of a new family of DNA-binding proteins bind to a conserved cis-element in the promoters of α-Amy2 genes. *Plant Mol. Biol.* 29, 691–702. doi: 10.1007/BF00041160

Rushton, P. J., Somssich, I. E., Ringler, P., and Shen, Q. J. (2010). WRKY transcription factors. *Trends Plant Sci.* 15, 247–258. doi: 10.1016/j.tplants.2010.02.006

Rushton, P. J., Torres, J. T., Parniske, M., Wernert, P., Hahlbrock, K., and Somssich, I. (1996). Interaction of elicitor-induced DNA-binding proteins with elicitor response elements in the promoters of parsley PR1 genes. *EMBO J.* 15, 5690–5700.

Sasaki, A., Yamaji, N., and Ma, J. F. (2014). Overexpression of OsHMA3 enhances Cd tolerance and expression of Zn transporter genes in rice. *J. Exp. Bot.* 65, 6013–6021. doi: 10.1093/jxb/eru340

Shanying, H., Xiaoe, Y., Zhenli, H., and Baligar, V. C. (2017). Morphological and physiological responses of plants to cadmium toxicity: a review. *Pedosphere* 27, 421–438.

Sheng, Y., Yan, X., Huang, Y., Han, Y., Zhang, C., Ren, Y., et al. (2019). The WRKY transcription factor, WRKY13, activates *PDR8* expression to positively regulate cadmium tolerance in *Arabidopsis*. *Plant Cell Environ.* 42, 891–903. doi: 10.1111/pce.13457

Smirnova, I. V., Bittel, D. C., Ravindra, R., Jiang, H., and Andrews, G. K. (2000). Zinc and cadmium can promote rapid nuclear translocation of metal response element-binding transcription factor-1. *J. Biol. Chem.* 275, 9377–9384. doi: 10.1074/jbc.275.13.9377

Solis, W. A., Childs, N. L., Weedon, M. N., He, L., Nebert, D. W., and Dalton, T. P. (2002). Retrovirally expressed metal response element-binding transcription factor-1 normalizes metallothionein-1 gene expression and protects cells against zinc, but not cadmium, toxicity. *Toxicol. Appl. Pharmacol.* 178, 93–101. doi: 10.1006/taap.2001.9319

Song, H., Wang, P., Hou, L., Zhao, S., Zhao, C., Xia, H., et al. (2016). Global analysis of WRKY genes and their response to dehydration and salt stress in soybean. *Front. Plant Sci.* 7:9. doi: 10.3389/fpls.2016.00009

Song, W.-Y., Martinoia, E., Lee, J., Kim, D., Kim, D.-Y., Vogt, E., et al. (2004). A novel family of cys-rich membrane proteins mediates cadmium resistance in Arabidopsis. *Plant Physiol.* 135, 1027–1039. doi: 10.1104/pp.103.037739

Sparkes, I. A., Runions, J., Kearns, A., and Hawes, C. (2006). Rapid, transient expression of fluorescent fusion proteins in tobacco plants and generation of stably transformed plants. *Nat. Protoc.* 1, 2019–2025. doi: 10.1038/nprot.2006.286

Szalai, G., Krantev, A., Yordanova, R., Popova, L. P., and Janda, T. (2013). Influence of salicylic acid on phytochelatin synthesis in *Zea mays* during Cd stress. *Turk. J. Bot.* 37, 708–714. doi: 10.1371/journal.pone.0160157

Tang, L., Mao, B. G., Li, Y. K., Lv, Q. M., Zhang, L. P., Chen, C. Y., et al. (2017). Knockout of *OsNramp5* using the CRISPR/Cas9 system produces low Cd-accumulating *indica* rice without compromising yield. *Sci. Rep.* 7:14438. doi: 10.1038/s41598-017-14832-9

Tang, W., Charles, T. M., and Newton, R. J. (2005). Overexpression of the pepper transcription factor CaPF1 in transgenic Virginia pine (*Pinus virginiana* Mill.) confers multiple stress tolerance and enhances organ growth. *Plant Mol. Biol.* 59, 603–617. doi: 10.1007/s11103-005-0451-z

Ülker, B., and Somssich, I. E. (2004). WRKY transcription factors: from DNA binding towards biological function. *Curr. Opin. Plant Biol.* 7, 491–498. doi: 10.1016/j.pbi.2004.07.012

Wu, H., Chen, C., Du, J., Liu, H., Cui, Y., Zhang, Y., et al. (2012). Co-overexpression FIT with *AtbHLH38* or *AtbHLH39* in Arabidopsis-enhanced cadmium tolerance via increased cadmium sequestration in roots and improved iron homeostasis of shoots. *Plant Physiol.* 158, 790–800. doi: 10.1104/pp.111.190983

Wu, X., Chen, J., Yue, X., Wei, X., Zou, J., Chen, Y., et al. (2019). The zinc-regulated protein (ZIP) family genes and glutathione s-transferase (GST) family genes play roles in Cd resistance and accumulation of pak choi (*Brassica campestris* ssp. *chinensis*). *Ecotoxicol. Environ. Saf.* 183:109571. doi: 10.1016/j.ecoenv.2019.109571

Xu, H., Watanabe, K. A., Zhang, L., and Shen, Q. J. (2016). WRKY transcription factor genes in wild rice *Oryza nivara*. *DNA Res.* 23, 311–323. doi: 10.1093/dnares/dsw025

Xu, Z., Ge, Y., Zhang, W., Zhao, Y., and Yang, G. (2018). The walnut *JrVHAG1* gene is involved in cadmium stress response through ABA-signal pathway and MYB transcription regulation. *BMC Plant Biol.* 18:19. doi: 10.1186/s12870-018-1231-7

Yang, G., Wang, C., Wang, Y., Guo, Y., Zhao, Y., Yang, C., et al. (2016). Overexpression of *ThVHAc1* and its potential upstream regulator, *ThWRKY7*, improved plant tolerance of Cadmium stress. *Sci. Rep.* 6:18752. doi: 10.1038/srep18752

Yang, J., Wang, Y., Liu, G., Yang, C., and Li, C. (2011). *Tamarix hispida* metallothionein-like *ThMT3*, a reactive oxygen species scavenger, increases tolerance against Cd 2+, Zn 2+, Cu 2+, and NaCl in transgenic yeast. *Mol. Biol. Rep.* 38, 1567–1574. doi: 10.1007/s11033-010-0265-1

Yang, Y., Zhou, Y., Chi, Y., Fan, B., and Chen, Z. (2017). Characterization of soybean WRKY gene family and identification of soybean WRKY genes that promote resistance to soybean cyst nematode. *Sci. Rep.* 7:17804. doi: 10.1038/s41598-017-18235-8

Yao, X., Cai, Y., Yu, D., and Liang, G. (2018). bHLH104 confers tolerance to cadmium stress in *Arabidopsis thaliana*. *J. Integr. Plant Biol.* 60, 691–702. doi: 10.1111/jipb.12658

Yi, S. Y., Kim, J.-H., Joung, Y.-H., Lee, S., Kim, W.-T., Yu, S. H., et al. (2004). The pepper transcription factor *CaPF1* confers pathogen and freezing tolerance in Arabidopsis. *Plant Physiol.* 136, 2862–2874. doi: 10.1104/pp.104.042903

Yu, Y., Wang, N., Hu, R., and Xiang, F. (2016). Genome-wide identification of soybean WRKY transcription factors in response to salt stress. *Springerplus* 5:920. doi: 10.1186/s40064-016-2647-x

Zhang, P., Wang, R., Ju, Q., Li, W., Tran, L.-S. P., and Xu, J. (2019). The R2R3-MYB transcription factor MYB49 regulates cadmium accumulation. *Plant Physiol.* 180, 529–542. doi: 10.1104/pp.18.01380

Zhang, Z. H., Zhou, T., Tang, T. J., Song, H. X., Guan, C. Y., Huang, J. Y., et al. (2019). A multiomics approach reveals the pivotal role of subcellular reallocation in determining rapeseed resistance to cadmium toxicity. *J. Exp. Bot.* 70, 5437–5455. doi: 10.1093/jxb/erz295

Zhao, F. J., and Huang, X. Y. (2018). Cadmium phytoremediation: call rice CAL1. *Mol. Plant* 11, 640–642. doi: 10.1016/j.molp.2018.03.016

Zheng, S., Wang, Q., Yuan, Y., and Sun, W. (2020). Human health risk assessment of heavy metals in soil and food crops in the Pearl River Delta urban agglomeration of China. *Food Chem.* 316:126213. doi: 10.1016/j.foodchem.2020.126213

Zhu, H., Ai, H., Cao, L., Sui, R., Ye, H., Du, D., et al. (2018). Transcriptome analysis providing novel insights for Cd-resistant tall fescue responses to Cd stress. *Ecotoxicol. Environ. Saf.* 160, 349–356. doi: 10.1016/j.ecoenv.2018.05.066

Zhu, Y. L., Pilon-Smits, E. A., Jouanin, L., and Terry, N. (1999a). Overexpression of glutathione synthetase in Indian mustard enhances cadmium accumulation and tolerance. *Plant Physiol.* 119, 73–80. doi: 10.1104/pp.119.1.73

Zhu, Y. L., Pilon-Smits, E. A., Tarun, A. S., Weber, S. U., Jouanin, L., and Terry, N. (1999b). Cadmium tolerance and accumulation in Indian mustard is enhanced by overexpressing γ-glutamylcysteine synthetase. *Plant Physiol.* 121, 1169–1177. doi: 10.1104/pp.121.4.1169

Conflict of Interest: The authors declare that the research was conducted in the absence of any commercial or financial relationships that could be construed as a potential conflict of interest.

frontiers in Plant Science

ORIGINAL RESEARCH
published: 26 June 2020
doi: 10.3389/fpls.2020.00888

K Fertilizers Reduce the Accumulation of Cd in *Panax notoginseng* (Burk.) F.H. by Improving the Quality of the Microbial Community

Yue Shi[1,2†], Lisha Qiu[3†], Lanping Guo[4], Jinhui Man[1], Bingpeng Shang[1], Rongfeng Pu[1], Xiaohong Ou[1], Chunyan Dai[1], Pengfei Liu[1], Ye Yang[1] and Xiuming Cui[1]**

[1] Yunnan Provincial Key Laboratory of Panax notoginseng, Key Laboratory of Panax notoginseng Resources Sustainable Development and Utilization of State Administration of Traditional Chinese Medicine, Kunming Key Laboratory of Sustainable Development and Utilization of Famous-Region Drug, Faculty of Life Science and Technology, Kunming University of Science and Technology, Kunming, China, [2] College of Chinese Materia Medica, Beijing University of Chinese Medicine, Beijing, China, [3] Analysis and Test Center, Kunming University of Science and Technology, Kunming, China, [4] Chinese Medica Resources Center, China Academy of Chinese Medicinal Sciences, Beijing, China

OPEN ACCESS

Edited by:
Basharat Ali,
University of Agriculture, Faisalabad, Pakistan

Reviewed by:
Shahbaz Atta Tung,
University of Agriculture, Faisalabad, Pakistan
Mumtaz Khan,
Gomal University, Pakistan
Jiang Xu,
Institute of Chinese Materia Medica, China Academy of Chinese Medical Sciences, China
Raza Waseem,
Nanjing Agricultural University, China

***Correspondence:**
Ye Yang
yangyekm@163.com
Xiuming Cui
sanqi37@vip.sina.com

†These authors share first authorship

Specialty section:
This article was submitted to Plant Nutrition, a section of the journal Frontiers in Plant Science

Received: 16 March 2020
Accepted: 29 May 2020
Published: 26 June 2020

Citation:
Shi Y, Qiu L, Guo L, Man J, Shang B, Pu R, Ou X, Dai C, Liu P, Yang Y and Cui X (2020) K Fertilizers Reduce the Accumulation of Cd in Panax notoginseng (Burk.) F.H. by Improving the Quality of the Microbial Community. Front. Plant Sci. 11:888. doi: 10.3389/fpls.2020.00888

The high background value of cadmium (Cd) in the *Panax notoginseng* planting soil is the main reason for the Cd content in *P. notoginseng* exceeding the limit standards. The main goal of this study was to reveal the mechanism by which potassium (K) reduces Cd accumulation in *P. notoginseng* from the perspective of the influences of soil microbial communities on soil pH, total organic matter (TOM) and cation exchange capacity (CEC). Pot experiments were conducted to study the effects of different types and amounts of applied K on the Cd content in *P. notoginseng*, and on the soil pH, TOM, CEC, and bioavailable Cd (bio-Cd) content in soil. Field experiments were conducted to study the effects of K_2SO_4 fertilizer on the microbial community, and its correlations with the soil pH, TOM and CEC were analyzed. A moderate application of K_2SO_4 (0.6 g·kg^{-1}) was found to be the most optimal treatment for the reduction of Cd in the pot experiments. The field experiments proved that K fertilizer (K_2SO_4) alleviated the decreases in pH, TOM and CEC, and reduced the content of bio-Cd in the soil. The application of K fertilizer inhibited the growth of Acidobacteria, but the abundances of Mortierellomycota, Proteobacteria and Bacteroidetes were promoted. The relative abundances of Acidobacteria and Proteobacteria in the soil bacteria exhibited significant negative and positive correlations with pH and CEC, respectively. In contrast, the relative abundance of Mortierellomycota was found to be positively correlated with the pH, TOM and CEC. The bio-Cd content was also found to be positively correlated with the relative abundance of Acidobacteriia but negatively correlated with the relative abundances of Proteobacteria and Mortierellomycota. The application of K fertilizer inhibited the abundance of Acidobacteria, which alleviated the acidification of the soil pH and CEC, and promoted increase in the abundances of Mortierellomycota, Proteobacteria and

Bacteroidetes, which ultimately increased the soil TOM and CEC. Soil microorganisms were found to mitigated decreases in the soil pH, TOM, and CEC and reduced the bio-Cd content in the soil, which significantly reduced the accumulation of Cd in *P. notoginseng*.

Keywords: bioavailable, cadmium, *Panax notoginseng*, potassium, soil microorganism

HIGHLIGHTS

- K fertilizers can change the composition and abundance of microbial community in soil.
- Soil microorganisms were found to mitigated decreases in the soil pH, TOM, and CEC.
- The bio-Cd content can be reduced by improving the soil pH, TOM, and CEC.

INTRODUCTION

The genuine producing area of *Panax notoginseng* (Burk.) F. H. is Yunnan Province, China (Yang et al., 2018), which generates approximately 98% of the *P. notoginseng* medicinal materials on the Chinese market (Liu, 2019). However, Yunnan Province accounts for 46% of China's Cd production (Liu et al., 2016). Its resulted in exceeding the standard rate by 35% and 23% of *P. notoginseng* planting soils and medicinal material, respectively (Ou et al., 2016; Shi et al., 2019). The ability to protect *P. notoginseng* from Cd has drawn considerable attention from consumers and regulatory departments (Lin et al., 2014). Thus, there is a need to develop a low-cost and high-efficiency Cd-blocking technology for *P. notoginseng* as well as to elucidate the underlying mechanisms by which Cd can be blocked.

Lowering the bioavailable Cd (bio-Cd) content in the soil is currently the main method for the reduction of the amount of Cd absorbed by plants (Guiwei et al., 2010). The soil pH, organic matter, cation exchange capacity (CEC) and other soil physical and chemical properties strongly influence on the bioavailability of heavy metals in the soil (Yuan, 2014) and thus affecting the migration of heavy metals from soil to crops (Huang et al., 2012). An increase in pH leads to a corresponding rise in OH^- levels and improves the ability of oxide colloids to adsorb and bind heavy metals. As a result, the soil adsorptive capacity for Cd^{2+} increases, thereby increasing the amount of Cd precipitation in the soil (Ardestani and Van Gestel, 2013; Hong et al., 2014). As the soil CEC increases, the soil's adsorption and retention of heavy metal cations increases, and its specific adsorption of anions weakens, resulting in a decrease in the bioavailability of heavy metals (e.g., Cd, Pb, Hg) in the soil (Chen et al., 2018). An increase in total organic matter (TOM) can increase pH in the soil and the solid organic matter adsorption of heavy metals (Belay et al., 2002). These changes can also decrease the exchangeable heavy metal content (Zeng et al., 2011).

Soil microorganisms can decompose organic matter and alter the TOM content (Neumann et al., 2014). Yang et al. (2011) found that bacterial biomass in orchard soil exhibited a significant positive correlation with soil organic matter. Soil microorganisms also significantly interacted with pH. Sait et al. (2006) found a significant negative correlation between colonial development in Acidobacteria and the soil pH. The number of soil fungi interacted with the soil CEC, pH, and available K content, and was significantly positively correlated with the available K content and CEC (Zhang et al., 2011). Therefore, soil microorganisms are an important index for the evaluation of the evaluating soil pH, TOM, and CEC (Sanusi, 2015).

Potassium is often considered as a quality element (Radulov et al., 2014). Simultaneously, the application of K as a fertilizer can reduce the exchangeable lead content in wheat planting soil, thus reducing the inhibition of the increase of the dry weight (Chen et al., 2007a,b). Zhao et al. (2004) found that K_2SO_4 fertilizer could decrease the carbonates fraction of Cd [F(Carb)] and the exchangeable fraction of Cd [F(EXC)] in wheat planting soil, resulting in the reduction of the Cd content in wheat. Wang et al. (2017) indicated that $KHCO_3$ fertilizer could reduce the Cd content in tobacco and alleviate Cd toxicity during growth. Thus, it is evident that K plays an important role in the reduction of the bio-Cd content in the soil, thereby reducing its accumulation in plants.

Duan et al. (2015) demonstrated that applying an appropriate amount of K fertilizer could also improve the diversity of fungal species in soil by restricting the growth of certain fungi and effectively preventing the over propagation of pathogenic fungi. Jia et al. (2004) proved that K fertilizers promoted the growth of soil microorganisms and contributed to the mineralization of the soil organic matter in buckwheat planting soil. In the present research, it was hypothesized that K fertilization can indirectly improve soil physical and chemical properties indirectly by influencing the soil microorganisms. Consequently, the bio-Cd content was found to be reduced in the soil. This process is a key mechanism for the reduction of the accumulation of Cd in *P. notoginseng* under the application of K fertilization. However, there currently exists no direct evidence to support this hypothesis.

Accordingly, pot experiments and 2-year field experiments were performed to explore the effects of different K fertilizers and application amounts on the soil on pH, CEC, TOM, soil microorganisms, and Cd content in *P. notoginseng*. The amount of K fertilizer applied in the cultivation of *P. notoginseng* was optimized, and soil improvement and utilization were combined to promote the reduction of Cd in *P. notoginseng*.

Abbreviations: Bio-Cd, Bioavailable Cd; CEC, Cation exchange capacity; F(Carb), Bound to carbonates fraction; F(EXC), Exchangeable fraction; F(Fe-MnOX), Bound to iron and manganese oxides fraction; F(OM), Bound to organic matter fraction; F(RES), Residual fraction; OTUs, Operational Taxonomic Units; RDA, Redundancy analysis; TOM, Total organic matter.

MATERIALS AND METHODS

Pot Experiments

Pot experiments were conducted from May 5 to September 5 in 2017, and the experimental site was located in faculty of life science and technology of Kunming university of science and technology (E 102.51, N 24.50, altitude 1982 m). Main environment of the greenhouse was as follows: soil moisture, 33–48%; air humidity, 35–82%; daytime temperature, 12–29°C; night temperature, 8–18°C; sunshine duration, 9–11 h.

Two-year-old *P. notoginseng* was planted in the plastic pot (70 × 40 × 28 cm) with 18 kg soil. The soil was the same as that of the greenhouse of tillage layers (0–20 cm). The soil was dried and crushed, separated from weeds, rocks and other debris, and then sifted and reserved. According to the conclusion of Li et al. (2015), 10 $mg{\cdot}kg^{-1}$ Cd treatment was set up. Under the same K treatment level, the amount of K input by different types of K fertilizer was consistent. Simultaneously, KCl and K_2SO_4 were adopted, respectively. Three K (K_2O) levels were used as follows, low application amount: 0.171 $g{\cdot}kg^{-1}$ (KCl1), 0.2 $g{\cdot}kg^{-1}$ (K_2SO_41); medium application amount: 0.513 $g{\cdot}kg^{-1}$ (KCl2), 0.6 $g{\cdot}kg^{-1}$ (K_2SO_42); high application amount: 1.026 $g{\cdot}kg^{-1}$ (KCl3), 1.2 $g{\cdot}kg^{-1}$ (K_2SO_43), respectively. The treatments were as follows: CK (control), Cd, Cd + KCl1, Cd + K_2SO_41, Cd + KCl2, Cd + K_2SO_42, Cd + KCl3, Cd + K_2SO_43.

Eight treatments were conducted, every treatment was repeated three times (three pots), every pot planted eight seedlings. Nitrogen (carbamide) and phosphate (P_2O_5) fertilizers were used at 0.30 and 0.10 $g{\cdot}kg^{-1}$, respectively. All of fertilizers were applied as basal fertilizer. Cd was soluted in distilled water, while basal fertilizers were mixed up with dry soil, and then added to the pots.

Field Experiments

In Qiubei County, Wenshan City, Yunnan Province, field experiments were performed from January to November of 2018 and 2019, respectively (Malishu, E: 103°61′, N: 23°87′, altitude: 1937 m; Longgaxinzhai, E: 104°1′, N: 24°11′, altitude: 1452 m). The basic soil physical and chemical properties of Malishu was as follows: pH, 5.76; TOM, 5.63 $g{\cdot}kg^{-1}$; CEC, 7.33 c $mol{\cdot}kg^{-1}$; total K 24.28 $g{\cdot}kg^{-1}$; total P, 0.52 $g{\cdot}kg^{-1}$; total N, 1.12 $g{\cdot}kg^{-1}$; alkali-hydrolyzed N 54.00 $mg{\cdot}kg^{-1}$; available P 1.15 $mg{\cdot}kg^{-1}$; and available K 83.00 $mg{\cdot}kg^{-1}$. The basic soil physical and chemical properties of Longgaxinzhai was as follows: pH, 5.88; TOM, 5.58 $g{\cdot}kg^{-1}$; CEC, 7.69 c $mol{\cdot}kg^{-1}$; total K 24.71 $g{\cdot}kg^{-1}$; total P, 0.35 $g{\cdot}kg^{-1}$; total N, 1.04 $g{\cdot}kg^{-1}$; alkali-hydrolyzed N 53.20 $mg{\cdot}kg^{-1}$; available P 1.08 $mg{\cdot}kg^{-1}$; and available K 87.00 $mg{\cdot}kg^{-1}$. The planting soil of *P. notoginseng* was red soil.

According to the optimum application type and amount of K fertilizer in the pot experiments, the optimum application amount of K fertilizer (K_2SO_4, 300 $kg{\cdot}ha^{-1}$ both in 2018 and 2019) in field experiment were performed according to the soil weight conversion of 20 cm deep plow layer. Simultaneously, the amount of K fertilizer (15 $kg{\cdot}ha^{-1}$ both in 2018 and in 2019) was set as the control. The treatments were as follows: K_{15}, K_{300}. All groups were repeated three times. The 15 $kg{\cdot}ha^{-1}$ (K_{15}) and 300 $kg{\cdot}ha^{-1}$ (K_{300}) were used as the application amounts. The 225 $kg{\cdot}ha^{-1}$ was used as the amount of P, N fertilizers. Thirty percent of the N and K fertilizers were applied as base, and 70% were applied as topdressing fertilizers. The topdressing fertilizer were applied at May, June, August and October, respectively, and the application rates were 20, 10, 20, and 20%, respectively. All P fertilizer was used as basal fertilizer. Around the experimental area, a protective row (width, 1 m) was set up to protect the performance of the experiments. The plot area was 2.30 m × 1.90 m, the transplant density was 15 cm × 15 cm, and seedlings were transplanted in January 2018 and 2019, respectively. In November 2018 and 2019, *P. notoginseng* and soil samples were collected. Field management was performed according to farmers' customary management.

Determination of Cd Content

Determination of Cd Content in *P. notoginseng*

According to Shi et al. (2019), microwave digestion with HNO_3-H_2O_2 was used to digest the Cd content in *P. notoginseng*. Dried sample (0.20 g) was accurately weighed (accurate to 0.0001 g) and placed it in the Teflon dissolving cup. Then, 10 ml 65% HNO_3 was added, and left overnight for pre-reaction and when 2 ml 30% H_2O_2 was added. Until the reaction was stable, the sample cup was covered, placed it in a high-pressure tank, and then putting into a microwave sample dissolving device. The step temperature increased to 180°C for 25 min (the power of the single tank was 600 w). While the sample was dissolved, the temperature was reduced to room temperature. The sample was transferred to a 10 ml volumetric flask, water was used to scale, and the sample was shaken well. And a blank control was made at the same time. The Cd content was determined by inductively coupled plasma atomic emission spectrometry (ICP-AES).

Speciation of Cd in the Soil and Determination of Cd Content

The soil Cd classification adopted the improved Tessier A five-step extraction method (Tessier et al., 1979). Soil was divided into the following five components:

F(EXC): The sediment was continuously extracted for 1 h with 8 ml 1 M $MgCl_2$ solution (pH = 7.00); then, centrifuged at 4000 r min^{-1} for 10 min and filled to constant volume to be measured.

F(Carb): The residue from previous was continuously extracted for 5 h with 8 ml 1 M NaAc solution (pH = 5.00), then 4000 r min^{-1} for 10 min centrifuged and made it constant volume to be measured.

F(Fe-MnOX): The residue from previous was continuously extracted for 6 h with 25% HAC solution of 20 ml 0.04 M $NH_2OH{\cdot}HCl$ at 96 ± 3°C; then, centrifuged at 4000 r min^{-1} for 10 min and filled to constant volume to be measured.

F(OM): The residue from previous was continuously extracted for 2 h with 3 ml 0.02 M HNO_3 and 5 ml 30% H_2O_2 solution (pH = 2.00) at 85 ± 3°C, continuously extracted for 3 h with 3 ml 30% H_2O_2, and cooled to room temperature; then, continuously extracted for 30 min with 5 ml 20% HNO_3 of 3.20 M NH_4AC; then, centrifuged at 4000 r min^{-1} for 10 min and filled to constant volume to be measured.

F(RES): The residue from previous was digested with HF-$HClO_4$.

Cd was analyzed using inductively coupled plasma mass spectroscopy (ICP-MS, X Series 2, Thermo Fisher Scientific, United States).

Determination of Soil pH, TOM, and CEC

Soil pH determination method refers to ISO 10390:2005 standard, which determined with a pH meter (FE20, Mettler, China) after mixing soil and water at a 1–2.5 ratio.

TOM determination method refers to ISO 23470–2011 standard, 0.10–0.50 g (0.001 g) soil sample was weighed, then mixed with 0.10 g $AgSO_4$, 5 ml 0.80 M $K_2Cr_2O_7$ solution and 5 ml H_2SO_4, then heated to 180°C for 5 min, and titrated with 0.20 M $(NH_4)_2$ Fe $(SO_4)_2$ standard solution.

CEC determination method refers to ISO 14235–2009 standard, 2.00 g soil sample was weighed, mixed with 60 ml 1 M ammonium acetate solution, centrifuged at 3000 r min^{-1} for 5 min, centrifugation was repeated until supernatant had no calcium ions. Then, 60 ml 95% ethanol was added and centrifuged, the above steps were repeated until the supernatant had no ammonium ions. The solution was distilled by Kjeldahl apparatus and titrated with HCl standard solution.

Determination of Microbial Diversity and Population Composition

The experimental samples were taken from the above *P. notoginseng* planting soil in field experiments. Total bacterial and fungal DNA were extracted from samples using the Power Soil DNA Isolation Kit (MO BIO Laboratories) according to the manufacturer's protocol. DNA quality and quantity were assessed by the ratios of 260 nm/280 nm and 260 nm/230 nm. Then DNA was stored at −80°C until further processing. The V3-V4 region of the bacterial 16S rRNA gene was amplified with the common primer pair (Forward primer, 5′-ACTCCTACGGGAGGCAGCA-3′; reverse primer, 5′-GGACTACHVGGGTWTCTAAT-3′) combined with adapter sequences and barcode sequences. The fungal ITS rRNA gene was amplified with the common primer pair (Forward primer, 5′-CTTGGTCATTTAGAGGAAGTAA-3′; reverse primer, 5′-GCTGCGTTCTTCATCGATGC-3′) combined with adapter sequences and barcode sequences. PCR amplification was performed in a total volume of 50 μl, which contained 10 μl Buffer, 0.2 μl Q5 High-Fidelity DNA Polymerase, 10 μl High GC Enhancer, 1 μl dNTP, 10 μM of each primer and 60 ng genome DNA. Thermal cycling conditions were as follows: an initial denaturation at 95°C for 5 min, followed by 15 cycles at 95°C for 1 min, 50°C for 1 min and 72°C for 1 min, with a final extension at 72°C for 7 min. The PCR products from the first step PCR were purified through VAHTSTM DNA Clean Beads. A second round PCR was then performed in a 40 μl reaction which contained 20 μl 2 × Phusion HF MM, 8 μl ddH_2O, 10 μM of each primer and 10 μl PCR products from the first step. Thermal cycling conditions were as follows: an initial denaturation at 98°C for 30 s, followed by 10 cycles at 98°C for 10 s, 65°C for 30 s and 72°C for 30 s, with a final extension at 72°C for 5 min. Finally, all PCR products were quantified by Quant-iT^{TM} dsDNA HS Reagent and pooled together. High-throughput sequencing analysis of bacterial and fungal rRNA genes were performed on the purified, pooled sample using the Illumina Hiseq 2500 platform (2 × 250 paired ends) at Biomarker Technologies Corporation, Beijing, China.

Statistical Analysis

Data were processed with Microsoft Excel software 2018, Graphpad Prism 7.0 SPSS 24.0 were applied to fit the curves and analyze statistics, respectively. Duncan's multiple range tests of one-way ANOVA were used to analyze data for separating means. When $P < 0.05$, differences were considered significant. The Spearman correlation analysis was used to assess the association of the relative abundance of microbial community with pH, TOM, CEC, and bio-Cd.

RESULTS

Effect of K Fertilizer on Cd Content in *P. notoginseng* in the Pot Experiments

The results of the pot experiment demonstrated that the Cd accumulation in *P. notoginseng* roots decreased under different types of K fertilizer treatments (**Figure 1**). Relative to that of Cd the treatment, the Cd content in the main root under the KCl2 and $K_2SO_4$2 treatments decreased by 28 and 44%, respectively; the Cd content in the rhizome decreased by 40 and 47%, respectively; and the Cd content in the rootlets decreased by 41 and 51%, respectively. The K_2SO_4 treatment resulted in the largest reduction in Cd accumulation and was thus adopted in the subsequent experimental treatments.

Relative to that under the Cd treatment, the Cd content in the main root under the $K_2SO_4$1, $K_2SO_4$2, and $K_2SO_4$3 treatments decreased by 46, 44, and 44%, respectively; that in the rhizome decreased by 47, 47, and 50%, respectively; that in the rootlets decreased by 47, 51, and 52%, respectively (**Figure 1**). The reduction in the accumulation of Cd in *P. notoginseng* under the moderate K fertilization treatment was similar to that under the high K fertilization treatment. Therefore, 0.6 g·kg^{-1} K_2SO_4 was converted into an application of 300 kg·ha^{-1} for the subsequent field verification experiment.

Effect of K Fertilizer on the pH, TOM, and CEC of *P. notoginseng* Planting Soil in the Pot Experiments

In the pot experiments, low K fertilizer treatments significantly improved the soil pH and TOM, but different types of K fertilizer treatments did not significantly affect the soil pH (**Figures 2A,D,G**). A moderate amount of K fertilizer was found to significantly promote the increase of the soil pH, TOM, and CEC. The pH levels of the soil under the KCl2 and $K_2SO_4$2 treatments increased by 5 and 6%, respectively; the TOM increased by 18 and 27%, respectively; and the CEC increased by 5 and 7%, respectively (**Figures 2C,E,H**).

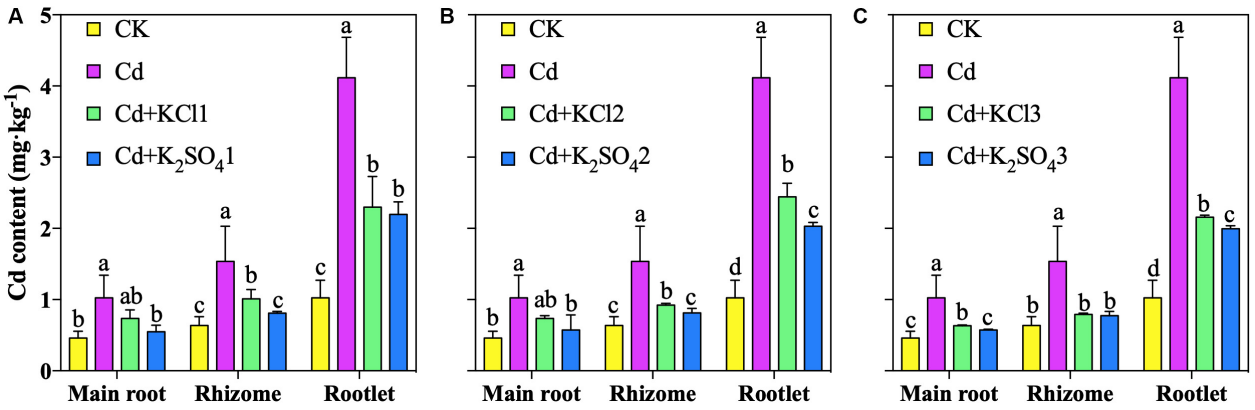

FIGURE 1 | Effect of different types of K on Cd content in *P. notoginseng* (**A** denoted low application amount, KCl1: 0.171, $K_2SO_4$1: 0.2 g·kg^{-1}; **B** denoted medium application amount, KCl2: 0.513, $K_2SO_4$2: 0.6 g·kg^{-1}; **C** denoted high application amount, KCl3: 1.026, $K_2SO_4$3: 1.2 g·kg^{-1}). Different lowercase letters indicate the means are significantly different at $P < 0.05$.

Effect of K Fertilizer on the Bio-Cd Content in *P. notoginseng* Planting Soil in the Pot Experiments

Compared with the Cd treatment, all K fertilizer treatments reduced the soil bio-Cd content in the soil (**Figure 3**). When a moderate amount of K fertilizer was applied, the bio-Cd contents under the KCl2 and $K_2SO_4$2 treatments decreased by 16 and 23%, respectively.

Effect of K_2SO_4 on Cd Accumulation in *P. notoginseng* in the Field Experiments

Relative to that under the K_{15} treatment, the Cd content in the main root under the K_{300} treatment decreased by 47%, that in the rhizome decreased by 41%, and that in the rootlets decreased by 23% in 2018; additionally, the Cd content in the main root decreased by 52% in 2019 (**Figure 4**). Regarding the K_{300} treatments in 2018 and 2019, the Cd content in the main root and rhizome were 0.20 (2018), 0.15 (2019) and 0.25 (2018), 0.25 (2019) mg·kg^{-1}, respectively, both of which were within the WM-T2-2004 standard (WM-T2-2004, 2004) (0.3 g·kg^{-1}).

Effect of K_2SO_4 on the pH, TOM, and CEC of *P. notoginseng* Planting Soil in the Field Experiments

Relative to those under the K_{15} treatment, the pH, TOM, and CEC of the soil under K_{300} treatment were increased by 14, 8, and 21%, respectively, in 2018; in 2019, the values of these increments were 13, 8, and 26%, respectively (**Figure 5**).

Effect of K_2SO_4 on Microbial Community Composition in *P. notoginseng* Planting Soil in the Field Experiments

The sequences were submitted to the SRA (Sequence Read Archive) at the National Center for Biotechnology Information (NCBI) under the accession number PRJNA626539 for 16S sequences (B1–B12) and ITS sequences (F1–F12). At the phylum level, 25 bacterial phyla and 10 fungal phyla were detected in eight samples under the two treatments. The bacterial communities in all treated samples primarily consisted of Proteobacteria, Acidobacteria, Gemmatimonadetes, Actinobacteria, Bacteroidetes, and other dominant phylum-level species with relative abundances of more than 5%. The fungal communities were primarily composed of Ascomycota, Mortierellomycota, and other dominant phylum-level species. The relative abundances of Proteobacteria and Verrucomicrobia increased under the K_2SO_4 treatment. The relative abundances of Proteobacteria significantly increased by 12% (2018) and 7% (2019), those of Acidobacteria significantly decreased by 13% (2018) and 6% (2019); and those of Chloroflexi significantly decreased by 17% (2018) and 21% (2019) (**Figures 6A**, **7A**). The relative abundances of Mortierellomycota significantly increased by 208% (2018) and 513% (2019), whereas those of Ascomycota significantly decreased by 22% (2018) and 21% (2019) (**Figures 6D**, **7D**).

Moreover, 65 bacterial classes and 23 fungal classes were detected in this study. The relative abundances of Acidobacteria decreased by 45% (2018) and 30% (2019) with the application of K_2SO_4 (**Figures 6B**, **7B**). The relative abundances of Mortierellomycetes increased by 208% (2018) and 515% (2019), whereas those of Sordariomycetes significantly decreased by 22% (2018) and 23% (2019) (**Figures 6E**, **7E**). A total of 348 bacterial genera (**Figures 6C**, **7C**) and 118 fungal genera (**Figures 6F**, **7F**)were detected in this study.

Correlation Analysis of Microbial Community Composition, pH, TOM, and CEC of *P. notoginseng* Planting Soil Under Different K_2SO_4 Treatments in the Field Experiments

At the phylum level, the relative abundances of Proteobacteria and Planctomycetes in the soil bacteria showed significant positive correlations with the pH and CEC, whereas the relative

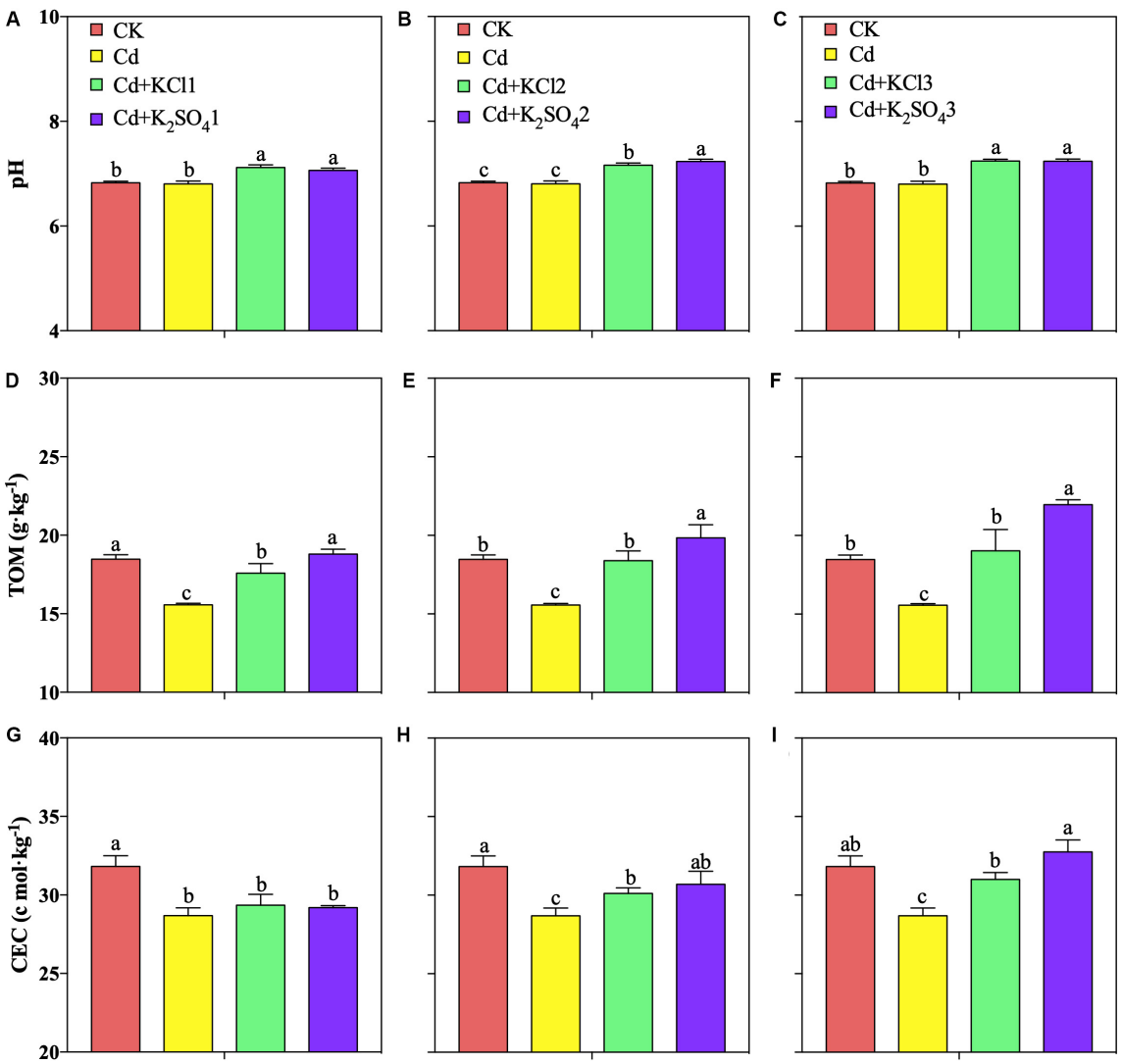

FIGURE 2 | Effect of different types and application amounts of K on pH, TOM, and CEC. **(A,D,G)** Denoted low application amount, KCl1:0.171, $K_2SO_4$1:0.2 g·kg^{-1}; **(B,E,H)** denoted medium application amount, KCl2:0.513, $K_2SO_4$2:0.6 g·kg^{-1}; **(C,F,I)** denoted high application amount, KCl3:1.026, $K_2SO_4$3:1.2 g·kg^{-1}. Different lowercase letters indicate the means are significantly different at $P < 0.05$.

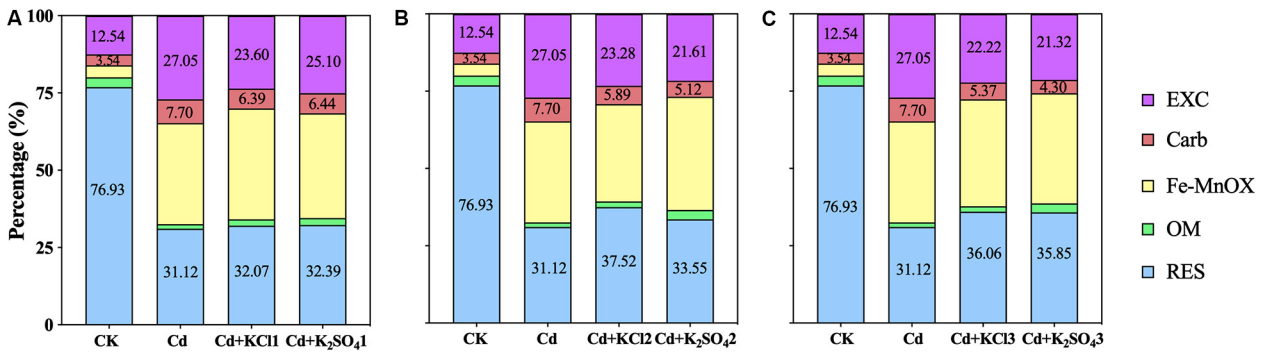

FIGURE 3 | Effect of different types and application amounts of K on Bio-Cd content in *P. notoginseng* planting soil **(A)** denoted low application amount, KCl1: 0.171, $K_2SO_4$1: 0.2 g·kg^{-1}; **(B)** denoted medium application amount, KCl2: 0.513, $K_2SO_4$2: 0.6 g·kg^{-1}; **(C)** denoted high application amount, KCl3: 1.026, $K_2SO_4$3: 1.2 g·kg^{-1}. Bio-Cd content is the sum of F(EXC) and F(Carb) Cd.

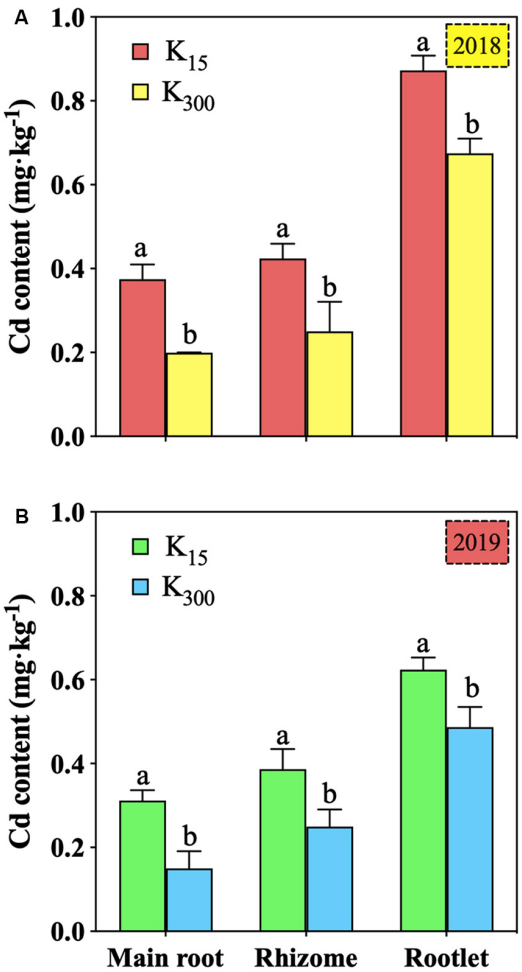

FIGURE 4 | Effect of different amounts of K_2SO_4 on the Cd content in *P. notoginseng* roots (K_{15}, 15 kg·ha^{-1}; K_{300}, 300 kg·ha^{-1}; **(A)** denoted experiment was conducted in 2018, **(B)** denoted experiment was conducted in 2019). Different lowercase letters indicate the means are significantly different at $P < 0.05$.

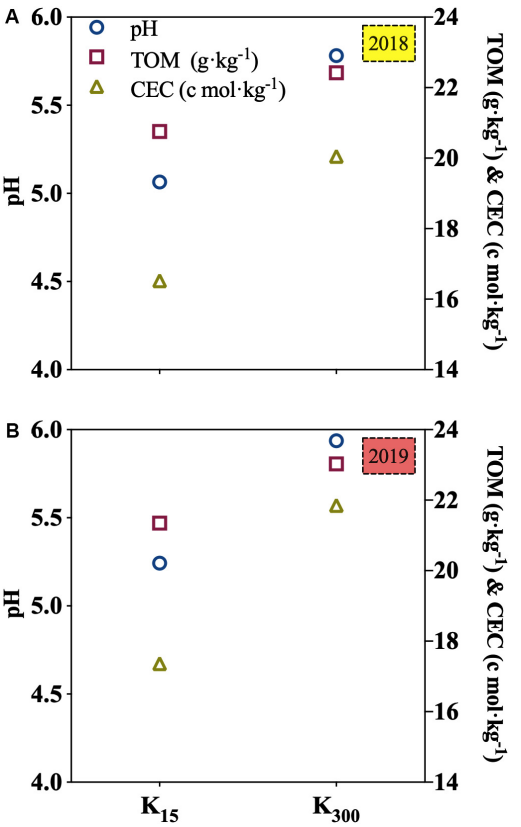

FIGURE 5 | Effect of different amounts of K_2SO_4 on pH, TOM and CEC in soil (K_{15}, 15 kg·ha^{-1}; K_{300}, 300 kg·ha^{-1}; **(A)** denoted experiment was conducted in 2018, **(B)** denoted experiment was conducted in 2019. Different lowercase letters indicate the means are significantly different at $P < 0.05$.

abundances of Chloroflexi exhibited a negative correlation with pH and CEC in both 2018 and 2019 (**Table 1**). The relative abundance of Mortierellomycota was found to exhibit significant positive correlations with the pH and CEC in the soil, whereas the relative abundance of Ascomycota exhibited a negative correlations with the pH, TOM, and CEC in the soil in 2018 and 2019.

At the class level, the relative abundance of Acidobacteriia in the soil bacteria was negatively correlated with the pH and CEC in 2018 and 2019. Moreover, the relative abundances of Verrucomicrobiae (2018) and Alphaproteobacteria (2018, 2019) respectively exhibited significant positive correlations with the pH and CEC, respectively. The relative abundance of Mortierellomycetes was positively correlated with the TOM, whereas the relative abundances of Sordariomycetes (2018, 2019) were negatively correlated with the pH and CEC of the soil (**Table 2**).

Redundancy analysis of dominant genus-level species of bacteria and the pH, TOM and CEC in *P. notoginseng* planting soil was conducted (**Figure 8**). The first ordination axis in **Figures 8A,C** explained 34% (2018) and 59% (2019) of the dominant genus-level species of soil bacteria, whereas the second ordination axis explained 19% (2018) and 22% (2019) of the same. This indicates that the amount of K_2SO_4 fertilizer was positively correlated with the pH, TOM, and CEC. The correlation *P*-values of the correlations between Holophaga (2018, 2019), Candidatus_Solibacter (2018), Bradyrhizobium (2018), Pseudolabrys (2019), and TOM were all less than 0.05 (**Figure 8**), indicating that the relative abundances of the aforementioned communities significantly affected the TOM content of the soil.

The first ordination axis in **Figures 8B,D** explained 22% (2018) and 57% (2019) of the variation in the dominant genus-level species of soil fungi, and the second ordination axis explained 16% (2018) and 25% (2019). The correlation *P*-values of the correlations between Mortierella (2018, 2019), Humicola (2018), Lecanicillium (2018), and Plectosphaerella (2019), and the pH and CEC were all less than 0.05 (**Figure 8**), indicating that the relative abundances of these communities significantly affected the pH and CEC of the soil.

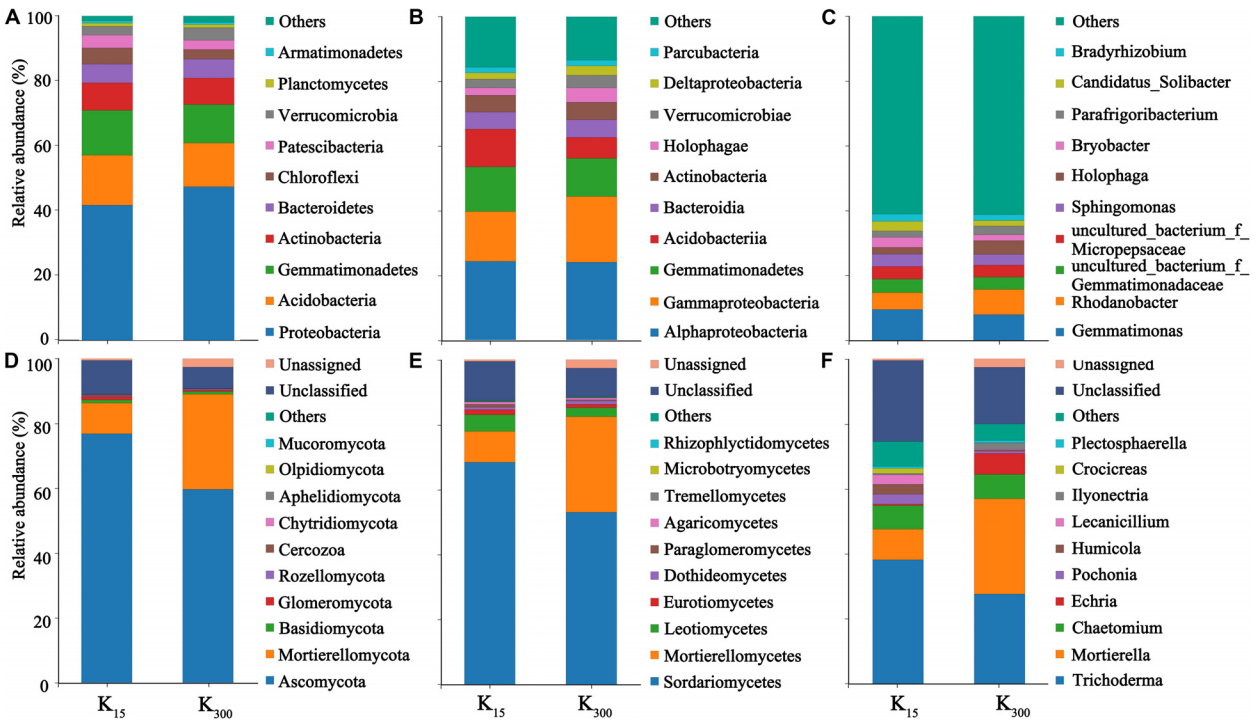

FIGURE 6 | Effect of different amounts of K_2SO_4 on the community composition and relative abundance of Bacteria (**A**, Phylum; **B**, Class; **C**, Genus), Fungi (**D**, Phylum; **E**, Class; **F**, Genus) in *P. notoginseng* planting soil in 2018 (K_{15}, 15 kg·ha^{-1}; K_{300}, 300 kg·ha^{-1}).

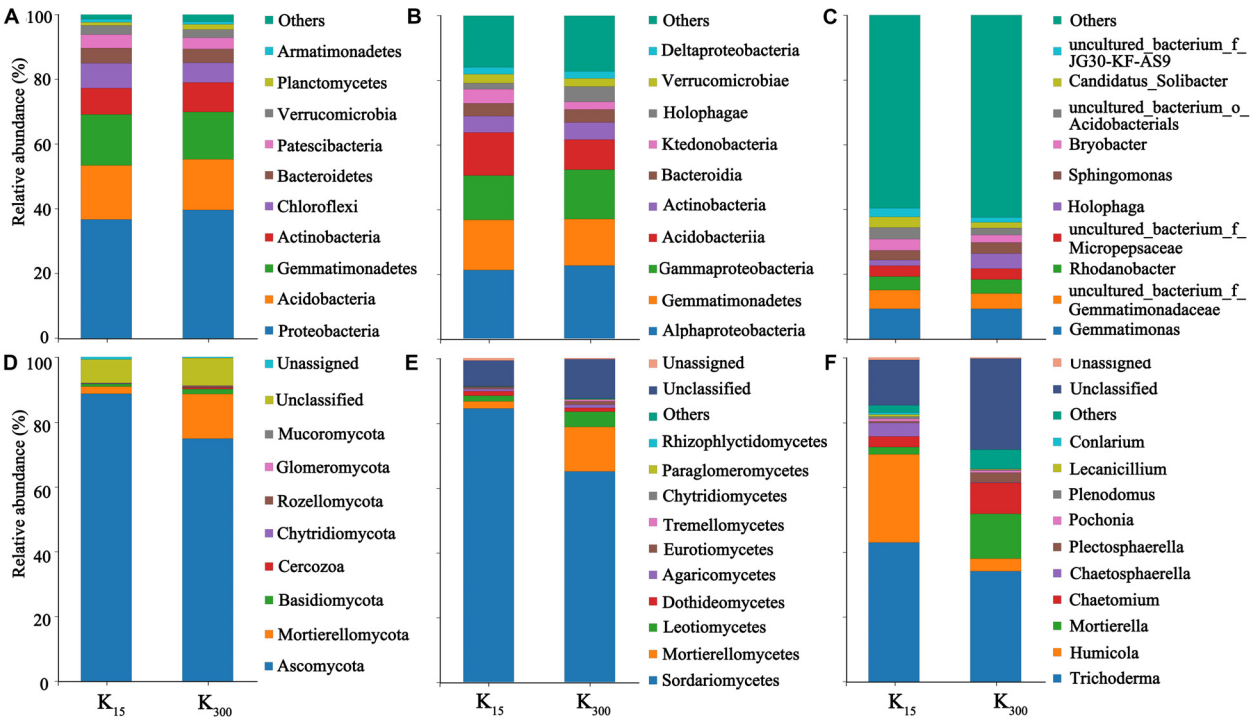

FIGURE 7 | Effect of different amounts of K_2SO_4 on the community composition and relative abundance of Bacteria (**A**, Phylum; **B**, Class; **C**, Genus), Fungi (**D**, Phylum; **E**, Class; **F**, Genus) in *P. notoginseng* planting soil in 2018 (K_{15}, 15 kg·ha^{-1}; K_{300}, 300 kg·ha^{-1}).

TABLE 1 | Correlation analysis of soil microbial communities at the phylum level and soil physical and chemical properties in *P. notoginseng* planting soil under different K_2SO_4 treatments.

	Bacterial				Fungal		
Community phylum	**pH**	**TOM**	**CEC**	**Community phylum**	**pH**	**TOM**	**CEC**
2018							
Proteobacteria	0.786*	0.857**	0.762*	Ascomycota	−0.833**	−0.667*	−0.857**
Acidobacteria	−0.095	0.214	−0.71	Mortierellomycota	0.714*	0.810	0.738*
Chloroflexi	−0.762*	−0.357	−0.738*	Chytridiomycota	−0.595	−0.810*	−0.643
Patescibacteria	−0.595	−0.810*	−0.571	–	–	–	–
Verrucomicrobia	0.786*	0.310	0.762*	–	–	–	–
2019							
Proteobacteria	0.935**	0.907**	0.882**	Ascomycota	−0.923**	−0.895**	−0.870**
Acidobacteria	−0.525	−0.509	−0.495	Mortierellomycota	0.970**	0.941**	0.914**
Chloroflexi	−0.987**	−0.948**	−0.922**	Basidiomycota	0.893**	0.866**	0.842**
Actinobacteria	0.934**	0.906**	0.881**	Rozellomycota	0.994**	0.964**	0.937**
Armatimonadetes	−0.763*	−0.741*	−0.720*	Glomeromycota	0.974**	0.945**	0.918**
Planctomycetes	0.823*	0.798*	0.776*	–	–	–	–

**Shows the correlation reached $P < 0.05$, **shows the correlation reached $P < 0.01$. TOM, total organic matter; CEC, cation exchange capacity.*

TABLE 2 | Correlation analysis of soil microbial communities at the class level and soil physical and chemical properties in *P. notoginseng* planting soil under different K_2SO_4 treatments.

	Bacterial				Fungal		
Community class	**pH**	**TOM**	**CEC**	**Community class**	**pH**	**TOM**	**CEC**
2018							
Alphaproteobacteria	0.500	0.095	0.548	Sordariomycetes	−0.833**	−0.667	−0.857**
Acidobacteriia	−0.905**	−0.643	−0.881**	Mortierellomycetes	0.714*	0.810*	0.738*
Verrucomicrobiae	0.786*	0.310	0.762*	Leotiomycetes	−0.810*	−0.738*	−0.762*
Deltaproteobacteria	0.881**	0.571	0.857**	–	–	–	–
2019							
Alphaproteobacteria	0.868**	0.842**	0.818*	Sordariomycetes	−0.930**	−0.902**	−0.877**
Acidobacteriia	−0.955**	−0.926**	−0.900*	Mortierellomycetes	0.970**	0.941**	0.914**
Actinobacteria	0.835**	0.810*	0.787*	Eurotiomycetes	0.940**	0.912**	0.886**
Gemmatimonadetes	−0.924*	−0.897*	−0.871*	–	–	–	–
Gammaproteobacteria	0.927*	0.899*	0.784*	–	–	–	–

**Shows the correlation reached $P < 0.05$, **shows the correlation reached $P < 0.01$. TOM, total organic matter; CEC, cation exchange capacity.*

Effect of K_2SO_4 on Bio-Cd Content in *P. notoginseng* Planting Soil in the Field Experiments

K_2SO_4 treatment can significantly decrease the bio-Cd content in *P. notoginseng* planting soil (**Figure 9**). Relative to that under the K_{15} treatment, the bio-Cd content under the K_{300} treatment decreased by 23% in 2018 and 37% in 2019. The bio-Cd content was found to be negatively correlated with pH, TOM and CEC in *P. notoginseng* planting soil in 2018 and 2019 (**Table 3**).

At the phylum level, the bio-Cd content in *P. notoginseng* planting soil was found to be positively correlated with the relative abundance of Acidobacteria (2018, 0.980*; 2019, 0.520); by contrast, the bio-Cd content was found to be negatively correlated with the relative abundances of Proteobacteria (2018, −0.781*; 2019, −0.925*) and Chloroflexi (2018, −0.781*; 2019, −0.967*) in the soil bacteria (**Table 4**). The bio-Cd content was also found to be negatively correlated with Mortierellomycota in the fungi (2018, −0.732*; 2019, −0.960*), but positively correlated with Ascomycota in 2018 (0.781*) and 2019 (0.913*).

At the class level, the bio-Cd content was found to be positively correlated with Acidobacteriia (2018, 0.927**; 2019, 0.945**), but negatively correlated with Verrucomicrobiae (2018, −0.781*) and Gammaproteobacteria (2019, −0.917**) in the soil bacteria. Moreover, the bio-Cd content was found to positively correlated with the relative abundance of Sordariomycetes (2018, 0.781*; 2019, 0.920**) and Leotiomycetes (2018, 0.781*), but negatively correlated with Mortierellomycetes (2018, −0.732*; 2019, −0.960**) in the soil fungi.

DISCUSSION

The bio-Cd content represents the portion of Cd in the soil that can be absorbed and utilized by plant. The pH, TOM, and CEC have been identified as the main factors that affect the

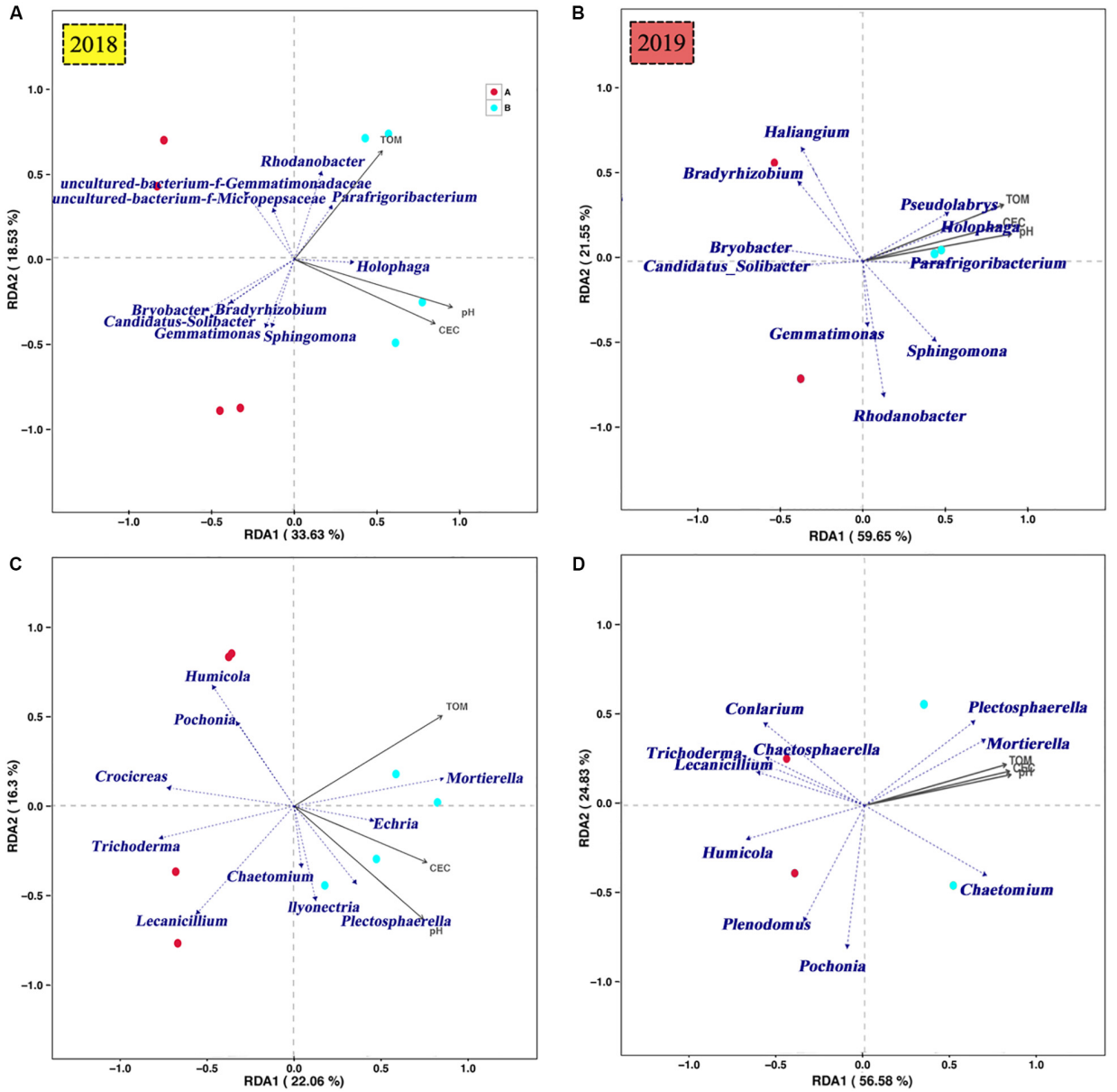

FIGURE 8 | RDA analysis of soil microbial community [**A**, bacteria (2018); **B**, fungi (2018); **C**, bacteria (2019); **D**, fungi (2019)] at the genus level and soil pH, TOM, and CEC in *P. notoginseng* planting soil under different K_2SO_4 treatments.

bioavailability of heavy metals in soil (Li and Song, 2003; Liang et al., 2013), and can be significantly regulated by fertilization. Agbede et al. (2010) found that the application of NPK mixture fertilizers can improve the pH and organic carbon content of yam (*Dioscorea rotundata Poir*) planting soil. K fertilizer can regulate the functional groups of acidic substances in tobacco planting soil and chelate heavy metal ions by adsorption and can thereby lowering the Cd activity and bio-Cd content in soil (Wu et al., 2012).

In the present study, pot experiments demonstrated that increases in the amount of applied K fertilizer significantly improved the pH, TOM, and CEC in *P. notoginseng* planting soil (**Figure 2**), resulting in a significant decrease in the bio-Cd content in the soil (**Figure 3**). The field experiments also verified the aforementioned results (**Figures 5**, **9**). The results indicated that pH, TOM, and CEC reduction were ameliorated under the K fertilizer treatment, reducing the bio-Cd content in the planting soil and ultimately reducing the migration of Cd from the soil to *P. notoginseng*.

Fertilization can also affect the compositions, abundances and activities of soil microbial species. Jiang (2017) found that N fertilizer could change bacterial soil into fungal soil and decrease the biomass and abundance of soil microbial communities. Zhang and Xu (2014) demonstrated that K

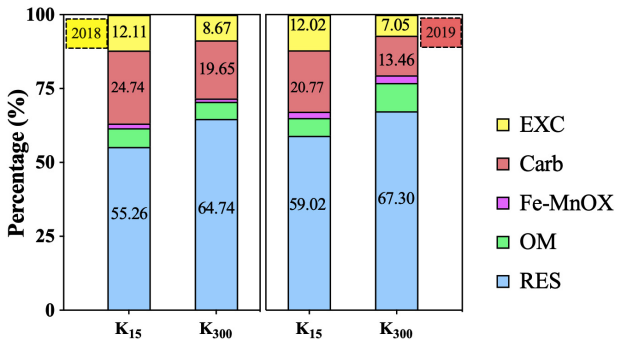

FIGURE 9 | Effect of different amounts of K_2SO_4 on Bio-Cd content in *P. notoginseng* planting soil [K_{15}, 15 kg·ha^{-1}; K_{300}, 300 kg·ha^{-1}. Bio-Cd content is the sum of F(EXC) and F(Carb) Cd].

TABLE 3 | Correlation analysis of bioavailable Cd content and soil physical and chemical properties in *P. notoginseng* planting soil under different K_2SO_4 treatments.

	2018 Bio-Cd content	2019 Bio-Cd content
pH	−0.976**	−0.986**
TOM	−0.683*	−0.984**
CEC	−0.976**	−0.906**

**Shows the correlation reached $P < 0.05$, **shows the correlation reached $P < 0.01$. TOM, total organic matter; CEC, cation exchange capacity; bio-Cd, bioavailable Cd.*

TABLE 4 | Correlation analysis of bioavailable Cd content and soil microbial community in *P. notoginseng* planting soil under different K_2SO_4 treatments.

2018	Bacterial	2018	Fungal
Community phylum	**Bioavailable Cd content**	**Community phylum**	**Bioavailable Cd content**
Proteobacteria	−0.781*	Ascomycota	0.781*
Acidobacteria	0.980*	Mortierellomycota	−0.732*
Chloroflexi	−0.781*	–	
Verrucomicrobia	0.781*	–	
Community class	**Bioavailable Cd content**	**Community class**	**Bioavailable Cd content**
Acidobacteriia	0.927**	Sordariomycetes	0.781*
Verrucomicrobiae	−0.781*	Mortierellomycetes	−0.732*
Deltaproteobacteria	−0.878**	Leotiomycetes	0.781*
2019	**Bacterial**	**2019**	**Fungal**
Community phylum	**Bioavailable Cd content**	**Community phylum**	**Bioavailable Cd content**
Proteobacteria	−0.925**	Ascomycota	0.913**
Acidobacteria	0.520	Mortierellomycota	−0.960**
Chloroflexi	−0.967**	Basidiomycota	−0.883*
Gemmatimonadete	0.921**	Rozellomycota	−0.983**
Actinobacteri	−0.924**	Glomeromycota	−0.963*
Community class	**Bioavailable Cd content**	**Community class**	**Bioavailable Cd content**
Acidobacteriia	0.945**	Sordariomycetes	0.920**
Holophagae	−0.976**	Mortierellomycetes	−0.960**
Alphaproteobacteria	−0.858**	Eurotiomycetes	−0.930**
Gemmatimonadete	0.914**	–	–
Gammaproteobacteria	−0.917**	–	–

**Shows the correlation reached $P < 0.05$, **shows the correlation reached $P < 0.01$.*

fertilizer (carbon enzyme K) could reduce the abundance and diversity of microbial communities in tomato planting soil. The application of K fertilizer can promote increases in soil nutrients and thereby lead to rapid increases in the abundances of microbial species that require large amounts of nutrients (richness groups) (Smith and Paul, 1990). Correspondingly, the application of K fertilizer can also reduce the abundances of microbial species that do not require large amounts of nutrients (Jia et al., 2004).

Essel et al. (2019) found a significant negative correlation between the abundances of bacteria, such as Holophagae, and pH in a 2-year spring wheat–pea rotation soil annually. In this study, the relative abundance of the class Acidobacteriia from the phylum Acidobacteria in *P. notoginseng* planting soil bacteria was found to be negatively correlated with the soil pH and CEC (**Table 2**). This pattern most likely resulted from the fact that most bacteria in Acidobacteria are acidophilic. However, increases in the application of K fertilizer inhibited the proliferation of the acidophilic population and thereby delayed decreases in the soil pH. Zhang et al. (2019) also indicated that the pH and TOM were significantly correlated with bacterial community abundance and that the pH was significantly correlated with fungal community composition, such as the abundance of Mortierellomycota.

The relative abundance of Mortierellomycota in *P. notoginseng* planting soil fungi was found to be positively correlated with the pH, TOM, and CEC (**Table 1**). This pattern can likely be attributed to the participation of Mortierellomycota in the mineralization of soil organic matter for the decomposition of crop residues into the soil and organic matter in organic fertilizers. Thus, the TOM content raised as the abundance of Mortierellomycota increased. Proteobacteria and Bacteroidetes belong to the richness groups, which can promote the mineralization of organic matter. Liu (2019) found that there are positive correlations of Proteobacteria and Bacteroidetes with the soil carbon availability. The present study found that the abundances of Proteobacteria and Bacteroidetes both increased as the amount of applied K fertilizer increased, which promoted the accumulation of the TOM (**Table 1**). This pattern shows that the abundances of Proteobacteria and Bacteroidetes of Fungi in the soil were promoted by K treatment, which facilitated the increases in the TOM.

Yao et al. (2019) determined that the bio-Cd content was significantly correlated with the diversity and abundance of microbial communities. In the present study, it was observed that the bio-Cd content was positively correlated with the

relative abundance of the class Acidobacteriia from the phylum Acidobacteria, but negatively correlated with the Proteobacteria and Mortierellomycota in the soil (**Table 4**). Therefore, as the amount of K fertilizer applied increased, the relative abundances of the dominant soil microbes in the community changed, thereby mitigating reductions in the pH, TOM, and CEC in the soil. As a result, the bio-Cd content in the soil and Cd content in *P. notoginseng* were reduced (**Figures 1**, **4**). According to traditional theories, K can change the bio-Cd content by altering the soil physical and chemical properties. However, the present study suggests another possibility: namely, that the effects of K on the bio-Cd content may be mediated by its effect on soil microorganisms, which, in turn, alter pH, TOM, and CEC.

The reduction of the Cd content by K may be achieved by (i) decreasing the bio-Cd content in soil via absorption via crops and by (ii) reducing the capability of crops to uptake Cd. Non-selective cation channels play a substantial role in root Cd uptake. This process is driven by the electrochemical gradient for Cd^{2+} on both sides of the plasma membrane. The membrane potential (between −70 and −90 mv) is often very close to the Nernst potential for K (available K, −70 mv); consequently, apoplast (soil) K^+ availability is increased, leading to membrane depolarization. Thus, reduced Cd accumulation in plants may also be caused by the weaker electrical gradient across the plasma membrane. However, these hypotheses require further verification.

CONCLUSION

A moderate K_2SO_4 treatment (pot experiment, 0.6 $g{\cdot}kg^{-1}$; field experiment, 300 $kg{\cdot}ha^{-1}$) provides the most optimal reduction of Cd accumulation in *P. notoginseng*. As the amount of applied K fertilizer increased, the relative abundances of Proteobacteria and Bacteroidetes increased, which promoted the accumulation of TOM; in addition, decreases in Acidobacteria alleviated the acidification of the soil. Such changes in these aforementioned soil microorganisms improved the pH, TOM, and CEC, which reduced the bio-Cd content in the soil and, in turn, the accumulation of Cd in the *P. notoginseng* roots was significantly reduced.

DATA AVAILABILITY STATEMENT

The datasets generated for this study can be found in the sequences were submitted to the SRA (Sequence Read Archive) at the National Center for Biotechnology Information (NCBI) under the accession number PRJNA626539 for 16S sequences (B1–B12) and ITS sequences (F1–F12).

AUTHOR CONTRIBUTIONS

YS was in charge of field experiment and pot experiment, and wrote the manuscript. LQ was in charge of determination of Cd content. LG was in charge of providing experimental ideas and revision the manuscript. JM was in charge of planting of Panax notoginseng. BS was in charge of harvesting of Panax notoginseng. RP was in charge of determination of soil physical and chemical properties. XO was in charge of determination of microbial diversity and population composition. CD was in charge of speciation of Cd in the soil and determination of Cd content. PL was in charge of statistical analysis. YY designed the whole experiment. XC was in charge of revision the manuscript. All authors contributed to the article and approved the submitted version.

FUNDING

This work was supported by the Key Project at Central Government Level: the ability establishment of sustainable use for valuable Chinese Medicine Resources (2060302), the Natural Science Foundation of China (Nos. 81960690, 81891014, and 81460580), the National Key Research and Development Plan (No: 2017YFC1700701), and the Ministry of Science and Technology of Yunnan Province, China (Nos. 2017ZF014 and 2016ZF001).

SUPPLEMENTARY MATERIAL

The Supplementary Material for this article can be found online at: https://www.frontiersin.org/articles/10.3389/fpls.2020.00888/full#supplementary-material

REFERENCES

Agbede, T. M., Oladitan, T. O., Alagha, S. A., Ojomo, A. O., and Ale, M. O. (2010). Comparative evaluation of poultry manure and NPK fertilizer on soil physical and chemical properties, leaf nutrient concentrations, growth and yield of yam (*Dioscorea rotundata* Poir) in Southwestern Nigeria. *World J. Agric. Sci.* 6, 540–546.

Ardestani, M. M., and Van Gestel, C. A. M. (2013). Using a toxicokinetics approach to explain the effect of soil ph on cadmium bioavailability to *Folsomia candida*. *Environ. Pollut. Environ. Pollut.* 180, 122–130. doi: 10.1016/j.envpol.2013.05.024

Belay, A., Claassens, A., and Wehner, F. (2002). Effect of direct nitrogen and potassium and residual phosphorus fertilizers on soil chemical properties, microbial components and maize yield under long-term crop rotation. *Biol. Fertil. Soils* 35, 420–427. doi: 10.1007/s00374-002-0489-x

Chen, J., Liu, B., Li, Z., Wang, P., and Chen, B. (2018). Soil heavy metal occurrence and its influencing factors in typical areas in Jianghan plain. *Res. Environ. Engin.* 32, 551–556.

Chen, S., Sun, L., Sun, T., Chao, L., and Yang, C. (2007a). Influence of potassium fertilizer on the phytoavailability of cadmium. *Environ. Sci.* 28, 182–188.

Chen, S., Sun, L., Sun, T., Yang, C., and Chao, L. (2007b). Effects of potash fertilizer on phytoavailability of lead. *J. Liaoning Tech. Univ.* 26, 285–288.

Duan, Y., Yang, Y., Jin, Y., Huang, J., and Chen, D. (2015). Effects of long-term potassium application on yield and quality of tobacco and soil physical and chemical properties. *Guizhou Agric. Sci.* 43, 100–104.

Essel, E., Xie, J., Deng, C., Peng, Z., Wang, J., Shen, J., et al. (2019). Bacterial and fungal diversity in rhizosphere and bulk soil under different long-term tillage

and cereal/legume rotation. *Soil. Till. Res.* 194:104302. doi: 10.1016/j.still.2019.1043020

Guiwei, Q., Varennes, A. D., Martins, L. L., Mourato, M. P., Cardoso, A. I., Mota, A. M., et al. (2010). Improvement in soil and sorghum health following the application of polyacrylate polymers to a cd-contaminated soil. *J. Hazard. Mater.* 173, 570–575. doi: 10.1016/j.jhazmat.2009.08.124

Hong, C. O., Owens, V. N., Kim, Y. G., Lee, S. M., Park, H. C., Kim, K. K., et al. (2014). Soil pH effect on phosphate induced cadmium precipitation in Arable soil. *Bull. Environ. Contam. Toxicol.* 93, 101–105. doi: 10.1007/s00128-014-1273-y

Huang, S., Zhang, Z., Zhang, J., and Pan, R. (2012). Effects of physical and chemical characteristics of soils on the adsorption of Cd. *J. Irrig. Drain.* 31, 19–22.

Jia, Z., Sun, M., Yang, Z., and MIao, G. (2004). Influence of different fertilizers to crop rhizosphere microorganisms. *Acta Agron. Sin.* 30, 491–495.

Jiang, J. (2017). *Effects of Excessive Fertilization On Soil Microbial Community Structure*. Shenyang: Shenyang Agricultural University.

Li, J., and Song, H. (2003). Effect of soil physicochemical properties on heavy metal behavior. *Environ. Sci. Trends* 1, 24–26.

Li, Z., Yang, Y., Cui, X., Liao, P., Ge, J., Wang, C., et al. (2015). Physiological response and bioaccumulation of *Panax notoginseng* to cadmium under hydroponic. *Chin J. Chin. Mater. Med.* 40, 2903–2908.

Liang, Z., Ding, Q., Wei, D., Li, J., Chen, S., and Ma, Y. (2013). Major controlling factors and predictions for cadmium transfer from the soil into spinach plants. *Ecotox. Environ. Saf.* 93, 180–185. doi: 10.1016/j.ecoenv.2013.04.003

Lin, L., Yan, X., Liao, X., and Zhang, Y. (2014). Accumulation of soil Cd,Cr,Cu,Pb by *Panax notoginseng* and its associated health risk. *Acta Ecol. Sin.* 11, 2868–2875.

Liu, Q. (2019). *Effects of Organic Mulching On Growth And Soil Nutrient And Microbial Diversity Of Panax Notoginseng (Burk.) F.H.Chen*. Kunming: Yunnan University.

Liu, X., Tian, G., Jiang, D., Zhang, C., and Kong, L. (2016). Cadmium (Cd) distribution and contamination in chinese paddy soils on national scale. *Environ. Sci. Pollut. Res.* 23, 1–12.

Neumann, D., Heuer, A., Hemkemeyer, M., Martens, R., and Tebbe, C. C. (2014). Importance of soil organic matter for the diversity of microorganisms involved in the degradation of organic pollutants. *ISME J.* 8, 1289–1300. doi: 10.1038/ismej.2013.233

Ou, X., Wang, L., Guo, L., Cui, X., Liu, D., and Yang, Y. (2016). Soil-plant metal relations in *Panax notoginseng:* an ecosystem health risk assessment. *Int. J. Environ. Res. Pub. Health* 13:1089. doi: 10.3390/ijerph13111089

Radulov, I., Berbecea, A., Imbrea, F., Lato, A., Crista, F., and Merghes, P. (2014). Potassium in soil-plant-human system. *J. Agric. Sci. Cambridge* 46, 47–52.

Sait, M., Davis, K., and Janssen, P. (2006). Effect of pH on isolation and distribution of members of subdivision 1 of the phylum *Acidobacteria* occurring in soil. *Appl. Environ. Microbiol.* 72, 1852–1857. doi: 10.1128/aem.72.3.1852-1857.2006

Sanusi, A. I. (2015). Impact of burning E-waste on soil physicochemical properties and soil microorganisms. *J. Limnol.* 8, 434–442. doi: 10.9734/bmrj/2015/16874

Shi, Y., Pu, R., Guo, L., Man, J., Shang, B., Ou, X., et al. (2019). Formula fertilization of nitrogen and potassium fertilizers reduces cadmium accumulation in Panax notoginseng. *Arch. Agron. Soil Sci.* 66, 343–357. doi: 10.1080/03650340.2019.1616176

Smith, L., and Paul, A. (1990). The significance of soil microbial biomass estimations. *Soil Biochem.* 6, 357–396.

Tessier, A., Campbell, P. G. C., and Bisson, M. (1979). Sequential extraction procedure for the speciation of particulate trace metals. *Anal. Chem.* 51, 844–851. doi: 10.1021/ac50043a017

Wang, X., Shi, M., Hao, P., Zheng, W., and Cao, F. (2017). Alleviation of cadmium toxicity by potassium supplementation involves various physiological and biochemical features in *Nicotiana tabacum* L. *Acta Physiol. Plant* 39:132.

WM-T2-2004 (2004). *Green Standards Of Medicinal Plants and Preparations for Foreign Trade and Economy*. China: Ministry of Commerce of the People's Republic of China.

Wu, S., Bai, H., Zhang, C., Wei, J., Zeng, X., Jiang, D., et al. (2012). Study on the effect of potassium fertilizer and the nutrition regulator on the contents of potassium and the heavy metals in flue-cured Tobacco leaves. *Chin. J. Soil Sci.* 43, 190–194.

Yang, H., Ying, T., Ning, Z., Zhao, F., and Wen, R. (2018). Human health risk assessment of heavy metals in the soil-*Panax notoginseng* system in Yunnan province, China. *Hum. Ecol. Risk Assess.* 24, 1312–1326. doi: 10.1080/10807039.2017.1411782

Yang, M., Tian, J., Sun, C., and Zhang, X. (2011). "Study on quantity of microorganism and fertility of orchard soil with different plant ages," in *Proceedings of the International Symposium on Water Resource and Environmental Protection*, Piscataway, NJ.

Yao, Y., Wang, P., and Wang, C. (2019). The influence on contaminant bioavailability and microbial abundance of lake hongze by the south-to-north water diversion project. *Int. J. Env. Res. Pub. Health* 16:3068. doi: 10.3390/ijerph16173068

Yuan, Y. (2014). Research progress in the effect of physical and chemical properties on heavy metal bioavailability in soil-crop system. *Adv. Geosci.* 4, 214–223. doi: 10.12677/ag.2014.44026

Zeng, F., Ali, S., Zhang, H., Ouyang, Y., Qiu, B., Wu, F., et al. (2011). The influence of pH and organic matter content in paddy soil on heavy metal availability and their uptake by rice plants. *Environ. Pollut.* 159, 84–91. doi: 10.1016/j.envpol.2010.09.019

Zhang, C., and Xu, C. (2014). Effect of different potassium fertilizers on tomato soil physical and chemical properties and microorganism. *J. Dezhou Univ.* 30, 80–82.

Zhang, Q., Wei, Q., Qi, H., Wang, X., Huang, W., Liu, J., et al. (2011). Optimal schemes and correlation analysis between soil nutrient, pH and miceoorganism population in orchard of Beijing suburb. *J. Fruit Sci.* 28, 15–19.

Zhang, X., Gao, G., Wu, Z., Wen, X., Zhong, H., Zhong, Z., et al. (2019). Agroforestry alters the rhizosphere soil bacterial and fungal communities of moso bamboo plantations in subtropical China. *Appl. Soil Ecol.* 143, 192–200. doi: 10.1016/j.apsoil.2019.07.019

Zhao, Z., Zhu, Y., Li, H., Smith, S., and Smith, A. (2004). Effects of forms and rates of potassium fertilizers on cadmium uptake by two cultivars of spring wheat (*Trictium aestivum*, L). *Environ. Int.* 29, 973–978. doi: 10.1016/s0160-4120(03)00081-3

Conflict of Interest: The authors declare that the research was conducted in the absence of any commercial or financial relationships that could be construed as a potential conflict of interest.

frontiers in Plant Science

ORIGINAL RESEARCH
published: 09 July 2020
doi: 10.3389/fpls.2020.01016

A Maize *ZmAT6* Gene Confers Aluminum Tolerance *via* Reactive Oxygen Species Scavenging

Hanmei Du[1†], Ying Huang[1†], Min Qu[1], Yihong Li[1], Xiaoqi Hu[1], Wei Yang[1], Hongjie Li[1], Wenzhu He[2], Jianzhou Ding[1], Chan Liu[1], Shibin Gao[1], Moju Cao[1], Yanli Lu[1] and Suzhi Zhang[1]*

[1] Key Laboratory of Biology and Genetic Improvement of Maize in Southwest China of Agricultural Department, Ministry of Agriculture, Maize Research Institute, Sichuan Agricultural University, Chengdu, China, [2] Crop Research Institute, Sichuan Academy of Agricultural Sciences, Chengdu, China

Aluminum (Al) toxicity is the primary limiting factor that affects crop yields in acid soil. However, the genes that contribute to the Al tolerance process in maize are still poorly understood. Previous studies have predicted that ZmAT6 is a novel protein which could be upregulated under Al stress condition. Here, we found that *ZmAT6* is expressed in many tissues and organs and can be dramatically induced by Al in both the roots and shoots but particularly in the shoots. The overexpression of *ZmAT6* in maize and *Arabidopsis* plants increased their root growth and reduced the accumulation of Al, suggesting the contribution of *ZmAT6* to Al tolerance. Moreover, the *ZmAT6* transgenic maize plants had lower contents of malondialdehyde and reactive oxygen species (ROS), but much higher proline content and even lower Evans blue absorption in the roots compared with the wild type. Furthermore, the activity of several enzymes of the antioxidant system, such as peroxidase (POD), superoxide dismutase (SOD), catalase (CAT), and ascorbate peroxidase (APX), increased in *ZmAT6* transgenic maize plants, particularly SOD. Consistently, the expression of *ZmSOD* in transgenic maize was predominant upregulated by Al stress. Taken together, these findings revealed that *ZmAT6* could at least partially confer enhanced tolerance to Al toxicity by scavenging ROS in maize.

Keywords: aluminum toxicity, *ZmAT6*, maize, reactive oxygen species, antioxidant

OPEN ACCESS

Edited by:
Rafaqat Ali Gill,
Chinese Academy of Agricultural Sciences, China

Reviewed by:
Hong Zhai,
China Agricultural University, China
Ling Xu,
Zhejiang Sci-Tech University, China

***Correspondence:**
Suzhi Zhang
suzhi1026@163.com

[†]These authors have contributed equally to this work

Specialty section:
This article was submitted to Plant Nutrition, a section of the journal Frontiers in Plant Science

Received: *24 April 2020*
Accepted: *22 June 2020*
Published: *09 July 2020*

Citation:
Du H, Huang Y, Qu M, Li Y, Hu X, Yang W, Li H, He W, Ding J, Liu C, Gao S, Cao M, Lu Y and Zhang S (2020) A Maize ZmAT6 Gene Confers Aluminum Tolerance via Reactive Oxygen Species Scavenging. Front. Plant Sci. 11:1016. doi: 10.3389/fpls.2020.01016

INTRODUCTION

Acidic soils refer to soil with pH ≤ 5.5, occupying almost 30% of the arable soil and 50% of the potential cultivated land (von Uexküll and Mutert, 1995). Aluminum (Al), the third abundant element in the earth's crust, can be converted into soluble and toxic Al^{3+} which is the major limiting factor for plants' growth in acidic soil (Kochian et al., 2004). Aluminum toxicity could rapidly inhibit the elongation of the root system even in a micromolar concentration, then affect the absorption of water and nutrients, and eventually resulting in the decline of crop yield (Kinraide, 1990; Ma and Furukawa, 2003; Kochian et al., 2004). Improving the physiological and genetic tolerance to Al in crops has long been a challenging problem for researchers.

To cope with Al stress, plants have evolved a series of aluminum resistant mechanisms. The primary Al-tolerance mechanisms in plants refer to the exclusion tolerance and internal tolerance (Kochian, 1995; Ma et al., 1997; Ma, 2000; Daspute et al., 2017). The common feature of the Al exclusion mechanisms is to prevent Al from entering the root apex by the excretion of detoxified organic acids (OAs) and Pi ligands to the apoplast or rhizosphere. The internal tolerance mechanism refers to the sequestration of Al into vacuoles and its detoxification by chelation (Ma, 2000; Zheng and Yang, 2005). Both mechanisms are controlled by the expression of a series of genes. In recent decades, many genes related to Al tolerance have been identified, such as organic acid transporter genes (*ALMTs* and *MATEs*) (Hoekenga et al., 2006; Furukawa et al., 2007; Liu et al., 2013), antioxidative stress-related genes (Wu et al., 2017), also including those encoding aluminum transporter (Nramps and ABC transporter, aquaporins) (Huang et al., 2012; Li et al., 2014; Kochian et al., 2015; Lu et al., 2017; Wang et al., 2017), enzymes related to cell wall polysaccharide metabolism (XTHs) (Zhu et al., 2012; Zhu et al., 2014), and transcription factor (STOP, WRKY, ASR, NAC) (Iuchi et al., 2007; Ding et al., 2013; Arenhart et al., 2016; Li et al., 2018; Lou et al., 2019).

Previous studies have reported that one of an important component of the plant's reaction to toxic levels of Al is oxidative stress, because Al^{3+} can induce the increase of active reactive oxygen species (ROS) and lipid peroxidase related enzyme activities in plants such as soybean, Arabidopsis, wheat, and maize (Cakmak and Horst, 1991; Keith et al., 1998; Giannakoula et al., 2010; Xu et al., 2012; Sun et al., 2017). In other words, the exposure of plants to an excessive amount of Al usually leads to the overproduction of ROS (Yamamoto et al., 2001; Exley, 2004) and lipid peroxidation, resulting in dysfunctional organelles, serious cell damage, and even cell death (Yamamoto et al., 2003; Šimonovičová et al., 2004; Kochian et al., 2005). The major source of ROS in Al stressed plants is the activated plasma membrane NAPDH oxidase which can lead to the production of $O_2^{\cdot-}$ and H_2O_2 (Sagi and Fluhr, 2001). Al^{3+} can quickly cross the plasma membrane and activate the Fenton reaction in the cytoplasm which increases the content of ROS in cells (Taylor et al., 2000).

To protect the plants from Al-triggered oxidative stress, they have evolved two defense ways, including enzyme-catalyzed antioxidant system and non-enzymatic system, to decrease ROS production, detoxify ROS, and stimulate the recovery from ROS-induced damages (Ahmad et al., 2010; Chowra et al., 2017; Daspute et al., 2017). The enzyme-catalyzed antioxidant system mainly improve the activity of antioxidant enzymes which include peroxidase (POD), superoxide dismutase (SOD), catalase (CAT), and ascorbate peroxidase (APX) (Ezaki et al., 2013), or increase the expression level of antioxidant enzyme genes (Irany et al., 2018). While the non-enzymatic antioxidants are ascorbate (AsA) and glutathione (GSH) (Xu et al., 2012). Ectopic overexpression of wheat *WMnSOD1* and alternative oxidase gene improved Al tolerance in transgenic *Brassica napus* plants and tobacco cells, respectively (Basu et al., 2001; Panda et al., 2013). Transgenic Arabidopsis plants, which overexpressed three glutathione S-transferase genes and two peroxidase genes of tobacco, were endowed with strong aluminum tolerance (Ezaki et al., 2000). Besides, it was also reported some upstream gene, such as *OsPIN2*, and *PEPC* and *PPDK*, which are in positive control of the expression of antioxidant enzyme gene, could also enhance the tolerance of transgenic rice plants to Al toxicity *via* reducing the production of ROS, improving the activity ROS-scavenging enzyme, and weakening lipid peroxidation (Wu et al., 2014; Zhang et al., 2018). Additionally, it was also believed that the synthesis of cysteine-rich proteins can reduce the production of ROS. Fortunately, one of this protein had been identified as an Al tolerance gene that regulated the transcription by STOP1-like protein (ART1) in rice (Xia et al., 2013).

ZmAT6 (aluminum tolerance 6) gene, which encodes an unknown protein and is upregulated by Al stress, was identified from gene chip data in our previous study (Xu et al., 2017). In this study, we aimed to investigate the role that *ZmAT6* played during Al stress. The Al tolerance-related phenotype of *ZmAT6* was assessed in transgenic maize plants and Arabidopsis, as well as various indices of Al tolerance. The mechanism underlining the involvement of ROS scavenging in the *ZmAT6*-mediated antagonization of Al toxicity was explored.

MATERIALS AND METHODS

Plant Materials and Growth Conditions

The Al-tolerant maize inbred line 178, which has a high value of relative root growth (RRG = 45%) in our previous study (Xu et al., 2017), was used in this study. The seeds of 178 were first sterilized with 75% (w/v) alcohol for 2 min, then with 2% (w/v) NaOCl for 8 min, and finally germinated in quartz sand for 7 d under 28°C, 60% relative humidity and a photoperiod of 16 h/8 h (light/dark) cycle. After germinating, the seedlings were transferred to Hoagland's solution (Hoagland and Arnon, 1950) and grown for 5 days to the three-leaf stage for further treatment. The nutrient solution was adjusted to pH 5.8 with HCl and renewed every two days. The greenhouse conditions were now set as 14 h/28°C and 10 h/22°C day–night cycle, 70% relative humidity and 300 μmol $m^{-2}s^{-1}$ intense luminosity.

Sequence Characteristic Analysis of *ZmAT6*

Multiple sequence alignment of ZmAT6 (GRMZM5G886177) and its homologs was performed using DNAMAN (LynonBiosoft). Promoter analysis was performed by PlantCARE (http://bioinformatics.psb.ugent.be/webtools/plantcare/html/), and the *cis*-elements are listed in **Table S2**.

Analysis of the Expression of *ZmAT6* by Semi-Quantitative RT-PCR and Real-Time PCR

The tissues and organs 10 days after pollination, including the roots, stems, leaves, ears, tassels, and kernels, were collected from 178; the seedlings were treated with 0.5 mM $CaCl_2$ solution (pH 4.2) at 28°C overnight before treatment with Al and then transferred into the same solution containing additively 60 μM $AlCl_3$ (pH 4.2) and treated for 0, 6, 12, 24, 48, and 96 h. All the tissues were immediately frozen in liquid nitrogen and stored at

−80°C. Semi-quantitative RT-PCR and real-time PCR were carried out as previously described (Lin et al., 2014). Three biological replicates were performed for each experiment. The primers used for *ZmAT6* were listed in **Table S3**.

Subcellular Location

The subcellular localization of the *ZmAT6* protein was predicted by the WoLF PSORT program (http://wolfpsort.org) (Horton et al., 2007). Moreover, the full length CDS of the*ZmAT6* gene was ligated to pCAMBIA2300 to establish the ZmAT6:GFP vector.

Overexpression of the *ZmAT6* Gene in Maize and *Arabidopsis*

The full length coding sequence of the *ZmAT6* gene was amplified and ligated to the CPB vector behind the cauliflower mosaic virus 35S (CaMV35S) promoter to construct the p35S:*ZmAT6* vector. The p35S:*ZmAT6* vector was transformed into immature maize callus of 18-599 by an *Agrobacterium*-mediated method (Huang et al., 2018) and into Arabidopsis by the flowering dip method (Clough and Bent, 1998). The transgenic plants of maize and Arabidopsis were confirmed by PCR amplification and harvested individually. The homozygous seeds of T4 generation were used for future experiments.

Assessment of the Plant Growth, Relative Root Growth, and Al Content

The seedlings of the transgenic maize and wild type (WT) 18-599 were transferred to Hoagland's solution with or without 200 μM $AlCl_3$ (pH 4.2). After two weeks of culture, the fresh weights of the underground part and the upper part of the ground were measured separately.

The root lengths of the transgenic maize plants and wild type were measured and treated as the initial length after pretreatment with 0.5 mM $CaCl_2$ for 12 h. The maize plants were exposed to 60 μM $AlCl_3$ for 3 days, the final length of the root was recorded, and the RRG was calculated (Sasaki et al., 2004; Sasaki et al., 2006). The root tips (approximately 1 cm) were collected and measured as previously described to determine the Al content (Osawa and Matsumoto, 2001).

Measurement of Cell Membrane Integrity, Lipid Peroxidation, and Proline Content

After treatment with 60 μM $AlCl_3$ for 24 h, the roots of transgenic maize plants and WT were immediately collected and dyed as described by Baker and Mock (Baker and Mock, 1994). Lipid peroxidation was determined by measuring the MDA content using the thiobarbituric acid method (Cakmak and Horst, 1991). Free proline determination was assessed as described by Bates (Bates et al., 1973).

Determination of ROS Related to Aluminum Stress

After treatment with 60 μM $AlCl_3$ for 24 h, the active oxygen content was measured in the seedlings of transgenic maize and WT (Jana and Choudhuri, 1982). The super oxygen free radical ($O_2^{\cdot-}$) was measured by the hydroxylamine method (Elstner and Heupel, 1976).

Antioxidant Enzyme Extractions, Activity Assessment Assay, and Gene Expression Detection

After Al treatment, roots were collected immediately, and 0.5 g of the root sample was homogenized with 50 mM sodium phosphate buffer (pH 7.0) containing 3 ml 1 mM ethylenediaminetetraacetic acid (EDTA). Homogenates were then centrifuged at 4°C for 20 min at 15,365 **g**, and the supernatants were used to determine the enzyme activity. The whole extraction procedure was carried out at 4°C.

The activities of SOD, POD, CAT, and APX were determined as previously described (Aebi, 1974; Giannopolitis and Ries, 1977; Nakano and Asada, 1981; Zheng and Huystee, 1992).

The relative expression of antioxidant enzyme genes in WT and one of the maize transgenic line L5 (**Figure S2**) was detected by RT-PCR, and the primers were listed in **Table S3**.

Statistical Analysis

All experiments were repeated at least three times, and data were represented as the mean ± SD of the replicates. Student's t tests at $p < 0.05$ and 0.01 were performed to identify significant differences between observation values using the SPSS21 software. The figures were drawn using the Origin 8.0 software (Origin Lab Corporation, Northampton, MA, USA).

RESULTS

Cloning and Molecular Characteristics of the ZmAT6 Sequence

Using gene specific primers, the complete CDS sequence of *ZmAT6* was isolated from the aluminum tolerance maize line 178. The 771 bp open reading frame (ORF) of *ZmAT6* has three exons and encodes a 27.79 kDa non-transmembrane protein with a predicted pI of 5.80 (**Figure S1**, **Table S1**). Multiple sequence alignment showed that ZmAT6 shared a higher similarity, up to 75.19%, with the rice homolog (Os01g0731600), higher than its Arabidopsis counterpart (At1g78780) (51.56%) (**Figure 1**). In addition, a promoter analysis of *ZmAT6* revealed that it included but was not limited to the binding sites GGN(T/g/a/C)V(C/A/g)S(C/G) of ART1 (**Table S2**), the major transcriptional factor that regulates the series of Al response genes in rice. However, protein prediction did not reveal any particular structure of ZmAT6.

Expression Pattern of *ZmAT6* in Different Organs and Under Al Treatment

To better understand the functions of *ZmAT6*, its expression patterns in several organs, including roots, stems, leaves, ears, tassels and kernels, at different growth stages were monitored using semi-quantitative reverse transcription PCR (RT-PCR).

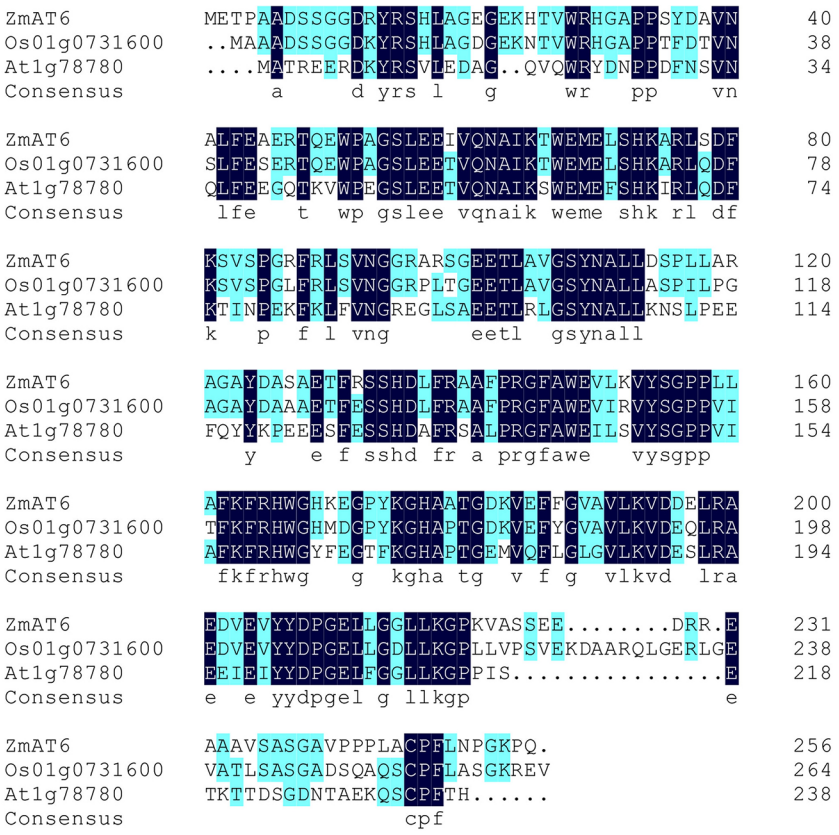

FIGURE 1 | ZmAT6 and its homologs are highly conservative.

ZmAT6 was moderately expressed in all the organs with the exception of its weak expression in ears (**Figure 2A**). Moreover, to investigate the pattern of expression of *ZmAT6* on Al exposure, the mRNA abundance of *ZmAT6* was monitored further in roots and shoots under a time-course Al stress treatment from 0 to 96 h. As shown in **Figure 2B**, the transcription of *ZmAT6* was dramatically upregulated after Al treatment in the roots or the shoots. The Al-inducted expression level of *ZmAT6* was quite stable in the roots during the whole process. Alternatively, *ZmAT6* in the shoots exhibited a much higher level of expression than in the roots. The mRNA abundance of *ZmAT6* peaked at time point six and then gradually decreased during prolonged Al stress. These results indicated that *ZmAT6* was sensitive to the fluctuating environmental Al^{3+} status in seedlings and was involved in the tolerance to aluminum toxicity in maize.

Subcellular Localization of ZmAT6

Using the WoLF PSORT program, ZmAT6 protein was predicted to be localized in the chloroplast or cytoplasm. To detect the subcellular localization of ZmAT6 protein, the coding region of *ZmAT6* was fused with the 3′ end of the *GFP* gene and driven by the *35S* promoter. The *GFP* gene alone under the control of the *35S* promoter served as the control. The subcellular localization of *ZmAT6* was determined in a transient expression system in *Nicotiana benthamiana* leaves. The result indicated that the 35S:ZmAT6:GFP fusion protein appeared to be localized in the chloroplast but not the cytoplasm (**Figure 3**).

Overexpression of *ZmAT6* in Maize Plants Conferred Improved Al Tolerance

To further investigate the function of *ZmAT6* under Al stress, the entire ORF of *ZmAT6* was inserted into the binary vector CPB (**Figures S2A, B**), and the recombinant expression vector p35S: *ZmAT6* was transformed into maize inbred line 18-599. Finally, 10 independent transgenic plants of T_0 generation were identified and confirmed by PCR detection (**Figure S2C**). Among them, three homozygous lines (L3, L5, and L10) of T3 generation with higher *ZmAT6* expression (**Figure S2D**) were propagated and selected for analysis.

To determine whether the overexpression of *ZmAT6* enhanced the tolerance of the transgenic plants to Al, we assessed the plant growth of the three overexpressed transgenic lines of *ZmAT6* (*OE-ZmAT6*) and the wild type (18-599, WT) under normal and Al stress conditions. At the beginning, the transgenic plants grew normally like the WT in a hydroponic

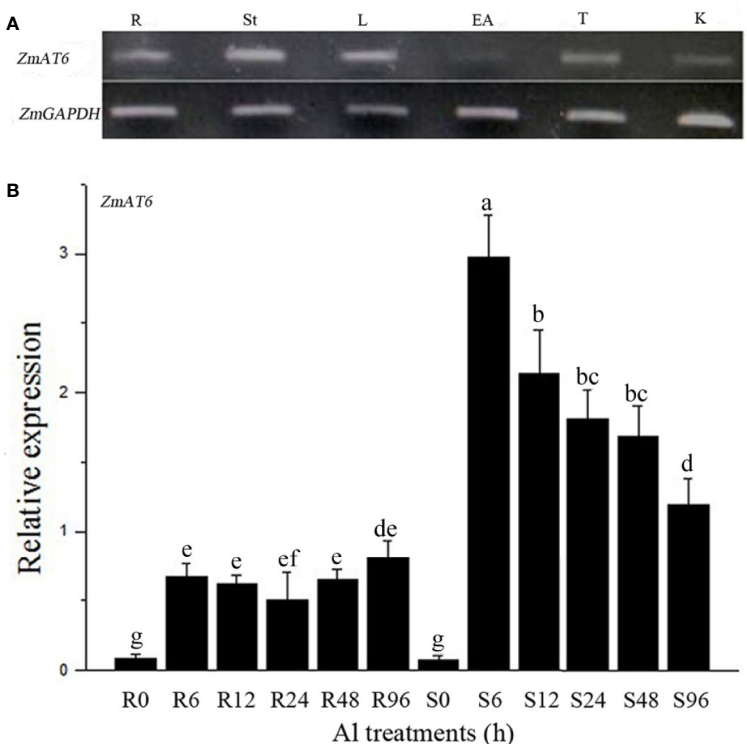

FIGURE 2 | The expression pattern of the *ZmAT6* gene. **(A)** Tissue and organ expression pattern of *ZmAT6* in adult maize plants. The letter above the columns of expression data refer to: R, root; St, stem; L, leaf; EA, ear; T, tassel; and K, kernel. **(B)** Transcription of *ZmAT6* in the roots (R) and shoot (S) was quantified at 0, 6, 12, 24, 48, and 96 h after Al treatment (60 μM $AlCl_3$, pH = 4.2). *ZmGAPDH* was used as internal reference gene. The values were presented as mean ± SD (n = 3) and marked with different letters to indicate statistic significant difference at $P < 0.05$ (student's *t* test).

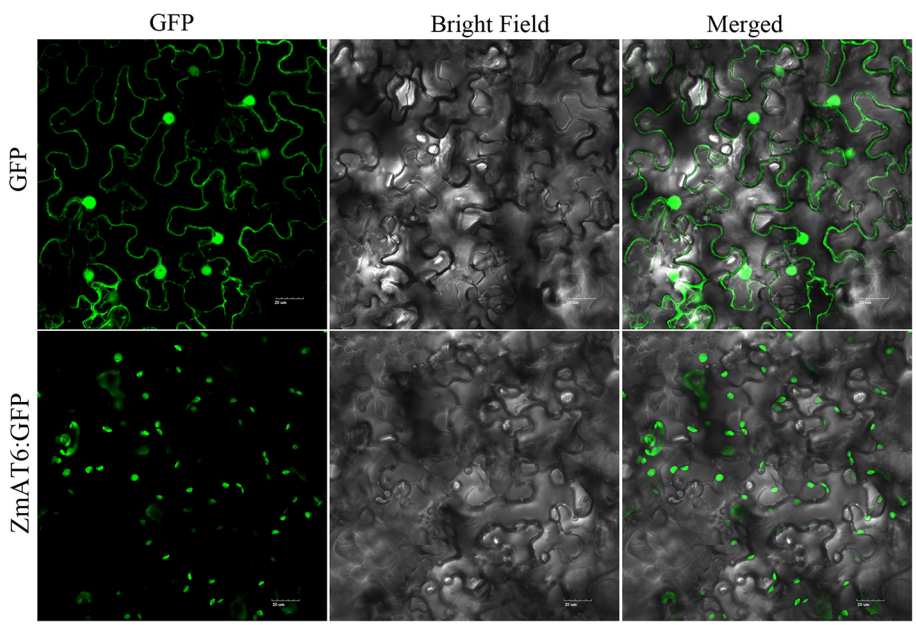

FIGURE 3 | Subcellular localization of ZmAT6.

culture (pH 4.2). Nevertheless, when cultivated in the same solution containing 200 μM $AlCl_3$, all of the *OE-ZmAT6* plants uniformly showed a high tolerance to Al. The mean value of RRG of *OE-ZmAT6* plants was 90%, much higher than that of the WT (70%) (**Figures 4A, D**). As for the root fresh weight, the mean value of *ZmAT6* transgenic lines was about 87% heavier than that of WT (**Figure 4B**), indicating a less inhibition of *OE-ZmAT6* plants when subjected to Al stress. Moreover, the vigorous leaf

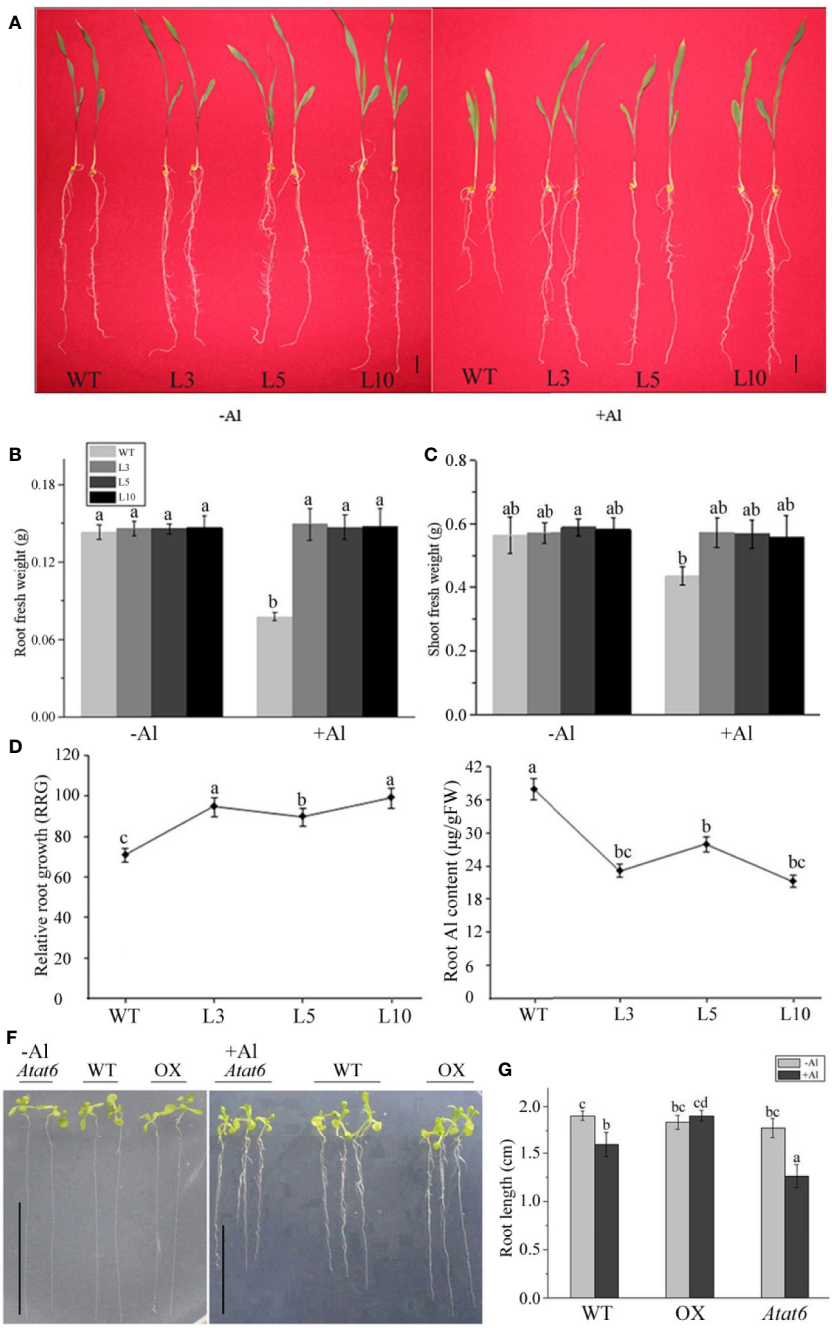

FIGURE 4 | *ZmAT6* overexpression enhanced aluminum tolerance in both transgenic maize and Arabidopsis. **(A)** Wild type (WT) and *OE-ZmAT6* transgenic plants were grown on hydroponic culture with or without Al treatment (60 μM $AlCl_3$, pH 4.2). The corresponding **(B)** root fresh weight, **(C)** shoot fresh weight, **(D)** relative root growth (RRG), and **(E)** aluminum (Al) content. Values represent mean ± SD (n = 3–5). Scale bar: 2.0 cm. Different letters indicate significant differences ($P < 0.01$) (multiple comparison). **(F)** Wild type Col-0 and mutants *Atat6* and *ZmAT6* overexpressed (OX) transgenic Arabidopsis plants grown with or without aluminum treatment (pH 4.2) and the corresponding **(G)** root length. Scale bar: 1.0 cm. Values represent mean ± SD ($n \geq 3$). Different letters indicate significant differences ($P < 0.01$) (multiple comparison).

growth of the *OE-ZmAT6* transgenic plants could also be verified by the significant increase in the shoot fresh weights (**Figures 4A, C**). Concerning the Al content in root tips, the mean value of 24.63 μg/g fresh weight (FW) was lower in the *OE-ZmAT6* plants than the 37.23μg/g FW in the WT (**Figure 4E**).

In addition, evidence from its Arabidopsis homolog *AtAT6* reinforced the fact that *AtAT6* could enhance or decrease aluminum tolerance *via* overexpression or mutation (**Figure S3**, **Figures 4F, G).** In comparison with the WT Col-0, the root length of the *Atat6* mutant (SALK_082224) was much shorter, while those of the *AtAT6*-overexpressed (OX) Arabidopsis plants were much longer on Al exposure (**Figure 4G**).

Furthermore, physiological indices related to Al-stress tolerance, including Evans blue staining, malondialdehyde (MDA) content, and proline (Pro) content, were also measured in three *OE-ZmAT6* transgenic lines and WT maize plants on Al exposure. As shown in **Figure 5** and **Figure S4**, the results indicated that the mean values of the Evans blue uptake (1.80 OD 600/g) and MDA content (3.14 μM/μg FW) in the *OE-ZmAT6* lines were significantly lower than those of the WT under Al treatment. In contrast, the Pro content (15.80 μM/g FW) was clearly higher than that in the WT (11.77 μM/g FW) when the plants suffered from Al toxicity (**Figure 5C**). These results verified the fact that overexpression of *ZmAT6* conferred tolerance to Al toxicity in *OE-ZmAT6* plants and reduced the oxidative damage of maize under Al stress.

ZmAT6 Is Related to the Scavenging of ROS

To investigate whether *ZmAT6* is related to the scavenging of ROS, we measured the content of hydrogen peroxide (H_2O_2) and the rate of production of the superoxide anion in the three *OE-ZmAT6* lines and the WT. Under normal conditions, no distinct difference could be detected between the *OE-ZmAT6* lines and WT regarding these two indices. Nevertheless, both H_2O_2 and the superoxide anion had increased in all the plants tested during Al stress, and the amplitude was even higher in the WT than in *OE-ZmAT6* plants (**Figures 6A, B**).The increase of H_2O_2 content and productive rate of superoxide anion in WT against *OE-ZmAT6* lines under Al stress were 0.38:0.09 (μM/L FW) and 0.24:0.11 (μM/mg) min, respectively. These results indicated that *ZmAT6* played an important role in the scavenging of the excessive ROS caused by Al stress, which endowed transgenic maize plants with the capacity to tolerate aluminum toxicity by ROS cleaning.

ZmAT6 Improved the Activity of Antioxidant Enzymes and the Expression Level of Antioxidant Genes in Transgenic Maize

To investigate the factors affecting the *ZmAT6*-mediated scavenging of ROS, we examined the activity of several enzymes usually involved in the antioxidant system. It was

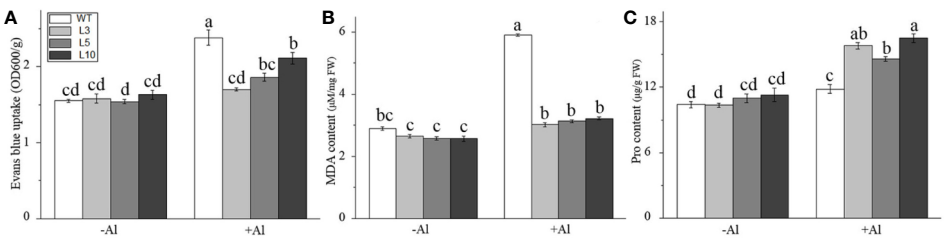

FIGURE 5 | Determination of physiological indexes related to aluminum tolerance. **(A)** Evans blue, **(B)** Malondialdehyde (MDA) and **(C)** Proline (Pro) in the wild type (WT) and three *OE-ZmAT6* transgenic maize lines (L3, l5, and L10). Values represent mean ± SD (n = 10). Different letters indicate significant differences ($P < 0.01$) (multiple comparison).

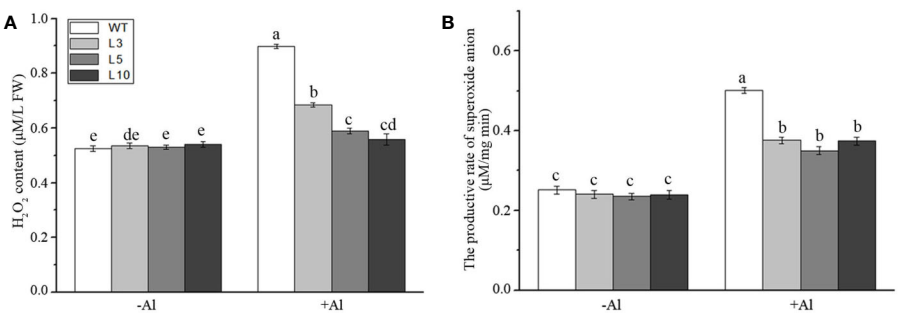

FIGURE 6 | Determination of ROS under aluminum stress. **(A)** Hydrogen peroxide content and **(B)** the productive rate of superoxide anion in wild type (WT) and three *OE-ZmAT6* transgenic maize lines (L3, L5, and L10). Values represent mean ± SD (n = 3). Different letters indicate significant differences ($P < 0.01$) (multiple comparison).

notable that the SOD activity of three *OE-ZmAT6* lines was significantly higher than that of the WT despite Al treatment. After treatment with 60 μM $AlCl_3$ (pH 4.2), the mean value of SOD activity of the *OE-ZmAT6* plants was dramatically increased, up to 244.4 U/g (**Figure 7A**). The activities of POD, CAT, and APX remained almost the same in the WT plants as in the *OE-ZmAT6* plants but decreased separately to 28.07, 22.92, and 14.77%, respectively, when subjected to Al stress (**Figures 7B–D**).

In addition, we also monitored the expression patterns of three antioxidant-enzyme genes on Al exposure. As shown in **Figures 8A, B**, the expression of *ZmSOD* and *ZmPOD* could be upregulated by Al stimulus in all tested plants with the exception of *ZmPOD* in WT, consistent with the enhanced activities of antioxidant enzymes (**Figure 7**). As for *ZmSOD* and *ZmPOD*, both of them exhibited a much higher level of expression either in the root or leaf of *OE-ZmAT6* plant than in WT. In particular, the expression of *ZmCAT* in the root of WT was higher than in *OE-ZmAT6* plant (**Figure 8C**). These results suggested that both the regulation on gene expression and activity of antioxidant enzymes contributed to the enhanced Al tolerance of *OE-ZmAT6* plant in maize.

DISCUSSION

ZmAT6 Is Involved in Al-Stress Related Responses

Some plants evolved many mechanisms to tolerate Al toxicity. *ZmAT6* was first identified as an Al-induced gene with an

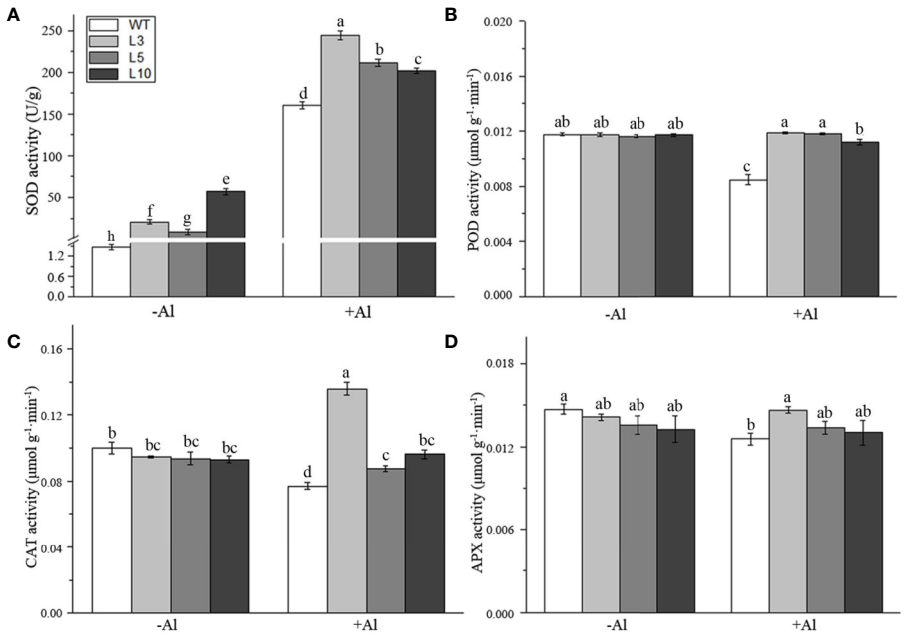

FIGURE 7 | Determination of the activity of several antioxidant enzymes. The activities of antioxidant-related enzymes **(A)** SOD, **(B)** POD, **(C)** CAT, and **(D)** APX were detected. Values represent mean ± SD (n = 4). Different letters indicate significant differences ($P < 0.05$) (multiple comparison).

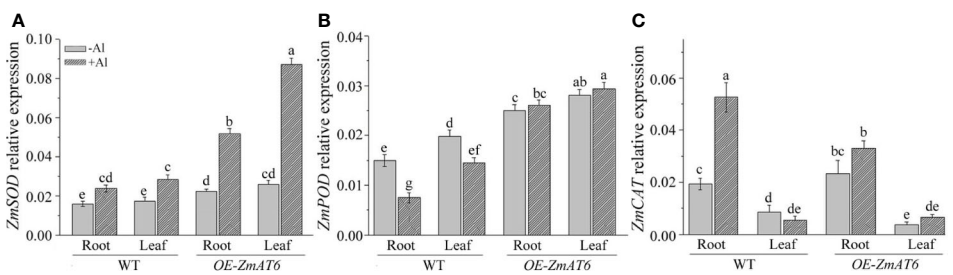

FIGURE 8 | The relative expression of antioxidant enzyme genes. The relative expression levels of **(A)** *ZmSOD*, **(B)** *ZmPOD*, and **(C)** *ZmCAT* were determined with or without Al treatment in WT and *OE-ZmAT6* transgenic maize (L5). *ZmGAPDH* was used as internal reference gene. Values represent mean ± SD (n = 3). Different letters indicate significant differences ($P < 0.05$) (multiple comparison).

unpredicted function from our previous microarray data (Xu et al., 2017). The unique indication was that its rice or tholog was regulated by OsART1, a master transcriptional factor that controls more than 30 Al response genes by binding to the GGTCC (GGN(T/g/a/C)V(C/A/g)S(C/G)) site of its promoter (Yamaji et al., 2009; Tsutsui et al., 2011). Similarly, we also found a GGNVS site in the promoter of *ZmAT6* (**Table S2**). In addition, *ZmAT6* expresses in many tissues and organs, and it could be rapidly induced by Al stress in both the roots and shoots of maize (**Figure 2**). These results suggested that *ZmAT6* may be a downstream gene in maize directly targeted by a transcription factor such as rice OsART1 when the plants are under Al stress. An exploration of the OsART1 equivalent in maize by strategies such as homolog query and gel shift assay could confirm this hypothesis.

Overexpression of *ZmAT6* Improved the Al Tolerance of Transgenic Maize Plants

The inhibition of the root length was an initial detection of Al toxicity in plants (Matsumoto and Motoda, 2012). Plants with strong Al tolerance usually exhibited high relative root growth (Ma et al., 2018; Badia et al., 2020). In this study, the RRG of *OE-ZmAT6* transgenic maize was more than 20% higher than those in the WT. Meanwhile, the mean value of the total fresh weight and the fresh weight of roots were more than 30% and even over 50% weightier than that of WT after exposure to Al, respectively (**Figures 4A–D**). Attributed to the ectopic overexpression of *ZmAT6*, the clear improvement of the Al tolerance was exhibited not only in transgenic maize plants but also in transgenic wild type Arabidopsis and *at6* mutant (**Figures 4F, G**). Moreover, the content of aluminum in the root of *OE-ZmAT6* plant is rather lower than that in the WT (**Figure 4E**), underlying an antagonism to Al toxicity.

In addition, a semi reduction of the superoxide radical ion caused by aluminum toxicity may lead to oxidative stress and serious cell damage. The enzyme-catalyzed antioxidant system and the non-enzymatic antioxidant system of plants could scavenge excessive ROS and reduce the cell damage caused by aluminum toxicity (Achary et al., 2008; Irany et al., 2018). The intensity of Evans blue staining and the content of MDA in the cells of target tissue could reflect the lipid peroxidation of the cell membrane. In this study, the significantly lower Evans blue uptake (**Figure 5A**, **Figure S4**) and MDA content (**Figure 5B**) of the *OE-ZmAT6* plants suggested that aluminum stress caused less damage to the cell membrane. This was consistent with the results of Sun (Sun et al., 2017) and Yu (Yu et al., 2018), who reported that the MDA content in the root tips of wheat increased significantly under aluminum treatment, particularly in sensitive genotype plants, and the higher Evans Blue uptake in the root apexes was due to the Al-induced oxidative stress. Moreover, proline, a type of antioxidant that favors ROS removal (Rodriguez and Redman, 2005), had a significantly higher content in tolerant plants than in sensitive ones (Ashraf and Foolad, 2007). The obviously increased content of proline in the *OE-ZmAT6* plants under Al stress in this study was highly consistent with the previous study of Giannakoula (Giannakoula et al., 2008), who found that the proline content in the Al-tolerant genotype maize increased with the concentration of Al.

Scavenging of ROS Favors *OE-ZmAT6* Maize Plants to Antagonize Al-Stress

Previous studies have documented that the excessive accumulation of ROS in plants under aluminum stress is the primary reason for oxidative stress and the decisive factor that inhibited root elongation (Tamás et al., 2006; Giannakoula et al., 2010). Giannakoula (Giannakoula et al., 2010) and Sun (Sun et al., 2017) had found that $O_2^{\cdot-}$ and H_2O_2 could predominantly accumulate in the roots of Al-sensitive maize and wheat, respectively, after exposure to Al. Compared with the wild type, overexpression of *AtPrx64* in transgenic tobacco also showed less root growth inhibition, lower H_2O_2 content, and less MDA accumulation following Al exposure (Wu et al., 2017). In our study, the content of H_2O_2 and the productive rate of the superoxide anion in the ROS of *OE-ZmAT6* maize plants were significantly lower than those in the WT under Al stress (**Figure 6**), indicating the involvement of AT6 in ROS scavenging. Indeed, the activities of the antioxidant enzymes POD, CAT, and APX of the *OE-ZmAT6* plants had no obvious change before and after Al treatment even though there was a significant difference between the transgenic lines and WT (**Figures 7B–D**). The only exception was SOD, which had significantly higher activities in the *OE-ZmAT6* plants than that in the WT before or after Al stress (**Figure 7A**). Consistently, the expression level of *ZmSOD* was also predominately upregulated by Al stimulus (**Figure 8A**), suggesting that SOD played a crucial role in effectively removing excess ROS from *OE-ZmAT6* maize cells and maintaining the balance of ROS.

Coincidentally, a number of studies also found that the enzyme-catalyzed antioxidant system is involved in Al stress antagonism even though the major scavenger enzyme was not the same. Darkó et al. (Darkó et al., 2004) found that the activity of the antioxidant enzymes in the wheat root tips changed noticeably under Al stress, and the activity of APX in Al-sensitive genotypes was significantly higher, while those of SOD and CAT were lower than those of the Al-tolerant genotype. However, the activities of SOD and POD were significantly improved in Al-sensitive maize after Al treatment, while the activities of SOD, POD and CAT exhibited no distinction in the Al-tolerant genotypes (Boscolo et al., 2003). Therefore, the ROS scavenging responses of antioxidant enzymes under Al stress conditions varied depending on the species and genotypes. Alternatively, the overexpression of genes encoding ROS-scavenging enzymes in several plant species had documented that their activities enhanced the tolerance of Al (Panda et al., 2013; Sun et al., 2017; Irany et al., 2018). In this study, *ZmAT6* enhanced the aluminum tolerance of maize by increasing the expression level of *ZmSOD* gene and improving the activity of the antioxidant enzymes SOD in the antioxidant enzymatic system.

In conclusion, we demonstrated that the chloroplast-located gene *ZmAT6* could be quickly induced by Al stress and could enhance the tolerance to Al toxicity when overexpressed in transgenic maize and Arabidopsis. *ZmAT6* could antagonize the Al toxicity *via* at least two ROS removal approaches:

increasing the activity of antioxidant enzymes SOD and the content of antioxidant proline.

DATA AVAILABILITY STATEMENT

The raw data supporting the conclusions of this article will be made available by the authors, without undue reservation.

AUTHOR CONTRIBUTIONS

HD and YH carried out the experiments, analyzed the data, and drafted the manuscript. JD, HL, XH, MQ, YLi, and WY contributed to sample collection and data analysis. WH, MC, SG, and YLu contributed with consultation. SZ designed the experiment and revised the manuscript. All authors contributed to the article and approved the submitted version.

FUNDING

This work was supported by the National Natural Science Foundation of China [No. 30800687, 31071434], and the Major Project of Education Department in Sichuan [No. 15ZA0022].

SUPPLEMENTARY MATERIAL

The Supplementary Material for this article can be found online at: https://www.frontiersin.org/articles/10.3389/fpls.2020.01016/full#supplementary-material

REFERENCES

Achary, V. M., Jena, S., Panda, K. K., and Panda, B. B. (2008). Aluminium induced oxidative stress and DNA damage in root cells of *Allium cepa* L. *Ecotoxicol. Environ. Saf.* 70, 300–310. doi: 10.1016/j.ecoenv.2007.10.022

Aebi, H. (1974). "Catalase, method of enzymatic analysis," in *Method of enzymatic analysis 3*. Ed. H. U. Bergmeyer (New York: Academic), 673–684.

Ahmad, P., Jaleel, C. A., Salem, M. A., Nabi, G., and Sharma, S. (2010). Roles of enzymatic and nonenzymatic antioxidants in plants during abiotic stress. *Crit. Rev. Biotechnol.* 30, 161–175. doi: 10.3109/07388550903524243

Arenhart, R. A., Schunemann, M., Bucker Neto, L., Margis, R., Wang, Z. Y., and Margis-Pinheiro, M. (2016). Rice ASR1 and ASR5 are complementary transcription factors regulating aluminium responsive genes. *Plant Cell Environ.* 39, 645–651. doi: 10.1111/pce.12655

Ashraf, M., and Foolad, M. R. (2007). Roles of glycine betaine and proline in improving plant abiotic stress resistance. *Environ. Exp. Bot.* 59, 206–216. doi: 10.1016/j.envexpbot.2005.12.006

Badia, M. B., Maurino, V. G., Pavlovic, T., Arias, C. L., Pagani, M. A., Andreo, C. S., et al. (2020). Loss of function of Arabidopsis NADP-malic enzyme 1 results in enhanced tolerance to aluminum stress. *Plant J.* 101, 653–665. doi: 10.1111/tpj.14571

Baker, C. J., and Mock, N. M. (1994). An improved methods for monitoring cell death in cell suspension and leaf disc assays using evans blue. *Plant Cell Tiss. Org. Cult.* 39, 7–12. doi: 10.1007/BF00037585

Basu, U., Good, A. G., and Taylor, G. J. (2001). Transgenic Brassica napus plants overexpressing aluminum-induced mitochondrial manganese superoxide dismutase cDNA are resistant to aluminum. *Plant Cell Environ.* 24, 1278–1269. doi: 10.1046/j.0016-8025.2001.00783.x

Bates, L. S., Waldren, R. P., and Teare, I. D. (1973). Rapid determination of free proline for water-stress studies. *Plant Soil* 39, 205–207. doi: 10.1007/BF00018060

Boscolo, P. R. S., Menossi, M., and Jorge, R. A. (2003). Aluminum-induced oxidative stress in maize. *Phytochemistry* 62, 181–189. doi: 10.1016/S0031-9422(02)00491-0

Cakmak, I., and Horst, W. J. (1991). Effect of aluminium on lipid peroxidation, superoxide dismutase, catalase, and peroxidase activities in root tips of soybean (*Glycine max*). *Physiol. Plant.* 83, 463–468. doi: 10.1111/j.1399-3054.1991.tb00121.x

Chowra, U., Yanase, E., Koyama, H., and Panda, S. K. (2017). Aluminium-induced excessive ROS causes cellular damage and metabolic shifts in black gram *Vigna mungo* (L.) Hepper. *Protoplasma* 254, 293–302. doi: 10.1007/s00709-016-0943-5

Clough, S. J., and Bent, A. F. (1998). Floral dip: a simplifed method for Agrobacterium -mediated transformation of *Arabidopsis thaliana*. *Plant J. Cell Mol. Biol.* 16, 735. doi: 10.1046/j.1365-313x.1998.00343.x

Darkó, É, Ambrus, H., Stefanovits-Bányai, É, Fodor, J., Bakos, F., and Barnabás, B. (2004). Aluminium toxicity, Al tolerance and oxidative stress in an Al-sensitive wheat genotype and in Al-tolerant lines developed by in vitro microspore selection. *Plant Sci.* 166, 583–591. doi: 10.1016/j.plantsci.2003.10.023

Daspute, A. A., Sadhukhan, A., Tokizawa, M., Kobayashi, Y., Panda, S. K., and Koyama, H. (2017). Transcriptional regulation of aluminum-tolerance genes in higher plants: clarifying the underlying molecular mechanisms. *Front. Plant Sci.* 8, 1358. doi: 10.3389/fpls.2017.01358

Ding, Z. J., Yan, J. Y., Xu, X. Y., Li, G. X., and Zheng, S. J. (2013). WRKY46 functions as a transcriptional repressor of ALMT1, regulating aluminum-induced malate secretion in Arabidopsis. *Plant J.* 76, 825–835. doi: 10.1111/tpj.12337

Elstner, E. F., and Heupel, A. (1976). Inhibition of nitrite formation from hydroxylammoniumchloride: a simple assay for superoxide dismutase. *Anal. Biochem.* 70, 616–620. doi: 10.1016/0003-2697(76)90488-7

Exley, C. (2004). The pro-oxidant activity of aluminum. *Free Radic. Biol. Med.* 36, 380–387. doi: 10.1016/j.freeradbiomed.2003.11.017

Ezaki, B., Gardner, R. C., Ezaki, Y., and Matsumoto, H. (2000). Expression of aluminum-induced genes in transgenic Arabidopsis plants can ameliorate aluminum stress and/or oxidative stress. *Plant Physiol.* 122, 657–665. doi: 10.1104/pp.122.3.657

Ezaki, B., Jayaram, K., Higashi, A., and Takahashi, K. (2013). A combination of five mechanisms confers a high tolerance for aluminum to a wild species of Poaceae, *Andropogon virginicus* L. *Environ. Exp. Bot.* 93, 35–44. doi: 10.1016/j.envexpbot.2013.05.002

Furukawa, J., Yamaji, N., Wang, H., Mitani, N., Murata, Y., Sato, K., et al. (2007). An aluminum-activated citrate transporter in barley. *Plant Cell Physiol.* 48, 1081–1091. doi: 10.1093/pcp/pcm091

Giannakoula, A., Moustakas, M., Mylona, P., Papadakis, I., and Yupsanis, T. (2008). Aluminum tolerance in maize is correlated with increased levels of mineral nutrients, carbohydrates and proline, and decreased levels of lipid peroxidation and Al accumulation. *J. Plant Physiol.* 165, 385–396. doi: 10.1016/j.jplph.2007.01.014

Giannakoula, A., Moustakas, M., Syros, T., and Yupsanis, T. (2010). Aluminum stress induces up-regulation of an efficient antioxidant system in the Al-tolerant maize line but not in the Al-sensitive line. *Environ. Exp. Bot.* 67, 487–494. doi: 10.1016/j.envexpbot.2009.07.010

Giannopolitis, C. N., and Ries, S. K. (1977). Superoxide dismutases I. Occurrence in higher plants. *Plant Physiol.* 59, 309–314. doi: 10.1104/pp.59.2.309

Hoagland, D. R., and Arnon, D.II (1950). The water-culture method for growing plants without soil. *Univ. Galif. Agric. Exp. Sta. Circ.* 347, 357–359. doi: 10.1016/S0140-6736(00)73482-9

Hoekenga, O. A., Maron, L. G., Piñeros, M. A., Cancado, G. M., Shaff, J., Kobayashi, Y., et al. (2006). *AtALMT1*, which encodes a malate transporter, is identified as one of several genes critical for aluminum tolerance in Arabidopsis. *PNAS* 103, 9738–9743. doi: 10.1073/pnas.0602868103

Horton, P., Park, K. J., Obayashi, T., Fujita, N., Harada, H., Adams-Collier, C. J., et al. (2007). WoLF PSORT: protein localization predictor. *Nucleic Acids Res.* 35, 585–587. doi: 10.1093/nar/gkm259

Huang, C. F., Yamaji, N., Chen, Z., and Ma, J. F. (2012). A tonoplast-localized half-size ABC transporter is required for internal detoxification of aluminum in rice. *Plant J.* 69, 857–867. doi: 10.1111/j.1365-313X.2011.04837.x

Huang, S., Gao, J., You, J., Liang, Y., Guan, K., Yan, S., et al. (2018). Identification of STOP1-like proteins associated with aluminum tolerance in sweet sorghum (*Sorghum bicolor* L.). *Front. Plant Sci.* 9, 258. doi: 10.3389/fpls.2018.00258

Irany, R. P., Anny , C. D. L., Tatiane , L. P., Raquel , A. A., and Maria , D. C. P. B. (2018). Gene expression and antioxidant enzymatic activity in passion fruit exposed to aluminum. *Afr. J. Agric. Res.* 13, 115–120. doi: 10.5897/ajar2017.12834

Iuchi, S., Koyama, H., Iuchi, A., Kobayashi, Y., Kitabayashi, S., Ikka, T., et al. (2007). Zinc finger protein STOP1 is critical for proton tolerance in Arabidopsis and coregulates a key gene in aluminum tolerance. *PNAS* 104, 9900–9905. doi: 10.1073/pnas.0700117104

Jana, S., and Choudhuri, M. A. (1982). Glycolate metabolism of three submersed aquatic angiosperms during ageing. *Aquat Bot.* 12, 345–354. doi: 10.1016/0304-3770(82)90026-2

Keith, D., Richards, E. J. S., Yogesh, K. S., Keith, R. D., and Richard, C. G. (1998). Aluminum induces oxidative stress genes in *Arabdopsis thaliana*. *Plant Physiol.* 116, 409–418. doi: 10.1104/pp.116.1.409

Kinraide, T. B. (1990). Assessing the rhizotoxicity of the aluminate ion, $Al(OH)^{4-}$. *Plant Physiol.* 93, 1620–1625. doi: 10.1104/pp.93.4.1620

Kochian, L. V., Hoekenga, O. A., and Pineros, M. A. (2004). How do crop plants tolerate acid soils? Mechanisms of aluminum tolerance and phosphorous efficiency. *Annu. Rev. Plant Biol.* 55, 459–493. doi: 10.1146/annurev.arplant.55.031903.141655

Kochian, L. V., Piñeros, M. A., and Hoekenga, O. A. (2005). The physiology, genetics and molecular biology of plant aluminum resistance and toxicity. *Plant Soil* 274, 175–195. doi: 10.1007/s11104-004-1158-7

Kochian, L. V., Pineros, M. A., Liu, J., and Magalhaes, J. V. (2015). Plant adaptation to acid soils: The molecular basis for crop aluminum resistance. *Annu. Rev. Plant Biol.* 66, 571–598. doi: 10.1146/annurev-arplant-043014-114822

Kochian, L. V. (1995). Cellular mechanisms of aluminum toxicity and resistance in plants. *Annu. Rev. Plant Biol.* 46, 237–260. doi: 10.1146/annurev.pp.46.060195.001321

Li, J. Y., Liu, J., Dong, D., Jia, X., McCouch, S. R., and Kochian, L. V. (2014). Natural variation underlies alterations in Nramp aluminum transporter (NRAT1) expression and function that play a key role in rice aluminum tolerance. *Proc. Natl. Acad. Sci. U. S. A.* 111, 6503–6508. doi: 10.1073/pnas.1318975111

Li, G. Z., Wang, Z. Q., Yokosho, K., Ding, B., Fan, W., Gong, Q. Q., et al. (2018). Transcription factor WRKY22 promotes aluminum tolerance via activation of OsFRDL4 expression and enhancement of citrate secretion in rice (Oryza sativa). *New Phytol.* 219, 149–162. doi: 10.1111/nph.15143

Lin, Y. A., Zhang, C. L., Lan, H., Gao, S. B., Liu, H. L., Liu, J., et al. (2014). Validation of potential reference genes for qPCR in maize across abiotic stresses, hormone treatments, and tissue types. *PloS One* 9, e95445. doi: 10.1371/journal.pone.0095445

Liu, M. Y., Chen, W. W., Xu, J. M., Fan, W., Yang, J. L., and Zheng, S. J. (2013). The role of *VuMATE1* expression in aluminium-inducible citrate secretion in rice bean (*Vigna umbellata*) roots. *J. Exp. Bot.* 64, 1795–1804. doi: 10.1093/jxb/ert039

Lou, H. Q., Fan, W., Jin, J. F., Xu, J. M., Chen, W. W., Yang, J. L., et al. (2019). A NAC-type transcription factor confers aluminium resistance by regulating cell wall-associated receptor kinase 1 and cell wall pectin. *Plant Cell Environ.* 43, 463–478. doi: 10.1111/pce.13676

Lu, M., Wang, Z., Fu, S., Yang, G., Shi, M., Lu, Y., et al. (2017). Functional characterization of the *SbNrat1* gene in sorghum. *Plant Sci.* 262, 18–23. doi: 10.1016/j.plantsci.2017.05.010

Ma, J. F., and Furukawa, J. (2003). Recent progress in the research of external Al detoxification in higher plants: a minireview. *J. Inorg. Biochem.* 97, 46–51. doi: 10.1016/s0162-0134(03)00245-9

Ma, J. F., Hiradate, S., Nomoto, K., Iwashlta, T., and Matsumoto, H. (1997). Internal detoxification mechanism of Al in hydrangea (identification of Al form in the leaves). *Plant Physiol.* 113, 1033–1039. doi: 10.1104/pp.113.4.1033

Ma, Q., Yi, R., Li, L., Liang, Z., Zeng, T., Zhang, Y., et al. (2018). *GsMATE* encoding a multidrug and toxic compound extrusion transporter enhances aluminum tolerance in. *Arabidopsis Thaliana BMC Plant Biol.* 18, 212. doi: 10.1186/s12870-018-1397-z

Ma, J. F. (2000). Role of organic acids in detoxification of aluminum in higher plants. *Plant Cell Physiol.* 41, 383–390. doi: 10.1093/pcp/41.4.383

Matsumoto, H., and Motoda, H. (2012). Aluminum toxicity recovery processes in root apices. Possible association with oxidative stress. *Plant Sci.* 185–186, 1–8. doi: 10.1016/j.plantsci.2011.07.019

Nakano, Y., and Asada, K. (1981). Hydrogen peroxide is pcavenged by ascorbate-specific peroxidase in spinach chloroplasts. *Plant Cell Physiol.* 22, 867–880. doi: 10.1093/oxfordjournals.pcp.a076232

Osawa, H., and Matsumoto, H. (2001). Possible involvement of protein phosphorylation in aluminum-responsive malate efflux from wheat root apex. *Plant Physiol.* 126, 411–420. doi: 10.1104/pp.126.1.411

Panda, S. K., Sahoo, L., Katsuhara, M., and Matsumoto, H. (2013). Overexpression of alternative oxidase gene confers aluminum tolerance by altering the respiratory capacity and the response to oxidative stress in tobacco cells. *Mol. Biotechnol.* 54, 551–563. doi: 10.1007/s12033-012-9595-7

Rodriguez, R., and Redman, R. (2005). Balancing the generation and elimination of reactive oxygen species. *PNAS* 102, 3175–3176. doi: 10.1073/pnas.0500367102

Sagi, M., and Fluhr, R. (2001). Superoxide production by plant homologues of the gp91(phox) NADPH oxidase. Modulation of activity by calcium and by tobacco mosaic virus infection. *Plant Physiol.* 126, 1281–1290. doi: 10.1104/pp.126.3.1281

Sasaki, T., Yamamoto, Y., Ezaki, B., Katsuhara, M., Ahn, S. J., Ryan, P. R., et al. (2004). A wheat gene encoding an aluminum-activated malate transporter. *Plant J.* 37, 645–653. doi: 10.1111/j.1365-313X.2003.01991.x

Sasaki, T., Ryan, P. R., Delhaize, E., Hebb, D. M., Ogihara, Y., Kawaura, K., et al. (2006). Sequence upstream of the wheat (Triticum aestivum L.) ALMT1 gene and its relationship to aluminum resistance. *Plant Cell Physiol.* 47, 1343–1354. doi: 10.1093/pcp/pcl002

Šimonovičová, M., Huttová, J., Mistrík, I., Široká, B., and Tamás, L. (2004). Root growth inhibition by aluminum is probably caused by cell death due to peroxidase-mediated hydrogen peroxide production. *Protoplasma* 224, 91–98. doi: 10.1007/s00709-004-0054-6

Sun, C., Liu, L., Zhou, W., Lu, L., Jin, C., and Lin, X. (2017). Aluminum Induces Distinct Changes in the Metabolism of Reactive Oxygen and Nitrogen Species in the Roots of Two Wheat Genotypes with Different Aluminum Resistance. *J. Age Food Chem.* 65, 9419–9427. doi: 10.1021/acs.jafc.7b03386

Tamás, L., Huttova, J., Mistrik, I., Simonovicova, M., and Siroka, B. (2006). Aluminium-induced drought and oxidative stress in barley roots. *J. Plant Physiol.* 163, 781–784. doi: 10.1016/j.jplph.2005.08.012

Taylor, G. J., McDonald-Stephens, J. L., Hunter, D. B., Bertsch, P. M., Elmore, D., Rengel, Z., et al. (2000). Direct Measurement of Aluminum Uptake and Distribution in Single Cells of. *Chara Corallina Plant Physiol.* 123, 987–996. doi: 10.1104/pp.123.3.987

Tsutsui, T., Yamaji, N., and Ma, J. F. (2011). Identification of a cis-acting element of ART1, a C2H2-type zinc-finger transcription factor for aluminum tolerance in rice. *Plant Physiol.* 156, 925–931. doi: 10.1104/pp.111.175802

von Uexküll, H. R., and Mutert, E. (1995). Global extent, development and economic-impact of acid soils. *Plant Soil* 171, 1–15. doi: 10.1007/bf00009558

Wang, Y., Li, R., Li, D., Jia, X., Zhou, D., Li, J., et al. (2017). NIP1;2 is a plasma membrane-localized transporter mediating aluminum uptake, translocation, and tolerance in Arabidopsis. *Proc. Natl. Acad. Sci. U. S. A.* 114, 5047–5052. doi: 10.1073/pnas.1618557114

Wu, D., Shen, H., Yokawa, K., and Baluska, F. (2014). Alleviation of aluminium-induced cell rigidity by overexpression of OsPIN2 in rice roots. *J. Exp. Bot.* 65, 5305–5315. doi: 10.1093/jxb/eru292

Wu, Y. S., Yang, Z. L., How, J. Y., Xu, H. N., Chen, L. M., and Li, K. Z. (2017). Overexpression of a peroxidase gene (AtPrx64) of *Arabidopsis thaliana in* tobacco improves plant's tolerance to aluminum stress. *Plant Mol. Biol.* 95, 157–168. doi: 10.1007/s11103-017-0644-2

Xia, J., Yamaji, N., and Ma, J. F. (2013). A plasma membrane-localized small peptide is involved in rice aluminum tolerance. *Plant J.* 76, 345–355. doi: 10.1111/tpj.12296

Xu, F. J., Li, G., Jin, C. W., Liu, W. J., Zhang, S. S., Zhang, Y. S., et al. (2012). Aluminum-induced changes in reactive oxygen species accumulation, lipid peroxidation and antioxidant capacity in wheat root tips. *Biol. Plant* 51, 89–96. doi: 10.1007/s10535-012-0021-6

Xu, L. M., Liu, W., Cui, B. M., Wang, N., Ding, J. Z., Liu, C., et al. (2017). Aluminium Tolerance Assessment of 141 Maize Germplasms in a Solution Culture. *Universal J. Agric. Res.* 5, 1–9. doi: 10.13189/ujar.2017.050101

Yamaji, N., Huang, C. F., Nagao, S., Yano, M., Sato, Y., Nagamura, Y., et al. (2009). A zinc finger transcription factor ART1 regulates multiple genes implicated in aluminum tolerance in rice. *Plant Cell.* 21, 3339–3349. doi: 10.1105/tpc.109.070771

Yamamoto, Y., Kobayashi, Y., and Matsumoto, H. (2001). Lipid peroxidation is an early symptom triggered by aluminum, but not the primary cause of elongation inhibition in pea roots. *Plant Physiol.* 125, 199–208. doi: 10.1104/pp.125.1.199

Yamamoto, Y., Kobayashi, Y., Devi, S. R., Rikiishi, S., and Matsumoto, H. (2003). Oxidative stress triggered by aluminum in plant roots. *Plant Soil* 255, 239–243. doi: 10.1023/A:1026127803156

Yu, Y., Zhou, W., Zhou, K., Liu, W., Liang, X., Chen, Y., et al. (2018). Polyamines modulate aluminum-induced oxidative stress differently by inducing or reducing H2O2 production in wheat. *Chemosphere* 212, 645–653. doi: 10.1016/j.chemosphere.2018.08.133

Zhang, Y. H., Wang, E. M., Zhao, T. F., Wang, Q. Q., and Chen, L. J. (2018). Characteristics of Chlorophyll Fluorescence and Antioxidant-Oxidant Balance in PEPC and PPDK Transgenic Rice under Aluminum Stress. *Russian J. Plant Physiol.* 65, 49–56. doi: 10.1134/s1021443718010211

Zheng, X., and Huystee, R. B. V. (1992). Peroxidase regulated elongation of segments from peanut hypocotyls. *Plant Sci.* 81, 47–56. doi: 10.1016/0168-9452(92)90023-F

Zheng, S. J., and Yang, J. L. (2005). Target sites of aluminum phytotoxicity. *Biol. Plant.* 49, 321–331. doi: 10.1007/s10535-005-0001-1

Zhu, X. F., Shi, Y. Z., Lei, G. J., Fry, S. C., Zhang, B. C., Zhou, Y. H., et al. (2012). *XTH31*, encoding an in vitro XEH/XET-active enzyme, regulates aluminum sensitivity by modulating in vivo XET action, cell wall xyloglucan content, and aluminum binding capacity in. *Arabidopsis Plant Cell.* 24, 4731–4747. doi: 10.1105/tpc.112.106039

Zhu, X. F., Wan, J. X., Sun, Y., Shi, Y. Z., Braam, J., Li, G. X., et al. (2014). Xyloglucan Endotransglucosylase-Hydrolase17 Interacts with Xyloglucan Endotransglucosylase-Hydrolase31 to Confer Xyloglucan Endotransglucosylase Action and Affect Aluminum Sensitivity in Arabidopsis. *Plant Physiol.* 165, 1566–1574. doi: 10.1104/pp.114.243790

Conflict of Interest: The authors declare that the research was conducted in the absence of any commercial or financial relationships that could be construed as a potential conflict of interest.

frontiers in Plant Science

ORIGINAL RESEARCH
published: 03 September 2020
doi: 10.3389/fpls.2020.565647

Seed Priming Improved Antioxidant Defense System and Alleviated Ni-Induced Adversities in Rice Seedlings Under N, P, or K Deprivation

Fahad Khan[1†], *Saddam Hussain*[1,2†], *Sehrish Khan*[3] *and Mingjian Geng*[1*]

[1] Microelement Research Center, College of Resources and Environment, Huazhong Agricultural University, Wuhan, China, [2] Department of Agronomy, University of Agriculture, Faisalabad, Pakistan, [3] Department of Environmental Sciences, University of Peshawar, Peshawar, Pakistan

OPEN ACCESS

Edited by:
Rafaqat Ali Gill,
Chinese Academy of Agricultural Sciences, China

Reviewed by:
Samiksha Singh,
University of Allahabad, India
Theodore Mulembo Mwamba,
Zhejiang University, China

***Correspondence:**
Mingjian Geng
mjgeng@mail.hzau.edu.cn

[†]These authors have contributed equally to this work

Specialty section:
This article was submitted to Plant Nutrition, a section of the journal Frontiers in Plant Science

Received: 25 May 2020
Accepted: 17 August 2020
Published: 03 September 2020

Citation:
Khan F, Hussain S, Khan S and Geng M (2020) Seed Priming Improved Antioxidant Defense System and Alleviated Ni-Induced Adversities in Rice Seedlings Under N, P, or K Deprivation. Front. Plant Sci. 11:565647. doi: 10.3389/fpls.2020.565647

Excess nickel (Ni) concentration in the growing medium severely hampers the plant growth by disturbing oxidative metabolism and nutrient status. The present study was carried out to investigate the individual and interactive effects of Ni toxicity (0.25 mM NiSO4.6H2O) and nutrient deprivation (no-N, no-P, or no-K) on growth, oxidative metabolism, and nutrient uptake in primed and non-primed rice seedlings. Rice seed was primed with distilled water (hydropriming), selenium (5 mg L^{-1}), or salicylic acid (100 mg L^{-1}). The Ni toxicity and deprivation of N, P, or K posed negative effects on the establishment of rice seedlings. The shoot length and fresh biomass were severely reduced by Ni toxicity and nutrient stresses; the minimum shoot growth was recorded for rice seedlings grown under Ni toxicity and no-N stress. The Ni toxicity reduced the root fresh biomass but did not significantly affect the root length of N-deprived seedlings. The rice seedlings with no-P or no-K recorded similar root fresh biomass compared with those grown with sufficient nutrient supply. The Ni toxicity alone or in combination with nutrient stresses triggered the production of reactive oxygen species (ROS) and caused lipid peroxidation in rice seedlings. Among antioxidants, only glutathione reductase and vitamin E were significantly increased by Ni toxicity under different nutrient stress treatments. The Ni toxicity also reduced the concentrations of N particularly in shoot of rice seedlings. The N-deprived (no-N) seedlings recorded maximum Ni concentration in shoot, while K-deprived (no-K) seedlings showed higher Ni concentrations in root. Seed priming with selenium or salicylic acid was effective to alleviate the detrimental effects of Ni toxicity and/or nutrient stresses on rice seedlings. The better growth and greater stress tolerance of primed seedlings was coordinately attributed to lower ROS production, higher membrane stability, strong antioxidative defense system, and maintenance of mineral nutrient status.

Keywords: seed priming, nutrient deprivation, nickel toxicity, oxidative damage, antioxidants

INTRODUCTION

Nickel (Ni) toxicity in plants is emerging as a worldwide problem threatening the agricultural sustainability. Generally, Ni is added into the environment by human activities like fossil fuel burning, metal mining, smelting, vehicle emissions, wastes disposal, and crop fertilization (Salt et al., 2000; Hussain et al., 2020a). Extremely high Ni concentrations in soil make the cultivatable land unfit for the cultivation of crops (Duarte et al., 2008). Higher range of Ni in the growing medium causes various changes in the different physiological and metabolic processes of plants, and leads to assorted toxicity indications (Kumar et al., 2007; Gajewska et al., 2009; Gajewska et al., 2013). Gajewska et al. (2013) found severe reductions in shoot and root growth of wheat under Ni stress, which were attributed restriction of cell division and elongation (Gajewska et al., 2009). Nickel stress may also reduce dry matter accumulation in different plant parts thus reduces the total plant biomass (Rao and Sresty, 2000; Pandey and Sharma, 2002; Rizwan et al., 2019).

Increasing evidences have suggested that the Ni toxicity in plants is also associated with the oxidative stress through increase in the production of reactive oxygen species (ROS) like hydrogen peroxide (H_2O_2), hydroxyl ion (OH^-), and super and nitric oxides anions (Galan et al., 2001; Gajewska et al., 2006; Hao et al., 2006; Gajewska and Sklodowska, 2007). These ROS may damage plant cell membrane, proteins, DNA and lipids, and cause lipid per oxidation (Bal and Kasprzak, 2002; Khaliq et al., 2015; Chen et al., 2016; Hussain et al., 2020b). Rao and Sresty (2000) observed increased production of a lipid peroxidation [malondialdehyde content (MDA)] in Ni exposed pigeon pea plants. Maize exposure to Ni stress significantly increased H_2O_2 production and antioxidants activity in the leaves (Kumar et al., 2007). Nickel cannot directly induce the production of ROS because it is not a redox-active metal, but indirectly it may play vital role in activation of antioxidant enzymes (Pandey and Sharma, 2002; Gajewska and Sklodowska, 2005) like superoxide dismutase (SOD), peroxidase (POD), catalase (CAT), glutathione peroxidase (GPX), and glutathione reductase (GR) (Gajewska and Sklodowska, 2005). Conversely, Zhao et al. (2008) and Gajewska and Sklodowska (2007) observed that Ni stress decreased the activities of several antioxidant enzymes and triggered the ROS accumulation and oxidative stress.

Imbalanced nutrient uptake is also a major response of plants in Ni toxic conditions (Pandey and Sharma, 2002; Ouzounidou et al., 2006; Hussain et al., 2020a). Gajewska et al. (2013) found the decrease in the concentration of nutrients in Ni exposed wheat, as Ni toxicity restricts nutrient uptake and causes nutrient deficiency (Chen et al., 2009) ultimately leading to disturbed physiological and biochemical processes in plant (Gajewska et al., 2006; Rizwan et al., 2019).

Seed priming is a method that manages the level of hydration within seeds and regulates the metabolic events in seed required for germination. Earlier researches have demonstrated that germination, seedling vigor, and survival of rice seedlings were enhanced by seed priming under normal and adverse soil and climatic conditions (Jisha et al., 2013; Hussain et al., 2016a; Hussain et al., 2016b; Hussain et al., 2016c; Zheng et al., 2016). Selenium (Se) is an important element, reported for the detoxification of toxic heavy metals in plants (Hasanuzzaman et al., 2010; Zembala et al., 2010), while salicylic acid (SA) is a phenolic compound and considered as an important growth regulator in the plants (Hayat et al., 2010). The positive effects of both Se and SA in plants under different abiotic stresses have been well reported (Sun et al., 2010; Hayat et al., 2010; Hasanuzzaman et al., 2010; Cui et al., 2012; Kumar et al., 2012; Gajewska et al., 2013). In our recent investigations, we found that Se and SA priming enhanced the rice tolerance against different stress factors including chilling, submergence, nutrient deprivation, and lead toxicity (Hussain et al., 2016a; Hussain et al., 2016b; Hussain et al., 2016c; Khan et al., 2018). However, little work has been done on the role of seed priming in enhancing the plant tolerance against combined Ni toxicity and nutrient deprivation. It was hypothesized that the toxic effects of Ni will be different with the supply of N, P, or K, and that the behavior of primed and non-primed rice seedlings regarding growth and oxidative metabolism will be variable under these stress factors. The present study was carried out to investigate the individual and interactive effects of Ni toxicity and N, P, or K-deprivation on growth, ROS production, antioxidant defense system, and nutrient homeostasis in primed and non-primed rice seedlings grown in hydroponic culture experiment.

MATERIAL AND METHODS

Growth Conditions, Treatments, and Experimental Set Up

Inbred rice cultivar "Huanghuazhan" seedlings were cultivated in plastic pots containing nutrient solution (pH: 6.6 ± 0.2) in a controlled growth chamber. The conditions of the growth chamber during the course of study were set as; temperature (day/night): 30/25°C, light intensity: 25,000 Lx, light period: 12 h; and humidity: 60%. Seed was treated with distilled water (hydropriming; HP), selenium (Se: 5 mg L^{-1}), and salicylic acid (SA: 100 mg L^{-1}) following standard procedure (Hussain et al., 2015; Hussain et al., 2016a; Hussain et al., 2016b). The Ni stress was applied through 0.25 mM NiSO4.6H2O from the start of experiment. The nutrient treatments were divided into four different groups as, sufficient nutrient supply (All nutrient), no-N (N deprivation), no-P (P deprivation), and no-K (K deprivation). The Hoagland's nutrient solution was used according to the recommendation of International Rice Research Institute (Yoshida et al., 1976), with some modifications as per treatment, as mentioned in our previous investigations (Hussain et al., 2016b; Khan et al., 2018). All the nutrients were refreshed after every alternate day. Plastic pots with 4 L of solution and a floating board with four separated sections (for different priming treatments) were used, and twenty seeds of each treatment were separately sown on the net attached with the floating board. All the treatments were arranged in completely randomized design (CRD) with three replications.

Observations

Eighteen days old rice seedlings were harvested and morphological growth attributes viz., shoot length, root length and their fresh weights were recorded using at least five seedlings randomly selected from each replicate. The maximum shoot and root lengths of the rice seedlings were recording using measuring tape, while digital electric balance was used for recording fresh weight. Fresh leaf samples were stored in -80°C refrigerator for analysis of different biochemical attributes.

The H_2O_2 and MDA contents (μM g^{-1} fresh weight) in the leaves were determined by the procedure of Patterson et al. (1984) and Bailly et al. (1996), respectively. Whereas, commercial O2•– assay kit-A052, OH– assay kit-A018, XOD assay kit-A034, and MAO assay kit-A002 were used for determination of superoxide anion radical (O2•– as U g^{-1} protein) content, hydroxyl ion (OH– as U mg^{-1} protein) content, xanthine oxidase (XOD as U g^{-1} protein) activity, and monoamine oxidase (MAO as U mg^{-1} protein) activity in the rice leaves, respectively.

The antioxidant activities/levels of SOD (U mg^{-1} protein), CAT (U mg^{-1} protein), POD (U mg^{-1} protein), GR (U g^{-1} protein), GPX (U mg^{-1} protein), GSH (reduced glutathione; μM g^{-1} protein), Vc (vitamin C; μg mg^{-1} protein), and Ve (vitamin E; μg g^{-1} tissue fresh weight in rice were recorded using commercial kits A001, A007-2, A084-3, A062, A005, A006, A009, and A008, respectively (Hussain et al., 2016a; Hussain et al., 2016b; Khan et al., 2018; Hussain et al., 2020b). All the kits used in the present study were purchased from Nanjing Jiancheng Bioengineering Institute, China (www.njjcbio.com), and were strictly used as per manufacturer's instructions. For determination of N, P, and K in shoots and roots, rice dry seedlings were digested with sulfuric acid. The N and P concentrations in the plant tissues were recorded by a continuous-flow injection analyzer, while K concentrations were analyzed using a flame photometer. For Ni determination, roots and shoots were digested in HNO3:HClO4 at 5:1 (v/v), and samples were analyzed using ICP-MS (Inductively coupled plasma mass spectrometry) technique.

Statistical Analysis

The replicated data were analyzed using analysis of variance (ANOVA) through Statistix 8.1 software. The treatment means were compared according to Tukey's HSD ($P \leq 0.05$) test.

RESULTS

Seedling Growth

Data regarding rice seedling growth as affected by Ni toxicity, seed priming and different nutrient stress treatments are shown in **Figure 1**. Compared with sufficient nutrient supply, shoot length, and shoot fresh weight were significantly ($p < 0.05$)

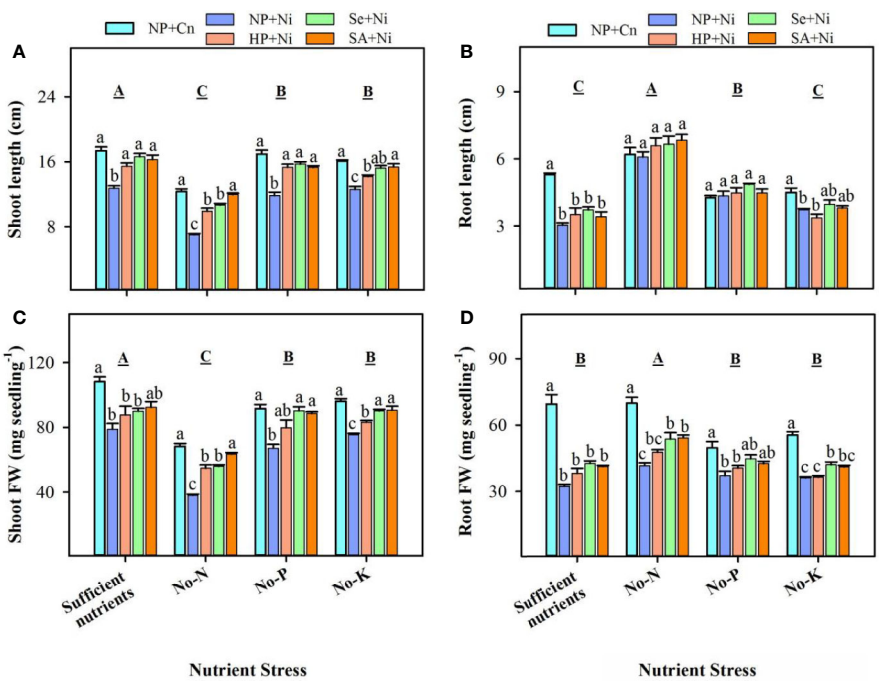

FIGURE 1 | Shoot length **(A)**, root length **(B)**, shoot fresh weight **(C)**, and root fresh weight **(D)** of primed and non-primed rice seedlings as influenced by different nutrient stress treatments and Ni toxicity. Vertical bars above mean indicate standard error of three replicates. Small alphabetical letters (a, b, c…) above mean bars show the differences among treatments within a specific nutrient stress treatment, while the capital alphabetical letter (A, B, C…) show the difference among nutrient stress treatments. NP+Cn, no priming and no Ni toxicity; NP+Ni, no priming with Ni toxicity; HP+Ni, hydropriming and Ni toxicity; Se+Ni, selenium priming and Ni toxicity; SA+Ni, salicylic acid priming and Ni toxicity; No-N, no nitrogen; No-P, no phosphorus; No-K, no potassium.

reduced in no-N, no-P, and no-K treatments; the minimum shoot growth was noted in no-N treatment. Root length was considerably increased in no-P or no-N treatments, but no-K did not significantly ($p > 0.05$) affect the root length. Rice seedlings with no-N recorded significantly ($p < 0.05$) higher root fresh weight compared with all other nutrient stress treatments. Exposure of Ni toxicity in non-primed seedlings (NP + Ni) recorded significantly ($p < 0.05$) lower shoot length and shoot fresh weight, compared with NP+Cn under all the nutrient stress treatments. The Ni induced reductions in shoot growth were more apparent in no-N treatment. The Ni toxicity did not significantly ($p > 0.05$) affect the root length of rice in no-N or no-P treatments, but root length was significantly ($p < 0.05$) reduced by Ni toxicity in rice seedlings with sufficient nutrient supply. Root fresh weight was significantly ($p < 0.05$) reduced by Ni toxicity in all nutrient stress treatments. Seed priming was found to alleviate the detrimental effects of Ni toxicity particularly on shoot growth, therefore, Se+Ni, and SA+Ni treatments recorded significantly ($p < 0.05$) higher shoot length and shoot fresh weight under no-N, no-P, and no-K treatments, compared with NP+Ni. Seed priming didn't significantly ($p > 0.05$) affect the root length; however, root fresh weight of rice in Se+Ni and SA+Ni under no-N, and Se+Ni under no-K was significantly ($p < 0.05$) higher with respect to NP+Ni (**Figure 1**).

Accumulation of ROS and Lipid Peroxidation Rate

Pronounced variations in the accumulation of ROS and lipid peroxidation rate in non-primed and primed rice seedlings were recorded under the influence of Ni toxicity and different nutrient stress treatments (**Figure 2**). The rate of lipid peroxidation (MDA contents) and the accumulation of O2•–, OH–, and H_2O_2 were significantly ($p < 0.05$) increased under no-N, no-P, and no-K treatments compared with sufficient nutrient supply (**Figure 2**). Nickel toxicity also significantly ($p < 0.05$) enhanced the accumulation of ROS and MDA contents in rice leaves regardless of the nutrient stress treatment. Seed priming was effective in decreasing ROS accumulation as well as lipid peroxidation in rice leaves under Ni toxicity and different nutrient stress treatments (**Figure 2**). Therefore, the accumulations of ROS and MDA were significantly ($p < 0.05$) lower in HP+Ni, Se+Ni, SA+Ni compared with NP+Ni under all nutrient stress treatments (**Figure 2**).

Activities of Xanthine Oxidase and Monoamine Oxidase

The activities of XOD and MAO in leaves of non-primed and primed rice seedlings significantly ($p < 0.05$) varied in response to Ni toxicity and nutrient stresses (**Figure 3**). Compared with

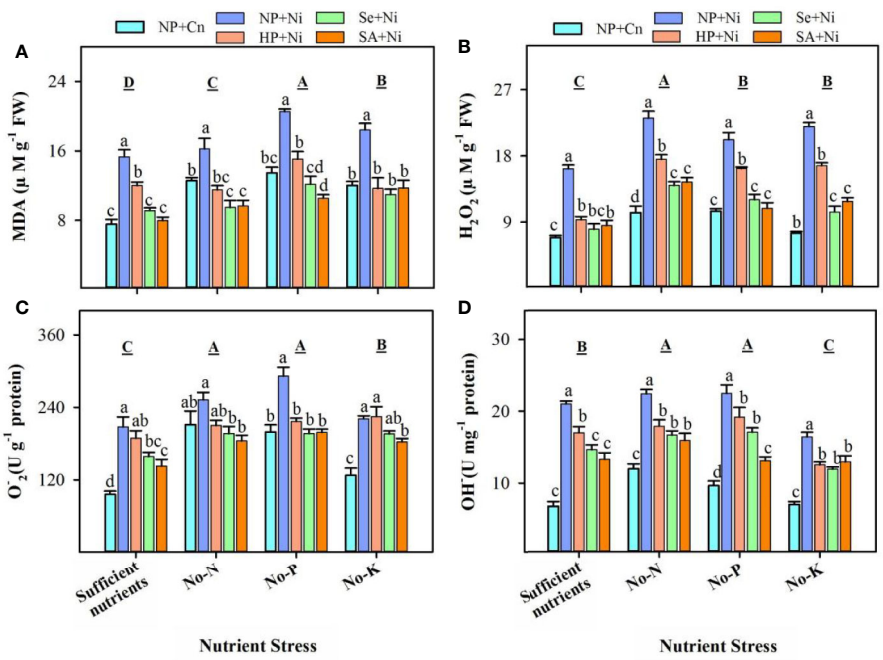

FIGURE 2 | The accumulation of reactive oxygen species and lipid peroxidation rate in the leaves of primed and non-primed rice seedlings as influenced by different nutrient stress treatments and Ni toxicity. **(A)** Malondialdehyde (MDA) content, **(B)** hydrogen peroxide (H_2O_2) content, **(C)** superoxide anion radical ($O_2^{\bullet}$–) content, **(D)** hydroxyl ion (OH^-) content. Details on statistical analysis and treatments are given in **Figure 1**. "The 1 U of OH^- was the amount required to reduce 1 M of H_2O_2 in the reaction mixture per minute at 37°C", while "1 U of O_2^- was equivalent of the value required to inhibit superoxide anion by 1 mg of Vc for 40 min at 37°C".

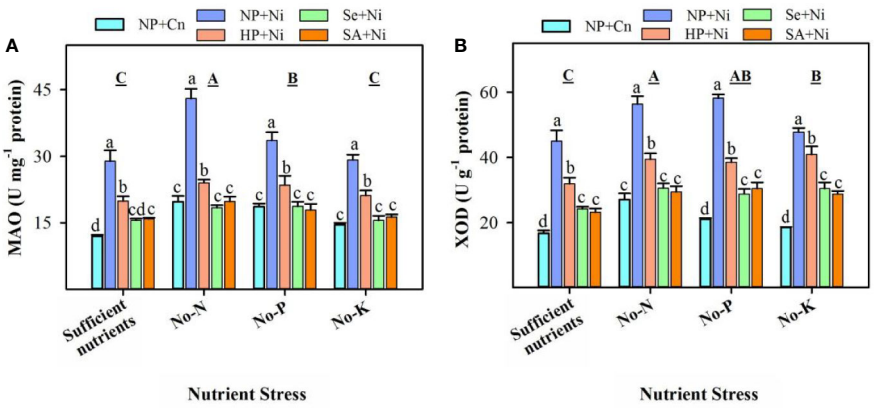

FIGURE 3 | Activities of monoamine oxidase (MAO) **(A)** and xanthine oxidase (XOD) **(B)** in the leaves of primed and non-primed rice seedlings as influenced by different nutrient stress treatments and Ni toxicity. Details on statistical analysis and treatments are given in **Figure 1**. "For MAO, 1 U was defined as the amount of enzyme that increased the absorbance by 0.01 at 37°C in 1 hour; while "for XOD, it was defined as 1 g of protein required to transform 1 μM of hypoxanthine to xanthine in 1 min at 37°C".

sufficient nutrient supply, MAO activities were significantly ($p < 0.05$) enhanced in no-N and no-P treatments, while XOD activities were increased significantly ($p < 0.05$) under the deprivation of N, P, or K (**Figure 3**). Among different nutrient stress treatments, the highest MAO and XOD activities were observed in rice seedlings grown in no-N. Effects of Ni toxicity were apparent in enhancing the MAO and XOD activities; NP+Ni recorded significantly higher activities of both these enzymes compared with NP+Cn under different nutrient stress treatments (**Figure 3**). The Ni-induced increases in MAO and XOD activities were more in no-P or no-N treatments. The activities of XOD and MAO in rice seedling were significantly ($p < 0.05$) decreased by seed priming. Compared to NP+Ni, all seed priming treatments significantly decreased the MAO and XOD activities in leaves under different nutrient stress treatments; however, Se+Ni and SA+Ni treatments were statistically ($p > 0.05$) similar, and were more effective than HP+Ni (**Figure 3**).

Enzymatic Antioxidants

Data on the activities of enzymatic antioxidants in non-primed and primed rice seedlings in response to Ni toxicity and nutrient stresses are presented in **Figure 4**. Compared with sufficient nutrient supply, SOD activities remained unaffected in no-N, but significantly ($p < 0.05$) decreased in no-P or no-K treatments. The activities of CAT were significantly ($p < 0.05$) higher in no-P, but remained unchanged in no-N or no-K, compared with sufficient nutrient supply. The GPX and POD activities were significantly ($p < 0.05$) decreased in no-K, but remained unchanged in no-N with respect to sufficient nutrient supply. The activities of GR were significantly ($p < 0.05$) decreased in no-N or no-P treatments. The Ni toxicity considerably affected the activities of enzymatic antioxidants, however, such effect varied with enzyme and nutrient stress. The SOD activity was unaffected, while GR activity was significantly ($p < 0.05$) increased in NP+Ni than NP+Cn, under all nutrient stress treatments. The CAT activity was significantly ($p < 0.05$) higher in NP+Ni under no-K or sufficient nutrient supply, while remained statistically similar ($p > 0.05$) to NP+Cn under no-N or no-P. Conversely, the NP+Ni significantly ($p < 0.05$) decreased the activity of POD under no-N or no-P, but it did not affect POD under no-K or sufficient nutrient supply compared to NP+Cn. The GPX activity was increased in NP+Ni under no-P, decreased under no-K, while did not change under no-N or sufficient nutrient supply, compared to NP+Cn (**Figure 4**). Seed priming (Se+Ni and SA+Ni) significantly ($p < 0.05$) increased the CAT and GR activities under different nutrient stress, compared with NP+Ni. The SOD, POD, and GPX activities were also significantly ($p < 0.05$) higher in both Se+Ni and SA+Ni treatments under no-N or no-P, compared with NP+Ni. Under no-K, Se+Ni recorded higher activities of GPX and POD compared with NP+Ni (**Figure 4**).

Non-Enzymatic Antioxidants

Compared with sufficient nutrient supply, the GSH, Vc, and Ve contents in rice seedlings were significantly ($p < 0.05$) reduced in no-N (**Figure 5**). The no-P didn't significantly ($p > 0.05$) affect GSH and Ve, but significantly ($p < 0.05$) declined the Vc concentration in rice leaves. The no-K significantly ($p < 0.05$) decreased the GSH content, but did not affect ($p > 0.05$) Vc and Ve content compared with sufficient nutrient supply (**Figure 5**). The Ni toxicity did not significantly ($p > 0.05$) alter the levels of GSH and Vc in all the nutrient stress treatments expect for GSH content in no-N. The Ve content was significantly ($p < 0.05$) increased by Ni stress (NP+Ni) under the deprivation of N, P, or K. Seed priming enhanced or at least maintained the levels of non-enzymatic antioxidants in the leaves of rice seedlings. All the seed priming treatments significantly ($p < 0.05$) enhanced the GSH content in no-P treatment, and Ve content in no-N and no-K treatments. Seed priming also significantly ($p < 0.05$) increased the Vc under sufficient nutrient supply, but did not change it under no-P, compared to NP+Ni. Significantly higher Vc contents in HP+Ni and Se+Ni under

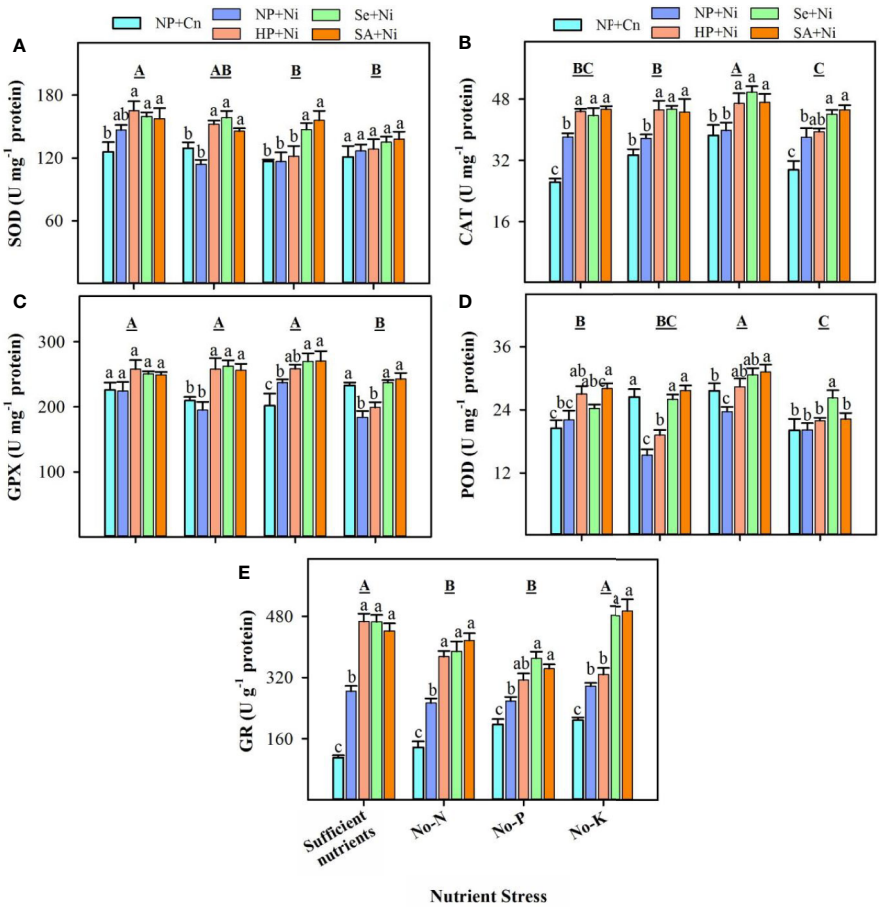

FIGURE 4 | Activities of various enzymatic antioxidants in the leaves of primed and non-primed rice seedlings as influenced by different nutrient stress treatments and Ni toxicity. **(A)** Superoxide dismutase (SOD), **(B)** catalase (CAT), **(C)** glutathione peroxidase (GPX), **(D)** peroxidase (POD), and **(E)** glutathione reductase (GR). Details on statistical analysis and treatments are given in **Figure 1**. One unit for different antioxidant enzymes was defined as follows; "I U of SOD activity was the amount of enzyme required to decrease the reference rate to 50% of maximum inhibition; 1 U of POD activity was defined as the amount of enzyme necessary for the decomposition of 1 μg substrate in 1 min at 37°C; 1 U of CAT activity was defined as the amount of enzyme required to decompose the 1 μM H_2O_2 in 1 second at 37°C; I U of GPX activity was the amount of enzyme required to oxidize 1 μM GSH in 1 minute at 37°C; 1 U of GR activity was defined as the amount of enzyme depleting 1 mM NADPH in 1 min".

no-N, and in SA+Ni under no-K were also observed compared with NP+Ni (**Figure 5**).

Macro-Nutrient Concentrations in Root and Shoot Tissues

The N concentrations in root and shoot of rice were significantly ($p < 0.05$) declined in no-N, but increased in no-K, compared with sufficient nutrient supply (**Figure 6**). The P-deprivation did not significantly ($p > 0.05$) affect the shoot N concentrations, but significantly ($p < 0.05$) increased the root N concentrations compared with sufficient nutrient supply. The P concentrations of both shoot and root in rice seedling were significantly ($p < 0.05$) decreased in no-P and no-K treatments, the shoot P concentrations were also significantly ($p < 0.05$) decreased in no-N with respect to sufficient nutrient supply. The shoot K concentration was significantly ($p < 0.05$) increased in no-N, but it was reduced in no-P or no-K treatments. The root K concentration was increased in no-N or no-P treatment, but significantly reduced in no-K compared with sufficient nutrient supply (**Figure 6**). The Ni toxicity significantly reduced both root and shoot N concentrations under all nutrient stress treatments, except for shoot N concentration in no-K treatment, compared with NP+Cn. The shoot and root P concentrations were significantly reduced by Ni toxicity in no-K and sufficient nutrients treatment. The Ni toxicity (NP+Ni) significantly decreased the shoot K concentrations in no-N or no-P treatments, while significantly increased root K concentrations in no-P or no-K treatments, compared with NP+Cn (**Figure 6**). Seed priming had positive effect on the uptake of primary macro-nutrients under different stress treatments. Compared with NP +Ni, seed priming treatments (NP+Ni, Se+Ni, SA+Ni) recorded statistically similar or higher concentration of N, P, and K in root

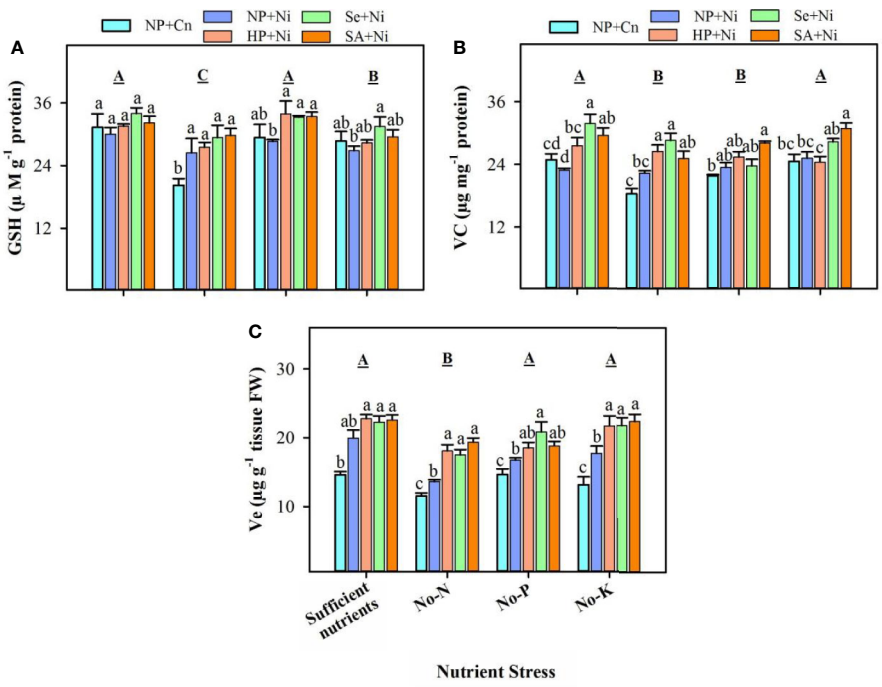

FIGURE 5 | The levels of various non-enzymatic antioxidants in the leaves of primed and non- primed rice seedlings as influenced by different nutrient stress treatments and Ni toxicity. **(A)** Reduced glutathione (GSH), **(B)** vitamin C (Vc), **(C)** vitamin E (Ve). Details on statistical analysis and treatments are given in **Figure 1**.

and shoot tissues of rice, under different nutrient stress treatments (**Figure 6**).

Nickel (Ni) Concentrations in Root and Shoot Tissues

Among different nutrient stress treatments, the Ni shoot concentrations were maximum in no-N treatment followed by no-P, while Ni root concentrations were maximum in rice seedlings with sufficient nutrient supply (**Figure 7**). The Ni concentration of shoot and root were significantly increased with application of Ni under all nutrient stress treatments. Seed priming (Se+Ni and SA+Ni) were effective to significantly decrease shoot Ni concentrations compared to NP+Ni under all nutrient stress treatments except no-P. The root Ni concentrations remained statistically similar in both primed and unprimed seedlings; only SA+Ni and HP+Ni recorded significantly lower root Ni concentrations in no-P and no-K treatments, respectively compared to NP+Ni (**Figure 7**).

DISCUSSION

Under natural conditions, multiple abiotic stresses often occur at a same time, and alter the growth of plants (Walter et al., 2012; Hussain et al., 2016b), however, the responses of plants to individual and combined stresses might be variable at physiological, biochemical, and molecular levels (Hussain et al., 2016b; Hussain et al., 2020b). The present study investigated the effects of different seed priming treatments on the growth, oxidative metabolism, and nutrient uptake in rice seedlings under individual and combined exposure of Ni toxicity and N, P, or K deprivation.

Ni Toxicity as Well N, P, or K Deprivation Triggered the Oxidative Damage in Rice Seedlings

The Ni toxicity as well as different nutrient stresses disrupted the oxidative metabolism in rice seedlings, and thus enhanced the production of ROS in rice leaves (**Figure 3**). The higher production of ROS also triggered the accumulation of MDA content and oxidative damage in rice leaves (**Figure 3A**) and ultimately reduced the growth. Although, the interactive influence of Ni and nutrient deprivation on oxidative metabolism in plants is rarely known previously, nevertheless, several studies have documented that individual application of Ni toxicity or N, P, K deficiency caused severe oxidative damage in various plants. For instance, Shin et al. (2005) documented that N, P, or K deprivation increased the accumulation of ROS in arabidopsis roots. Gajewska et al. (2006) reported that Ni toxicity in plants caused oxidative stress in wheat. In pigeon pea, Ni toxicity from 0.5 to 1.5 mM promoted the accumulation of O2•−, OH−, H_2O_2 and MDA content in both shoot and root (Rao and Sresty, 2000). Many enzymatic sources like XOD, MAO, and NADPH oxidase have also been reported to control the production of ROS under stress (Hussain et al., 2016b), in addition to non-enzymatic sources of ROS production (limitation of CO_2 fixation, photorespiration etc.). Hao et al.

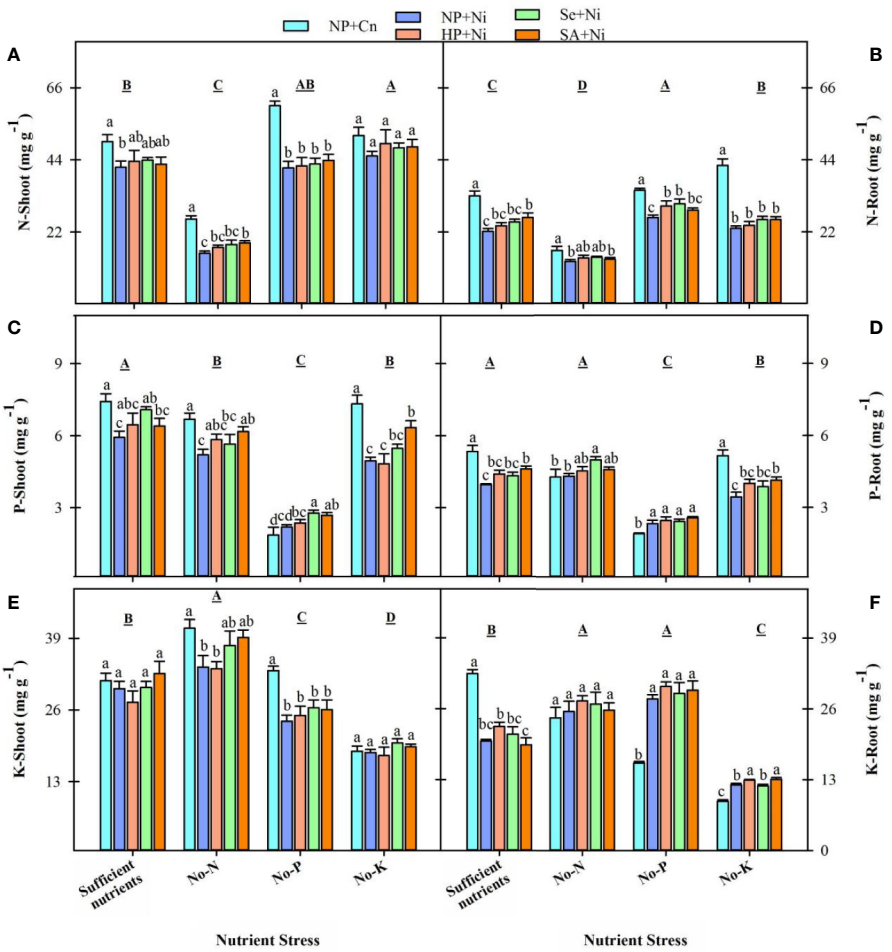

FIGURE 6 | Shoot and root concentrations of nitrogen **(A, B)**, phosphorus **(C, D)**, and potassium **(E, F)** in primed and non-primed rice seedlings as influenced by different nutrient stress treatments and Ni toxicity. Details on statistical analysis and treatments are given in **Figure 1**.

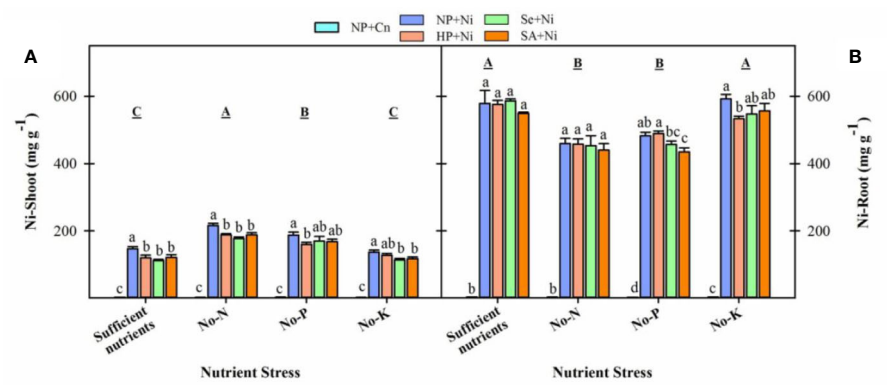

FIGURE 7 | Shoot **(A)** and root **(B)** concentrations of nickel in primed and non-primed rice seedlings as influenced by different nutrient stress treatments and Ni toxicity. Details on statistical analysis and treatments are given in **Figure 1**.

(2006) described that the Ni stress regulated the NADPH oxidase activity, which induced ROS production in the roots of 5-day-old wheat seedlings. In the present study, the activities of XOD and MAO in rice leaves were enhanced under Ni toxicity and different nutrient stresses, and activities of both these enzymes were concomitant with ROS accumulation (**Figures 2** and **3**), which indicated that XOD and MAO also contributed in the production of ROS under stress conditions. Plants overcome the excessive production of ROS through coordinated action of different enzymatic (such as SOD, CAT, POD, GPX, GR, and GST) and non-enzymatic antioxidant (such as GSH, Vc, and Ve) (Gill and Tuteja, 2010; Hasanuzzaman and Fujita, 2011; Chen et al., 2016; Hussain et al., 2016a; Hussain et al., 2016b; Hussain et al., 2020b). In the present study, the responses of different antioxidants varied with the enzyme and stress conditions. For instance, compared with NP+Cn, the SOD activity in NP+Ni was generally unaffected, the CAT activity was triggered under no-K, while the POD activity in NP+Ni was decreased under no-N or no-P. The lower activities of CAT and POD enzymes in NP+Ni under P or N-deprivation were well linked with higher oxidative damage in these treatments (**Figures 2** and **4**). Previously, differential responses of these antioxidant enzymes were observed under Ni toxicity by different researchers. For example, Gajewska and Sklodowska (2007) found that SOD and CAT activities were markedly reduced in wheat in response to 100 μM Ni treatment. Likewise, Pandey and Sharma (2002) reported that exposure of cabbage to 0.5 mM Ni for 8 days reduced the CAT and POD activities. Papadopoulos et al. (2007) found that exposure of *Hydrocharis dubia* to 0.5, 1, 2, 3, 4 mM Ni for 3 days caused reductions in the activities of SOD, POD, and CAT in leaves. In disparity, Rao and Sresty (2000) stated that activities of SOD and POD were increased at 0.5 mM Ni concentration while CAT activity was declined in 6-day-old pigeon pea seedlings. In the present study, GR activity was considerably enhanced by Ni toxicity under different nutrient stress treatments, suggesting that this enzyme was more responsive to Ni stress. Similar results regarding GR activity were also found by Rao and Sresty (2000) in pigeon pea.

Along with enzymatic antioxidants, the significant role of GSH, Vc, and Ve in the tolerance of plants to abiotic stresses has been well proven (Foyer and Noctor, 2005; Gill and Tuteja, 2010; Hussain et al., 2016a; Hussain et al., 2016b; Hussain et al., 2020b). In this study, variable response of Ve, GSH and Vc in rice leaves were detected under Ni toxicity and nutrient deprivation (**Figure 5**). Among different nutrient stresses, the accumulations of all these non-enzymatic antioxidants were significantly decreased in no-N treatments, indicating that N availability is critical for synthesis and accumulation of these molecules. Exposure of Ni stress generally triggered the Ve content, but did not alter the Vc and GSH content under all the nutrient treatments except GSH under N-deprivation (**Figure 5**). Although GR was considerably increased by Ni toxicity, minimal effect of Ni on GSH content suggests that biosynthesis of GSH might have been limited by Ni stress. Several researchers have observed that the Ni toxicity decreased the Vc and GSH concentrations, which may cause higher oxidative stress in plants (Kukkola et al., 2000; Rao and Sresty, 2000).

Seed Priming Triggered the Antioxidant Defense System and Alleviated the Stress-Evoked Adversities in Rice Seedlings

Seed priming significantly decreased the accumulation of ROS and rate of lipid peroxidation (**Figure 2**), which indicated that oxidative stress and seedling damage, induced by Ni toxicity and/or nutrient deprivation, were effectively assuaged by seed priming. Various researches on different abiotic stresses have reported the similar priming-induced effects on ROS accumulation and MDA content (Jisha et al., 2013; Hussain et al., 2016a; Hussain et al., 2016b; Zheng et al., 2016; Hussain et al., 2018; Hussain et al., 2020b). The activities of ROS producing enzymes such as, XOD and MAO were also restricted by seed priming (**Figure 3**). The SA and Se priming recorded higher activities/levels of SOD, CAT, POD, GR, GSH, Vc, and Ve under Ni toxicity and nutrient deprived conditions over no priming (**Figures 4** and **5**). The significantly higher activities/contents of these antioxidants in primed rice seedlings were associated with the lower buildup of ROS in rice leaves. All the antioxidants triggered by seed priming were effective in controlling the ROS, which are very important for inducing tolerance to abiotic stresses (Gill and Tuteja, 2010; Miller et al., 2010). Previously, many studies revealed that seed priming enhanced antioxidant levels in seed which help to cope with stress induced adversities after germination (Bailly et al., 2008; Khaliq et al., 2015; Hussain et al., 2016a; Hussain et al., 2016b).

Ni Toxicity Disrupted the Mineral Nutrient Status of Non-Primed Rice Seedlings Under Different Nutrient Stress Treatments

The Ni toxicity is well known to inhibit the nutrient (such as N, P, and K) uptake in plants (Pandey and Sharma, 2002; Ouzounidou et al., 2006). In the present study, Ni toxicity caused macro-nutrients deficiency in rice seedlings; however, the effects varied with plant parts and nutrient stress treatments (**Figure 6**). The Ni induced reductions in N, P, and K concentrations were more for shoot compared with root particularly under no-N, indicating that Ni stress mainly limited the translocation of these elements. These findings are in agreement to Brune and Deitz (1995) who also observed that Ni toxicity caused P and K deficiency in leaves and roots. Athar and Ahmad (2002) reported that Ni toxicity reduced root and shoots N content in mungbean and chickpea plants, and P content in *Helianthus annus* and *Hyptis suaveolens*, and these effects were attributed to increased activity of acid phosphatase and ATPase under Ni toxicity (Pillay et al., 1996). Heavy metals including Ni alter the functions and structure of membrane (Gajewska et al., 2006), which decrease the nutrient uptake and translocation to root and shoot. Seed priming was found to improve the uptake of N, P, and K under Ni toxicity. The growth of primed rice seedlings was significantly higher than non-primed rice seedlings (**Figure 1**), while the nutrient

concentrations were generally similar or higher in primed rice seedlings (**Figure 6**). When considering the overall nutrient content per seedlings, primed rice seedlings were able to accumulate higher quantity of nutrients in its plant parts. Previously, several researchers (Gunes et al., 2007; Shah et al., 2012; Shah et al., 2013; Ahmad et al., 2015; Khan et al., 2018) have concluded that seed priming improved uptake and translocation of mineral nutrients in plants. Ahmad et al. (2015) noted improved root and shoot concentrations of N, P, and K by seed priming with ascorbic acid and hydrogen peroxide, and attributed it to vigorous and well developed root system.

Ni Accumulation in Rice Seedlings Varied With Nutrient Stress Treatment and Seed Priming

Exposure of Ni toxicity triggered its concentrations in both plant parts of rice seedlings, nevertheless, the Ni concentrations varied greatly with N, P, or K deprivation and seed priming (**Figure 7**). Differences were also apparent between plant parts, as more Ni was accumulated in the root, which is the common tolerance mechanism of different plant species including rice to heavy metals. Interestingly, the shoot Ni concentrations were higher in no-N or no-P treatments, while root Ni concentrations were higher in treatments with no-K or sufficient nutrient supply. It might be suspected that the better seedling performance and higher tolerance in treatments with no-K or sufficient nutrient supply might also be due to the lower Ni translocation. In the present study, the total shoot and root Ni concentrations were recorded, therefore, it is not known whether N, P, or K- deprivation altered the Ni distribution between vacuolar compartments and the other parts of the cell. In the future studies, determining the effect of nutrient deprivation/deficiency on Ni concentration in different cellular compartments will provide a better understanding. The seed priming treatments generally recorded similar root concentrations, but lower shoot concentrations than non-primed treatment. Overall, the lower Ni accumulations in primed rice seedlings were reflected in the maintenance of growth characteristics and nutrient's status on the level close to the control (**Figures 1**, **6**, and **7**). The seed priming with Se and SA was found to be more effective against Ni toxicity than hydropriming. By now, a number of evidences have revealed the effectiveness of Se (Hasanuzzaman et al., 2010; Sun et al., 2010; Zembala et al., 2010; Kumar et al., 2012; Gajewska et al., 2013) and SA (Hayat et al., 2010; Cui et al., 2012) for controlling heavy metal stress in different plants.

CONCLUSIONS

Conclusively, Ni toxicity and deprivation of N, P, or K enhanced the production of ROS and caused lipid peroxidation thus, restricted the rice growth and mineral nutrient uptake. The negative effects of Ni toxicity were more with the interaction of N- or P- deprivation. However, seed priming of rice counteracted the Ni induced stress adversities in rice seedlings. The better growth and greater stress tolerance of primed rice seedlings was coordinately attributed to lower ROS production and accumulation, higher membrane stability, strong antioxidative defense system, and maintenance of mineral nutrient status.

DATA AVAILABILITY STATEMENT

The original contributions presented in the study are included in the article/supplementary material; further inquiries can be directed to the corresponding author.

AUTHOR CONTRIBUTIONS

FK: data curation, methodology, software, writing-original draft preparation. SH: conceptualization, methodology, supervision, writing—reviewing and editing. SK: software, writing—original draft preparation. MG: investigation, supervision, writing—reviewing and editing.

FUNDING

The authors are thankful to Special Fund for Agro-scientific Research in the Public Interest of China (Project No. 201103005 & 201503122) for funding this study.

REFERENCES

Ahmad, I., Basra, S. M. A., Hussain, S., Hussain, S. A., Rehman, H., Rehman, A., et al. (2015). Priming with ascorbic acid, salicylic acid and hydrogen peroxide improves seedling growth of spring maize at suboptimal temperature. *J. Environ. Agric. Sci.* 3, 14–22

Athar, R., and Ahmad, M. (2002). Heavy metal toxicity in legume microsymbiont system. *J. Plant Nutr.* 25, 369–386. doi: 10.1081/PLN-100108842

Bailly, C., Benamar, A., Corbineau, F., and Dome, D. (1996). Changes in malondialdehyde contents and in superoxide dismutase, catalase, glutathione reductase activities in sunflower seeds related to accelerated seed aging. *Physiol. Plant* 97, 104–110. doi: 10.1111/j.1399-3054.1996.tb00485.x

Bailly, C., El-Maarouf-Bouteau, H., and Corbineau, F. (2008). From intracellular signaling networks to cell death: the dual role of reactive oxygen species in seed physiology. *C. R. Biol.* 331, 806–814. doi: 10.1016/j.crvi.2008.07.022

Bal, W., and Kasprzak, K. S. (2002). Induction of oxidative DNA damage by carcinogenic metals. *Toxicol. Lett.* 127, 55–62. doi: 10.1016/S0378-4274(01)00483-0

Brune, A., and Deitz, K. J. (1995). A comparative analysis of element composition of roots and leaves of barley seedlings grown in the presence of toxic cadmium, molybdenum, nickel and zinc concentrations. *J. Plant Nutr.* 18, 853–868. doi: 10.1080/01904169509364943

Chen, C., Huang, D., and Liu, J. (2009). Functions and toxicity of nickel in plants: recent advances and future prospects. *Clean.* 37, 304–313. doi: 10.1002/clen.200800199

Chen, W., Guo, C., Hussain, S., Zhu, B., Deng, F., Xue, Y., et al. (2016). Role of xylo-oligosaccharides in protection against salinity-induced adversities in Chinese cabbage. *Environ. Sci. Pollut. Res.* 23, 1254–1264. doi: 10.1007/s11356-015-5361-2

Cui, W., Li, L., Gao, Z., Wu, H., Xie, Y., and Shen, W. (2012). Haem oxygenase-1 is involved in salicylic acid-induced alleviation of oxidative stress due to cadmium stress in Medicago sativa. *J. Exp. Bot.* 63, 695–709. doi: 10.1093/jxb/ers201

Duarte, B., Delgado, M., and Ca ador, I. (2008). The role of citric acid in cadmium and nickel uptake and translocation, in Halimione portulacoides. *Chemosphere*. 69, 836–840. doi: 10.1016/j.chemosphere.2007.05.007

Foyer, C. H., and Noctor, G. (2005). Oxidant and antioxidant signaling in plants: a re-evaluation of the concept of oxidative stress in a physiological context. *Plant Cell. Environ.* 28, 1056–1071. doi: 10.1111/j.1365-3040.2005.01327.x

Gajewska, E., and Sklodowska, M. (2005). Antioxidative responses and proline level in leaves and roots of pea plants subjected to nickel stress. *Acta Physiol. Plant* 27, 329–339. doi: 10.1007/s11738-005-0009-3

Gajewska, E., and Sklodowska, M. (2007). Effect of nickel on ROS content and antioxidative enzyme activities in wheat leaves. *Bio. Metals.* 20, 27–36. doi: 10.1007/s10534-006-9011-5

Gajewska, E., Sklodowska, M., Slaba, M., and Mazur, J. (2006). Effect of nickel on antioxidative enzyme activities, proline and chlorophyll contents in wheat shoots. *Biol. Plant* 50, 653–659. doi: 10.1007/s10535-006-0102-5

Gajewska, E., Wielanek, M., Bergier, K., and Skłodowska, M. (2009). Nickel-induced depression of nitrogen assimilation in wheat roots. *Acta Physiol. Plant* 31, 1291–1300. doi: 10.1007/s11738-009-0370-8

Gajewska, E., Drobik, D., Wielanek, M., Sekulska-Nalewajko, J., Gocławski, J., Mazur, J., et al. (2013). Alleviation of nickel toxicity in wheat (Triticum aestivum L.) seedlings by selenium supplementation. *Biological Lett.* 50 (2), 63–76.

Gajewska, E., Drobik, D., Wielanek, M., Sekulska-Nalewajko, J., Gocławski, J., Mazur, J., and Skłodowska, M. (2013). Alleviation of nickel toxicity in wheat (*Triticum aestivum* L.) seedlings by selenium supplementation. *Biological Lett.* 50 (2), 63–76.

Galan, A., García-Bermejo, L., Troyano, A., Vilaboa, N. E., Fernández, C., de Blas, E., and Aller, P.. (2001). The role of intracellular oxidation in death induction (apoptosis and necrosis) in human promonocytic cells treated with stress inducers (cadmium, heat, X- rays). *Eur. J. Cell Biol.* 80, 312–320. doi: 10.1078/0171-9335-00159

Gill, S. S., and Tuteja, N. (2010). Reactive oxygen species and antioxidant machinery in abiotic stress tolerance in crop plants. *Plant Physiol. Biochem.* 48, 909–930. doi: 10.1016/j.plaphy.2010.08.016

Gunes, A., Inal, A., Alpaslan, M., Eraslan, F., Bagci, E. G., and Cicek, N. (2007). Salicylic acid induced changes on some physiological parameters symptomatic for oxidative stress and mineral nutrition in maize (Zea mays L.) grown under salinity. *J. Plant Physiol.* 164, 728–736. doi: 10.1016/j.jplph.2005.12.009

Hao, F., Wang, X., and Chen, J. (2006). Involvement of plasma-membrane NADPH oxidase in nickel- induced oxidative stress in roots of wheat seedlings. *Plant Sci.* 170, 151–158. doi: 10.1016/j.plantsci.2005.08.014

Hasanuzzaman, M., and Fujita, M. (2011). Selenium pretreatment up regulates the antioxidant defense and methylglyoxal detoxification system and confers enhanced tolerance to drought stress in rapeseed seedlings. *Biol. Trace Element Res.* 143, 1758–1776. doi: 10.1007/s12011-011-8998-9

Hasanuzzaman, M., Anwar Hossain, M., and Fujita, M. (2010). Selenium in higher plants: physiological role, antioxidant metabolism and abiotic stress tolerance. *J. Plant Sci.* 5, 354–375. doi: 10.3923/jps.2010.354.375

Hayat, Q., Hayat, S., Irfan, M., and Ahmad, A. (2010). Effect of exogenous salicylic acid under changing environment: A review. *Environ. Exp. Bot.* 68, 14–25. doi: 10.1016/j.envexpbot.2009.08.005

Hussain, S., Zheng, M., Khan, F., Khaliq, A., Fahad, S., Peng, S., Huang, J., Cui, K., and Nie, L. (2015). Benefits of rice seed priming are offset permanently by prolonged storage and the storage conditions. *Sci. Rep.* 5 (1), 1–12.

Hussain, S., Khan, F., Hussain, H. A., and Nie, L. (2016a). Physiological and biochemical mechanisms of seed priming-induced chilling tolerance in rice cultivars. *Front. Plant Sci.* 7:116. doi: 10.3389/fpls.2016.00116

Hussain, S., Khan, F., Cao, W., Wu, L., and Geng, M. (2016b). Seed priming alters the production and detoxification of reactive oxygen intermediates in rice seedlings grown under sub-optimal temperature and nutrient supply. *Front. Plant Sci.* 7, 439. doi: 10.3389/fpls.2016.00439

Hussain, S., Yin, H., Peng, S., Khan, F. A., Khan, F., Sameeullah, M., et al. (2016c). Comparative transcriptional profiling of primed and non-primed rice seedlings under submergence stress. *Front. Plant Sci.* 7, 1125. doi: 10.3389/fpls.2016.01125

Hussain, S., Khaliq, A., Tanveer, M., Matloob, A., and Hussain, H. A. (2018). Aspirin priming circumvents the salinity-induced effects on wheat emergence and seedling growth by regulating starch metabolism and antioxidant enzyme activities. *Acta Physiol. Plant* 40, 68. doi: 10.1007/s11738-018-2644-5

Hussain, S., Khaliq, A., Noor, M. A., Tanveer, M., Hussain, H. A., Hussain, S., et al. (2020a). "Metal Toxicity and Nitrogen Metabolism in Plants: An Overview," in *Carbon and Nitrogen Cycling in Soil* (Singapore: Springer), 221–248.

Hussain, H. A., Men, S., Hussain, S., Zhang, Q., Ashraf, U., Anjum, S. A., et al. (2020b). Maize tolerance against drought and chilling stresses varied with root morphology and antioxidative defense system. *Plants* 9, 720. doi: 10.3390/plants9060720

Jisha, K. C., Vijayakumari, K., and Puthur, J. T. (2013). Seed priming for abiotic stress tolerance: An overview. *Acta Physiol. Planta.* 35, 1381–1396. doi: 10.1007/s11738-012-1186-5

Khaliq, A., Aslam, F., Matloob, A., Hussain, S., Geng, M., Wahid, A., et al. (2015). Seed priming with selenium: consequences for emergence, seedling growth, and biochemical attributes of rice. *Biol. Trace Elem. Res.* 166, 236–244. doi: 10.1007/s12011-015-0260-4

Khan, F., Hussain, S., Tanveer, M., Khan, S., Hussain, H. A., Iqbal, B., et al. (2018). Coordinated effects of lead toxicity and nutrient deprivation on growth, oxidative status, and elemental composition of primed and non-primed rice seedlings. *Environ. Sci. Pollut. Res.* 25, 21185–21194. doi: 10.1007/s11356-018-2262-1

Kukkola, E., Rautio, P., and Huttunen, S. (2000). Stress indications in copper- and nickel-exposed Scots pine seedlings. *Environ. Exp. Bot.* 43, 197–210. doi: 10.1016/S0098-8472(99)00057-X

Kumar, P., Tewari, R. K., and Sharma, P. N. (2007). Excess nickel-induced changes in antioxidative processes in maize leaves. *J. Plant Nutr. Soil Sci.* 170, 796–802. doi: 10.1002/jpln.200625126

Kumar, M., Bijo, A. J., Baghel, R. S., Reddy, C. R. K., and Jha, B. (2012). Selenium and spermine alleviate cadmium induced toxicity in the red seaweed *Gracilaria dura* by regulating antioxidants and DN A methylation. *Plant Physiol. Biochem.* 51, 129–138. doi: 10.1016/j.plaphy.2011.10.016

Miller, G. A. D., Suzuki, N., Ciftci-Yilmaz, S., and Mittler, R. O. N. (2010). Reactive oxygen species homeostasis and signalling during drought and salinity stresses. *Plant Cell Environ.* 33, 453–467. doi: 10.1111/j.1365-3040.2009.02041.x

Ouzounidou, G., Moustakas, M., Symeonidis, L., and Karataglis, S. (2006). Response of wheat seedlings to Ni stress: Effects of supplemental calcium. *Arch. Environ. Contam. Toxicol.* 50, 346–352. doi: 10.1007/s00244-005-5076-3

Pandey, N., and Sharma, C. P. (2002). Effect of heavy metals Co2+, Ni2+ and Cd2 +on growth and metabolism of cabbage. *Plant Sci.* 163, 753–758. doi: 10.1016/S0168-9452(02)00210-8

Papadopoulos, A., Prochaska, C., Papadopoulos, F., Gantidis, N., and Metaxa, E. (2007). Determination and evaluation of cadmium, copper, nickel, and zinc in agricultural soils of western Macedonia, Greece. *Environ. Manage.* 40, 719–726. doi: 10.1007/s00267-007-0073-0

Patterson, B. D., MacRae, E. A., and Ferguson, I. B. (1984). Estimation of hydrogen peroxide in plant extracts using titanium (IV). *Anal. Biochem.* 139, 487–492. doi: 10.1016/0003-2697(84)90039-3

Pillay, S. V., Rao, V. S., and Rao, K. V. N. (1996). Effect of nickel toxicity in *Hyptis suareeolens* (L.) Poit and Helianthus annuus L. *Indian J. Plant Physiol.* 1, 153–156.

Rao, K. V. M., and Sresty, T. V. (2000). Antioxidative parameters in the seedlings of pigeonpea (*Cajanus cajan* (L.) Millspaugh) in response to Zn and Ni stresses. *Plant Sci.* 157, 113–128. doi: 10.1016/S0168-9452(00)00273-9

Rizwan, M., Mostofa, M. G., Ahmad, M. Z., Zhou, Y., Adeel, M., Mehmood, S., et al. (2019). Hydrogen sulfide enhances rice tolerance to nickel through the prevention of chloroplast damage and the improvement of nitrogen metabolism under excessive nickel. *Plant Physiol. Biochem.* 138, 100–111. doi: 10.1016/j.plaphy.2019.02.023

Salt, D. E., Prince, R. C., Pickering, I. J., and Raskin, I. (2000). *In Phytoremediation of Contaminated Soil and Water*. Eds. N. Terry and G. Banuelos (Boca Raton, FL: Lewis Publishers), 189–200.

Shah, H., Jalwat, T., Arif, M., and Miraj, G. (2012). Seed priming improves early seedling growth and nutrient uptake in mungbean. *J. Plant Nutr.* 35, 805–816. doi: 10.1080/01904167.2012.663436

Shah, Z., Haq, I. U., Rehman, A., Khan, A., and Afzal, M. (2013). Soil amendments and seed priming influence nutrients uptake, soil properties, yield and yield

components of wheat (*Triticum aestivum* L.) in alkali soils. *Soil Sci. Plant Nutr.* 59 (2), 262–270. doi: 10.1080/00380768.2012.762634

Shin, R., Berg, R. H., and Schachtman, D. P. (2005). Reactive oxygen species and root hairs in Arabidopsis root response to nitrogen, phosphorus and potassium deficiency. *Plant Cell Physiol.* 46, 1350–1357. doi: 10.1093/pcp/pci145

Sun, H. W., Ha, S. J., Liang, X., and Kang, W. J. (2010). Protective role of selenium on garlic growth under cadmium stress. *Commun. Soil Sci. Plant Anal.* 41, 1195–1204. doi: 10.1080/00103621003721395

Walter, J., Jentsch, A., Beierkuhnlein, C., and Kreyling, J. (2012). Ecological stress memory and cross stress tolerance in plants in the face of climate extremes. *Environ. Exp. Bot.* 94, 3–8. doi: 10.1016/j.envexpbot.2012.02.009

Yoshida, S., Forno, D. A., Cook, J. H., and Gomez, K. A. (1976). *Laboratory Manual for Physiological Studies of Rice. 3rd ed.* (Los Banos, Philippines: The International Rice Research Institute), 61–66.

Zembala, M., Filek, M., Walas, S., Mrowiec, H., Kornas, A., Miszalski, Z., et al. (2010). Effect of selenium on macro- and microelement distribution and physiological parameters of rape and wheat seedlings exposed to cadmium stress. *Plant Soil.* 329 (1-2), 457–468. doi: 10.1007/s11104-009-0171-2

Zhao, J., Shi, G., and Yuan, Q. (2008). Polyamines content and physiological and biochemical responses to ladder concentration of nickel stress in Hydrocharis dubia (Bl.) Backer leaves. *BioMetals.* 21, 665–674.

Zheng, M., Tao, Y., Hussain, S., Jiang, Q., Peng, S., and Huang, J. (2016). Seed priming in dry direct- seeded rice: consequences for emergence, seedling growth and associated metabolic events under drought stress. *Plant Growth Regul.* 78, 167–178. doi: 10.1007/s10725-015-0083-5

Conflict of Interest: The authors declare that the research was conducted in the absence of any commercial or financial relationships that could be construed as a potential conflict of interest.

frontiers in Plant Science

ORIGINAL RESEARCH
published: 09 September 2020
doi: 10.3389/fpls.2020.559059

Novel Insights Into the Hyperaccumulation Syndrome in *Pycnandra* (Sapotaceae)

Sandrine Isnard[1,2], Laurent L'Huillier[3], Adrian L. D. Paul[4], Jérôme Munzinger[1], Bruno Fogliani[3,5], Guillaume Echevarria[4,6], Peter D. Erskine[4], Vidiro Gei[4], Tanguy Jaffré[1,2] and Antony van der Ent[4,6]*

[1] AMAP, Université Montpellier, IRD, CIRAD CNRS, INRAE, Montpellier, France, [2] AMAP, IRD, Herbier de Nouvelle-Calédonie, Nouméa, New Caledonia, [3] Institut Agronomique néo-Calédonien (IAC), Equipe ARBOREAL (AgricultuRe BiOdiveRsité Et vAlorisation), Paita, New Caledonia, [4] Centre for Mined Land Rehabilitation, Sustainable Minerals Institute, The University of Queensland, St Lucia, QLD, Australia, [5] Institute of Exact and Applied Sciences (ISEA), Université de la Nouvelle-Calédonie, Nouméa, New Caledonia, [6] Université de Lorraine – INRAE, Laboratoire Sols et Environnement, Vandoeuvre-lès-Nancy, France

The discovery of nickel hyperaccumulation, in *Pycnandra acuminata*, was the start of a global quest in this fascinating phenomenon. Despite recent advances in the physiology and molecular genetics of hyperaccumulation, the mechanisms and tolerance of Ni accumulation in the most extreme example reported to date, *P. acuminata*, remains enigmatic. We conducted a hydroponic experiment to establish Ni tolerance levels and translocation patterns in roots and shoots of *P. acuminata*, and analyzed elemental partitioning to gain insights into Ni regulation. We combined a phylogeny and foliar Ni concentrations to assess the incidence of hyperaccumulation within the genus *Pycnandra*. Hydroponic dosing experiments revealed that *P. acuminata* can resist extreme Ni concentrations in solution (up to 3,000 μM), and dosing at 100 μM Ni was beneficial to growth. All plant parts were highly enriched in Ni, but the latex had extreme Ni concentrations (124,000 μg g^{-1}). Hyperaccumulation evolved independently in only two subgenera and five species of the genus *Pycnandra*. The extremely high level of Ni tolerance is posited to derive from the unique properties of laticifers. The evolutionary and ecological significance of Ni hyperaccumulation in *Pycnandra* is discussed in light of these findings. We suggest that Ni-rich laticifers might be more widespread in the plant kingdom and that more investigation is warranted.

Keywords: hydroponic, hyperaccumulation, laticifers, nickel, Pycnandra, X-ray fluorescence spectroscopy

OPEN ACCESS

Edited by:
Andre Rodrigues dos Reis, São Paulo State University, Brazil

Reviewed by:
Matthew John Milner, National Institute of Agricultural Botany (NIAB), United Kingdom
José Lavres Junior, University of São Paulo, Brazil

****Correspondence:***
Sandrine Isnard
sandrine.isnard@ird.fr

Specialty section:
This article was submitted to Plant Nutrition, a section of the journal Frontiers in Plant Science

Received: *02 June 2020*
Accepted: *13 August 2020*
Published: *09 September 2020*

Citation:
Isnard S, L'Huillier L, Paul ALD, Munzinger J, Fogliani B, Echevarria G, Erskine PD, Gei V, Jaffré T and van der Ent A (2020) Novel Insights Into the Hyperaccumulation Syndrome in Pycnandra (Sapotaceae). Front. Plant Sci. 11:559059. doi: 10.3389/fpls.2020.559059

INTRODUCTION

The seminal report by Jaffré et al. (1976) on the nickel (Ni)-rich latex of *Pycnandra acuminata* (previously *Sebertia acuminata*; Sapotaceae) introduced the term "hyperaccumulator" and gave rise to a new field of research (Jaffré et al., 1976; Jaffré et al., 2018). Hyperaccumulators are unusual plants that accumulate metals or metalloids (*e.g.* Ni, Co, Mn, Zn) in their living tissues to levels that may be hundreds or thousands of times greater than what is normal for most plants (Reeves, 2003; van der Ent et al., 2013). While most plants only contain ≤10 μg g^{-1} of Ni in their tissues, Ni-hyperaccumulators are

capable of accumulating ≥ 1,000 μg g^{-1} of Ni in their tissues (Brooks et al., 1977). The remarkable syndrome of hyperaccumulation is a response to the elevated Ni concentrations typically found in soils derived from ultramafic rocks (*i.e.* Mg- and Fe-rich) (Brooks, 1987). *Pycnandra acuminata*, a large tree endemic to New Caledonia, has attracted the attention of scientists for nearly five decades because of its vivid blue-green latex (**Figures 1A, D**) that contains up to 257,000 μg g^{-1} Ni (Jaffré et al., 1976), the highest Ni concentration ever found in a living organism (Sagner et al., 1998; Rascio and Navari-Izzo, 2011).

Nickel is an essential mineral element for higher plants, even though it is usually required in extremely low concentrations (Brown et al., 1987). One key function of Ni is as an essential component of urease, an enzyme which catalyzes urea hydrolysis for the release of ammonia (Gerendás et al., 1999; Taiz and Zeiger, 2006). This activity contributes to the recycling of endogenous nitrogen for plant growth (Gerendás et al., 1999). In contrast, the exposure of normal plants to elevated Ni concentrations alters the uptake of Fe and Mg provoking chlorosis, and depressing plant growth (Tan et al., 2000; Seregin and Kozhevnikova, 2006; Nishida et al., 2011). The critical toxicity level for Ni in normal plants is about 10 to 50 μg g^{-1} (Krämer, 2010). Nickel hyperaccumulator plant species have extraordinarily high levels of resistance and can tolerate high concentrations of Ni in soil and in solution in cultivation. In hydroponics experiments, the biomass production of hyperaccumulators (*e.g. Alyssum bertolonii*, *Noccaea goesingense*, *Berkheya coddii*) remains unaffected by Ni concentrations of up to several hundred μM in the hydroponic solution (Gabbrielli et al., 1991; Krämer et al., 1997; Robinson et al., 2003).

Several hypotheses have been put forth to explain the selective advantage of the hyperaccumulation syndrome, ranging from simple sequestration of toxic metals, physiological benefits,

FIGURE 1 | Hyperaccumulator species in the genus *Pycnandra* (Sapotaceae) from New Caledonia. All three species have a blue-green Ni-rich latex. **(A)** Mature specimen of *Pycnandra acuminata* with a tree height of approximately 24 m in the Parc de la Rivière Bleue. **(B)** Individual of *P. caeruleilatex* in Kuebini, Yate. **(C)** Individual of *P. kouakouensis* in Mount Kouakoué. Green-blue Ni-rich latex exuding from the main trunk of *Pycnandra acuminata* **(D)**, white Ni-poor latex exuding from the main trunk of *P. caeruleilatex* **(E)**, green-blue Ni-rich latex exuding a small cut branch of *P. caeruleilatex* **(G)**, green-blue Ni-rich latex exuding a small cut branch and broken petiole of *P. kouakouensis* in **(F–H)**.

drought stress protection, allelopathic effects and "elemental defence". However there is no consensus, and hyperaccumulation may have evolved for different reasons in different lineages in the plant kingdom (Martens and Boyd, 1994; Boyd and Martens, 1998; Boyd and Jaffré, 2001; Bhatia et al., 2005). To date, most studies regarding the mechanisms of uptake and tolerance of Ni hyperaccumulation have been limited to few model herbaceous species (*Berkheya* (Asteraceae); *Noccaea* and *Alyssum* (Brassicaceae)). Very little is comparatively known about woody hyperaccumulators that represent a large proportion of the diversity of Ni hyperaccumulators in tropical regions of the world (Reeves et al., 2018).

In most hyperaccumulator plants studied to date Ni is preferentially accumulated in foliar epidermal cells (Leitenmaier and Küpper, 2013). In *P. acuminata*, cryo-scanning electron microscopy with energy-dispersive X-ray spectroscopy (SEM-EDS) has shown that (stem) laticifers are highly Ni-enriched, and laticifers were suggested to constitute the main accumulation location (Sagner et al., 1998). Nickel accumulation in laticiferous plants might be particularly high, with the total Ni content of a single mature *P. acuminata* tree estimated at 5.15 kg (van der Ent and Mulligan, 2015). Because *P. acuminata* grows in forested areas over peridotitic alluvia or colluvia relatively rich in Ni (Jaffré et al., 1976; Perrier et al., 2004), but deprived of Ni-ore potential, bio-accumulation of Ni in *P. acuminata* could represent an additional source of highly enriched Ni fluid. More globally, laticifer cells represent natural biofactories for the production of several types of compounds and chemicals offering multiple commercial possibilities (Castelblanque et al., 2017). Nickel-rich laticifers are not only limited to *P. acuminata* and have also been described from several species belonging to the Euphorbiaceae and Phyllanthaceae (Berazaín et al., 2007; Reeves et al., 2007).

Enhanced levels of metal transport in hyperaccumulators has predominantly been shown to involve long-distance transport in the xylem (Lasat et al., 1996; Lasat et al., 1998; Rascio and Navari-Izzo, 2011), and extreme accumulation in the phloem bundles is described as a common feature of most tropical woody hyperaccumulators (van der Ent et al., 2017). The physiology of laticifer cells still remains a *terra incognita* (Pickard, 2008), and laticiferous hyperaccumulators might bring much insight into unexplored long-distance transport of natural products in plants.

New Caledonia is recognized as a global hotspot for metal hyperaccumulator plants, and the territory offers significant opportunities to broaden our understanding of the mechanisms involved in Ni hyperaccumulation (Jaffré et al., 2013; van der Ent et al., 2015; Isnard et al., 2016). Apart from *P. acuminata*, two other recently described *Pycnandra* species from New Caledonia also have a blue-green Ni-rich latex: *P. kouakouensis* and *P. caeruleilatex* (Swenson and Munzinger, 2016) (**Figure 1**), suggesting that hyperaccumulation is not an isolated phenomenon in the genus.

Discoveries of trace element hyperaccumulator plants have historically required time-consuming destructive chemical analysis of fragments from herbarium specimens (for examples in the New Caledonian context, see Brooks et al. (1977); Jaffré et al. (1979); Kersten et al. (1979)), which severely constrained the collection of large datasets. Recent advances in handheld X-ray fluorescence spectroscopy (XRF) systems have enabled non-destructive analysis of herbarium specimens (McCartha et al., 2019; van der Ent et al., 2019b), and this approach has been successfully applied to assess the incidence of hyperaccumulation in the ultramafic flora of New Caledonia (Gei et al., 2020). This work has permitted mass measurements of tens of thousands of samples in herbaria in a relatively short time span at low-cost (van der Ent et al., 2019a). Another advantage of XRF analysis is that the raw data (*e.g.* energy-dispersive X-ray fluorescence spectra) can be reprocessed when more accurate calibration models become available (van der Ent et al., 2019a).

Here, we combine experimental and field approaches to gain insight into the mechanisms of hyperaccumulation in *P. acuminata*. Nickel dosing hydroponic experiments were undertaken to establish Ni tolerance levels and translocation patterns in the roots and shoots of *P. acuminata*. Considering the extremely high accumulation capacity of this species, tolerance was studied using very high Ni concentrations (up to 3,000 μM Ni in solution), thus differing from previous studies that did not exceed several hundred μM in the hydroponic solution (Gabbrielli et al., 1991; Krämer et al., 1997; Robinson et al., 2003). We measured multi-element concentrations in different plant tissues and transport fluids of plants in nature, to gain insight into Ni accumulation partitioning relative to other essential and non-essential elements. Finally, we undertook a systematic XRF re-assessment of the full *Pycnandra* genus, in combination with a resolved phylogeny, to investigate the phylogenetic incidence of hyperaccumulation in this genus.

MATERIALS AND METHODS

Nickel Dosing Experiment With *Pycnandra acuminata* Seedlings

Pycnandra acuminata seeds were germinated at 27°C in vermiculite moistened with demineralized water. After a period of 4 weeks, seedlings with their cotyledons and 2 young leaves were transferred to 5-L containers (4 seedlings per container) containing one-tenth strength modified Hoagland's solution at pH 5.3 (Ca, 0.25 mM; Mg, 0.06 mM; K, 0.37 mM; NH_4, 0.12 mM; NO_3, 0.87 mM; PO_4, 0.12 mM; SO_4, 0.06 mM; Cl, 3.1 μM; B, 1.5 μM; Mn, 0.1 μM; Zn, 0.1 μM; Cu, 0.03 μM; Mo, 0.03 μM; Fe-EDTA, 1.2 μM), in order to be close to the natural soil solution (Becquer et al., 2010). The nutrient solutions were supplemented with 0, 100, 300, 1,000, or 3,000 μM Ni as $NiSO_4.6H_20$. They were continuously aerated and renewed every 7 days. Growth conditions were 25:21 ± 1°C (light (L): dark (D)), 70:80 ± 5% (L:D) relative humidity, 14 h L: 10 h D daily photoperiod, with 200 ± 10 μmol m^{-2} s^{-1} photon flux density at leaf level. A randomized block factorial design with five Ni concentrations, and five replicates was used.

After 180 days of growth under these conditions, the plants were harvested and separated into roots and shoots, rinsed twice in distilled water, dried at 105°C, and finally weighed. *Pycnandra acuminata* fruits are known to contain 3,000 to 5,000 μg g^{-1} Ni

(Jaffré et al., 1976; Sagner et al., 1998), with 5,000 μg g^{-1} in the cotyledons (Sagner et al., 1998). Seedlings can translocate Ni from the cotyledons into the shoots during development (Chaney et al., 2009), therefore, shoots were separated into two compartments to distinguish between the portion of stem that grew in the presence of cotyledons (Pre-Cotyledons-Shoots, PrCS) and the younger portion of stems that grew after the fall of the cotyledons (Post-Cotyledons Shoots; PstCS). For this purpose, the position of the last leaves was marked, once cotyledon fell. This sampling procedure was used to assess Ni translocation within the shoot. Shoot length was measured from cotyledon marks to the apical meristem. Plant samples (PrCS, PstCS, roots) were then ground, dry-ashed at 485°C, and further oxidized and re-dissolved in HNO_3. Elemental concentrations of Ca, K, Mg, P, and Ni were determined by Inductively coupled plasma atomic emission spectroscopy (ICP-AES).

Field Collection and Chemical Analysis of Plant Tissue Samples

Pycnandra acuminata (Baill.) Swenson & Munzinger (formerly *Sebertia acuminata* and known locally as "Sève bleue" tree) is rare and restricted to lowland humid forest on ultramafic soils, mainly in the southern ultramafic massif but also on the east side and in the northwest of the main island (Swenson and Munzinger, 2010).

Plant tissue samples (leaves, twigs, wood, bark, phloem, latex, xylem sap) for bulk chemical analysis were collected in the field, from a population located at the Plaine des Lacs (22°16′27.94"S, 166°54′12.44"E) in the southern massif. Bark and wood samples were taken from small diameter branches (2–3 cm) by stripping the bark with a sharp stainless-steel knife, whereas phloem samples were collected by stripping sections from beneath the bark using a razor blade. Latex samples were obtained by slicing a groove into the bark of the tree (**Figure 1D**). Xylem sap was collected with a handheld vacuum pump from excised branches, after bark removal to prevent contamination by phloem sap.

These samples were dried at 70°C for five days in a drying oven, gamma irradiated and subsequently ground and digested using 4 ml HNO_3 (70%) in a microwave oven (Milestone Start D) for a 45-minute program. After dilution to 30 ml with ultrapure water (Millipore 18.2 MΩ·cm at 25°C) they were analyzed with ICP-AES with a Thermo Scientific iCAP 7400 instrument for macro-elements (Mg, P, K, Ca) and trace-elements (Mn, Fe, Co, Ni, Zn) in radial and axial modes depending on the element and expected analyte concentration. All elements were calibrated with a 4-point curve covering analyte ranges in the samples. In-line internal addition standardization using yttrium was used to compensate for matrix-based effects.

Additional material from the two other recently described *Pycnandra* species with a blue-green Ni-rich latex: *P. kouakouensis* and *P. caeruleilatex* (Swenson and Munzinger, 2016) (**Figure 1**), were analyzed and presented in **Supplementary Table 1**.

Herbarium X-Ray Fluorescence Spectroscopy

The foliar elemental concentrations of the herbarium specimens were measured using a Thermo Fisher Scientific Niton XL3t 950 GOLDD+. After the initial large-scale study reported in Gei et al. (2020) was completed, efforts were made to further improve the calibration model for XRF measurements of New Caledonian plants, many of which have atypical morphological characteristics (such as thick coriaceous leaves), which can affect the accuracy of XRF measurements which is "matrix sensitive." A substantially improved newer calibration was used in this study to re-evaluate the distribution of Ni hyperaccumulation within the Sapotaceae and to finely assess the phylogenetic distribution of Ni hyperaccumulation in the genus *Pycnandra*. This new calibration was obtained from 221 specimens from the Herbarium of New Caledonia (NOU) that were intentionally chosen to cover a very wide concentration range (low range to hyperaccumulation range for Mn, Co, Ni, Zn) on the basis of the earlier study (**Supplementary material**). From each specimen a 1-cm^2 area was destructively excised from each specimen, analyzed by XRF and after digestion by ICP-AES. The resulting regression equation used for "calibration" were substantially improved (for instance R^2 improved from 0.87 to 0.98), and the newer calibration was used in this study (**Supplementary Figure 1**).

In total, 2,148 specimens of the Sapotaceae, including 847 specimens of *Pycnandra*, were analyzed. The XRF analysis was undertaken on a sheet of "herbarium cardboard" on a pure titanium plate (~99.995%, 2 mm thick ×10 × 10 cm) to provide a uniform background and block transmitted X-rays. The XRF analysis used the "Soils Mode" in the "Main filter" configuration for 30 s duration (Gei et al., 2020). For each herbarium specimen, one XRF measurement was taken from a mature leaf (**Supplementary Material 1**).

The molecular phylogenetic trees of *Pycnandra* was simplified and adapted from Swenson et al. (2007, 2015), including 57 of the 59 described species, plus 4 undescribed species (*Pycnandra fastuosa* W (=open-veined), P. Munzinger 3385, P. Butaud 3343, P. Munzinger 5673, see Swenson and Munzinger, 2016 for details). *Niemeyera whitei* was used as outgroup (Swenson et al., 2007).

Data Processing

The matching XRF and ICP-AES data was used to obtain calibration curves. The apparent limits of detection (LOD) were estimated by visual inspection of the log-transformed regression models of the XRF data against corresponding ICP-AES measurements and set at XRF values: 107 μg g^{-1} for Ni (range, 107–113,987, n = 149), 426 μg g^{-1} for Co (372–9,532, n = 50), 455 μg g^{-1} for Mn (455–176,396, n = 159), and 27 μg g^{-1} for Zn (range, 27–1,238, n = 117). The residuals *vs.* fitted values were inspected for each linear regression analysis, and outliers (± 3 SD of the residual) were identified and removed. Secondary linear regression models were then derived after the samples with XRF values below the limit of detection were removed. The regression models (y = calculated ICP-AES; x = measured XRF) are: Ni: $y = 0.2351x^{1.0969}$ (R^2 0.98), Mn: $y = 0.7869x^{0.9165}$ (R^2 0.98), Co: $y = 0.429x^{0.9809}$ (R^2 0.92), and Zn: $y = 0.3766x^{1.1259}$ (R^2 0.88) (**Supplementary Figure 1**). The data from the Ni dosing experiment were analyzed by ANOVA after being checked for homogeneity of variance. Significance of differences between means was performed using *t*-test at the 95% confidence limit.

The Waller-Duncan k-ratio t-test ($\alpha = 0.05$) was used to determine the effect of treatments for all the measured parameters in the hydroponics experiment.

RESULTS

Nickel Dosing Experiment on *Pycnandra acuminata* Seedlings

Pycnandra acuminata plants were cultivated in hydroponic solutions (spiked with 0, 100, 300, 1,000, or 3,000 μM Ni) for 6 months and growth, biomass production, and elemental concentrations in roots and shoots were analyzed. The total mean Ni concentrations in shoots ranged from ~500 to 12,900 μg g^{-1} across treatments and shoot compartments (**Table 1**). In the control treatment, the plants had translocated Ni stored in the original seed to their shoots, and to a lesser extent in their roots, Ni concentration was consequently strongly compartmentalized as indicated by significantly higher values in the basal part of the shoots (PreCS) followed by PstC and roots (**Table 1**). No significant difference in Ni concentration between the shoot compartments were found in the other treatments, except in the 3,000 μM Ni treatment, where Ni accumulates at significantly higher concentrations in the apical shoot (11,200 μg g^{-1} *vs.* 8,700 μg g^{-1}) (**Table 1**). The apical shoot/root concentration ratio (TF) was significantly higher in the control treatment (**Figure 2D**) but did not vary with increasing Ni treatment (from 100 μM to 3,000 μM). TF mean values were around 1 (0.97<TF<1.62) across Ni treatments, meaning that the average Ni concentration in the shoots is (almost) always greater than the corresponding root Ni concentration.

Nickel concentrations increased significantly across all treatments in the apical compartment (PstCS) while in the older compartment (PreCS) Ni concentrations were not affected by treatments above 300 μM, and a significant increase was found only between the 100 and 300 μM treatments (**Figures 2A, B**). In the roots, Ni concentrations increased in the 100, 300, and 1,000 μM Ni treatments, but was not affected by treatments above 1,000 μM (**Figure 2C**).

The exposure of *P. acuminata* to increasing Ni concentrations induced different growth reduction in the shoots and roots (**Figure 3**). Shoots have a higher sensitivity to concentration in the solution above 100 μM Ni, while roots exhibited greater ability to tolerate Ni up to 1,000 μM Ni in the nutrient solution. Only the extreme 3,000 μM Ni treatment significantly impacted the root biomass (**Figure 3C**). Shoot growth was significantly stimulated in the 100 μM Ni treatment (+40% shoot mass), with more individual variation, and similar to the control in the 300 and 1,000 μM Ni treatment (**Figure 5B**). Plant shoot biomass was significantly impacted by Ni in the 3,000 μM Ni treatment (**Figure 3B**), but no symptoms of toxicity, such as chlorosis, were observed across treatments (**Figure 3A**). Similar results were obtained for the shoot length and the daily growth rate although there was no significant difference between the 300, 1,000, and 3,000 μM treatments (**Figures 3D, E**). Macronutrient concentrations in plant parts were not affected by the Ni treatment, although there was a decrease in Ca in the roots and a decrease in Mg concentrations in the different parts of the plants with increasing Ni concentrations in the solution (**Table 2**).

Elemental Concentrations in *Pycnandra acuminata*

In *P. acuminata* trees Ni was highly enriched in all parts of the measured, including the leaves, twigs, but exceptionally high Ni was found only in the latex (**Table 3**). The latex had extreme Ni concentrations, reaching 66,000 μg g^{-1} (**Table 3**). The twigs, both bark (including phloem) and wood had high Ni concentrations (up to 11,800 μg g^{-1} Ni in bark). The xylem sap was distinctively Ni-enriched, but the concentration was limited to ~1,430 μg ml^{-1} (**Table 3**). In the leaves, nutrient concentrations (Ca, K, Mg) were relatively high, whereas concentrations of trace-elements were lower (Co, Mn and Zn). All the different plant parts had concentrations below 200 μg g^{-1} and Co was particularly low with no tissue with a mean >15 μg g^{-1}. The low Fe concentration indicated that tissues did not have soil particle contamination. Calcium was particularly enriched in the bark (mean 5,690 μg g^{-1}) while wood had ~1,500 μg g^{-1} on average. Phosphorus concentrations were low in all plant parts. The latex, besides being strongly enriched in Ni, also had rather high concentrations of Ca, and was Zn enriched compared to other plant tissues. Other elemental concentrations (Mg, P, K, Mn, Fe, Co) were very low in the latex. Compared to Ni, elemental concentration for other elements were also low in the xylem sap.

In *P. kouakouensis* another "blue-latex" hyperaccumulator species, the Ni concentrations in leaves were not particularly high (mean value, 3,610 μg g^{-1}) but the latex had extreme Ni concentrations (124,000 μg g^{-1}) (**Supplementary Table 1**). In *P. caeruleilatex*, Ni concentrations were relatively low with the highest value in the apical tip (2,470 μg g^{-1}).

TABLE 1 | Nickel concentrations in the different plant compartment (PreC-Shoots, PstC-Shoots and roots) of *Pycnandra acuminata* after 180 days of growth in hydroponics for different Ni concentration in the nutrient solution.

Treatment (μmol L^{-1} Ni)	n	Tissue nickel concentrations		
		PreC-Shoots	PstC-Shoots	Roots
0	5	2,360–3,230 [2,770]a	508–1,260 [948]b	102–250 [176]c
100	5	2,900–5,600 [4,190]a	2,500–6,910 [4,070]a	1,230–3,690 [2,550]a
300	5	4,990–8,160 [6,850]a	4,580–7,100 [5,900]a	4,340–7,620 [6,150]a
1000	5	6,050–12,200 [8,350]a	7,110–10,600 [8,640]a	5,835–12,300 [8,980]a
3000	5	6,390–11,500 [8,730]a	9,460–12,900 [11,200]b	7,970–11,700 [10,200]ab

Letters indicate significant difference between tissues for each treatment, at 5% level (Waller-Duncan k-ratio t-test). All values in in μg g^{-1} dry weight.

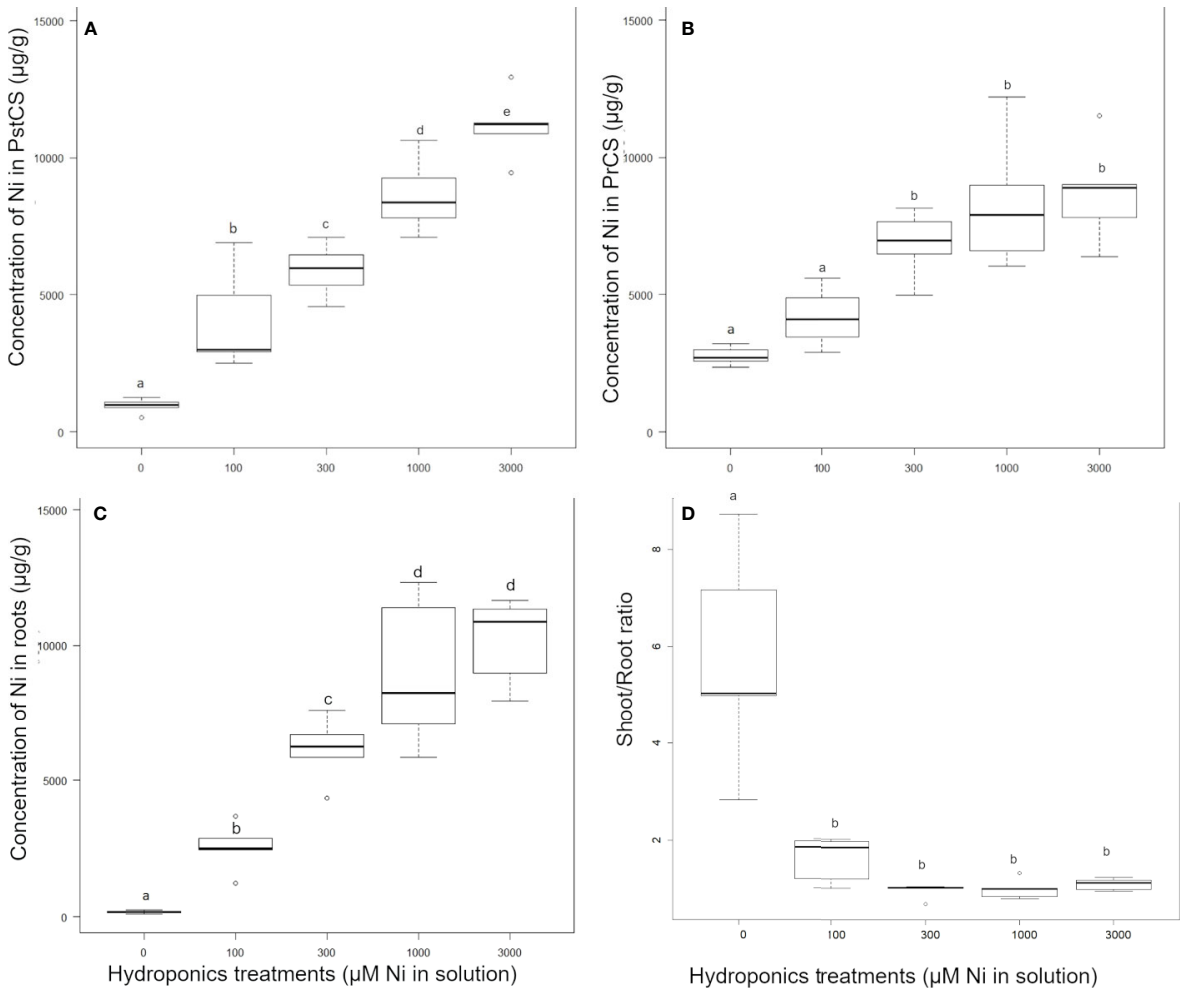

FIGURE 2 | Effect of nickel concentrations in the nutrient solution on the nickel concentration in *Pycnandra acuminata*, after 180 days of growth in hydroponics (n=5). **(A)** PrCS, **(B)** PstCS, **(C)** root and **(D)** shoot to root ratio. Letters indicate significant difference at 5% level (Waller-Duncan k-ratio t-test).

Incidence of Hyperaccumulation in the New Caledonian Sapotaceae

Herbarium X-ray fluorescence (XRF) scanning was undertaken on all specimens of the Sapotaceae (covering 6 genera) held at the Herbarium of New Caledonia (NOU), totaling 2,148 specimens. The holdings included all genera occurring in New Caledonia, *Manilkara* (1 species), *Mimusops* (1 species), *Pichonia* (7 species), *Planchonella* (36 species), *Pleioluma* (17 species), and *Pycnandra* (62 taxa). Hyperaccumulation of Ni was found with exceedances of the nominal Ni hyperaccumulation threshold (>1,000 µg g^{-1}) in the genera *Pichonia, Planchonella* and *Pycnandra* (**Supplementary Figure 2**). In the two former genera, only one to two specimens exceeded this threshold, while in *Pycnandra* many specimens exhibited exceptional [Ni] values. None of the Sapotaceae specimens had a [Mn] above the hyperaccumulation threshold (>10,000 µg g^{-1}, (Baker and Brooks, 1989)) (**Supplementary Figure 2**). Values exceeding Zn hyperaccumulation threshold (>3,000 µg g^{-1}, (van der Ent et al., 2013)) were recorded in only two specimens of *Pycnandra petiolata* out of 47 specimens (**Supplementary Figure 1**). None of the measured specimens had Co concentration values above the limit of detection.

Following the XRF assessment, we focused on Ni hyperaccumulation in the genus *Pycnandra*. For most species, concentration values did not exceed the limit of detection, and few species had Ni concentrations around few hundred µg g^{-1} (**Figure 4**). Only five species had incidences of Ni hyperaccumulation: *P. acuminata, P. caeruleilatex, P. canaliculata, P. kouakouensis*, and *P. sessilifolia* (**Figure 4**). For the three blue-green latex species, *P. acuminata, P. caeruleilatex*, and *P. kouakouensis* all specimens exceeded the Ni hyperaccumulation threshold. These species belong to different clades (two subgenus *Trouettia* and *Sebertia*). *Pycnandra acuminata, P. kouakouensis* and *P. canalicula* belong to the same, through unresolved, clade. The highest median foliar Ni concentrations were recorded in *P. acuminata* with 42,000 µg g^{-1}

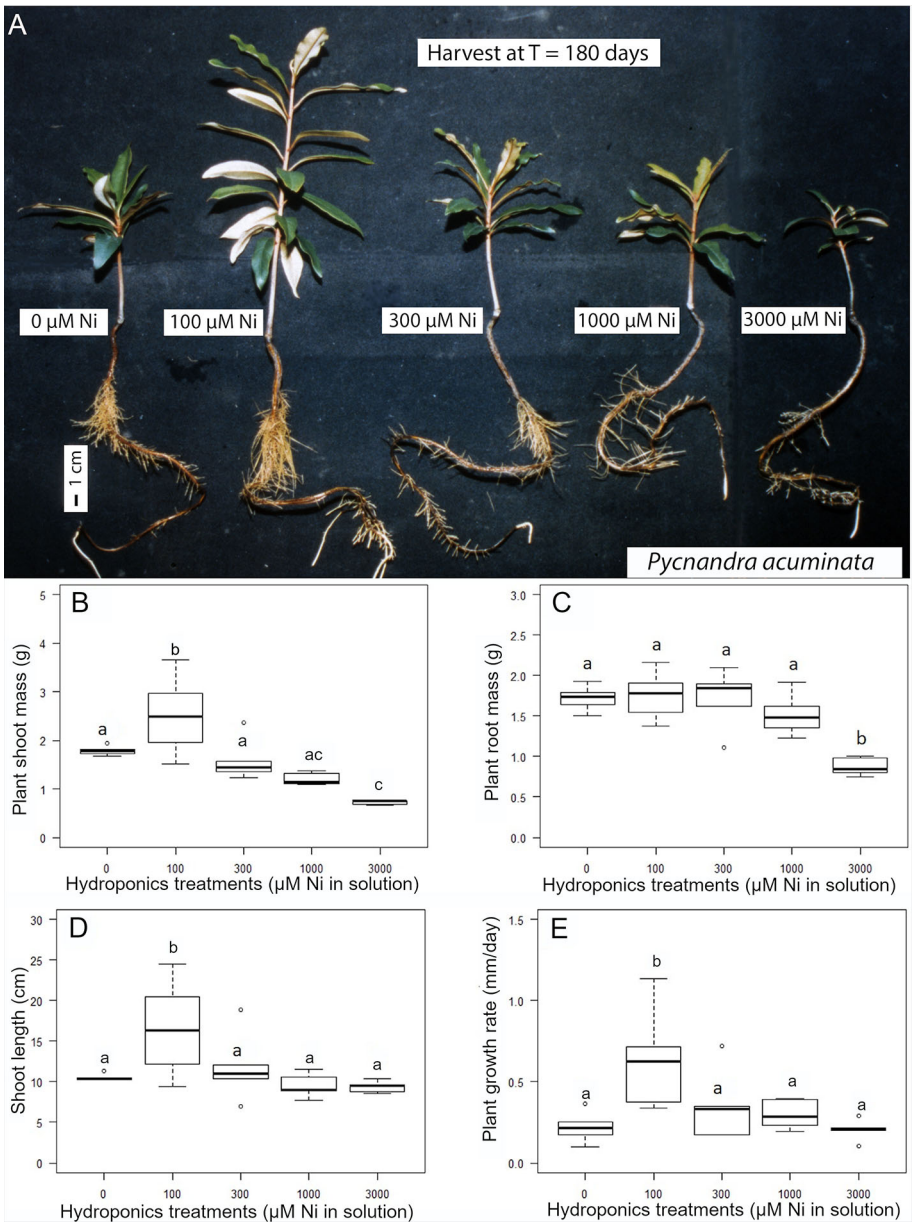

FIGURE 3 | Nickel tolerance of *Pycnandra acuminata* in hydroponic culture. **(A)** Plants exposed to the indicated concentration of Ni for 180 days. **(B–E)** Effect of nickel concentration in the nutrient solution on growth (n = 5). **(B)** Plant shoot biomass, **(C)** plant root mass, **(D)** plant shoot height and **(E)** plant mean relative growth rate. Letters indicate significant difference at 5% level (Waller-Duncan k-ratio t-test).

TABLE 2 | Bulk elemental concentrations (ICP-AES) of macronutrients in PreC-Shoots, PstC-Shoots, and roots of 180 days *Pycnandra acuminata* plants as a function of the Ni concentration in the nutrient solution.

Treatment (µmol L^{-1} Ni)	Tissue macronutrient concentrations											
	PreC-Shoots				PstC-Shoots				Roots			
	Mg	P	K	Ca	Mg	P	K	Ca	Mg	P	K	Ca
0	1,100	2,400	15,800	5,900	1,700	1,500	25,200	4,000	1,200	4,600	14,100	5,100
100	600	2,500	14,500	6,200	1,000	1,500	22,100	4,500	1,300	4,300	14,500	3,700
300	700	3,000	17,700	5,300	600	1,800	26,200	4,100	800	4,400	13,500	2,300
1000	500	2,700	17,300	3,100	600	1,900	35,600	3,400	600	4,200	12,800	1,200

All values in in µg g^{-1} dry weight.

TABLE 3 | Bulk elemental concentrations (ICP-AES) in different plant parts and fluids of *Pycnandra acuminata* (values as means and ranges in μg g^{-1} dry weight).

Plant species	Plant tissue	n	Elemental concentrations									
			Mg	P	K	Ca	Mn	Fe	Co	Ni	Zn
Pycnandra acuminata	Old leaves	5	1,560 (1,240–2,440)	276 (244–308)	8,220 (5,800–11,400)	2,660 (1880–3490)	50.8 (30.1–72.8)	137 (34.6–279)	4.77 (0.70–11.0)	6,530 (536–16,900)	43.2 (3.14–109)
	Young leaves	5	2,490 (1,490–3,730)	389 (283–478)	10,700 (8,040–12,400)	3,700 (970–8,400)	72.0 (35.9–145)	80.0 (32.7–139)	10.2 (1.29–37.7)	7,570 (4,260–12,900)	49.8 (24.9–84.4)
	Twigs	5	3,970 (1,060–8,790)	369 (255–489)	9,400 (7,360–13,300)	13,300 (7,550–30,200)	126 (39.8–204)	182 (105–391)	12.6 (1.11–58.1)	10,700 (3,170–14,100)	112 (98.9–139
	Bark (including phloem)	5	666 (441–960)	142 (103–206)	4,670 (3,060–6,890)	5,690 (2,720–12,100)	67.0 (32.7–150)	225 (58.1–349)	2.09 (0.34–4.49)	7,520 (1,280–11,800)	74.4 (9.37–114)
	Wood	5	430 (316–677)	103 (46.2–231)	3,700 (1,780–7,430)	1,610 (548–2,930)	20.1 (11.9–28.0)	24.0 (12.2–36.1)	0.51 (0.14–0.73)	2,930 (1,510–5,180)	26.7 (14.1–49.3)
	Latex	5	177 (121–278)	20.5 (15.9–23.9)	184 (98.2–392)	4,000 (1,310–9,600)	31.1 (13.6–56.6)	23.4 (13.1–31.7)	4.36 (3.78–5.57)	62,800 (57,100–66,300)	367 (330–392)
	Xylem sap (μg ml^{-1})	3	15.4 (9.09–30.7)	0.90 (0.09–1.75)	110 (61.0–160)	124 (71.2–172)	0.85 (0.43–1.74)	0.62 (0.27–0.81)	0.08 (0.03–0.18)	813 (313–1,426)	4.87 (2.00–7.83)

Ni (14 out of 18 specimens had a [Ni] >10,000 μg g^{-1}) and *P. kouakouensis* with values between 18,900 and 37,400 μg g^{-1} Ni in the three measured specimens. *Pycnandra caeruleilatex* also reached high [Ni] (up to 11,300 μg g^{-1} Ni) with the four measured specimens exceeding the nominal Ni hyperaccumulation threshold. Almost 50% of the measured specimens of *P. sessiliflora* had foliar concentrations above the hyperaccumulation threshold, but values did not exceed 2,500 μg g^{-1} Ni. The last species, *P. canaliculata*, is a marginal hyperaccumulator, with only one specimen (out of 28) exceeding the hyperaccumulation threshold. While foliar Ni concentrations measured by XRF in herbarium specimens are commonly high for hyperaccumulators species (median, 15,400 μg g^{-1}; maximum, 42,000 μg g^{-1} in *P. acuminata*), the bulk foliar Ni concentration did not exceed 16,900 μg g^{-1} in our field collected leaves (**Table 3**) (while up to 25,000 μg g^{-1} has been reported in the literature, Jaffré et al., 2013). This is due to the high sensitivity of XRF measurement and the leaf morphology of *Pycnandra*, as Ni is highly concentrated in the dense laticifer network.

DISCUSSION

Nickel Tolerance and Translocation Throughout the Plant

In this study we report extremely high levels of Ni tolerance in cultivated *P. acuminata* plants that did not show any phytotoxicity symptoms when exposed to Ni concentrations as high as 1,000 μM in solution for a long-time (180 days). The concentrations in the growth medium were much more elevated than in experiments on other Ni hyperaccumulator plants (*e.g. Noccaea*, *Alyssum*) where Ni concentrations did not exceed several hundred μM in hydroponic solution (Gabbrielli et al., 1991; Krämer et al., 1997; Robinson et al., 2003). The decrease of root biomass suggests the first visible symptom of metal toxicity (Kahle, 1993; Shah et al., 2010), but is significant only in the 3,000 μM treatment. No other obvious toxicity symptoms (*i.e.* no interveinal chlorosis) were observed at concentrations as high as 3,000 μM and Ni continued to accumulate in the apical shoots up to 12,000 μg g^{-1}, although the growth of both root and shoots was reduced. Experimental levels of Ni accumulation were similar to concentrations measured in leaves or twigs of trees collected in the field.

As a consequence of the high endogenous Ni content reported from *P. acuminata* seeds (up to 5,000 μg g^{-1} Ni in the cotyledons, Jaffré et al., 1976; Sagner et al., 1998) (**Figure 5**), foliar Ni concentrations were high in plants of the control treatment (the solution contained at most nanomolar concentrations of Ni). The relatively high Ni concentrations in the shoots and to a lesser extent in the roots of plants, 180 days after germination, is due to translocation of Ni from the seed store. Seed Ni supply has also been reported in another hyperaccumulator species and can provide the young plant with enough Ni to meet the potentially higher Ni requirement of hyperaccumulators (Chaney et al., 2009). The precise location of Ni within the seed tissue of *P. acuminata* is unclear, but bulk analyses of fruits showed that Ni was found in high concentrations in the cotyledons (5,000 μg g^{-1}) while concentrations in the embryo were below the detection limit (Sagner et al., 1998).

FIGURE 4 | Phylogenetic distribution of hyperaccumulation in the endemic genus *Pycnandra* (Sapotaceae) from New Caledonia. On the left, phylogenetic tree of *Pycnandra*, simplified and adapted from Swenson et al. (Swenson et al., 2007; Swenson et al., 2015), including 57 of the 59 described species, plus 4 undescribed species (*Pycnandra fastuosa* W (=open-veined), P. Munzinger 3385, P. Butaud 3343, P. Munzinger 5673, see Swenson and Munzinger, 2016 for details). Subgenera are indicated vertically, *Niemeyera whitei* is kept as outgroup. On the right, boxplot of [Ni] for each species, based on XRF measurements. Species unavailable for XRF measurements are indicate in grey color. The red vertical dash-line indicates the hyperaccumulation threshold ([Ni] >1,000 µg g^{-1}).

Laticifers, where most of the Ni is stored in *P. acuminata* (Sagner et al., 1998), are specialized cells known to occur in immature embryos, at the base of emerging cotyledons (Evert, 2006; Castelblanque et al., 2016). It can therefore be reasonably assumed that the laticifers cells in the cotyledons contain a large fraction of the Ni in the seedling (**Figure 5**), and that Ni is

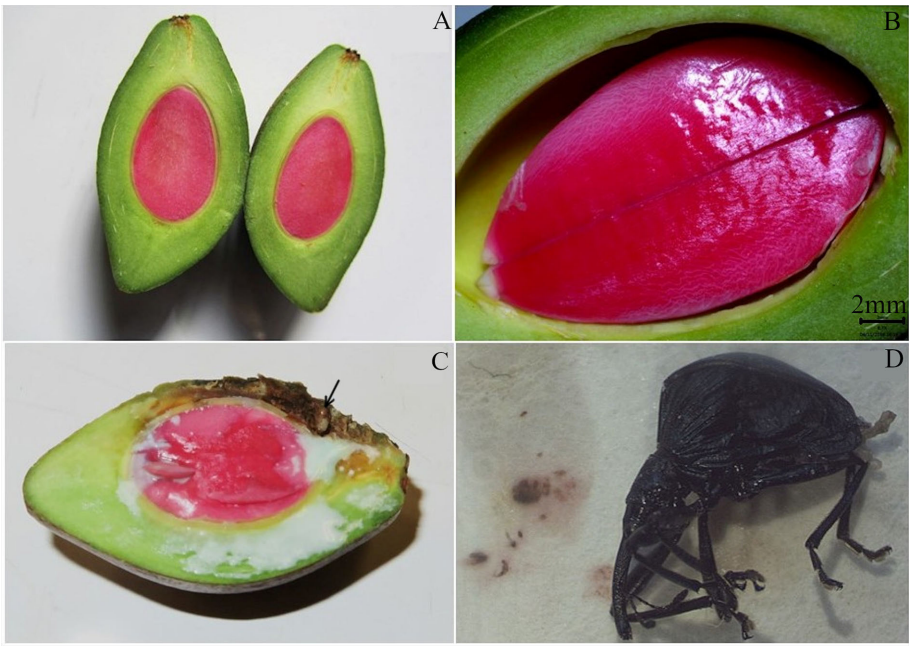

FIGURE 5 | Cut fruit of *Pycnandra acuminata* **(A)**, showing detail of the seed, note laticifer network visible in the cotyledons **(B)**, and **(C)** exuding latex and Apionidae larva (black arrow). **(D)** Adult Apionidae that developed within the fruit. The pressed insect had a positive dimethylglyoxime impregnated-paper staining (red/brown stained), revealing it high Ni content (>1,000 μg g^{-1}).

transferred from cotyledons to leaves after germination. In our control experiment, Ni in seedlings was preferentially accumulated in old parts of the shoots (PreCS) in comparison to the later developed apical compartment (PstC) (*i.e.* the shoot that developed after cotyledons fall) and root. This Ni partitioning can be explained by the high sequestration function of leaves (laticifers) in *P. acuminata*. Nickel in seedlings is first accumulated in the shoot that develops in the presence of cotyledons, only a small fraction of Ni was transferred to the shoot that developed after cotyledon fall. Increasing Ni in the solution tends to increase Ni concentrations in both shoot compartments and roots, a common physiology of hyperaccumulators plants (Shah et al., 2010). A saturation threshold was reached in the roots and basal part of the shoots (above 1,000 μM Ni treatment), but not in the more recently developed shoots (PstCS), where Ni concentrations continued to increase in the 3,000 μM treatment. This probably reflects a saturation of sequestration capacity of old leaves and roots, and the dynamics of metal uptake and transport that depends on the concentration in the external medium (Gabbrielli et al., 1991; Shah et al., 2010). Note that this also reveals the high sequestration capacity of the roots (up to ~12,000 μg g^{-1}), that we infer to be linked to storage in laticifers. Whilst the capacity to translocate and accumulate more metal in the shoots than in the roots is often used as a criteria to identify hyperaccumulator plants (Baker et al., 1994), we found that in *P. acuminata* a large fraction of the Ni can be stored in the roots, when Ni availability is high.

Nickel transport from roots to the shoots in hyperaccumulator plants has been attributed to the xylem (Alves et al., 2011; Rascio and Navari-Izzo, 2011). Accordingly, we found that the Ni concentrations in the xylem sap of *P. acuminata* trees was particularly high (313–1,426 μg g^{-1}) (**Supplementary Table 2**), implying Ni transport in the xylem. In our experiment the control treatment was devoid of Ni and Ni in seedlings, most probably derived from cotyledons, was only partially transferred to the shoot. Translocation of Ni through the phloem has been suggested to occur in hyperaccumulators (Deng et al., 2016), and was revealed by tissues-level analysis that showed high concentrations of Ni in the phloem of hyperaccumulators (Mesjasz-Przybylowicz et al., 2016; van der Ent et al., 2017). High Ni concentrations have also been found in the sap of hyperaccumulators species, but phloem sap sampling is a technically challenging task (Álvarez-Fernández et al., 2014). In plants with laticifers or other ducts, Ni could also be preferentially stored in these cells that are found in all plant tissues and sometime in the phloem itself (Evert, 2006). Whether Ni translocation, from cotyledons to leaves and from old leaves to young leaves, in *P. acuminata* occurs *via* the phloem and/or the laticifer network remains an intriguing question. Current understanding suggests that laticifers provide an effective location to store a wide array of secondary compounds, but very little is known about putative ion trafficking through laticifer networks (Hagel et al., 2008; Castelblanque et al., 2016). Translocation through laticifers has been advocated but not investigated (Kutchan, 2005).

Based on our results, we posit that at low Ni concentrations in the solution, Ni accumulated preferentially in old leaves in comparison to the apical shoot and root. At high Ni concentrations in the

solution, the maximum storage capacity in roots and old leaves is reached and Ni is actively transported to the apical shoots. At the whole plant scale, this physiology would reflect a tendency for higher Ni concentrations in the shoots when bioavailable Ni is high. Interestingly, the unique whole-plant scale accumulation pattern of Ni in *P. caeruleilatex* gives insights into this physiology. *Pycnandra caeruleilatex* has latex in the main trunk and older branches that is uncolored and thus apparently Ni-poor, but the latex in the apical shoots and petioles of apical leaves is distinctly blue-green (*i.e.* Ni-rich) (**Figures 1E, G**). This [Ni] distribution pattern could reflect the dynamics of Ni transport and translocation, but more investigation in this remarkable model species is required.

Evolution of Hyperaccumulation in *Pycnandra*

This study highlights repeated, but infrequent, evolution of hyperaccumulation within the genus *Pycnandra*, the syndrome being variously expressed in the different species. Hence, hyperaccumulation evolved at least two times within the genus, in the subgenera *Sebertia* and *Trouettia*, while it is (nearly) absent in subgenera *Achradotypus, Pycnandra*, and *Leptostylis*. The divergence between *Pycnandra* and its sister group *Niemeyera*, an Australian endemic, is estimated to 29.8 Myr (22.3–38 Myr) (Swenson et al., 2014), the genus being the oldest lineages estimated to date in the flora of New Caledonia (Pillon, 2012). In the sister genus *Niemeyera*, no species are known to occur on ultramafic soils (Atlas of Living Australia, ala.org.au), and hyperaccumulation does not occur in the genus. The genus *Pycnandra* has been estimated to have colonized the main island (Grande Terre) between 29.8–16.2 Ma (stem and crown-node age) ago (Swenson et al., 2014). Altogether, this suggests that constitutive hyperaccumulation in *Pycnandra* has evolved *in situ*, during a very long period of exposure to New Caledonian ultramafic soils. The infrequent evolution of hyperaccumulation in the genus *Pycnandra*, despite a long evolutionary time since island colonization, suggests that the syndrome might be strongly physiologically constrained and/or has a complex selective advantage. A drawback is that in *Pycnandra*, no clade is strictly associated with ultramafic soils. Instead, soil preference is labile within clades (Swenson and Munzinger, 2016). This is in accordance with the few studies, where ultramafic preference has been mapped onto phylogenies, showing its highly labile evolutionary origin (Anacker, 2011). Nickel hyperaccumulation is a syndrome of ultramafic soil that has evolved repeatedly in many clades in the flora of New Caledonia (Pillon et al., 2010; Jaffré et al., 2013; Gei et al., 2020) as elsewhere (Reeves et al., 1999; Borhidi, 2001; Krämer, 2010; Cappa and Pilon-Smits, 2014). It has, however not been shown to lead to adaptive radiation or important diversification within a clade. For example, in neotropical *Psychotria* hyperaccumulation probably occurs in only a few distantly related species (McCartha et al., 2019). Under ultramafic conditions, hyperaccumulation might maximize fitness and competitive ability but this selective advantage is subtle and depends on species physiology, environment, and probably biotic pressures. A gradient from accumulation to hyperaccumulation is found in many clades inclined to tolerate high Ni concentrations. The evolution of hyperaccumulation might thus be a gradual evolutionary process (Boyd, 2012), and this explains why it is so challenging to understand the evolution of this syndrome.

The Evolutionary Advantage of Ni Hyperaccumulation in *P. acuminata*

It is striking that only three species with Ni-rich laticifers, and two marginal hyperaccumulators, occur in *Pycnandra*, which is the largest endemic genus of New Caledonia (Munzinger et al., 2020. [continuously updated]) and frequently occurs on ultramafic soils (Swenson and Munzinger, 2016). Several hypotheses have been put forth to explain the selective advantage of hyperaccumulation, ranging from tolerance (sequestration), disposal from the plant through leaf abscission, drought resistance, interference (allelopathy), or pathogen/herbivore defence (Martens and Boyd, 1994; Boyd and Martens, 1998; Boyd and Jaffré, 2001; Bhatia et al., 2005). The defensive enhancement hypothesis has received most research attention and is backed up with experimental evidence for some species (see Boyd, 2012 for a review). The principal roles of laticifers are in wound healing, defence against herbivory, and pathogen defence (Agrawal and Konno, 2009). The high-pressure laticifers ducts of *P. acuminata* are effectively weaponized with toxic Ni-citrate salt to which sap sucking or browsing insects are exposed, suggesting a role in elemental defence. Spectacular internal excretion (deposition) of inorganic compounds in laticifers could provide an effective way to gain defence metabolites at potentially lower cost. During field work, however, we found many fruits of *P. acuminata* infested by Apionidae larvae that reached maturity (**Figures 5C, D**), suggesting insect specialization with high levels of tolerance, and important seed predation. Several host associations between genera of Apionidae (weevil family) and Sapotaceae have already been documented, including with several species of *Pycnandra* (Wanat and Munzinger, 2012), but never with hyperaccumulator species. Herbivore interactions and Ni-tolerant insects have also been reported for *P. acuminata* fruits, whose fleshy pericarp is highly Ni-enriched (Sagner et al., 1998; Boyd et al., 2006). Although so-called "high-Ni insects" are known, community-level studies show that bioaccumulation of Ni does not occur at the plant-herbivore or herbivore-predator steps. (Boyd et al., 2006; Migula et al., 2007).

A major finding of the hydroponics experiment, apart from the unreported extremely high levels of Ni tolerance, is the enhanced growth at 100 μM Ni at Ni concentrations exceeding values previously reported (Nishida et al., 2011; Iori et al., 2013; Deng et al., 2014). It is known that Ni has a stimulatory effect on some plants, but at very low prevailing concentrations (Mishra and Kar, 1974). Purely growth stimulatory effects at high Ni concentrations (100 μM) have not previously been reported, even in Ni hyperaccumulator plants. The question then arises as to why Ni has a growth promoting effect at concentrations millions of times greater than is required for urease activity (< 5 μg g^{-1} foliar Ni, Eskew et al., 1983)? Because *P. acuminata* stores a large portion of Ni in laticifer and epidermal cells (Sagner et al., 1998), only a small fraction of Ni in the plant might actually be involved in urease activity, but perhaps enough to stimulate the recycling of endogenous nitrogen and stimulate growth, at least in the first developmental stages.

The ecological significance of hyperaccumulation in *P. acuminata* could also be related to interference and allelopathy benefits. Phyto-enrichment of the litter, leading to an increase in bioavailable Ni in the soil, has been suggested to affect the germination and growth of competing plant species (Boyd and Jaffré, 2001), and may provide an ecological advantage for hyperaccumulator plants if they need more Ni than other plants. Hyperaccumulators might benefit from *in situ* (fruit and seed) high Ni concentrations at the seedlings stage and phytoenrichment from others hyperaccumulator in latter stage of growth. Chaney et al. (2009) failed to obtain proof of a functional Ni deficiency in *Alyssum* because seeds supplied enough Ni for growth, in a 6-week growth period. We believe that Ni contained in seeds plays an essential role in the seedling phase of hyperaccumulator plants, such as *P. acuminata*.

The Incidence of Nickel-Rich Laticifers May Have Been Overlooked

One of the major physiological constrains of hyperaccumulation is the ability to store metal in high concentrations without interfering with basic plant metabolism. Such physiological constraints could limit the evolution of hyperaccumulation to few clades. The fact that *P. acuminata* (and *P. kouakouensis* and *P. caeruleilatex*) can accumulate extraordinary levels of Ni in their tissues is because of the storage capacity of laticifers (that account for a large volume in stem, leaves and roots, *unpublished data*), and this might constitute a physiological advantage for the evolution of hyperaccumulation.

Laticifers are defined as internal secretory structures for secondary metabolites (Hagel et al., 2008). Accumulation of Ni in laticifers of hyperaccumulator plants demonstrates that they might extend their physiology to extreme levels of internal excretion (deposition) of inorganic compounds for metal detoxification and possibly transport (van der Ent et al., unpublished). This "novel function" connects to the concept of exaptation *(i.e.* "function of object now being used in another way") (Gould and Vrba, 1982).

Nickel-rich laticifers have also been described from *Euphorbia helenae* subsp. *grandifolia* (Euphorbiaceae) which has a latex with 30,900 μg g^{-1} Ni (Reeves et al., 1996) and two *Phyllanthus* species from Cuba (Berazaín et al., 2007). Another example is *Cnidoscolus* cf. *bahianus* (Euphorbiaceae) from Brazil which produces a latex that contains 13,500 μg g^{-1} Ni, whereas the leaves are much less Ni-rich with only 100 to 1,020 μg g^{-1} Ni (Reeves et al., 2007). Field qualitative testing of several other species belonging to *Euphorbia, Chamaesyce*, and *Manihot* also revealed latex containing >1,000 μg g^{-1} Ni (Reeves et al., 2007). Observation of Ni-rich latex have also been made in *Planchonella roxburghiana* (Sapotaceae) and *Ficus trachypison* (Moraceae) from Halmahera (Indonesia) (Lopez et al., 2019). Hyperaccumulator plants with Ni-rich laticifers appear to be rare in the plant kingdom, but the phenomenon could have been largely overlooked. Many Ni hyperaccumulator plant species are in families known to produce laticifer cells (*e.g.* Asteraceae, Phyllanthaceae, Euphorbiaceae, Metcalfe, 1967) suggesting that more investigations into this phenomenon may be warranted.

CONCLUSION

Our study reveals outstanding Ni tolerance in a woody hyperaccumulator that is related to the plant scale distribution and large internal volume of laticifer cells. We also showed that growth is stimulated by Ni concentrations in the solution as high 100 μM Ni and Ni in the seed store of the cotyledons is translocated to the young shoots. These results strongly suggest a higher Ni requirement of this species, although the underlying function(s) remain elusive. Our study relied on a rare species, but the observation of Ni-rich latex in other hyperaccumulators species, suggest that this mechanism of Ni storage might be more common than previously thought. Future research is needed to elucidate how laticifer networks are involved in Ni trafficking throughout the plant.

DATA AVAILABILITY STATEMENT

The raw data supporting the conclusions of this article will be made available by the authors, without undue reservation.

AUTHOR CONTRIBUTIONS

AE and SI conceived the research. SI, VG, PE, and AE collected the plant samples in New Caledonia. LL'H performed the hydroponic experiments. VG conducted the XRF screening. AP and AE conducted the chemical analysis of plant tissue samples; JM made the matrix for the phylogenetic tree. SI, LL'H, and AP analyzed the data. SI and AE wrote the article with contributions from all authors. SI is the corresponding author for this work.

FUNDING

AE was the recipient of a Discovery Early Career Researcher Award (DE160100429) from the Australian Research Council. VG was the recipient of an Australia Awards PhD Scholarship from the Australian Federal Government. This work was supported by UMR AMAP.

ACKNOWLEDGMENTS

We thank the herbarium of New Caledonia (NOU) for assistance and permission to study material. We thank Hervé Jourdan for Apionidae identification, and Gilles Le Moguédec for valuable assistance with R software for the phylogeny. Authors thank the Province Sud de Nouvelle-Calédonie for permission to collect plant material (APA-NCPS-2018-11, 3058-2018).

SUPPLEMENTARY MATERIAL

The Supplementary Material for this article can be found online at: https://www.frontiersin.org/articles/10.3389/fpls.2020.559059/full#supplementary-material

REFERENCES

Agrawal, A. A., and Konno, K. (2009). Latex: a model for understanding mechanisms, ecology, and evolution of plant defense against herbivory. *Annu. Rev. Ecol. Evol. Syst.* 40 (1), 311–331. doi: 10.1146/annurev.ecolsys.110308.120307

Álvarez-Fernández, A., Díaz-Benito, P., Abadía, A., Lopez-Millan, A.-F., and Abadía, J. (2014). Metal species involved in long distance metal transport in plants. *Front. Plant Sci.* 5, 105. doi: 10.3389/fpls.2014.00105

Alves, S., Nabais, C., Simoes Goncalves Mde, L., and Correia Dos Santos, M. M. (2011). Nickel speciation in the xylem sap of the hyperaccumulator *Alyssum serpyllifolium* ssp. *lusitanicum* growing on serpentine soils of northeast Portugal. *J. Plant Physiol.* 168 (15), 1715–1722. doi: 10.1016/j.jplph.2011.04.004

Anacker, B. (2011). "Phylogenetic patterns of endemism and diversity," in *Serpentine: The Evolution and Ecology of a Model System*. Eds. S. P. Harisson and N. Rajakaruna (Berkeley, California, USA: University of California Press), 49–79.

Baker, A. J. M., and Brooks, R. R. (1989). Terrestrial higher plants which hyperaccumulate metallic elements - a review of their distribution, ecology and phytochemistry. *Biorecovery* 1, 81–126. doi: 10.1080/01904168109362867

Baker, A. J. M., Reeves, R. D., and Hajar, A. S. M. (1994). Heavy metal accumulation and tolerance in British populations of the metallophyte *Thlaspi caerulescens* J. & C. Presl (Brassicaceae). *New Phytol.* 127 (1), 61–68. doi: 10.1111/j.1469-8137.1994.tb04259.x

Becquer, T., Quantin, C., and Boudot, J. (2010). Toxic levels of metals in Ferralsols under natural vegetation and crops in New Caledonia. *Eur. J. Soil Sci.* 61, 994–1004. doi: 10.1111/j.1365-2389.2010.01294.x

Berazaín, R., de la Fuente, V., Sánchez-Mata, D., Rufo, L., Rodríguez, N., and Amils, R. (2007). Nickel localization on tissues of hyperaccumulator species of *Phyllanthus* L. (Euphorbiaceae) from Ultramafic Areas of Cuba. *Biol. Trace Elem. Res.* 115 (1), 67–86. doi: 10.1385/bter:115:1:67

Bhatia, N. P., Baker, A. J., Walsh, K. B., and Midmore, D. J. (2005). A role for nickel in osmotic adjustment in drought-stressed plants of the nickel hyperaccumulator *Stackhousia tryonii* Bailey. *Planta* 223 (1), 134–139. doi: 10.1007/s00425-005-0133-8

Borhidi, A. (2001). Phylogenetic trends in Ni-accumulating plants. *South Afr. J. Sci.* 97 (11-12), 544–547.

Boyd, R. S., and Jaffré, T. (2001). Phytoenrichment of soil content by *Sebertia acuminata in* New Caledonia and concept of elemental allelopathy. *S. Afr. J. Sci.* 97, 535–538. Available online at: https://hdl.handle.net/10520/EJC97252

Boyd, R. S., and Martens, S. N. (1998). The significance of metal hyperaccumulation for biotic interactions. *Chemoecology* 8 (1), 1–7. doi: 10.1007/s000490050002

Boyd, R. S., Wall, M. A., and Jaffré, T. (2006). Nickel levels in arthropods associated with Ni hyperaccumulator plants from an ultramafic site in New Caledonia. *Insect Sci.* 13 (4), 271–277. doi: 10.1111/j.1744-7917.2006.00094.x

Boyd, R. S. (2012). Plant defense using toxic inorganic ions: conceptual models of the defensive enhancement and joint effects hypotheses. *Plant Sci.* 195, 88–95. doi: 10.1016/j.plantsci.2012.06.012

Brooks, R. R., Lee, J., Reeves, R. D., and Jaffré, T. (1977). Detection of nickeliferous rocks by analysis of herbarium specimens of indicator plants. *J. Geochem. Explor.* 7, 49–57. doi: 10.1016/0375-6742(77)90074-7

Brooks, R. R. (1987). *Serpentine and its vegetation: a multidisciplinary approach* (Portland OR: Dioscorides Press).

Brown, P. H., Welch, R. M., and Cary, E. E. (1987). Nickel: a micronutrient essential for higher plants. *Plant Physiol.* 85 (3), 801–803. doi: 10.1104/pp.85.3.801

Cappa, J. J., and Pilon-Smits, E. A. H. (2014). Evolutionary aspects of elemental hyperaccumulation. *Planta* 239 (2), 267–275. doi: 10.1007/s00425-013-1983-0

Castelblanque, L., Balaguer, B., Marti, C., Rodriguez, J. J., Orozco, M., and Vera, P. (2016). Novel insights into the organization of laticifer cells: a cell comprising a unified whole system. *Plant Physiol.* 172 (2), 1032–1044. doi: 10.1104/pp.16.00954

Castelblanque, L., Balaguer, B., Marti, C., Rodriguez, J. J., Orozco, M., and Vera, P. (2017). Multiple facets of laticifer cells. *Plant Signal. Behav.* 12 (7), e1300743. doi: 10.1080/15592324.2017.1300743

Chaney, R. L., Fellet, G., Torres, R., Centofanti, T., Green, C. E., and Marchiol, L. (2009). Using chelator-buffered nutrient solutions to limit Ni phytoavailability to the Ni-hyperaccumulator *Alyssum murale*. *Northeast. Nat.* 16 (sp5), 215–222. doi: 10.1656/045.016.0517

Deng, T. H., Cloquet, C., Tang, Y. T., Sterckeman, T., Echevarria, G., Estrade, N., et al. (2014). Nickel and zinc isotope fractionation in hyperaccumulating and nonaccumulating plants. *Environ. Sci. Technol.* 48 (20), 11926–11933. doi: 10.1021/es5020955

Deng, T.-H.-B., Tang, Y.-T., van der Ent, A., Sterckeman, T., Echevarria, G., Morel, J.-L., et al. (2016). Nickel translocation via the phloem in the hyperaccumulator *Noccaea caerulescens* (Brassicaceae). *Plant Soil* 404, 35–45. doi: 10.1007/s11104-016-2825-1

Eskew, D. L., Welch, R. M., and Cary, E. E. (1983). Nickel: an essential micronutrient for legumes and possibly all higher plants. *Science* 222 (4624), 621–623. doi: 10.1126/science.222.4624.621

Evert, R. F. (2006). *Esau"s Plant Anatomy* (Hoboken, New Jersey, USA: A John Wiley & Sons, Inc).

Gabbrielli, R., Mattioni, C., and Vergnano, O. (1991). Accumulation mechanisms and heavy metal tolerance of a nickel hyperaccumulator. *J. Plant Nutr.* 14 (10), 1067–1080. doi: 10.1080/01904169109364266

Gei, V., Isnard, S., Erskine, P., Echevarria, G., Fogliani, B., Jaffré, T., et al. (2020). A systematic assessment of the occurrence of trace element hyperaccumulation in the flora of New Caledonia. *Bot. J. Linn. Soc.* 194 (1), 1–22. doi: 10.1093/botlinnean/boaa029. boaa029.

Gerendás, J., Polacco, J. C., Freyermuth, S. K., and Sattelmacher, B. (1999). Significance of nickel for plant growth and metabolism. *J. Plant Nutr. Soil Sci.* 162 (3), 241–256. doi: 10.1002/(sici)1522-2624(199906)162:3<241::Aid-jpln241>3.0.Co;2-q

Gould, S. J., and Vrba, E. S. (1982). Exaptation - a missing term in the science of form. *Palaeobiology* 8, 4–15.

Hagel, J. M., Yeung, E. C., and Facchini, P. J. (2008). Got milk? The secret life of laticifers. *Trends Plant Sci.* 13 (12), 631–639. doi: 10.1016/j.tplants.2008.09.005

Iori, V., Pietrini, F., Cheremisina, A., Shevyakova, N. I., Radyukina, N., Kuznetsov, V. V., et al. (2013). Growth responses, metal accumulation and phytoremoval capability in *Amaranthus* plants exposed to nickel under hydroponics. *Water Air Soil Pollut.* 224 (2). doi: 10.1007/s11270-013-1450-3

Isnard, S., L'huillier, L., Rigault, F., and Jaffré, T. (2016). How did the ultramafic soils shape the flora of the New Caledonian hotspot? *Plant Soil* 403 (1-2), 53–76. doi: 10.1007/s11104-016-2910-5

Jaffré, T., Brook, R. R., Lee, J., and Reeves, R. G. (1976). *Sebertia acuminata*: A hyperaccumulator of nickel from New Caledonia. *Science* 193 (4253), 579–580. doi: 10.1126/science.193.4253.579

Jaffré, T., Kersten, W., Brooks, R. R., and Reeves, R. D. (1979). Nickel uptake by Flacourtiaceae of New Caledonia. *Proc. R. Soc Lond. Ser. B.: Biol. Sci.* 205 (1160), 385–394. doi: 10.1098/rspb.1979.0072

Jaffré, T., Pillon, Y., Thomine, S., and Merlot, S. (2013). The metal hyperaccumulators from New Caledonia can broaden our understanding of nickel accumulation in plants. *Front. Plant Physiol.* 4, 279. doi: 10.3389/fpls.2013.00279

Jaffré, T., Reeves, R. D., Baker, A. J. M., Schat, H., and van der Ent, A. (2018). The discovery of nickel hyperaccumulation in the New Caledonian tree Pycnandra acuminata 40 years on: an introduction to a Virtual Issue. *New Phytol.* 218 (2), 397–400. doi: 10.1111/nph.15105

Kahle, H. (1993). Response of roots of trees to heavy metals. *Environ. Exp. Bot.* 33 (1), 99–119. doi: 10.1016/0098-8472(93)90059-O

Kersten, W. J., Brooks, R. R., Reeves, R. D., and Jaffré, T. (1979). Nickel uptake by New Caledonian species of *Phyllanthus*. *Taxon* 28 (5-6), 529–534. doi: 10.2307/1219791

Krämer, U., Smith, R. D., Wenzel, W. W., Raskin, I., and Salt, D. E. (1997). The role of metal transport and tolerance in nickel hyperaccumulation by *Thlaspi goesingense* Halàcsy. *Plant Physiol.* 115 (4), 1641–1650. doi: 10.1104/pp.115.4.1641

Krämer, U. (2010). Metal hyperaccumulation in plants. *Annu. Rev. Plant Biol.* 61 (1), 517–534. doi: 10.1146/annurev-arplant-042809-112156

Kutchan, T. M. (2005). A role for intra- and intercellular translocation in natural product biosynthesis. *Curr. Opin. Plant Biol.* 8 (3), 292–300. doi: 10.1016/j.pbi.2005.03.009

Lasat, M. M., Baker, A., and Kochian, L. V. (1996). Physiological Characterization of Root Zn2+ Absorption and Translocation to Shoots in Zn Hyperaccumulator and Nonaccumulator Species of Thlaspi. *Plant Physiol.* 112 (4), 1715–1722. doi: 10.1104/pp.112.4.1715

Lasat, M. M., Baker, A. J., and Kochian, L. V. (1998). Altered Zn Compartmentation in the Root Symplasm and Stimulated Zn Absorption into the Leaf as Mechanisms Involved in Zn Hyperaccumulation in *Thlaspi caerulescens*. *Plant Physiol.* 118 (3), 875–883. doi: 10.1104/pp.118.3.875

Leitenmaier, B., and Küpper, H. (2013). Compartmentation and complexation of metals in hyperaccumulator plants. *Front. Plant Sci.* 4:374. doi: 10.3389/fpls.2013.00374

Lopez, S., van der Ent, A., Erskine, P., Echevarria, G., Morel, J. L., Lee, G., et al. (2019). Rhizosphere chemistry and above-ground elemental fractionation of nickel hyperaccumulator species from Weda Bay (Indonesia). *Plant Soil*. 436, 543–563. doi: 10.1007/s11104-019-03954-w

Martens, S. N., and Boyd, R. S. (1994). The ecological significance of nickel hyperaccumulation: a plant chemical defense. *Oecologia* 98 (3), 379–384. doi: 10.1007/bf00324227

McCartha, G. L., Taylor, C. M., van der Ent, A., Echevarria, G., Navarrete Gutierrez, D. M., and Pollard, A. J. (2019). Phylogenetic and geographic distribution of nickel hyperaccumulation in neotropical *Psychotria*. *Am. J. Bot.* 106 (10), 1377–1385. doi: 10.1002/ajb2.1362

Mesjasz-Przybylowicz, J., Przybyłowicz, W., Barnabas, A., and van der Ent, A. (2016). Extreme nickel hyperaccumulation in the vascular tracts of the tree *Phyllanthus balgooyi* from Borneo. *New Phytol.* 209 (4), 1513–1526. doi: 10.1111/nph.13712

Metcalfe, C. R. (1967). Distribution of latex in the plant kingdom. *Econ. Bot.* 21 (2), 115–127. doi: 10.1007/bf02897859

Migula, P., Przybyłowicz, W. J., Mesjasz-Przybyłowicz, J., Augustyniak, M., Nakonieczny, M., Głowacka, E., et al. (2007). Micro-PIXE studies of elemental distribution in sap-feeding insects associated with Ni hyperaccumulator, Berkheya coddii. *Plant Soil* 293 (1-2), 197–207. doi: 10.1007/s11104-007-9231-7

Mishra, D., and Kar, M. (1974). Nickel in plant growth and metabolism. *Bot. Rev.* 40 (4), 395–452. doi: 10.1007/BF02860020

Munzinger, J., Morat, P., Jaffré, T., Gâteblé, G., Pillon, Y., Rouhan, G., et al. (2020). *[continuously updated]). FLORICAL: Checklist of the vascular indigenous flora of New Caledonia*. Available at: http://publish.plantnet-project.org/project/florical. doi: 10.13140/RG.2.1.1760.6007

Nishida, S., Tsuzuki, C., Kato, A., Aisu, A., Yoshida, J., and Mizuno, T. (2011). AtIRT1, the primary iron uptake transporter in the root, mediates excess nickel accumulation in *Arabidopsis thaliana*. *Plant Cell Physiol.* 52 (8), 1433–1442. doi: 10.1093/pcp/pcr089

Perrier, N., Colin, F., Jaffré, T., Ambrosi, J.-P., Rose, J., and Bottero, J.-Y. (2004). Nickel speciation in *Sebertia acuminata*, a plant growing on a lateritic soil of New Caledonia. *C. R. Geosci.* 336 (6), 567–577. doi: 10.1016/j.crte.2003.12.014

Pickard, W. F. (2008). Laticifers and secretory ducts: two other tube systems in plants. *New Phytol.* 177 (4), 877–888. doi: 10.1111/j.1469-8137.2007.02323.x

Pillon, Y., Munzinger, J., Amir, H., and Lebrun, M. (2010). Ultramafic soils and species sorting in the flora of New Caledonia. *J. Ecol.* 98, 1108–1116. doi: 10.1111/j.1365-2745.2010.01689.x

Pillon, Y. (2012). Time and tempo of diversification in the flora of New Caledonia. *Bot. J. Linn. Soc* 170 (3), 288–298. doi: 10.1111/j.1095-8339.2012.01274.x

Rascio, N., and Navari-Izzo, F. (2011). Heavy metal hyperaccumulating plants: how and why do they do it? and what makes them so interesting? *Plant Sci.* 180 (2), 169–181. doi: 10.1016/j.plantsci.2010.08.016

Reeves, R. D., Baker, A. J. M., Borhidi, A., and Berazain, R. (1996). Nickel-accumulating plants from the ancient serpentine soils of Cuba. *New Phytol.* 133 (2), 217–224. doi: 10.1111/j.1469-8137.1996.tb01888.x

Reeves, R. D., Baker, A. J. M., Borhidi, A., and Berazaín, R. (1999). Nickel hyperaccumulation in the serpentine flora of Cuba. *Ann. Bot.* 83 (1), 29–38. doi: 10.1006/anbo.1998.0786

Reeves, R. D., Baker, A. J. M., Becquer, T., Echevarria, G., and Miranda, Z. J. G. (2007). The flora and biogeochemistry of the ultramafic soils of Goiás state, Brazil. *Plant Soil* 293 (1-2), 107–119. doi: 10.1007/s11104-007-9192-x

Reeves, R. D., Baker, A. J. M., Jaffré, T., Erskine, P., Echevarria, G., and van der Ent, A. (2018). A database for plants that hyperaccumulate metals and metalloid trace elements. *New Phytol.* 218, 407–411. doi: 10.1111/nph.14907

Reeves, R. D. (2003). Tropical hyperaccumulators of metals and their potential for phytoextraction. *Plant Soil* 249 (1), 57–65. doi: 10.1023/a:1022572517197

Robinson, B. H., Lombi, E., Zhao, F. J., and McGrath, S. P. (2003). Uptake and distribution of nickel and other metals in the hyperaccumulator *Berkheya coddii*. *New Phytol.* 158 (2), 279–285. doi: 10.1046/j.1469-8137.2003.00743.x

Sagner, S., Kneer, R., Wanner, G., Cosson, J. P., Deus-Neumann, B., and Zenk, M. H. (1998). Hyperaccumulation, complexation and distribution of nickel in *Sebertia acuminata*. *Phytochemistry* 47 (3), 339–347. doi: 10.1016/s0031-9422(97)00593-1

Seregin, I. V., and Kozhevnikova, A. D. (2006). Physiological role of nickel and its toxic effects on higher plants. *Russian J. Plant Physiol.* 53 (2), 257–277. doi: 10.1134/s1021443706020178

Shah, F. U. R., Ahmad, N., Masood, K. R., Peralta-Videa, J. R., and Ahmad, F. (2010). "Heavy metal toxicity in plants," in *Plant Adaptation and Phytoremediation*. Eds. M. Ashraf, M. Ozturk and M. S. A. Ahmad (Dordrecht: Springer Netherlands), 71–97.

Swenson, U., and Munzinger, J. (2010). Revision of *Pycnandra* subgenus *Sebertia* (Sapotaceae) and a generic key to the family in New Caledonia. *Adansonia* 32 (2), 239–249 211. doi: 10.5252/a2010n2a5

Swenson, U., and Munzinger, J. (2016). Five new species and a systematic synopsis of *Pycnandra* (Sapotaceae), the largest endemic genus in New Caledonia. *Aust. Syst. Bot.* 29 (1), 1–40. doi: 10.1071/SB16001

Swenson, U., Bartish, I. V., and Munzinger, J. (2007). Phylogeny, diagnostic characters, and generic limitation of Australasian Chrysophylloideae (Sapotaceae, Ericales): Evidence from ITS sequence data and morphology. *Cladistics* 23, 201–228. doi: 10.1111/j.1096-0031.2006.00141.x

Swenson, U., Nylinder, S., and Munzinger, J. (2014). Sapotaceae biogeography supports New Caledonia being an old Darwinian island. *J. Biogeogr.* 41 (4), 797–809. doi: 10.1111/jbi.12246

Swenson, U., Munzinger, J., Lowry, P. P.II, Cronholm, B., and Nylinder, S. (2015). Island life – classification, speciation and cryptic species of *Pycnandra* (Sapotaceae) in New Caledonia. *Bot. J. Linn. Soc* 179 (1), 57–77. doi: 10.1111/boj.12308

Taiz, L., and Zeiger, E. (2006). *Plant Physiology*. *4th edn* (Sunderland: Sinauer Associates, Inc.).

Tan, X. W., Ikeda, H., and Oda, M. (2000). Effects of nickel concentration in the nutrient solution on the nitrogen assimilation and growth of tomato seedlings in hydroponic culture supplied with urea or nitrate as the sole nitrogen source. *Sci. Hortic.* 84 (3-4), 265–273. doi: 10.1016/s0304-4238(99)00107-7

van der Ent, A., and Mulligan, D. (2015). Multi-element concentrations in plant parts and fluids of Malaysian nickel hyperaccumulator plants and some economic and ecological considerations. *J. Chem. Ecol.* 41 (4), 396–408. doi: 10.1007/s10886-015-0573-y

van der Ent, A., Baker, A. J. M., Reeves, R. D., Pollard, A. J., and Schat, H. (2013). Hyperaccumulators of metal and metalloid trace elements: Facts and fiction. *Plant Soil* 362 (1-2), 319–334. doi: 10.1007/s11104-012-1287-3

van der Ent, A., Jaffré, T., L'Huillier, L., Gibson, N., and Reeves, R. D. (2015). The flora of ultramafic soils in the Australia–Pacific region: state of knowledge and research priorities. *Aust. J. Bot.* 63 (4), 173–190. doi: 10.1071/BT15038

van der Ent, A., Callahan, D. L., Noller, B. N., Mesjasz-Przybylowicz, J., Przybylowicz, W. J., Barnabas, A., et al. (2017). Nickel biopathways in tropical nickel hyperaccumulating trees from Sabah (Malaysia). *Sci. Rep.* 7, 41861. doi: 10.1038/srep41861

van der Ent, A., Echevarria, G., Pollard, A. J., and Erskine, P. (2019a). X-Ray fluorescence ionomics of herbarium collections. *Sci. Rep.* 9, 4746. doi: 10.1038/s41598-019-40050-6

van der Ent, A., Ocenar, A., Tisserand, R., Sugau, J. B., Echevarria, G., and Erskine, P. D. (2019b). Herbarium X-ray fluorescence screening for nickel, cobalt and manganese hyperaccumulator plants in the flora of Sabah (Malaysia, Borneo Island). *J. Geochem. Explor.* 202, 49–58. doi: 10.1016/j.gexplo.2019.03.013

Wanat, M., and Munzinger, J. (2012). Biology of the Apionidae (Coleoptera: Curculionoidea) in New Caledonia, a preliminary report. *Zootaxa* 3554, 59–74. doi: 10.11646/zootaxa.3717.4.5

Conflict of Interest: The authors declare that the research was conducted in the absence of any commercial or financial relationships that could be construed as a potential conflict of interest.

frontiers in Plant Science

ORIGINAL RESEARCH
published: 09 September 2020
doi: 10.3389/fpls.2020.01297

Glutamic Acid-Assisted Phytomanagement of Chromium Contaminated Soil by Sunflower (*Helianthus annuus* L.): Morphophysiological and Biochemical Alterations

Mujahid Farid[1], Sheharyaar Farid[2], Muhammad Zubair[3], Muhammad Awais Ghani[4], Muhammad Rizwan[2], Hafiz Khuzama Ishaq[1], Saad Alkahtani[5], Mohamed M. Abdel-Daim[5,6] and Shafaqat Ali[2,7]**

[1] Department of Environmental Sciences, University of Gujrat, Gujrat, Pakistan, [2] Department of Environmental Sciences and Engineering, Government College University, Faisalabad, Pakistan, [3] Department of Chemistry, University of Gujrat, Gujrat, Pakistan, [4] Department of Agronomy, University of Agriculture Faisalabad, Institute of Horticultural Science, Faisalabad, Pakistan, [5] Department of Zoology, College of Science, King Saud University, Riyadh, Saudi Arabia, [6] Pharmacology Department, Faculty of Veterinary Medicine, Suez Canal University, Ismailia, Egypt, [7] Department of Biological Sciences and Technology, China Medical University, Taichung, Taiwan

OPEN ACCESS

Edited by:
Mukesh Kumar Kanwar, Zhejiang University, China

Reviewed by:
Neil J. Willey, University of the West of England, United Kingdom
Durgesh Kumar Tripathi, Amity University, India

***Correspondence:**
Mujahid Farid
mujahid726@yahoo.com
Shafaqat Ali
shafaqataligill@yahoo.com; shafaqat@mail.cmuh.org.tw

Specialty section:
This article was submitted to Plant Nutrition, a section of the journal Frontiers in Plant Science

Received: *19 March 2020*
Accepted: *07 August 2020*
Published: *09 September 2020*

Citation:
Farid M, Farid S, Zubair M, Ghani MA, Rizwan M, Ishaq HK, Alkahtani S, Abdel-Daim MM and Ali S (2020) Glutamic Acid-Assisted Phytomanagement of Chromium Contaminated Soil by Sunflower (Helianthus annuus L.): Morphophysiological and Biochemical Alterations. Front. Plant Sci. 11:1297. doi: 10.3389/fpls.2020.01297

Chelator-assisted phytoremediation is an economical, sustainable, and ecologically friendly method of extracting heavy metals and metalloids from the soil. Organic chelators are thought to enhance metal availability and mobility in contaminated media, thereby improving phytoextraction. The aim of the present study was to examine whether exogenous application of glutamic acid (GA) could improve chromium (Cr) phytoextraction by sunflower plants (*Helianthus annuus* L.). Seeds were planted in plastic pots filled with 5 kg of local agricultural soil spiked with increasing concentrations of Cr (1, 2, and 5 mg kg^{-1}). Glutamic acid (5 mM) was applied to soil in solution according to a completely randomized experimental design, and the sunflower plants were harvested after 8 weeks. The results indicated that increasing Cr-induced stress significantly inhibited plant growth, leading to reduced biomass, photosynthetic pigment content, activities of antioxidant enzymes, and leaf area of the sunflower plants. However, exogenous addition of GA significantly reduced the Cr-associated toxic effects while also increasing the accumulation of Cr in the plants. Moreover, increasing concentrations of Cr in the soil increased the generation of reactive oxygen species (ROS) responsible for the altered antioxidant enzyme activities. The results revealed that GA application to the topsoil enhanced the Cr concentration and accumulation in the root, stem, and leaves by up to 254, 225, 355, and 47, 59, 150% respectively. Further the GA addition reduced the Cr-induced toxicity in plants and might be helpful for enhancing Cr phytoextraction by sunflower plants.

Keywords: accumulation, chromium, glutamic acid, photosynthetic pigments, phytoextraction, sunflower

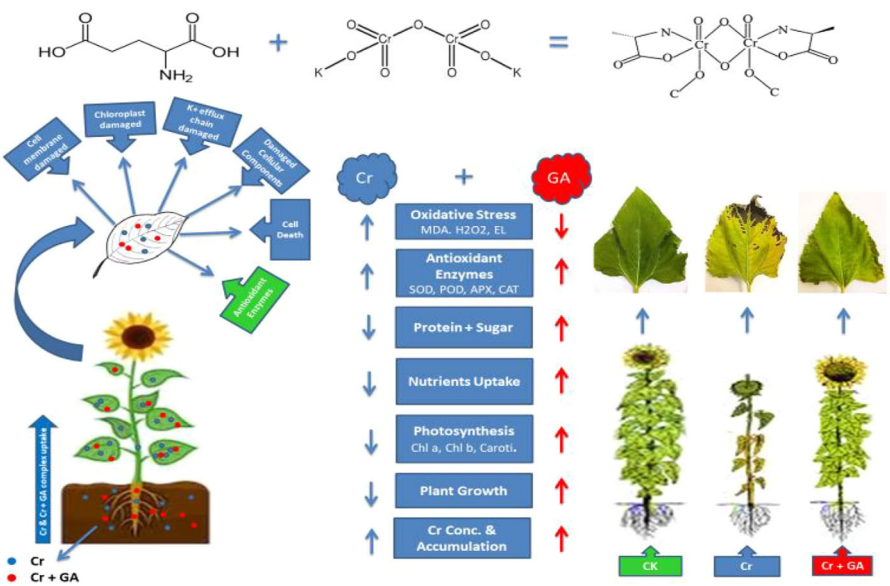

GRAPHICAL ABSTRACT |

INTRODUCTION

Topsoil provides macro- and micronutrients that are essential for plants and serves as a sink for toxic heavy metals. Among the heavy metals, cadmium (Cd), lead (Pb), chromium (Cr), arsenic (As), and mercury (Hg) are known to be some of the most harmful poisonous elements in the environment (Ali et al., 2013; Adrees et al., 2015a; Shakoor et al., 2014; Ali et al., 2015). Numerous natural and anthropogenic activities result in the escape of hazardous substances into the air, water, and soil that can harm both human health and the environment. Under natural conditions, many crops are vulnerable to a variety of stresses, including those associated with heavy metals, drought, salinity, and disease (Shahid et al., 2017). Heavy metal toxicity is the most common problem affecting plant growth and yield. Heavy metals can also enter the food chain and accumulate in plant and human body tissues (Rizwan et al., 2016). Chromium is a relatively abundant heavy metal in the topsoil owing to its utility in various industrial processes (Farid et al., 2018a). It is used both in the electroplating industry as an anticorrosive and antibiofouling agent, as well as in steel and automobile manufacturing (Farid et al., 2017a). Chromium-mediated toxicity to plants depends on its valence state, with Cr(VI) being very toxic to plants, and Cr(III) less so (Ali et al., 2013; Ali et al., 2015). There is evidence that plants grown on Cr-polluted soil undergo changes in the germination process and exhibit retarded growth (Farid et al., 2017a; Habiba et al., 2018). Additionally, Cr causes many physiological disorders in plants by altering nutrient uptake and the activity of the photosynthetic machinery (Nguyen et al., 2017).

The process of microbial conversion of hexavalent Cr to its trivalent form is cost-effective. The continuous monitoring of microbial activity is essential for this process due to higher sensitivity (Narayania and Shetty, 2012). Although alkaline digestion is used for extracting assimilated and soluble Cr(VI) from soil media (Forte and Mutiti, 2017), this method does not allow for the complete recovery of metals owing to limitations such as the oxidation of Cr(III) (Shahid et al., 2017).

Plants are increasingly used for the remediation of contaminated soil and water as a substitute for the more expensive conventional purifying techniques (Nguyen et al., 2017). Phytoremediation refers to the use of plants for minimizing the concentration of toxic metals in contaminated soil. Plants that are used for phytoremediation and that have an enhanced capacity to accumulate metals from contaminated soil with greater ability to translocate metals in the above ground biomass generally considered as translocation factor greater than 1 (TF > 1) are known as hyperaccumulator plants (Cunningham et al., 1995; Mantry and Patra, 2017). Generally, metals cannot be easily extracted from soil media in great quantities because they form complex bonds with ligands in the soil. Recent studies have shown that plants used for remediation accumulate larger amounts of heavy metals in their roots and then transfer them to above-ground biomass (Wei et al., 2011; Saleem et al., 2015; Lukina et al., 2016). This suggests that plants with greater biomass, such as mustard, rapeseed, maize and sunflower plants, can be beneficial in the field and can survive in the presence of toxic heavy metals (Cekic et al., 2017; Rizwan et al., 2017a). Along with higher biomass plants, many vegetables, ornamental and floating plant species also showed greater accumulation potential (Amir et al., 2020; Khair et al., 2020; Khalid et al., 2020) Phytoremediation refers to the use of plants for the extractive removal of metal contamination from soil and aquatic media. (Salt et al., 1998; USEPA, 2000). An increasing number of studies have shown that specific plant species can

remove, degrade, and immobilize a wide range of harmful contaminants (Lasat, 2000). Phytostabilization is used to treat Cr (VI) by converting it into the less toxic Cr(III) with the help of pre-existing plant species (Ali et al., 2013; Farid et al., 2015; Farid et al., 2017b). Different amendments are used worldwide, including organic and inorganic acids (Rizwan et al., 2017a). However, the focus is currently centered on organic acids due to their rapid degradation and potential to enhance metal bioavailability and plant growth (Wiszniewska et al., 2016). Several studies have demonstrated the potential of glutamic acid (GA) as a biodegradable chelating agent (Farid et al., 2018b), such as its ability to enhance the capacity of plants for phytoremediation of different heavy metals (Wei et al., 2011). The success of phytoextraction is mainly reliant on the ability of plants to produce enough aboveground biomass and on their hyperaccumulation potential (translocation of metals from root to shoot) (Yeh and Pan, 2012; Fatima et al., 2020). The results of recent studies have demonstrated the potential of the sunflower plant for the phytoextraction of heavy metals such as Pb, Cd, Cr, Hg, and nickel (Ni) (Yeh and Pan, 2012; De Maria et al., 2013; Farid et al., 2018a; Farid et al., 2018b). Furthermore, the added-value of edible oil yield from the sunflower reduces the costs of phytoremediation (Nehnevajova et al., 2007; 2012). Chemical mutagenesis can also help to increase the capacity of the sunflower to extract heavy metals (Nehnevajova et al., 2009). However, there are only few studies reported on the chelating effect of glutamic acid (GA). Farid et al. (2018a; 2018b) reported that the translocation and accumulation of Cr and Ni were increased in sunflower plants treated with organic chelating acids. Artificially prepared chelators have been extensively used for the plant-mediated extraction of toxic metals in both water and soil media (Huang et al., 1997; Epstein et al., 1999); however, the risks of leaching into groundwater and heavy metal persistence renders them unsuitable for this technique (Farid et al., 2015). The application of gallic acid to the soil of growing sunflower seedlings greatly enhances growth parameters such as oil yield and carbohydrate and protein contents of the plants, as well as the uptake of Ni (Farid et al., 2017b).

The use of GA as a mediator to improve plant growth for enhanced metal extraction has not been comprehensively investigated (Barros-Galvao et al., 2017). Therefore, the aim of the current study was a) to observe the influence of metal concentration on growth characteristics of sunflower (b) to measure the effect of GA on the growth and physiology of sunflower under Cr stress, and (c) to evaluate the phytoextraction potential of sunflower for Cr with AA amendment.

MATERIALS AND METHODS

Plant Resources and Growing Conditions

In the present study, loamy clay soil (52% clay, 26% silt, 22% sand) was collected from the botanical garden of the University of Gujrat, Pakistan, at a depth of 0–20 cm. To eliminate debris and plant residues, the soil was passed through a 2-mm sieve. Healthy seeds of the sunflower (*Helianthus annuus* L.) genotype Faisalabad Hybrid FH-614 were collected from the Oilseeds Research Institute, AARI, Faisalabad (Farid et al., 2017b). Experiments were carried out in the botanical garden of the University of Gujrat under controlled semi-dry weather conditions. The seeds were washed and rinsed with 10% hydrogen peroxide (H_2O_2) to remove germs and then rinsed with distilled water. Ten seeds were sown per pot filled with 5 kg of soil, and after 15 days of germination the plants were thinned to five plants per pot to give five experimental replicates. The plants that were removed were then crushed and mixed in the same pot for green manure. The experiment was performed under a complete randomized design (CRD). After 15 and 30 days of germination, each pot was supplied with a 500-ml solution of fertilizer comprising 2.14 g L^{-1} K (as K_2SO_4), 2.19 g L^{-1} N [as $(NH_2)_2CO$], and 0.5 g L^{-1} P [as $(NH_4)_2HPO_4$].

Treatments

At 4 weeks post-germination, juvenile plants grown in Cr-spiked soil (1, 2, and 5 mg kg^{-1}) were treated with GA (5 mM). The following eight combinations consisting five replicated for each treatment were used in the present study: T1, Cr (0 mg kg^{-1}) + GA (0 mM); T2, Cr (1 mg kg^{-1}); T3, Cr (2 mg kg^{-1}); T4, Cr (5 mg kg^{-1}); T5, GA (5 mM); T6, Cr (1 mg kg^{-1}) + GA (5 mM); T7, Cr (2 mg kg^{-1}) + GA (5 mM); T8, Cr (5 mg kg^{-1}) + GA (5 mM). The Cr(VI) background level was 0.12 mg kg^{-1} of soil. The GA was dissolved in deionized water and exogenously applied to the soil by pouring into the pot weekly for the following 8 consecutive weeks.

Plant Sampling and Analysis

After 8 weeks of treatment, three biological replicate plants were harvested to provide a mean for each of the five experimental replicates. All the samples were washed with deionized water, and leftover water was absorbed using a napkin. All the plants were systematically separated into leaves, stems, and roots. Agronomic traits such as root length, plant height, number of flowers and leaves per plant, leaf area, and dry and fresh weight of all parts (leaf, stem, and root) were measured. An electric scale was used for the measurement of fresh and dry biomass. After drying at 90°C in an electric oven, the samples were used for further analysis.

Plant Accessory Pigment Assay

After 8 weeks of treatment, the fully expanded sunflower leaves were collected to assess the chlorophyll (Chl a, Chl b, total Chl) and carotenoid contents using a spectrophotometer (Halo DB20/DB-20S, Dynamica Labs, London, UK) according to the method of Metzner et al. (1965) with some modifications. Leaf pigments were collected by normalizing with an 85% (v/v) solution of acetone at 4°C with continuous stirring in the dark until staining was completed.

The extracted pigment was centrifuged for 10 min at 4,000 rpm, and the resulting pigment was placed in a spectrophotometer to record the absorbance at the wavelengths of 663, 644, and 452.5 nm against a blank of 85% acetone (v/v) solution. To estimate chlorophyll a and b and carotenoid

contents, the results were integrated according to the adjusted extinction constants and the equation given by Lichtenthaler (1987) as follows:

$$\text{Chlorophyll a}(\text{mg kg}^{-1}) = 10.3 \times E663 - 0.98b \times bE644$$

$$\text{Chlorophyll b}(\text{mg kg}^{-1}) = 19.7 \times E644 - 3.87b \times bE663$$

$$\text{Total chlorophyll} = \text{chlorophyll a} + \text{chlorophyll b}$$

$$\text{Total carotenoids}\ (\text{mg kg}^{-1}) = 4.2 \times \text{E452.5} - \{(0.0264 \times \text{chlorophyll a}) + (0.426 \times \text{chlorophyll b})\}$$

The pigment quantities were expressed as milligrams per gram fresh weight.

Analysis of Chromium Content

A known weight of leaves, stems, or roots samples dehydrated at 90°C was placed in a muffle-type furnace for 7 h at 650°C then the remnants were mixed with nitric acid (HNO_3) and hydrochloric acid (HCl) at a 3:1 ratio, and the samples were then diluted to 50 ml with deionized water and examined using an atomic absorption spectrometer (NOVA A400 Analytik Jena, Germany) to measure the Cr concentration, as described by Ehsan et al. (2013).

The amount of Cr was calculated as follows:

$$\text{Cr concentration}\ (\text{mg kg}^{-1}) = \text{metal reading of digested sample}\ (\text{mg L} - 1) \times \text{dilution factor}$$

Cr accumulation was measured with the following formula:

$$\text{Cr accumulation}\ (\text{mg plant}^{-1}) = \text{Cr concentration in each organ}\ (\text{mg kg}^{-1}) \times \text{dry weight of the organ (kg)}$$

Determination of Electrolyte Leakage and Levels of MDA and H_2O_2

Electrolyte leakage (EL) was estimated using a technique defined by Dionisio-Sese and Tobita (1998). After 8 weeks of treatment, the uppermost and fully stretched sunflower leaves were cut into 5-mm long pieces and then inserted into test tubes filled with 8 ml of deionized water. The initial electrical conductivity (EC1) was then measured after incubation in a water bath at 32°C for 2 h. To discharge all the electrolytes into the solution, the test tubes containing the same samples as of EC1 were first autoclaved at 121°C for 20 min; when the samples had cooled to room temperature (25°C), the second electrical conductivity (EC2) was measured using a pH/conductivity meter (INCO-LAB, Model 720, Kuwait). The following equation was used to compute EL:

$$\text{EL} = (\text{EC1}/\text{EC2}) \times 100$$

The malondialdehyde (MDA) concentration in the roots and leaves of the sunflower was determined by the thiobarbituric acid (TBA) reaction method (Heath and Packer, 1968) modified by Dhindsa et al. (1981) and Zhang and Kirkham (1994). Root and leaf samples (0.25 g) were homogenized with 5 ml (0.1%) of trichloroacetic acid (TCA). The resulting mixture was centrifuged at 10,000 × *g* for 5 min, and an additional 4 ml of TCA (20%) containing TBA (0.5%) was mixed into 1 ml of the supernatant solution. The solution was heated for 30 min at 95°C and subsequently cooled in an ice bath. The post-centrifugation absorbance at 600 nm was subtracted from the absorbance at 532 nm of the same mixture. An extinction coefficient of 155 mM^{-1} cm^{-1} was used to compute MDA content.

The H_2O_2 concentration was measured using the colorimetric method of Jana and Choudhuri, 1981. To extract the H_2O_2, leaf and root samples (50 mg) were homogenized with 3 ml of 50 mM phosphate buffer (pH 6.5) and subsequently centrifuged at 6,000 × *g* for 25 min. To measure the concentration of H_2O_2, the supernatant was mixed with 1 ml of titanium sulfate (0.1%) and 20% H_2SO_4 (v/v), and 3 ml of the solution was again centrifuged at 6000 × *g* for 15 min until the supernatant turned yellow. The supernatant was subsequently analyzed at 410 nm to determine the concentration of H_2O_2 which was calculated using the extinction coefficient 0.28 μmol^{-1} cm^{-1}.

SPAD Value

One week before plant harvest, leaf greenness (chlorophyll) was measured in the second uppermost fully expanded leaf using a SPAD chlorophyll meter SPAD-502 (Zhejiang Top Cloud-Agri Technology Co., Ltd.).

Evaluation of Antioxidant Enzymes and Protein Content

The contents of antioxidant enzymes (SOD, POD, APX, and CAT) in the roots and leaves were determined using a UV-Visible spectrophotometer (Halo DB20/DB-20S, Dynamica Labs, London, UK). Samples of roots and fully expanded leaves were collected after 8 weeks of treatment to measure the enzyme content. Leaf and root samples (1 g) were snap-frozen in liquid nitrogen and ground using a precooled mortar and pestle and then mixed with 0.05 M phosphate buffer (pH 7.8). The prepared samples were then filtered through four layers of muslin cloth and the homogenates centrifuged at 12,000 × *g* for 10 min at 4°C. The final supernatant was directly used to measure the SOD and POD contents according to the method described by Zhang (1992). The same supernatant was used for measurement of the soluble protein content using standard albumin and dye (Coomassie brilliant blue G-250) as reported by Bradford (Bradford, 1976).

The CAT (EC 1.11.1.6) content was measured following the protocol of Aebi (1984). The assay mixture was prepared by adding 100 µl of the extract of each enzyme and H_2O_2 (300 mM) to 2.8 ml of 50 mM phosphate buffer (2 mM citric acid (CA), pH 7.0). The CAT concentration was recorded by measuring the decrease in absorbance at 240 nm as a consequence of the

consumption of H_2O_2 ($\epsilon = 39.4\ mM^{-1}\ cm^{-1}$). Similarly, APX (EC 1.11.1.11) content was assessed by mixing 100 µl of enzyme extract, 100 µl of H_2O_2 (300 mM), 2.7 ml of 25 mM potassium phosphate buffer (2 mM CA, pH 7.0), and 100 µl of ascorbic acid (7.5 mM) (Nakano and Asada, 1981). The oxidation pattern of ascorbate was estimated from the variations in wavelength at 290 nm ($\epsilon = 2.8\ mM^{-1}\ cm^{-1}$).

Statistical Analysis

Data are expressed as the average values of five replicates for each treatment. One-way Analysis-of-variance (ANOVA) followed by Tukey's *post-hoc* test, and significant differences were calculated by all pairwise comparison to determine significant differences and standard deviation (SD). The different small letters in figures and tables describe values that are significantly different at $p \leq 0.05$. All analyses were carried out using Statistix 10.0 software.

RESULTS

Plant Agronomic Traits

Significant variation was observed in biomass and growth parameters, including fresh and dry mass of the root, stem, and leaf, along with root length, plant height, leaf area, leaf number, and total number of flowers (**Table 1**). All the plants showed reduced growth and impaired agronomic traits resulting from Cr toxicity. Compared with controls, the most severe effects were seen at the highest concentration of Cr used (5 mg kg^{-1}).

Chromium application at 5 mg kg^{-1} reduced root length, plant height, and leaf area by 71, 63, and 51%, respectively, when compared with controls. Similarly, fresh and dry mass of the leaf, stem, and root declined by 69 and 61%, 73 and 68%, and 68 and 73%, respectively, compared with control. However, GA application reduced the Cr-induced toxicity and exerted an ameliorative effect on the morphology of the sunflower plants (**Table 1**). The addition of GA (5 mM) alone or with Cr (1, 2, or 5 mg kg^{-1}) significantly improved the agronomic traits of the plants. Root length (40%) and plant height (55%) were both increased under combined GA (5 mM) and Cr (5 mg kg^{-1}) treatment when compared with Cr treatment alone (5 mg kg^{-1}). A similar trend was observed for fresh and dry biomass of the leaf, stem, and root (44 and 54%, 53 and 53%, and 77 and 87%, respectively) under T8 (5 mg kg^{-1} Cr and 5 mM GA) when compared with the respective controls.

Plant Accessory Pigments

Increasing the Cr concentration in the treatments led to a significant reduction in the chlorophyll and carotenoid contents compared with the controls (**Figure 1**). Extreme reductions of 82 and 71% in the carotenoid and total chlorophyll contents, respectively, were observed with Cr addition at 5 mg kg^{-1} when compared with the controls. Co-amendment of GA and Cr decreased the Cr-induced toxicity in terms of improved chlorophyll and carotenoid contents. Maximum increases were observed in Chl a (79%), Chl b (55%), total Chl (69%), and carotenoid (109%) contents under T8 (5 mg kg^{-1} Cr and 5 mM GA). Plants co-treated with Cr and GA showed greater potential to tolerate Cr stress, as evidenced by their ability to retain greater amounts of carotenoid and chlorophyll contents.

Soluble Protein and SPAD Value

Soluble protein content in the leaf and root and the SPAD value of the sunflower plants were significantly reduced with increasing Cr concentrations compared with the control (**Figure 2**). At the higher level of Cr used (5 mg kg^{-1}), the

TABLE 1 | Effect of different concentrations of Cr alone and/or in combination with GA on agronomic traits of sunflower.

Treatments	Cr Concentration (mg kg^{-1})				Cr Concentration (mg kg^{-1})			
	Cr 0	Cr 1	Cr 2	Cr 5	Cr 0	Cr 1	Cr 2	Cr 5
	Root Fresh Weight (g)				**Stem Fresh Weight (g)**			
GA 0	21.43 ± 1.17a	14.50 ± 1.32c	10.83 ± 0.76d	6.16 ± 1.52e	50.59 ± 1.52a	31.96 ± 0.51bc	24.13 ± 2.80de	12.4 ± 0.86f
GA 5 mM	22.36 ± 1.20a	17.60 ± 0.65b	14.43 ± 0.51c	10.93 ± 0.95d	51.73 ± 2.41a	39.13 ± 0.80b	30.00 ± 1.30cd	20.60 ± 1.60ef
	Root Dry Weight (g)				**Stem Dry Weight (g)**			
GA 0	7.90 ± 0.52a	5.06 ± 0.20c	2.76 ± 0.51d	2.10 ± 0.1e	17.56 ± 1.00a	11.26 ± 0.60c	9.06 ± 0.40de	5.49 ± 0.50f
GA 5 mM	8.26 ± 0.25a	6.36 ± 0.40b	5.13 ± 0.15c	3.93 ± 0.30d	16.36 ± 0.70a	14.10 ± 0.55b	10.73 ± 0.40cd	8.43 ± 0.40e
	Leaf Fresh Weight (g)				**Leaf Dry Weight (g)**			
GA 0	24.76 ± 1.50a	17.20 ± 1.25bc	12.00 ± 1.94d	7.60 ± 1.49e	7.86 ± 0.15a	5.26 ± 0.25c	4.23 ± 0.25d	3.03 ± 0.05e
GA 5 mM	24.43 ± 0.75a	20.63 ± 0.70b	16.00 ± 0.50c	11.00 ± 1.50de	7.9 ± 0.10a	6.86 ± 0.15b	4.56 ± 0.40cd	4.66 ± 0.49cd
	Plant Height (cm)				**Root Length (cm)**			
GA 0	99.16 ± 5.20a	71.6 ± 3.04c	55.50 ± 2.68d	36.63 ± 5.29e	35.73 ± 2.27a	24.76 ± 3.95bc	19.7 ± 1.44cd	10.13 ± 1.04e
GA 5 mM	101.5 ± 3.77a	86.21 ± 3.43b	78.13 ± 6.19bc	56.9 ± 2.50d	36.46 ± 0.60a	30.5 ± 1.93ab	25.03 ± 3.06bc	14.23 ± 1.44de
	No. of Leaves Plant^{-1}				**No. of Flowers Plant^{-1}**			
GA 0	16.66 ± 1.15b	13.66 ± 0.57c	8.33 ± 0.57e	7.00 ± 0.00e	8.66 ± 0.57a	6.16 ± 0.57bc	4.34 ± 0.57d	2.00 ± 0.00e
GA 5 mM	19.00 ± 1.00a	16.00 ± 1.00b	13.33 ± 0.57cd	11.33 ± 0.57d	8.00 ± 1.00a	7.34 ± 0.57ab	5.34 ± 0.57cd	3.67 ± 0.57de
	Leaf Area (cm^2)							
GA 0	154.37 ± 6.24a	124.03 ± 13.4b	96.56 ± 2.21c	75.4 ± 5.04d				
GA 5 mM	156.13 ± 1.97a	140.1 ± 4.41ab	125.90 ± 2.40b	88.05 ± 5.28cd				

Values are means of five replicates ± S.D. Mean values followed by small different letters are significantly different from each-others at P ≤ 0.05.

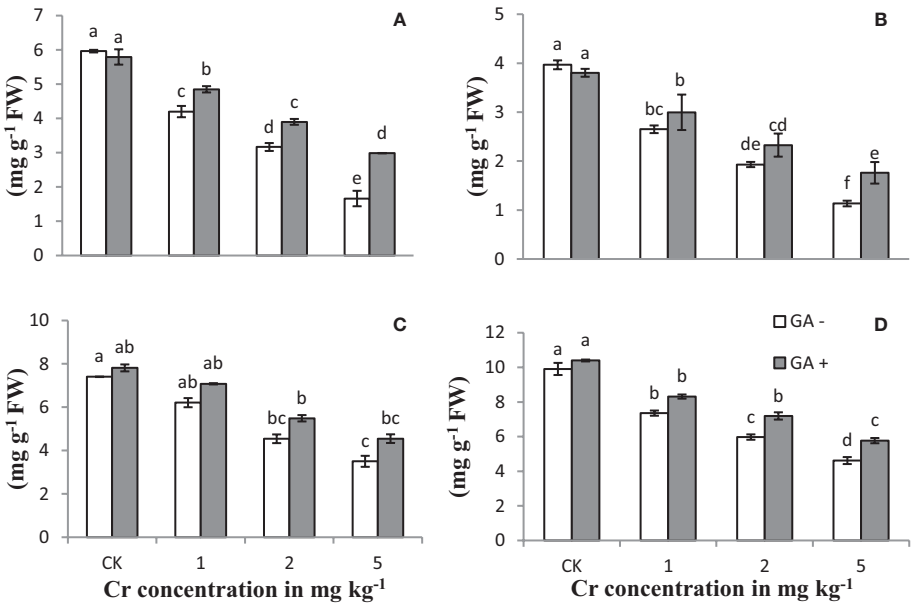

FIGURE 1 | Effect of Cr and GA on chlorophyll a **(A)**, chlorophyll b **(B)**, total chlorophylls **(C)** and carotenoids **(D)** in Sunflower grown in soil with increasing Cr concentrations (0, 1, 2 and 5 mg kg^{-1}) and GA (0 and 5mM). Values are demonstrated as means of five replicates along with standard deviation. Different small letters indicate that values are significantly different at $P < 0.05$.

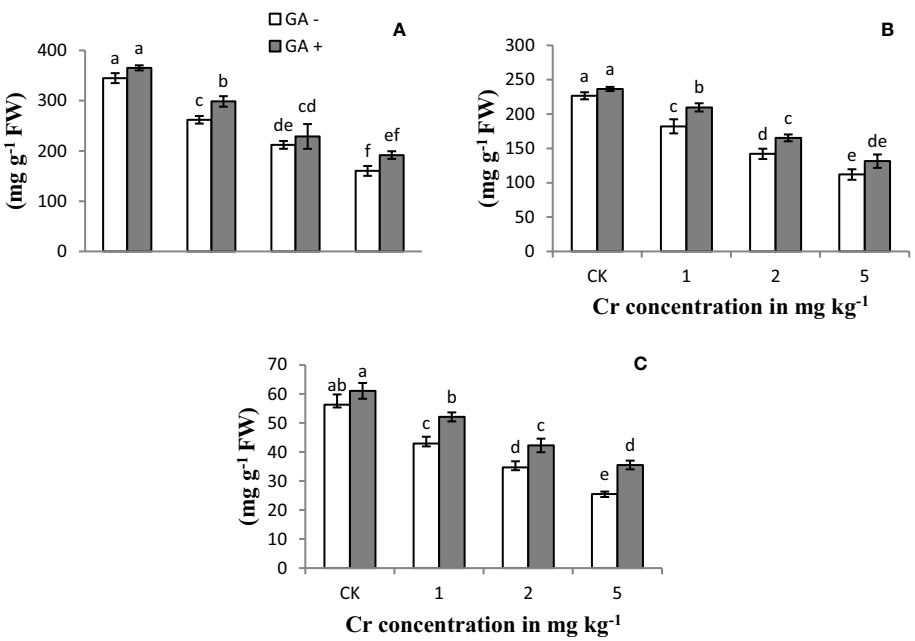

FIGURE 2 | Effect of Cr and GA on SP in leaves **(A)**, SP in root **(B)** and SPAD value **(C)** in Sunflower grown in soil with increasing Cr concentrations (0, 1, 2 and 5 mg kg^{-1}) and GA (0 and 5 mM). Values are demonstrated as means of five replicates along with standard deviation. Different small letters indicate that values are significantly different at $P < 0.05$.

protein content in the root and leaf was reduced by 74 and 38%, respectively, compared with the control samples. In addition, the greatest decrease in the SPAD value (68%) was recorded at the highest Cr concentration. The application of GA resulted in a gradual improvement in the SPAD rate and the protein content in the leaves and roots under Cr-induced stress conditions. Glutamic acid treatment led to increases in the soluble protein content of roots and leaves of 40 and 20%, receptively, under 5 mg kg^{-1} Cr treatment. Similarly, the maximum SPAD value also increased by 60% with T8 (5 mg kg^{-1} Cr and 5 mM GA) compared with the other GA treatments.

Electrolyte Leakage and MDA and Hydrogen Peroxide Content

The levels of reactive oxygen species (ROS) and EL in the roots and leaves of the sunflower plants treated with Cr and/or GA are shown in **Figure 3**. H_2O_2 and MDA content and EL of the plants increased with increasing Cr concentrations (1, 2, and 5 mg kg^{-1}) compared with control. The largest increases in H_2O_2, MDA content, and EL were 143, 153, and 148% in leaves and 108, 176, and 116% in roots, respectively, in soils treated with Cr (5 mg kg^{-1}). Glutamic acid application significantly attenuated the Cr-induced oxidative stress in both roots and leaves by reducing ROS production at all Cr levels tested, while a slight increase was also noted in control plants under GA treatment (**Figure 3**). Under combined Cr and GA treatment, the major decrease in H_2O_2 generation was 16% in leaves and 14% in roots in soil treated with 2 mg kg^{-1} Cr; for MDA production, the greatest decrease was 14% in leaves with 2 mg kg^{-1} Cr treatment and 23% in roots with 1 mg kg^{-1} at Cr; and for EL, the maximum reduction was 17% in leaves with 2 mg kg^{-1} Cr and 18% in roots at 1 mg kg^{-1} Cr.

Antioxidant Enzyme Activities

The activities/concentrations of antioxidant enzymes, including APX, CAT, POD, and SOD, in both leaves and roots were

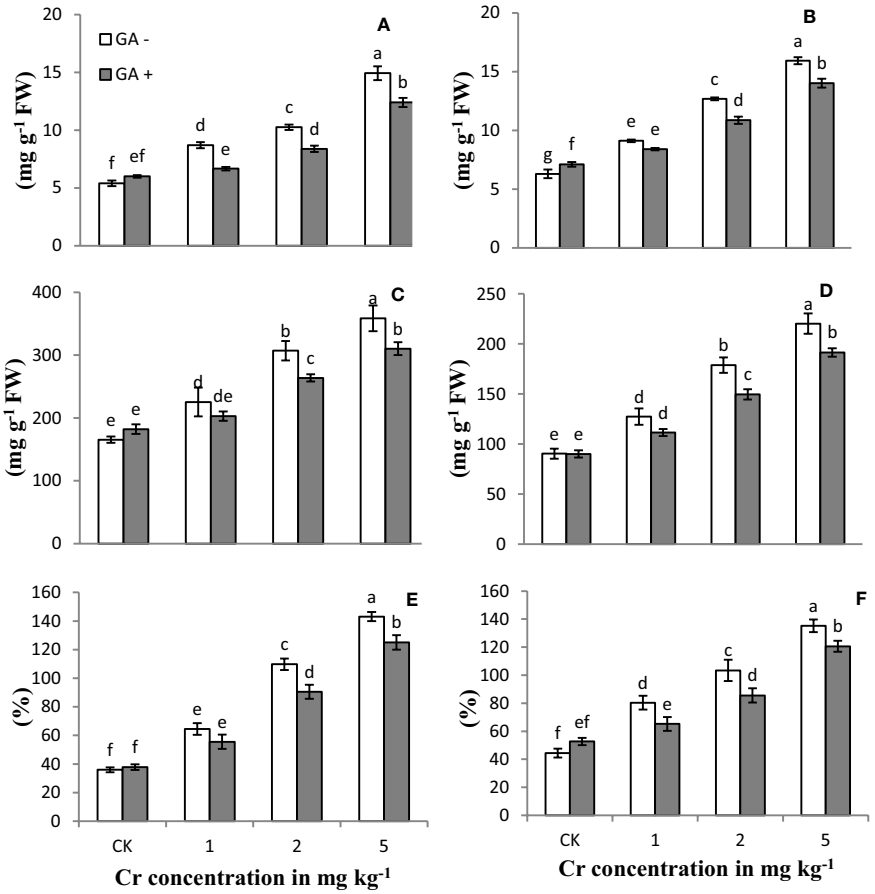

FIGURE 3 | Effect of Cr and GA on MDA in root **(A),** MDA in leaves **(B),** H_2O_2 in root **(C),** H_2O_2 in leaves **(D),** EL in roots **(E)** and EL in leaves **(F)** of Sunflower grown in soil with increasing Cr concentrations (0, 1, 2 and 5 mg kg^{-1}) and GA (0 and 5mM). Values are demonstrated as means of five replicates along with standard deviation. Different small letters indicate that values are significantly different at $P<0.05$.

measured under Cr and GA co-application (**Figure 4**). Compared with the control, soil spiked with 1 and 2 mg kg^{-1} Cr significantly improved the activities of all antioxidant enzymes in both roots and leaves (231 and 311% for SOD; 124 and 88% for POD; 106 and 163% for APX; and 114 and 123% for CAT, respectively). At the highest concentration of Cr tested (5 mg kg^{-1}), the activities of these enzymes tended to decrease in both roots and leaves (26 and 34% for SOD; 18 and 20% for POD; 15 and 14% for APX; and 14 and 15% for CAT, respectively) compared with Cr treatment at 2 mg kg^{-1}. Glutamic acid application further increased the activities of these antioxidant enzymes and exerted an additive effect under Cr stress. The greatest antioxidant enzyme activities were observed in both roots and leaves of the sunflower when GA was co-applied with 2 mg kg^{-1} Cr. Under combined Cr and GA treatment, the largest increase in SOD activity was 15% in roots

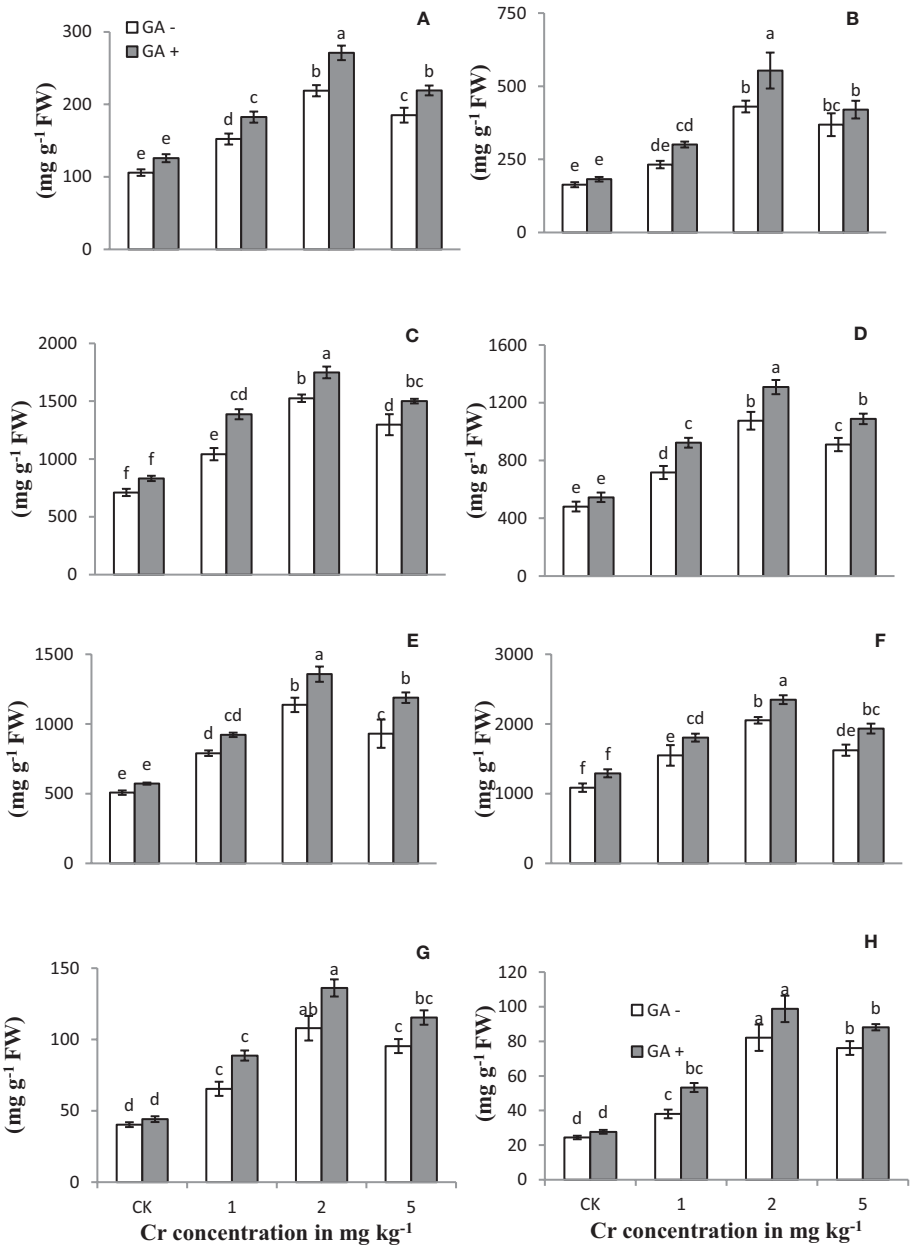

FIGURE 4 | Effect of Cr and GA on APX in root **(A)**, APX in leaves **(B)**, CAT in root **(C)**, CAT in leaves **(D)**, POD in root **(E)**, POD in leaves **(F)**, SOD in root **(G)** and SOD in leaves **(H)** of Sunflower grown in soil with increasing Cr concentrations (0, 1, 2 and 5 mg kg^{-1}) and GA (0 and 5 mM). Values are demonstrated as means of five replicates along with standard deviation. Different small letters indicate that values are significantly different at $P < 0.05$.

and 31% in leaves at 1 mg kg^{-1} Cr; for POD activity, the largest increase was 27% in roots and 19% in leaves at 5 mg kg^{-1} Cr; for APX activity, the largest increase was 23% in roots at 2 mg kg^{-1} Cr and 29% in leaves at 1 mg kg^{-1} Cr; and for CAT activity, the largest increase was 33% in roots and 28% in leaves at 1 mg kg^{-1} Cr.

Chromium Uptake

Chromium addition at the concentrations of 1, 2, and 5 mg kg^{-1} significantly enhanced the Cr concentration and accumulation in the roots, stems, and leaves of the sunflower plants (**Table 2**). Trace levels of Cr were detected in control plants, likely due to background Cr concentrations in the soil. The highest concentration and accumulation of Cr in the root, stem, and leaf were observed at the greatest concentration of Cr tested (5 mg kg^{-1}) (increases of 254, 225, 355 and 47, 59, 150%, respectively, compared with Cr treatment at 1 mg kg^{-1}). The combined GA and Cr treatment further markedly enhanced the absorption and accumulation of Cr in the root, stem, and leaf of the sunflower plant. At the highest concentrations of Cr (5 mg kg^{-1}) and GA (5mM), the concentration and accumulation increased by 24 and 132% in the root, 31 and 59% in the stem, and 19 and 150% in the leaf, respectively.

DISCUSSION

Agronomic Traits

The increased Cr concentrations led to a significant decrease in the growth of the sunflower plants (**Table 1**). Several studies regarding Cr-induced toxic effects on sunflower plant have been widely reported (Farid et al., 2017a; Farid et al., 2018a; Farid et al., 2018b). Chromium-induced toxicity was shown to severely impair nutrient uptake in plants, leading to reduced biomass production and stunted growth (Tauqeer et al., 2016; Fozia et al., 2008). Similarly, Cr stress has been reported to inhibit the growth (Atta et al., 2013) and reduce the fresh and dry biomass of sunflower plants (Saleem et al., 2015). In addition to Cr, sunflower plants also show suppressed growth under Ni (Lin et al., 2003), Ag (Farid et al., 2018a), Cd (Junior et al., 2015), As (Farid et al., 2016), and Cu stress (Imran et al., 2013). Chromium-associated toxicity has also been reported in different plants such as *Braccisa napus* L. (Afshan et al., 2015), *Pisum sativum* L. (Tripathi et al., 2015), *Lemna minor* L. (Sallah-Ud-Din et al., 2017), *Echinochloa colona* (Rout et al., 2000), pea (Rodriguez et al., 2012), and wheat (Ali B. et al., 2015; Mathur et al., 2016). A significant reduction in the quality and yield has been observed in carrots grown on Cr-contaminated soil exceeding the permissible limit (Ding et al., 2014). In our study, plants treated with GA showed improved growth and greater biomass when compared with those treated with Cr alone. Moreover, at the greatest Cr concentrations tested, GA application alleviated the Cr-induced stress in the sunflower. The growth- moderating role of GA under cold stress for rice (Jia et al., 2017) and under drought stress for wheat (Liu et al., 2011) has previously been reported. The addition of GA was shown to regulate plant nutrient uptake and translocation by enhancing nutrient availability (Farid et al., 2018b). As depicted in **Table 1**, GA exerted a growth-moderating effect on sunflower plants at all Cr concentrations applied. Similar stress-alleviating effects were observed when GA was applied to sunflower plants under Ag stress (Farid et al., 2018a). This growth-moderating role of GA is very similar to that of other organic chelators such as citric acid, aminolaevulinic acid, and abscisic acid (Barros-Galvao et al., 2017; Farid et al., 2018a; Farid et al., 2018b). In the present study, we confirmed the growth- moderating and growth-regulatory effects of GA on sunflower plants under heavy metal stress.

Chlorophyll Content

In plants, Cr-related toxicity is similar to that of Ag, Ni, Cd, Pb, as well as other metals (Habiba et al., 2015; Farooq et al., 2016; Farid et al., 2018a). The increasing concentrations of Cr applied and the associated toxicity significantly reduced the performance of the photosynthetic machinery (**Figure 1**). This decrease in chlorophyll and carotenoid contents in sunflower plants is in agreement with the results reported by Farid et al. (2017a) and Fozia et al. (2008). Atta et al. (2013) and Saleem et al. (2015) both reported that Cr stress can disrupt water translocation and cause nutrient deficiency in plants, whereas Singh et al. (2013) and Najeeb et al. (2011) described that reduced chlorophyll and carotenoid content might result from an impaired electron chain due to the deterioration of the photosynthetic system. Disruption of the photosynthetic machinery linked to Cr toxicity has also been reported in wheat (Jabeen et al., 2016), *Brassica*

TABLE 2 | Effect of different concentrations of Cr alone and/or in combination with GA on Cr concentration and accumulation in sunflower.

Treatments	Cr Concentration (mg kg^{-1})			Cr accumulation (µg $plant^{-1}$)		
	Leaf	Stem	Root	Leaf	Stem	Root
CK	2.06 ± 0.15g	10.71 ± 3.12f	13.53 ± 0.51g	18.40 ± 1.32f	190.41 ± 67.44e	106.88 ± 6.90e
GA	3.16 ± 0.04g	12.66 ± 2.08f	22.48 ± 0.54g	29.18 ± 0.225f	207.90 ± 40.88e	185.82 ± 3.79e
Cr 1	62.46 ± 8.19f	142.15 ± 13.01e	175.49 ± 12.78f	328.99 ± 50.77e	1598.03 ± 101.17d	887.70 ± 39.70d
Cr 1+ GA	100.50 ± 5.25e	189.36 ± 13.24e	237.33 ± 24.96e	690.10 ± 28.02cd	2667.36 ± 196.17c	1506.29 ± 116.88c
Cr 2	151.24 ± 3.11d	258.33 ± 17.23d	360.01 ± 17.32d	640.24 ± 32.23d	2344.83 ± 237.35c	1360.33 ± 238.03c
Cr 2+GA	193.83 ± 12.98c	378.33 ± 17.55c	478.33 ± 17.55c	885.17 ± 54.92b	4071.50 ± 533.58b	2457.16 ± 161.94b
Cr 5	271.76 ± 10.52b	462.33 ± 42.85b	622.33 ± 30.27b	824.35 ± 28.94bc	2545.16 ± 359.40c	1307.66 ± 106.20cd
Cr 5+GA	325.61 ± 15.01a	606.10 ± 24.24a	772.66 ± 24.07a	1519.54 ± 105.67a	5104.33 ± 80.50a	3043.33 ± 328.51a

Values are means of five replicates ± S.D. Mean values followed by small different letters are significantly different from each-others at $P \leq 0.05$.

napus (Afshan et al., 2015), *Lemna minor* (Sallah-Ud-Din et al., 2017), and mung bean (Adrees et al., 2015a). In the current study, the decreased levels of carotenoids and photosynthetic pigments might be a consequence of exacerbated electrolyte leakage and ROS generation (**Figure 3**). The results clearly demonstrated that the introduction of GA markedly improved the Cr-associated toxic effects and the functioning of the photosynthetic machinery of the plants, an idea that is supported by the similar findings of Farid et al. (2018a). Forde et al. (2007) also reported that the chlorophyll and carotenoid contents were increased in plants under GA supply.

Soluble Protein and SPAD

Both the soluble protein content and SPAD value of the sunflower decreased in the leaves and roots with increasing Cr concentrations (**Figure 2**). Our findings are in line with the conclusions of Farid et al. (2017a; 2018a; 2018b) and Saleem et al. (2015) who reported a decline in soluble protein content and SPAD value of sunflower plants exposed to Cr stress. In agreement with the present findings, many plant species also show reduced soluble protein content and SPAD values, such as cotton exposed to Pb (Anwaar et al., 2015), wheat exposed to Cr (Adrees et al., 2015b), and maize and mung bean exposed to Cd (Hussain et al., 2006; Sabir et al., 2014). Rizwan et al. (2017a) stated that the SPAD value is directly associated with the leaf chlorophyll content, suggesting that a decrease in chlorophyll content and water translocation might be responsible for the observed decrease in the SPAD value. The results indicated that the application of GA alone or in combination with Cr greatly increased the soluble protein content and SPAD value (**Figure 3**), which was in close agreement with the results of studies by Jia et al. (2017) and Farid et al. (2018a). Increased enzymatic activities (**Figure 4**) are the indication of damage to the soluble protein levels in plant (Forde and Mutiti, 2017). Increased soluble protein content under GA application has been observed for plants under different heavy metal stresses, such as Cd, Cu, Pb, and Zn, as reported by Doumett et al. (2010).

Reactive Oxygen Species

Exposure of sunflower plants to Cr resulted in oxidative damage, which was attributable to electrolyte leakage and ROS generation (**Figure 4**; Farid et al., 2018a; Farid et al., 2018b). Ahmad et al. (2017) also reported oxidative damage in sunflower plants exposed to Cr stress. This response of sunflower plants to stress induced by various heavy metals is concisely reviewed by Rizwan et al. (2017b). Similar to sunflower plants, *Brassica napus*, soybean, barley, and wheat also show higher ROS production under Cr stress (Adrees et al., 2015b; Gill et al., 2016). Chromium-induced toxicity was shown to alter K^+ efflux and impair the electron transport chain in plants, leading to increased production of OH^- and O^- free radicals, further enhancing EL (Fozia et al., 2008; Rizwan et al., 2017a). Recent studies reported that high levels of EL and ROS generation were observed in plants exposed to biotic and abiotic stresses, such as salinity (Noman et al., 2015), drought (Arshad et al., 2016), pathogen attack (Giovanini et al., 2006), and herbicide application (Song et al., 2007). Gallic acid application to soil reduced EL and ROS generation in plants under Cr stress. This decrease might be due to the activation of the antioxidant defense system and repair of the plant electron transport chain and water translocation system, similar to the findings of Sallah-Ud-Din et al. (2017). Furthermore, GA is reported to act like other organic chelators in scavenging ROS by improving the natural protection system of plants. In this study, the improvements in plant growth, biomass, and photosynthetic machinery might have resulted from decreased EL and ROS production caused by the addition of GA.

Antioxidant Defense System

The sunflower is known to activate its antioxidant enzyme defense system under biotic and abiotic stresses (Farid et al., 2018a). Activation of these enzymes was also observed in the current study (**Figure 4**). Increasing the Cr concentration significantly enhanced the activities of POD, SOD, CAT, and APX. Interestingly, at the highest Cr concentration used (5 mg kg^{-1}), the activities of these enzymes tended to decrease. This behavior of the sunflower plant under Cr stress has also been previously reported by Farid et al. (2017a; 2018a; 2018b). Additionally, the sunflower also showed a similar trend under Pb, Cu, and Cd stress (Li et al., 2011; Shamsi et al., 2014). Rizwan et al. (2017a; 2017b) reported an increase in antioxidant enzyme activity resulting from ROS production under heavy metal stress. Demidchik (2012) reported that plants activate the ROS scavenging defense system by regulating the electron transport chain and K^+ efflux. At lower Cr concentrations, antioxidant enzymes favored normal plant activity; however, the antioxidant defense system could not cope with the higher Cr concentrations. This phenomenon has been observed in sunflower plants under the stress of various heavy metals, as summarized by Rizwan et al. (2017a), as well as in sunflower plants under drought, salinity, and heat stress (Naeem et al., 2012; Kanto et al., 2015). Similar to that observed with other organic acids, GA application led to a significant increase in the activities of all antioxidant enzymes in sunflower plants supplemented with Cr (Sallah-Ud-Din et al., 2017; Farid et al., 2018a).

Chromium Concentration and Accumulation

The sunflower plant is widely reported to be a hyperaccumulator plant for various heavy metals due to its height and root structure (Farid et al., 2017a, Rizwan et al., 2017a; Rizwan et al., 2017b; Farid et al., 2018a; Farid et al., 2018b). In this study, Cr accumulation gradually increased in all the plant organs with increasing Cr content in the soil (**Table 2**), which is similar to the findings reported by Fozia et al. (2008) and Saleem et al. (2015). Several studies have reported that Cr can be readily absorbed by different plants, including *Lemna minor* (Sallah-Ud-Din et al., 2017), *Brassica napus* (Afshan et al., 2015), wheat (Adrees et al., 2015b), and mung bean (Jabeen et al., 2016). Chromium uptake and accumulation are mainly dependent on its availability and mobility in the soil (Ali et al., 2011; Ali et al., 2013) and can be affected by the addition of exogenously applied chelators

(Shahid et al., 2017). Similarly, the addition of GA under Cr stress significantly enhanced Cr uptake and accumulation in our study. This increased accumulation could be attributed to the chelating properties of GA, which has the ability to detach metals from organic fractions in the soil as reported by Doumett et al. (2010). The chelating properties of GA have also been reported by Farid et al. (2018a) and Jia et al. (2017). The greater the plant biomass, the higher the accumulation of metal in plant tissues. Relatively few studies have investigated the chelating ability of GA for heavy metals and the response of the sunflower at the genetic and molecular levels. Our results were broadly in agreement with our stated hypothesis that GA can enhance metal accumulation, growth, and biomass in plants.

Conclusions

The results of the present study indicated that sunflower growth, biomass, and biochemical attributes were significantly reduced as a result of Cr-induced toxicity. Increasing the concentration of applied Cr significantly increased Cr concentration and accumulation in the root, stem and leaf of sunflower plant. Meanwhile, we also found a positive role of GA due to its ability to regulate normal functioning and plant growth. Glutamic acid markedly ameliorated the Cr-induced toxicity in the sunflower, improving its morphological, physiological, and biochemical attributes. Our results indicated that the sunflower might be a suitable and potential candidate for Cr phytoextraction under GA application in Cr contaminated soils. Future studies are required to elucidate the associated molecular and genetic mechanisms.

DATA AVAILABILITY STATEMENT

The raw data supporting the conclusions of this article will be made available by the authors, without undue reservation, to any qualified researcher.

AUTHOR CONTRIBUTIONS

All authors contributed to the article and approved the submitted version.

FUNDING

This work was funded by Researchers Supporting Project number (RSP 2020/26), King Saud University, Riyadh, Saudi Arabia.

ACKNOWLEDGMENTS

This work was funded by Researchers Supporting Project number (RSP 2020/26), King Saud University, Riyadh, Saudi Arabia. The authors are also grateful to the University of Gujrat, Gujrat Pakistan and Higher Education Commission (HEC) of Pakistan.

REFERENCES

Adrees, M., Ali, S., Rizwan, M., Zia-ur-Rehman, M., Ibrahim, M., Abbas, F., et al. (2015a). Mechanisms of silicon-mediated alleviation of heavy metal toxicity in plants: a review. *Ecotoxicol. Environ. Saf.* 119, 186–197. doi: 10.1016/j.ecoenv.2015.05.011

Adrees, M., Ali, S., Rizwan, M., Ibrahim, M., Abbas, F., Farid, M., et al. (2015b). The effect of excess copper on growth and physiology of important food crops: a review. *Environ. Sci. Pollut. Res.* 22, 8148–8162. doi: 10.1007/s11356-015-4496-5

Aebi, H. (1984). Catalase in vitro methods. *Enzymology* 105, 121–126. doi: 10.1016/S0076-6879(84)05016-3

Afshan, S., Ali, S., Bharwana, S. A., Rizwan, M., Farid, M., Abbas, F., et al. (2015). Citric acid enhances the phytoextraction of chromium, plant growth, and photosynthesis by alleviating the oxidative damages in *Brassica napus* L. *Environ. Sci. Pollut. Res.* 22, 11679–11689. doi: 10.1007/s11356-015-4396-8

Ahmad, R., Ali, S., Hannan, F., Rizwan, M., Iqbal, M., Hassan, Z., et al. (2017). Promotive role of 5-aminolevulinic acid on chromium-induced morphological, photosynthetic, and oxidative changes in cauliflower (*Brassica oleracea botrytis* L.). *Environ. Sci. Pollut. Res.* 24, 8814–8824. doi: 10.1007/s11356-017-8603-7

Ali, S., Bai, P., Zeng, F., Cai, S., Shamsi, I. H., Qiu, B., et al (2011). The ecotoxicological and interactive effects of chromium and aluminum on growth, oxidative damage and antioxidant enzymes on two barley genotypes differing in Al tolerance. *Environ. Exp. Bot.* 70, 2–3. doi: 10.1016/j.envexpbot.2010.09.002

Ali, S., Farooq, M. A., Yasmeen, T., Hussain, S., Arif, M. S., Abbas, F., et al. (2013). The influence of silicon on barley growth, photosynthesis and ultra-structure under chromium stress. *Ecotoxicol. Environ. Saf.* 89, 66–72. doi: 10.1016/j.ecoenv.2012.11.015

Ali, B., Gill, R. A., Yang, S., Gill, M. B., Farooq, M. A., Liu, D., et al. (2015). Regulation of cadmium-induced proteomic and metabolic changes by 5 aminolevulinic acid in leaves of *Brassica napus* L. *PloS One* 10 (4), p.e0123328. doi: 10.1371/journal.pone.0123328

Amir, W., Farid, M., Ishaq, H. K., Farid, S., Zubair, M., Alharby, H. F., et al. (2020). Accumulation potential and tolerance response of Typha latifolia L. under citric acid assisted phytoextraction of lead and mercury. *Chemosphere* 257, 127247. doi: 10.1016/j.chemosphere.2020.127247

Anwaar, S. A., Ali, S., Ali, S., Ishaque, W., Farid, M., Farooq, M. A., et al. (2015). Silicon (Si) alleviates cotton (*Gossypium hirsutum* L.) from zinc (Zn) toxicity stress by limiting Zn uptake and oxidative damage. *Environ. Sci. Pollut. Res.* 22, 3441–3450. doi: 10.1007/s11356-014-3938-9

Arshad, M., Ali, S., Noman, A., Ali, Q., Rizwan, M., Farid, M., et al. (2016). Phosphorus amendment decreased cadmium (Cd) uptake and ameliorates chlorophyll contents, gas exchange attributes, antioxidants, and mineral nutrients in wheat (*Triticum aestivum* L.) under Cd stress. *Arch. Agron. Soil Sci.* 62, 533–546. doi: 10.1080/03650340.2015.1064903

Atta, M. I., Bokhari, T. Z., Malik, S. A., Wahid, A., Saeed, S., and Gulshan, A. B. (2013). Assessing Some Emerging Effects of Hexavalent Chromium on Leaf Physiological Performance in Sunflower (*Helianthus annuus* L.). *Int. J. Sci. Eng. Res.* 4, 945–949.

Barros-Galvao, T., Oliveira, D. F. A., Macedo, C. E. C., and Voigt, E. L. (2017). Modulation of Reserve Mobilization by Sucrose, Glutamine, and Abscisic Acid During Seedling Establishment in Sunflower. *J. Plant Growth Regul.* 36, 11–21. doi: 10.1007/s00344-016-9611-4

Bradford, M. M. (1976). A rapid and sensitive method for the quantification of microgram quantities of protein utilizing the principle of proteindye binding. *Anal. Biochem.* 72, 248–254. doi: 10.1016/0003-2697(76)90527-3

Cekic, F. O., Ekinci, S., Inal, M. S., and Unal, D. (2017). Silver nanoparticles induced genotoxicity and oxidative stress in tomato plants. *Turk. J. Biol.* 41, 700–707. doi: 10.3906/biy-1608-36

Cunningham, S. D., Berti, W. R., and Huang, J. W. (1995). Phytoremediation of contaminated soils. *Trend. Biotechnol.* 13 (9), 393–397. doi: 10.1016/s0167-7799(00)88987-8

De Maria, S., Puschenreiter, M., and Rivelli, A. R. (2013). Cadmium accumulation and physiological response of sunflower plants to Cd during the vegetative growing cycle. *J. Plant Soil Environ.* 59, 254–261. doi: 10.17221/788/2012-PSE

Demidchik, V. (2012). *Reactive oxygen species and oxidative stress in plants* (CAB Inter. Oxford: Plant Stress Physiol), 24–58.

Dhindsa, R. S., Plumb-Dhindsa, P., and Thorpe, T. A. (1981). Leaf senescence: correlated with increased levels of membrane permeability and lipid peroxidation, and decreased levels of superoxide dismutase and catalase. *J. Exp. Bot.* 32 (1), 93–101. doi: 10.1093/jxb/32.1.93

Ding, C., Li, X., Zhang, T., Ma, Y., and Wang, X. (2014). Phytotoxicity and accumulation of chromium in carrot plants and the derivation of soil thresholds for Chinese soils. *Ecotoxicol. Environ. Saf.* 108, 179–186. doi: 10.1016/j.ecoenv.2014.07.006

Dionisio-Sese, M. L., and Tobita, S. (1998). Antioxidant responses of rice seedlings to salinity stress. *Plant Sci.* 135, 1–9. doi: 10.1016/S0168-9452(98)00025-9

Doumett, S., Fibbi, D., Azzarello, E., Mancuso, S., Mugnai, S., Petruzzelli, G., et al. (2010). Influence of the application renewal of glutamate and tartrate on Cd, Cu, Pb and Zn distribution between contaminated soil and *Paulownia tomentosa* in a pilot-scale assisted phytoremediation study. *Inter. J. Phyto.* 13 (1), 1–17. doi: 10.1080/15226510903567455

Ehsan, S., Ali, S., Noureen, S., Farid, M., Shakoor, M. B., Aslam, A., et al. (2013). Comparative assessment of different heavy metals in urban soil and vegetables irrigated with sewage/industrial waste water. *Ecoterra* 35, 37–53.

Epstein, A. L., Gussman, C. D., Blaylock, M. J., Yermiyahu, U., Huang, J. W., Kapulnik, Y., et al. (2012). EDTA and Pb—EDTA accumulation in Brassica juncea grown in Pb—amended soil. *Plant Soil* 208 (1), 87–94. doi: 10.1023/A:1004539027990

Farid, M., Ali, S., Ishaque, W., Shakoor, M. B., Niazi, N. K., Bibi, I., et al. (2015). Exogenous application of ethylenediamminetetraacetic acid enhanced phytoremediation of cadmium by *Brassica napus* L. *Inter. J. Environ. Sci. Technol.* 12 (12), 3981–3992. doi: 10.1007/s13762-015-0831-0

Farid, M., Ali, S., and Rizwan, M. (2016). "Citric acid assisted phytoremediation of copper by Brassica napus L.," in *Arsenic Research and Global Sustainability.* (Stockholm, Sweden, Arsenic Research and Global Sustainability: CRC Press, Taylor and Francis Group, London), June 19-23, 2016.

Farid, M., Ali, S., Rizwan, M., Ali, Q., Abbas, F., Bukhari, S. A. H., et al. (2017a). Citric acid assisted phytoextraction of chromium by sunflower; morpho-physiological and biochemical alterations in plants. *Ecotoxicol. Environ. Saf.* 145, 90–102. doi: 10.1016/j.ecoenv.2017.07.016

Farid, M., Ali, S., Akram, N. A., Rizwan, M., Abbas, F., Bukhari, S. A. H., et al. (2017b). Phyto-management of Cr-contaminated soils by sunflower hybrids: physiological and biochemical response and metal extractability under Cr stress. *Environ. Sci. Pollut. Res.* 24 (20), 16845–16855. doi: 10.1007/s11356-017-9247-3

Farid, M., Ali, S., Zubair, M., Saeed, R., Rizwan, M., Sallah-Ud-Din, R., et al. (2018a). Glutamic acid assisted phyto-management of silver contaminated soils through sunflower; physiological and biochemical response. *Environ. Sci. Pollut. Res.* 25 (25), 25390–25400. doi: 10.1007/s11356-018-2508-y

Farid, M., Ali, S., Rizwan, M., Ali, Q., Saeed, R., Nasir, T., et al. (2018b). Phyto-management of chromium contaminated soils through sunflower under exogenously applied 5-aminolevulinic acid. *Ecotoxicol. Environ. Saf.* 151 (30), 255–265. doi: 10.1016/j.ecoenv.2018.01.017

Farooq, M. A., Detterbeck, A., Clemens, S., and Dietz, K. J. (2016). Silicon-induced reversibility of cadmium toxicity in rice. *J. Exp. Bot.* 67, 3573–3585. doi: 10.1093/jxb/erw175

Fatima, A., Farid, M., Alharby, H. F., Bamagoos, A. A., Rizwan, M., and Ali, S. (2020). Efficacy of fenugreek plant for ascorbic acid assisted phytoextraction of copper (Cu); A detailed study of Cu induced morpho-physiological and biochemical alterations. *Chemosphere* 251, 126424. doi: 10.1016/j.chemosphere.2020.126424

Forde, B. G., and Lea, P. J. (2007). Glutamate in plants: metabolism, regulation, and signaling. *J. Exp. Bot.* 58 (9), 2339–2358. doi: 10.1093/jxb/erm121

Forte, J., and Mutiti, S. (2017). Phytoremediation Potential of *Helianthus annuus* and Hydrangea paniculata in Copper and Lead-Contaminated Soil. *Water Air Soil Pollut.* 228, 77. doi: 10.1007/s11270-017-3249-0

Fozia, A., Muhammad, A. Z., Muhammad, A., and Zafar, M. K. (2008). Effect of chromium on growth attributes in sunflower (*Helianthus annuus* L.). *J. Environ. Sci.* 20, 1475–1480. doi: 10.1016/S1001-0742(08)62552-8

Gill, R. A., Ali, B., Cui, P., Shen, E., Farooq, M. A., Islam, F., et al. (2016). Comparative transcriptome profiling of two Brassica napus cultivars under chromium toxicity and its alleviation by reduced glutathione. *BMC Genom.* 17, 885. doi: 10.1186/s12864-016-3200-6

Giovanini, M. P., Puthoff, D. P., Nemacheck, J. A., Mittapalli, O., Saltzmann, K. D., Ohm, H. W., et al. (2006). Gene-for-gene defense of wheat against the hessian fly lacks a classical oxidative burst. *Mole. Plant-Microbe Interact.* 19, 1023–1033. doi: 10.1094/MPMI-19-1023

Habiba, U., Ali, S., Farid, M., Shakoor, M. B., Rizwan, M., Ibrahim, M., et al. (2015). EDTA enhanced plant growth, antioxidant defense system, and phytoextraction of copper by *Brassica napus* L. *Environ. Sci. Pollut. Res.* 22, 1534–1544. doi: 10.1007/s11356-014-3431-5

Habiba, U., Ali, S., Rizwan, M., Hussain, M. B., Hussain, A., Alam, P., et al. (2018). The Ameliorative Role of 5-Aminolevulinic Acid (ALA) Under Cr Stress in Two Maize Cultivars Showing Differential Sensitivity to Cr Stress Tolerance. *J. Plant Growth Regul.* 38 (3), 788–795. doi: 10.1007/s00344-018-9890-z

Heath, R. L., and Packer, L. (1968). Photoperoxidation in isolated chloroplasts: I. Kinetics and stoichiometry of fatty acid peroxidation. *Arch. Biochem. Biophys.* 125, 189–198. doi: 10.1016/0003-9861(68)90654-1

Huang, J. W., Chen, J., Berti, W. R., and Cunningham, S. D. (1997). Phytoremediation of lead-contaminated soils: role of synthetic chelates in lead phytoextraction. *Environ. Sci. Technol.* 31 (3), 800–805. doi: 10.1021/es9604828

Hussain, M., Ahmad, M. S. A., and Kausar, A.B.I.D.A. (2006). Effect of lead and chromium on growth, photosynthetic pigments and yield components in mash bean [*Vigna mungo* (L.) Hepper]. *Pak. J. Bot.* 38, 1389–1396.

Imran, M. A., Nawaz Ch, M., Khan, R. M., and Ali, Z. (2013). Toxicity of arsenic (As) on seed germination of sunflower (*Helianthus annuus* L.). *Int. J. Phys. Sci.* 8, 840–847. doi: 10.5897/IJPS12.20

Jabeen, N., Abbas, Z., Iqbal, M., Rizwan, M., Jabbar, A., Farid, M., et al. (2016). Glycinebetaine mediates chromium tolerance in mung bean through lowering of Cr uptake and improved antioxidant system. *Arch. Agron. Soil Sci.* 62, 648–662. doi: 10.1080/03650340.2015.1082032

Jana, S., and Choudhuri, M. (1981). Glycolate metabolism of three submerged aquatic angiosperms during aging. *Aqua. Bot.* 12, 345–354. doi: 10.1016/0304-3770(82)90026-2

Jia, Y., Zou, D., Wang, J., Sha, H., Liu, H., Inayat, M. A., et al. (2017). Effects of γ-Aminobutyric Acid, Glutamic Acid, and Calcium Chloride on Rice (Oryza sativa L.) Under Cold Stress During the Early Vegetative Stage. *J. Plant Growth Regul.* 36, 240–253. doi: 10.1007/s00344-016-9634-x

Junior, C. A., Barbosa, H., de, S., Moretto Galazzi, R., Ferreira Koolen, H. H., Gozzo, F. C., et al. (2015). Evaluation of proteome alterations induced by cadmium stress in sunflower (*Helianthus annuus* L.) cultures. *Ecotoxicol. Environ. Saf.* 119, 170–177. doi: 10.1016/j.ecoenv.2015.05.016

Kanto, U., Jutamanee, K., Osotsapar, Y., Chai-arree, W., and Jattupornpong, S. (2015). Promotive effect of priming with 5-aminolevulinic acid on seed germination capacity, seedling growth and antioxidant enzyme activity in rice subjected to accelerated ageing treatment. *Plant Prod. Sci.* 18, 443–454. doi: 10.1626/pps.18.443

Khair, K. U., Farid, M., Ashraf, U., Zubair, M., Rizwan, M., Farid, S., et al. (2020). Citric acid enhanced phytoextraction of nickel (Ni) and alleviate *Mentha piperita* (L.) from Ni-induced physiological and biochemical damages. *Environ. Sci. Pollut. Res.* 27, 27010–27022. doi: 10.1007/s11356-020-08978-9

Khalid, A., Farid, M., Zubair, M., Rizwan, M., Iftikhar, U., Ishaq, H. K., et al. (2020). Efficacy of Alternanthera bettzickiana to Remediate Copper and Cobalt Contaminated Soil Physiological and Biochemical Alterations. *Int. J. Environ. Res.* 14, 243–255. doi: 10.1007/s41742-020-00251-8

Lasat, M. M. (2000). Phytoextraction of metals from contaminated soil: a review of plant/soil/metal interaction and assessment of pertinent agronomic issues. *J. Hazard Subst. Res.* 2, 1–25. doi: 10.4148/1090-7025.1015

Li, X., Xing, W., Zhuo, S., Zhou, J., Li, F., Qiao, S. Z., et al. (2011). Preparation of capacitor's electrode from sunflower seed shell. *Biores. Technol.* 102, 1118–1123. doi: 10.1016/j.biortech.2010.08.110

Lichtenthaler, H. K. (1987). Chlorophyll sand carotenoids: pigments of photosynthetic bio membranes. *Method Enzymol.* 148, 350–382. doi: 10.1016/0076-6879(87)48036-1

Lin, J., Jiang, W., and Liu, D. (2003). Accumulation of copper by roots, hypocotyls, cotyledons and leaves of sunflower (*Helianthus annuus* L.). *Biores. Technol.* 86, 151–155. doi: 10.1016/S0960-8524(02)00152-9

Liu, C., Zhao, L., and Yu, G. (2011). The Dominant Glutamic Acid Metabolic Flux to Produce γ-Amino Butyric Acid over Proline in *Nicotiana tabacum* Leaves under Water Stress Relates to its Significant Role in Antioxidant Activity. *J. Integr. Plant Biol.* 53, 608–618. doi: 10.1111/j.1744-7909.2011.01049.x

Lukina, A. O., Boutin, C., Rowland, O., and Carpenter, D. J. (2016). Evaluating trivalent chromium toxicity on wild terrestrial and wetland plants. *Chemosphere.* 162, 355–364. doi: 10.22215/etd/2015-11076

Mantry, P., and Patra, H. K. (2017). Combined effect of Cr+ 6 and chelating agents on growth and Cr bioaccumulation in flood susceptible variety of rice *Oryza sativa* (L.) cv. Swarna. *Annal. Plant Sci.* 6, 1573–1578. doi: 10.21746/aps.2017.02.008

Mathur, S., Kalaji, H. M., and Jajoo, A. (2016). Investigation of deleterious effects of chromium phytotoxicity and photosynthesis in wheat plant. *Photosynth* 54, 185–192. doi: 10.1007/s11099-016-0198-6

Metzner, H., Rau, H., and Senger, H. (1965). Untersuchungenzur synchronisierbaketieinzel-nerpigmentmangel-mutation von chlorella. *Planta* 65, 186–194. doi: 10.1007/BF00384998

Naeem, M. S., Warusawitharana, H., Liu, H., Liu, D., Ahmad, R., Waraich, E. A., et al. (2012). 5-Aminolevulinic acid alleviates the salinity-induced changes in *Brassica napus* as revealed by the ultrastructural study of chloroplast. *Plant Physiol. Biochem.* 57, 84–92. doi: 10.1016/j.plaphy.2012.05.018

Najeeb, U., Jilani, G., Ali, S., Sarwar, M., Xu, L., and Zhou, W. J. (2011). Insight into cadmium induced physiological and ultra-structural disorders in *Juncus effusus* L. and its remediation through exogenous citric acid. *J. Hazard. Mater.* 186, 565–574. doi: 10.1016/j.jhazmat.2010.11.037

Nakano, Y., and Asada, K. (1981). Hydrogen peroxide scavenged by ascorbate specific peroxidase in spinach chloroplasts. *Plant Cell Physiol.* 22, 867–880. doi: 10.1093/oxfordjournals.pcp.a076232

Narayani, M., and Shetty, V. (2012). Characteristics of a novel Acinetobacter sp. and its kinetics in hexavalent chromium bioreduction. *J Microbiol. Biotechnol.* 22 (5), 690–698. doi: 10.4014/jmb.1110.10073

Nehnevajova, E., Herzig, R., Federer, G., Erismann, K. H., and Schwitzguébel, J. P. (2007). Chemical mutagenesis—a promising technique to increase metal concentration and extraction in sunflowers. *Int. J Phytorem.* 9 (2), 149–165. doi: 10.1080/15226510701232880

Nehnevajova, E., Herzig, R., Bourigault, C., Bangerter, S., and Schwitzguébel, J. P. (2009). Stability of enhanced yield and metal uptake by sunflower mutants for improved phytoremediation. *Int. J. Phyto.* 11 (4), 329–346. doi: 10.1080/15226510802565394

Nehnevajova, E., Lyubenova, L., Herzig, R., Schröder, P., Schwitzguébel, J. P., and Schmülling, T. (2012). Metal accumulation and response of antioxidant enzymes in seedlings and adult sunflower mutants with improved metal removal traits on a metal-contaminated soil. *Environ. Exp. Bot.* 76, 39–48. doi: 10.1016/j.envexpbot.2011.10.005

Nguyen, K. L., Nguyen, H. A., Richter, O., Pham, M. T., and Nguyen, V. P. (2017). Ecophysiological responses of young mangrove species *Rhizophora apiculata* (Blume) to different chromium contaminated environments. *Sci. Total Environ.* 574, 369–380. doi: 10.1016/j.scitotenv.2016.09.063

Noman, A., Ali, S., Naheed, F., Ali, Q., Farid, M., Rizwan, M., et al. (2015). Foliar application of ascorbate enhances the physiological and biochemical attributes of maize (*Zea mays* L.) cultivars under drought stress. *Arch. Agron. Soil Sci.* 61, 1659–1672. doi: 10.1080/03650340.2015.1028379

Rizwan, M., Ali, S., Rizvi, H., Rinklebe, J. T., Sang, D. C., Meers, E., et al. (2016). Phytomanagement of heavy metals in contaminated soils using sunflower: a review. *Crit. Rev. Environ. Sci. Technol.* 46, 1498–1528. doi: 10.1080/10643389.2016.1248199

Rizwan, M., Ali, S., Abbas, F., Adrees, M., Zia-ur-Rehman, M., Farid, M., et al. (2017a). "Role of organic and inorganic amendments in alleviating heavy metal stress in oil seed crops," in *Oil Seed Crops: Yield and Adaptations under Environmental Stress*, *1st ed.*, vol. 12 . Ed. P. Ahmad (USA: John Wiley & Sons, Ltd), 224–235. Published 2017 by John Wiley & Sons, Ltd. doi: 10.1002/9781119048800

Rizwan, M., Ali, S., Qayyum, M. F., Ok, Y. S., Adrees, M., Ibrahim, M., et al. (2017b). Effect of metal and metal oxide nanoparticles on growth and physiology of globally important food crops: a critical review. *J. Hazard. Mater.* 322, 2–16. doi: 10.1016/j.jhazmat.2016.05.061

Rodriguez, E., Santos, C., Azevedo, R., Moutinho-Pereira, J., Correia, C., and Dias, M. C. (2012). Chromium (VI) induces toxicity at different photosynthetic levels in pea. *Plant Physiol. Biochem.* 53, 94–100. doi: 10.1016/j.plaphy.2012.01.013

Rout, G. R., Samantaray, S., and Das, P. (2000). Effects of chromium and nickel on germination and growth intolerant and non-tolerant populations of *Echinochloa colona* (L.) link. *Chemosphere* 40, 855–859. doi: 10.1016/S0045-6535(99)00303-3

Sabir, M., Hanafi, M. M., Zia-Ur-Rehman, M., Saifullah, Ahmad, H. R., Hakeem, K. R., et al. (2014). Comparison of low-molecular-weight organic acids and ethylenediaminetetraacetic acid to enhance phytoextraction of heavy metals by maize. *Commun. Soil Sci. Plant Anal.* 45, 42–52. doi: 10.1080/00103624.2013.848879

Saleem, M., Asghar, H. N., Khan, M. Y., and Zahir, Z. A. (2015). Gibberellic acid in combination with pressmud enhances the growth of sunflower and stabilizes chromium (VI) contaminated soil. *Environ. Sci. Pollut. Res.* 22, 10610–10617. doi: 10.1007/s11356-015-4275-3

Sallah-Ud-Din, R., Farid, M., Saeed, R., Ali, S., Rizwan, M., Tauqeer, H. M., et al. (2017). Citric acid enhanced the antioxidant defense system and chromium uptake by *Lemna minor* L. grown in hydroponics under Cr stress. *Environ. Sci. Pollut. Res.* 24 (21), 17669–17675. doi: 10.1007/s11356-017-9290-0

Salt, D. E., Smith, R. D., and Raskin, I. (1998). Phytoremediation. *Anal. Plant Bio.* 49 (1), 643–668. doi: 10.1146/annurev.arplant.49.1.643

Shahid, M., Shamshad, S., Rafiq, M., Khalid, S., Bibi, I., Niazi, N. K., et al. (2017). Chromium speciation, bioavailability, uptake, toxicity and detoxification in soil-plant system: A review. *Chemosphere* 178, 513–533. doi: 10.1016/j.chemosphere.2017.03.074

Shakoor, M. B., Ali, S., Hameed, A., Farid, M., Hussain, S., Yasmeen, T., et al. (2014). Citric acid improves lead (Pb) phytoextraction in *Brassica napus* L. by mitigating Pb-induced morphological and biochemical damages. *Ecotoxicol. Environ. Saf.* 109, 38–47. doi: 10.1016/j.ecoenv.2014.07.033

Shamsi, I. H., Zhang, G. P., Hu, H. L., Xue, Q. Y., Hussain, N., Ali, E., et al. (2014). Assessment of the hazardous effects of Cd on physiological and biochemical characteristics of soybean genotypes. *Int. J. Agric. Biol.* 16, 41–48.

Singh, H. P., Mahajan, P., Kaur, S., Batish, D. R., and Kohli, R. K. (2013). Chromium toxicity and tolerance in plants. *Environ. Chem. Lett.* 11, 229–254. doi: 10.1007/s10311-013-0407-5

Song, N. H., Yin, X. L., Chen, G. F., and Yang, H. (2007). Biological responses of wheat (*Triticum aestivum*) plants to the herbicide chlorotoluron in soils. *Chemosphere* 68, 1779–1787. doi: 10.1016/j.chemosphere.2007.03.023

Tauqeer, H. M., Ali, S., Rizwan, M., Ali, Q., Saeed, R., Iftikhar, U., et al. (2016). Phytoremediation of heavy metals by *Alternanthera bettzickiana*: growth and physiological response. *Ecotoxicol. Environ. Saf.* 126, 138–146. doi: 10.1016/j.ecoenv.2015.12.031

Tripathi, D. K., Singh, V. P., Prasad, S. M., Chauhan, D. K., and Dubey, N. K. (2015). Silicon nanoparticles (SiNp) alleviate chromium (VI) phytotoxicity in *Pisum sativum* (L.) seedlings. *Plant Physiol. Biochem.* 96, 189–198. doi: 10.1016/j.plaphy.2015.07.026

USEPA. United States Environmental Protection Agency Reports (2000). Introduction to Phytoremediation, – EPA 600/R-99/107, National Service Center for Environmental Publications (NSCEP), USA.

Wei, Z. B., Guo, X. F., Wu, Q. T., Long, X. X., and Penn, C. J. (2011). Phytoextraction of heavy metals from contaminated soil by co-cropping with chelator application and assessment of associated leaching risk. *Int. J. Phyto.* 13 (7), 717–729. doi: 10.1080/15226514.2010.525554

Wiszniewska, A., Hanus-Fajerska, E., Muszyńska, E., and Ciarkowska, K. (2016). Natural organic amendments for improved phytoremediation of polluted soils: a review of recent progress. *Pedosphere* 26, 1–12. doi: 10.1016/S1002-0160(15)60017-0

Yeh, T. Y., and Pan, C. T. (2012). Effect of chelating agents on copper, zinc, and lead uptake by sunflower, Chinese cabbage, cattail, and reed for different organic contents of soils. *J. Environ. Anal. Toxicol.* 2, 2161–0525. doi: 10.4172/2161-0525.1000145

Zhang, J., and Kirkham, M. B. (1994). Drought-stress-induced changes in activities of superoxide dismutase, catalase, and peroxidase in wheat species. *Plant Cell Physiol.* 35, 785–791. doi: 10.1093/oxfordjournals.pcp.a078658

Zhang, X. Z. (1992). "The measurement and mechanism of lipid peroxidation and SOD POD and CAT activities in biological system," in *Research Methodology of Crop Physiology*. Ed. X. Z. Zhang (Beijing Agric: Press), 208–221.

Conflict of Interest: The authors declare that the research was conducted in the absence of any commercial or financial relationships that could be construed as a potential conflict of interest.

frontiers in Plant Science

ORIGINAL RESEARCH
published: 15 September 2020
doi: 10.3389/fpls.2020.571157

Photosynthesis Performance and Antioxidative Enzymes Response of *Melia azedarach* and *Ligustrum lucidum* Plants Under Pb–Zn Mine Tailing Conditions

XinHao Huang[1], *Fan Zhu*[1,2*], *ZhiXiang He*[1], *XiaoYong Chen*[2,3], *GuangJun Wang*[1,2], *MengShan Liu*[2] *and HongYang Xu*[2]

[1] College of Life Science and Technology, Central South University of Forestry and Technology, Changsha, China, [2] National Engineering Laboratory for Applied Forest Ecological Technology in Southern China, Central South University of Forestry and Technology, Changsha, China, [3] College of Arts and Sciences, Governors State University, University Park, IL, United States

OPEN ACCESS

Edited by:
Basharat Ali,
University of Agriculture, Faisalabad, Pakistan

Reviewed by:
Mujahid Farid,
University of Gujrat, Pakistan
Theodore Mulembo Mwamba,
Zhejiang University, China

***Correspondence:**
Fan Zhu
csuftzf@163.com

Specialty section:
This article was submitted to Plant Nutrition, a section of the journal Frontiers in Plant Science

Received: *12 June 2020*
Accepted: *27 August 2020*
Published: *15 September 2020*

Citation:
Huang X, Zhu F, He Z, Chen X, Wang G, Liu M and Xu H (2020) Photosynthesis Performance and Antioxidative Enzymes' Response of Melia azedarach and Ligustrum lucidum Plants Under Pb–Zn Mine Tailing Conditions. Front. Plant Sci. 11:571157. doi: 10.3389/fpls.2020.571157

Lead–zinc (Pb–Zn) mine tailings pose a great risk to the natural environment and human health because of their high toxicity. In this study, the responses of photosynthesis, chlorophyll fluorescence, and antioxidative enzyme of *Melia azedarach* and *Ligustrum lucidum* in the soil contaminated by Pb–Zn mine tailings were investigated. Results showed that Pb–Zn mine tailings significantly reduced net photosynthetic rates and leaf photosynthetic pigment content of both trees, and the reduction of net photosynthetic rates was mainly caused by their biochemical limitation (BL). The chlorophyll fluorescence parameters from Pb–Zn tailing stressed leaves indicated that Pb–Zn tailings affected PSII activity which was evident from the change values of energy fluxes per reaction center (RC): probability that an electron moves further than Q_A^- (ET_O/TR_O), maximum quantum yield for primary photochemistry (TR_O/ABS), the density of PSII RC per excited cross-section (RC/CS_O), the absorption of antenna chlorophylls per PSII RC (ABS/RC), and the turnover number of Q_A reduction events (N). Pb–Zn mine tailings also affected the oxidation and reduction of PSI, which resulted in a great increase of reactive oxygen species (ROS) contents and then stimulated the rate of lipid peroxidation. Both trees exhibited certain antioxidative defense mechanisms as elevated superoxide dismutase (SOD), peroxidase (POD), and catalase (CAT) activities, then declined under high level of Pb–Zn tailing treatment. Comparatively, *L. lucidum* showed less extent effect on photosynthesis and higher antioxidative enzyme activities than *M. azedarach*; thus *L. lucidum* was more tolerant than *M. azedarach* at least under the described Pb–Zn tailing treatment. These results indicate that the effect of Pb–Zn mine tailings on photosynthesis performance mainly related to imbalance of the PSII activity and PSI redox state in both trees. We propose that *M. azedarach* and *L. lucidum* could relieve the oxidative stress for phytoremediation under the appropriate Pb–Zn mine tailing content.

Keywords: antioxidative enzymes, *Ligustrum lucidum*, *Melia azedarach*, Pb–Zn tailings, photosynthesis

INTRODUCTION

Plants require certain heavy metals (HMs) as essential elements for their growth, development, and yield production, but excess amount of these metals can become phytotoxic and cause adverse effects on plant biomass production, crop yield, and food safety (Pierattini et al., 2017). The major sources of HMs originated from anthropogenic activities; mining activities seem to be the largest contributor of HM pollutions in many places, and it is a particular case in China (Ha et al., 2011; Han et al., 2013; Zhuang et al., 2014; Chen et al., 2015). It was recently reported that the mining activities have resulted in about 40,000 ha mining wastelands in this country, and the wastelands have been continuously expanded at a rate of 3,300 ha per year (Li, 2006; Luo et al., 2015; Yu et al., 2019). Mining activities generated a large amount of mine tailings in the mining sites where high concentrations of Pb, Zn, and other HMs were detected in local environments, which caused a wide range of environmental problems (Han et al., 2013). Therefore, it is urgent and necessary to reestablish vegetation in mining wasteland for ecological restoration (Yu et al., 2019).

Various methods have been identified and employed to the restoration of HM-polluted soils (Teng et al., 2015). Phytoremediation technology has been widely considered as an efficient, inexpensive, and environmental-friendly approach to clean up the contaminated environments by HMs (Han et al., 2016). Trees have the great potential use in remediation of HM-polluted soil in view of large biomass and massive root systems (Pulford and Watson, 2003). However, Tang et al. (2019) demonstrated that the Pb–Zn mine tailing significantly reduced plant growth and chlorophyll contents in three woody plants (*Castanopsis fissa*, *Daphniphyllum calycinum* and *Pinus massoniana*). The limitation in tree growth might thus be associated with photosynthesis which was sensitive to HM stress (Çiçek et al., 2017; Zhong et al., 2018; Huang et al., 2019; Liang et al., 2019). Evidence showed that the reduction of leaf photosynthesis under HM toxicity might be attributed to the limitation of stomatal opening (Gs) and CO_2 diffusion in mesophyll (Gm), the suppression of photochemistry and biochemistry, or synthetic combinations of these factors (Kosobrukhov et al., 2004; Kola and Wilkinson, 2005; Krantev et al., 2008; Deng et al., 2014). Sagardoy et al. (2010) reported the main limitation to photosynthesis rate in sugar beet was likely due to the reduction of Gs under Zn stress. Lin and Jin (2018) found similar results in an experiment with three vegetables (*B. chinensis*, *C. coronarium*, and *B. alboglabra*) under Cu stress. However, Velikova et al. (2011) studied the impact of Ni on the photosynthesis of *Populus nigra* and found the limitation to photosynthesis rates of this species resulted from the restriction in Gm, not in Gs. Gm influenced photosynthetic capacity and determined the available CO_2 concentration for photosynthesis in the chloroplasts (Centritto et al., 2009). Some studies showed that the electron transfer was inhibited by Pb pollutant at the photosystem I (PSI) donor side because Pb affected activity of PSI (Belatik et al., 2013; Bernardini et al., 2016), but some studies suggested the activity of PSI in *Microcystis aeruginosa* and *Chlorella pyrenoidosa* had no inhibition with Cd treatment (Zhou et al., 2006; Wang et al., 2013). And some studies indicated that Cd affected the whole electron transport in photosystem II (PSII): on the donor side, it inhibited the OEC, while on the acceptor side, it inhibited electron transport between Q_A^- and Q_B^-. (Mallick and Mohn, 2003; Sigfridsson et al., 2004; Chu et al., 2018). Additionally, a number of studies also reported that HMs exhibited less effect of photosynthetic rate, electron transport, conversion of light energy, and photochemical efficiency in tolerant plant species than those in sensitive ones (Guo et al., 2018; Sorrentino et al., 2018; Huang et al., 2019).

Reactive oxygen species (ROS) can highly increase in the chloroplasts when photosynthetic electron transport chain was blocked by HM toxicity (Zhang et al., 2018). ROS like superoxide (O_2^-) and hydrogen peroxide (H_2O_2) could lead to lipid peroxidation, protein oxidation, membrane and nucleic acid damage, and inactivation of enzymes (Bi et al., 2016; Bezerril et al., 2017; Lu et al., 2017). To prevent an oxidative damage, plants activated enzymatic ROS scavenging mechanisms, such as superoxide dismutase (SOD), peroxidase (POD) and catalase (CAT), ascorbic acid and glutathione, to keep ROS at a basal non-toxic level (Israr et al., 2011; Štefanić et al., 2018; Du et al., 2020). In the past two decades, many studies have estimated the direct link between the oxidative stress in metal toxicity and metal-tolerant plants (Boominathan and Doran, 2003; Chiang et al., 2006). A large proportion of studies have indicated that metal tolerant plants were linked to superior constitutive antioxidative defense (Srivastava and Doran, 2005; Chiang et al., 2006; Nie et al., 2016). Although great progress has been made in supporting the HM toxicity to plant photosynthesis and its redox balance, the effects of HM stress on photosynthetic performance varied depending on the plant species, metal ion and concentration. Meanwhile, these available data provide a restricted view on single metal contamination or herbaceous plants (Mobin and Khan, 2007; Wali et al., 2016). Therefore, the photosynthesis and redox responses of trees to HM tailing stress still need to be studied further.

Melia azedarach is a fast-growing, deciduous broad-leaved tree species and is widely distributed in the southern regions of China. It is mainly planted for reforestation as a useful timber production species or as an ornamental plant. *Ligustrum lucidum* is a commonly-seen evergreen broad-leaved tree species in South China. This species is often planted as an ornamental tree in the urban. Moreover, both *M. azedarach* and *L. lucidum* are native plants in the southern regions of China, Frérot et al. (2006) pointed out that native plants could be a useful option to phytoremediation because native plants are better adapted to local climate conditions than plants introduced from other environments, and they were previously found to have high tolerance in Cd or Mn contaminated soils (Trikshiqi and Rexha, 2015; Su et al., 2017; Liang et al., 2019). However, the metal toxicity manifestations and mechanisms behind tolerance need further investigation, so the specific goals of this study were: 1) to investigate the contributions of Gs, Gm, and biochemical component respectively to the photosynthesis reduction in two

tested plants by photosynthesis limitation analysis, 2) to identify the impact of Pb–Zn stress on the whole photosynthetic electron flow chain from PSII to PSI and the state of PSI, 3) to explore the tolerant mechanisms of both trees to Pb–Zn tailing stress in terms of the redox responses of photosystems and antioxidative enzymes. Based on the above studies, the differences of tolerance between *M. azedarach* and *L. lucidum* were discussed. Results could provide a theoretical basis for selecting and breeding the resistant trees species grown in Pb–Zn polluted environments.

MATERIALS AND METHODS

The Physicochemical Properties of Pb–Zn Tailings and Experimental Soil

The study was conducted in the Central South University of Forestry and Technology (CSUFT), Changsha City, Hunan Province, China (28°8′12″N, 112°59′36″E). The Pb–Zn mine tailing samples were collected from a Pb–Zn mining site in Suxian district, Chenzhou City, Hunan Province, China (25°30′38″–25°00′19″N, 112°16′41″–112°53′23″E). The soil samples were collected from the top soil (5–20 cm) in a garden field of CSUFT campus. Both Pb–Zn mine tailing samples and top soil samples were air-dried at room temperature. The large debris, stones, and pebbles were manually removed before being applied to the pot experiment. The soil pH value, soil total carbon (TC), total nitrogen (TN), total phosphorus (TP), and soil heavy metal content were measured in laboratory according to Bao (2000), the basic physicochemical properties of soil were as follows: pH 4.95, total C 5.82 g kg^{-1}, total N 0.33 g kg^{-1}, total P 0.16 g kg^{-1}, Pb 0.002 g kg^{-1}, Zn 0.003 g kg^{-1}. The properties of Pb–Zn mine tailing samples were determined: pH 3.89, total C 13.89 g kg^{-1}, total N 1.25 g kg^{-1}, P 0.82 g kg^{-1}, Pb 8.92 g kg^{-1}, Zn 14.41 g kg^{-1}.

Plant Seedlings

Two-year-old young plants of *M. azedarach* (mean tree height: ~73.5 cm, mean stem base diameter: ~0.6 cm) and *L. lucidum* (mean tree height: ~130.0 cm, mean stem base diameter: ~0.9 cm) were purchased from a local nursery.

Experimental Design

Pb–Zn mine tailings represent a poor spoil substrate characterized by high contents of Pb and Zn, low levels of organic nutrients, and poor physical structure and water retention capacity (Meeinkuirt et al., 2012); few plants can survive in such harsh environmental condition. Mixing mine tailings with garden soil helps decrease the bioavailability of metals and improves mine tailing structure and ultimately upgrades the physical properties and nutrient status of mine tailings. Moreover, this method has been commonly used in many studies of phytoremediation in mine tailing (Chen et al., 2015; Han et al., 2016; Tang et al., 2019). In the present study, four treatments were set up in the pot experiment with different weighted proportions of Pb–Zn mine tailings and garden soils. Each pot contained 10 kg mixed soils. The four treatments were: (1) 90% garden soils + 10% Pb–Zn mine tailings (designed as L1, the 10 kg mixed soils were 9 kg garden soil and 1 kg mine tailings, the same as below); (2) 75% garden soils + 25% Pb–Zn mine tailings (L2); (3) 50% garden soils + 50% Pb–Zn mine tailings (L3), and (4) 100% garden soils + 0% Pb–Zn mine tailings as the control (C). The Pb–Zn mine tailings and garden soils were completely mixed and then the *M. azedarach* and *L. lucidum* young plants were transplanted into the pots with one plant per pot. Each treatment was replicated six times. The temperatures of the greenhouse were set at 30/25°C (day temperature for 10 h and night temperature for 14 h), and relative humidity was 65/85%. During the study period, each pot was supplied with equal quantity of pure water every 1 to 2 days until the young plants were harvested. Both trees were measured for all physiological parameters after growing for 425 days (from June 15th, 2017 to September 13th, 2018) in Pb–Zn tailing treatments.

Relative Growth Rate (RGR)

Plant biomass was measured using a harvesting method. The plant was divided into leaves, stem, and root components; the fresh weights of each component were measured by using an electronic balance and then dried at 70°C until constant weight was reached. The dry weight (DW) of each component was determined by using an electronic balance. Six individual plants were selected for biomass measurement for each of *M. azedarach* and *L. lucidum* species at the beginning of the treatment, respectively, as initial dry weight (DW). The biomass of each component was determined as initial dry weight (DW). After 425 days of treatment (from June 15th, 2017 to September 13th, 2018), all examined plants were harvested and the biomass was measured as final DW. The determination of relative growth rate (RGR) is based on the method of Environment Canada (2007) guidelines as follows:

$$RGR = (ln \quad X_j - \ln X_i)/(t_j - t_i);$$

where X_i and X_j represent the values of final DW and initial DW, respectively; t_j and t_i represent initial time and final time, respectively.

Gas Exchange Measurements

Three new, similar size and fully expanded leaves per plant were chosen for the measurements of photosynthesis for each treatment. The leaf gas exchange and Chl fluorescence were measured by using an open gas exchange system (LI-COR 6400XT, Lincoln, USA) at the same time with an integrated Chl fluorescence chamber head in the morning (8:00–10:00 am). For all measurements, the following conditions were set up: leaf temperature of 25–32°C, PAR of 1,000 μmol (photon) m^{-2} s^{-1}, and vapor pressure deficit (VPD) of 2.0 ± 0.2 kPa.

For developing the relationships between leaf photosynthesis and intercellular CO_2 concentrations (A–Ci curves), the steady-state rates of leaf maximum net photosynthesis rate (P_n, μmol m^{-2} s^{-1}), stomatal conductance (Gs, mol m^{-2} s^{-1}) and intercellular CO_2 concentration (Ci, μmol m^{-2} s^{-1}) were measured. The A–Ci curves were developed by measuring P_n at 15 reference CO_2 concentrations: 400, 300, 250, 200, 150, 100, 50, 25, 0, 400, 600, 800, 1,000, 1,200, 1,400 μmol mol^{-1} as described by Centritto et al.

(2003). The maximum carboxylation rate allowed by Rubisco (V_{cmax}), day respiration (R_d), and electron transfer rate of photosynthesis based on NADPH requirement (J_{max}) were estimated based on the modeling methods (Farquhar et al., 1980; Sharkey et al., 2007).

Mesophyll conductance to CO_2 (Gm) was calculated by using 'variable J method' (Harley et al., 1992; Sagardoy et al., 2010) as:

$$Gm = P_n/(Ci)(\Gamma*(J_{flu} + 8(P_n + R_d))/((J_{flu})4(P_n + R_d)) \quad (1)$$

where, P_n and Ci were obtained from gas exchange measurements under saturating light, Γ∗ was the CO_2 concentration at the compensation point in the absence of mitochondrial respiration and was obtained according to Bernacchi et al. (2002), R_d was calculated based on the A–Ci curve on the same leaf according to Pinelli and Loreto (2003).

J_{flu} represented the rate of electron transport and was calculated as:

$$J_{flu} = 0.5 \cdot \varphi PSII \cdot \alpha \cdot PPFD \quad (2)$$

where, α was total leaf absorbance in the visible light range (taken as 0.85, Grassi and Magnani, 2005), 0.5 was a factor to account for the distribution of light between the two photosystems (Laisk and Loreto, 1996). The actual chloroplastic CO_2 concentration (Cc) was calculated from the g_m value as Cc = Ci – (P_n/Gm) (Harley et al., 1992).

Photosynthesis Limitation Analysis

The inhibition of Pb–Zn stress on plant photosynthesis was further assessed based on the contribution made by various functional components to the photosynthetic limitations (Sagardoy et al., 2010). The functional components were stomatal (SL), mesophyll conductance (MCL), and leaf biochemical characteristics (BL). The relative contributions of these functional components to the photosynthesis limitations were evaluated when compared with a reference status in which the photosynthesis limitations were ignorable, and the Gs, Gm, and V_{cmax} were at their maximum. In this study, the corresponding values of Gs, Gm, and V_{cmax} taken from C treatments were as reference values; thus the photosynthesis limitations were set to 0.

The Kinetics of Prompt Fluorescence and Modulated 820 nm Reflection

Fast chlorophyll a fluorescence was measured by using M-PEA (Multifunctional Plant Efficiency Analyser, Hansatech Instrument, UK). After 1 h dark adaptation using dark adaptation clips, leaves were exposed to a pulse of saturating red light (5,000 μmol m^{-2} s^{-1}, peak at 625 nm, duration from 50 μs to 2 s, records of 128 points), and the measurements were carried out during a period of 8:30–11:00 am. The OJIP transient was analyzed based on the JIP test (Strasser et al., 2004). The values of fluorescence intensity from the original measurements were used in this study: fluorescence intensity at 20 μs (at the O step, considering as the minimum fluorescence, F_O); 300 μs ($F_{300\mu s}$) used for calculation of the initial slope of the relative variable fluorescence kinetics; 2 ms (at the J step, F_J); 30 ms (at the I step, F_I), and the P step (considering as the maximum fluorescence, F_m). The description and calculation of standardization formula of OJIP transients and formula of parameters were listed in **Table 1**.

Modulated 820 nm reflection was also expressed as MR/MR_O. The value of MR and MR_O were determined by the method of Zhou et al. (2019). The PSI redox was denoted by V_{PSI} (maximum PSI oxidation rate) and $V_{PSII–PSI}$ (maximum PSI reduction rate, respectively, and were obtained according to Gao et al. (2014).

Evaluation of Chlorophyll and Carotenoid Contents

Leaf chlorophylls and carotenoid content were extracted using 95% ethanol and then placed in the dark for at least 72 h at 4°C. The extracts were measured at wavelengths of 665, 649, and 470 nm spectrophotometrically and was then calculated as milligram per gram of fresh weight (Ji et al., 2018).

Assay of Superoxide Anion (O_2^-) Production Rate, H_2O_2 Content, and Malondialdehyde (MDA)

The O_2^- production rate was measured using a reagent kit (Beijing Solarbio Science and Technology, China). H_2O_2 content was measured using the method of Okuda et al. (1991). The MDA level was assayed as a thiobarbituric acid reactive substance according to the method of Dhindsa et al. (1981). A 0.25 g fresh leaf sample was homogenized; supernatant was collected and measured at the wave length of 532, 600, and 450 nm using a UV/visible spectrophotometer.

Estimation of Proline and Antioxidative Enzymes

Proline content was determined using Pure Pro as a standard (Gao, 2006). A 0.1 g fresh leaf sample was homogenized with 5 ml of 3% aqueous sulfosalicylic acid and was then extracted in a boiling bath.

For determination of SOD, POD, and CAT, a 0.3 g fresh leaf sample was grounded in 3 ml extraction buffer containing 25 mM Hepes, 2% polyvinyl-pyrrolidone (PVP), 0.2 mM EDTA, and 2 mM ascorbate (pH 7.8) and was centrifuged at 12,000 g for 20 min at 4°C. The supernatants were collected for enzyme analysis.

SOD activity was determined according to Giannopolitis and Ries (1977). The 3 ml reaction mixture contained 0.05 M phosphate buffer solution (pH 7.8), 0.06 M Riboflavin, 0.195 M Met, 0.003 M EDTA, 1.125 mM NBT, and 0.2 ml enzyme supernatants. The measurements were performed at 25°C. The tested samples were incubated for 10–20 min under 10,000 lx irradiance; inhibition rate of nitro blue tetrazolium (NBT) reached to 50% represented one unit of SOD activity as by spectrophotometer at 560 nm.

POD activity was assessed as in Beffa et al. (1990). The reaction mixture contained 0.1 M sodium-acetic buffer (pH 5.0), 0.25% (w/v) guaiacol, 0.75% H_2O_2, and 0.05 ml enzyme supernatants. One unit of POD activity was represented as an increase of 0.01 ΔOD value a minute at 470 nm.

CAT activity was determined according to Aebi (1984). The reaction mixture contained 0.05 M phosphate buffer (pH 7.0)

TABLE 1 | Formulae and definitions the technical data of the OJIP curves, the selected JIP-test parameters and the selected PF parameters used in this study.

Technical fluorescence	
F_t	Fluorescence at time t after onset of actinic illumination
$F_O \cong F_{20\mu s}$ or $F_{50\mu s}$	Minimal fluorescence, when all PSII RCs are open
$F_K = F_{300\mu s}$	Fluorescence intensity at the K-step (300 μs) of OJIP
$F_J = F_{20ms}$	Fluorescence intensity at the J-step (2 ms) of OJIP
$F_I = F_{30ms}$	Fluorescence intensity at the I-step (30 ms) of OJIP
$F_P(=F_M)$	Maximal recorded fluorescence intensity, at the peak P of OJIP
N	the turnover number of QA reduction events
$F_v = F_t - F_O$	Variable fluorescence at time t
$F_V = F_M - F_O$	Maximal variable fluorescence
$V_I = (F_M - F_I)/(F_M - F_O)$	Relative variable fluorescence at time t
$V_K = (F_K - F_O)/(F_M - F_O)$	Relative variable fluorescence at the K-step
$V_J = (F_J - F_O)/(F_M - F_O)$	Relative variable fluorescence at the J-step
$W_K = W_{300\mu s} = (F_{300\mu s} - F_O)/(F_J - F_O)$	Relative variable fluorescence at the K-step to the amplitude F_J-F_O
$\varphi_{Po} = PHI(P_0) = TR_0/ABS = 1 - F_O/F_M$	Maximum quantum yield for primary photochemistry
$\psi_{Eo} = PSI_0 = ET_0/TR_0 = (1 - V_J)$	Probability that an electron moves further than QA^-
$\varphi_{Eo} = PHI(E_0) = ET_0/ABS = (1 - F_O/F_M)/(1 - V_J)$	Quantum yield for electron transport (ET)
$\varphi_{Ro} = RE_0/ABS = \varphi_{Po} \times \psi_{Eo} \times \delta_{Ro} = \varphi_{Po} \times (1 - V_I)$	Quantum yield for reduction of the end electron acceptors on the PSI acceptor side (RE)
$\delta_{Ro} = RE_0/ET_0 = (1 - V_I)/(1 - V_J)$	Probability that an electron is transported from the reduced intersystem electron acceptors to the final electron acceptors of PSI (RE)
ABS/CS = CH1/CS	Absorption flux per CS
$RC/CS = \varphi_{Po} \times (V_J/M_0) \times (ABS/CS)$	Q_A-reducing RCs per CS
$PI_{ABS} = \frac{\gamma RC}{1 - \gamma RC} \times \frac{\varphi Po}{1 - \varphi Po} \times \frac{\varphi Eo}{1 - \varphi Eo}$	Performance index (potential) for energy conservation from photons absorbed by PSII to the reduction of intersystem electron acceptors
$\Delta V_{IP} = 1 - V_I$	Amplitude of the I to P phase of the OJIP fluorescence transient (associated with PSI reaction center content).
Abbreviations	
P_n	net photosynthetic rate
Gs	stomatal conductance
Ci	intercellular CO_2 concentration
Gm	mesophyll conductance to CO_2
Rd	day respiration
Cc	chloroplastic CO_2 concentration
V_{cmax}	Maximum carboxylation rate allowed by Rubisco
J_{max}	rate of photosynthetic electron transport based on NADPH requirement
SL	stomatal conductance
MCL	mesophyll conductance
BL	biochemical limitation
MDA	malondialdehyde
SOD	superoxide dismutase
POD	peroxidase
CAT	Catalase

and 0.45 M H_2O_2 and 0.2 ml enzyme supernatants. One unit of CAT activity was represented as decrease of ΔOD value a minute at 240 nm. The measurement for each antioxidative enzyme was repeated three times.

Assay of Leaf Total Rubisco Activity

Ribulose-1, 5-bisphosphate carboxylase/oxygenase (Rubisco) of leaves from the tested plants was assayed according to the method of Chen et al. (2005). After centrifugation at 13,000 $r{\cdot}min^{-1}$ 40 s at 2°C, the supernatant was used immediately for assays of Rubisco activity (Jiang et al., 2008).

Total Metal Content

For the determination of the metal contents in plant, the different dried plant components were powdered and passed through an 80-mesh sieve. About 0.1 g of plant material was digested with 1 ml of HNO_3 and H_2O_2 (8:2, v/v). Then, the tube with plant material was on the block at 200°C for 0.75–1 h. The residue was taken up in 10 ml of demineralized water. The concentrations of Pb and Zn were determined by atomic absorption spectrophotometry (AA-6800, Shimadzu, Kyoto, Japan) (Huang et al., 2019). The measurement for each sample was repeated six times, and the mean value was calculated.

The metal translocation factor (TF) in the leaves was represented as the metal concentration ratio of plant leaves and stems to roots (Han et al., 2016).

Statistical Analyses

Two-way analysis of variance (ANOVA) was performed on the data using SPSS (20.0). Differences among the eight treatment combinations (two species × four Pb–Zn mine tailing treatments) were analyzed by two-way analysis of variance; eight means were separated by Duncan's new multiple range test at $P < 0.05$ level. Data were presented as means ± SD (n = 6). The principal component analysis (PCA) used CANOCO version 5.0.

RESULTS

RGR, Pb/Zn Contents in Roots, Stems, and Leaves

As Pb–Zn tailing portions increased, RGR of *M. azedarach* and *L. lucidum* was decreased progressively compared with the control group ($P < 0.05$) (**Table 2**), the RGR values were reduced by 10–90% and 6–70% in *M. azedarach* and *L. lucidum*, respectively, in Pb–Zn treatments when compared with the C plants (**Table 2**). The concentrations of Pb and Zn in the leaves, stems, and roots increased with the increase of the proportion of Pb–Zn tailings in both tested plants compared to the C (**Table 2**). The Pb and Zn concentrations were significantly higher in the roots than in the leaves and stems. The Pb and Zn concentrations showed as Zn > Pb in the leaves, stems, and roots in all Pb–Zn tailing treatments. TFs of Pb and Zn were higher in *M. azedarach* than those in *L. lucidum*.

TABLE 2 | Relative growth rate (RGR), Pb and Zn concentrations and translocation coefficient of *M. azedarach* and *L. lucidum* grown in soil mixed with different proportions of Pb–Zn mine tailings.

		RGR	Pb content				Zn content			
			Root	Leaf	Stem	TF	Root	Leaf	Stem	TF
M. azedar-ach	C	0.010 ± 0.002a	0.57 ± 0.04a	0.31 ± 0.06a	0.15 ± 0.05a	0.80 ± 0.27a	27.32 ± 1.98a	30.36 ± 1.56a	31.44 ± 0.91a	2.26 ± 0.22a
	L1	0.009 ± 0.004a	15.93 ± 0.41b	9.68 ± 0.78b	8.01 ± 0.35b	1.11 ± 0.31b	49.12 ± 2.32b	70.5 ± 3.34b	33.88 ± 1.05a	2.13 ± 0.35a
	L2	0.005 ± 0.003b	43.96 ± 2.18c	26.08 ± 2.56c	13.67 ± 3.32c	0.90 ± 0.16a	101.49 ± 3.22c	126.41 ± 4.78c	41.81 ± 2.25b	1.66 ± 0.27b
	L3	0.001 ± 0.000c	105.13 ± 6.83d	50.98 ± 1.45d	16.39 ± 0.41c	0.65 ± 0.22a	236.14 ± 7.63d	177.88 ± 8.34d	62.15 ± 3.04c	1.01 ± 0.18c
L. lucidu-m	C	0.018 ± 0.002a	0.31 ± 0.04a	0.41 ± 0.04a	0.22 ± 0.02a	2.02 ± 0.11a	24.15 ± 2.02a	28.46 ± 0.57a	24.36 ± 1.12a	2.19 ± 0.33a
L1		0.017 ± 0.001b	20.84 ± 1.22b	5.48 ± 0.63b	5.41 ± 0.22b	0.52 ± 0.09b	69.51 ± 4.41b	50.32 ± 4.32b	33.12 ± 0.76b	1.20 ± 0.25b
L2		0.009 ± 0.002c	59.78 ± 3.54c	15.64 ± 1.15c	8.46 ± 0.76c	0.40 ± 0.12b	158.45 ± 5.67c	78.16 ± 4.09c	36.39 ± 1.77b	0.72 ± 0.21b
L3		0.005 ± 0.003d	141.04 ± 4.32d	36.75 ± 1.93d	9.13 ± 0.55c	0.33 ± 0.04b	288.12 ± 8.91d	99.65 ± 3.88d	51.12 ± 2.09c	0.53 ± 0.11c

TF = the metal concentration ratio of plant leaves and stems to roots. Data are means ± SE, n = 6. Values with different letters within the same column indicate significant differences at the p < 0.05 level between Pb–Zn treatments. C: 100% garden soil, L1: 90% garden soil + 10% Pb–Zn tailings, L2: 75% garden soil + 25% Pb–Zn tailings, L3: 50% garden soil + 50% Pb–Zn tailings.

Pigment Contents

The photosynthetic pigment contents of the two tested plants were found to decline with increasing Pb–Zn tailing portions (**Figures 1A–D**). A significant reduction in chlorophylls a, b, and total chlorophyll in the two tested plants was observed under Pb–Zn tailing stress as compared to the C, respectively. Carotenoid content was notably affected by Pb–Zn tailing stress when the Pb–Zn treatment exceeded a portion of 10%. Compared with *L. lucidum*, *M. azedarach* showed a faster increase and a greater extent of chlorophylls a, b, total chlorophyll, and carotenoid content. When compared to the C groups, Chl a decreased by a range of 18 to 50%, Chl b from 9 to 35%, total chlorophyll from 16 to 46%, and the carotenoids from 5 to 37% in *L. lucidum* in L1–L3 treatments. The corresponding values decreased in *M. azedarach* from 4to 42% in Chl a, from 5 to 21% in Chl b, from 5 to 37% in total chlorophyll, and from 3 to 34% in carotenoids.

Gas Exchange

The Pb–Zn tailing treatments had an inhibitory effect on Pn, Gs, Gm, V_{cmax}, J_{max}, and Rubisco activity, but had promotion effect on Ci and Cc in both examined plants (**Figure 2**). Pn, V_{cmax}, J_{max} significantly decreased after Pb–Zn mine tailing treatment. The Gm of the leaves from the two plants gradually decreased with the increase of Pb–Zn tailing portions. For *M. azedarach*, Gs showed a significant difference between C and L1 treatments and then gradually decreased when the plants were grown in L2 treatments, and eventually reached the minimum value at L3 treatments. In *L. lucidum*, Gs was decreased slightly as Pb–Zn tailing portions increased. Both plants exhibited the similar tendency in Ci and Cc as Pb–Zn tailing portions increased. Ci and Cc decreased slightly when the plants were in L1 treatments and then significantly increased in L2 and L3 treatments ($P < 0.05$), but the change of Ci was higher in *L. lucidum* (increased from −5 to 58%) than in *M. azedarach* (increased from −4 to 5%). The decrease of P_n, Gm, V_{cmax}, and J_{max} in *M. azedarach* showed a greater extent than that in *L. lucidum*. When compared to the C groups, the Pn decreased by a range of 12 to 56%, the Gm from 7 to 18%, the V_{cmax} from 9 to 43%, the J_{max} from 19 to 64%, and the Rubisco activity from 10 to 52% in *L. lucidum* in L1–L3 treatments. The corresponding values decreased in *M. azedarach* from 31 to 67% in Pn, from 10 to 28% in Gm, from 16 to 59% in V_{cmax}, from 21 to 72% in J_{max}, and from 31 to 62% in the Rubisco activity.

Under Pb–Zn tailing treatments, biochemical limitations (BLs) increased in the two tested plants. The BL values of *M. azedarach* increased 12, 34, and 53% in the L1, L2, and L3 treatments compared to the C, respectively (**Table 3**). The corresponding values increased 6, 23, and 36% in L1, L2, and L3 treatments in *L. lucidum*, respectively. The stomatal conductance limitation (SL) and the mesophyll conductance (MCL) of leaves in both trees increased slightly under Pb–Zn treatments. The SL values increased 4–6% and the MCL values increased 0.4–0.8% for *M. azedarach* and *L. lucidum* when compared to C.

Prompt Fluorescence OJIP Transient Analysis

The Pb–Zn stress had a considerable effect on fluorescent OJIP transients in two tested plants (**Figure 3**). The F_o values were

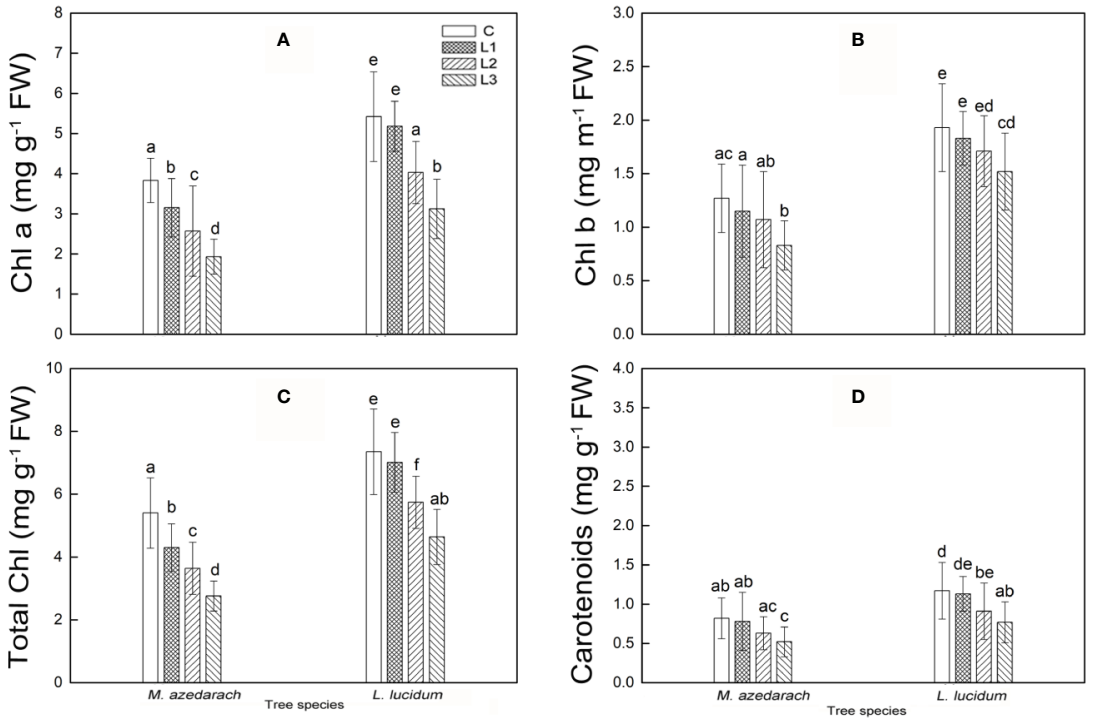

FIGURE 1 | Chlorophyll a **(A)**, chlorophyll b **(B)**, total chlorophyll **(C)** and carotenoids **(D)** in leaves of *M. azedarach* and *L. lucidum* grown in soil mixed with different proportions of Pb–Zn mine tailings. C (control), L1, L2, and L3 represent 100% garden soil, 90% garden soil + 10% Pb–Zn tailings, 75% garden soil + 25% Pb–Zn tailings, 50% garden soil + 50% Pb–Zn tailings, respectively. Different letters above the bars indicate a significant difference at $P < 0.05$. Values are means of n = 6; bar indicates standard error.

significantly reduced under Pb–Zn treatments in *M. azedarach* compared to the C (**Figure 3A**, inset). However, the F_o values of *L. lucidum* had no significant increase under Pb–Zn tailing treatments compared to the C (**Figure 3B**, inset). Three Pb–Zn tailing treatments did not affect W_k in *L. lucidum* compared to the C (**Figure 4A**). In *M. azedarach*, W_k was similar for both C and L1 treatments and significantly increased in L2 and L3 treatments (**Figure 4A**). Pb–Zn stress treatments significantly decreased performance index (PIabs) in *M. azedarach* and *L. lucidum* (**Figure 4B**) but distinctly increased the turnover number of Q_A reduction events (N) and absorption flux (ABS/RC) (**Figures 4F, G**). Meanwhile, RC/CS_O, TR_O/ABS, and ET_O/TR_O were decreased dramatically by Pb–Zn stress (**Figures 4C–E**).

The value of φR_o, δR_o and ΔV_{IP} significantly decreased in *M. azedarach* and *L. lucidum* as Pb–Zn tailing portions increased (**Figures 4H–J**). When compared to the C groups, the φR_o decreased by 21, 34, and 40%, the δR_o decreased by 32, 33, and 47%, and the ΔV_{IP} decreased by 18, 33, and 53% in *M. azedarach* in L1, L2, and L3 treatments, respectively. The corresponding values decreased 19, 24, and 36% in φR_o, 17, 30 and 35 in δR_o, 17, 26, and 37% in ΔV_{IP} in *L. lucidum*.

MR/MR_O Transient Analysis

After Pb–Zn tailing treatments, the shape of the MR/MR_O kinetics was obviously changed in the two tested plants. The lowest points represented a turning point of PSI oxidation state (**Figure 5**). When compared to the C, the lowest points on the reflection curve of both tested plants increased with rising Pb–Zn tailing portions. The V_{PSI} and $V_{PSII-PSI}$ of both tested plants declined significantly with the rising Pb–Zn tailing portions (**Table 4**). V_{PSI} and $V_{PSII-PSI}$ of both tested plants significantly decreased in the treated groups than in the C groups. Compared with *L. lucidum*, *M. azedarach* showed a greater decrease of V_{PSI} and $V_{PSII-PSI}$.

PI_{abs}, ΔV_{IP} in Relation to V_{cmax}

A significant positive relationship of PI_{abs}, ΔV_{IP} and V_{cmax} was observed in both tested plants under Pb–Zn mine tailing treatments (**Figure 6**). As V_{cmax} decreased, PI_{abs}, ΔV_{IP} decreased linearly in *M. azedarach* and *L. lucidum*, respectively.

O_2^- Production Rate, H_2O_2, MDA and Proline Content in Leaves

With an increase of Pb–Zn mine tailing portions, the O_2^- production rate, H_2O_2, and MDA contents of two tested plant leaves increased notably (**Figures 7A, C, D**). Compared with *L. lucidum*, *M. azedarach* showed a faster increase and a greater extent O_2^- production rate, H_2O_2, and MDA contents. The proline content in *M. azedarach* and *L. lucidum* reached the peak at L2 treatments (**Figure 7B**), where the proline content was 1.96 and 1.36 times higher than that in the C treatments,

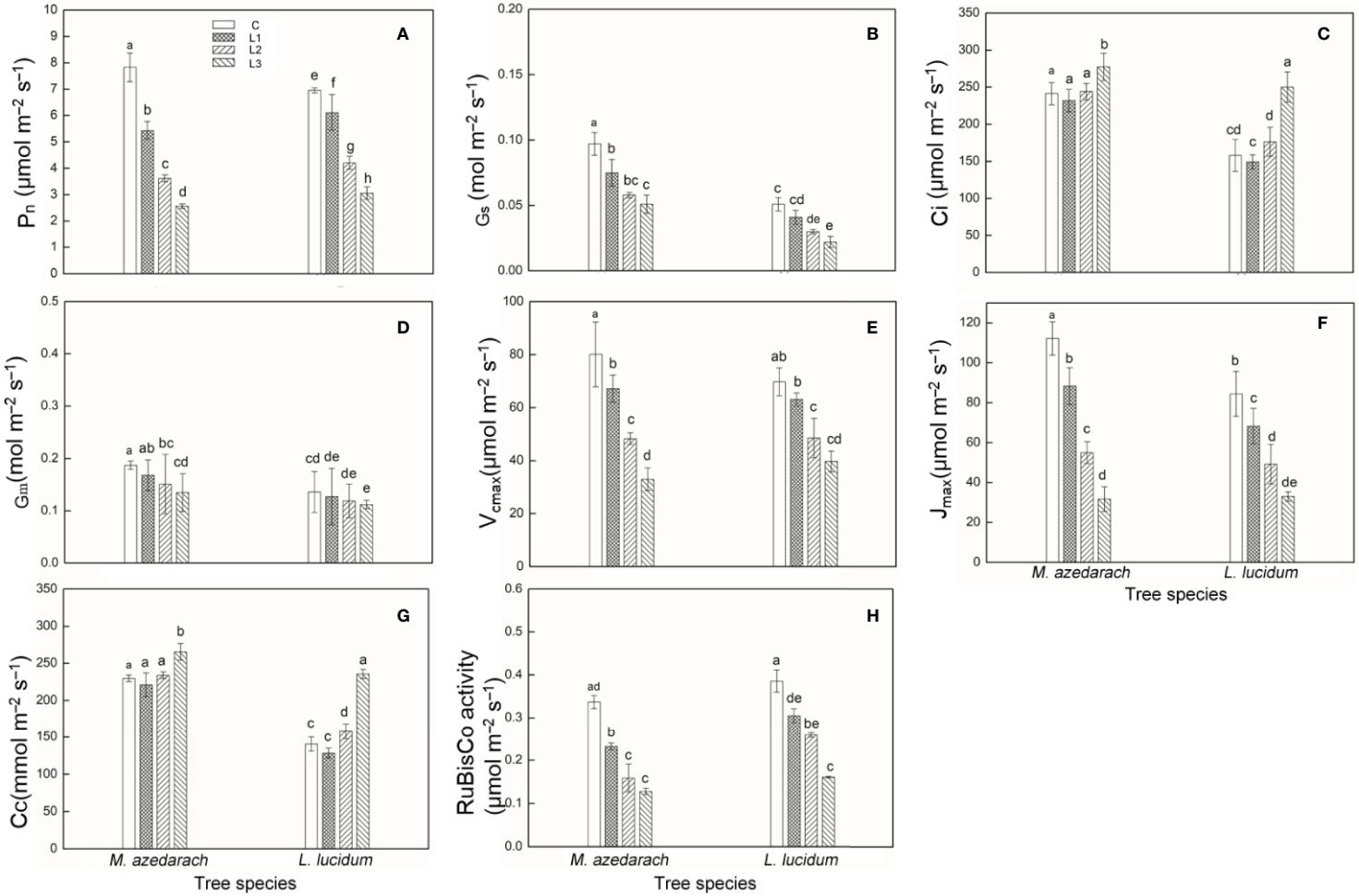

FIGURE 2 | Photosynthetic parameters measured with a Li-6400 gas exchange system and rubisco activity in *M. azedarach* and *L. lucidum* grown in soil mixed with different proportions of Pb–Zn mine tailings. **(A)** Pn, net photosynthetic rate; **(B)** Gs, stomatal conductance; **(C)** Ci, intercellular CO_2 concentration; **(D)** Gm, mesophyll conductance to CO_2; **(E)** V_{cmax}, maximum carboxylation rate allowed by Rubisco; **(F)** J_{max}, rate of photosynthetic electron transport based on NADPH requirement; **(G)** Cc, chloroplastic CO2 concentration; **(H)** Rubisco activity. C (control), L1, L2, and L3 represent 100% garden soil, 90% garden soil + 10% Pb–Zn tailings, 75% garden soil + 25% Pb–Zn tailings, 50% garden soil + 50% Pb–Zn tailings, respectively. Different letters above the bars indicate a significant difference at $P < 0.05$. Values are means of $n = 6$; bar indicates standard error.

TABLE 3 | Photosynthesis limitation parameters (%) in *M. azedarach* and *L. lucidum* grown in soil mixed with different proportions of Pb–Zn mine tailings.

	C	Pb–Zn tailings treatments		
		L1	L2	L3
M. azedarach				
SL	0.0%	5.1%	5.6%	4.0%
MCL	0.0%	0.5%	0.5%	0.8%
BL	0.0%	12.2%	33.6%	53.1%
L. lucidum				
SL	0.0%	5.0%	6.0%	6.4%
MCL	0.0%	0.4%	0.5%	0.4%
BL	0.0%	5.8%	23.1%	35.9%

Data are means ± SE, n = 6. The control (C) was taken as a reference, for which all limitations were set to 0. SL: stomatal conductance limitation, MCL: mesophyll conductance, BL: biochemical limitations. L1: 90% garden soil + 10% Pb–Zn tailings, L2: 75% garden soil + 25% Pb–Zn tailings, L3: 50% garden soil + 50% Pb–Zn tailings.

respectively. Under L3 treatments, the proline content in *M. azedarach* and *L. lucidum* decreased by 16 and 13% of that in the C, respectively.

Antioxidant Enzyme Activity in Leaves

The SOD, POD, and CAT displayed similar trends in activity in both tested trees with the increase of Pb–Zn mine tailing portions (**Figures 8A–C**). Compared with the C, the activities of SOD and POD in both tested trees significantly increased under L1 and L2 treatments and decreased under L3 treatment. The CAT activity in both tested trees under all Pb–Zn treatments was significantly higher than that in the C plants. Notably, the activities of SOD, POD, and CAT in *L. lucidum* were significantly higher than that in *M. azedarach* under all Pb–Zn mine tailing treatments.

Principal Component Analysis

PCA was used to understand Pb–Zn tailings affecting the photosynthetic characteristics including RGR, PSII performance, PSI content, net photosynthesis rates (Pn), and the antioxidative enzymes of leaves in both trees (**Figure 9**). The first two components comprised 90.0% (50.3% for PC1 and 39.7% for PC2), 91.4% (62.9% for PC1 and 28.5% for PC2), and 90.9% (36.7% for PC1 and 54.2% for PC2) of the total variations in L1, L2, and L3 treatments, respectively. Under L1 and L2 treatments, PIabs, ΔV_{IP}, and Pn were the most influential in the PC1; and SOD, POD and CAT in the PC2. Under L3 treatments, SOD, POD, and CAT were the most influential in the PC1, and PIabs and ΔV_{IP} in the PC2. Evidently, two tested plans were more closely to photosynthetic parameters (PIabs, ΔV_{IP}, and Pn) than to antioxidative enzymes (SOD, POD and CAT) under L1 and L2 treatments, but were more closely to antioxidative enzymes than to photosynthetic parameters under L3 treatment. In addition, RGR was positively related to the photosynthetic parameters in the tested plants.

DISCUSSION

The Reduction of Plant Growth Is Attributed to the Depression of Photosynthesis

When plants were grown in Pb–Zn contaminated soils, plant growth and development were retarded and eventually the biomass production decreased (Ha et al., 2011; Han et al., 2013). In this study, the RGR values for the two tested trees decreased under Pb–Zn treatments (**Table 2**). It was well known that plant biomass productivity was dependent on the photosynthetic assimilating accumulation which provided energy and carbon sources (Liu et al., 2017). A positive correlation was found between Pn and RGR in this study (**Figure 9**), suggesting the photosynthetic processes were inhibited by Pb–Zn stress in the tested tree species.

The Photosynthesis Limitation Is Mainly Attributed to the Biochemical Limitation

A significant decrease of gas exchange parameters was observed in the Pb–Zn treated plants (**Figure 2**). Photosynthesis limitations might be derived from different physiological

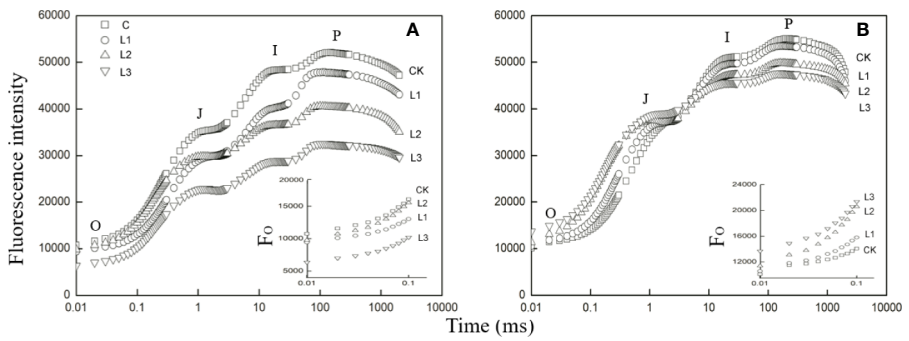

FIGURE 3 | Fast induction curves of chlorophyll fluorescence (OJIP) in *M. azedarach* **(A)** and *L. lucidum* **(B)** grown in soil mixed with different proportions of Pb–Zn mine tailings. The letters O, J, I, and P refer to the selected time points used by the JIP-test for the calculation of structural and functional parameters. The used signals are: the fluorescence intensity at $F_O \cong F_{20\mu s}$ or $F_{50\mu s}$; at 3 ms = F_J; and at 30 ms = F_I; the maximal fluorescence intensity, $F_P = F_M$. C (control); L1, L2, and L3 represent 100% garden soil, 90% garden soil + 10% Pb–Zn tailings, 75% garden soil + 25% Pb–Zn tailings, 50% garden soil + 50% Pb–Zn tailings, respectively. In the insets of the two panels, the F_O of the fluorescence rise is compared between measurements on control and Pb–Zn treated leaves.

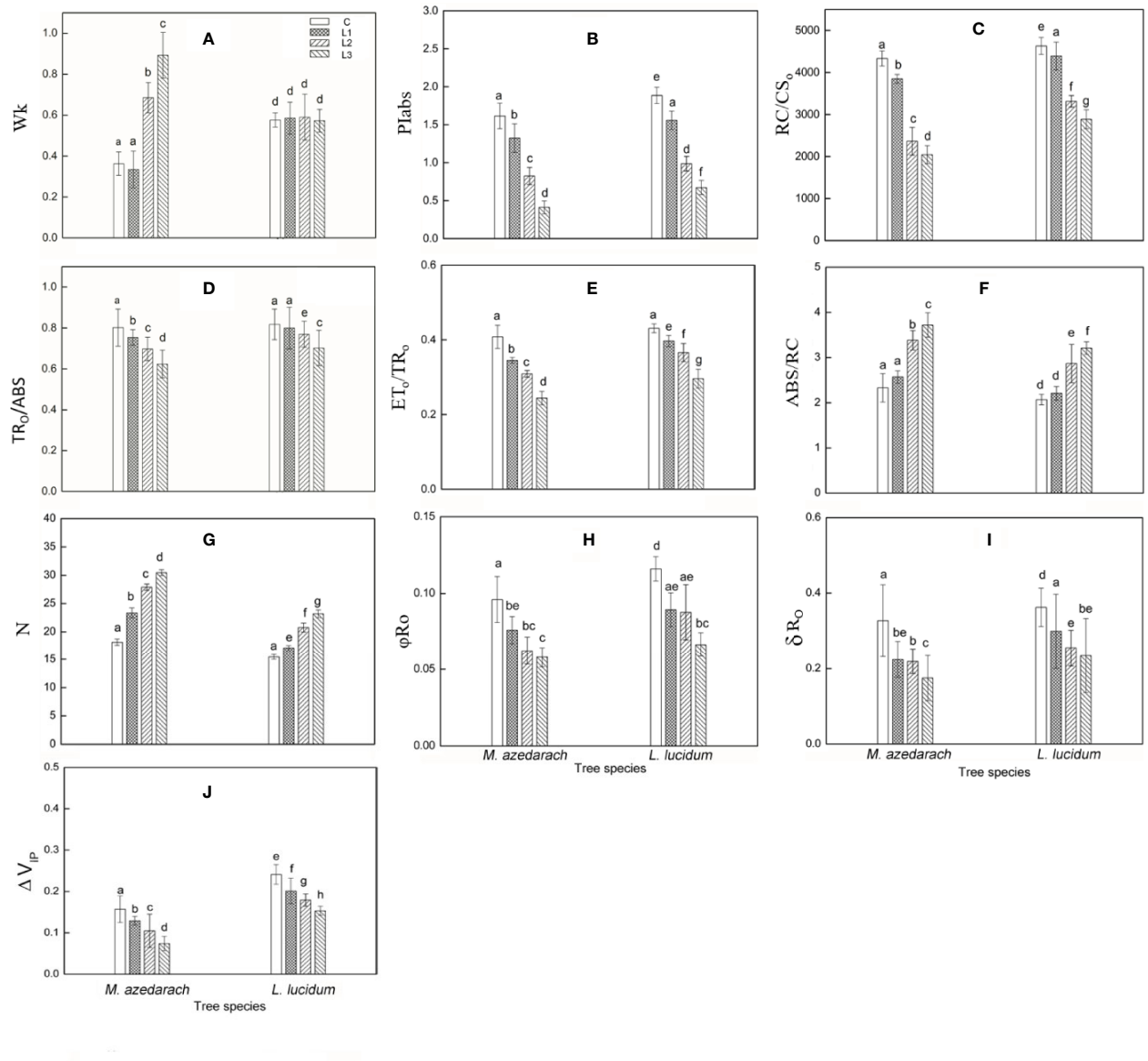

FIGURE 4 | Parameters derived from OJIP transients of *M. azedarach* and *L. lucidum* grown in soil mixed with different proportions of Pb–Zn mine tailings. **(A)** W_K, relative variable fluorescence at the K-step to the amplitude F_J–F_O; **(B)** PI_{ABS}, performance index (potential) for energy conservation from photons absorbed by PSII to the reduction of intersystem electron acceptors; **(C)** RC/CS_O, the density of PSII reaction center (RC) per excited cross-section (at t = 0); **(D)** TR_O/ABS, maximum quantum yield for primary photochemistry; **(E)** ET_O/TR_O, probability that an electron moves further than QA^-; **(F)** ABS/CS, absorption flux per unit area; **(G)** N, the turnover number of Q_A reduction events; **(H)** φ_{Ro}, quantum yield for reduction of the end electron acceptors on the PSI acceptor side (RE); **(I)** δ_{Ro}, probability that an electron is transported from the reduced intersystem electron acceptors to the final electron acceptors of PSI (RE); **(J)** ΔV_{IP}, amplitude of the I to P phase of the OJIP fluorescence transient (associated with PSI reaction center content). C (control); L1, L2, and L3 represent 100% garden soil, 90% garden soil + 10% Pb–Zn tailings, 75% garden soil + 25% Pb–Zn tailings, 50% garden soil + 50% Pb–Zn tailings, respectively. Different letters above the bars indicate a significant difference at $P < 0.05$. Values are means of $n = 6$, bar indicates standard error.

processes, such as stomatal opening, mesophyll conductance to CO_2, and the carboxylation capacity (Flexas et al., 2008; Centritto et al., 2009). In this study, although Gs and Gm significantly decreased (**Figures 2B, D**), they probably played a minor role in limiting photosynthesis because Ci and Cc increased simultaneously (**Table 3**, **Figures 2C, G**). The biochemical limitation was likely the major factor affecting photosynthesis in *M. azedarach* and *L. lucidum* (**Table 3**). Change for the results were in line with the findings of other studies (Seregin and Kozhevnikova, 2006; Velikova et al., 2011). The biochemical limitations were related to the considerable declines in V_{cmax} and J_{max} with increasing Pb–Zn stresses. The *M. azedarach* suffered more metabolic damage than that in *L. lucidum* (**Figures 2E, F**), indicating that the supply of energy source and carbon skeleton

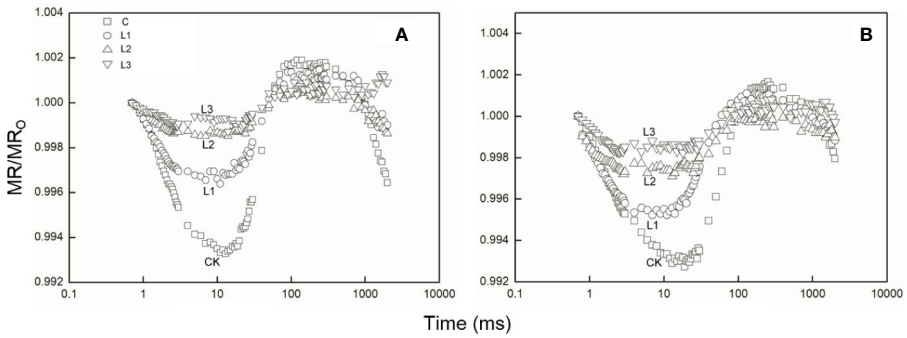

FIGURE 5 | The 820 nm light reflection curves of *M. azedarach* **(A)** and *L. lucidum* **(B)** in soil mixed with different proportions of Pb–Zn mine tailings. Modulated 820 nm reflection was expressed as MR/MR$_O$, where MR$_O$ is the modulated reflection value at the onset of actinic illumination (taken at 0.7 ms, the first reliable MR measurement) and MR is the modulated reflection signal during illumination. C (control); **(A)** L1, **(B)** L2, and **(C)** L3 represent 100% garden soil, 90% garden soil + 10% Pb–Zn tailings, 75% garden soil + 25% Pb–Zn tailings, 50% garden soil + 50% Pb–Zn tailings, respectively.

for plant growth and development was lower in *M. azedarach* than in *L. lucidum* (Imsande and Touraine, 1994). The decrease of V_{cmax} values might be ascribed to a reduction of Rubisco activity in the photosynthetic process (**Figure 2H**). The influence of Rubisco activity due to adverse environmental conditions has been reported by other studies (Bah et al., 2010). The J_{max} inhibition in the leaves under Pb–Zn tailing treatments observed from the changes in A/Cc curves indicated the photochemical limitation occurred in our study. The results were in line with the finding which Velikova et al. (2011) reported that alterations in the electron transport rate from PSII to PSI under heavy metals stresses result in a J_{max} limitation.

In addition, there was a decrease in chlorophyll and carotenoid content with the rising Pb–Zn stress in *M. azedarach* and *L. lucidum*, which illustrated that Pb–Zn stress had harmed the photosynthetic apparatus for these two tree species. The decrease of chlorophyll content might be attributed to HMs interfering Fe metabolism, inhibiting chlorophyll synthetase activity and enhancing chlorophyll enzyme activity (Rana, 2015). As a result, chlorophyll degradation ultimately inactivated photosynthesis (Hajihashemi and Ehsanpour, 2013). We found that the decrease degree of chlorophyll content was higher than that of carotenoid content by HMs. The results were in line with the previous finding by Amir et al. (2020) who reported that chlorophylls were more susceptible to the negative impact of HMs as compared to carotenoids.

TABLE 4 | Parameters derived from the modulated 820-nm reflection (MR/MR$_O$) of the *M. azedarach* and *L. lucidum* grown in soil mixed with different proportions of Pb–Zn mining tailings.

M. azedarach	V_{PSI}	$V_{PSII-PSI}$	V_{PSII}
C	2.065 ± 0.212a	0.095 ± 0.008a	2.160 ± 0.145a
L1	1.309 ± 0.088b	0.063 ± 0.014b	1.372 ± 0.056b
L2	0.561 ± 0.107c	0.019 ± 0.007c	0.580 ± 0.009c
L3	0.413 ± 0.069d	0.005 ± 0.000d	0.418 ± 0.011d
L. lucidum			
C	2.046 ± 0.054a	0.036 ± 0.004a	2.082 ± 0.094a
L1	1.544 ± 0.131b	0.021 ± 0.006b	1.565 ± 0.083b
L2	1.804 ± 0.009c	0.010 ± 0.002c	1.814 ± 0.115c
L3	0.681 ± 0.102d	0.008 ± 0.001d	0.699 ± 0.057d

Data are means ± SE, n = 6. Different small letters in the same column indicate significant difference at 0.05 level by Duncan's new multiple test. V_{PSI}: maximum slope decrease of MR/MR$_O$; $V_{PSII-PSI}$: maximum slope increase of MR/MR$_O$; $V_{PSII} = V_{PSI} + V_{PSII-PSI}$. L1 90% garden soil + 10% Pb–Zn tailings, L2: 75% garden soil + 25% Pb–Zn tailings, L3: 50% garden soil + 50% Pb–Zn tailings.

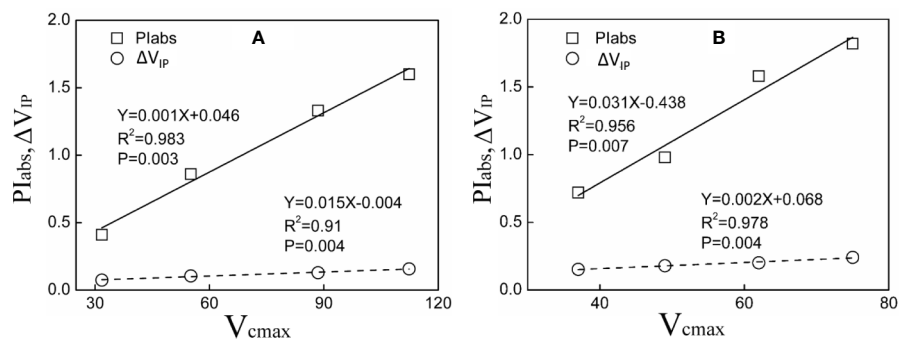

FIGURE 6 | Relationship between Plabs, ΔV_{IP} and V_{cmax} for *M. azedarach* **(A)** and *L. lucidum* **(B)** in soil mixed with different proportions of Pb–Zn mine tailings.

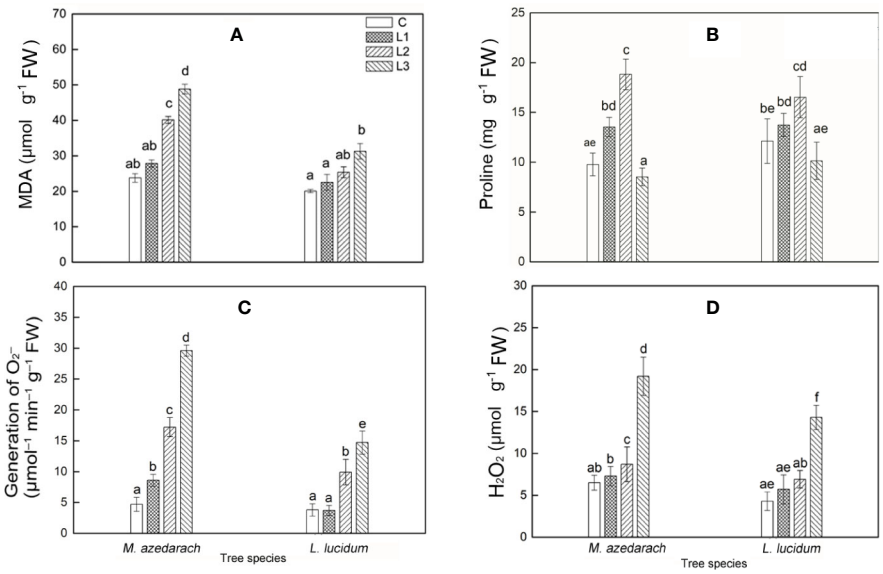

FIGURE 7 | Malondialdehyde (MDA) **(A)**, Proline **(B)**, O_2^- production rate **(C)**, H_2O_2 content **(D)** in leaves of *M. azedarach* and *L. lucidum* grown in soil mixed with different proportion of Pb–Zn mine tailings. C (control); L1, L2, and L3 represent 100% garden soil, 90% garden soil + 10% Pb–Zn tailings, 75% garden soil + 25% Pb–Zn tailings, 50% garden soil + 50% Pb–Zn tailings, respectively. Different letters above the bars indicate a significant difference at $P < 0.05$. Values are means of $n = 6$; bar indicates standard error.

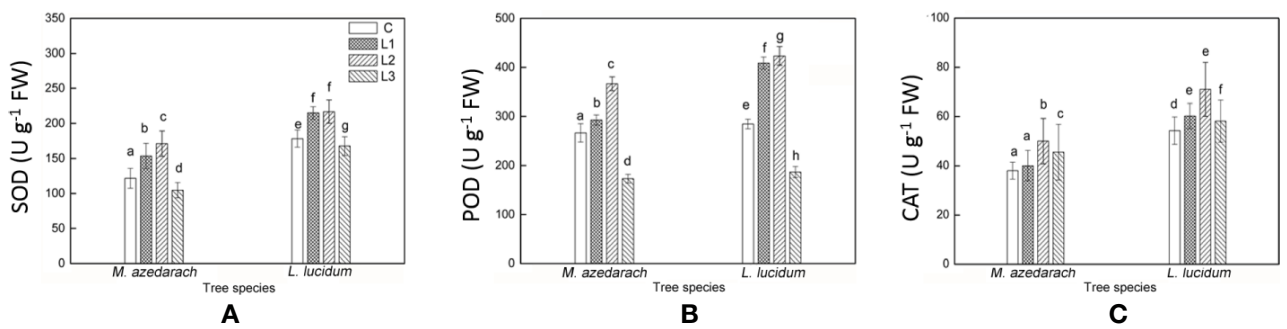

FIGURE 8 | Superoxide dismutase (SOD) **(A)**, Peroxidase (POD) **(B)** and Catalase (CAT) **(C)** in leaves of *M. azedarach* and *L. lucidum* grown in soil mixed with different proportions of Pb–Zn mine tailings. C (control); L1, L2, and L3 represent 100% garden soil, 90% garden soil + 10% Pb–Zn tailings, 75% garden soil + 25% Pb–Zn tailings, 50% garden soil + 50% Pb–Zn tailings, respectively. Different letters above the bars indicate a significant difference at $P < 0.05$. Values are means of $n = 6$; bar indicates standard error.

The Photosynthetic Electron Transport Is Altered by the Pb–Zn Tailing Stress

Changes in environmental factors could affect photosynthetic performance (Ji et al., 2018). The impacts of HM stresses on the electron transfer and energy balance in photosynthetic processes are quantified by OJIP fluorescence (Li and Zhang, 2015; Guo et al., 2018). In this study, the chlorophyll fluorescence transient curves of the two tested plants were all modified by Pb–Zn mine tailings (**Figure 3**). With the increase of proportions of Pb–Zn mine tailings, F_O values were significantly reduced in *M. azedarach*, but increased in *L. lucidum* compared to the control (**Figure 3**); the value of F_P decreased in the two tested plants. The F_O decrease in *M. azedarach* was likely attributed to the photoinhibitory damage on PSII acceptor (Setlik et al., 1990), and the increase of F_O in *L. lucidum* might be caused by increasing amount of free chlorophylls to the PSII RC (Gilmore et al., 1996). The decrease in F_P was observed in other heat and salt stress studies due to the increased fraction of inactive RCs (Jedmowski and Brüggemann, 2015; Oukarroum et al., 2015). W_K was the donor site parameter of PSII, which has been widely used to analyze damage to OEC by HM stresses (Li and Zhang, 2015). In this study, an increase of W_k value in *M. azedarach* (**Figure 4A**) suggested that Pb–Zn stress not only impaired the OEC; the process of electron transfer was also impaired at the P680 donor site (Jiang et al., 2008; Dąbrowski et al., 2016). However, the OEC and the donor side of PSII were

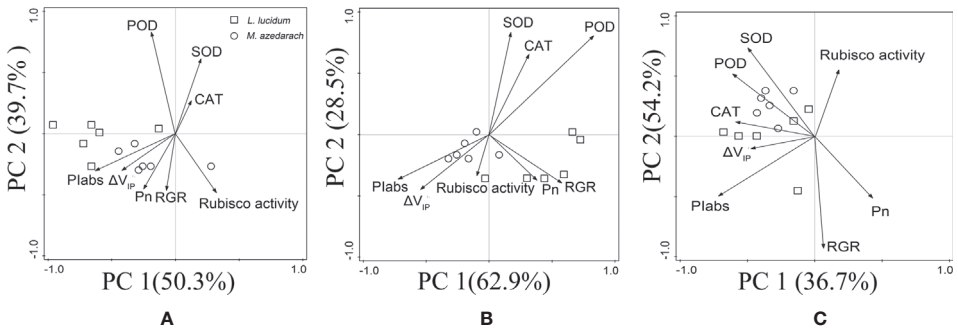

FIGURE 9 | Principal component analysis (PCA) of antioxidant enzymes, PSII performance, PSI content, net photosynthesis rates (Pn), and the relative growth rate (RGR) of *M. azedarach* and *L. lucidum* exposed to different proportions of Pb–Zn mine tailings. **(A)** L1, **(B)** L2, and **(C)** L3 represent 100% garden soil, 90% garden soil + 10% Pb–Zn tailings, 75% garden soil + 25% Pb–Zn tailings, 50% garden soil + 50% Pb–Zn tailings, respectively.

not impaired by Pb–Zn stress in *L. lucidum* since W_k values did not show a significant change.

Here, several important JIP-test parameters based on the OJIP transient were used to detect and quantify the changes of the photosystem status under Pb-Zn mine tailings stresses. The reduction of the maximum quantum yield of primary photochemistry (TRo/ABS) (**Figure 4D**) and the electron numbers moved further than the Q_A^- (ET_O/TR_O) (**Figure 4E**) indicating that Pb–Zn stress resulted in a fast accumulation of Q_A^- in the PSII reaction centers. The results suggested the photosynthetic electron transport was impaired in the acceptor side of PSII, and the electron flow beyond Q_A^- was blocked (Bernardini et al., 2016). It was reported that photoinhibition process can be more accurately assessed by the changes between flux ratios and specific fluxes per reaction center (RC) (Baker and Rosenqvist, 2004; Mlinarić et al., 2017). It was worth noting that the RC/CS_O was diminished and ABS/RC was risen in the two tested plants (**Figures 4C, F**), suggesting that although the numbers of active PSII RCs were decreased under Pb–Zn stress, the photochemical reaction efficiency of the remaining RCs was improved by maintaining the regular photosynthesis ability (Paunov et al., 2018). Due to the inactivation of a number of reaction centers, the remaining RCs had to increase their turnover in order to completely reduce the PQ pool (Zhou et al., 2019) as shown by a rise in parameter N (**Figure 4G**). *M. azedarach* had lower values of PIabs, RC/CS_O, TR_O/ABS, and ET_O/TR_O and higher values of ABS/RC than that in *L. lucidum*, indicating that Pb–Zn stress may affect, to a greater extent, the PSII activity in *M. azedarach* species.

ΔV_{IP} has been used to describe the changes in content of PSI reaction center under detrimental conditions (Oukarroum et al., 2009; Ceppi et al., 2012). The drought and Zn stress conditions declined ΔV_{IP} in *Hordeum spontaneum* (Oukarroum et al., 2009) and *Phragmites australis* (Bernardini et al., 2016). In this study, ΔV_{IP} was significantly lower for the two plants grown in Pb–Zn contaminated soil when compared to C (**Figure 4J**), indicating that Pb–Zn stress decreased the PSI reaction center in the two tested tree species. The significant reductions of φR_o and δR_o (**Figures 4H, I**) indicated that the effect of Pb–Zn stress on electron flow occurred in the acceptor side of PSI because of the reduction of the PSI content (Hu et al., 2018). In addition, the values of V_{PSI} of the two tested plants decreased in the Pb–Zn treated groups when compared to the C (**Figure 5**, **Table 4**), indicating that the oxidization reactions were inhibited due to the Pb–Zn stress. The decline in the $V_{PSII-PSI}$ suggested that the reduction activity of PSI activity was injured by the Pb–Zn stress. Therefore, the decreases in maximum oxidization and reduction activity of PSI reaction center were observed since Pb–Zn stress affected PSI content.

In this study, a positive linear relation was found between PI_{abs} and V_{cmax} in this study suggesting that PSII performance was positively related to CO_2 assimilation (**Figure 6**). The result was in accordance with the suggestions provided by Ghotbi-Ravandi et al. (2014); they reported that the reduction in PSII performance played an important role in the decrease of CO_2 assimilation rate in *Morocco* under mild and severe drought stresses. Meanwhile, ΔV_{IP} also decreased linearly with the decrease of V_{cmax}; the result suggested that PSI content might limit the capacity of CO_2 assimilation (**Figure 6**). Because the decrease of PSI content could disturb the electron flow from PSII to PSI and limited the synthesis of ATP and NADPH (Brestic et al., 2015), the inhibition of CO_2 assimilation rate can be suggested as a result of the excessive excitation energy that damage the photosystems and especially impeded the photochemical activity of PSI (Zivcak et al., 2013). Specifically, *M. azedarach* suffered more serious effects on the photosynthetic electron transport chain than *L. lucidum* under Pb–Zn stress. This finding was supported by the fact that photosynthetic parameters (PIabs, ΔV_{IP}, and Pn) were more affected in *M. azedarach* than that in *L. lucidum* in PCA analysis (**Figure 9**).

L. lucidum May Be More Tolerant to Pb–Zn Stress Than *M. azedarach*

It is previously demonstrated that adverse conditions impaired PSII electron transport; the excess electron resulted in increasing the levels of ROS and consequently caused oxidative stress (Pospíšil, 2009; Guo et al., 2018). The malondialdehyde (MDA) content represents level of lipid peroxidation, which was able to indicate

oxidative damage of membrane lipids under stress conditions (Sharma and Dubey, 2005). In this study, with the increase of proportion of Pb–Zn mine tailings, the O_2^- production rate and H_2O_2 content in both tested tree leaves increased significantly, contributing to a significant increase of MDA content. This result was in line with the previous reports where MDA content increased in *Peganum harmala*, *Kandelia obovate*, and *Alternanthera bettzickiana* under HMs stress (Lu et al., 2010; Cheng et al., 2017). In this study, proline contents increased in *M. azedarach* and *L. lucidum* leaves in L1 and L2 treatments but decreased at L3 treatments when compared to the C (**Figure 7B**). The phenomena suggested the increase of proline contents at low and medium Pb–Zn treatments could maintain the integrity of cellular membranes, protect proton pump, and eliminate ROS (Dhir et al., 2012). The decrease of proline contents in L3 treatments might be explained by the fact that the physiological functions and metabolisms of plants were seriously damaged at high concentration of Pb–Zn toxicity (Chen et al., 2003). When the equilibrium between ROS generation and detoxification was disrupted by abiotic stresses, the induction of antioxidative enzyme defense activities played a crucial role in HM tolerance in plants (Ashraf, 2009). SOD was the first defense line against oxidative stresses, and superoxide radicals (O_2^-) were scavenged by SOD. CAT was recognized as the most important enzyme for scavenging H_2O_2 produced in plant cells and was primarily associated with the maintenance steady of cellular. POD enzyme can detoxify H_2O_2 and thereby was conducive to maintaining the integrity of cellular membranes (Liu et al., 2017). In this study, SOD, POD, and CAT activity in *M. azedarach* and *L. lucidum* initially increased and then declined under Pb–Zn stress (**Figure 8**). The same patterns were found in *Iris halophila* exposed to Pb mine tailing treatments (Han et al., 2016). The SOD, POD, and CAT activities were higher in the L1 and L2 treatments than those in the C, indicating that the antioxidative system can effectively mitigate oxidative damage (Nie et al., 2016). The reduction of antioxidative enzyme activity under the highest Pb–Zn tailing treatments might be ascribed to the fact that the gene expression of SOD, POD and CAT enzymes was impacted by strong Pb–Zn stress (Hu et al., 2015). Another account for the decrease in SOD, POD, and CAT activity was that these variables were exhausted to alleviate the detrimental effects of ROS under higher Pb–Zn stress (Nie et al., 2016).

Under Pb–Zn stress, *L. lucidum* had a lower level of lipid peroxidation and higher activities of the antioxidative enzyme when compared to *M. azedarach*. As the tolerance to HMs was linked with the low level of lipid peroxidation and high activities of antioxidative enzymes (Ma et al., 2001; Sharma and Dietz, 2009), *L. lucidum* likely possessed a higher tolerability to HMs than *M. azedarach*. Additionally, less influence occurred on PSII and PSI in *L. lucidum* than in *M. azedarach* (**Figure 4**), which was probably attributed to the lower MDA content and higher antioxidative enzyme activities in *L. lucidum* (Iqbal et al., 2019). It should be noted that the TFs for Pb and Zn in stems and leaves were lower in *L. lucidum* than in *M. azedarach*, and more Pb and Zn were retained in *L. lucidum* roots, indicating that *L. lucidum* has more excellent metal exclusion strategy under Pb–Zn mine tailing treatments.

CONCLUSION

The current study showed that Pb–Zn mine tailing had a crucial negative influence on two tested plants' development and biomass production by inhibiting the chlorophyll synthesis and photosynthetic metabolism. The reduction of net photosynthetic rates in *M. azedarach* and *L. lucidum* due to HM stress was mainly caused by their biochemical limitation, including decreases of V_{cmax} and J_{max}. Pb–Zn stress damaged multiple locations along the photosynthetic electron transport chain. Specifically, it impaired the OEC (only in *M. azedarach*) and blocked electron flow of acceptor side of PSII and disturbed the PSI oxidation and reduction in both tested trees. Moreover, the increase of ROS content in both plant species was directly related to the obstruction of the electron transfer. Meanwhile, *M. azedarach* and *L. lucidum* could maintain high levels of SOD, POD, CAT, and proline contents to effectively relieve oxidative stress. The more tolerance of *L. lucidum* might be attributed to these facts: (1) higher RGR; (2) more accumulation of Pb–Zn in roots; (3) a less extent effect occurred on PSII and PSI activity; and (4) lower ROS and MDA content and higher antioxidative enzymes activities.

DATA AVAILABILITY STATEMENT

All datasets presented in this study are included in the article.

AUTHOR CONTRIBUTIONS

Idea and study designed: FZ. Performed the experiments: ML and HX. Wrote the paper: XH. Helped revise original paper: XC, ZH, and GW.

FUNDING

This work was financially supported by the Key Research and Development Project of Hunan Province (2017NK2171), the "948" introduction project of The State Bureaucracy of Forestry (2014-4-62), the Hunan Provincial Innovation Foundation For Postgraduate (CX2018B434), the Scientific Innovation Fund for Post-graduates of Central South University of Forestry and Technology (20181007), and the Scientific Innovation Fund for Post-graduates of Central South University of Forestry and Technology (CX20192062).

ACKNOWLEDGMENTS

We thank Dr. DaYong Fan for stimulating discussions and critical readings of the manuscript.

REFERENCES

Aebi, H. (1984). Catalase in vitro. *Methods Enzymol.* 105, 121–126. doi: 10.1016/S0076-6879(84)05016-3

Amir, W., Farid, M., Ishaq, H. K., Farid, S., Zubair, M., Alharby, H. F., et al. (2020). Accumulation potential and tolerance response of Typha latifolia L. under citric acid assisted phytoextraction of lead and mercury. *Chemosphere* 157, 127247–127261. doi: 10.1016/j.chemosphere.2020.127247

Ashraf, M. (2009). Biotechnological approach of improving plant salt tolerance using antioxidants as markers. *Biotechnol. Adv.* 1, 84–93. doi: 10.1016/j.biotechadv.2008.09.003

Bah, A. M., Sun, H., Chen, F., Zhou, J., Dai, H. X., Zhang, G. P., et al. (2010). Comparative proteomic analysis of typha angustifolia leaf under chromium, cadmium and lead stress. *J. Hazard. Mater.* 184, 191–203. doi: 10.1016/j.jhazmat.2010.08.023

Baker, N. R., and Rosenqvist, E. (2004). Applications of chlorophyll fluorescence can improve crop production strategies: An examination of future possibilities. *J. Exp. Bot.* 55, 1607–1621. doi: 10.1093/jxb/erh196

Bao, S. D. (2000). *The Soil Agricultural Chemistry Analysis* (Beijing: Chinese Agriculture Press). (in chinese).

Beffa, R., Martin, H. V., and Pilet, P. E. (1990). In vitro oxidation of indoleacetic acid by soluble auxin-oxidases and peroxidases from maize root. *Plant Physiol.* 94, 485–491. doi: 10.1104/pp.94.2.485

Belatik, A., Hotchandani, S., Tajmir-Riahi, H.-A., and Carpentier, R. (2013). Alteration of the structure and function of photosystem I by Pb^{2+}. *J. Photochem. Photobiol. B.* 123, 41–47. doi: 10.1016/j.jphotobiol.2013.03.010

Bernacchi, C. J., Portis, A. R., Nakano, H., Caemmerer, S. V., and Long, S. P. (2002). Temperature response of mesophyll conductance. Implications for the determination of Rubisco enzyme kinetics and for limitations to photosynthesis in vivo. *Plant Physiol.* 130, 1992–1998. doi: 10.1104/pp.008250

Bernardini, A., Salvatori, E., Guerrini, V., Fusaro, L., Canepari, S., and Manes, F. (2016). Effects of high Zn and Pb concentrations on Phragmites australis (Cav.) Trin. Ex. Steudel: Photosynthetic performance and metal accumulation capacity under controlled conditions. *Int. J. Phytoremediat.* 1, 16–24. doi: 10.1080/15226514.2015.1058327

Bezerril, F. N. M., Otoch, M. D. L. O., Gomes-Rochette, N. F., Sobreira, A.C.de M., Barreto, A. A. G. C., de Oliveira, F. D. B., et al. (2017). Effect of lead on physiological and antioxidant responses in two Vigna unguiculata cultivars differing in Pb-accumulation. *Chemosphere* 176, 397–404. doi: 10.1016/j.chemosphere.2017.02.072

Bi, A., Fan, J., Hu, Z., Wang, G., Amombo, E., Fu, J., et al. (2016). Differential acclimation of enzymatic antioxidant metabolismand photosystem II photochemistry in Tall Fescue under drought and heat and the combined stresses. *Front. Plant Sci.* 7, 453. doi: 10.3389/fpls.2016.00453

Boominathan, R., and Doran, P. M. (2003). Cadmium tolerance and antioxidative defenses in hairy roots of the cadmium hyperaccumulator, Thlaspi caerulescens. *Biotechnol. Bioeng.* 83, 158–167. doi: 10.1002/bit.10656

Brestic, M., Zivcak, M., Kunderlikova, K., Sytar, O., Shao, H., Kalaji, H. M., et al. (2015). Low PSI content limits the photoprotection of PSI and PSII in early growth stages of chlorophyll b-deficient wheat mutant lines. *Photosynth. Res.* 125, 151–166. doi: 10.1007/s11120-015-0093-1

Centritto, M., Loreto, F., and Chartzoulakis, K. (2003). The use of low [CO_2] to estimate diffusional and non-diffusional limitations of photosynthetic capacity of salt-stressed olive saplings. *Plant Cell Environ.* 26, 585–594. doi: 10.1046/j.1365-3040.2003.00993.x

Centritto, M., Lauteri, M., Monteverdi, M. C., and Serraj, R. (2009). Leaf gas exchange, carbon isotope discrimination, and grain yield in contrasting rice genotypes subjected to water deficits during the reproductive stage. *J. Exp. Bot.* 60, 2325–2339. doi: 10.1093/jxb/erp123

Ceppi, M. G., Oukarroum, A., Çiçek, N., Strasser, R. J., and Schansker, G. (2012). The IP amplitude of the fluorescence rise OJIP is sensitive to changes in the photosystem I content of leaves: a study on plants exposed to magnesium and sulfate deficiencies, drought stress and salt stress. *Physiol. Plant* 144, 277–288. doi: 10.1111/j.1399-3054.2011.01549.x

Chen, Y. X., He, Y. F., Luo, Y. M., Yu, Y. L., Lin, Q., and Wong, M. H. (2003). Physiological mechanism of plant roots exposed to cadmium. *Chemosphere* 6, 780–793. doi: 10.1016/s0045-6535(02)00220-5

Chen, L. S., Qi, Y. P., Smith, B. R., and Liu, X. H. (2005). Aluminum-induced decrease in CO_2 assimilation in citrus seedlings is unaccompanied by decreased activities of key enzymes involved in CO_2 assimilation. *Tree Physiol.* 25, 317–324. doi: 10.1093/treephys/25.3.317

Chen, F. L., Wang, S. Z., Mu, S. Y., Azimuddin, I., Zhang, D. Y., Pan, X. L., et al. (2015). Physiological responses and accumulation of heavy metals and arsenic of Medicago sativa L. growing on acidic copper mine tailings in arid lands. *J. Geochem. Explor.* 157, 27–35. doi: 10.1016/j.gexplo.2015.05.011

Cheng, S. S., Tam, N. F. Y., Li, R. L., Shen, X. X., Niu, Z. Y., Chai, M. W., et al. (2017). Temporal variations in physiological responses of Kandelia obovata seedlings exposed to multiple heavy metals. *Mar. Pollut. Bull.* 2, 1089–1095. doi: 10.1016/j.marpolbul.2017.03.060

Chiang, H. C., Lo, J. C., and Yeh, K. C. (2006). Genes Associated with Heavy MetalTolerance and Accumulation in Zn/Cd Hyperaccumulator Arabidopsis halleri: A GenomicSurvey with cDNA Microarray. *Environ. Sci. Technol.* 40, 6792–6798. doi: 10.1021/es061432y

Chu, J. J., Zhu, F., Chen, X. Y., Liang, H. Z., Wang, R. J., Wang, X. X., et al. (2018). Effects of cadmium on photosynthesis of Schima superba young plant detected by chlorophyll fluorescence. *Environ. Sci. Pollut. R.* 25, 10679–10687. doi: 10.1007/s11356-018-1294-x

Çiçek, N., Oukarroum, A., Strasser, R. J., and Schansker, G. (2017). Salt stress effects on the photosynthetic electron transport chain in two chickpea lines differing in their salt stress tolerance. *Photosynth. Res.* 136, 291–301. doi: 10.1007/s11120-017-0463-y

Dąbrowski, P., Baczewska, A. H., and Pawluśkiewicz, B. (2016). Prompt chlorophyll a fluorescence as a rapid tool for diagnostic changes in PSII structure inhibited by salt stress in Perennial ryegrass. *J. Photochem. Photobiol. B.* 157, 22–31. doi: 10.1016/j.jphotobiol.2016.02.001

Deng, G., Li, M., Li, H., Yin, L., and Li, W. (2014). Exposure to cadmium causes declines in growth and photosynthesisin the endangered aquatic fern (*Ceratopteris pteridoides*). *Aquat. Bot.* 1, 23–32. doi: 10.1016/j.aquabot.2013.07.003

Dhindsa, R. S., Plumb-Dhindsa, P., and Thorpe, T. A. (1981). Leaf senescence: correlated with increased levels of membrane permeability and lipid peroxidation, and decreased levels of superoxide dismutase and catalase. *J. Exp. Bot.* 32, 93–101. doi: 10.1093/jxb/32.1.93

Dhir, B., Nasim, S. A., Samantary, S., and Srivastava, S. (2012). Assessment of osmolyte accumulation in heavy metal exposed *Salvinia Natans*. *Int. J. Bot.* 8, 153–158. doi: 10.3923/ijb.2012.153.158

Du, H. M., Huang, Y., Qu, M., Li, Y. H., Hu, X. Q., Yang, W., et al. (2020). A Maize ZmAT6 gene confers Aluminum tolerance via reactive oxygen species scavenging. *Front. Plant Sci.* 11, 1016. doi: 10.3389/fpls.2020.01016

Farquhar, G. D., Caemmerer, S. V., and Berry, J. A. (1980). A biochemical model of photosynthetic CO_2 assimilation in leaves of C3 species. *Planta* 149, 78–90. doi: 10.1007/BF00386

Flexas, J., Ribas-Carbò, M., Diaz-Espejo, A., Galmés, J., and Medrano, H. (2008). Mesophyll conductance to CO_2: current knowledge and future prospects. *Plant Cell Environ.* 31, 602–621. doi: 10.1111/j.1365-3040.2007.01757.x

Frérot, H., Lefèbvre, C., Gruber, W., Collin, C., Santos, A. D., and Escarré, J. (2006). Specific Interactions between Local Metallicolous Plants Improve the Phytostabilization of Mine Soils. *Plant Soil.* 282, 53–65. doi: 10.1007/s11104-005-5315-4

Gao, J., Li, P., Ma, F., and Goltsev, V. (2014). Photosynthetic performance during leaf expansion in Malus micromalus probed by chlorophyll a fluorescence and modulated 820 nm reflection. *J. Photochem. Photobiol. B.* 137, 144–150. doi: 10.1016/j.jphotobiol.2013.12.005

Gao, J. F. (2006). *Experimental Guidance For Plant Physiology* (Beijing, China (in chinese: Higher Education Press). doi: 10.4236/oalib.preprints.1200091

Ghotbi-Ravandi, A. A., Shahbazi, M., Shariati, M., and Mulo, P. (2014). Effects of Mild and Severe Drought Stress on Photosynthetic Efficiency in Tolerant and Susceptible Barley (*Hordeum vulgare* L.) Genotypes. *J. Agron. Crop Sci.* 26, 403–415. doi: 10.1111/jac.12062

Giannopolitis, C. N., and Ries, S. K. (1977). Superoxide dismutases I. Occurrence in higher plants. *Plant Physiol.* 59, 309–314. doi: 10.1104/pp.59.2.309

Gilmore, A. M., Hazlett, T. L., and Debrunner, P. G. (1996). Comparativetime-resolved photosystem II chlorophyll a fluorescence analyses revealdistinctive differences between photoinhibitory reaction center damage andxanthophyll cycle-dependent energy dissipation. *Photochem. Photobiol.* 64, 552–563. doi: 10.1111/j.1751-1097.1996.tb03105.x

Grassi, G., and Magnani, F. (2005). Stomatal, mesophyll conductance and biochemical limitations to photosynthesis as affected by drought and leaf

ontogeny in ash and oak trees. *Plant Cell Environ.* 28, 834–849. doi: 10.1111/j.1365-3040.2005.01333.x

Guo, P., Qi, Y. P., Cai, Y. T., Yang, T. Y., Yang, L. T., Huang, Z. R., et al. (2018). Aluminum effects on photosynthesis, reactive oxygen species and methylglyoxal detoxification in two *citrus* species differing in aluminum tolerance. *Tree Physiol.* 38, 1548–1565. doi: 10.1093/treephys/tpy035

Ha, N. T. H., Sakakibara, M., Sano, S., and Nhuan, M. T. (2011). Uptake of metals and metalloids by plants growing in a lead–zinc mine area, northern vietnam. *J. Hazard. Mater.* 186, 1384–1391. doi: 10.1016/j.jhazmat.2010.12.020

Hajihashemi, S., and Ehsanpour, A. A. (2013). Influence of exogenously applied paclobutrazol on some physiological traits and growth of Stevia rebaudiana under in vitro drought stress. *Biologia* 68, 414–420. doi: 10.2478/s11756-013-0165-7

Han, Y. L., Huang, S. Z., Yuan, H. Y., Zhao, J. Z., and Gu, J. G. (2013). Organic acids on the growth, anatomical structure, biochemical parameters and heavy metal accumulation of Iris lactea var. chinensis seedling growing in Pb mine tailings. *Ecotoxicology* 22, 1033–1042. doi: 10.1007/s10646-013-1089-2

Han, Y. L., Zhang, L. L., Yang, Y. H., Yuan, H. Y., Zhao, J. Z., Gu, J. G., et al. (2016). Pb uptake and toxicity to Iris halophila tested on Pb mine tailing materials. *Environ. Pollut.* 214, 510–516. doi: 10.1016/j.envpol.2016.04.048

Harley, P. C., Loreto, F., Dimarco, G., and Sharkey, T. D. (1992). Theoretical considerations when estimating the mesophyll conductance to CO_2 flux by analysis of the response of photosynthesis to CO_2. *Plant Physiol.* 98, 1429–1436. doi: 10.1104/pp.98.4.1429

Hu, Z. R., Fan, J. B., Chen, K., Amombo, E., Chen, L., and Fu, J. M. (2015). Effects of ethylene on photosystem II and antioxidant enzyme activity in Bermuda grass under low temperature. *Photosynth. Res.* 128, 59–72. doi: 10.1007/s11120-015-0199-5

Hu, W., Snider, J. L., Chastain, D. R., Slaton, W., and Tishchenko, V. (2018). Sub-optimal emergence temperature alters thermotolerance of thylakoid component processes in cotton seedlings. *Environ. Exp. Bot.* 155, 360–367. doi: 10.1016/j.envexpbot.2018.07.020

Huang, X. H., Zhu, F., Yan, W. D., Chen, X. Y., Wang, G. J., and Wang, R. J. (2019). Effects of Pb and Zn toxicity on chlorophyll fluorescence and biomass production of *Koelreuteria paniculata* and *Zelkova schneideriana* young plants. *Photosynthetica* 52, 688–697. doi: 10.32615/ps.2019.050

Imsande, J., and Touraine, B. (1994). Demand and the regulation of nitrate uptake. *Plant Physiol.* 105, 3–7. doi: 10.1104/pp.105.1.3

Iqbal, N., Hussain, S., Raza, M. A., Yang, C. Q., Safdar, M. E., Brestic, M., et al. (2019). Drought tolerance of soybean (*Glycine max L. Merr.*) by improved photosynthetic characteristics and an efficient antioxidant enzyme activities under a split-root system. *Front. Physiol.* 10, 786. doi: 10.3389/fphys.2019.00786

Israr, M., Jewell, A., Kumar, D., and Sahi, S. V. (2011). Interactive effects of lead, copper, nickel and zinc on growth, metal uptake and antioxidative metabolism of Sesbania drummondii. *J. Hazard. Mater.* 186, 1520–1526. doi: 10.1016/j.jhazmat.2010.12.021

Jedmowski, C., and Brüggemann, W. (2015). Imaging of fast chlorophyll fluorescence induction curve (OJIP) parameters, applied in a screening study with wild barley (*Hordeum spontaneum*) genotypes under heat stress. *J. Photoch. Photobio. B.* 151, 153–160. doi: 10.1016/j.jphotobiol.2015.07.020

Ji, X., Cheng, J., Gong, D. H., Zhao, X. J., Qi, Y., Su, Y. N., et al. (2018). The effect of NaCl stress on photosynthetic efficiency and lipid production in freshwater microalg—*scenedesmus obliquus*, xj002. *Sci. Total Environ.* 633, 593–599. doi: 10.1016/j.scitotenv.2018.03.240

Jiang, H., Chen, L., Zheng, J. G., Han, S., Tang, N., and Smith, B. R. (2008). Aluminum-induced effects on photosystem II photochemistry in citrus leaves assessed by the chlorophyll a fluorescence transient. *Tree Physiol.* 28, 1863–1871. doi: 10.1093/treephys/28.12.1863

Kola, H., and Wilkinson, K. J. (2005). Cadmium uptake by a green alga can be predicted by equilibrium modelling. *Environ. Sci. Technol.* 9, 3040–3047. doi: 10.1021/es048655d

Kosobrukhov, A., Knyazeva, I., and Mudrik, V. (2004). Plantago major plants responses to increase content of lead in soil: growth and photosynthesis. *Plant Growth Regul.* 2, 145–151. doi: 10.1023/b:grow.0000017490.59607.6b

Krantev, A., Yordanova, R., Janda, T., Szalai, G., and Popova, L. (2008). Treatment with salicylic acid decreases the effect of cadmium on photosynthesis in maize plants. *J. Plant Physiol.* 9, 920–931. doi: 10.1016/j.jplph.2006.11.014

Laisk, A., and Loreto, F. (1996). Determining photosynthetic parameters from leaf CO_2 exchange and chlorophyll fluorescence–Ribulose-1,5-bisphosphate carboxylase oxygenase specificity factor, dark respiration in the light, excitation distribution between photosystems, alternative electron transport and mesophyll diffusion resistance. *Plant Physiol.* 110, 903–912. doi: 10.1104/pp.110.3.903

Li, X. M., and Zhang, L. H. (2015). Endophytic infection alleviates Pb^{2+} stress effects on photosystem II functioning of *Oryza sativa* leaves. *J. Hazard. Mater* 295, 79–85. doi: 10.1016/j.jhazmat.2015.04.015

Li, M. S. (2006). Ecological restoration of mineland with particular reference to the metalliferous mine wasteland in China: a review of research and practice. *Sci. Total Environ.* 357, 38–53. doi: 10.1016/j.scitotenv.2005.05.003

Liang, H. Z., Zhu, F., Wang, R. J., Huang, X. H., and Chu, J. J. (2019). Photosystem II of Ligustrum lucidumin response to different levels of manganese exposure. *Sci. Rep.* 9, 12568–12578. doi: 10.1038/s41598-019-48735-8

Lin, M. Z., and Jin, M. F. (2018). Soil Cu contamination destroys the photosynthetic systems and hampers the growth of green vegetables. *Photosynthetica* 56, 1336–1345. doi: 10.1007/s11099-018-0831-7

Liu, H., Zhang, C., Wang, J., Zhou, C., Feng, H., Mahajan, M. D., et al. (2017). Influence and interaction of iron and cadmium on photosynthesis and antioxidative enzymes in two rice cultivars. *Chemosphere* 171, 240–247. doi: 10.1016/j.chemosphere.2016.12.081

Lu, Y., Li, X. R., He, M. Z., Zhao, X., Liu, Y. B., Cui, Y., et al. (2010). Seedlings growth and antioxidative enzymes activities in leaves under heavy metal stress differ between two desert plants: a perennial (Peganum harmala) and an annual (*Halogeton glomeratus*) grass. *Acta Physiol. Plant* 3, 583–590. doi: 10.1007/s11738-009-0436-7

Lu, T., Meng, Z., Zhang, G., Qi, M., Sun, Z., Liu, Y., et al. (2017). Sub-high Temperature and High Light Intensity Induced Irreversible Inhibition on Photosynthesis System of Tomato Plant (*Solanum lycopersicum* L.). *Front. Plant Sci.* 8, 365. doi: 10.3389/fpls.2017.00365

Luo, Z. H., Tian, D. L., Ning, C., Yan, W. D., Xiang, W. H., and Peng, C. H. (2015). Roles of *Koelreuteria bipinnata* as a suitable accumulator tree species in remediating Mn, Zn, Pb, and Cd pollution on Mn mining wastelands in southern China. *Environ. Earth Sci.* 74, 4549–4559. doi: 10.1007/s12665-015-4510-8

Ma, L. Q., Komar, K. M., Tu, C., Zhang, W., Cai, Y., and Kennelley, E. D. (2001). A fern that hyperaccumulates arsenic: a hardy, versatile, fast growing plant helps to remove arsenic from contaminated soils. *Nature* 6820, 579. doi: 10.1038/35054664

Mallick, N., and Mohn, F. H. (2003). Use of chlorophyll fluorescence in metalstress research: a case study with the green microalga Scenedesmus. *Ecotoxicol. Environ. Saf.* 55, 64–69. doi: 10.1016/s0147-6513(02)00122-7

Meeinkuirt, W., Pokethitiyook, P., Kruatrachue, M., Tanhan, P., and Chaiyarat, R. (2012). Phytostabilization of a pb-contaminated mine tailing by various tree species in pot and field trial experiments. *Int. J. Phytoremediat.* 14, 925–938. doi: 10.1080/15226514.2011.636403

Mlinarić, S., Antunović Duni, J., Skendrović Babojelić, M., Cesar, V., and Lepeduš, H. (2017). Differential accumulation of photosynthetic proteins regulates diurnal photochemical adjustments of PSII in common fig (*Ficus carica* L.) leaves. *J. Plant Physiol.* 209, 1–10. doi: 10.1016/j.jplph.2016.12.002

Mobin, M., and Khan, N. A. (2007). Photosynthetic activity, pigment composition and antioxidative response of two mustard (*Brassica juncea*) cultivars differing in photosynthetic capacity subjected to cadmium stress. *J. Plant Physiol.* 164, 601–610. doi: 10.1016/j.jplph.2006.03.003

Nie, J., Liu, Y. G., Zeng, G. M., Zheng, B. H., Tan, X. F., Liu, H., et al. (2016). Cadmium accumulation and tolerance of macleaya cordata: a newly potential plant for sustainable phytoremediation in cd-contaminated soil. *Environ. Sci. Pollut. R.* 23, 10189–10199. doi: 10.1007/s11356-016-6263-7

Okuda, T., Matsuda, Y., Yamanaka, A., and Sagisaka, S. (1991). Abrupt increase in the level of hydrogen peroxide in leaves of winter wheat is caused by cold treatment. *Plant Physiol.* 97, 1265–1267. doi: 10.1104/pp.97.3.1265

Oukarroum, A., Schansker, G., and Strasser, R. J. (2009). Drought stress effects on photosystem I content and photosystem II thermotolerance analyzed using Chl a fluorescence kinetics in barley varieties differing in their drought tolerance. *Physiol. Plant* 137, 188–199. doi: 10.1111/j.1399-3054.2009.01273.x

Oukarroum, A., Bussotti, F., Goltsev, V., and Kalaji, H. M. (2015). Correlation between reactive oxygen species production and photochemistry of

photosystems I and II in Lemna gibba l plants under salt stress. *Environ. Exp. Bot.* 109, 80–88. doi: 10.1016/j.envexpbot.2014.08.005

Paunov, M., Koleva, L., Vassilev, A., Vangronsveld, J., and Goltsev, V. (2018). Effects of different metals on photosynthesis: cadmium and zinc affect chlorophyll fluorescence in Durum Wheat. *Int. J. Mol. Sci.* 19, 787–800. doi: 10.3390/ijms19030787

Pierattini, E. C., Francini, A., Raffaelli, A., and Sebastiani, L. (2017). Surfactant and heavy metal interaction in poplar: a focus on SDS and Zn uptake. *Tree Physiol.* 38, 109–118. doi: 10.1093/treephys/tpx155

Pinelli, P., and Loreto, F. (2003). $^{12}CO_2$ emission from different metabolic pathways measured in illuminated and darkened C3 and C4 leaves at low, atmospheric and elevated CO_2 concentration. *J. Exp. Bot.* 54, 1761–1769. doi: 10.1093/jxb/erg187

Pospíšil, P. (2009). Production of reactive oxygen species by photosystem II. *Biochim. Biophys. Acta* 1787, 1151–1160. doi: 10.1016/j.bbabio.2009.05.005

Pulford, I. D., and Watson, C. (2003). Phytoremediation of heavy metal-contaminated land by trees—a review. *Environ. Int.* 29, 529–540. doi: 10.1016/s0160-4120(02)00152-6

Rana, S. (2015). Plant response towards cadmium toxicity: an overview. *Ann. Plant Sci.* 7, 1162–1172.

Sagardoy, R., Vázquez, S., Florez-Sarasa, I. D., Albacete, A., Ribas-Carbó, M., Flexas, J., et al. (2010). Stomatal and mesophyll conductances to CO_2 are the main limitations to photosynthesis in sugar beet (beta vulgaris) plants grown with excess zinc. *New Phytol.* 187, 145–158. doi: 10.1111/j.1469-8137.2010.03241.x

Seregin, I. V., and Kozhevnikova, A. D. (2006). Physiological role of nickel and its toxic effects on higher plants. *Russ. J. Plant Physiol.* 53, 257–277. doi: 10.1134/s1021443706020178

Setlik, I., Allakhveridiev, S.II, Nedbal, L., Setlikova, E., and Klimov, V. V. (1990). Three types of Photosystem II photoinactivation-I. Damaging process on the acceptor side. *Photosynth. Res.* 23, 39–48. doi: 10.1007/BF00030061

Sharkey, T. D., Bernacchi, C. J., Farquha, G. D., and Singsaas, E. L. (2007). Fitting photosynthetic carbon dioxide response curves for C3 leaves. *Plant Cell Environ.* 30, 1035–1040. doi: 10.1111/j.1365-3040.2007.01710.x

Sharma, S. S., and Dietz, K. J. (2009). The relationship between metal toxicity and cellular redox imbalance. *Trends Plant Sci.* 1, 0–50. doi: 10.1016/j.tplants.2008.10.007

Sharma, P., and Dubey, R. S. (2005). Lead toxicity in plants. *Toxic Met. Plants* 17, 35–52. doi: 10.1515/9783110434330-015

Sigfridsson, K. G., Bernat, G., Mamedov, F., and Styring, S. (2004). Molecular interference of Cd^{2+} with photosystem II. *BBA-Biomembranes* 1659, 19–31. doi: 10.1016/j.bbabio.2004.07.003

Sorrentino, M. C., Capozzi, F., Amitrano, C., Giordano, S., Arena, C., and Spagnuolo, V. (2018). Performance of three cardoon cultivars in an industrial heavy metal-contaminated soil: Effects on morphology, cytology and photosynthesis. *J. Hazard. Mater* 351, 131–137. doi: 10.1016/j.jhazmat.2018.02.044

Srivastava, M., and Doran, P. M. (2005). Antioxidant responses of hyperaccumulator and sensitive fern species to arsenic. *J. Exp. Bot.* 56, 1335–1342. doi: 10.1093/jxb/eri134

Štefanić, P. P., Cvjetko, P., Biba, R., Domijan, A. M., Letofsky-Papst, I., Tkalec, M., et al. (2018). Physiological, ultrastructural and proteomic responses of tobacco seedlings exposed to silver nanoparticles and silver nitrate. *Chemosphere* 209, 640–653. doi: 10.1016/j.chemosphere.2018.06.128

Strasser, R. J., Tsimilli-Michael, M., and Srivastava, A. (2004). "Analysis of the chlorophyll a fluorescence transient," in *Chlorophyll fluorescence: a signature of photosynthesis*. Eds. G. C. Papageorgiou and Govindjee, (Netherlands: Kluwer Academic Publishers Press), 321–362. doi: 10.1007/978-1-4020-3218-9_12

Su, M. J., Cai, S. Z., Deng, H. M., Long, C. Y., Ye, C., Song, H. X., et al. (2017). Effects of cadmium and acid rain on cell membrane permeability and osmotic adjustment substance content of *Melia azedarach* L. seedlings. *Acta Sci. Circumstantiae* 37, 4436–4443. doi: 10.13671/j.hjkxxb.2017.0216. (in chinese).

Tang, C. F., Chen, Y. H., Zhang, Q. N., Li, J. B., Zhang, F. Y., and Liu, Z. M. (2019). Effects of peat on plant growth and lead and zinc phytostabilization from lead-zinc mine tailing in southern China: Screening plant species resisting and accumulating metals. *Ecotox. Environ. Safe.* 176, 42–49. doi: 10.1016/j.ecoenv.2019.03.078

Teng, Y., Luo, Y., Ma, W. T., Zhu, L. J., Ren, W. J., Luo, Y. M., et al. (2015). *Trichoderma reesei* FS10-C enhances phytoremediation of Cd-contaminated soil by *Sedum plumbizincicola* and associated soil microbial activities. *Front. Plant Sci.* 6, 438. doi: 10.3389/fpls.2015.00438

Trikshiqi, R., and Rexha, M. (2015). Heavy metal monitoring by Ligustrum lucidum, Fam: Oleaceae vascular plant as bio-indicator in Durres city. *Int. J. Curr. Res.* 7, 14415–14422.

Velikova, V., Tsonev, T., Loreto, F., and Centritto, M. (2011). Changes in photosynthesis, mesophyll conductance to CO_2, and isoprenoid emissions in *Populus nigra* plants exposed to excess nickel. *Environ. Pollut.* 159, 1058–1066. doi: 10.1016/j.envpol.2010.10.032

Wali, M., Gunsè, B., Llugany, M., Corrales, I., Abdelly, C., Poschenrieder, C., et al. (2016). High salinity helps the halophyte Sesuvium portulacastrum in defense against Cd toxicity by maintaining redox balance and photosynthesis. *Planta* 2, 1–14. doi: 10.1007/s00425-016-2515-5

Wang, S. Z., Zhang, D. Y., and Pan, X. L. (2013). Effects of cadmium on the activities of photosystems of Chlorella pyrenoidosa and the protective role of cyclic electron flow. *Chemosphere* 2, 230–237. doi: 10.1016/j.chemosphere.2013.04.070

Yu, P. Y., Sun, Y. P., Huang, Z. L., Zhu, F., Sun, Y. J., and Jiang, L. J. (2019). The effects of ectomycorrhizal fungi on heavy metals' transport in pinus massoniana and bacteria community in rhizosphere soil in mine tailing area. *J. Hazard. Mater* 381, 121203–121215. doi: 10.1016/j.jhazmat.2019.121203

Zhang, H. H., Xu, N., Li, X., Long, J. H., Sui, X., Wu, Y. N., et al. (2018). Arbuscular Mycorrhizal Fungi (*Glomus mosseae*) improves growth, photosynthesis and protects photosystem II in leaves of *Lolium perenne* L. @ in cadmium contaminated soil. *Front. Plant Sci.* 9, 1156. doi: 10.3389/fpls.2018.01156

Zhong, X., Li, Y. T., Che, X. K., Zhang, Z. S., Li, Y. M., Liu, B. B., et al. (2018). Significant inhibition of photosynthesis and respiration in leaves of *Cucumis sativus* L. by oxybenzone, an active ingredient in sunscreen. *Chemosphere* 219, 456–462. doi: 10.1016/j.chemosphere.2018.12.019

Zhou, W. B., Juneau, P., and Qiu, B. S. (2006). Growth and photosynthetic responses of the bloom-forming cyanobacterium Microcystis aeruginosa to elevated levels of cadmium. *Chemosphere* 10, 1738–1746. doi: 10.1016/j.chemosphere.2006.04.078

Zhou, R. H., Kan, X., Chen, J. J., Hua, H. L., Li, Y., Ren, J. J., et al. (2019). Drought-induced changes in photosynthetic electron transport in maize probed by prompt fluorescence, delayed fluorescence, P700 and cyclic electron flow signals. *Environ. Exp. Bot.* 158, 51–62. doi: 10.1016/j.envexpbot.2018.11.005

Zhuang, P., Hu, H. P., Li, Z. A., Zou, B., and McBride, M. B. (2014). Multiple exposure and effects assessment of heavy metals in the population near mining area in south China. *PloS One* 9, 1–11. doi: 10.1371/journal.pone.0094484

Zivcak, M., Brestic, M., Balatova, Z., Drevenakova, P., Olsovska, K., and Kalaji, H. M. (2013). Photosynthetic electron transport and specific photoprotective responses in wheat leaves under drought stress. *Photosynth. Res.* 1–3, 529–546. doi: 10.1007/s11120-013-9885-3

Conflict of Interest: The authors declare that the research was conducted in the absence of any commercial or financial relationships that could be construed as a potential conflict of interest.

frontiers in Plant Science

ORIGINAL RESEARCH
published: 23 October 2020
doi: 10.3389/fpls.2020.547133

Indigenous Tocopherol Improves Tolerance of Oilseed Rape to Cadmium Stress

Essa Ali[1], Zeshan Hassan[2], Muhammad Irfan[3], Shabir Hussain[3], Haseeb-ur-Rehman[3], Jawad Munawar Shah[2], Ahmad Naeem Shahzad[3], Murtaza Ali[4], Saad Alkahtani[5], Mohamed M. Abdel-Daim[5,6], Syed Asad Hussain Bukhari[3] and Shafaqat Ali[7,8]**

[1] Department of Food Science and Technology, Zhejiang University of Technology, Hangzhou, China, [2] College of Agriculture, Bahauddin Zakariya University, Layyah, Pakistan, [3] Department of Agronomy, Bahauddin Zakariya University, Multan, Pakistan, [4] Department of Basic Sciences and Humanities, University of Engineering and Technology, Mardan, Pakistan, [5] Department of Zoology, College of Science, King Saud University, Riyadh, Saudi Arabia, [6] Department of Pharmacology and Toxicology, Faculty of Veterinary Medicine, Suez Canal University, Ismailia, Egypt, [7] Department of Environmental Sciences and Engineering, Government College University, Faisalabad, Pakistan, [8] Department of Biological Science and Technology, China Medical University, Taichung, Taiwan

OPEN ACCESS

Edited by:
Mukesh Kumar Kanwar, Zhejiang University, China

Reviewed by:
Matthew John Milner, National Institute of Agricultural Botany (NIAB), United Kingdom
Harminder Pal Singh, Panjab University, India

***Correspondence:**
Syed Asad Hussain Bukhari
bukhariasad@yahoo.com
Shafaqat Ali
shafaqataligill@yahoo.com

Specialty section:
This article was submitted to Plant Nutrition, a section of the journal Frontiers in Plant Science

Received: *30 March 2020*
Accepted: *17 September 2020*
Published: *23 October 2020*

Citation:
Ali E, Hassan Z, Irfan M, Hussain S, Rehman H-u, Shah JM, Shahzad AN, Ali M, Alkahtani S, Abdel-Daim MM, Bukhari SAH and Ali S (2020) Indigenous Tocopherol Improves Tolerance of Oilseed Rape to Cadmium Stress. Front. Plant Sci. 11:547133. doi: 10.3389/fpls.2020.547133

Two oilseed rape genotypes (Jiu-Er-13XI and Zheyou-50), differing in seed oil content, were subjected to cadmium (Cd) stress in hydroponic experiment. Genotypic differences were observed in terms of tolerance to Cd exposure. Cd treatment negatively affected both genotypes, but the effects were more devastating in Jiu-Er-13XI (low seed oil content) than in Zheyou-50 (high seed oil content). Jiu-Er-13XI accumulated more reactive oxygen species (ROS), which destroyed chloroplast structure and decreased photosynthetic pigments, than Zheyou-50. Total fatty acids, especially 18:2 and 18:3, severely decreased as suggested by increase in MDA content. Roots and shoots of Jiu-Er-13XI plants accumulated more Cd content, while less amount of tocopherol (Toc) was observed under Cd stress, than Zheyou-50. Conversely, Zheyou-50 was less affected by Cd stress than its counterpart. It accumulated comparatively less amount of Cd in roots and shoots, along with reduced accumulation of malondialdehyde (MDA) and ROS under Cd stress, than Jiu-Er-13XI. Further, the level of Toc, especially α-Tocopherol, was much higher in Zheyou-50 than in Jiu-Er-13XI, which was also supported by high expression of Toc biosynthesis genes in Zheyou-50 during early hours. Toc not only restricted the absorption of Cd by roots and its translocation to shoot but also scavenged the ROS generated during oxidative stresses. The low level of MDA shows that polyunsaturated fatty acids in chloroplast membranes remained intact. In the present study the tolerance of Zheyou-50 to Cd stress, over Jiu-Er-13XI, is attributed to the activities of Toc. This study shows that plants with high seed oil content are tolerant to Cd stress due to high production of Toc.

Keywords: cadmium stress, oilseed rape, pigments, ultrastructure, tocopherols

INTRODUCTION

Heavy metals are major environmental pollutants due to their detrimental effects on life. Severe concerns, related to ecology, evolution, nutrition, and environment, are associated with heavy metals (Hawkes, 1997). Due to exorbitantly increasing industrialization and urbanization, heavy metals are constantly penetrating the environment as industrial effluents and household wastes, posing a potential threat to the ecosystem. Heavy metals enter the food chain through plants grown on polluted soil or irrigated with contaminated water (Bukhari et al., 2016). Cadmium (Cd) is one of such hazardous metals piercing the environment by anthropogenic, as well as natural means (Lima et al., 2006). Cadmium becomes a part of the soil–plant environment as plants absorb water and nutrients from the soil. Cadmium can affect plants in many ways, especially by damaging their photosynthetic apparatus (Ali et al., 2015), reducing gas exchange ability (Jia et al., 2011), causing nutrient imbalance (Feng et al., 2013), subcellular changes like chloroplast, mitochondrial, and nuclear membrane disintegration (Liu et al., 1995; Wang et al., 2011; Ali et al., 2018), and destroying antioxidant defense systems (Ahmad et al., 2011). Moreover, exposure of plants to Cd stress inhibits cell growth (Di Toppi and Gabbrielli, 1999) and alters root morphology (Jia et al., 2011). In short, contamination of soil and water bodies with Cd and its subsequent absorption by plants are serious concerns threatening the agricultural production and human health globally (Wu et al., 2005). Cd-induced damage to plants is an outcome of overgeneration of reactive oxygen species (ROS). Cadmium cannot directly generate free radicals via Fenton and/or Haber Weiss reactions in biological systems. However, the accumulation of ROS in Cd-treated plants has been reported in literature (Pathak and Khandelwal, 2006; Zhou et al., 2009). Actually, Cd produces ROS indirectly by increasing the concentration of free Fe by replacing it in different proteins, compromising the integrity of the membranes by lipid peroxidation, which can be demonstrated by the increase in malondialdehyde (MDA) content (Scholz et al., 1990; Dorta et al., 2003). Plants combat Cd stress by virtue of certain enzymatic and non-enzymatic systems. In plants, tocopherols are considered as an important component of non-enzymatic protection against stresses.

Oilseed rape (*Brassica napus* L.), an important crop of temperate regions, provides edible oil, animal feed, and biodiesel. Its dry seed contains about 40–50% oil content (Hüsken et al., 2005). Besides, oilseed rape contains lipid soluble tocopherols, also called vitamin E, which is a well-known antioxidant against reactive oxygen species (ROS), and an essential nutrient for human beings and animals. Tocopherols, the constituents of compounds having vitamin E, are synthesized by photosynthetic organisms only (Mène-Saffrané and DellaPenna, 2010). Tocopherols are lipid-soluble molecules with four structural derivatives [alpha (α), beta (β), gamma (γ), and delta (δ)] having diverse biological functions. Tocopherols serve as antioxidants by annihilating singlet oxygen and neutralizing the harmful radicals to inhibit lipid peroxidation of membranes (Sattler et al., 2004a; Krieger-Liszkay, 2005). *In vitro*, each molecule of α-, β-, γ-, and δ-tocopherol can protect up to 220, 120, 100, and 30 molecules of polyunsaturated fatty acids (PUFAs), respectively (Fukuzawa et al., 1982). Plant tissues vary massively in their tocopherol content and composition (Grusak et al., 1999). Photosynthetic tissues contain 10 to 50 mg tocopherol/g fresh weight (FW), with α- tocopherol the dominant one, while seeds vary from 300 to 2,000 mg tocopherol/g oil, where γ-tocopherol is a main constituent (Grusak, 1999). This variation in tocopherol content and composition is attributed to a variety of environmental and genetic factors. Photosynthetic tissues, especially leaves, are highly responsive to environmental variations. However, tolerant plants generally exhibit enhanced tocopherol levels, while susceptible ones display net reduction in tocopherol content under stress. Alpha tocopherol shows a remarkable increase under water deficit conditions (Garcia-Plazaola and Becerril, 2000; Munne-Bosch and Alegre, 2001). Further, tocopherol content of plants increase in response to various abiotic stresses like salinity, light, cold, and heavy metals, which may offer a supplementary line of defense against oxidative deterioration (Havaux et al., 2000; Munne-Bosch and Alegre, 2002b; Tang et al., 2016; Gramegna et al., 2019; Nowicka et al., 2020). Based on increasing tocopherol content in response to abiotic stresses (Kim et al., 2019), it is believed that protection of PUFAs from oxidative damage is the main function of tocopherols (Havaux et al., 2000; Collakova and DellaPenna, 2003; Abbasi et al., 2007; Collin et al., 2008). The current study was designed to probe the response of two *Brassica napus* genotypes, differing in oil content, to Cd stress in terms of fatty acids and tocopherol levels.

MATERIALS AND METHODS

Plant Materials and Treatments

A hydroponic trial was carried out under natural light conditions in a net house of the Zijingang campus, Zhejiang University, Hangzhou, China. Two rapeseed genotypes, Zheyou-50 (high seed oil content) and Jiu-Er-13XI (low seed oil content), were used in the experiment (Du et al., 2015). The seeds were sown in trays containing 50% compost, 25% vermiculite, and 25% sand in the growth chamber. After 1 month, seedlings were transferred to the wire house to adapt to the outside environment. Morphologically similar and healthy seedlings were shifted to 5-L buckets having 4.5 L of nutrient solution (mg L^{-1}): $(NH_4)_2SO_4$, 48.2; $MgSO_4$, 65.9; K_2SO_4, 15.9; KNO_3, 18.5; $Ca(NO_3)_2$, 59.9; KH_2PO_4, 24.8; Fe-citrate, 7; $MnCl_2$–$4H_2O$, 0.9; $ZnSO_4$–$7H_2O$, 0.11; $CuSO_4$–$5H_2O$, 0.04; HBO_3, 2.9; H_2MoO_4, 0.01. The pH of the nutrient solution was maintained at 5.8 ± 0.1 using HCl or NaOH. The containers were covered with plates having eight evenly spaced holes (one seedling per hole) and placed in a net house. One week after transplantation, Cd (as $CdCl_2.2.5H_2O$) was added to the corresponding containers to form two treatments: basal nutrient solution (control), and 100 μM Cd (Cd). The containers were continuously aerated using pumps, and the nutrient solution was renewed after every 5 days. The experimental treatments were adjusted in randomized complete block design (RCBD) with

three replications. Samples for gene expression and quantification of ROS were collected at 12, 24, and 48 h after treatment (HAT). For other parameters, samples were harvested at 3, 6, and 9 days after treatment (DAT) and stored at −80°C for subsequent analysis.

Quantifying Leaf Photosynthetic Pigments

Photosynthetic pigment contents (Chl a, Chl b, and carotenoids) were determined according to the method described by Wang et al. (2009). Briefly, 10 fresh leaf disks (diameter, 1 cm) were placed in a glass tube containing a mixture of ethanol, acetone, and distilled water (4.5:4.5:1) and stored at 4°C for 48 h in the dark. The absorbance of the extract was noted at 645 and 663 nm on a spectrophotometer.

Formula for chlorophyll determination (mg/g FW):

$$\text{Chl. (a)} = 12.71 \times \text{OD663} - 2.59 \times \text{OD645}/100$$
$$\text{Chl. (b)} = 22.88 \times \text{OD645} - 4.67 \times \text{OD663}/100$$
$$\text{Total chlorophyll} = \text{Chl. (a)} + \text{Chl. (b)}$$

Determination of MDA Content

Leaf tissues (0.5 g) were crushed and blended with 8 ml of 50 mM phosphate buffer (PBS, pH 7.8) solution under ice-cold conditions. Homogenate was subjected to centrifugation at 12,000 rpm and 4°C for 15 min. The supernatant was collected to determine malondialdehyde (MDA) content as described by Hodges et al. (1999). The mixture of reaction solution (5% TCA solution with 2.5 g TBA) and sample extract was heated at 95°C for 15 min in a water bath, followed by immediate cooling on ice. After centrifugation at 4,800 rpm for 10 min, the supernatant was run on a spectrophotometer to record the absorbance at 532 nm ($E532 = 1.55 \times 10^{-1}$ mM cm^{-1}). Non-specific turbidity was corrected by subtracting the value of absorbance taken at 600 nm.

Determination of Cd Accumulation

About 0.1 g of oven-dried (at 65–70°C for 72 h) tissues of shoot and root were crushed for the determination of Cd concentration. Mineralization was performed by heating 5 ml of 65% HNO_3 using a microwave digester (Microwave 3000; AntoonPaar). The volume of the digested samples was raised to 10 ml by adding Milli-Q water. Specimens were run on inductively coupled plasma-optical emission spectrometer (ICP-OES; Optima 8000DV; PerkinElmer) to quantify the Cd content.

Leaf Tissue Reactive Oxygen Species Staining and Quantification

Leaves harvested at 12, 24, and 48 h after treatment were processed for ROS quantification. H_2O_2 and O_2^- contents were quantified using the method suggested by Jiang and Zhang (2001) and Gong et al. (2008), respectively.

Determination of Tocopherol Content

Tocopherols were extracted and analyzed by the method suggested by Li et al. (2013) with minor changes. About 100 mg of fresh leaf discs were placed in a 2-ml skirted screw-cap microtube having 1.3 ml of n-hexane. Samples were macerated using bead mill homogenizer (Bead Ruptor-24, Omni, Kennesaw, GA, United States) at 8 m s^{-1} for 30 s and incubated for 15 h under dark conditions. The supernatant (20 μl) was subjected to normal-phase high-performance liquid chromatography machine (model 600, Waters, Milford, MA, United States) fitted with a Zorbax Rx-SIL column (4.6 mm × 250 mm × 5 μm; Agilent, Englewood, CO, United States) and a fluorescence detector (λex = 295 nm; λem = 330 nm). The mobile phase of hexane/tert-butyl methyl ether (95:5, v/v) was transported at a constant rate of 1 ml min^{-1}. Isoforms of tocopherol were quantified using the curves derived from pure standards of tocopherol. The peaks of the tocopherol standards (α-, β, γ-, and δ- tocopherol) were distinguished by their retention times. To determine tocopherol contents of experimental samples, standard curve was calibrated in accordance with the corresponding peaks of individual tocopherol derivatives. Tocopherol contents were expressed in mg per g of sample, and the total amount of tocopherol was calculated as the sum of α- and γ-tocopherol.

Determination of Fatty Acid Composition and Content

Fatty acids (FAs) were analyzed according to the protocol described by Chen et al. (2012) with slight modifications. Approximately 200 mg of leaf samples were ground in a 12-mL screw-top glass tube having 5 ml of extraction solution (chloroform/isopropanol, 2:1, v/v), followed by incubation at 80°C for 2 h. Upon cooling down the samples to room temperature, 1 ml of n-hexane and 2 ml of NaCl solution (0.9%) were added to the tubes. The specimens were centrifuged at 2,300 rpm for 5 min. The supernatant (1 ml) was used to analyze the FA components on GC-FID. The samples (2 μl) were auto-injected into the gas chromatograph (GC, 6890N, Agilent, United States) system, having a fused silica capillary column Rtx-Wax (30 m × 0.25 mm × 0.50 μm, Restek, United States) and FID detector. Initially, the column temperature was set to 160°C for 1 min, following a gradual increase to 240°C at the rate of 4°C/min, and maintained for 16 min.

Quantitative Real-Time PCR Analyses

About 100 mg of leaf tissues were crushed, and total RNA was extracted using Miniprep kit, following the manufacturer's instructions. RNeasy Mini Kit (Qiagen, Hilden, Germany) was used to remove genomic DNA. ReverTra AceqPCR RT kit (Toyobo, Japan) was utilized to synthesize cDNA. Based on mRNA or expressed sequence tag (EST), gene-specific primers were designed for qRT-PCR. SYBR Green PCR Master Mix (Applied Biosystems) was used to amplify the PCR products, in triplicate, in 25 μl qRT-PCRs in an iCycleriQ^{TM} 96-well real-time PCR detection system (Bio-Rad, Hercules, CA, United States). PCR conditions were as follows: denaturation at 95°C for 3 min; 40 cycles of denaturation at 95°C for 30 s; annealing at 58°C for 30 s; extension at 72°C for 30 s. Threshold cycle values were calculated by employing the software provided with the

PCR machine and mRNA levels were quantified by following the method described by Livak and Schmittgen (2001).

Subcellular Analysis by Transmission Electron Microscopy (TEM)

Fresh leaf sections (~1 mm^2) were excised at 9 days after treatment (DAT) from the topmost fully expanded leaves of plants and processed for TEM studies. Samples were fixed in 2.5% glutaraldehyde (v/v) overnight and washed three times with 0.1 M SPB (sodium phosphate buffer, pH 7.0). The specimens were post-fixed in 1% osmium tetroxide (OsO_4) for 1 h and washed with 0.2 M SPB (pH 7.2) for 1–2 h. Dehydration was carried out in a graded series of ethanol (50, 60, 70, 80, 90, 95, and 100%) and acetone (100%). The samples were then infiltrated and embedded in Spurr's resin. Ultrathin sections (80 nm) were prepared and mounted on copper grids and viewed under transmission electron microscope (JEOL TEM-1230EX) at an accelerating voltage of 60.0 kV.

Statistical Analysis

Data were statistically analyzed using MSTAT-C software version 2.10 and expressed as means ± standard error (SE). Data were subjected to one-way ANOVA, and LSD test was used to compare the treatments at $P \leq 0.01$ or $P \leq 0.05$ (Steel and Torrie, 1980). Figures were prepared using OriginPro v7.5 (OriginLab, Northampton, MA, United States) software.

RESULTS

Photosynthetic Pigment Composition

Chlorophyll is the main component of green plants. The amount and composition of chlorophyll differ from genotype to genotype and also depend on environmental conditions. In the present study, total chlorophyll content of Zheyou-50 was 52.3 mg g^{-1} FW, which was considerably higher than that of Jiu-Er-13XI (38.1 mg g^{-1} FW). Chl a and Chl b contents also varied between two genotypes. Zheyou-50 and Jiu-Er-13XI contained 32.1 and 23.5 mg g^{-1} FW chl a, and 21.1 and 14.6 mg g^{-1} FW chl b, respectively (**Table 1**). Cd treatment adversely affected pigment contents in both genotypes. Chl a, chl b, and total chl decreased by 32.35, 21.27, and 30% respectively, with respect to control treatment. The detrimental effect of Cd became prominent with increasing treatment time duration. Total chlorophyll content reduced by 10 and 20% at 6 DAT and 9 DAT, respectively, compared to 3 DAT (**Table 1**). All sole factors were significantly different for photosynthetic pigment composition and content.

Interactive effect showed a conspicuous decline in chlorophyll content in both genotypes subjected to Cd stress. However, the decrease was more pronounced in Jiu-Er-13XI than in Zheyou-50. Jiu-Er-13XI showed 47.9, 34.10, and 43% reduction in chl a, chl b, and total chlorophyll, respectively, compared to control treatment (**Figure 1**). However, both genotypes showed a non-significant decrease in pigment content with increase in treatment timing (**Supplementary Table S2**).

TABLE 1 | Sole effect of genotype, treatment, and timings on photosynthetic pigments in rapeseed.

	Chl a [mg/g fresh weight (FW)]	Chl b (mg/g FW)	Chla + b (mg/g FW)
Genotypes			
Jiu-Er-13XI	23.5 ± 2.07 b	14.6 ± 0.99 b	38.1 ± 2.95 b
Zheyou-50	32.1 ± 1.15 a	21.1 ± 0.88 a	52.3 ± 2.03 a
Significance	**	**	**
Treatments			
Ck	33.2 ± 1.08 a	20.0 ± 0.85 a	53.2 ± 1.79 a
Cd	22.4 ± 1.79 b (−32.35%)	15.7 ± 1.32 b (−21.27%)	37.2 ± 2.83 b (−30%)
Significance	**	**	**
Timings			
3DAT	31.1 ± 2.10 a	19.3 ± 1.31	50.4 ± 3.19 a
6DAT	27.1 ± 2.54 b (−12%)	17.9 ± 1.47 (−7.33%)	45.0 ± 3.72 ab (−10.7%)
9DAT	25.2 ± 2.35 b (−18%)	16.4 ± 1.66 (−14.84%)	40.1 ± 3.83 b (−20.36%)
Significance	**	ns	**

*DAT, days after treatment; ns, non-significant. **Significant at $P \leq 0.01$; numbers in parenthesis show percent increase (+) or decrease (−).*

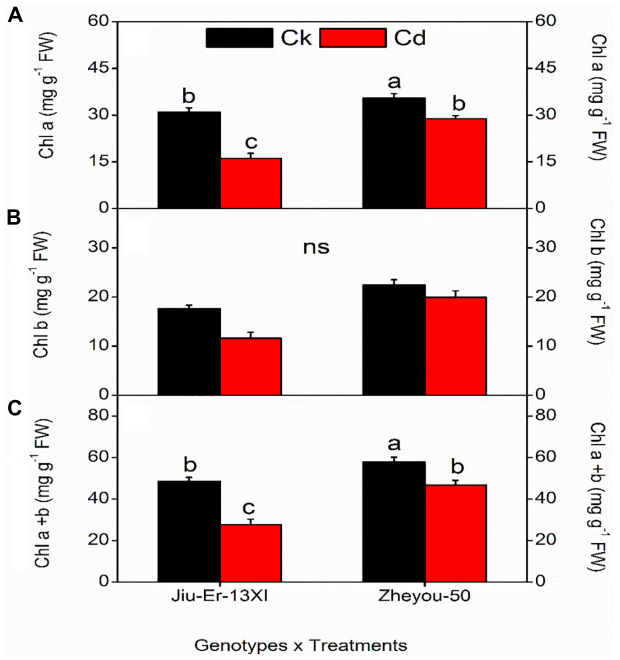

FIGURE 1 | Interactive effect of genotype and treatment on photosynthetic pigments in rapeseed. Lettering indicates statistical difference ($p \leq 0.01$) among the treatments for each parameter. Data represent the mean ± SE of three measurements. Ck, Cd, and ns represent control, 100 μM Cd, and non-significant, respectively.

Cadmium Accumulation and MDA Content

Malondialdehyde is the oxidative product of membrane lipids and its accumulation in plant tissues is an indicator of lipid

peroxidation during environmental stresses. In the present study, Cd-treated plants accumulated up to 53% higher MDA content than the Cd-untreated ones, showing the deleterious effects of Cd on membrane lipids. Nonetheless, Zheyou-50 exhibited tolerance to Cd by accumulating less amount of MDA (18.72 nM g^{-1} FW) than Jiu-Er-13XI (22.27 nM g^{-1} FW). Maximum increase (63.15%) in MDA content was seen at 9 DAT, compared with 3 DAT, suggesting a rise in oxidative stress on membrane lipids with increasing time duration (**Table 2**). Interactive effects for MDA accumulation are presented in **Supplementary Table S3** and **Figure 2**. Cd treatment deleteriously affected Jiu-Er-13XI and showed 72% higher MDA content than the control treatment. Conversely, Zheyou-50 depicted only 32% increase in MDA content under cd treatment compared to control. Moreover, 43.49, 58.63, and 46.93% increase was recorded for MDA accumulation at 3, 6, and 9 DAT, respectively, under Cd treatment. Roots are in direct contact with metals whether in the soil or in a hydroponic system. In the present study, root and shoot accumulated 15.7 and 0.17 mg Cd/g DW, respectively, under Cd treatment. Cd accumulation significantly increased with treatment timings as 9.9 mg/g DW (root) and 0.11 mg/g DW (shoot) Cd content was recorded at 9 DAT, which was considerably higher than that observed after 3 days of treatment (**Table 2**). Under Cd treatment, Jiu-Er-13XI plants accumulated Cd at the rate of 0.019 and 17.30 mg/g DW in shoot and root, respectively. However, Zheyou-50 showed only 0.017 and 14 mg/g DW Cd in shoot and root, under Cd treatment, respectively (**Figure 2**). Jiu-Er-13XI exhibited 89.80%, while Zheyou-50 showed only 48% rise in Cd accumulation at 9 DAT compared to 3 DAT.

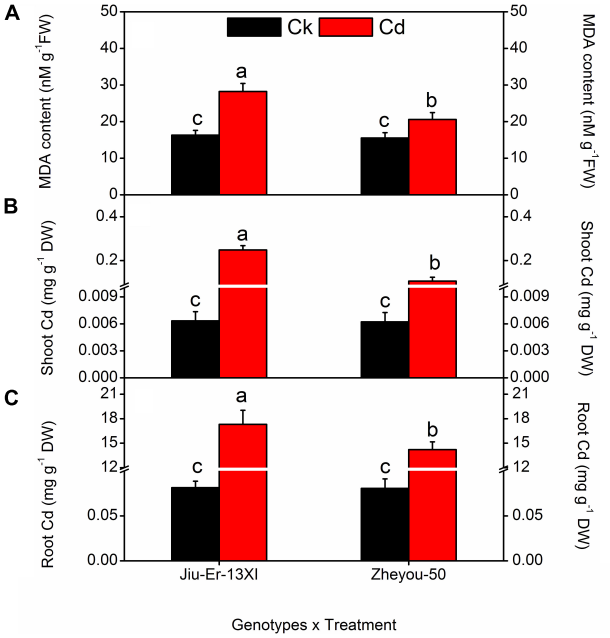

FIGURE 2 | Interactive effects of genotypes and treatments on root, shoot, Cd accumulation, and leaf malondialdehyde (MDA) content in rapeseed. Lettering indicates statistical difference ($p \leq 0.01$) among the treatments for each parameter. Data represent the mean ± SE of three measurements. Ck and Cd represent control and 100 μM Cd, respectively.

Accumulation of Reactive Oxygen Species

Reactive oxygen species (ROS), produced during oxidative stress, are harmful to plants. ROS, especially hydrogen peroxide (H_2O_2) and superoxide radicals ($O_2^{\bullet}$), generated during stresses directly attack membrane lipids and compromise the integrity of the membrane system. In the current study, H_2O_2 and $O_2^{\bullet}$ contents increased by 36.30 and 18.68%, respectively, under Cd stress compared to the control treatment. Increase in treatment duration elevated the accumulation of ROS. At 48 HAT, H_2O_2 and $O_2^{\bullet}$ contents increased up to 32 and 14.20% compared to 12 HAT (**Table 3**).

Moreover, Jiu-Er-13XI was more severely affected by Cd stress than Zheyou-50. Jiu-Er-13XI showed 50 and 25.70%, while Zheou-50 exhibited only 20 and 11.32% increase in H_2O_2 and $O_2^{\bullet}$ contents, respectively, in comparison with their respective control treatments (**Figure 3**). Treatment duration aggravated the outcomes of Cd stress on both genotypes. However, the impact was more pronounced in Jiu-Er-13XI, with a 43% increase in H_2O_2 content at 48 HAT, compared to 12 HAT (**Supplementary Table S4**).

TABLE 2 | Sole effect of genotype, treatment and timings on root shoot cadmium (Cd) accumulation and leaf malondialdehyde (MDA) content in rapeseed.

Factors	Cd (root) (mg/g DW)	Cd (shoot) (mg/g DW)	MDA (nM g^{-1} FW)
Genotypes			
Jiu-Er-13XI	8.69 ± 2.24 a	0.12 ± 0.03 a	22.27 ± 1.89 a
Zheyou-50	7.14 ± 1.77 b	0.05 ± 0.01 b	18.05 ± 1.31 b
Significance	**	**	**
Treatments			
Ck	0.08 ± 0.006 b	0.007 ± 0.0007 b	15.92 ± 0.94 b
Cd	15.76 ± 1.02 a	0.17 ± 0.02 a	24.40 ± 1.68 a (+53.18%)
Significance	**	**	**
Timings			
3DAT	5.88 ± 1.78 c	0.05 ± 0.02 c	15.67 ± 1.15 c
6DAT	7.90 ± 2.39 b	0.09 ± 0.03 b	19.25 ± 1.81 b (+22.9%)
9DAT	9.97 ± 3.08 a	0.11 ± 0.03 a	25.56 ± 2.08 a (+63.15%)
Significance	**	**	**

*DAT, days after treatment; ns, non-significant. **Significant at P ≤ 0.01.*

Expression of Tocopherol Biosynthesis Genes

Tocopherol biosynthesis pathway consists of six genes. Expression of these genes was measured at 12, 24, and 48 HAT. A significant difference was seen in the expression of all genes, except BnPDS1, in both genotypes. Moreover, Cd stress increased the expression of all genes compared to control treatment. An average increase of 52.7% was seen in BnVTE4, which codes for α-tocopherol. The increase in gene expression was time dependent (**Table 4**). Cadmium treatment affected

TABLE 3 | Sole effects of genotypes, treatments, and timings on leaf reactive oxygen species (ROS) accumulation in rapeseed.

	H_2O_2 (μmol g^{-1} FW)	O_2^- (nmol m^{-1} g^{-1} FW)
Genotypes		
Jiu-Er-13XI	42.7 ± 2.7 a	61.1 ± 2.0 a
Zheyou-50	33.2 ± 1.2 b	54.6 ± 1.2 b
Significance	**	**
Treatments		
Ck	32.1 ± 1.1	52.9 ± 1.0 b
Cd	43.8 ± 2.5a (+36%)	62.8 ± 1.7a (+18%)
Significance	**	**
Timings		
12HAT	32.4 ± 1.7 b	53.1 ± 1.7 b
24HAT	38.5 ± 2.9a (+18%)	59.7 ± 1.9a (+12%)
48HAT	43.0 ± 3.4 a (+32%)	60.7 ± 2.6a (+14%)
Significance	**	**

*HAT, hours after treatment. **Significant at $P \leq 0.01$.*

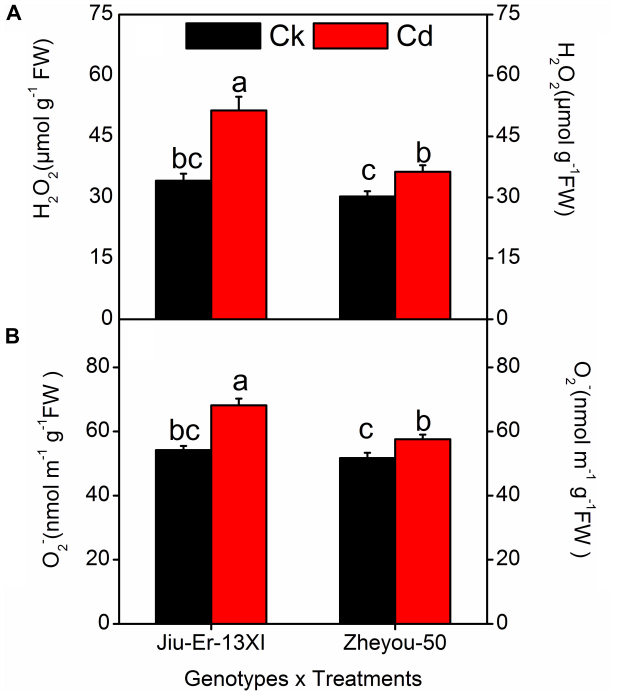

FIGURE 3 | Interactive effects of genotypes and treatments on leaf reactive oxygen species (ROS) accumulation in rapeseed. Lettering indicates statistical difference ($p \leq 0.01$) among the treatments for each parameter. Data represent the mean ± SE of three measurements. Ck and Cd represent control and 100 μM Cd, respectively.

the expression of tocopherol biosynthesis pathway genes in different manners in both genotypes. A prominent increase in BnVTE4 (87%) and BnVTE5 (65%) was observed in Zheyou-50 and Jiu-Er-13XI, respectively, under Cd stress, indicating the accumulation of α-tocopherol in Zheyou-50 and degradation of chlorophyll in Jiu-Er-13XI (**Figure 4**). Besides, a significant interaction was observed between genotypes and treatment as well as treatment and time duration except for BnVTE1 (**Supplementary Table S5**).

Fatty Acid Contents and Composition

Cadmium stress affected fatty acid contents and composition in a genotype-dependent manner. Compared with normal growth conditions, Jiu-Er-13XI showed about 21% decrease, while Zheyou-50 depicted 3.40% increase in total fatty acid content under Cd stress (**Figure 5**). Cd stress caused a reduction in 18:2 and 18:3 fatty acid contents of Jiu-Er-13XI by 41.11 and 49.21%, respectively, indicating a detrimental effect of Cd on polyunsaturated fatty acids (PUFA). In contrast, no such adversity was recorded for Zheyou-50. Instead, a 10.20 and 3.34% increase was detected in 18:2 and 18:3 fatty acids, respectively, suggesting a normal metabolism in this genotype. Sole and interactive effects are also presented in **Table 5** and **Supplementary Table S6**.

Tocopherol Contents and Composition

Jiu-Er-13XI and Zheyou-50 showed a differential response to Cd in terms of tocopherol composition. Jiu-Er-13XI revealed 2.82, 0.08, and 3.07 mg g^{-1} FW of alpha, gamma, and total tocopherol, respectively, whereas Zheyou-50 exhibited a higher concentration of alpha (4.32 mg g^{-1} FW), gamma (0.09 mg g^{-1} FW) and total tocopherol (4.42 mg g^{-1} FW) than its counterpart. On average basis, Cd increased alpha and total tocopherol by 22.11 and 25.31%, respectively, while decreased gamma tocopherol content by 27.44% with respect to control. Moreover, treatment duration also enhanced the total tocopherol by 19.69 and 44.05% at 3 DAT and 9 DAT, respectively, with reference to the control treatment (**Table 6**). Considering interactive effects, Cd treatment increased total and α-tocopherol contents in both genotypes, while it decreased gamma tocopherol. However, the increase was prominent in Zheyou-50 as it accumulated 45.33 and 47.43% higher total and α-tocopherol under Cd stress than the control treatment. Conversely, Jiu-Er-13XI accumulated only 22.61 and 32.74% higher content of alpha and total tocopherol under Cd treatment than the normally grown plants (**Figure 6**). Treatment duration also induced the accumulation of α-tocopherol, which was higher (46.74%) in Zheyou-50 than in Jiu-Er-13XI (29.30%), with reference to their respective control treatments. The increase in total tocopherol was directly proportional to treatment duration. After 9 days of treatment, total and α-tocopherol increased by 41.86 and 36.20%, respectively. Interestingly, increase in α-tocopherol was accompanied by a corresponding decline in γ-tocopherol. Cd treatment decreased γ-tocopherol by 35.16 and 28.16% in Zheyou-50 and Jiu-Er-13XI, respectively. After 9 days of treatment, the decrease was considerably prominent in Zheyou-50 (51.08%), suggesting the impact of time duration on the fate of γ-tocopherol (**Supplementary Table S7**).

Subcellular Study

Molecular and biochemical changes observed in rapeseed genotypes under Cd stress reflected at subcellular level as well. The leaf cells of the Jiu-Er-13XI and Zheyou-50 control plants were metabolically active, as suggested by the presence

TABLE 4 | Sole effects of genotypes, treatments, and timings on tocopherol (Toc) biosynthesis genes.

	BnVTE1	BnVTE2	BnVTE3	BnVTE4	BnVTE5	BnPDS1
Genotypes						
Jiu-Er-13XI	1.11 ± 0.11	0.93 ± 0.1 b	1.38 ± 0.16 a	0.96 ± 0.05 b	1.6 ± 0.1 a	6.4 ± 1.4
Zheyou-50	1.09 ± 0.08	1.98 ± 0.3 a	0.84 ± 0.07 b	1.17 ± 0.10 a	0.8 ± 0.06 b	7.0 ± 1.4
Significance	Ns	**	**	**	**	ns
Treatments						
Ck	0.89 ± 0.06 b	1.28 ± 0.23 b	0.86 ± 0.05 b	0.84 ± 0.05 b	1.06 ± 0.07b	3.0 ± 0.4b
Cd	1.31 ± 0.09 a	1.63 ± 0.28 a	1.36 ± 0.17 a	1.29 ± 0.07 a	1.37 ± 0.17a	10.3 ± 1.5a
Significance	**	**	**	**	**	**
Timing						
3HAT	1.15 ± 0.07	0.89 ± 0.08 b	1.11 ± 0.09	1.17 ± 0.07 a	1.17 ± 0.16	3.3 ± 1.1c
6HAT	1.09 ± 0.15	0.98 ± 0.17 b	1.08 ± 0.11	0.93 ± 0.1 ab	1.23 ± 0.13	5.7 ± 1.0b
9HAT	1.07 ± 0.11	2.50 ± 0.34 a	1.14 ± 0.27	1.09 ± 0.1b	1.26 ± 0.21	11.0 ± 0.02a
Significance	Ns	**	ns	**	Ns	**

*HAT, hours after treatment; ns, non-significant. **Significant at $P \leq 0.01$.*

of well-developed chloroplasts with the normal shape and size. There were no starch granules in cells of both genotypes under control treatment, indicating a normal carbohydrate metabolism. Furthermore, the structure of granal and stromal lamella remained intact under normal growth environment (**Figures 7A,C**). Contrarily, subcellular structure of Cd-treated plants, especially Jiu-Er-13XI (low oil rapeseed genotype), was severely affected by stress. The chloroplast structure changed from normal elongated to big round-shaped one. The thylakoid membrane system was completely destroyed by Cd stress. Accumulation of starch granules in chloroplast is a clear sign of disrupted starch metabolism. Increase in number and size of plastoglobules suggests the accumulation of tocopherols under stress (**Figures 7B,D**). Unlike Jiu-Er-13XI, the genotype with high oil content (Zheyou-50) showed a moderate level of Cd-induced damage to chloroplast structure. The thylakoid membrane network showed comparatively better arrangements, with no starch granules, showing undisturbed carbohydrate metabolism under Cd stress.

DISCUSSION

Comprehensive study on tolerance of plants to Cd stress is of utmost importance to elucidate the underlying mechanisms to develop Cd-tolerant genotypes. Ability of plants to detoxify ROS is one of the main strategies to combat heavy metal-induced oxidative stress. Tocopherols are regarded as the non-enzymatic component of the plant defense system and play major roles in protecting plants against stresses at cellular and subcellular level (Collakova and DellaPenna, 2003; Li et al., 2010). The current investigation is focused on illuminating the role of tocopherols in response to oxidative stress, induced by Cd, in two oilseed rape genotypes, differing in fatty acid content.

Current study indicates Cd accumulation in roots and its translocation to upper parts of plants in both genotypes. However, the degree of absorption and translocation is higher in Jiu-Er-13XI (low seed oil content) than in Zheyou-50 (high seed oil content), suggesting the tolerance of Zheyou-50 to Cd stress. Usually, tolerant genotypes either inhibit the absorption of heavy metals via roots or restrict their translocation to the leaves. The effect of Cd on photosynthetic pigments is well documented (Ali et al., 2015). Cd is believed to replace metals in metal-containing enzymes, e.g., substituting Ca ion in PSII leads to the inhibition of water splitting systems. Damage to structure of chloroplast, reduction in chlorophyll synthesis and its deterioration are the major reasons for reduction in chlorophyll content (López-Millán et al., 2009). The net loss of chlorophyll was much higher in Jiu-Er-13XI than in Zheyou-50. The main reason behind this tolerance is the reduced absorption and restricted translocation of Cd ions in Zheyou-50.

Accumulation of ROS in Cd-treated plants has been reported in the literature (Pathak and Khandelwal, 2006; Zhou et al., 2009). Though Cd cannot directly generate free radicals, it produces ROS indirectly by increasing the free Fe-concentration, possibly via replacement in various proteins (Scholz et al., 1990; Dorta et al., 2003). Quantification of H_2O_2 and O_2^- in this study indicates an immediate accumulation of ROS upon Cd exposure. The degree of accumulation is treatment duration and genotype dependent, as Zheyou-50 accumulated less ROS than Jiu-Er-13XI. Upregulation of BnVTE5 in Jiu-Er-13XI shows the increased degradation of chlorophyll by ROS.

Polyunsaturated fatty acids, such as linolenic acid and linoleic acid in membrane lipids are very sensitive to oxidation caused by Cd-induced ROS (Frankel, 2005). Current experiment reveals a decline in total fatty acid content of Cd-treated plants of Jiu-Er-13XI, compared to the normally grown plants. This reduction in total fatty acids is ascribed to decrease in 18:2 and 18:3 fatty acids in Cd-treated Jiu-Er-13XI plants. Stressed plants of Jiu-Er-13XI indicate increase in content of other fatty acids like, 16:0, 18:0, and 18:1, suggesting an inhibition in desaturation ability of enzymes. Contrary to that, no such effect on fatty acid composition of Zheyou-50 plants is observed. Instead, considerable enhancement in total fatty acid content under Cd treatment suggests the tolerance of this genotype to Cd stress. The increase in expression level of BnVTE4 in Zheyou-50 may protect PUFA under stressed environment. In a current investigation, decrease in 18:2 and 18:3 fatty acid contents

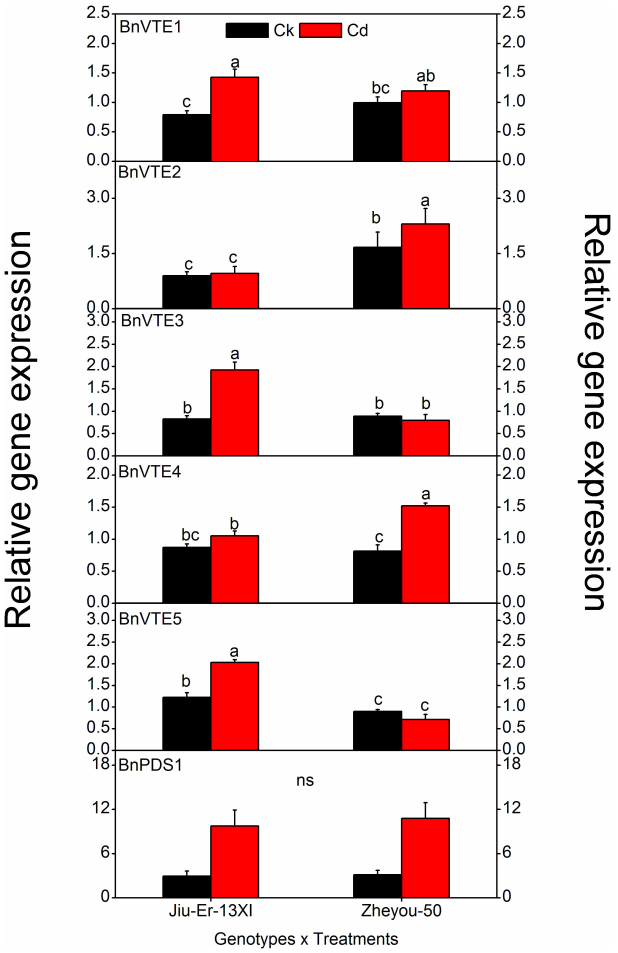

FIGURE 4 | Interactive effects of genotypes and treatments on Toc genes expression in rapeseed. Lettering indicates statistical difference ($p \leq 0.01$) among the treatments for each parameter. Data represent the mean ± SE of three measurements. Ck, Cd, and ns indicate control, 100 μM Cd, and non-significant, respectively.

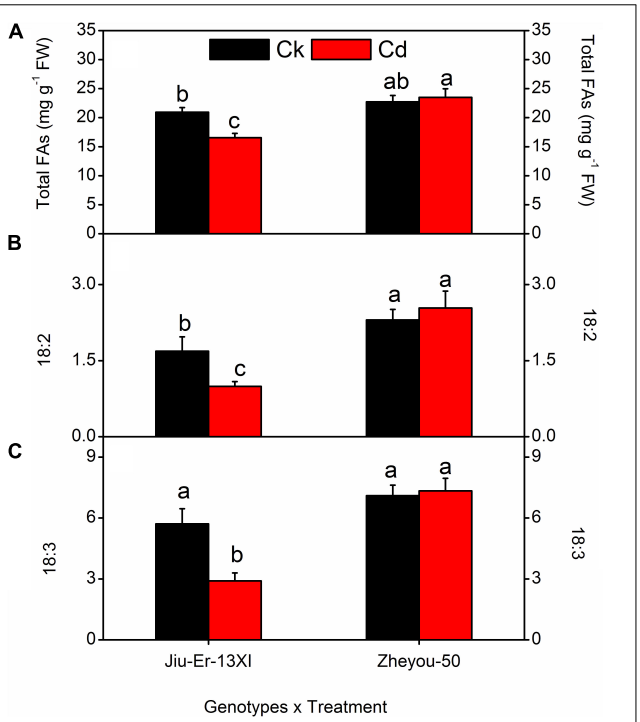

FIGURE 5 | Interactive effects of genotypes and treatments on leaf fatty acid content and composition in rapeseed. Lettering indicates statistical difference ($p \leq 0.01$) among the treatments for each parameter. Data represent the mean ± SE of three measurements. Ck and Cd represent control and 100 μM Cd, respectively.

of Jiu-Er-13XI is accompanied by the accumulation of MDA. MDA is the product of oxidation of 18:3 fatty acid, which is regarded as an important indicator of fatty acid oxidation under stress (Sattler et al., 2003). With increase in treatment duration, marked increase can be seen in MDA content. Conversely, MDA accumulation is low in Zheyou-50 because Cd stress had no such effects on the fatty acid composition of this genotype.

A study of anatomical disorders under a stressful environment is highly important to understand the tolerance mechanism of plants at subcellular level. Studies on barley (Wang et al., 2011) and tomato (Gratão et al., 2009) indicate that chloroplast is highly vulnerable to Cd stress. The present study reveals a severe damage to chloroplast structure of plants of Jiu-Er-13XI under Cd stress. The damaging effect can be explained as disruption in chloroplast structure (Borges et al., 2004), with completely deformed thylakoid membranes (Vijaranakul et al., 2001). Abnormal chloroplast, having reduced amounts of chlorophyll, is unlikely to possess surplus energy. Therefore, the presence of starch granules in Jiu-Er-13XI genotype indicates the incapability of chloroplasts to metabolize reserve carbohydrates (Uzunova and Popova, 2000), indicating the vulnerability of this genotype to Cd. In contrast, Zheyou-50 is not much affected by Cd stress.

Tocopherols are vitamin E group of lipid-soluble compounds having multifunctional properties. Tocopherols are believed to protect PUFA from ROS, produced during oxidative stress either by quenching superoxide radicals or by terminating the chain reaction (Sattler et al., 2004b; Krieger-Liszkay, 2005). Having said that tocopherols are produced by the oxygenic organisms and are an essential component of human nutrition, their function is not well investigated in plants. The reason behind the scarcity of literature could be the disappointing results obtained in certain studies where complete absence of tocopherol did not show any significant influence on plant growth and metabolism (Havaux et al., 2005; Maeda et al., 2005). Therefore, the role of tocopherol in mitigating oxidative damage remained unexplored. Instead, its role in other processes like transport of sugars, cellular signaling, and seed germination and dormancy are reported (Sattler et al., 2004b). However, with the advent of mutation and transgenic techniques in *Arabidopsis* and *Synechocystis* sp. PCC6803, study on functions of tocopherols became possible by eliminating (Schledz et al., 2001) or increasing the concentration of tocopherol (Collakova and DellaPenna, 2001;

TABLE 5 | Sole effects of genotypes, treatments, and timings on leaf fatty acid (FA) content and composition in rapeseed.

	16:0	18:0	18:1	18:2	18:3	Total FA
Genotypes						
Jiu-Er-13XI	3.4 ± 0.09	1.39 ± 0.11	3.41 ± 0.18	1.34 ± 0.16	4.3	18.7 ± 0.74
Zheyou-50	3.3 ± 0.16	1.56 ± 0.07	2.85 ± 0.07	2.41 ± 0.19	7.2	23.1 ± 0.90
Significance	ns	ns	**	**	**	**
Treatments						
Ck	3.3 ± 0.14	1.33 ± 0.09	3.05 ± 0.15	1.99 ± 0.18	6.40	21.8 ± 0.69
Cd	3.5 ± 0.12 (+5%)	1.61 ± 0.08 (+21.4%)	3.21 ± 0.15 (+5.13%)	1.76 ± 0.25 (−11.5%)	5.11 (−21%)	20.0 ± 1.16 (−8.29%)
Significance	*	**	ns	**	**	**
Timings						
3DAT	2.9 ± 0.05	1.13 ± 0.13	3.48 ± 0.12	1.02 ± 0.12	4.72	17.6 ± 0.56
6DAT	3.3 ± 0.11 (+14.4%)	1.55 ± 0.07 (+37.2)	3.34 ± 0.19 (−3.9%)	2.12 ± 0.20 (107%)	5.49 (+16%)	21.2 ± 0.89 (+20.2%)
9DAT	4.0 ± 0.10 (+21.2%)	1.74 ± 0.06 (+12.3)	2.56 ± 0.10 (−26.5%)	2.4 ± 0.25 (141%)	7.06 (49%)	23.9 ± 1.24 (+12.9%)
Significance	**	**	**	**	**	**

*DAT, days after treatment; ns, non-significant. *Significant at $P \leq 0.05$; **significant at $P \leq 0.01$.*

Savidge et al., 2002) or replacing them with biosynthetic intermediates (Porfirova et al., 2002; Sattler et al., 2003) to uncover the underlying mechanism in plants. Accumulation of tocopherol can be observed in response to multiple abiotic stresses (Havaux et al., 2000; Munne-Bosch and Alegre, 2002a). In the present study, the concentration of total and α-tocopherol improved under Cd stress compared to the control treatment, suggesting its role during oxidative stresses. The role of tocopherols in ameliorating Cd stress is attributed to the activity of α-tocopherol. Alpha tocopherol content increased in both genotypes under stress. However, the magnitude of increase was considerably lower in Jiu-Er-13XI than in Zheyou-50, strengthening the idea that sensitive plants show net loss of tocopherol during oxidative stresses (Munne-Bosch, 2005). The increase in α-tocopherol was accompanied by the decrease in γ-tocopherol, suggesting the upregulation of VTE4.

The role of α-tocopherol is well known in protecting PUFA from oxidative damage (Sattler et al., 2004a). In the current experiment, the decrease in total fatty acid content of Jiu-Er-13XI might be due to the low production of tocopherol, while in Zheyou-50, the increase in net fatty acid content was attributed to the protection provided by α-tocopherol. Alpha tocopherol provided protection to PUFA in Zheyou-50 by quenching the

TABLE 6 | Sole effects of genotypes, treatments, and timings on leaf tocopherol content and composition in rapeseed.

	Alpha (mg g^{-1} FW)	Gamma (mg g^{-1} FW)	Total Toc (mg g^{-1} FW)
Genotypes			
Jiu-Er-13XI	2.8 ± 0.1 b	0.08 ± 0.006b	3.0 ± 0.19 b
Zheyou-50	4.3 ± 0.2 a	0.09 ± 0.006a	4.4 ± 0.19 a
Significance	**	**	**
Treatments			
Ck	3.2 ± 0.1 b	0.10 ± 0.007 a	3.3 ± 0.19 b
Cd	3.9 ± 0.2 a (+22%)	0.07 ± 0.005 b (−27%)	4.1 ± 0.26 a (+25%)
Significance	**	**	**
Timings			
3DAT	2.9 ± 0.1c	0.11 ± 0.009 a	3.0 ± 0.18 c
6DAT	3.6 ± 0.2 b (+21%)	0.08 ± 0.006 b (−24%)	3.7 ± 0.25 b (+19.6%)
9DAT	4.1 ± 0.3 a (+14%)	0.06 ± 0.003 c (−43%)	4.4 ± 0.34 a (+44.0%)
Significance	**	**	**

*DAT, days after treatment; ns, non-significant. **Significant at $P \leq 0.01$.*

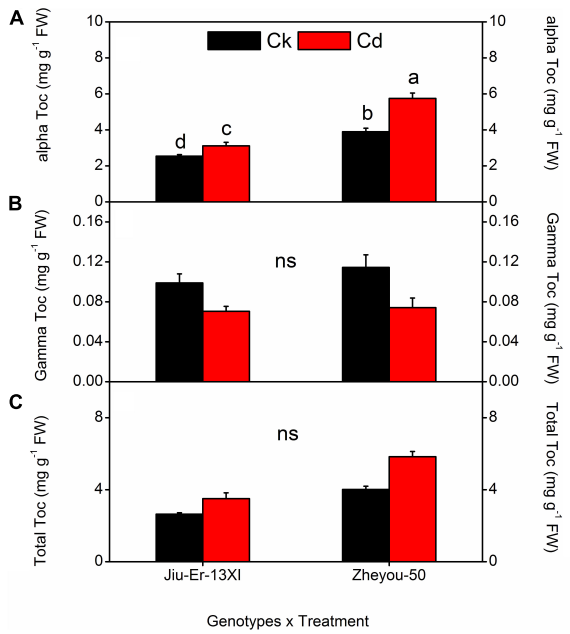

FIGURE 6 | Interactive effects of genotypes and treatments on leaf tocopherol content and composition in rapeseed. Lettering indicates statistical difference ($p \leq 0.01$) among the treatments for each parameter. Data represent the mean ± SE of three measurements. Ck, Cd, and ns represent control, 100 μM Cd, and non-significant, respectively.

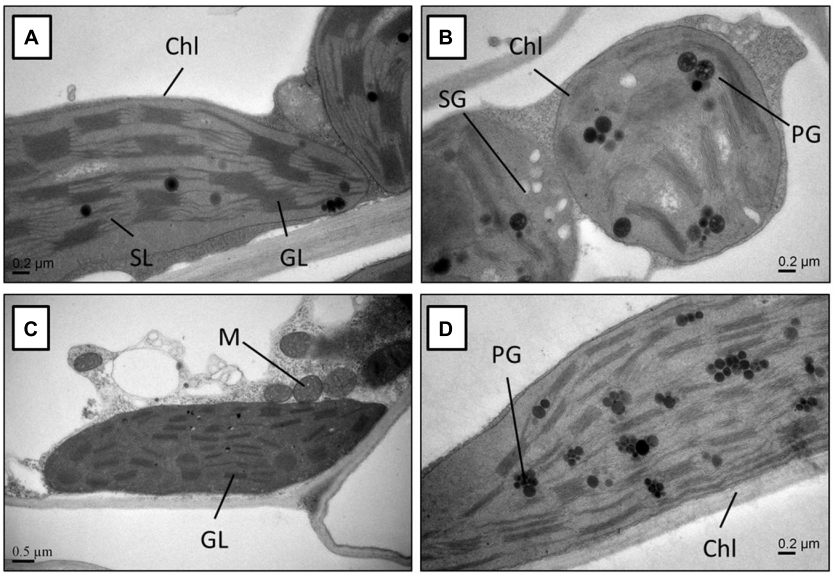

FIGURE 7 | Transmission electron micrograph of the leaf mesophyll cells from Jiu-Er-13XI (A = Ck, B = 100 µM Cd), and Zheyou-50 (C = Ck, D = 100 µM Cd). Labels: Ch, chloroplast; SG, starch grain; PG, plastoglobule; M, mitochondrion; GL, granallamella; SL, stromal lamella.

superoxide radicals, as ROS accumulation was reduced in this genotype compared to the Jiu-Er-13XI. MDA is the oxidative product of linolenic acid (Farmer 2007). In Jiu-Er-13XI, decrease in linolenic acid was accompanied by increase in MDA, showing the peroxidation of lipid membranes, while there was no such increase or decrease shown by Zheyou-50 for MDA and linolenic acid, respectively.

This view is further strengthened by the structure of chloroplast (**Figure 7**). In Jiu-Er-13XI, the chloroplast is completely deformed with destroyed thylakoid membranes and accumulation of starch granules, suggesting the oxidation of PUFA by ROS, and abnormality in sugar transport (**Figure 7B**). Abnormality in starch metabolism of Jiu-Er-13XI under Cd stress suggests the alternate function of tocopherol other than antioxidant (Maeda et al., 2006). The function of tocopherols in restricting the absorption of Cd and inhibiting its transport to upper parts of plant is not well documented. However, in the present study, reduction in absorption of Cd by roots and its limited translocation to aerial plant parts in Zheyou-50 might have been mediated by tocopherols.

CONCLUSION

The current study concludes that genotypic differences were observed in Cd tolerance of two oilseed rape varieties. Zheyou-50, with higher tocopherol content, exhibited better tolerance to Cd stress than Jiu-Er-13XI in terms of all studied parameters. The reduction in absorption and translocation of Cd and scavenging of reactive oxygen species by tolerant genotypes indicate the involvement of tocopherol in Cd stress amelioration. The current study suggests that the plants having high tocopherol content can withstand Cd stress effectively. The outcomes of the present investigation will serve as a source of valuable information for the scientific fraternity engaged in developing Cd-tolerant oilseed rape genotypes. However, further studies must be conducted in order to explore the underlying mechanism of tolerance to Cd stress in plants.

DATA AVAILABILITY STATEMENT

All datasets for this study are included in the article/**Supplementary Material**.

AUTHOR CONTRIBUTIONS

EA conceived and oversaw the work. EA, JMS, and SAHB executed the trial. ZH, MI, and SH made the figures and tables. HR, ANS, and MA analyzed the data. EA, MA-D, and SAHB wrote the manuscript. SAk and SAi revised the manuscript. All authors have carefully read and approved the article.

FUNDING

The study was funded by Researchers Supporting Project number (RSP 2020/26), King Saud University, Riyadh, Saudi Arabia, Key Project of Research and Development Plan of Zhejiang (2018C02SA780973), and Natural Science Foundation of China (31401506).

SUPPLEMENTARY MATERIAL

The Supplementary Material for this article can be found online at: https://www.frontiersin.org/articles/10.3389/fpls.2020.547133/full#supplementary-material

REFERENCES

Abbasi, A., Hajirezaei, M., Hofius, D., Sonnewald, U., and Voll, L. M. (2007). Specific roles of α- and γ-tocopherol in abiotic stress responses of transgenic tobacco (*Nicotiana tabacum* L.). *Plant Physiol.* 143, 1720–1738. doi: 10.1104/pp.106.094771

Ahmad, P., Nabi, G., and Ashraf, M. (2011). Cadmium-induced oxidative damage in mustard (*Brassica juncea* L.) Czern & Coss) plants can be alleviated by salicylic acid. *South Afr. J. Bot.* 77, 36–44. doi: 10.1016/j.sajb.2010.05.003

Ali, E., Hussain, N., Shamsi, I. H., Jabeen, Z., Siddiqui, M. H., and Jiang, L. (2018). Role of jasmonic acid in improving tolerance of rapeseed (*Brassica napus* L.) to Cd toxicity. *J. Zhejiang Univ. Sci. B* 19, 130–146. doi: 10.1631/jzus.b1700191

Ali, E., Maodzeka, A., Hussain, N., Shamsi, I. H., and Jiang, L. (2015). The alleviation of cadmium toxicity in oilseed rape (*Brassica napus*) by the application of salicylic acid. *Plant Growth Regul.* 75, 641–655. doi: 10.1007/s10725-014-9966-0

Borges, R., Miguel, E. C., Dias, J. M. R., Da, C. M., Ricardo, E. B. S., Oliveira, J. G., et al. (2004). Ultrastructural, physiological and biochemical analyses of chlorate toxicity on rice seedlings. *Plant Sci.* 166, 1057–1062. doi: 10.1016/j.plantsci.2003.12.023

Bukhari, S. A. H., Zheng, W., Xie, L., Zhang, G., Shang, S., and Wu, F. (2016). Cr-induced changes in leaf protein profile, ultrastructure and photosynthetic traits in the two contrasting tobacco genotypes. *Plant Growth Regul.* 79, 147–156. doi: 10.1007/s10725-015-0120-4

Chen, M. X., Wang, Z., Zhu, Y., Li, Z. L., Hussain, N., Zhang, G. P., et al. (2012). Effect of TRANSPARENT TESTA 2 on seed fatty acid biosynthesis and tolerance to environmental stresses during young seedling establishment in *Arabidopsis*. *Plant Physiol.* 160, 1023–1036. doi: 10.1104/pp.112.202945

Collakova, E., and DellaPenna, D. (2001). Isolation and functional analysis of homogentisate phytyltransferase from *Synechocystis* sp. PCC 6803 and *Arabidopsis*. *Plant Physiol.* 127, 1113–1124. doi: 10.1104/pp.010421

Collakova, E., and DellaPenna, D. (2003). The role of homogentisate phytyltransferase and other tocopherol pathway enzymes in the regulation of tocopherol synthesis during abiotic stress. *Plant Physiol.* 133, 930–940. doi: 10.1104/pp.103.026138

Collin, V. C., Eymery, F., Genty, B., Rey, P., and Havaux, M. (2008). Vitamin E is essential for the tolerance of *Arabidopsis thaliana* to metal-induced oxidative stress. *Plant Cell Environ.* 31, 244–257.

Di Toppi, L. S., and Gabbrielli, R. (1999). Response to cadmium in higher plants. *Environ. Exp. Bot.* 41, 105–130. doi: 10.1016/s0098-8472(98)00058-6

Dorta, D. J., Leite, S., and DeMarco, K. C. (2003). A proposed sequence of events for cadmium-induced mitochondrial impairment. *J. Inorg. Biochem.* 97, 251–257. doi: 10.1016/s0162-0134(03)00314-3

Du, X., Hussain, N., Li, Z., Chen, X., Hua, S., Zhang, D., et al. (2015). Effect of Gibberellin on the biosynthesis of tocopherols in oilseed rape (*Brassica napus* L.) and *Arabidopsis*. *J. Agric. Food Chem.* 63, 360–369. doi: 10.1021/jf505312c

Feng, R. W., Wei, C. Y., Tu, S. X., Ding, Y. Z., and Song, Z. G. (2013). A dual role of Se on Cd toxicity: evidences from the uptake of Cd andsome essential elements and the growth responses in paddyrice. *Biol. Trace Elem. Res.* 151, 113–121. doi: 10.1007/s12011-012-9532-4

Frankel, E. N. (2005). *Lipid Oxidation*. Philadelphia, PA:Woodhead Publishing Ltd.

Fukuzawa, K., Tokumura, A., Ouchi, S., and Tsukatani, H. (1982). Antioxidant activities of tocopherols on Fe2-ascorbate-induced lipid peroxidation in lecithin liposomes. *Lipids* 17, 511–513. doi: 10.1007/bf02535334

Garcia-Plazaola, J. I., and Becerril, J. M. (2000). Effects of drought on photoprotective mechanisms in European beech (*Fagus sylvatica* L.) seedlings from different provenances. *Trees Strut. Funct.* 14, 485–490. doi: 10.1007/s004680000068

Gong, H. J., Chen, K. M., Zhao, Z. G., Chen, G. C., and Zhou, W. J. (2008). Effects of silicon on defense of wheat against oxidative stress under drought at different developmental stages. *Biol. Plant.* 52, 592–596. doi: 10.1007/s10535-008-0118-0

Gramegna, G., Rosado, D., Sánchez Carranza, A. P., Cruz, A. B., Simon-Moya, M., Llorente, B., et al. (2019). PHYTOCHROME-INTERACTING FACTOR 3 mediates light-dependent induction of tocopherol biosynthesis during tomato fruit ripening. *Plant Cell Environ.* 42, 1328–1339. doi: 10.1111/pce.13467

Gratão, P. L., Monteiro, C. C., Rossi, M. L., Martinelli, A. P., Peres, L. E. P., Medici, L. O., et al. (2009). Differential ultra structural changes in tomato hormonal mutants exposed to cadmium. *Environ. Exp. Bot.* 67, 387–394. doi: 10.1016/j.envexpbot.2009.06.017

Grusak, M. A. (1999). Genomics-assisted plant improvement to benefit human nutrition and health. *Trends Plant Sci.* 4, 164–166. doi: 10.1016/s1360-1385(99)01400-4

Grusak, M. A., DellaPenna, D., and Welch, R. M. (1999). Physiologic processes affecting the content and distribution of phytonutrients in plants. *Nutr. Rev.* 57, S27–S33.

Havaux, M., Bonfils, J. P., Lütz, C., and Niyogi, K. K. (2000). Photodamage of the photosynthetic apparatus and its dependence on the leaf developmental stage in the npq1 *Arabidopsis* mutant deficient in the xanthophyll cycle enzyme violaxanthin de-epoxidase. *Plant Physiol.* 124, 273–284. doi: 10.1104/pp.124.1.273

Havaux, M., Eymery, F., Porfirova, S., Rey, P., and Dormann, P. (2005). Tocochromanol protects against photo inhibition and oxidative stress in *Arabidopsis thaliana*. *Plant Cell* 17, 3451–3469. doi: 10.1105/tpc.105.037036

Hawkes, J. S. (1997). Heavy metals. *J. Chem. Edu.* 74, 1369–1374.

Hodges, D. M., DeLong, J. M., Forney, C. F., and Prange, R. K. (1999). Improving the thiobarbituric acid-reactive-substances assay for estimating lipid peroxidation in plant tissues containing anthocyanin and other interfering compounds. *Planta* 207, 604–611. doi:10.1007/s004250050524

Hüsken, A., Baumert, A., Strack, D., Becker, H. C., Möllers, C., and Milkowski, C. (2005). Reduction of sinapate ester content in transgenic oilseed rape (*Brassica napus*) by dsRNAi-based suppression of *BnSGT1* gene expression. *Mol. Breeding* 16, 127–138. doi: 10.1007/s11032-005-6825-8

Jia, Y., Tang, S. R., Ju, X. H., Shu, L. N., Tu, S. X., Feng, R. W., et al. (2011). Effects of elevated CO_2 levels on root morphological traitsand Cd uptakes of two *Lolium* species under Cd stress. *J. Zhejiang Univ. Sci. B* 12, 313–325. doi: 10.1631/jzus.b1000181

Jiang, M., and Zhang, J. (2001). Effect of abscisic acid on active oxygen species, antioxidative defence system and oxidative damage in leaves of maize seedlings. *Plant Cell Physiol.* 42, 1265–1273. doi: 10.1093/pcp/pce162

Kim, S. E., Lee, C. J., Ji, C. Y., Kim, H. S., Park, S. U., Lim, Y. H., et al. (2019). Transgenic sweetpotato plants overexpressing tocopherol cyclase display enhanced α-tocopherol content and abiotic stress tolerance. *Plant Physiol. Biochem.* 144, 436–444. doi: 10.1016/j.plaphy.2019.09.046

Krieger-Liszkay, A. (2005). A singlet oxygen production in photosynthesis. *J. Exp. Bot.* 56, 337–346. doi: 10.1093/jxb/erh237

Li, F., Wu, Q. Y., Sun, Y. L., Wang, L. Y., Yang, X. H., and Meng, Q. W. (2010). Overexpression of chloroplastic monodehydroascorbate reductase enhanced tolerance to temperature and methyl viologen-mediated oxidative stresses. *Physiol. Plant.* 139, 421–434.

Li, Y. L., Hussain, N., Zhang, L. M., Chen, X. Y., Ali, E., and Jiang, L. X. (2013). Correlations between tocopherol and fatty acid components in germplasm collections of Brassica oilseeds. *J. Agri. Food Chem.* 61, 34–40. doi: 10.1021/jf3042837

Lima, A. I. G., Pereira, S. I. A., de Almeida Paula Figueira, E. M., Caldeira, G. C. N., and de Matos Caldeira, H. D. Q. (2006). Cadmium detoxification in roots of *Pisum sativum* seedlings: relationship between toxicity levels, thiol pool alterations and growth. *Environ. Exp. Bot.* 55, 149–162. doi: 10.1016/j.envexpbot.2004.10.008

Liu, D., Jiang, W., Wang, W., and Zhai, L. (1995). Evaluation of metal ion toxicity on root tip cells by the Allium test. *Isr. J. Plant Sci.* 43, 125–133. doi: 10.1080/07929978.1995.10676598

Livak, K. J., and Schmittgen, T. D. (2001). Analysis of relative gene expression data using real-time quantitative PCR and the $2^{-}\Delta\Delta C$ method. *Methods* 25, 402–408. doi: 10.1006/meth.2001.1262

López-Millán, A. F., Sagardoy, R., Solanas, M., and Abadía, A. (2009). Cadmium toxicity in tomato (*Lycopersicon esculentum*) plants grown in hydroponics. *Environ. Exp. Bot.* 65:376. doi: 10.1016/j.envexpbot.2008.11.010

Maeda, H., Sakuragi, Y., Bryant, D. A., and DellaPenna, D. (2005). Tocopherols protect *Synechocystis* sp. strain PCC 6803 from lipid peroxidation. *Plant Physiol.* 138, 1422–1435. doi: 10.1104/pp.105.061135

Maeda, H., Song, W., Sage, T. L., and DellaPenna, D. (2006). Tocopherols play a crucial role in low temperature adaptation and phloem loading in *Arabidopsis*. *Plant Cell* 18, 2710–2732. doi: 10.1105/tpc.105.039404

Mène-Saffrané, L., and DellaPenna, D. (2010). Biosynthesis, regulation and functions of tocochromanols in plants. *Plant Physiol. Biochem.* 48, 301–309. doi: 10.1016/j.plaphy.2009.11.004

Munne-Bosch, S. (2005). The role of α-tocopherol in plant stress tolerance. *J. Plant Physiol.* 162, 743–748. doi: 10.1016/j.jplph.2005.04.022

Munne-Bosch, S., and Alegre, L. (2001). Subcellular compartmentation of the diterpene carnosic acid and its derivatives in the leaves of rosemary. *J. Plant Physiol.* 125, 1094–1102. doi: 10.1104/pp.125.2.1094

Munne-Bosch, S., and Alegre, L. (2002a). Interplay between ascorbic acid and lipophilic antioxidant defences in chloroplasts of water-stressed *Arabidopsis* plants. *FEBS Lett.* 524, 145–148. doi: 10.1016/s0014-5793(02)03041-7

Munne-Bosch, S., and Alegre, L. (2002b). The function of tocopherols and tocotrienols in plants. *Crit. Rev. Plant Sci.* 21, 31–57. doi: 10.1201/9781420080391-8

Nowicka, B., Fesenko, T., Walczak, J., and Kruk, J. (2020). The inhibitor-evoked shortage of tocopherol and plastoquinol is compensated by other antioxidant mechanisms in *Chlamydomonas reinhardtii* exposed to toxic concentrations of cadmium and chromium ions. *Ecotoxicol. Environ. Saf.* 191:110241. doi: 10.1016/j.ecoenv.2020.110241

Pathak, N., and Khandelwal, S. (2006). Oxidative stress and apoptotic changes in murine splenocytes exposed to cadmium. *Toxicology* 220, 26–36. doi: 10.1016/j.tox.2005.11.027

Porfirova, S., Bergmuller, E., Tropf, S., Lemke, R., and Dormann, P. (2002). Isolation of an *Arabidopsis* mutant lacking vitamin E and identification of a cyclase essential for all tocopherol biosynthesis. *Proc. Natl. Acad. Sci. U.S.A.* 99, 12495–12500. doi: 10.1073/pnas.182330899

Sattler, S. E., Cahoon, E. B., Coughlan, S. J., and DellaPenna, D. (2003). Characterization of tocopherol cyclases from higher plants and cyanobacteria. Evolutionary implications for tocopherol synthesis and function. *Plant Physiol.* 132, 2184–2195. doi: 10.1104/pp.103.024257

Sattler, S. E., Cheng, Z., and DellaPenna, D. (2004a). From *Arabidopsis* to agriculture: engineering improved vitamin E content in soybean. *Trends Plant Sci.* 9, 365–367. doi: 10.1016/j.tplants.2004.06.002

Sattler, S. E., Gilliland, L. U., Magallanes-Lundback, M., Pollard, M., and DellaPenna, D. (2004b). Vitamin E is essential for seed longevity and for preventing lipid peroxidation during germination. *Plant Cell* 16, 1419–1432. doi: 10.1105/tpc.021360

Savidge, B., Weiss, J. D., Wong, Y. H., Lassner, M. W., Mitsky, T. A., Shewmaker, C. K., et al. (2002). Isolation and characterization of homogentisate phytyltransferase genes from *Synechocystis* sp.PCC 6803 and *Arabidopsis*. *Plant Physiol.* 129, 321–332. doi: 10.1104/pp.010747

Schledz, M., Seidler, A., Beyer, P., and Neuhaus, G. (2001). A novel phytyltransferase from *Synechocystis* sp.PCC 6803 involved in tocopherol biosynthesis. *FEBS Lett.* 499, 15–20. doi: 10.1016/s0014-5793(01)02508-x

Scholz, R. W., Graham, K. S., and Wynn, M. K. (1990). "Interaction of glutathione and a-tocopherol in the inhibition of lipid peroxidation of rat liver microsomes," in *Biological Oxidation Systems*, eds C. C. Eddy, G. A. Hamilton, and K. M. Madyastha (San Diego, CA: Academic Press), 841–867. doi: 10.1016/b978-0-12-584552-6.50027-6

Steel, R. G. D., and Torrie, J. H. (1980). *Principles and Procedures of Statistics: a Biometrical Approach*, 2nd Edn. New York, NY: McGraw-Hill.

Tang, Y., Fu, X., Shen, Q., and Tang, K. (2016). Roles of MPBQ-MT in promoting α/γ-tocopherol production and photosynthesis under high light in lettuce. *PLoS One* 11:e0148490. doi: 10.1371/journal.pone.0148490

Uzunova, A. N., and Popova, L. P. (2000). Effect of salicylic acid on the leaf anatomy and chloroplast ultrastructure of barley plants. *Photosynthetica* 38, 243–250. doi: 10.1023/a:1007226116925

Vijaranakul, U., Jayaswal, R. K., and Nadakavukaren, M. J. (2001). Alteration in chloroplast ultrastructure of suspension cultured *Nicotiana tabacum* cells by cadmium. *Sci. Asia* 27, 227–231.

Wang, F., Chen, F., Cai, Y., Zhang, G., and Wu, F. (2011). Modulation of exogenous glutathione in ultrastructure and photosynthetic performance against Cd stress in the two barley genotypes differing in Cd tolerance. *Biol. Trace Elem. Res.* 144, 1275–1288. doi: 10.1007/s12011-011-9121-y

Wang, L. S., Wang, L., Wang, L., Wang, G., Li, Z. H., and Wang, J. J. (2009). Effect of 1-butyl-3-methylimidazolium tetrafluoroborate on the wheat (*Triticuma estivum* L.) seedlings. *Environ. Toxicol.* 24, 296–303. doi: 10.1002/tox.20435

Wu, F. B., Dong, J., Qian, Q. Q., and Zhang, G. P. (2005). Subcellular distribution and chemical form of Cd and Cd-Zn interaction in different barley genotypes. *Chemosphere* 60, 1437–1446. doi: 10.1016/j.chemosphere.2005.01.071

Zhou, Y. J., Zhang, S. P., and Liu, C. W. (2009). The protection of selenium on ROS-mediated apoptosis by mitochondria dysfunction in cadmium-induced LLC-PK1 cells. *Toxicol. In Vitro* 23, 288–294. doi: 10.1016/j.tiv.2008.12.009

Conflict of Interest: The authors declare that the research was conducted in the absence of any commercial or financial relationships that could be construed as a potential conflict of interest.

The handling editor declared a shared affiliation with one of the authors EA at the time of review.

frontiers in Plant Science

ORIGINAL RESEARCH
published: 30 October 2020
doi: 10.3389/fpls.2020.568887

Plant Cadmium Resistance 2 (SaPCR2) Facilitates Cadmium Efflux in the Roots of Hyperaccumulator *Sedum alfredii* Hance

Jiayu Lin[1†], Xiaoyu Gao[1†], Jianqi Zhao[1], Jie Zhang[1], Shaoning Chen[1,2] and Lingli Lu[1,3]*

[1] Key Laboratory of Environment Remediation and Ecological Health, College of Environmental & Resource Science, Zhejiang University, Hangzhou, China, [2] College of Life Sciences and Medicine, Zhejiang Sci-Tech University, Hangzhou, China, [3] Key Laboratory of Subtropic Soil and Plant Nutrition, College of Environmental & Resource Science, Zhejiang University, Hangzhou, China

Hyperaccumulators are the preferred materials for phytoremediation. *Sedum alfredii* Hance is a cadmium (Cd) hyperaccumulator plant in China, although its detoxification mechanism remains unresolved. In our study, we cloned a gene belonging to the plant cadmium resistance (*PCR*) family, named *SaPCR2*, from the hyperaccumulating ecotype (HE) of *S. alfredii*. Sequence analysis indicated that *SaPCR2* contained a cysteine-rich domain highly conserved in the *PCR* family and played an important role in Cd detoxification. Based on the relative quantitative results, *SaPCR2* was highly expressed in the roots of HE *S. alfredii*, but not the shoots and Cd exposure did not significantly affect *SaPCR2* expression. In contrast, the expression level of *SaPCR2* was very low in plants of its non-hyperaccumulating ecotype (NHE). The subcellular localization of SaPCR2 in tobacco leaves and yeasts showed that SaPCR2 was localized on the plasma membrane and the expression of the SaPCR2 protein in a Zn/Cd-sensitive yeast Δ*zrc1* significantly increased its tolerance to Cd stress by decreasing the Cd content in cells. Heterologous expression of *SaPCR2* in plants of both *Arabidopsis thaliana* and NHE *S. alfredii* significantly reduced the Cd levels in the roots, but not in the shoots. These results suggest that the overexpression of *SaPCR2* in plants provides a route for Cd leak out of the root cells and protects the root cells against phytotoxicity of Cd stress. To the best of our knowledge, this is the first study of transporter-mediated root efflux of Cd in hyperaccumulator *S. alfredii*.

Keywords: cadmium, plant cadmium resistance family, hyperaccumulator, *Sedum alfredii*, efflux

OPEN ACCESS

Edited by:
Rafaqat Ali Gill,
Chinese Academy of Agricultural Sciences, China

Reviewed by:
Qingyu Wu,
Chinese Academy of Agricultural Sciences (CAAS), China
Shiu Cheung Lung,
The University of Hong Kong, Hong Kong

****Correspondence:***
Lingli Lu
linglilulu@gmail.com;
lulingli@zju.edu.cn

† These authors have contributed equally to this work

Specialty section:
This article was submitted to Plant Nutrition, a section of the journal Frontiers in Plant Science

Received: *04 June 2020*
Accepted: *09 October 2020*
Published: *30 October 2020*

Citation:
Lin J, Gao X, Zhao J, Zhang J, Chen S and Lu L (2020) Plant Cadmium Resistance 2 (SaPCR2) Facilitates Cadmium Efflux in the Roots of Hyperaccumulator Sedum alfredii Hance. Front. Plant Sci. 11:568887. doi: 10.3389/fpls.2020.568887

INTRODUCTION

Cadmium (Cd) is one of the most toxic elements for plants, animals, and human beings. High Cd exposure to crops via the biogeochemical behavior of soil-plant systems significantly threatens human health (Godt et al., 2006; Marisela Fernandez-Valverde et al., 2010; Shahid et al., 2017). During the past few decades, heavy metals (including Cd) have become the greatest pollutants worldwide due to the rapid development of the chemical industry, metallurgy, and electroplating

Abbreviations: HE, hyperaccumulating ecotype; NHE, non-hyperaccumulating ecotype; PCR, Plant cadmium resistance.

(Hu et al., 2016). For instance, Cd is reported to be the most severe pollutant for agricultural soils in China (Li et al., 2014; Zhao et al., 2015; Shi et al., 2019). Phytoremediation of heavy metals is an efficient and economical soil remediation technique to clear or alleviate heavy metal pollution in soils (Liu et al., 2018). Hyperaccumulators can accumulate 100–1,000-fold higher heavy metals than normal plants without toxic consequences (Rascio and Navari-Izzo, 2011) and, therefore, are of high scientific interest as a representative plant material to extract heavy metals with great ability (Pollard et al., 2014).

To grow healthily in highly contaminated soils, a sophisticated detoxification system must exist in the plants of hyperaccumulators, especially for the root systems, which suffer first from heavy metal toxicity. Therefore, high root tolerance is the precondition for hyperaccumulating plants to grow well under high Cd stress. Roots of hyperaccumulators might present superior antioxidative defenses under Cd condition (Boominathan and Doran, 2003; Chiang et al., 2006; Wu et al., 2015) or sequestrated Cd in vacuoles and cell walls (Fu et al., 2011; Parrotta et al., 2015). However, the most important strategy for the root resistance of hyperaccumulators is to efflux Cd out of the root cells and subsequently translocate to the aboveground parts of plants. In hyperaccumulator *Noccaea caerulescens*, the great ability of xylem loading is one of the main processes participating in Cd hyperaccumulation (Sterckeman et al., 2015). High expression of *HMA4* in *Arabidopsis halleri* supports the enhanced metal flux from the root symplasm into the xylem vessels necessary for shoot metal hyperaccumulation (Hanikenne et al., 2008). This is different from the strategies of some regular or resistant plants to prevent heavy metals from accumulating in plants. For example, OsZIP1 can function as a metal exporter in rice when zinc (Zn), copper (Cu), and Cd are present in excess in the environment and decrease the metal accumulation in plants (Liu et al., 2019). Therefore, the investigation of transporters involved in the efflux of Cd in the roots of hyperaccumulators may facilitate our understanding of metal tolerance in roots as well as its hyperaccumulation in shoots.

Plant cadmium resistance (PCR) family transporters, especially *PCR1* and *PCR2*, are involved in the efflux of Cd and other bivalent cations from cells to the outside, mainly via the lateral transport and xylem loading in the roots. The first PCR family gene found in *A. thaliana*, named *AtPCR1*, showed a strong tolerance for Cd in the selection of Cd-tolerant genes of *A. thaliana* using yeast Cd-sensitive mutants (Song et al., 2004). The study of OsPCR1 in rice showed that the *OsPCR1* knockdown lines decreased the weight and Cd content of grains (Song et al., 2015). AtPCR2 is mainly distributed on the epidermis of the root hair zone, as well as the vascular and epidermal cells of the elongation zone, which plays a very important role in the translocation of Zn (Song et al., 2010). In *Brassica juncea*, BjPCR1 was found to be localized on the plasma membrane of the root epidermal cells at the subcellular level and is mainly responsible for the absorption and root-to-shoot transportation of calcium (Ca) (Song et al., 2011). However, to the best of our knowledge, no study has been undertaken on the function of the PCR family protein in hyperaccumulating plants.

Sedum alfredii Hance, a Chinese native Zn/Cd hyperaccumulator belonging to the Crassulaceae family (Yang et al., 2004, 2006), has a high capacity for tolerating, translocating, and accumulating high amounts of Cd (Lu et al., 2008; Tian et al., 2011, 2017). The Cd concentration in the shoots of HE *S. alfredii* is as high as 9,000 mg/kg (Yang et al., 2004). However, the molecular mechanisms involved in root resistance and translocation of Cd remain unknown. In the present study, a high expression gene belonging to the PCR family, named *SaPCR2*, was cloned from this plant species and the functions of this gene were investigated.

MATERIALS AND METHODS

Plant Materials and Growth Conditions

The hyperaccumulating ecotype (HE) *S. alfredii* and its non-hyperaccumulating ecotype (NHE) were originally collected from a Zn/Cd mine in Quzhou (Zhejiang province, China) and tea plantation in Hangzhou (Zhejiang province, China), respectively. The plant materials used in this experiment were cultured after several generations of asexual cuttings. The same seedlings were cut and exposed to deionized water until rooting and were then added to 1/4, 1/2, and full nutrient solution gradually, which was replaced every 3 days. The formulation of the full nutrient solution contained 2.0 mM $Ca(NO_3)_2$, 0.7 mM K_2SO_4, 0.1 mM KH_2PO_4, 0.1 mM KCl, 0.5 mM $MgSO_4$, 20 μM Fe-EDTA, 5 μM $ZnSO_4$, 10 μM H_3BO_3, 5 μM $ZnSO_4$, 0.5 μM $MnSO_4$, 0.2 μM $CuSO_4$, and 0.01 μM $(NH_4)_6Mo_7O_{24}$. The temperature of incubation was set at 25–28°C, with a 16 h light/8 h dark cycle. Three-week-old seedlings were used in subsequent experiments.

SaPCR2 Cloning and Sequence Analysis

The results of the previous transcriptome sequence of HE *S. alfredii* illustrated that the sequence (Sa_Contig10958, GenBank: HE728063) was predicted to encode the gene from the *PCR* family (Gao et al., 2013). According to this sequence (Sa_Contig10958), we designed RACE primers to clone the full-length sequence from HE and NHE *S. alfredii* using the Smart RACE cDNA amplification kit (Clontech). The cDNA sequences of *SaPCR2* are the same in two ecotypes (**Supplementary Figure S1**), so we named this gene as *SaPCR2*. The primer used for *SaPCR2* 5′-RACE was 5′-CACGGAGACTCTTGTAGATCATAC-3′ and the primer used for *SaPCR2* 3′-RACE was 5′-TGCCATCTACGGCCTGATTT-3′. The transmembrane domain of SaPCR2 was predicted using the TMHMM Online analysis tool[1]. The protein sequence alignment analysis was compared with ClustalX. The phylogenetic tree analysis was performed using MEGA5.0 with the neighbor-joining method.

Expression Pattern of *SaPCR2*

Two ecological types of *S. alfredii* were treated by $CdCl_2$ with different concentrations (HE: 10 and 100 μM, NHE: 10 μM)

[1]http://www.cbs.dtu.dk/services/TMHMM/

and times (0, 6, 24 h, 3, and 7 days). The roots, stems, and leaves of each plant were separated and frozen rapidly in liquid nitrogen. The total RNA was extracted using a Spin Column Plant Total RNA Purification Kit (Sangon) and then synthesized to cDNA with a HiScript II Q RT SuperMix for qPCR (+ gDNA wiper) (Vazyme). Real-time quantitative PCR (RT-qPCR) was performed using a ChamQ SYBR Color qPCR Master Mix (Without ROX) (Vazyme), with LightCycler 480 System (Roche, United States). The RT-qPCR protocol was as follows: 95°C for 3 min, 40 cycles of 95°C for 10 s, 60°C for 30 s. The melting-curve analysis was included to verify the specificity of the primer. The mean amplification efficiency was analyzed with the LinReg software (Ruijter et al., 2009). The specific primers for RT-qPCR were designed according to the *SaPCR2* sequence as follows: *SaPCR2* forward 5′-GCGGTGGGATGTGGTCTAC-3′ and *SaPCR2* reverse 5′-CGATAATCTCGGCTATTTGGC-3′, *SaACTIN1* forward 5′-TGTGCTTTCCCTCTATGCC-3′, and reverse: 5′-CGCTCAGCAGTGGTTGTG-3′ (Chao et al., 2010). The relative expression levels were calculated using $2^{-\Delta Ct}$ method.

Plasmid Construction

All the *SaPCR2* sequences for reconstruction were amplified using the ClonExpress II One Step Cloning Kit (Vazyme), and the primers used are listed in **Table 1**. To generate yeast expression vectors, the open reading frame of *SaPCR2* was cloned into the *Spe*I and *Eco*RI sites of the pDR196 (*pDR196-SaPCR2* vector), which contained a uracil amino acid selection marker. To produce the green fluorescent protein (*GFP*)-fused *SaPCR2* expression vector ($35S_{pro}$-*SaPCR2-GFP* vector) for transient expression in tobacco, the open reading frame of *SaPCR2* sequence without stop codon was cloned into the pCAMBIA 1300-eGFP vector between the *Kpn*I and *Bam*HI sites, which was controlled by the cauliflower mosaic virus (CaMV) 35S promoter. Taking pCAMBIA 1300 as the plant overexpression vector, we cloned the full-length *SaPCR2* into the *Acc*I and *Xba*I restriction sites.

Subcellular Localization of SaPCR2

The tobacco leaves were used to observe the subcellular localization of SaPCR2. *Agrobacterium tumefaciens* GV3101 monoclonal containing the $35S_{pro}$-*SaPCR2-GFP* vector was picked, activated, and suspended in 10 mM $MgCl_2$ and 10 mM MES (pH = 5.6). The final OD_{600} of the bacteria concentration was adjusted to approximately 0.4 and it was then injected into the epidermis of the tobacco leaves using a needleless syringe, cultured for 24–36 h. The epidermis was treated with 0.8 M mannitol for at least 10 min to induce plasmolysis and the fluorescence was detected using a confocal microscopy (LSM700, Carl Zeiss, Germany). FM 4–64 fluorescence was used as a plasma membrane marker.

TABLE 1 | Primers used for vector construction of *SaPCR2*.

Yeast expression vector (*pDR196-SaPCR2* vector)	Forward	tataccccagcctcgactagt ATGTATCCATCTTTGTCTG
	Reverse	gataagcttgatatcgaattc TCATCTACTCATCCCCTGC
GFP expression vector ($35S_{pro}$-*SaPCR2-GFP* vector)	Forward	tacgaattcgagctcggtaccATGTATCC ATCTTTGTCTGAAAATGAG
	Reverse	catgtcgactctagaggatcc TCTACTCATCCCCTGCGGAA
Plant expression vector ($35S_{pro}$-*SaPCR2* vector)	Forward	aagcttatcgataccgtcgac ATGTATCCATCTTTGTCTG
	Reverse	gggggatccactagttctaga TCATCTACTCATCCCCTGC

The lowercase indicates recombinant sequences.

Cd Resistance in Yeast Strains Expressing *SaPCR2*

To express the SaPCR2 in yeast, the *pDR196-SaPCR2* vector or pDR196 empty vector were transformed into the wild type BY4743 and Zn/Cd-sensitive mutant Δ*zrc1* (MAT1; his3; leu2; met15; ura3; YMR243c: kanMX4) using the LiAc/PEG/ssDNA method (Gietz and Schiestl, 2007). The positive strains were screened out by selected synthetic dropout (SD) solid media (absence of uracil amino acid) and verified by PCR with specific primers: forward 5′-GCGGTGGGATGTGGTCTAC-3′ and reverse 5′-CGATAATCTCGGCTATTTGGC-3′. For Cd tolerance assay, yeast cells were cultured in selected liquid SD until OD_{600} = 1. Then, 5 μL serial dilutions (OD_{600} = 1.0, 0.1, 0.01, and 0.001) were spotted on SD with 0, 10, and 60 μM $CdCl_2$ at 30°C. Photographs were taken after 3-days incubation. For Cd accumulation testing, the yeast was cultured overnight to OD_{600} = 0.1 and then added to the SD liquid medium with 2.5, 5.0, and 10.0 μM $CdCl_2$ for 24 h at 30°C. The yeast cells were collected via centrifugation and washed three times with ultra-pure water. The cells were dried for 2 days at 85°C and digested in HNO_3 to determine the heavy metal concentration in the yeast strains by inductively coupled plasma mass spectrometry (Agilent, United States).

Plant Transformations

To investigate *SaPCR2* in *S. alfredii*, the transgenic system of NHE *S. alfredii* was constructed. The seeds of NHE *S. alfredii* were sterilized in 0.1% $HgCl_2$ for 5 min and washed with sterile water five to six times and were then spotted on 1/2 Murashige and Skoog (MS) medium (Murashige and Skoog, 1962). After approximately 8 weeks, young stems of the aseptic seedlings were cut into approximately 1–2 cm and transferred to callus-inducing medium (**Table 2**) with 6-benzylaminopurine (6-BA) and 1.0 mg/L 2,4-dichlorophenoxyacetic acid (2,4-D). When the stem segments appeared to be differentiated and enlarged, *A. tumefaciens* GV3101 (OD_{600} = 0.6) was used for transfection. Then the explants were co-cultured with *Ag. tumefaciens* containing the $35S_{pro}$-*SaPCR2* vector for 2 days and then removed to the selection medium (**Table 2**). The hyg-resistant explants were moved to differential medium (**Table 2**). After emergence, the medium was changed to 1/2 MS-agar medium. Then, the well-rooted plants were moved to nutrient solution for subsequent experiments. *SaPCR2* overexpressing *A. thaliana* was obtained using the *Agrobacterium*-mediated floral dip method (Clough and Bent, 1998).

TABLE 2 | Optimization of the transgenic system of *S. alfredii*.

Process	Medium	Main operation
Seed germination	1/2 MS	Sterilize seed and spot on medium for 8 weeks.
Induction	MS + 0.5 mg/L 6-BA + 1.0 mg/L 2,4-D	Cut stem into 1–2 cm sections and culture for 3 days.
Cocultivation	MS + 0.5 mg/L 6-BA + 1.0 mg/L 2,4-D + 100 mg/L acetosyringone (AS)	Cultivate bacterial solution until OD_{600} reaching 0.6, then resuspend by resuspension (MS + 100 mg/L AS) and infect for 15 mins. The total cocultivation time should not exceed 2 days.
Selection	MS + 0.5 mg/L 6-BA + 1.0 mg/L 2,4-D + 100 mg/L Timentin + 30 mg/L hygromycin (Hyg)	Soak the explants into three 100 mg/L Timentin for 15 mins, then wash three to four times using sterile water.
Differentiation	MS + 0.5 mg/L 6-BA + 0.1 mg/L 1-Naphthaleneacetic acid (NAA) + 100 mg/L Timentin + 30 mg/L Hyg	Cut healthy callus and transfer to differentiation medium, change medium once at 14 days.
Rooting	1/2 MS + 100 mg/L Tim + 30 mg/L Hyg	Move robust differentiated shoots to rooting medium.

The total plant genomic DNA was extracted from the fresh leaves of transgenic plants and their wild type using the CTAB method, identified by the following primers: forward 5′-ATGTATCCATCTTTGTCTG-3′ and reverse 5′-TCATCTACTCATCCCCTGC-3′. The expression level of *SaPCR2* in the transgenic NHE *S. alfredii* was investigated by RT-qPCR as mentioned above. Two independent transgenic lines of NHE *S. alfredii* (SaPCR2-L1, SaPCR2-L2) and *A. thaliana* of T2 plants (SaPCR2-OX1, SaPCR2-OX2) were identified as *SaPCR2* overexpressing lines for subsequent analysis.

Cd Concentration of Plants

The seeds of the transgenic *A. thaliana* were collected and spotted on 1/2 MS solid medium and then 4-days-old seedlings were transferred to nutrient agar plates with 15 or 30 μM $CdCl_2$ for 7 days. There were 20 plants for one treatment and each treatment was repeated three times. Well-rooted transgenic NHE *S. alfredii* lines and their corresponding wild type plants in the same growth states were hydroponically cultured for 3 weeks and then treated with 10 μM $CdCl_2$ for 5 days. For Cd concentration determination, all the plant samples were rinsed in 20 mM Na_2-EDTA to remove excess Cd^{2+} attached to the surface and were then separated into roots, stems, and leaves for drying and digesting in HNO_3-H_2O_2. The Cd concentration was analyzed using an inductively coupled plasma optical emission spectrometer (Agilent, United States).

The Cd uptake (μg/kg root FW) = Total Cd in the plants (μg)/Fresh weight of roots (kg).

Plasma Membrane Integrity and Lipid Peroxidation of Roots

The plants were exposed to 10 μM $CdCl_2$ for 7 days. The plasma membrane integrity and lipid peroxidation of roots were

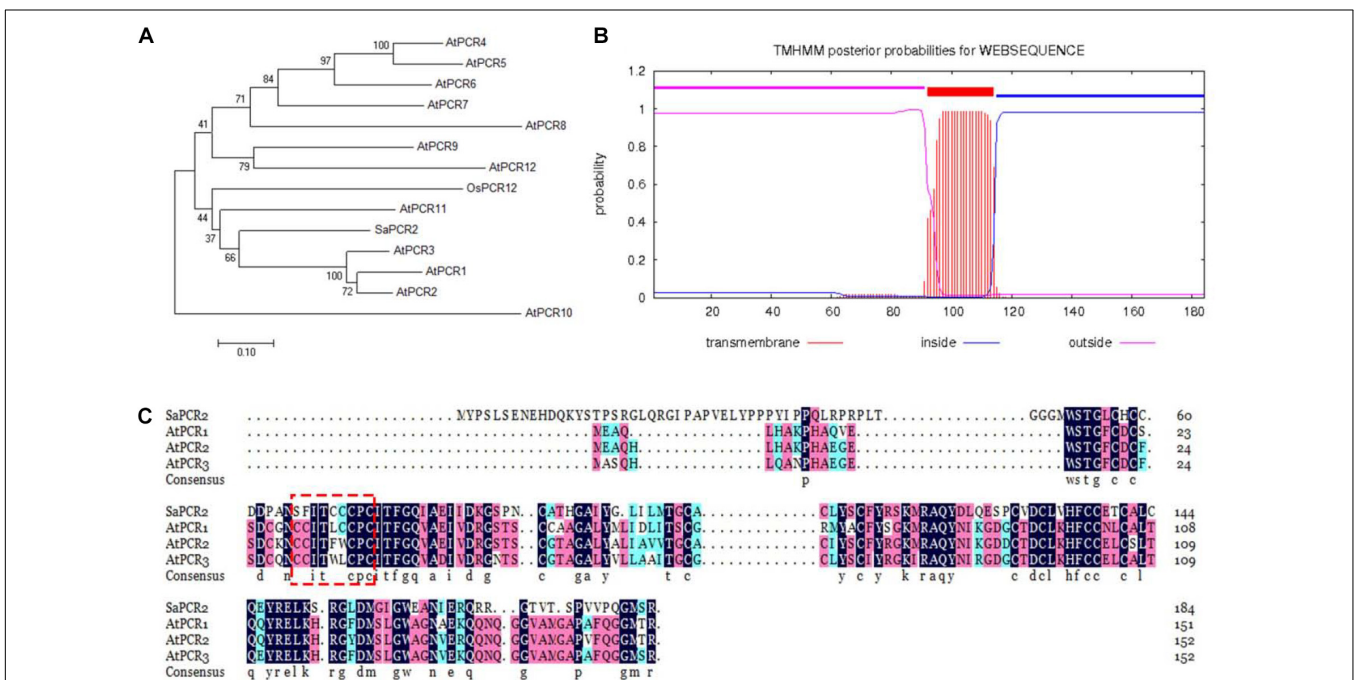

FIGURE 1 | Sequence analysis of SaPCR2. **(A)** Phylogenic tree of SaPCR2 proteins in *Arabidopsis thaliana*, *Oryza sativa,* and *Sedum alfredii*. The 0.1 scale showed substitution distance. **(B)** SaPCR2 protein transmembrane topology prediction. **(C)** Amino acid sequence alignment of SaPCR2, AtPCR1, AtPCR2, and AtPCR3. Identical residues are shown in black, residues with a similarity over 70% are shown in red, and 50% or more are shown in blue. The fully conserved CCXXXXCPC domains are framed by the red box.

investigated using the analysis of Evans blue uptake, MDA content, as well as Schiff's reagent staining (Tian et al., 2012).

RESULTS AND DISCUSSION

Sequence Analysis of SaPCR2

As an unessential element, Cd is suggested to enter/exit plant cells through the transporters of bivalent cations for nutrient elements, such as Zn/Mn/Fe (Ueno et al., 2008; Willems et al., 2010; Sasaki et al., 2012). The PCR family has been confirmed as membrane transporters not only for the transportation of Cd, but also for Zn, Fe, and Ca (Song et al., 2004, 2010, 2011). In this study, the putative *PCR* gene was cloned from *S. alfredii* according to the published transcription sequence (Gao et al., 2013). Phylogenetic analysis revealed that the putative PCR amino acid sequence was 44.68% similar to AtPCR2 belonging to *A. thaliana* (**Figure 1A**). Therefore, we named this PCR transporter *SaPCR2*. The SaPCR2 protein sequence contained 184 amino acids and a transmembrane domain predicted with the TMHMM Online analysis tool (**Figure 1B**). A multiple sequence alignment with PCR from *A. thaliana* was undertaken, showing that the SaPCR2 protein exhibited the same familial signature (**Figure 1C**). Analysis of the amino acid sequences showed that SaPCR2 contained a highly conserved CCXXXXCPC domain. This small cysteine-rich protein may play an important role in the detoxification mechanisms of Cd (Song et al., 2004). Therefore, SaPCR2 identified in the HE *S. alfredii* may be of great importance in Cd transportation.

SaPCR2 Is Highly Expressed in the Roots of HE *S. alfredii*

To understand the expression characteristics of *SaPCR2* gene, we analyzed its expression in the roots and shoots of the two *S. alfredii* ecotypes using RT-qPCR. High expression of *SaPCR2* was observed in the roots of the HE *S. alfredii*, but not in the shoots (**Figure 2A**). The expression level of *SaPCR2* in the roots was approximately 33-fold higher than that in the stems of the HE (**Figure 2A**). This differed from that of *AtPCR1*, which was exclusively expressed in the aboveground parts of *A. thaliana* (Song et al., 2004), yet similar to that of *BjPCR1* in *Brassica juncea* (Song et al., 2011). To investigate the effects of

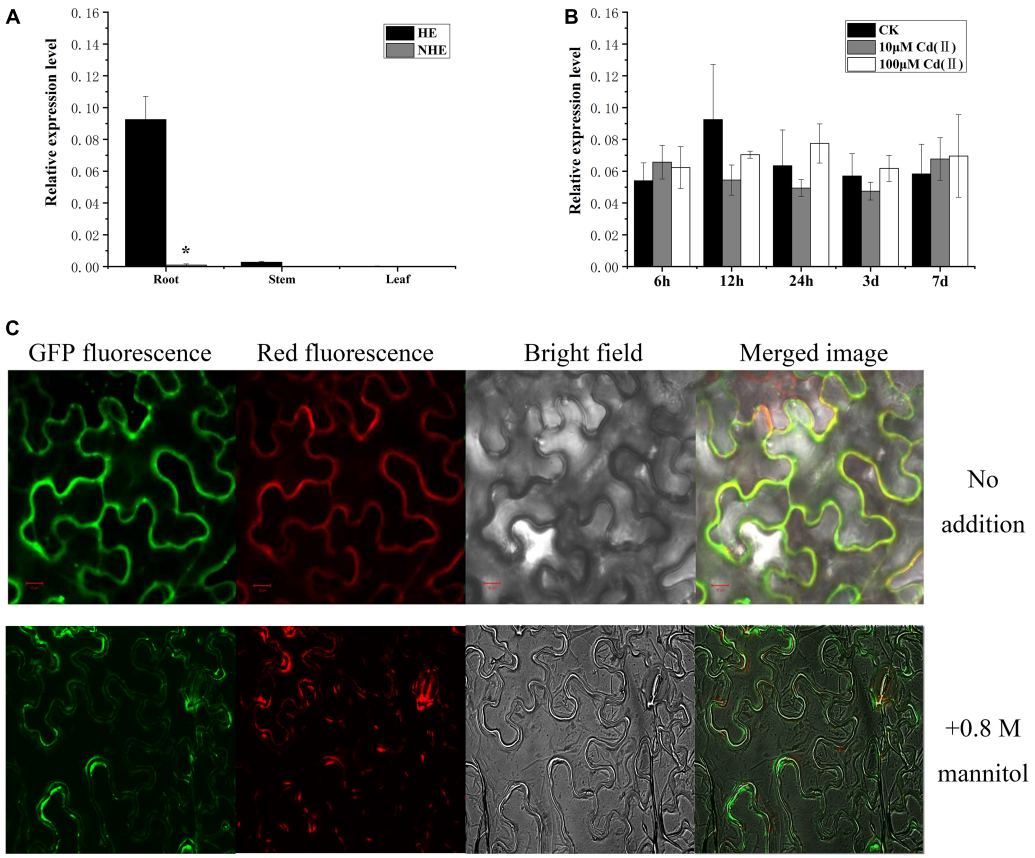

FIGURE 2 | Expression of *SaPCR2* and subcellular location of SaPCR2. **(A)** Expression level of *SaPCR2* in roots, stems, and leaves of two ecotypes (HE and NHE) of *Sedum alfredii*. **(B)** Expression levels of *SaPCR2* in the roots of the HE *S. alfredii* at different time points. The plants were treated with 0, 10, or 100 μM $CdCl_2$ for 6, 12, 24 h, 3, or 7 days. Error bars are ± SE of $n = 3$. Relative expression levels were normalized to the level of constitutively expressed gene *SaACTIN1*. *Indicates significant difference between ecotypes ($p < 0.05$). **(C)** Subcellular location of SaPCR2 in epidermal cells of tobacco. Distribution of green fluorescent protein (GFP)-SaPCR2 fusion protein and red fluorescent protein (plasma membrane marker) in tobacco leaf epidermis cells. Scale bar = 10 μm.

Cd exposure on *SaPCR2* expression, we analyzed the variations in the *SaPCR2* expression levels in the HE roots after different Cd exposure for 6 h to 7 days. Cd exposure did not result in any significant variation of the *SaPCR2* expression levels in the HE roots (**Figure 2B**). Therefore, this gene is not induced by Cd stress. In plants of NHE *S. alfredii*, the *SaPCR2* expression was not observed in either roots or shoots regardless of Cd treatments (**Figure 2A**).

These results are similar to the transcript levels of several reported Cd-related transporters in plants of HE *S. alfredii*. The high expression of these genes may result from the adaption of high Cd exposure during long-term evolution. For example, *SaHMA3* plays an essential role in Cd detoxification and its expression in HE *S. alfredii* was also significantly higher than that in NHE plants (Zhang et al., 2016), however, no significant difference was observed after Cd treatment (Liu et al., 2017). The high expression levels of these transporters in plants of HE *S. alfredii* may result from the long-term adaption and evolution of this plant species exposed to the high heavy metal levels in its natural habitat soils.

SaPCR2 Localizes to the Plasma Membrane and Enhances Cd Resistance in Yeast

To determine the subcellular location of SaPCR2, *GFP* fused to *SaPCR2* under the control of the CaMV 35S promoter (*35S$_{pro}$-SaPCR2-GFP*) construct was generated for the transient expression in epidermal cells of tobacco leaves. The green fluorescence signal of the SaPCR2-GFP fusion protein was observed in the plasma membrane showing co-localization with the plasma membrane marker dye FM 4-64 (**Figure 2C**). When exposed to a high concentration of sucrose, the green fluorescence signal was in close to the cell wall, but not organelle membrane, which was similar with BjPCR1 (Song et al., 2011).

The effect of SaPCR2 on Cd resistance was assayed in Δ*zrc1* yeast strains. The *SaPCR2* transcript was recombined in the yeast expression vector pDR196. In the absence of Cd, there was no significant difference between the transgenic yeast strains (**Figure 3A**). On the SD solid medium supplemented

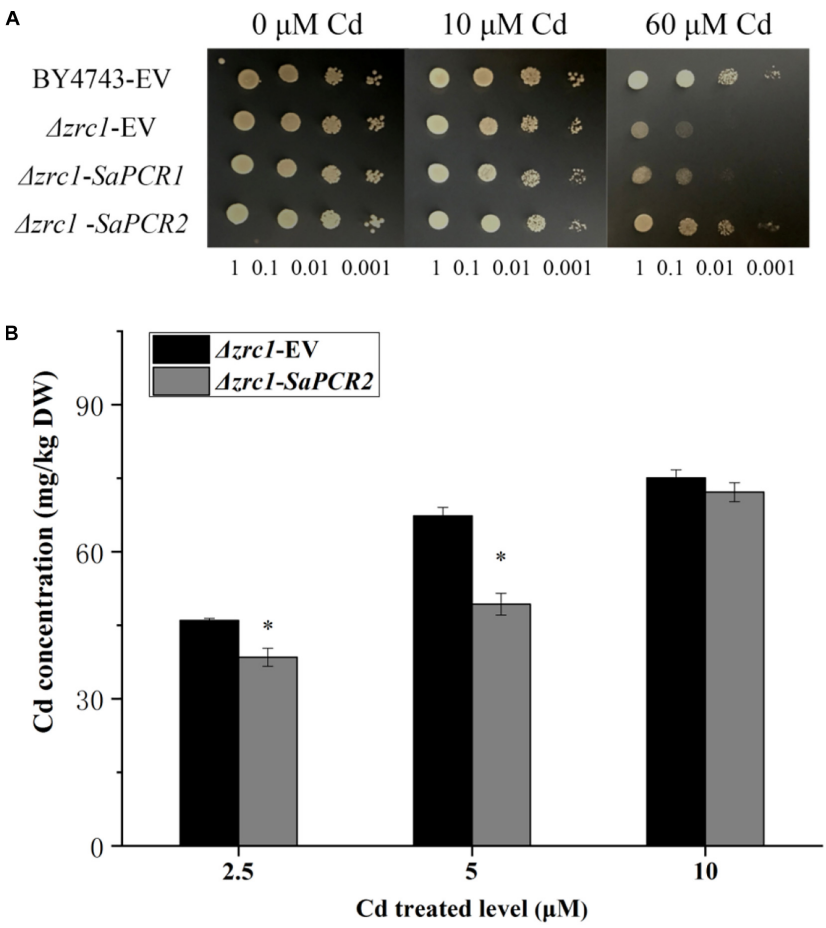

FIGURE 3 | Expressing *SaPCR2* enhanced cadmium (Cd) tolerance in yeast mutant Δ*zrc1* by reducing Cd concentration. **(A)** The yeast strain BY4743 and Δ*zrc1* transformed with *pDR196-SaPCR2* vector or *pDR196* empty vector (EV) were diluted (OD_{600} = 1.0, 0.1, 0.01, and 0.001) and spotted on SD medium with 0, 10, and 60 μM $CdCl_2$ for 3 days at 30°C. **(B)** Cd concentration in yeasts. Δ*zrc1* strains expressed EV and *pDR196-SaPCR2* were cultured in SD liquid medium with 2.5, 5, and 10 μM $CdCl_2$ for 24 h at 30°C. Error bars are ± SE of $n = 4$. *Indicates significant differences between Δ*zrc1*-EV and Δ*zrc1-SaPCR2* ($p < 0.05$).

with 60 μM $CdCl_2$, the growth of the empty vector (EV) and *SaPCR2*-expressing lines in the Δ*zrc1* backgrounds were inhibited. However, the Δ*zrc1* strain transfected with EV showed higher sensitivity to Cd than the Δ*zrc1* strain expressing *SaPCR2* (**Figure 3A**). To test the Cd-transporting activity of SaPCR2, we determined the Cd concentration in the *SaPCR2*-expressing Δ*zrc1* mutant strain treated with Cd. When cultured in the presence of 2.5 or 5.0 μM $CdCl_2$, SaPCR2-expressing Δ*zrc1*

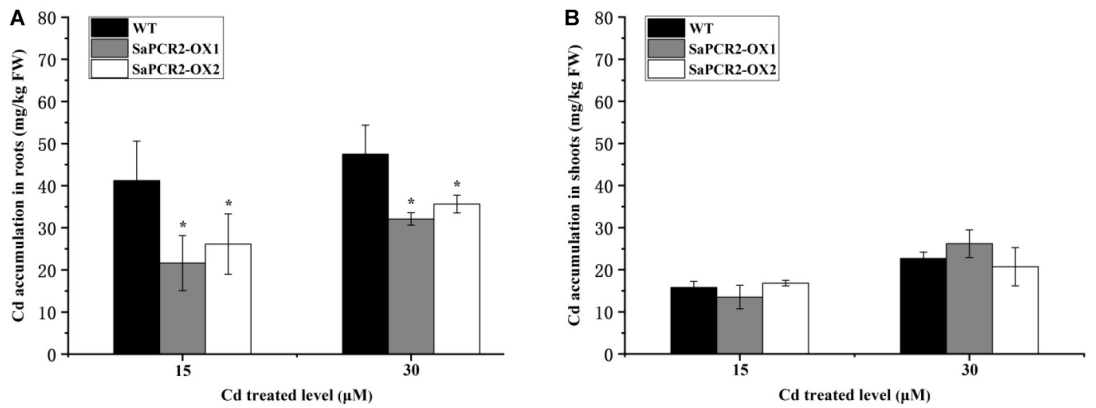

FIGURE 4 | Cd concentration in *SaPCR2* overexpressing *Arabidopsis thaliana*. Cd concentration of **(A)** roots and **(B)** shoots in wild type, OX1, and OX2. Plants were cultured on 1/2 MS solid medium with 15 and 30 μM $CdCl_2$ for 7 days, every 20 plants for one treatment, each treatment repeated three times. Error bars are ± SD of $n = 3$. *Indicates significant difference between genotypes ($p < 0.05$).

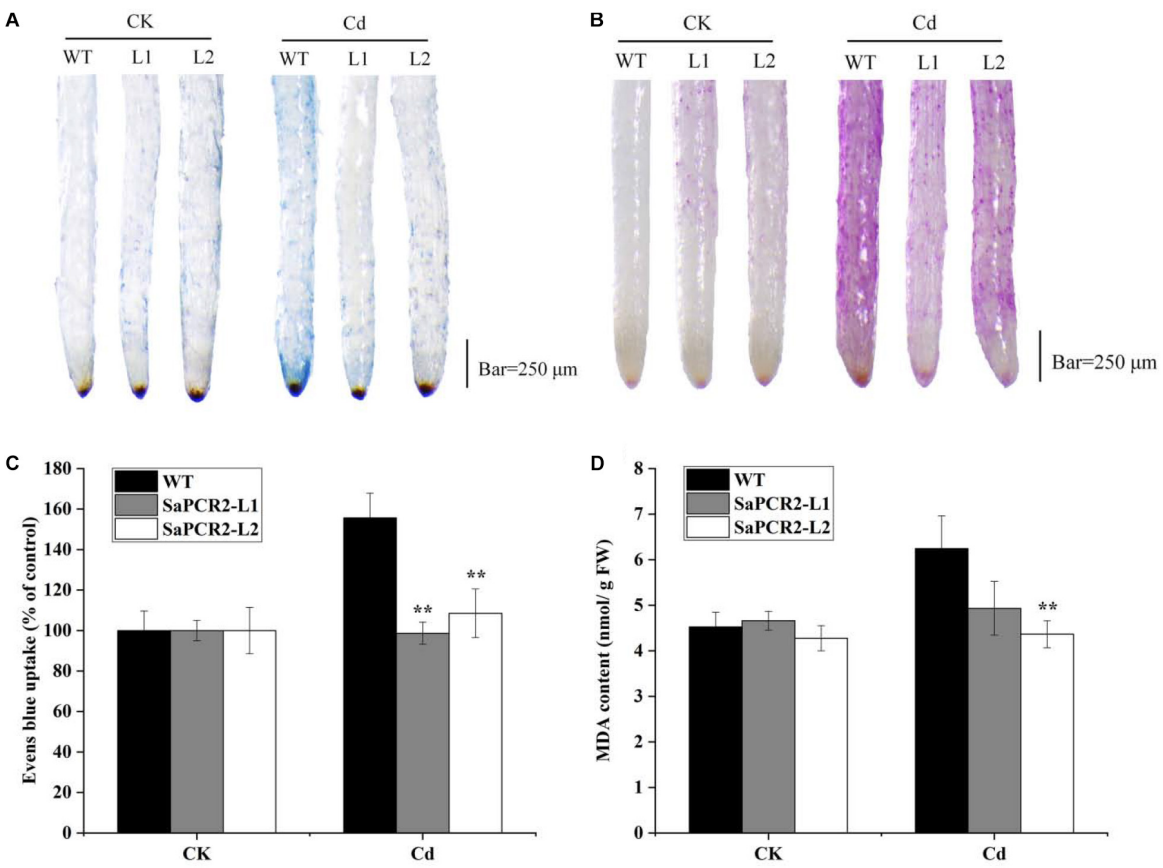

FIGURE 5 | Cd-induced loss of plasma membrane integrity **(A,C)** and lipid peroxidation **(B,D)** in the root tips of *SaPCR2* overexpressing NHE *Sedum alfredii* line (L1 and L2). The plants were cultured in nutrient solution with 10 μM $CdCl_2$ for 7 days, each treatment was repeated three times. Error bars are ± SD of $n = 3$. **Indicates significant difference between genotypes ($p < 0.01$). Scale bar = 250 μm.

cells accumulated lower Cd than EV-transformed control cells ($p < 0.05$) (**Figure 3B**). These results indicate that SaPCR2 enhanced yeast Cd resistance by reducing Cd concentration in cells. Therefore, the SaPCR2 may function as a transporter at plasma membrance in the roots of HE *S. alfredii*, which mediates Cd reduction in cells.

Heterologous of *SaPCR2* Reduced Cd Accumulation in *A. thaliana* and NHE *S. alfredii*

To further determine the effects of *SaPCR2* under Cd stress, we overexpressed *SaPCR2* in *A. thaliana*. Two lines transfected with *SaPCR2* (OX1 and OX2) were selected for subsequent experiments (**Supplementary Figure S2A**). The root lengths of transgenic lines were similar to the wild type in each treatment (**Supplementary Figures S2B,C**). However, the overexpressed *SaPCR2* significantly decreased Cd concentration in the roots compared with the wild type when plants were grown with 15 or 30 μM $CdCl_2$ ($p < 0.05$) (**Figure 4**). The Cd accumulations in the roots of two independent overexpressing lines were 27–37% and 18–21% lower than the wild type, respectively (**Figure 4A**). By contrast, there was no significant difference in the accumulations of Cd in the shoots (**Figure 4B**). These results suggest that the overexpressed *SaPCR2* decreased Cd accumulation in the roots of *A. thaliana*.

Due to the much higher expression levels of *SaPCR2* in HE plants than that of NHE, we generated *SaPCR2* NHE *S. alfredii* overexpressing lines (L1 and L2) to test the effect of *SaPCR2* in NHE plants under Cd exposure. Higher expression levels of *SaPCR2* were observed in L1 and L2. Compared with the wild type, the transcript levels of the *SaPCR2* in the roots of overexpressing lines were 109–114-fold higher (**Supplementary Figures S3A,B**). After culturing in nutrient solution with 10 μM $CdCl_2$, the leaves of wild type (NHE *S. alfredii*) wilted and the biomass showed a downtrend (**Supplementary Figure S3D**), whereas the L1 and L2 plants showed little toxicity phenomenon, especially in the roots (**Figure 5**). The Cd concentrations in the roots of the wild type were significantly higher than those of the *SaPCR2* overexpressing lines ($p < 0.05$) (**Figure 6**). In the stems, L2 contained approximately 26% lower concentrations than the wild type; however, there was no significant difference in the leaves (**Figure 5**). Therefore, the heterologous overexpressing of

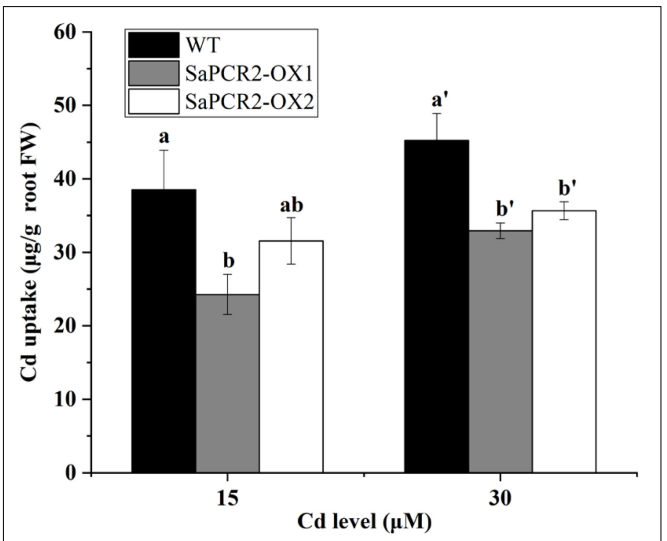

FIGURE 7 | Cd uptake in wild type and *SaPCR2*-overexpressed transgenic *Arabidopsis thaliana* lines (OX1 and OX2). The plants were cultured on 1/2 MS solid medium with 15 and 30 μM $CdCl_2$ for 7 days, every 20 plants for one treatment, each treatment repeated three times. Error bars are ± SE of $n = 3$. Different letters indicate significant differences between genotypes ($p < 0.05$).

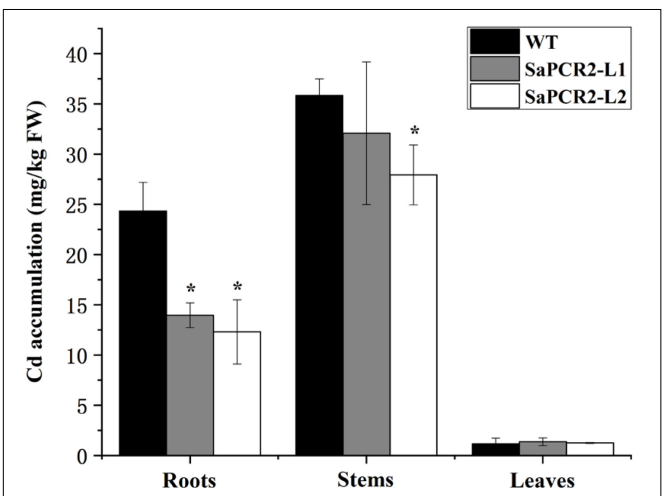

FIGURE 6 | Cd concentration in the root, stem, and leaf of wild type and *SaPCR2*-overexpressed transgenic NHE *Sedum alfredii* lines (L1 and L2). The plants were cultured in nutrient solution with 10 μM $CdCl_2$ for 5 days, each treatment was repeated three times. Error bars are ± SD of $n = 3$. *Indicates significant difference between genotypes ($p < 0.05$).

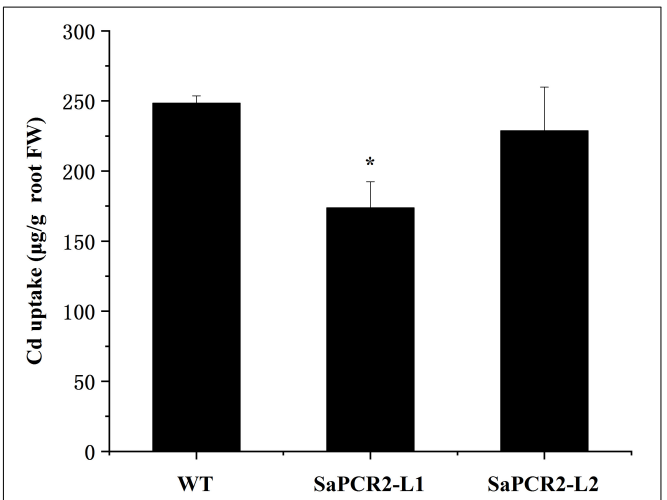

FIGURE 8 | Cd uptake in wild type and *SaPCR2*-overexpressed transgenic NHE *Sedum alfredii* lines (L1 and L2). The plants were cultured in nutrient solution with 10 μM $CdCl_2$ for 5 days, each treatment repeated three times. Error bars are ± SE of $n = 3$. *Indicates significant difference between genotypes ($p < 0.05$).

SaPCR2 significantly reduced Cd accumulation in the roots of the transgenic NHE *S. alfredii*, without translocating increased Cd to its shoots.

Overexpression of *SaPCR2* Provides a Route to Leak Cd Out of the Root Cells

Currently, many studies on the physiological mechanisms of Cd tolerance in the roots of hyperaccumulators have been undertaken, which have shown three main mechanisms in the roots of HE *S. alfredii* that play an important role in Cd homeostasis, including (1) transportation: Cd could be transformed from root to shoot to avoid excess Cd accumulation in roots (Lu et al., 2008, 2009; Tian et al., 2017); (2) segmentation: HE *S. alfredii* can transfer Cd from the cytoplasm to the vacuole or cell wall (Tian et al., 2010, 2017); (3) chelation and anti-oxidation: small molecule compounds and intracellular Cd^{2+} are combined to reduce the ion concentration and the antioxidant system is activated to alleviate the Cd stress at the same time (Tian et al., 2012). Many transporters have been used to testify the mechanisms mentioned above. For example, ZIP, HMA, or YSL proteins are implicated in Cd transport across membranes (Gallego et al., 2012). P-type ATPases HMA2 and HMA4, localizing to the plasma membrane, play essential roles in controlling Cd translocation (Hussain et al., 2004; Wong and Cobbett, 2009; Nocito et al., 2011). CAL1 acts by chelating Cd in the cytosol and facilitating Cd secretion to extracellular spaces, thus lowering the cytosolic Cd concentration while driving long-distance Cd transport via xylem vessels (Luo et al., 2018). Therefore, in hyperaccumulating plants, the capacity to translocate Cd to the shoots is a comprehensively proved mechanism involved in the tolerance of the roots. However, further calculation showed that overexpressing *A. thaliana* and NHE *S. alfredii* lines of *SaPCR2* had lower Cd uptake than the wild type (**Figures 7**, **8**). Therefore, the Cd decrease in roots not only depends on the efficient translocation systems, but is also attributed to the limit of Cd uptake and accumulation. For plants, there are two approaches to reduce the Cd concentration in roots—rapid root-to-shoot translocation and efficient efflux out of plants, both of which essentially protect the roots from too much Cd poison. For instance, heavy metal P-type ATPase OsHMA6 in rice, which is likely a Cu efflux protein (Zou et al., 2020). Therefore, we proposed a mechanism that has not been reported in the mechanism of Cd tolerance in HE *S. alfredii*, "leaking Cd out of plants."

CONCLUSION

The present study identified a gene coding SaPCR2 from HE *S. alfredii* expressed in roots. This transporter was localized to the plasma membrane. Heterologous overexpression of *SaPCR2* reduced Cd uptake and accumulation in plants. Therefore, these findings improve the Cd detoxification mechanisms of hyperaccumulators and may contribute to the development of phytoremediation and food safety in the future.

DATA AVAILABILITY STATEMENT

The datasets presented in this study can be found in online repositories. The names of the repository/repositories and accession number(s) can be found in the article/**Supplementary Material**.

AUTHOR CONTRIBUTIONS

XG, JL, JiaZ, and JieZ performed the experiments. JL, LL, and SC wrote and revised the manuscript. LL designed, supervised, and obtained funding for the project. All authors gave final approval for publication.

FUNDING

This work was supported by projects from the National Natural Science Foundation of China (41977130 and 31672235), a project from the National Key Research and Development Program of China (2016YFD0800401).

ACKNOWLEDGMENTS

We sincerely thank Prof. Tian Shengke for providing the seeds of NHE *S. alfredii* and Editage (www.editage.cn) for language editing.

SUPPLEMENTARY MATERIAL

The Supplementary Material for this article can be found online at: https://www.frontiersin.org/articles/10.3389/fpls.2020.568887/full#supplementary-material

REFERENCES

Boominathan, R., and Doran, P. M. (2003). Cadmium tolerance and antioxidative defenses in hairy roots of the cadmium hyperaccumulator, *Thlaspi caerulescens*. *Biotechnol. Bioeng.* 83, 158–167. doi: 10.1002/bit.10656

Chao, Y. E., Zhang, M., Feng, Y., Yang, X. E., and Islam, E. (2010). cDNA-AFLP analysis of inducible gene expression in zinc hyperaccumulator *Sedum alfredii* Hance under zinc induction. *Environ. Exp. Bot.* 68, 107–112. doi: 10.1016/j.envexpbot.2009.11.013

Chiang, H. C., Lo, J. C., and Yeh, K. C. (2006). Genes associated with heavy metal tolerance and accumulation in Zn/Cd hyperaccumulator *Arabidopsis halleri*: a genomic survey with cDNA microarray. *Environ. Sci. Technol.* 40, 6792–6798. doi: 10.1021/es061432y

Clough, S. J., and Bent, A. F. (1998). Floral dip: a simplified method for *Agrobacterium*-mediated transformation of *Arabidopsis thaliana*. *Plant J.* 16, 735–743. doi: 10.1046/j.1365-313x.1998.00343.x

Fu, X., Dou, C., Chen, Y., Chen, X., Shi, J., Yu, M., et al. (2011). Subcellular distribution and chemical forms of cadmium in *Phytolacca americana* L. *J. Hazard. Mater.* 186, 103–107. doi: 10.1016/j.jhazmat.2010.10.122

Gallego, S. M., Pena, L. B., Barcia, R. A., Azpilicueta, C. E., Lannone, M. F., Rosales, E. P., et al. (2012). Unravelling cadmium toxicity and tolerance in

plants: Insight into regulatory mechanisms. *Environ. Exp. Bot.* 83, 33–46. doi: 10.1016/j.envexpbot.2012.04.006

Gao, J., Sun, L., Yang, X., and Liu, J. X. (2013). Transcriptomic analysis of cadmium stress response in the heavy metal hyperaccumulator *Sedum alfredii* Hance. *PLoS One* 8:e64643. doi: 10.1371/journal.pone.0064643

Gietz, R. D., and Schiestl, R. H. (2007). High-efficiency yeast transformation using the LiAc/SS carrier DNA/PEG method. *Nat. Protoc.* 2, 31–34. doi: 10.1038/nprot.2007.13

Godt, J., Scheidig, F., Grosse-Siestrup, C., Esche, V., Brandenburg, P., Reich, A., et al. (2006). The toxicity of cadmium and resulting hazards for human health. *J. Occup. Med. Toxicol.* 1:22. doi: 10.1186/1745-6673-1-22

Hanikenne, M., Talke, I. N., Haydon, M. J., Lanz, C., Nolte, A., Motte, P., et al. (2008). Evolution of metal hyperaccumulation required cis-regulatory changes and triplication of *HMA4*. *Nature* 453, 391–U344. doi: 10.1038/nature06877

Hu, Y., Cheng, H., and Tao, S. (2016). The challenges and solutions for cadmium-contaminated rice in China: a critical review. *Environ. Int.* 92-93, 515–532. doi: 10.1016/j.envint.2016.04.042

Hussain, D., Haydon, M. J., Wang, Y., Wong, E., Sherson, S. M., Young, J., et al. (2004). P-Type ATPase heavy metal transporters with roles in essential zinc homeostasis in *Arabidopsis*. *Plant Cell* 16, 1327–1339. doi: 10.1105/tpc.020487

Li, Z., Ma, Z., van der Kuijp, T. J., Yuan, Z., and Huang, L. (2014). A review of soil heavy metal pollution from mines in China: pollution and health risk assessment. *Sci. Total Environ.* 468, 843–853. doi: 10.1016/j.scitotenv.2013.08.090

Liu, H., Zhao, H., Wu, L., Liu, A., Zhao, F.-J., and Xu, W. (2017). Heavy metal ATPase 3 (HMA3) confers cadmium hypertolerance on the cadmium/zinc hyperaccumulator *Sedum plumbizincicola*. *New Phytol.* 215, 687–698. doi: 10.1111/nph.14622

Liu, L., Li, W., Song, W., and Guo, M. (2018). Remediation techniques for heavy metal-contaminated soils: principles and applicability. *Sci. Total Environ.* 633, 206–219. doi: 10.1016/j.scitotenv.2018.03.161

Liu, X. S., Feng, S. J., Zhang, B. Q., Wang, M. Q., Cao, H. W., Rono, J. K., et al. (2019). OsZIP1 functions as a metal efflux transporter limiting excess zinc, copper and cadmium accumulation in rice. *BMC Plant Biol.* 19:283. doi: 10.1186/s12870-019-1899-3

Lu, L. L., Tian, S. K., Yang, X. E., Li, T. Q., and He, Z. L. (2009). Cadmium uptake and xylem loading are active processes in the hyperaccumulator *Sedum alfredii*. *J. Plant Physiol.* 166, 579–587. doi: 10.1016/j.jplph.2008.09.001

Lu, L. L., Tian, S. K., Yang, X. E., Wang, X. C., Brown, P., Li, T. Q., et al. (2008). Enhanced root-to-shoot translocation of cadmium in the hyperaccumulating ecotype of *Sedum alfredii*. *J. Exp. Bot.* 59, 3203–3213. doi: 10.1093/jxb/ern174

Luo, J. S., Huang, J., Zeng, D. L., Peng, J. S., Zhang, G. B., Ma, H. L., et al. (2018). A defensin-like protein drives cadmium efflux and allocation in rice. *Nat. Commun.* 9:645. doi: 10.1038/s41467-018-03088-0

Marisela Fernandez-Valverde, S., Ordonez-Regil, E., Cabanas-Moreno, G., and Solorza-Feria, O. (2010). Electrochemical behavior of Ni-Mo electrocatalyst for water electrolysis. *J. Mex. Chem. Soc.* 54, 169–174.

Murashige, T., and Skoog, F. (1962). A Revised medium for rapid growth and bio assays with tobacco tissue cultures. *Physiol. Plant.* 15, 473–497. doi: 10.1111/j.1399-3054.1962.tb08052.x

Nocito, F. F., Lancilli, C., Dendena, B., Lucchini, G., and Sacchi, G. A. (2011). Cadmium retention in rice roots is influenced by cadmium availability, chelation and translocation. *Plant Cell Environ.* 34, 994–1008. doi: 10.1111/j.1365-3040.2011.02299.x

Parrotta, L., Guerriero, G., Sergeant, K., Cal, G., and Hausman, J. F. (2015). Target or barrier? The cell wall of early- and later-diverging plants vs cadmium toxicity: differences in the response mechanisms. *Front. Plant Sci.* 6:133. doi: 10.3389/fpls.2015.00133

Pollard, A. J., Reeves, R. D., and Baker, A. J. M. (2014). Facultative hyperaccumulation of heavy metals and metalloids. *Plant Sci.* 217, 8–17. doi: 10.1016/j.plantsci.2013.11.011

Rascio, N., and Navari-Izzo, F. (2011). Heavy metal hyperaccumulating plants: how and why do they do it? And what makes them so interesting? *Plant Sci.* 180, 169–181. doi: 10.1016/j.plantsci.2010.08.016

Ruijter, J. M., Ramakers, C., Hoogaars, W. M., Karlen, Y., Bakker, O., van den Hoff, M. J., et al. (2009). Amplification efficiency: linking baseline and bias in the analysis of quantitative PCR data. *Nucleic Acids Res.* 37:e45. doi: 10.1093/nar/gkp045

Sasaki, A., Yamaji, N., Yokosho, K., and Ma, J. F. (2012). Nramp5 Is a major transporter responsible for manganese and cadmium uptake in rice. *Plant Cell* 24, 2155–2167. doi: 10.1105/tpc.112.096925

Shahid, M., Dumat, C., Khalid, S., Niazi, N. K., and Antunes, P. M. C. (2017). "Cadmium bioavailability, uptake, toxicity and detoxification in soil-plant system," in *Rev. Environ. Contam. Toxicol*, ed. P. DeVoogt (New York, NY: Springer), 73–137. doi: 10.1007/398_2016_8

Shi, T., Ma, J., Wu, F., Ju, T., Gong, Y., Zhang, Y., et al. (2019). Mass balance-based inventory of heavy metals inputs to and outputs from agricultural soils in Zhejiang Province. *China. Sci. Total Environ.* 649, 1269–1280. doi: 10.1016/j.scitotenv.2018.08.414

Song, W. Y., Choi, K. S., Alexis, D. A., Martinoia, E., and Lee, Y. (2011). *Brassica juncea* plant cadmium resistance 1 protein (BjPCR1) facilitates the radial transport of calcium in the root. *Proc. Natl. Acad. Sci. U.S.A.* 108, 19808–19813. doi: 10.1073/pnas.1104905108

Song, W. Y., Choi, K. S., Kim, D. Y., Geisler, M., Park, J., Vincenzetti, V., et al. (2010). *Arabidopsis* PCR2 is a zinc exporter involved in both zinc extrusion and long-distance zinc transport. *Plant Cell* 22, 2237–2252. doi: 10.1105/tpc.109.070185

Song, W. Y., Lee, H. S., Jin, S. R., Ko, D., Martinoia, E., Lee, Y., et al. (2015). Rice PCR1 influences grain weight and Zn accumulation in grains. *Plant Cell Environ.* 38, 2327–2339. doi: 10.1111/pce.12553

Song, W. Y., Martinoia, E., Lee, J., Kim, D., Kim, D. Y., Vogt, E., et al. (2004). A novel family of cys-rich membrane proteins mediates cadmium resistance in *Arabidopsis*. *Plant Physiol.* 135, 1027–1039. doi: 10.1104/pp.103.037739

Sterckeman, T., Goderniaux, M., Sirguey, C., Cornu, J. Y., and Nguyen, C. (2015). Do roots or shoots control cadmium accumulation in the hyperaccumulator *Noccaea caerulescens*? *Plant Soil* 392, 87–99. doi: 10.1007/s11104-015-2449-x

Tian, S. K., Lu, L. L., Labavitch, J., Yang, X. E., He, Z., Hu, H., et al. (2011). Cellular sequestration of cadmium in the hyperaccumulator plant species *Sedum alfredii*. *Plant Physiol.* 157, 1914–1925. doi: 10.1104/pp.111.183947

Tian, S. K., Lu, L. L., Yang, X. E., Huang, H. G., Wang, K., and Brown, P. H. (2012). Root adaptations to cadmium-induced oxidative stress contribute to Cd tolerance in the hyperaccumulator *Sedum alfredii*. *Biol. Plant.* 56, 344–350. doi: 10.1007/s10535-012-0096-0

Tian, S. K., Lu, L. L., Yang, X. E., Webb, S. M., Du, Y., and Brown, P. H. (2010). Spatial imaging and speciation of lead in the accumulatorpPlant *Sedum alfredii* by microscopically focused synchrotron X-ray investigation. *Environ. Sci. Technol.* 44, 5920–5926. doi: 10.1021/es903921t

Tian, S. K., Xie, R. H., Wang, H. X., Hu, Y., Hou, D. D., Liao, X. C., et al. (2017). Uptake, sequestration and tolerance of cadmium at cellular levels in the hyperaccumulator plant species *Sedum alfredii*. *J. Exp. Bot.* 68, 2387–2398. doi: 10.1093/jxb/erx112

Ueno, D., Iwashita, T., Zhao, F. J., and Ma, J. F. (2008). Characterization of Cd translocation and identification of the Cd form in xylem sap of the Cd-hyperaccumulator *Arabidopsis halleri*. *Plant Cell Physiol.* 49, 540–548. doi: 10.1093/pcp/pcn026

Willems, G., Frerot, H., Gennen, J., Salis, P., Saumitou-Laprade, P., and Verbruggen, N. (2010). Quantitative trait loci analysis of mineral element concentrations in an *Arabidopsis halleri* x *Arabidopsis lyrata* petraea F-2 progeny grown on cadmium-contaminated soil. *New Phytol.* 187, 368–379. doi: 10.1111/j.1469-8137.2010.03294.x

Wong, C. K. E., and Cobbett, C. S. (2009). HMA P-type ATPases are the major mechanism for root-to-shoot Cd translocation in *Arabidopsis thaliana*. *New Phytol.* 181, 71–78. doi: 10.1111/j.1469-8137.2008.02638.x

Wu, Z., Zhao, X., Sun, X., Tan, Q., Tang, Y., Nie, Z., et al. (2015). Antioxidant enzyme systems and the ascorbate-glutathione cycle as contributing factors to cadmium accumulation and tolerance in two oilseed rape cultivars (*Brassica napus* L.) under moderate cadmium stress. *Chemosphere* 138, 526–536. doi: 10.1016/j.chemosphere.2015.06.080

Yang, X. E., Li, T. Q., Long, X. X., Xiong, Y. H., He, Z. L., and Stoffella, P. J. (2006). Dynamics of zinc uptake and accumulation in the hyperaccumulating and non-hyperaccumulating ecotypes of *Sedum alfredii* Hance. *Plant Soil* 284, 109–119. doi: 10.1007/s11104-006-0033-0

Yang, X. E., Long, X. X., Ye, H. B., He, Z. L., Calvert, D. V., and Stoffella, P. J. (2004). Cadmium tolerance and hyperaccumulation in a new Zn-hyperaccumulating plant species (*Sedum alfredii* Hance). *Plant Soil* 259, 181–189. doi: 10.1023/B:PLSO.0000020956.24027.f2

Zhang, J., Zhang, M., Shohag, M. J. I., Tian, S. K., Song, H., Feng, Y., et al. (2016). Enhanced expression of SaHMA3 plays critical roles in Cd hyperaccumulation and hypertolerance in Cd hyperaccumulator *Sedum alfredii* Hance. *Planta* 243, 577–589. doi: 10.1007/s00425-015-2429-7

Zhao, F. J., Ma, Y. B., Zhu, Y. G., Tang, Z., and McGrath, S. P. (2015). Soil contamination in China: current status and mitigation strategies. *Environ. Sci. Technol.* 49, 750–759. doi: 10.1021/es5047099

Zou, W. L., Li, C., Zhu, Y. J., Chen, J. G., He, H. H., and Ye, G. Y. (2020). Rice heavy metal P-type ATPase OsHMA6 is likely a copper efflux protein. *Rice Sci.* 27, 143–151. doi: 10.1016/j.rsci.2020.01.005

Conflict of Interest: The authors declare that the research was conducted in the absence of any commercial or financial relationships that could be construed as a potential conflict of interest.

frontiers in Plant Science

REVIEW
published: 07 January 2021
doi: 10.3389/fpls.2020.545453

Role of Exogenous and Endogenous Hydrogen Sulfide (H_2S) on Functional Traits of Plants Under Heavy Metal Stresses: A Recent Perspective

Muhammad Saleem Arif[1], Tahira Yasmeen[1], Zohaib Abbas[1], Shafaqat Ali[1,2]*, Muhammad Rizwan[1], Nada H. Aljarba[3], Saad Alkahtani[4] and Mohamed M. Abdel-Daim[4,5]*

[1] Department of Environmental Science and Engineering, Government College University Faisalabad, Faisalabad, Pakistan, [2] Department of Biological Sciences and Technology, China Medical University, Taichung, Taiwan, [3] Department of Biology, College of Science, Princess Nourah Bint Abdulrahman University, Riyadh, Saudi Arabia, [4] Department of Zoology, College of Science, King Saud University, Riyadh, Saudi Arabia, [5] Pharmacology Department, Faculty of Veterinary Medicine, Suez Canal University, Ismailia, Egypt

OPEN ACCESS

Edited by:
Mukesh Kumar Kanwar, Zhejiang University, China

Reviewed by:
Elke Bloem, Julius Kühn-Institut, Germany
Syed Tahir Ata-Ul-Karim, The University of Tokyo, Japan

***Correspondence:**
Tahira Yasmeen
rida_akash@hotmail.com; tahirayasmeen@gcuf.edu.pk
Shafaqat Ali
shafaqataligill@yahoo.com; shafaqataligill@gcuf.edu.pk

Specialty section:
This article was submitted to Plant Nutrition, a section of the journal Frontiers in Plant Science

Received: *25 March 2020*
Accepted: *27 November 2020*
Published: *07 January 2021*

Citation:
Arif MS, Yasmeen T, Abbas Z, Ali S, Rizwan M, Aljarba NH, Alkahtani S and Abdel-Daim MM (2021) Role of Exogenous and Endogenous Hydrogen Sulfide (H_2S) on Functional Traits of Plants Under Heavy Metal Stresses: A Recent Perspective. Front. Plant Sci. 11:545453. doi: 10.3389/fpls.2020.545453

Improving growth and productivity of plants that are vulnerable to environmental stresses, such as heavy metals, is of significant importance for meeting global food and energy demands. Because heavy metal toxicity not only causes impaired plant growth, it has also posed many concerns related to human well-being, so mitigation of heavy metal pollution is a necessary priority for a cleaner environment and healthier world. Hydrogen sulfide (H_2S), a gaseous signaling molecule, is involved in metal-related oxidative stress mitigation and increased stress tolerance in plants. It performs multifunctional roles in plant growth regulation while reducing the adverse effects of abiotic stress. Most effective function of H_2S in plants is to eliminate metal-related oxidative toxicity by regulating several key physiobiochemical processes. Soil pollution by heavy metals presents significant environmental challenge due to the absence of vegetation cover and the resulting depletion of key soil functions. However, the use of stress alleviators, such as H_2S, along with suitable crop plants, has considerable potential for an effective management of these contaminated soils. Overall, the present review examines the imperative role of exogenous application of different H_2S donors in reducing HMs toxicity, by promoting plant growth, stabilizing their physiobiochemical processes, and upregulating antioxidative metabolic activities. In addition, crosstalk of different growth regulators with endogenous H_2S and their contribution to the mitigation of metal phytotoxicity have also been explored.

Keywords: biochemical properties, physiological activities, heavy metal stress, hydrogen sulfide, signaling molecule, oxidative impairment

INTRODUCTION

Heavy metals are a group of metal elements having peculiar physical and chemical properties, which are also known to possess higher specific gravity > 4 g cm^{-3} in nature (Grant and Grant, 1987; Duffus, 2002). Environmental occurrence of heavy metal can be of both natural and anthropogenic origin; however, unprecedented release and their strong ecological persistence have now become a

serious toxicological and public health challenge worldwide (Arif et al., 2019; Zheng et al., 2020). Under natural conditions, heavy metals are the intrinsic component of earth crust and are often dispersed in soil, water, and atmosphere as a result of many geological processes, i.e., forest fire and volcanic eruption (Lado et al., 2008). A range of anthropogenic activities, such as intensive pesticides, as well as fertilizers use, vehicular emissions, mining activities, and industrial wastes, are the main contributors of heavy metal pollution across various domains of environment. Besides this, heavy environmental loading of metal toxicants also emanates from different wastewater sources. Globally, large volume of untreated wastewater is being discharged directly into waterways and soil, where they pose serious concerns for ecosystem stability (Mataka et al., 2006).

In soil, level of individual heavy metal concentration is a primary indicator often used to determine the degree of ecotoxicological effects on plants. For instance, some metals, such as nickel (Ni), molybdenum (Mo), zinc (Zn), and copper (Cu), are plant micronutrients and are phytotoxic only if their concentration is higher in soil (Lasat, 2002), whereas few other metallic elements, in particular chromium (Cr), lead (Pb), and cadmium (Cd), are hazardous to plants even at low soil concentrations. Heavy metals can either be found in dissolved or immobilized form; however, high immobilization rates can cause stronger detrimental effects on plants because of their *in situ* persistence and concentration buildup over time (Alloway, 1995, 2013). Consequently, they tend to impair various growth attributes of plants (Ahmad et al., 2012). Furthermore, some of these metals, such as Cr, Cd, Mn, and Zn, are also recognized to exert hormetic responses, which are reflected by a positive growth response at low concentrations and by phytotoxicity at higher metal concentrations (Azevedo and Lea, 2005). Detrimental effects of heavy metals on plants may involve oxidative stress, stunted growth, and toxicity-induced metabolic anomalies.

After nitric oxide and carbon monoxide, hydrogen sulfide (H_2S) is the third most important naturally occurring gaseous molecule known for its cellular signaling in biology (Yang et al., 2008). In plants, synthesis and release of H_2S typically occur during different stages of metabolic activities. It is generally formed in cut branches, tissue cultures, and leaf discs, whereas it is discharged into the surrounding environment from green cells of the plants (Rennenberg et al., 1990). Under normal growth conditions, numerous plants such as soybean, pumpkin, cotton, cantaloupe, squash, corn, and cucumber were found to release H_2S from leaf into the exterior environment (Wilson et al., 1978). Besides increasing enzymatic activity of vigorous cysteine (Cys), H_2S secretion is also recognized to enhance sulfite and sulfate metabolic activities (Rennenberg, 1983, 1984). However, numerous reports have observed paradoxical functions of H_2S in the regulation of plants physiological and biochemical traits. For instance, H_2S has been established to act as sulfur source at lower concentration, while promoting phytotoxic effects on plant growth at elevated level (De Kok et al., 2002; Li, 2013; Hancock and Whiteman, 2016; Li et al., 2016; Hancock, 2017; Huo et al., 2018). In most plants, elongated exposure to higher H_2S level eventually caused leaf removal after developing leaf injury, which can lead to overall deterioration of plant growth. Likewise, H_2S triggered O_2 obstruction and subsequent impaired nutrient acquisition in rice seedlings were reported by Wang et al. (2012). Positive influence of H_2S on various plants has also been reported in literature. Shoot deposited sulfur (S) from H_2S appears to provide major site-specific S regulation for plants to improve plant growth, particularly under sulfur-deprived conditions. In many plants, H_2S is reported to be involved in the regulation of key physiological and growth functions, such as formation of adventitious root in cucumber, stomatal conductance in *Arabidopsis thaliana*, enhanced tolerance against salinity in alfalfa during seed germination, and regulation of thiol levels in *A. thaliana* (Riemenschneider et al., 2005a,b; Lisjak et al., 2010; Lin et al., 2012).

The H_2S is a convenient stress signaling molecule, as its biosynthesis process can take place in various cellular components once plants experience stress such as heavy metal exposure (Zulfiqar and Hancock, 2020). Upon its production, H_2S can be highly mobile across plant membranes and can either be influxed in or effluxed out of the plant system as a way out against heavy metal stress (Shivaraj et al., 2020). Plant stress adaptation against heavy metal in H_2S-treated plant is initiated via antioxidant activities (Kushwaha and Singh, 2019), accumulation of osmoregulators (Tian et al., 2016), cell signaling protein (He et al., 2019), and by different gene expressions (Pandey and Gautam, 2019). Overall, it enables plants to combat against stress factor such as heavy metals via effective removal of reactive oxygen species (ROS) by adjusting intracellular redox balance.

A plant experiment with nickel spiking has demonstrated that H_2S can enhance rice nickel tolerance prompted mainly by preventing chloroplast damage as a result of improved N metabolism under excessive nickel contamination (Rizwan et al., 2019). However, the role of H_2S as a signaling molecule in plants is still not fully understood despite the fact that the release of H_2S has been demonstrated in many plant species. Notably, desulfhydrases (H_2S-releasing enzymes) have functionally been endorsed as key H_2S volatile in plants (Riemenschneider et al., 2005b). In another case, enhanced L-Cys desulfhydrase (LCD) activity under biotic stress further reaffirms its significant potency as an adaptive defense approach under stress agriculture (Rausch and Wachter, 2005). H_2S was also involved in a promotional role of superior root organogenesis in *Ipomoea batatas*, *Salix matsudana*, and *Glycine max* L. (Zhang et al., 2009).

The antioxidant enzymes are another type of stress mediator in plants, which are often activated as a key defense response after recognition of given stressor, including heavy metals (Zhang et al., 2010a,b). Foliar application of sodium hydrosulfide (NaHS), an H_2S donor, led to an upscale induction response of different antioxidant enzymes and reduced the concentration of H_2O_2 in wheat seedlings to enhance resistance against heat stress. Also, Zhang et al. (2011) emphasized that H_2S can have an effective role in plant protection against different types of oxidative stress. Water-soluble antioxidants, such as ascorbic acid and glutathione, were expressed at enhanced level upon fumigation with H_2S, which consequently delivered higher water stress tolerance in wheat plants (Shan et al., 2011). As NaHS is characterized as key antioxidant inducer; therefore, plant

growth promotive activities including root organogenesis (Zhang et al., 2009), stomatal regulation (Lisjak et al., 2010), and seed germination (Zhang et al., 2010a,b) were substantially improved in response to heavy metal stresses. Interestingly, exogenously applied H_2S (100 ppb) has shown striking effect on plant growth improvement of beet, alfalfa, and lettuce (Thompson and Kats, 1978). Furthermore, H_2S foliar spraying has also improved the accumulation of vital nutrients in plant (Wang et al., 2012).

As a secondary messenger, nitric oxide and H_2S can collectively trigger signal transduction resulting in higher intracellular buildup of these molecules, which are indeed a plant's necessity to cope with metal-induced oxidative stress. In this way, use of H_2S with nitric oxide could exert a regulatory response to transporters and antioxidant systems to alleviate phytotoxic effects of heavy metals (Li et al., 2012; Wang et al., 2019). Considering all the background information about the role of H_2S in biological system and, most importantly, its interaction with crop plants under stress agriculture, we aimed to get an advanced overview of H_2S-related growth promotive effects on crop plants. Soil contamination by heavy metals imposes greater ecological concern because of lack of plant cover and resultant land degradation. However, use of stress alleviators, such as H_2S, along with suitable crop plant holds a great potential for the successful restoration of these contaminated soils. We also focus on how the use of H_2S and other precursor compounds interacts with plants to counteract heavy metal toxicity. Moreover, our discussion also focuses H_2S-mediated response mechanisms exhibited by plants toward heavy metal toxicity.

CHEMISTRY OF H_2S

H_2S is a weak acid with good water solubility and commonly exists in neutral molecular form (H_2S). Although HS^- is a major ionic form of H_2S involved in most of its biological reactions, S^{2-} also exists in minor concentration due to higher dissociation constant for second ionization (Filipovic et al., 2018). Despite being a highly water-soluble compound, H_2S tends to be unstable under natural conditions as it slowly oxidizes to elemental sulfur having a weak solubility in aqueous solution. Moreover, the volatile nature of H_2S exacerbates its experimental use in the environment. For instance, nearly half-dose of H_2S could be lost in 5 min from open cell culture wells (DeLeon et al., 2012). Consequently, H_2S handling imposes greater challenge of its precise measurement under field conditions (Wang et al., 2014; Peng and Xian, 2015).

$$H_2S \rightleftharpoons HS^- + H^+ \rightleftharpoons S^{2-} + 2H^+ \text{ (in aqueous solution)}$$

OCCURRENCE AND BIOSYNTHESIS OF H_2S IN PLANTS

There has been a proposition long ago that plants can produce and release H_2S themselves, particularly when exposed to external sulfur (S) stimuli, i.e., Cys, sulfate, sulfite, or SO_2 (Wilson et al., 1978; Sekiya et al., 1982a,b). This was thought to be a mechanism for regulating sulfur homeostasis (Calderwood and Kopriva, 2014). However, mechanistic understanding of H_2S generation in plants and its interaction with other cellular components remains elusive. In higher plants, H_2S biosynthesis pathway emerges in different subcellular compartments, where main enzymes linked to sulfur metabolism have the potential to initiate H_2S biogenesis (Corpas et al., 2019b; Chen et al., 2020). In plants, most common enzymes involved in the H_2S biosynthesis enzymes include LCD, D-Cys desulfhydrase (DCD), l-3-cyanoalaninesynthase, sulfite reductase, and Cys synthase (Yamasaki and Cohen, 2016). Among various plant cellular organelles, chloroplast serves as the major H_2S production site due to localization of sulfite reductase enzyme, which catalyzes the reduction of sulfite to sulfide during sulfate assimilation pathway. In addition to this, cytosol can also generate H_2S by the action of DCD and LCD, accompanied by ammonia and pyruvate production. In chloroplast, sulfide concentration is two times greater than that found into the cytosol (Krueger et al., 2009). However, this sulfide is dissociated into its ionized forms due to the basic physiological conditions and therefore unable to pass through the membranes to the cytosol (Kabil and Banerjee, 2010). In mitochondria, the synthesis of H_2S can be regulated by β-cyanoalanine synthase (a pyridoxal phosphate-dependent enzyme), which transforms both cyanide and L-Cys into β-cyanoalanine and H_2S in order to degrade toxic cyanogen (Gotor et al., 2019). Recently, Corpas et al. (2019a) also provided an evidence of H_2S generation in the peroxisomes of *Arabidopsis*; however, it is still unclear whether its generation pathway is endogenous or recruited from other cellular compartments (e.g., cytosol). Additionally, the expression of plant cellular proteins [L-Cys desulfurase such as *O*-acetylserine thiol lyase (OAS-TL) and Nifs-like proteins] also processes the H_2S synthesis in different cellular organelles (Gotor et al., 2019). These enzymes, with their varied expression, are therefore involved in controlling the production of H_2S across various cellular compartments of the plant. On the other hand, occurrence of H_2S in these cellular organelles with strong lipophilic characteristic promotes its translocation in the lipid bilayer of cell membranes (Cuevasanta et al., 2017).

H_2S is a flammable-toxic gaseous molecule that is often distinguished by stinky rotten eggs smell. It has also shown strong concentration dependent affinity for reactions as it can disrupt mitochondrial cytochrome activity and even reduce mitochondrial respiration (Mancardi et al., 2009). Surprisingly, research in recent years has unraveled the significance of H_2S as a gasotransmitter that promotes plant growth and development at various stages of plant life cycle (Xuan et al., 2020). Other than algae, fungi, and few prokaryotes, plants are known to take leverage of taking up the naturally occurring sulfate (SO_4^{2-}) source of S from soil and incorporate it into organic forms (Takahashi et al., 2011). In S assimilation process, sulfate taken up by plant roots is initially reduced to H_2S by catalytic activity of adenosine 5′-phosphosulfate reductase and sulfite reductase and eventually transformed into Cys via O-OAS-TL. Therefore, H_2S is an extremely important intermediate in the thiometabolism pathway.

The use of H_2S as signaling molecule has now become very common; thus, basic mechanism of its functional activities has been decrypted (Mustafa et al., 2009; Aroca et al., 2015). Some recent proteomic analyses have described a new posttranslational modification of proteins, where reactive Cys residues (as an H_2S signal) can modify protein function by converting the thiol group (-SH) into a persulfide group (-SSH) known as persulfidation. In most cases, persulfide adducts exhibit higher nucleophilicity relative to the thiol group, and as a result, modified Cys displayed highly complex reactivity (Paul and Snyder, 2012). This might be the rationale of widespread persulfidation in nature, which largely affects protein over O_2 and N species (Ida et al., 2014) (**Figure 1**). Overall, complex functional interactions of H_2S based on its donor, concentration gradient, and plant section tend to describe actions of specific protein after translational modification.

The nature of H_2S-mediated specific cellular modifications still lacks clarity, because thermodynamic reaction involving H_2S and a thiol is unfavorable. Sulfane sulfur is a sulfur atom that has the peculiar ability to bind reversibly to other sulfur atoms to form hydropersulfides (R-S-SH) and polysulfides (-S-Sn-S-). These polysulfides tend to be far more efficient in persulfidation, as they are more nucleophilic than H_2S (Toohey, 2011). Recently, new molecular weight persulfides were identified as possible mediator of sulfide signaling. In this relation, Cys-persulfide (Cys-SSH), glutathione persulfide, and its persulfurated species Cys-SSnH and GSSnH have been designated as redox regulators (Kasamatsu et al., 2016; Kimura et al., 2017). Recently, the endogenous Cys-SSH production synthetized by prokaryotic and mammalian cysteinyl-tRNA synthetases using L-Cys as substrate has been described. The Cys polysulfides bound to tRNA are incorporated into polypeptides that are synthesized *de novo* in the ribosomes, suggesting that these enzymes are the principal Cys persulfide synthases *in vivo* (Akaike et al., 2017).

PROMOTIVE ROLE OF H_2S IN REGULATING PLANT HEAVY METAL STRESS

Of various abiotic stresses in environment, heavy metal-triggered stress always has very serious repercussions for plant growth and productivity. Like other abiotic stress, heavy metal stress is also associated with unregulated overproduction of ROS, which can influence plant metabolism and physiological activities by inflicting range of oxidative stress damages. Among the signaling molecules, H_2S is now an established regulator of growth in plants exposed to plethora of abiotic stresses, including heavy metal stress (Rather et al., 2020).

EXOGENOUS H_2S APPLICATION: A PRECURSOR OF HEAVY METAL STRESS ALLEVIATION IN PLANTS

Given a suite of heavy metal mitigation approaches competing for an effective stress management in agriculture, it is extremely pertinent to consider only those measures that can provide plant benefits only in an eco-friendly way. Although H_2S is toxic for many living organisms as evidenced by mitochondrion inhibition (Wang et al., 2019), its central role in key plant physiological functions and therapeutic use in various human ailments have been well developed in recent times (Aroca et al., 2020). The H_2S in gaseous form is the simplest method of its usage in the laboratory; however, it is not realistic practice due to non-targeted ecotoxicological consequences both for the humans and environment (Rubright et al., 2017). In most cases, NaHS and/or sodium sulfide (Na_2S) are used as H_2S donor molecules specifically due to their higher dissolution, resulting in a short albeit sustained pulse of H_2S (**Table 1**).

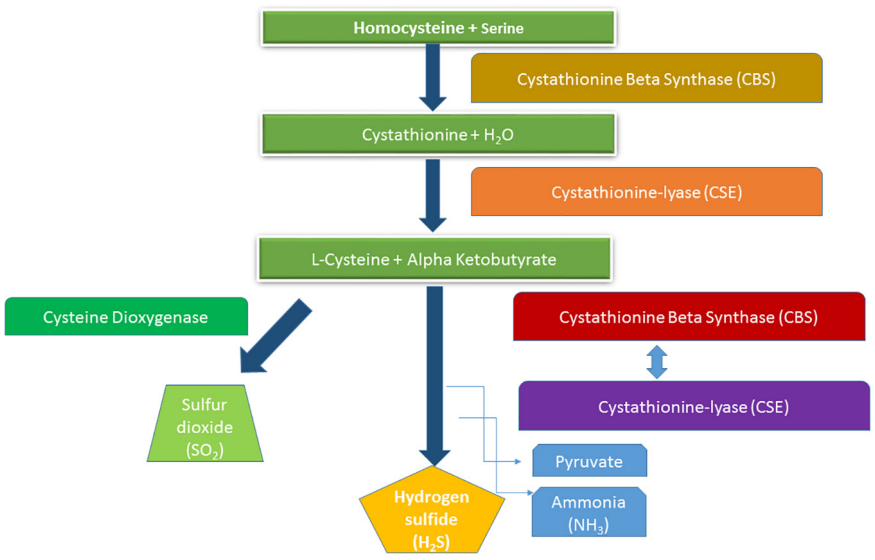

FIGURE 1 | Hydrogen sulfide production through homocysteine metabolism.

TABLE 1 | Effects of exogenous application of different H_2S sources on plant growth regulations under heavy metals stress.

H_2S source	H_2S conc.	Plant species	Experiment	Duration/ growth stage	Heavy metal/source	Exposure level	Tolerance mechanisms involved	References
Sodium hydrosulfide (NaHS)	100 μM	Alfalfa (*Medicago sativa* L.)	Potted soil	60 days/ young plant	Lead, cadmium	217 mg kg^{-1} of Pb 4.95 mg kg^{-1} of Cd	Upscaled antioxidant activity (POD, CAT, APX, SOD) and reduced oxidative damage (MDA, H_2O_2, O^-_2) decreased the absorption of metal ions	Fang et al., 2020
Sodium hydrosulfide (NaHS)	100 μM	Zucchini (*Cucurbita pepo* L.)	Potted soil	14 days/ young seedlings	Nickel: Ni $(NO_3)_2$	50 mg of Ni	Decreased metal ions accumulation, restored ionic homeostasis and averted oxidative membrane damages by upregulation of phenolic and flavonoid metabolites	Valivand and Amooaghaie, 2020
Sodium sulfite (Na_2SO_3)	0.5 mM	Foxtail millet (*Setaria italica* L.)	Hydroponic culture	12 days/ young seedlings	Cadmium	100 μM	Suppressed nitrate reductase and nitric oxide synthase–dependent endogenous nitric oxide (NO), which further enhanced the enzyme activities, i.e., SOD and POD, leading to the rescue of Cd related root growth inhibition	Han et al., 2020
Sodium hydrosulfide (NaHS)	200 μM	Cauliflower (*Brassica oleracea* L.)	Potted soil	42 days/ transplants	Chromium: $K_2Cr_2O_7$	10–100 μM	Restricted oxidative stress damages (EL, MDA, H_2O_2), increased antioxidant activity (SOD, CAT, APX, POD) in leaves and root tissues	Ahmad et al., 2020
Sodium hydrosulfide (NaHS)	150 μM	Woad plant (*Isatis indigotica* L.)	Hydroponic culture	28 days/ young seedlings	Cadmium	22.5 μM	Decreased intracellular metal ion toxicity and induced production of metallothioneins (metal-binding protein) restricting root-to-shoot Cd translocation	Jia et al., 2020
Sodium hydrosulfide (NaHS)	0.2 mM	Cauliflower (*Brassica oleracea* L.)	Hydroponic culture	24 days/ young seedlings	Lead: Pb $(CH_3COO)_2{\cdot}3H_2O$	0.5 mM	Scavenging of ROS through antioxidant activity and Pb ion chelation by non-protein thiol and total glutathione	Chen et al., 2018
Sodium hydrosulfide (NaHS)	0.2 mM	Pepper (*Capsicum annuum* L.)	Sand, peat, and perlite mixed pots	70 days/ mature plants	Zinc: $ZnSO_4 \cdot 7H_2O$	O.5 mM	Reduced metal ions uptake, improved N, P, and Fe uptake and promoted antioxidant activities for limiting membrane oxidative stress damage	Kaya et al., 2018
Sodium hydrosulfide (NaHS)	500 μM	Maize (*Zea mays* L.)	Hydroponic culture	19 days/ young seedlings	Chromium	200 μM	Alleviated Cr toxicity by reducing the production of cyto-toxic methylglyoxal via glutathione-S-transferase (GST) detoxification	Kharbech et al., 2020
Sodium hydrosulfide (NaHS)	50 μM	Oilseed rape (*Brassica napus* L.)	Hydroponic culture	18 days/ young seedlings	Cadmium: $CdCl_2$	20 μM	Prompted higher L-cysteine desulfhydrase (LCD) for S-metabolism, minimized Cd translocation to shoots–leaves and prevented chlorosis	Yu et al., 2019

(Continued)

TABLE 1 | Continued

H_2S source	H_2S conc.	Plant species	Experiment	Duration/ growth stage	Heavy metal/source	Exposure level	Tolerance mechanisms involved	References
Sodium hydrosulfide (NaHS)	100 μM	Coriander (*Coriandrum sativum* L.)	Hydroponic culture	18 days/ young seedlings	Copper: $CuSO_4$	100 μM	Reduced electrolyte leakage by regulating antioxidant enzyme activity via ascorbate–glutathione cycle	Karam and Keramat, 2017
Sodium hydrosulfide (NaHS)	200 μM	Black night shade (*Solanum nigrum* L.)	Hydroponic culture	21 days/ young seedlings	Zinc: $ZnCl_2$	400 μM	Reduced free cytosolic metal content in roots by upregulated metallothioneins mediated Zn-chelation and antioxidant response mechanism	Liu et al., 2016
Sodium hydrosulfide (NaHS)	0.8 mM	Wheat (*Triticum aestivum* L.)	Plastic trays/ sand-vermiculite	14 days/ young seedlings	Copper: $CuSO_4$	100 μM	Ascorbate and glutathione metabolism minimized Cu toxicity by reducing malondialdehyde content and limiting electrolyte leakage	Shan et al., 2012
Sodium hydrosulfide (NaHS)	200 μM	Cotton (*Gossypium hirsutum* L.)	Hydroponic culture	28 days/ young seedlings	Lead: Pb $(NO_3)_2$	50 μM	Improved photosynthetic pigmentation, enhanced antioxidant activities and eventually decreasing malondialdehyde (MDA), electrolyte leakage, and H_2O_2 production	Bharwana et al., 2014
Sodium hydrosulfide (NaHS)	100 μM	Pea (*Pisum sativum* L.)	Hydroponic culture	30 days/ young seedlings	Arsenate: $Na_2HAsO_4 \times 7H_2O$	50 μM	Revitalized redox cell status against arsenate toxicity by promoting ascorbate–glutathione metabolism and counteract ROS induced membrane damage	Singh et al., 2015
Sodium hydrosulfide (NaHS)	100 μM	Rice (*Oryza sativa* L.)	Hydroponic culture	35 days/ young seedlings	Nickel: $NiSO_4 \cdot 6H_20$	200 μM	Enhanced chloroplast biogenesis and regulate nitrogen (N) metabolism via enzymes, i.e., nitrate reductase, nitrite reductase, glutamate synthase, glutamate oxaloacetate transaminase, glutamine synthetase, and glutamate pyruvate transaminase, and boost plant tolerance under Ni stress	Rizwan et al., 2019
Sodium hydrosulfide (NaHS)	200 μM	Rice (*Oryza sativa* L.)	Hydroponic culture	28 days/ young seedlings	Mercury: $HgCl_2$	100 μM	Sequestered metal ions in roots and prevented plant oxidative damages by maintaining low MDA and H_2O_2	Chen et al., 2016

POD, peroxidase; SOD, superoxide dismutase; CAT, catalase; APX, ascorbate peroxidase; MDA, malondialdehyde; H_2O_2, hydrogen peroxide, EL, electrolyte leakage.

Production of ROS, by-product of physiological metabolism, is a typical plant response under abiotic stress including heavy metal stress. Nevertheless, plants vary in their response against the different oxidative stresses linked to ROS in species-cultivar-specific ways. In plants, a robust antioxidative defense system (enzymatic and non-enzymatic) has been evolved to scavenge the excessive ROS accumulation, which can in turn counteract the harmful impacts of oxidative stress. Increasing evidence demonstrated that NaHS treatment can ameliorate and repair oxidative stress caused by heavy metal toxicity (Luo et al., 2020). Exogenous application of H_2S can suppress the burst of ROS by activating enzymatic and non-enzymatic defense components of ascorbate–glutathione cycle and eventually avert oxidative stress damage to plants.

Legume plants are of considerable significance for the remediation of heavy metal-polluted soil due to the unique symbiotic assemblage of N-fixing bacteria (rhizobia) with leguminous host plant (Reichman, 2007; Shen et al., 2019). In alfalfa, exogenous application of NaHS (100 μM) has mitigated the compounding effects of dual metal stress (Pb/Cd) on legume-rhizobium symbiosis (**Table 1**; Fang et al., 2020). Application of H_2S donor molecule boosted up the survival rate of rhizobia by enhancing soil enzyme activity, facilitating

nutrient transformations, and shifting both composition and diversity of soil microbial population. This study concludes that H_2S-mediated symbiosis has resulted in development of greater plant resistance to metal-induced toxicity as evident by increased antioxidant enzyme activity and reduced metal ion absorption. Similar to these findings, Mostofa et al. (2015) investigated a rice–cadmium interaction model, where H_2S provided further evidence of being an efficient growth regulator to mitigate Cd-related growth suppression and reduction in biomass. Moreover, rice growth revitalization performance was primarily triggered by a three-way Cd alleviation process, including low Cd uptake/accumulation, mineral nutrient upregulation, and photosynthetic functions and timely induction of antioxidant response.

Heavy metals, such as Ni, are known to cause disruption in the absorption and utilization of key mineral elements in plants (Sharma and Dhiman, 2013). Importantly, Ni metal ions demonstrate a strong competitive affinity for bivalent cations, i.e., Ca, Mg, Mn, Fe, Zn, which could reduce uptake of these essential elements and obstruct normal plant growth and development (Ahmad et al., 2011). In hydroponic culture, NaHS (100 μM)-treated young seedlings of Zucchini plant showed a decrease in Ni accumulation by reviving essential mineral homeostasis (Valivand and Amooaghaie, 2020). Furthermore, this study validates the role of H_2S in osmotic adjustment, as indicated by the proline and sugar content of plant exposed to heavy metal stress. Clearly, NaHS facilitated an increase in flavonoid and phenolic secretions likely to reduce the oxidative damage due to ROS scavenging, which in turn led to the improved Ni tolerance in *Zucchini* seedlings.

Phenolic and flavonoid are not the solitary metabolites those are exuded by heavy metal–stressed plants. Ahmad et al. (2020) demonstrated that NaHS treatment can upregulate antioxidant enzyme activity in Cr-exposed cauliflower seedlings, which is central to the amelioration of Cr-related oxidative damages, as well as reduction in metal ion translocation, to aerial plant parts. Root growth is an important predictor of plant productivity in agriculture, while impaired root growth has often been distinguished as one of the most common and earliest symptoms of plant exposure to metal toxicity (Liu et al., 2018). In foxtail millet, Cd-induced root growth inhibition was reversed by an SO_2 derivative compound Na_2SO_3 (Han et al., 2020). This study concludes the existence of crosstalk between SO_2 and nitric oxide (NO) for nitrate reductase (NR)–nitric oxide synthase-dependent endogenous NO signaling that prompted an upregulated antioxidant enzyme activity and suppressed genes associated with the Cd uptake (SiNRAMP1, SiNRAMP6, SiIRT1, and SiIRT2).

Plant cell wall is a first architectural barrier to avert transmembrane movements of toxic materials, such as heavy metals (Krzesłowska, 2011), as it can allow cellular compartmentation of the metal ions and reduce the phytotoxic effects of heavy metal exposure (Lai, 2015). Metal-tolerant proteins such as metallothionein and phytochelatins are crucial metal-binding ligand that regulates cationic homeostasis of plant cell wall (Yu et al., 2018; Zhi et al., 2020). In Woad plants, Jia et al. (2020) identified strict connection between Cd chelation and S metabolic products based on the weakening of metal ion translocation from root to shoot. The study confirmed that NaHS stimulated the endogenous metal binding proteins, i.e., metallothionein 1A and phytochelatins, which in turn promoted Cd accumulation in the cell wall by modifying its contents, thus reducing intracellular metal ion mobility for detoxification. Previously, Jia et al. (2016) established an intertwining effect of H_2S and Cys in *A. thaliana* L. They found that sulfur metabolism has key role to play in the growth and development of plants exposed to Cd toxicity. Collectively, plant stress alleviators such as H_2S and Cys have been shown to resurrect root growth, as well as to increase plant Cd tolerance via S metabolite feedback loop. An active synergy between H_2S and proline pulls together millet plant from negative effects of Cd toxicity, as evidenced by induced Cd tolerance and stimulated biomass production (Tian et al., 2016). Apart from higher proline accumulation, as well as proline dehydrogenase (PDH) and proline-5-carboxylate reductase (P5CR) activities, the transcript levels of PDH and P5CR were also enhanced after H_2S treatment.

Also, Yu et al. (2019) have shown that exogenous NaHS application can increase Cd retention into the root cell wall of oilseed rape by stimulating LCD activity. Furthermore, NaHS led to increase in cellular pectin, and root methylesterase activity validates higher metal-binding capacity of root cell that repressed Cd translocation to aerial plant sections. In another study, downregulated metal homeostasis and uptake were recorded when young seedlings of black night shade plant were treated with NaHS under Zn stress (Liu et al., 2016). It has been noted that expression of the metallothionein was increased, leading to an improvement in plant Zn tolerance as shown by the chelation of excessive Zn in the cytoplasm. Moreover, elevated expression of antioxidant enzyme, CAT2, also prevented oxidative stress damages in metal-stressed plants as a result of H_2S treatment.

Seed viability is one of the crucial determinants of healthy plant growth and increased production. Seed germination and its emergence and subsequent seedling establishment contribute proportionally to achieve sustainability, growth, and productivity. Exogenous NaHS application has improved both seed germination and seedling emergence in cauliflower by scavenging Pb-induced ROS (Chen et al., 2018). Interestingly, H_2S-led exhibition of plant protection against Pb stress was comparable to ROS scavengers, i.e., 4,5-dihydroxy-1,3-benzene disulfonic acid and N, N′-dimethylthiourea. They concluded that non-enzymatic antioxidants, such as non-protein thiol and total glutathione, were upregulated by H_2S and improved Pb tolerance by ROS-scavenging and/or directly chelating metal ions. Plant exposure to metal ions often represses the activity of transporters, resulting in ionic imbalance and reduced nutrients assimilation in plants (Vaculík et al., 2020). In Zn-exposed pepper plants, exogenous NaHS treatment reduced Zn plant accumulation and enhanced the absorption of key mineral elements, i.e., Fe, N, P (Kaya et al., 2020). Moreover, mitigating effects of NaHS have been further up-scaled by antioxidant activity and osmotic adjustment to minimize membrane oxidative damage. Methylglyoxal (MG), a cytotoxic metabolic by-product of glycolytic pathways, usually interacts with macromolecules to trigger protein inactivation and induces oxidative damages

to plant under abiotic stress, such as heavy metals (Hoque et al., 2016; Bhuyan et al., 2020). In maize, Cr tolerance of young seedlings was linked to the suppression of NADPH oxidase activity, resulting in restricted ROS accumulation following exogenous application of NaHS (Kharbech et al., 2020). This study illustrated the potential function of glutathione in minimizing Cr toxicity by reducing MG content while preserving glutathione–ascorbate homeostasis for additional S metabolism, as demonstrated by the activity of glutathione S-transferase and reductase enzymes. Similarly, NaHS pretreatment also reduced the lipid peroxidation and electrolyte leakage in coriander seedling exposed to Cu toxicity (Karam and Keramat, 2017). These results further substantiate that NaHS-led changes in endogenous H_2S were presumably involved in the prevention of oxidative damages via cellular ascorbate–glutathione cycle. Similarly, mitigation of Cu toxicity in wheat has been linked to H_2S-related ascorbate–glutathione cycle (Shan et al., 2012). Moreover, decrease in lipid peroxidation and electrolyte leakage further implies a systemic defense response activated by NaHS application.

Photosynthesis is a key physiological process for plant productivity and directly provides energy for plant growth. Photosynthetic pigments are very sensitive to various abiotic stress including heavy metals, which can negatively affect rate of photosynthesis via chlorophyll and carotenoid degradation (Amari et al., 2017). RuBISCO (a multi-meric photosynthetic enzyme), reflects potential for plant productivity and the efficiency of resource use by its net C assimilation rate. There is some substantial evidence in literature that described about H_2S role of being a key regulator of plant photosynthetic apparatus (Carmo-Silva et al., 2015; Cummins et al., 2018). In spinach, Chen et al. (2011) found that NaHS-treated plants had significant increase in chlorophyll content alongside higher soluble protein content and biomass yield. This possibly highlights the significance of RuBISCO activity, which promotes chloroplast biogenesis, photosynthetic enzyme expression, and thiol redox alterations. Also, Bharwana et al. (2014) reported that NaHS application could regulate the photosynthetic activity of cotton seedlings under Pb toxicity. They concluded that higher photosynthesis is obviously a defense mechanism intended to minimize metal toxicity by accelerating rate of photosynthesis, which ultimately contribute to cope with predictable oxidative stress. Further results showed that H_2S also promoted the reversal of electrolyte leakage in cotton seedlings caused by Pb toxicity, as shown by reduced H_2O_2 and MDA contents. In another study, Rizwan et al. (2019) reported NaHS-induced upregulation of chloroplast biogenesis and N metabolism in rice plant exposed to Ni stress. The NaHS application has been found to increase the activities of various N-related enzymes, i.e., NR, nitrite reductase, glutamate synthase, glutamate oxaloacetate transaminase, glutamine synthetase, and glutamate pyruvate transaminase. Furthermore, key involvement of H_2S in Ni stress regulation of rice plant was also validated by the expression of genes abundance associated with N metabolism. Also, Chen et al. (2016) revealed the molecular basis of rice stress adaptation against mercury (Hg) contamination. In their study, H_2S pretreatment extended membrane transcriptional expression of bZIP60 and OsMT-1, which were involved in Hg localization in roots. In addition, Hg-related plant membrane damages were attenuated by scavenging ROS and downregulation of H_2O_2 and MDA, which eventually led to growth promotion of rice seedlings. The redox status of plant cell can be disrupted by accumulation of ROS associated with metal toxicity, resulting in a cascade of retarded physiological and morphological functions (Schutzendubel and Polle, 2002). In pea seedlings, H_2S application restored the cellular redox status of pea suffering from arsenate toxicity (Singh et al., 2015). It appears that H_2S-mediated recovery of ascorbate–glutathione enzymes pool was a pivotal contributor to plant defense, as depicted by suppression of oxygen free radicals and membrane damage.

STRESS ALLEVIATORS AND ENDOGENOUS H_2S: A COMBATING TOOL TOWARD METAL DETOXIFICATION

In some recent reports, enrolment of different plant growth regulators has also unveiled endogenous H_2S synthesis in plant that eventually provide a protective role in crop plants under stress (**Table 2**). NO has been deemed to be an important signaling compound that can stimulate plant growth and development in agriculture. A plethora of studies has investigated the key involvement of NO in activating plant defense response to heavy metal stress (Bai et al., 2014; Rizwan et al., 2018; Hu et al., 2019; Sharma et al., 2020a). A strong synergic association between exogenously applied NO and resultant endogenous synthesis of H_2S was involved in enhanced Cr resistance of tomato seedlings (Alamri et al., 2020). It appears that increased S assimilation and related enzyme metabolic activities have mitigated the depressing effect of metal ions in both cellular and molecular levels. Salicylic acid (SA), a phenolic compound, has been known to control a broad range of physiological and biochemical functions in plants to combat stressful conditions, including heavy metals (Hasanuzzaman et al., 2019; Sharma et al., 2020b). The exogenous application of Na_2SiO_3, a silicon derivative compound, endorsed a functional relationship between NO and H_2S in regulating the Cd stress of pepper plant (Kaya et al., 2020). It was evident that upregulation of endogenous NO and H_2S was central to metal stress alleviation as confirmed by lower Cd content of leaves. In addition, improvement in plant antioxidant activities, nutrients uptake (e.g., Ca, K), photosynthesis activity, and water relations upscaled the plant metal tolerance. In pepper experiment, SA prompted 66% higher buildup of endogenous H_2S in Pb-exposed leaves over untreated control (Kaya, 2020). It was further elucidated that efficient crosstalk between SA and H_2S averted induced phytotoxicity effect by minimizing Cd accumulation in leaves via upregulated metabolisms of the enzymes involved in ascorbate–glutathione cycle. Furthermore, SA and H_2S augmented leaf relative water, water potential, and proline content, which has key contribution in restoring the

TABLE 2 | Use of different stress alleviators and their interactions with endogenous H_2S for higher metal tolerance in plants.

Stress alleviator	Exogenous H_2S	Plant species	Experiment	Duration/ growth stage	Heavy metal/source	Exposure level	Endogenous H_2S	Stress alleviating symptoms	References
Silicon (Na_2SiO_3) 2.0 mM	NO	Pepper (*Capsicum annuum* L.)	Potted soil	35 days/ young seedlings	Cadmium: $CdCl_2$	0.1 mM	Upregulated ~10 μmol g^{-1} fresh weight	Reduced leaf Cd content and oxidative stress Improved K and Ca uptake	Kaya et al., 2020
Nitric oxide (NO) 50 μM	NO	Tomato (*Solanum lycopersicum* L.)	Pot filled with vermiculite-perlite	21 days/ young seedlings	Chromium: $K_2Cr_2O_7$	100 μM Cr (VI)	Upregulated ~98 nmol g^{-1} fresh weight	Increased S assimilation and kinked enzyme metabolism averted DNA and oxidative damages.	Alamri et al., 2020
Thiamine (THI) 50 mgL^{-1}	0.2 mM sodium hydrosulfide (NaHS)	Strawberry (*Fragaria* × *ananassa* Duch)	Hydroponic culture	28 days	Cadmium: $CdCl_2$	0.1 mM	Upregulated ~15 μmol g^{-1} fresh weight	Upregulated endogenous NO and hydrogen sulfide (H_2S); Enhanced Ca and K uptake	Kaya and Aslan, 2020
0.5 mM salicylic acid (SA)	0.2 mM sodium hydrosulfide (NaHS)	Pepper (*Capsicum annuum* L.)	Perlite pot	28 days/ young seedlings	Lead; $PbCl_2$	0.1 mM	Upregulated ~23 μmol g^{-1} fresh weight	Pb induced phytotoxicity was alleviated by SA + NaHS related upregulation in ascorbate–glutathione cycle	Kaya, 2020
Calcium ($CaCl_2$) 15 mM	100 μM sodium hydrosulfide (NaHS)	Zucchini (*Cucurbita pepo* L.)	Hydroponic culture	14 days/ young seedlings	Nickel: Ni $(NO_3)_2$	50 mg L^{-1}	Upregulated ~323 nmol g^{-1} fresh weight	Both extracellular (Ca^{2+}) and intracellular (CaM) complex activated crosstalk of Ca^{2+} and H_2S to revert plant oxidative damages	Valivand et al., 2019
0.5 mM salicylic acid (SA)	0.5 mM sodium hydrosulfide (NaHS	Maize (*Zea mays* L.)	Potted sand–perlite	9 days/ young seedlings	Lead: Pb $(NO_3)_2$	2.5 mM	Not detected	Regulated metal toxicity by increasing glycine betaine and NO at the expense of S-amino acids metabolism, i.e., arginine, methionine	Zanganeh et al., 2018
0.5 mM salicylic acid (SA)	NO	Maize (*Zea mays* L.)	Potted sand–perlite	9 days/ young seedlings	Lead: Pb $(NO_3)_2$	2.5 mM	Upregulated ~3.5 μmol g^{-1} fresh weight	Minimized chlorophyll related damages, built-up ascorbic acid glutathione and upregulation of antioxidant enzyme activity	Zanganeh et al., 2019
1 μM methyl jasmonate (MeJA)	50 μM sodium hydrosulfide (NaHS)	Foxtail millet (*Setaria italica* L.)	Hydroponic culture	14 days/ young seedlings	Cadmium chloride ($CdCl_2$)	200 μM	Upregulated 75–120 nm g^{-1} fresh weight	Alleviated growth retardations by decreasing H_2O_2 and malondialdehyde content, also repressed Cd accumulation in seedlings	Tian et al., 2017

phenotypic appearance of Pb-stressed plants. In another study with maize exposed to Pb stress, Zanganeh et al. (2018) pointed out the synergic effect of SA and H_2S, which contributed to the relegation of metal-induced phytotoxicity by augmenting glycine-betaine and NO signaling. It was found that SA and NO signaling play an instrumental role in plant growth regulation as they boosted the S-assimilation via arginine–methionine metabolism and thus prevented Pb-induced oxidative stress injury in plants.

Thiamine (THI) is another unique biomolecules that can effectively control plant growth by facilitating the synthesis of carbohydrate, nucleic acids, adenosine triphosphate, and nicotinamide adenine dinucleotide phosphate (Nosaka, 2006). At the same time, it can also activate defensive responses in plants as a non-cofactor (Bettendorff and Wins, 2013; Yusof et al., 2015). Recent work utilizing THI as growth regulators in strawberry transplants exposed to Cd stress has revealed a 1.7-fold increase in endogenous H_2S levels and displayed enhanced metal tolerance (Kaya and Aslan, 2020). They found that endogenous NO levels have also demonstrated the similar rise following THI treatment. The increase in leaf H_2S concentration caused the upregulation of MDA and H_2O_2, while antioxidant enzyme activities were downregulated to overcome Cd toxicity. Furthermore, endogenous H_2S improved mechanical stability and physiological functions of strawberry plants by markedly increasing the uptake of key nutrient elements, i.e., calcium and potassium. Although calcium (Ca) is typically an essential macronutrient required for normal plant growth, it can act as a universal messenger to establish systemic defense response and tolerance acquisition under stressful conditions (Jalmi et al., 2018). Several studies confirmed that exogenous Ca application can lead to higher stress tolerance in plants upon heavy metal exposure (Gonzalez et al., 2012; Ahmad et al., 2015; Aziz et al., 2015). According to Valivand et al. (2019), two-sided crosstalk between exogenous Ca and endogenous H_2S appears to mediate defense response in *Zucchini* plant exposed to Ni stress. The Ca signaling cascade from roots to leaves has been involved in endogenous H_2S synthesis that contributes toward a systemic acclimation against Ni stress. At the same time, antioxidant enzyme activities and genetic expression of calmodulin (CaM) protein further strengthen the metal ion tolerance of young seedlings, as demonstrated by reduced electrolyte leakage and oxidative injury. This study further supports the fact that both intracellular and extracellular Ca-based complexes are important for the synthesis of endogenous H_2S to improve plant metal tolerance. Ascorbate–glutathione metabolism involves antioxidant defense system that perceives stress and regulates plant growth by coordinating the activities of detoxification of ROS by its key enzymes–ascorbate peroxidase, monodehydroascorbate reductase, dehydroascorbate reductase, and glutathione reductase (Hasanuzzaman et al., 2017). In maize, Zanganeh et al. (2019) showed that endogenous H_2S positively regulated early growth of young seedlings via SA-mediated Pb detoxification. Plant exposure to metal ion significantly deteriorated chlorophyll content and restricted nutrients uptake, whereas H_2S-SA crosstalk was instrumental in reversal of selected plant physiological and biochemical attributes, indicated by higher plant expression of ascorbic acid–glutathione metabolic activities. Methyl jasmonate (MeJA), a volatile derivative of jasmonic acid, serves as main cell signaling molecule mediating various key plant processes and also triggers plant defense in response to wide array of abiotic stresses (Raza et al., 2020). In foxtail millet, exogenous MeJA and NaHS showed an increase in endogenous H_2S (75–120 nm g FW^{-1}) and restore seedling growth under Cd stress (Tian et al., 2017). The results suggest that endogenous H_2S buildup was a pivotal component of ROS mitigation, thus hindering the accumulation of Cd in young seedlings. In addition, positive interplay between MeJA and H_2S augmented Cd-induced expression of the homeostasis-related genes (MTP1, MTP12, CAX2, and ZIP4).

CONCLUSION AND FUTURE PROSPECTIVE

In agriculture, abiotic stress involving heavy metals contributes to major production losses globally. It is broadly acknowledged that H_2S can mitigate the abiotic stresses including heavy metal stress. This review provides insight into beneficial aspects of H_2S on plant biochemical and physiological responses against heavy metal stress. After a thorough review of the available literature, we found that heavy metals inhibit plant growth, which unfortunately disturbs food production and eventually leads to food shortfall. Application of H_2S has shown effective mitigation of heavy metals related by strengthening the biochemical and physiological functions of plants. Treatment of H_2S devotedly leads to the enhancement in plant growth, photosynthetic pigments, biomass, nutrient uptake, gas exchange parameters, and antioxidant enzymes of plants.

Taking due account of the above findings and studies, it is strongly concluded that H_2S treatment effectively reduces the harmful effects of many heavy metals (Al, Cd, B, Pb, Cr, and Cu) by obstructing the accumulation of heavy metals in various plants. Such results strongly indicate that H_2S treatment could be used effectively as a signal molecule to inhibit the oxidative stress caused by heavy metal contamination. Recently, interaction of certain signal molecules and growth regulators with H_2S application has been investigated in order to regulate plant growth against heavy metal stress. Nonetheless, future work on other emerging signaling molecules and phytohormones is highly desirable, which can provide us a better understanding of these signaling molecules that affect the concentration of plant hormones and thus control the toxicity of metals in plants. Moreover, further investigations

at genomics, transcriptomic, and metabolomics scale are required to explore the particular H_2S-generated tolerance mechanism in various plants against heavy metal stress. On the other hand, effective, widespread, and ongoing field trials using organic amendments and/or metal-tolerant microbial inoculant can also be tested for their protective role against the exposed contaminants, which can also upscale the effectiveness of H_2S in heavy metal-contaminated degraded land.

AUTHOR CONTRIBUTIONS

All authors listed have made a substantial, direct and intellectual contribution to the work, and approved it for publication.

FUNDING

This research was funded by the Deanship of Scientific Research at Princess Nourah Bint Abdulrahman University through the Fast-track Research Funding Program.

ACKNOWLEDGMENTS

The authors highly acknowledge the Government College University, Faisalabad, Pakistan for its support. This work was financially supported by Fast-track Research Funding Program under the Deanship of Scientific Research at Princess Nourah Bint Abdulrahman University.

REFERENCES

Ahmad, I., Akhtar, M. J., Zahir, Z. A., and Jamil, A. (2012). Effect of cadmium on seed germination and seedling growth of four wheat (*Triticum aestivum* L.) cultivars. *Pak. J. Bot.* 5, 1569–1574.

Ahmad, M. S., Ashraf, M., and Hussain, M. (2011). Phytotoxic effects of nickel on yield and concentration of macro- and micro-nutrients in sunflower (*Helianthus annuus* L.) achenes. *J. Hazard. Mater.* 185, 1295–1303. doi: 10.1016/j.jhazmat.2010.10.045

Ahmad, P., Sarwat, M., Bhat, N. A., Wani, M. R., Kazi, A. G., Tran, L. S., et al. (2015). Alleviation of cadmium toxicity in *Brassica juncea* L. by calcium application involves various physiological and biochemical strategies. *PLoS One* 10:e0114571. doi: 10.1371/journal.pone.0114571

Ahmad, R., Ali, S., Rizwan, M., Dawood, M., Farid, M., Hussain, A., et al. (2020). Hydrogen sulfide alleviates chromium stress on cauliflower by restricting its uptake and enhancing antioxidative system. *Physiol. Plant.* 168, 289–300.

Akaike, T., Ida, T., Wei, F.-Y., Nishida, M., Kumagai, Y., Alam, M. M., et al. (2017). Cysteinyl-tRNA synthetase governs cysteine polysulfidation and mitochondrial bioenergetics. *Nat. Commun.* 8:1177.

Alamri, S., Ali, H. M., Khan, M. I. R., Singh, V. P., and Siddiqui, M. H. (2020). Exogenous nitric oxide requires endogenous hydrogen sulfide to induced the resilience through sulfur assimilation in tomato seedlings under hexavalent chromium toxicity. *Plant Physiol. Biochem.* 155, 20–34. doi: 10.1016/j.plaphy.2020.07.003

Alloway, B. J. (1995). *Heavy Metals in Soils*. Glasgow: Blackie Academic and Professional.

Alloway, B. J. (2013). *Heavy Metals in Soils: Trace Metals and Metalloids in Soils and Their Bioavailability*, 3rd Edn. Glasgow: Blackie Academic and Professional.

Amari, T., Ghnaya, T., and Abdelly, C. (2017). Nickel, cadmium and lead phytotoxicity and potential of halophytic plants in heavy metal extraction. *South Afr. J. Bot.* 111, 99–110. doi: 10.1016/j.sajb.2017.03.011

Arif, M. S., Yasmeen, T., Shahzad, S. M., Riaz, M., Rizwan, M., Iqbal, S., et al. (2019). Lead toxicity induced phytotoxic effects on mung bean can be relegated by lead tolerant *Bacillus subtilis* (PbRB3). *Chemosphere* 234, 70–80. doi: 10.1016/j.chemosphere.2019.06.024

Aroca, A., Gotor, C., Bassham, D. C., and Romero, L. C. (2020). Hydrogen sulfide: from a toxic molecule to a key molecule of cell life. *Antioxidants.* 9:621. doi: 10.3390/antiox9070621

Aroca, A., Serna, A., Gotor, C., and Romero, L. C. (2015). S-sulfhydration: a cysteine posttranslational modification in plant systems. *Plant Physiol.* 168, 334–342. doi: 10.1104/pp.15.00009

Azevedo, R. A., and Lea, P. J. (2005). Toxic metals in plants. *Br. J. Plant Physiol.* 17:1. doi: 10.1590/s1677-04202005000100001

Aziz, H., Sabir, M., Ahmad, H. R., Aziz, T., Zia-ur-Rehman, M., Hakeem, K. R., et al. (2015). Alleviating effect of calcium on nickel toxicity in rice. *Clean Soil Air Water* 43, 787–866.

Bai, X. Y., Dong, Y. J., Wang, Q. H., Xu, L. L., Kong, J., and Liu, S. (2014). Effects of lead and nitric oxide on photosynthesis, antioxidative ability, and mineral element content of perennial ryegrass. *Biol. Plant.* 59, 163–170. doi: 10.1007/s10535-014-0476-8

Bettendorff, L., and Wins, P. (2013). Thiamine triphosphatase and the CYTH superfamily of proteins. *FEBS J.* 280, 6443–6455. doi: 10.1111/febs.12498

Bharwana, S. A., Ali, S., Farooq, M. A., Ali, B., Iqbal, N., Abbas, F., et al. (2014). Hydrogen sulfide ameliorates lead-induced morphological, photosynthetic, oxidative damages and biochemical changes in cotton. *Environ. Sci. Pollut. Res.* 21, 717–731. doi: 10.1007/s11356-013-1920-6

Bhuyan, M. H. M. B., Parvin, K., Mohsin, S. M., Mahmud, J. A., Hasanuzzaman, M., and Fujita, M. (2020). Modulation of cadmium tolerance in rice: insight into vanillic acid-induced upregulation of antioxidant defense and glyoxalase systems. *Plants* 9:188. doi: 10.3390/plants9020188

Calderwood, A., and Kopriva, S. (2014). Hydrogen sulfide in plants: from dissipation of excess sulfur to signaling molecule. *Nitric Oxide* 41, 72–78. doi: 10.1016/j.niox.2014.02.005

Carmo-Silva, E., Scales, J. C., Madgwick, P. J., and Parry, M. A. J. (2015). Optimizing Rubisco and its regulation for greater resource use efficiency. *Plant Cell Environ.* 38, 1817–1832. doi: 10.1111/pce.12425

Chen, J., Wu, F. H., Wang, W. H., Zheng, C. J., Lin, G. H., Dong, X. J., et al. (2011). Hydrogen sulfide enhances photosynthesis through promoting chloroplast biogenesis, photosynthetic enzyme expression, and thiol redox modification in *Spinacia oleracea* seedlings. *J. Exp. Bot.* 62, 4481–4493. doi: 10.1093/jxb/err145

Chen, T., Tian, M., and Han, Y. (2020). Hydrogen sulfide: a multi-tasking signal molecule in the regulation of oxidative stress responses. *J. Exp. Bot.* 71, 2862–2869. doi: 10.1093/jxb/eraa093

Chen, Z., Chen, M., and Jiang, M. (2016). Hydrogen sulfide alleviates mercury toxicity by sequestering it in roots or regulating reactive oxygen species productions in rice seedlings. *Plant Physiol. Biochem.* 111, 179–192. doi: 10.1016/j.plaphy.2016.11.027

Chen, Z., Yang, B., Hao, Z., Zhu, J., Zhang, Y., and Xu, T. (2018). Exogenous hydrogen sulfide ameliorates seed germination and seedling growth of cauliflower under lead stress and its antioxidant role. *J. Plant Growth Regul.* 37, 5–15. doi: 10.1007/s00344-017-9704-8

Corpas, F. J., Barroso, J. B., Gonzalez-Gordo, S., Munoz-Vargas, M. A., and Palma, J. M. (2019a). Hydrogen sulfide: a novel component in *Arabidopsis* peroxisomes which triggers catalase inhibition. *J. Integr. Plant Biol.* 61, 871–883.

Corpas, F. J., González-Gordo, S., Cañas, A., and Palma, J. M. (2019b). Nitric oxide and hydrogen sulfide in plants: which comes first? *J. Exp. Bot.* 70, 4391–4404. doi: 10.1093/jxb/erz031

Cuevasanta, E., Moller, M. N., and Alvarez, B. (2017). Biological chemistry of hydrogen sulfide and persulfides. *Arch. Biochem. Biophys.* 617, 9–25. doi: 10.1016/j.abb.2016.09.018

Cummins, P. L., Kannappan, B., and Gready, J. E. (2018). Directions for optimization of photosynthetic carbon fixation: RuBisCO's efficiency may not be so constrained after all. *Front. Plant Sci.* 9:183.

De Kok, L. J., Castro, A., Durenkamp, M., Stuiver, C. E. E., Westerman, S., Yang, L., et al. (2002). "Sulphur in plant physiology," in *Proceedings No 500, The International Fertiliser Society*, New York, NY. doi: 10.1016/j.plaphy.2016.12.024

DeLeon, E. R., Stoy, G. F., and Olson, K. R. (2012). Passive loss of hydrogen sulfide in biological experiments. *Anal. Biochem.* 421, 203–207. doi: 10.1016/j.ab.2011.10.016

Duffus, J. H. (2002). "Heavy metals" a meaningless term? (IUPAC Technical Report). *Pure appl. Chem.* 74, 793–807. doi: 10.1351/pac200274050793

Fang, L., Ju, W., Yang, C., Jin, X., Liu, D., Li, M., et al. (2020). Exogenous application of signaling molecules to enhance the resistance of legume-rhizobium symbiosis in Pb/Cd-contaminated soils. *Environ. Pollut.* 265:114744. doi: 10.1016/j.envpol.2020.114744

Filipovic, M. R., Zivanovic, J., Alvarez, B., and Banerjee, R. (2018). Chemical biology of H_2S signaling through persulfidation. *Chem. Rev.* 118, 1253–1337. doi: 10.1021/acs.chemrev.7b00205

Gonzalez, A., Cabrera, M., de, L., Henriquez, M. J., Contreras, R. A., Morales, B., et al. (2012). Cross talk among calcium, hydrogen peroxide, and nitric oxide and activation of gene expression involving calmodulins and calcium-dependent protein kinases in *Ulva compressa* exposed to copper excess. *Plant Physiol.* 158, 1451–1462. doi: 10.1104/pp.111.191759

Gotor, C., García, I., Aroca, Á, Laureano-Marín, A. M., Arenas-Alfonseca, L., Jurado-Flores, A., et al. (2019). Signaling by hydrogen sulfide and cyanide through post-translational modification. *J. Exp.Bot.* 70, 4251–4265. doi: 10.1093/jxb/erz225

Grant, R., and Grant, C. (1987). *Grant and Hackh's Chemical Dictionary*. New York, NY: McGraw-Hill.

Han, Y., Yin, Y., and Yi, H. (2020). Decreased endogenous nitric oxide contributes to sulfur dioxide derivative alleviated cadmium toxicity in *Foxtail millet* roots. *Environ. Exp. Bot.* 177:104144. doi: 10.1016/j.envexpbot.2020.104144

Hancock, J. T. (2017). Harnessing evolutionary toxins for signaling: reactive oxygen species, nitric oxide and hydrogen sulfide in plant cell regulation. *Front. Plant. Sci.* 8:189.

Hancock, J. T., and Whiteman, M. (2016). Hydrogen sulfide signaling: interactions with nitric oxide and reactive oxygen species. *Ann. N. Y. Acad. Sci.* 1365, 5–14. doi: 10.1111/nyas.12733

Hasanuzzaman, M., Matin, M. A., Fardus, J., Hasanuzzaman, M., Hossain, M. S., and Parvin, K. (2019). Foliar application of salicylic acid improves growth and yield attributes by upregulating the antioxidant defense system in Brassica campestris plants grown in lead-amended soils. *Acta Agro. Bot.* 72:1765.

Hasanuzzaman, M., Nahar, K., Anee, T. I., and Fujita, M. (2017). Exogenous silicon attenuates cadmium-induced oxidative stress in *Brassica napus* L. by modulating AsA-GSH pathway and glyoxalase system. *Front. Plant Sci.* 8:1061.

He, H., Li, Y., and He, L. F. (2019). Role of nitric oxide and hydrogen sulfide in plant aluminum tolerance. *Biometals* 32, 1–9. doi: 10.1007/s10534-018-0156-9

Hoque, T. S., Hossain, M. A., Mostofa, M. G., Burritt, D. J., Fujita, M., and Tran, L. S. P. (2016). Methylglyoxal: an emerging signaling molecule in plant abiotic stress responses and tolerance. *Front. Plant Sci.* 7:1341.

Hu, Y., Lu, L., Tian, S., Li, S., Liu, X., Gao, X., et al. (2019). Cadmium-induced nitric oxide burst enhances Cd tolerance at early stage in roots of a hyperaccumulator *Sedum alfredii* partially by altering glutathione metabolism. *Sci. Total Environ.* 650, 2761–2770. doi: 10.1016/j.scitotenv.2018.09.269

Huo, J., Huang, D., Zhang, J., Fang, H., Wang, B., Wang, C., et al. (2018). Hydrogen sulfide: a gaseous molecule in postharvest freshness. *Front. Plant Sci.* 27:1172.

Ida, T., Sawa, T., Ihara, H., Tsuchiya, Y., Watanabe, Y., Kumagai, Y., et al. (2014). Reactive cysteine persulfides and S-polythiolation regulate oxidative stress and redox signaling. *Proc. Natl. Acad. Sci. U.S.A.* 111, 7606–7611. doi: 10.1073/pnas.1321232111

Jalmi, S. K., Bhagat, P. K., Verma, D., Noryang, S., Tayyeba, S., Singh, K., et al. (2018). Traversing the links between heavy metal stress and plant signaling. *Front. Plant Sci.* 9:12.

Jia, H., Wang, X., Dou, Y., Liu, D., Si, W., Fang, H., et al. (2016). Hydrogen sulfide - cysteine cycle system enhances cadmium tolerance through alleviating cadmium-induced oxidative stress and ion toxicity in *Arabidopsis* roots. *Sci. Rep.* 6:39702.

Jia, H., Wang, X., Shi, C., Guo, J., Ma, P., Wei, T., et al. (2020). Hydrogen sulfide decreases Cd translocation from root to shoot through increasing Cd accumulation in cell wall and decreasing Cd^{2+} influx in *Isatis indigotica*. *Plant Physiol. Biochem.* 155, 605–612. doi: 10.1016/j.plaphy.2020.08.033

Kabil, O., and Banerjee, R. (2010). Redox biochemistry of hydrogen sulfide. *J. Biol. Chem.* 285, 21903–21907. doi: 10.1074/jbc.r110.128363

Karam, E. A., and Keramat, B. (2017). Hydrogen sulfide protects coriander seedlings against copper stress by regulating the ascorbate-glutathione cycle in leaves. *J. Plant Process Funct.* 5, 59–64.

Kasamatsu, S., Nishimura, A., Morita, M., Matsunaga, T., Abdul Hamid, H., and Akaike, T. (2016). Redox signaling regulated by cysteine persulfide and protein polysulfidation. *Molecules* 21:E1721.

Kaya, C. (2020). Salicylic acid-induced hydrogen sulphide improves lead stress tolerance in pepper plants by upraising the ascorbate-glutathione cycle. *Physiol. Plant* [Epub ahead of print]. doi: 10.1111/ppl.13159

Kaya, C., Akram, N. A., Ashraf, M., Alyemeni, M. N., and Ahmad, P. (2020). Exogenously supplied silicon (Si) improves cadmium tolerance in pepper (*Capsicum annuum* L.) by up-regulating the synthesis of nitric oxide and hydrogen sulfide. *J. Biotechnol.* 316, 35–45. doi: 10.1016/j.jbiotec.2020.04.008

Kaya, C., Ashraf, M., and Akram, N. A. (2018). Hydrogen sulfide regulates the levels of key metabolites and antioxidant defense system to counteract oxidative stress in pepper (*Capsicum annuum* L.) plants exposed to high zinc regime. *Environ. Sci. Pollut. Res.* 25, 12612–12618. doi: 10.1007/s11356-018-1510-8

Kaya, C., and Aslan, M. (2020). Hydrogen sulphide partly involves in thiamine-induced tolerance to cadmium toxicity in strawberry (Fragaria x ananassa Duch) plants. *Environ. Sci. Pollut. Res.* 27, 941–953. doi: 10.1007/s11356-019-07056-z

Kharbech, O., Massoud, M. B., Sakouhi, L., Djebali, W., Mur, L. A. J., and Chaoui, A. (2020). Exogenous application of hydrogen sulfide reduces chromium toxicity in maize seedlings by suppressing NADPH oxidase activities and methylglyoxal accumulation. *Plant Physiol. Biochem.* 154, 646–656. doi: 10.1016/j.plaphy.2020.06.002

Kimura, Y., Koike, S., Shibuya, N., Lefer, D., Ogasawara, Y., and Kimura, H. (2017). 3-Mercaptopyruvate sulfurtransferase produces potential redox regulators cysteine- and glutathione-persulfide (Cys-SSH and GSSH) together with signaling molecules H_2S_2, H_2S_3 and H_2S. *Sci. Rep.* 7:10459.

Krueger, S., Niehl, A., Martin, M. C., Steinhauser, D., Donath, A., Hildebrandt, T., et al. (2009). Analysis of cytosolic and plastidic serine acetyltransferase mutants and subcellular metabolite distributions suggests interplay of the cellular compartments for cysteine biosynthesis in *Arabidopsis*. *Plant Cell Environ.* 32, 349–367. doi: 10.1111/j.1365-3040.2009.01928.x

Krzesłowska, M. (2011). The cell wall in plant cell response to trace metals: polysaccharide remodeling and its role in defense strategy. *Acta Physiol. Plant.* 33, 35–51. doi: 10.1007/s11738-010-0581-z

Kushwaha, B. K., and Singh, V. P. (2019). Glutathione and hydrogen sulfide are required for sulfur-mediated mitigation of Cr (VI) toxicity in tomato, pea and brinjal seedlings. *Physiol. Plant* 168, 406–421.

Lado, L. R., Hengl, T., and Reuter, H. I. (2008). Heavy metals in European soils: a geostatistical analysis of the FOREGS geochemical database. *Geoderma* 148, 189–199. doi: 10.1016/j.geoderma.2008.09.020

Lai, H. Y. (2015). Subcellular distribution and chemical forms of cadmium in *Impatiens walleriana* in relation to its phytoextraction potential. *Chemosphere* 138, 370–376. doi: 10.1016/j.chemosphere.2015.06.047

Lasat, M. M. (2002). Phytoextraction of toxic metals A review of biological mechanism. *J Environ. Qual.* 31, 109–120. doi: 10.2134/jeq2002.1090

Li, L., Wang, Y., and Shen, W. (2012). Roles of hydrogen sulphide and nitric oxide in the alleviation of cadmium-induced oxidative damage in alfalfa seedling roots. *Biometals* 25, 617–631. doi: 10.1007/s10534-012-9551-9

Li, Z. G. (2013). Hydrogen sulfide: a multifunctional gaseous molecule in plants. *Russ. J. Plant Physiol.* 60, 733–740. doi: 10.1134/s1021443713060058

Li, Z. G., Min, X., and Zhou, Z. H. (2016). Hydrogen sulfide: a signal molecule in plant cross-adaptation. *Front. Plant Sci.* 7:1621.

Lin, Y. T., Li, M. Y., Cui, W. T., Lu, W., and Shen, W. B. (2012). Haem oxygenase-1 is involved in hydrogen sulfide-induced cucumber adventitious root formation. *J. Plant Growth Regul.* 3, 519–528. doi: 10.1007/s00344-012-9262-z

Lisjak, M., Srivastava, N., Teklic, T., Civale, L., Lewandowski, K., Wilson, I., et al. (2010). A novel hydrogen sulfide donor causes stomatal opening and reduces nitric oxide accumulation. *Plant Physiol. Biochem.* 48, 931–935. doi: 10.1016/j.plaphy.2010.09.016

Liu, T. J., Liu, X. N., Liu, M. L., and Wu, L. (2018). Evaluating heavy metal stress levels in rice based on remote sensing phenology. *Sensors* 18:860. doi: 10.3390/s18030860

Liu, X., Chen, J., Wang, G.-H., Wang, W.-H., Shen, Z.-J., Luo, M.-R., et al. (2016). Hydrogen sulfide alleviates zinc toxicity by reducing zinc uptake and regulating genes expression of antioxidative enzymes and metallothioneins in roots of the cadmium/zinc hyperaccumulator *Solanum nigrum* L. *Plant Soil* 400, 177–192. doi: 10.1007/s11104-015-2719-7

Luo, S., Calderón-Urrea, A., Yu, J., Liao, W., Xie, J., Lv, J., et al. (2020). The role of hydrogen sulfide in plant alleviates heavy metal stress. *Plant Soil* 449, 1–10. doi: 10.1007/s11104-020-04471-x

Mancardi, D., Penna, C., Merlino, A., Del Soldato, P., Wink, D. A., and Pagliaro, P. (2009). Physiological and pharmacological features of the novel gasotransmitter: hydrogen sulfide. *BBA Bioenerget.* 1787, 864–872. doi: 10.1016/j.bbabio.2009.03.005

Mataka, L. M., Henry, E. M. T., Masamba, W. R. L., and Sajidu, S. M. (2006). Lead remediation of contaminated water using *Moringa stenopetala* sp., and *Moringa oleifera* sp., seed powder. *Inter. J. Environ. Sci. Tech.* 2, 131–139. doi: 10.1007/bf03325916

Mostofa, M. G., Rahman, A., Ansary, M. M. U., Watanabe, A., Fujita, M., and Tran, L. S. P. (2015). Hydrogen sulfide modulates cadmium-induced physiological and biochemical responses to alleviate cadmium toxicity in rice. *Sci. Rep.* 5:14078.

Mustafa, A. K., Gadalla, M. M., Sen, N., Kim, S., Mu, W., Gazi, S. K., et al. (2009). H_2S signals through protein S-sulfhydration. *Sci. Signal.* 2:ra72. doi: 10.1126/scisignal.2000464

Nosaka, K. (2006). Recent progress in understanding thiamin biosynthesis and its genetic regulation in *Saccharomyces cerevisiae*. *Appl. Microbiol. Biotechnol.* 72, 30–40. doi: 10.1007/s00253-006-0464-9

Pandey, A. K., and Gautam, A. (2019). Stress responsive gene regulation in relation to hydrogen sulfide in plants under abiotic stress. *Physiol. Plant* 168, 511–525.

Paul, B. D., and Snyder, S. H. (2012). H2S signalling through protein sulfhydration and beyond. *Nat. Rev. Mol. Cell Biol.* 13, 499–507. doi: 10.1038/nrm3391

Peng, B., and Xian, M. (2015). Hydrogen sulfide detection using nucleophilic substitution-cyclization-based fluorescent probes. *Methods Enzymol.* 554, 47–62. doi: 10.1016/bs.mie.2014.11.030

Rather, B. A., Mir, I. R., Sehar, Z., Anjum, N. A., Masood, A., and Khan, N. A. (2020). The outcomes of the functional interplay of nitric oxide and hydrogen sulfide in metal stress tolerance in plants. *Plant Physiol. Biochem.* 155, 523–534. doi: 10.1016/j.plaphy.2020.08.005

Rausch, T., and Wachter, A. (2005). Sulfur metabolism: a versatile platform for launching defence operations. *Trends Plant Sci.* 10, 503–509. doi: 10.1016/j.tplants.2005.08.006

Raza, A., Charagh, S., Zahid, Z., Mubarik, M. S., Javed, R., Siddiqui, M. H., et al. (2020). Jasmonic acid: a key frontier in conferring a biotic stress tolerance in plants. *Plant Cell Rep.* [Epub ahead of print]. doi: 10.1007/s00299-020-02614-z

Reichman, S. M. (2007). The potential use of the legume-rhizobium symbiosis for the remediation of arsenic contaminated sites. *Soil Biol. Biochem.* 39, 2587–2593. doi: 10.1016/j.soilbio.2007.04.030

Rennenberg, H. (1983). Role of O-acetylserine in hydrogen sulfide emission from pumpkin leaves in response to sulfate. *Plant Physiol.* 73, 560–565. doi: 10.1104/pp.73.3.560

Rennenberg, H. (1984). The fate excess of sulfur in higher plants. *Annu. Rev. Plant Physiol.* 35, 121–153. doi: 10.1146/annurev.pp.35.060184.001005

Rennenberg, H., Huber, B., Schroder, P., Stahl, K., Haunold, W., Georgii, H. W., et al. (1990). Emission of volatile sulfur compounds from spruce trees. *Plant Physiol.* 92, 560–564. doi: 10.1104/pp.92.3.560

Riemenschneider, A., Nikiforova, V., Hoefgen, R., De Kok, L. J., and Papenbrock, J. (2005a). Impact of elevated H_2S on metabolite levels, activity of enzymes and expression of genes involved in cysteine metabolism. *Plant Physiol. Biochem.* 43, 473–448. doi: 10.1016/j.plaphy.2005.04.001

Riemenschneider, A., Riedel, K., Hoefgen, R., Papenbrok, J., and Hesse, H. (2005b). Impact of reduced *O*-acetylserine (thiol) lyase iso-form contents on potato plant metabolism. *Plant Physiol.* 137, 892–900. doi: 10.1104/pp.104.057125

Rizwan, M., Mostofa, M. G., Ahmad, M. Z., Imtiaz, M., Mehmood, S., Adeel, M., et al. (2018). Nitric oxide induces rice tolerance to excessive nickel by regulating nickel uptake, reactive oxygen species detoxification and defense- related gene expression. *Chemosphere* 191, 23–35. doi: 10.1016/j.chemosphere.2017.09.068

Rizwan, M., Mostofa, M. G., Ahmad, M. Z., Zhou, Y., Adeel, M., Mehmood, S., et al. (2019). Hydrogen sulfide enhances rice tolerance to nickel through the prevention of chloroplast damage and the improvement of nitrogen metabolism under excessive nickel. *Plant Physiol. Biochem.* 138, 100–111. doi: 10.1016/j.plaphy.2019.02.023

Rubright, S. L. M., Pearce, L. L., and Peterson, J. (2017). Environmental toxicology of hydrogen sulfide Nitric Oxide. *Biol. Chem.* 71:1. doi: 10.1016/j.niox.2017.09.011

Schutzendubel, A., and Polle, A. (2002). Plant responses to abiotic stresses: heavy metal-induced oxidative stress and protection by mycorrhization. *J. Exp. Bot.* 53, 1351–1365. doi: 10.1093/jexbot/53.372.1351

Sekiya, J., Schmidt, A., Wilson, L. G., and Filner, P. (1982a). Emission of hydrogen sulfide by leaf tissue in response to L-cysteine. *Plant Physiol.* 70, 430–436. doi: 10.1104/pp.70.2.430

Sekiya, J., Wilson, L. G., and Filner, P. (1982b). Resistance to injury by sulfur dioxide: correlation with its reduction to, and emission of, hydrogen sulfide in Cucurbitaceae. *Plant Physiol.* 70, 437–441. doi: 10.1104/pp.70.2.437

Shan, C., Dai, H., and Sun, Y. (2012). Hydrogen sulfide protects wheat seedlings against copper stress by regulating the ascorbate and glutathione metabolism in leaves. *Aust. J. Crop Sci.* 6, 248–254.

Shan, C. J., Zhang, S. L., Li, D. F., Zhao, Y. Z., Tian, X. L., Zhao, X. L., et al. (2011). Effects of exogenous hydrogen sulfide on the ascorbate and glutathione metabolism in wheat seedlings leaves under water stress. *Acta. Physiol. Plant.* 33, 2533–2540. doi: 10.1007/s11738-011-0746-4

Sharma, A., and Dhiman, A. (2013). Nickel and cadmium toxicity in plants. *J. Pharm. Sci. Innov.* 2, 20–24. doi: 10.7897/2277-4572.02213

Sharma, A., Sidhu, G. P. S., Araniti, F., Bali, A. S., Shahzad, B., Tripathi, D. K., et al. (2020b). The role of salicylic acid in plants exposed to heavy metals. *Molecules* 25:540. doi: 10.3390/molecules25030540

Sharma, A., Soares, C., Sousa, B., Martins, M., Kumar, V., Shahzad, B., et al. (2020a). Nitric oxide-mediated regulation of oxidative stress in plants under metal stress: a review on molecular and biochemical aspects. *Physiol. Planta.* 168, 318–344. doi: 10.1111/ppl.13004

Shen, G. T., Ju, W. L., Liu, Y. Q., Guo, X. B., Zhao, W., and Fang, L. C. (2019). Impact of urea addition and rhizobium inoculation on plant resistance in metal contaminated soil. *Int. J. Environ. Res. Publ. Health* 16:1955. doi: 10.3390/ijerph16111955

Shivaraj, S. M., Vats, S., Bhat, J. A., Dhakte, P., Goyal, V., Khatri, P., et al. (2020). Nitric oxide and hydrogen sulfide crosstalk during heavy metal stress in plants. *Physiol. Planta* 168, 437–455.

Singh, V. P., Singh, S., Kumar, J., and Prasad, S. M. (2015). Hydrogen sulfide alleviates toxic effects of arsenate in pea seedlings through up-regulation of the ascorbate-glutathione cycle: possible involvement of nitric oxide. *J. Plant Physiol.* 181, 20–29. doi: 10.1016/j.jplph.2015.03.015

Takahashi, H., Kopriva, S., Giordano, M., Saito, K., and Hell, R. (2011). Sulfur assimilation in photosynthetic organisms: molecular functions and regulations of transporters and assimilatory enzymes. *Annu. Rev. Plant Biol.* 62, 157–184. doi: 10.1146/annurev-arplant-042110-103921

Thompson, C. R., and Kats, G. (1978). Effects of continuous hydrogen sulphide fumigation on crop and forest plants. *Environ. Sci. Technol.* 12, 550–553. doi: 10.1021/es60141a001

Tian, B., Qiao, Z., Zhang, L., Li, H., and Pei, Y. (2016). Hydrogen sulfide and proline coperate to alleviate cadmium stress in foxtail millet seedlings. *Plant Physiol. Biochem.* 109, 293–299. doi: 10.1016/j.plaphy.2016.10.006

Tian, B., Zhang, Y., Jin, Z., Liu, Z., and Pei, Y. (2017). Role of hydrogen sulfide in the methyl jasmonate response to cadmium stress in *Foxtail millet*. *Front. Biosci. Landmark* 225:30–538.

Toohey, J. I. (2011). Sulfur signaling: is the agent sulfide or sulfane? *Anal. Biochem.* 413, 1–7. doi: 10.1016/j.ab.2011.01.044

Vaculík, M., Lukačová, Z., Bokor, B., Martinka, M., Tripathi, D. K., and Lux, A. (2020). Alleviation mechanisms of metal(loid) stress in plants by silicon: a review. *J. Exp. Bot.* 71, 6744–6757. doi: 10.1093/jxb/eraa288

Valivand, M., and Amooaghaie, R. (2020). Sodium hydrosulfide modulates membrane integrity, cation homeostasis, and accumulation of phenolics and osmolytes in Zucchini under nickel stress. *J. Plant Growth Regul.* [Epub ahead of print]. doi: 10.1007/s00344-020-10101-8

Valivand, M., Amooaghaie, R., and Ahadi, A. M. (2019). Interplay between hydrogen sulfide and calcium/calmodulin enhances systemic acquired acclimation and antioxidative defense against nickel toxicity in zucchini. *Environ. Exp. Bot.* 158, 40–50. doi: 10.1016/j.envexpbot.2018.11.006

Wang, H., Ji, F., Zhang, Y., Hou, J., Liu, W., Huang, J., et al. (2019). Interactions between hydrogen sulphide and nitric oxide regulate two soybean citrate transporters during the alleviation of aluminium toxicity. *Plant Cell Environ.* 42, 2340–2356. doi: 10.1111/pce.13555

Wang, K., Peng, H., and Wang, B. (2014). Recent advances in thiol and sulfide reactive probes. *J. Cell Biochem.* 115, 1007–1022. doi: 10.1002/jcb.24762

Wang, S., Chi, Q., Hu, X., Cong, Y., and Li, S. (2019). Hydrogen sulfide-induced oxidative stress leads to excessive mitochondrial fission to activate apoptosis in broiler myocardia. *Ecotoxicol. Environ. Saf.* 183, 1–9.

Wang, Y. Q., Li, L., Cui, W. T., Xu, S., Shen, W. B., and Wang, R. (2012). Hydrogen sulfide enhances alfalfa (*Medicago sativa*) tolerance against salinity during seed germination by nitric oxide pathway. *Plant Soil* 351, 107–119. doi: 10.1007/s11104-011-0936-2

Wilson, L. G., Bressan, R. A., and Filner, P. (1978). Light-dependent emission of hydrogen sulfide from plants. *Plant Physiol.* 61, 184–189. doi: 10.1104/pp.61.2.184

Xuan, L., Li, J., Wang, X., and Wang, C. (2020). Crosstalk between hydrogen sulfide and other signal molecules regulates plant growth and development. *Int. J. Mol. Sci.* 21:4593. doi: 10.3390/ijms21134593

Yamasaki, H., and Cohen, M. F. (2016). Biological consilience of hydrogen sulfide and nitric oxide in plants: gases of primordial earth linking plant, microbial and animal physiologies. *Nitric Oxide* 55, 91–100. doi: 10.1016/j.niox.2016.04.002

Yang, G., Wu, L., Jiang, B., Yang, W., Qi, J., Cao, K., et al. (2008). H_2S as a physiologic vasorelaxant, hypertension in mice with deletion of cystathionine γ-lyase. *Science* 322, 587–590. doi: 10.1126/science.1162667

Yu, X. Z., Ling, Q. L., Li, Y. H., and Lin, Y. J. (2018). mRNA analysis of genes encoded with *Phytochelatin Synthase* (PCS) in rice seedlings exposed to chromium: the role of phytochelatins in Cr detoxification. *Bull. Environ. Contam. Toxicol.* 101, 257–261. doi: 10.1007/s00128-018-2362-0

Yu, Y., Zhou, X. Y., Zhu, Z. H., and Zhou, K. J. (2019). Sodium hydrosulfide mitigates cadmium toxicity by promoting cadmium retention and inhibiting its translocation from roots to shoots in *Brassica napus*. *J. Agric. Food Chem.* 67, 433–440. doi: 10.1021/acs.jafc.8b04622

Yusof, Z. N. B., Borhan, F. P., Mohamad, F. A., and Rusli, M. H. (2015). The effect of *Ganoderma boninense* infection on the expressions of thiamine (vitamin B1) biosynthesis genes in oil palm. *J. Oil Palm Res.* 27, 12–18.

Zanganeh, R., Jamei, R., and Rahmani, F. (2018). Impacts of seed priming with salicylic acid and sodium hydrosulfide on possible metabolic pathway of two amino acids in maize plant under lead stress. *Mol. Biol. Res. Comm.* 7, 83–87.

Zanganeh, R., Jamei, R., and Rahmani, F. (2019). Role of salicylic acid and hydrogen sulfide in promoting lead stress tolerance and regulating free amino acid composition in *Zea mays* L. *Acta Physiol. Plant.* 41:94.

Zhang, H., Hua, S. L., Zhang, Z. J., Hua, L. Y., Jiang, C. X., Wei, Z. J., et al. (2011). Hydrogen sulfide acts as a regulator of flower senescence in plants. *Postharvest Biol. Technol.* 60, 251–257. doi: 10.1016/j.postharvbio.2011.01.006

Zhang, H., Hu, L. Y., Hu, K. D., Jiang, C. X., and Luo, J. P. (2010a). Hydrogen sulfide alleviated chromium toxicity in wheat. *Biol. Plant.* 54, 743–747. doi: 10.1007/s10535-010-0133-9

Zhang, H., Tan, Z. Q., Hu, L. Y., Wang, S. H., Luo, J. P., and Jones, R. L. (2010b). Hydrogen sulfide alleviates aluminum toxicity in germinating wheat seedlings. *J. Integr. Plant Biol.* 52, 556–567. doi: 10.1111/j.1744-7909.2010.00946.x

Zhang, H., Tang, J., Liu, X. P., Wang, Y., Yu, W., Peng, W. Y., et al. (2009). Hydrogen sulfide promotes root organogenesis in Ipomoea batatas, *Salix matsudana* and *Glycine max*. *J. Integr. Plant Biol.* 51, 1084–1092.

Zheng, S., Wang, Q., Yuan, Y., and Sun, W. (2020). Human health risk assessment of heavy metals in soil and food crops in the Pearl River Delta urban agglomeration of China. *Food Chem.* 316:126213. doi: 10.1016/j.foodchem.2020.126213

Zhi, J., Liu, X., Yin, P., Yang, R., Liu, J., and Xu, J. (2020). Overexpression of the metallothionein gene PaMT3-1 from *Phytolacca americana* enhances plant tolerance to cadmium. *Plant Cell Tissue Organ. Cult.* 143, 211–218. doi: 10.1007/s11240-020-01914-2

Zulfiqar, F., and Hancock, J. T. (2020). Hydrogen sulfide in horticulture: emerging roles in the era of climate change. *Plant Physiol. Biochem.* 155, 667–675. doi: 10.1016/j.plaphy.2020.08.010

Conflict of Interest: The authors declare that the research was conducted in the absence of any commercial or financial relationships that could be construed as a potential conflict of interest.

frontiers in Plant Science

REVIEW
published: 04 February 2021
doi: 10.3389/fpls.2020.587785

Lead Toxicity in Cereals: Mechanistic Insight Into Toxicity, Mode of Action, and Management

*Muhammad Aslam[1], Ayesha Aslam[1], Muhammad Sheraz[1], Basharat Ali[2], Zaid Ulhassan[3], Ullah Najeeb[4], Weijun Zhou[3] and Rafaqat Ali Gill[5]**

[1] Department of Plant Breeding and Genetics, University of Agriculture, Faisalabad, Pakistan, [2] Department of Agronomy, University of Agriculture, Faisalabad, Pakistan, [3] Zhejiang Key Laboratory of Crop Germplasm, Institute of Crop Science, Zhejiang University, Hangzhou, China, [4] Queensland Alliance for Agriculture and Food Innovation, Centre for Crop Science, University of Queensland, Brisbane, QLD, Australia, [5] Oil Crops Research Institute of the Chinese Academy of Agricultural Sciences/The Key Laboratory of Biology and Genetic Improvement of Oil Crops, The Ministry of Agriculture and Rural Affairs, Wuhan, China

OPEN ACCESS

Edited by:
Victoria Fernandez, Polytechnic University of Madrid, Spain

Reviewed by:
Smouni Abdelaziz, Mohammed V University, Morocco
Balal Yousaf, University of Science and Technology of China, China

***Correspondence:**
Rafaqat Ali Gill
drragill@caas.cn;
rafaqatalipbg@yahoo.com

Specialty section:
This article was submitted to Plant Nutrition, a section of the journal Frontiers in Plant Science

Received: *27 July 2020*
Accepted: *21 December 2020*
Published: *04 February 2021*

Citation:
Aslam M, Aslam A, Sheraz M, Ali B, Ulhassan Z, Najeeb U, Zhou W and Gill RA (2021) Lead Toxicity in Cereals: Mechanistic Insight Into Toxicity, Mode of Action, and Management. Front. Plant Sci. 11:587785. doi: 10.3389/fpls.2020.587785

Cereals are the major contributors to global food supply, accounting for more than half of the total human calorie requirements. Sustainable availability of quality cereal grains is an important step to address the high-priority issue of food security. High concentrations of heavy metals specifically lead (Pb) in the soil negatively affect biochemical and physiological processes regulating grain quality in cereals. The dietary intake of Pb more than desirable quantity *via* food chain is a major concern for humans, as it can predispose individuals to chronic health issues. In plant systems, high Pb concentrations can disrupt several key metabolic processes such as electron transport chain, cellular organelles integrity, membrane stability index, PSII connectivity, mineral metabolism, oxygen-evolving complex, and enzymatic activity. Plant growth-promoting rhizobacteria (PGPR) has been recommended as an inexpensive strategy for remediating Pb-contaminated soils. A diverse group of *Ascomycetes* fungi, i.e., dark septate endophytes is successfully used for this purpose. A symbiotic relationship between endophytes and host cereal induces Pb tolerance by immobilizing Pb ions. Molecular and cellular modifications in plants under Pb-stressed environments are explained by transcription factor families such as bZIP, ERF, and GARP as a regulator. The role of metal tolerance protein (MTP), natural resistance-associated macrophage protein (NRAMP), and heavy metal ATPase in decreasing Pb toxicity is well known. In the present review, we provided the contemporary synthesis of existing data regarding the effects of Pb toxicity on morpho-physiological and biochemical responses of major cereal crops. We also highlighted the mechanism/s of Pb uptake and translocation in plants, critically discussed the possible management strategies and way forward to overcome the menace of Pb toxicity in cereals.

Keywords: bioremediation, cereals, lead toxicity, mechanism, management, plant growth and development

INTRODUCTION

Heavy metals (HMs) naturally exist in the Earth's crust as soil constituents (Lasat, 2002). In the environment, HMs persistently accumulate due to stability and non-degradability. As a result of industrialization and anthropogenic activities (mining, electroplating and leather tanning, etc.), and disruptions in the natural marine and terrestrial habitats, this accumulation is growing rapidly (Meagher, 2000). Depending on their geological origin in the soil or human and industrial contamination, the concentration of HMs in soil can vary from 1 to 100,000 mg kg^{-1} (Blayock, 2000). For example, approximately 20 million hectares of agricultural land is irrigated with industrial effluents which contain traces of different elements as reviewed in Khalid et al. (2018).

These rapid changes in soil climate driven by anthropogenic activities override the natural adaptability of plants. Given the dependence of plants on soil media for acquiring essential elements for completing their life cycle, a high degree of versatility is needed to acclimatize the rapidly evolving conditions. Along with essential nutrients, plants uptake unknown toxic elements; some of them are HMs such as mercury, chromium, cadmium, arsenic, and lead (Pb). Heavy metals can enter into human body by consuming these contaminated foods and pose health risks (kidney diseases, renal tubular dysfunction, and bone damage) (Xie et al., 2018). Similarly, HMs disrupt physiological and biochemical processes in plants, such as photosynthesis, protein synthesis, redox balance, and energy transduction, as they accelerate generation of reactive oxygen species (Kopyra and Gwóźdź, 2003; Ali et al., 2015a,b). By disrupting the biological processes of plants, HMs may induce excessive micronutrient uptake and toxicity in plants (Peralta-Videa et al., 2009). There are several plant species that show tolerance to higher concentrations of HMs and toxic substances and are well adaptable to metalliferous soils, i.e., *Juncus effusus* (Kiran and Prasad, 2017; Najeeb et al., 2017).

Lead (Pb) is a very soft, dense, ductile metal with relatively low electrical conductivity than other metals. Lead is a nonessential element and when taken up by plants can negatively affect plant metabolic processes (Ali et al., 2014a,b). As it is an anthropogenic environmental pollutant, the crops cultivated on Pb-contaminated soils suffer poor germination, root growth, and biomass production. In nature, Pb forms minerals by interacting with other elements, and therefore is rarely present in native forms. The use of Pb for various purposes since ancient Rome is clarified by archeological findings. Whereas, its environmental concentration has risen more than 1,000 times over the last three centuries due to human interventions, with the largest rise from 1950 to 2000. Mineral deposits, along with copper and zinc, are typically the primary source of Pb. Globally, Pb contamination is expected to further increase due to its high application in the automotive and electric bicycle industries (Roberts, 2003). Urban agriculture, which relies on crop production in the vicinity of industries often cultivates food crops on polluted soils. Food demand is strong in urban areas, so the trend towards using polluted arable soils for cereal cultivation is rising (Peralta-Videa et al., 2009; **Table 1**).

TABLE 1 | Lead production and reserves.

Country	Production (1,000 m^3 ton)	Reserves	Country	Production (1,000 m^3 ton)	Reserves
USA	400	7,000	Peru	280	6,000
Australia	620	27,000	Poland	35	1,500
Bolivia	90	1,600	Russia	90	9,200
Canada	65	650	South Africa	50	300
China	1,600	13,000	Sweden	65	1,100
India	95	2,600	Other	330	4,000
Ireland	45	600	**Total**	**4,100**	**80,000**
Mexico	185	5,600			

Source: Geological Society of America (http://geology.com/usgs/lead/).

In most parts of the globe, cereals are the main staple food and play a crucial role in global food security. The key goal to meet an ever-increasing demand for food for more than 9 billion people by 2050 is expected to increase pressure on grain industry (Akinyele and Shokunbi, 2015). Typically, cereals contain 75% starch, 15% protein, and 3% fat; they also contain vitamins (folate and tocotrienols), minerals, phytochemicals (lignans, alkylresorcinols, and sterols), and antioxidants in different concentrations (Ragaee et al., 2006). Micronutritional constituents, trace elements, and dietary fibers are rich in bran and cereal semen (65–85%, Akinyele and Shokunbi, 2015). Phytochemicals present in bran play a key role in reducing the risks of coronary diseases. Likewise, by modulating cellular oxidative status, the phenolic compounds of cereal grains protect the body from oxidative harm. Dietary fibers enhance food's functional properties, such as viscosity, retaining capacity for water and oil, and swelling capacity. The adverse effects of high use of cereal-based dietary fibers are minimized by various processing technologies (microfluidization, grinding methods, thermal treatment, and bioprocessing) (Sen et al., 2020; **Table 2**). In most cereals, roots only penetrate into the soil from where the HMs are absorbed to a depth of 25 cm. The transfer of HMs to commercially valuable crop plants (particularly cereals) is of great concern, which can lead to biomagnification *via* entry into the food chain (Peralta-Videa et al., 2009).

LEAD UPTAKE MECHANISM

In order to maintain nutrient homeostasis, plants must regulate nutrient uptake and respond to changes in the soil as well as within the plant. Plants utilize different strategies for mobilization and uptake of nutrients as well as chelation, transport between the various cells and organs of the plant and storage to achieve whole-plant nutrient homeostasis. Metal bioavailability is regulated by: (a) soil mineral status; (b) mineralization; and (c) membrane transporters. The following are the two major routes for plant metal uptake: (i) passive uptake, powered by membrane concentration gradient, and (ii) inducible substrate-specific and energy-dependent uptake (Williams et al., 2000).

TABLE 2 | Contribution of cereals in energy consumed by humans.

Consumption or energy	World	Asia	Africa	South America	North America	Europe	Oceania
g capita^{-1} day^{-1}	403	426	414	318	293	362	249
kcal capita^{-1} day^{-1}	1,292	1,422	1,284	967	812	1,007	764

Source: FAO. Food Consumption Database (FAO, 2013).

A total of 17 different types of mineral elements needed for plants are transported to various organs according to their needs (Marschner, 2012). Many variables, such as soil physical and chemical properties, soil metal concentration, soil pH, redox status, and soil permeability play a direct or indirect role in the mobility of essential and nonessential elements in the soil (Dong et al., 2009). In the form of complexes, Pb is immobilized in the soil and thus becomes unavailable for plant uptake (Peralta-Videa et al., 2009). As it is a nonessential element for plants, there is no specific channel for Pb uptake. Plant species have different abilities and pathways for absorbing and transporting Pb ions. On root tips, this element is found within the soil as linked to carboxylic groups of mucilage uronic acids (Sharma and Dubey, 2005). Lead ions differently affect uptake of other essential nutrients i.e., it has a positive effect on Ca and K and negative effect on Mg absorption.

The Rhizosphere, Root Exudates, and Element Uptake

As an active part of soil, the rhizosphere is directly affected by numerous organic compounds and root exudates (Jones et al., 2009). For example, 10–40% of the plants' (organic and inorganic) photosynthetically fixed carbon is released in this part of the soil (McNear, 2013). Mucilage, sloughed off root cap, boundary cells, and exudates constitute the rhizodeposition. Mucilage assists in soil lubrication, root defense from desiccation, soil quality improvement, and nutrient uptake during root tip development (McNear, 2013). In the availability and absorption of metals by plants, the rhizosphere and soil microorganisms play a key role. By catalyzing the redox reaction, microbial activity alters the trend of HM uptake process (Dinh et al., 2020). The microenvironment formed by various discharged compounds contributes to the toxicity of HMs in nutrient absorption, including Pb as tested in Jitendra et al. (2017).

Root exudates consist of compounds of low and high molecular weight which are released actively and passively. Components of low molecular weight help to attract and use soil biota, which promote the rhizosphere through colonization or symbiosis on roots (Hawes et al., 2002). In inter- and intraplant interactions, root exudates play a role, helping to signal events (Kumar and Bais, 2012). The important micronutrients in metallic soils become accessible to plant roots due to the discharge of metal chelators. By improving their mobility and solubility, these chelators enhance the bioavailability of metals, and this is achieved by breaking the bonds between metals and soil particles (Rao et al., 2018).

Lead, widely available in the plant rhizosphere, has poor bioavailability for plants to be absorbed as it precipitates as sulfates and phosphates (Blaylock and Huang, 2000). Furthermore, the translocation of Pb is restricted by the roots, which accumulate maximum Pb contents. As recently reported by Li et al. (2020), the bioavailability of Pb depends on its concentration in the soil, the physical and chemical state of the soil, and the particular genotype of specific plant species. Lead mobility is strongly influenced by soil pH levels, i.e., increased mobility and Pb absorption has been recorded in low pH soils (3.9). Isotopes labeling techniques showed that more than 90% of Pb produced from ryegrass and wheat passed through the atmosphere (Alexander et al., 2006).

In the cell wall or in the form of extracellular precipitates on root tissues, much of the absorbed Pb occurs as bound to exchangeable ion sites (Sahi et al., 2002). For Pb movement under low concentration in roots, the endodermis acts as a partial barrier. Lead ions settle on the cell wall in the case of wheat roots and can be extracted by using citric acid (Xie et al., 2018). After getting into the root cortex, Pb ions transfer to the apoplastic space through the conductive transpiration system. Furthermore, it gives symplastic access to the region of lateral root initiation and young roots that grow. Its mobility is regulated by cross-membrane movement within the cytoplasm and membrane protein (Dong et al., 2009).

Transporters that are present in xylem parenchyma cells or phloem companion cells primarily facilitate the long-distance transport of Pb from roots to shoots (Dong et al., 2009). The transport of Pb occurs from the soil into root epidermal cells, followed by loading into the root xylem vessels for distribution into other plant organs. All plant transporter proteins are membrane proteins with Pb homeostasis as their responsibility (Romanowska et al., 2012). Vacuole sequestration potential (VSC) also plays a major role in the transport and sequestration of metals over long distances (Williams et al., 2000). *Via* mutual cooperation, tonoplast-localized transporters and ion chelators automatically change the available metal ions in the surrounding region (Peng and Gong, 2014; **Figure 1**).

Translocation/transport phenomena of Pb slightly differ from other HMs. Normally, 5% of Pb is transported into aerial components (Kiran and Prasad, 2017) and 95% remains accumulated in roots (Chandra et al., 2018). The possible mechanism is that in plant roots, ion-transferable cell wall sites mediate extracellular Pb binding. In this way, with the carboxyl group, Pb forms stable binding complexes and remains located in the roots. The components of the cell wall, such as glucuronic acid, limit apoplastic transport into the above plant components (Inoue et al., 2013). Lead efflux is regulated by P-type transporters or Pb cellular complexes that decrease the toxicity of Pb by endorsing sequestration into a specific organelle (Jiang et al., 2017). Previous studies have indicated that leucine-rich repeat (LRR), ATM1, and PDR12 the

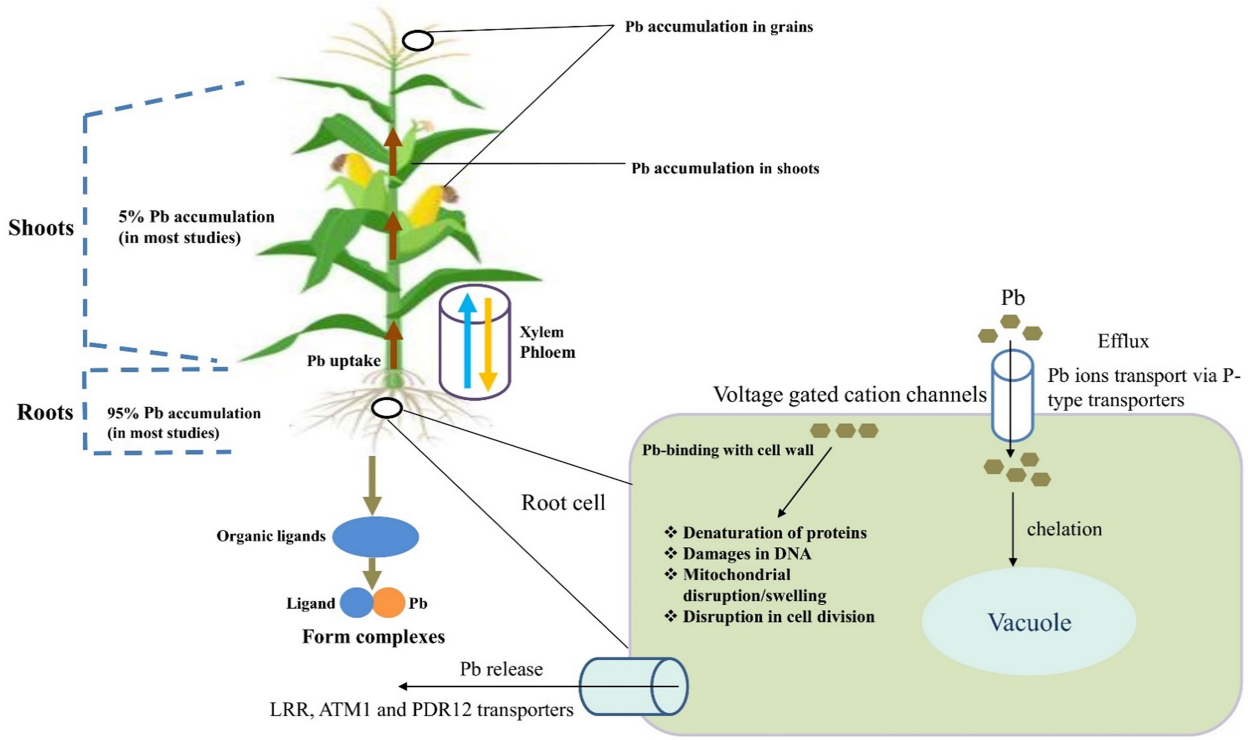

FIGURE 1 | Potential uptake mechanisms and accumulation of lead (Pb) in plant parts. The sequence of Pb accumulation in different organs of cereals particularly in wheat is as; roots > shoots > shells > grains. Relatively higher Pb accumulation in root tissues could be an inactivate Pb in root cell walls. However, accumulation of Pb in grain is of main concern regarding its entry in food chain. Bioconcentration factor (BCF) and translocation factor (TF) are very important characteristics to be focused regarding accumulation and translocation of Pb. The heavy-metal mobility factor (MF) is equal to the ratio of the sum of labile fractions (exchangeable and bound-to-carbonate fractions) to the sum of all fractions, which is a good index to describe the relative mobility and bioavailable form of the metals in soils.

transporters may be associated with cell cellular Pb extrusion (Zhu et al., 2013).

TOXICITY LEVEL AND MODE OF ACTION

Heavy metal is defined as "a metal with a density greater than 5 g cm^{-3}." Of a total of 53 HMs that occur naturally, 17 are biologically available and are important for the ecosystem (Alamri et al., 2018). For plants, Pb is a nonessential element, so it becomes toxic even at low concentrations. It is transferred from the atmosphere to plants quickly (Mishra et al., 2020). In cereal grains, the allowable Pb amount is >0.20 mg kg^{-1} (WHO/FAO, 2016). In response to varying Pb levels, genotypic variations are observed among species. For example, 30 ppm of Pb in the soil could reduce the production of maize genotypes by about 76 to 85% (Ghani et al., 2010). Maize plants translocate 2 to 5% of the soil absorbed Pb from roots to leaves. The root endodermis barrier may be the explanation for this small amount of translocation (Ghani et al., 2010). The low penetration capacity of Pb through the endodermis layer in maize was verified by historochemical observations (Sharma and Dubey, 2005). There is a weak bonding between Pb compounds and phytochelatins due to the large ion radius and high concentration number (Sharma and Dubey, 2005). The plants do not allow Pb to freely penetrate to the protoplast through cell wall tissues. Actively dividing cells are relatively susceptible to Pb concentration. Pb concentrations above 100 μM typically become toxic for callus induction (Krishania and Agarwal, 2012). In addition, high Pb concentrations in soil media minimize the supply of other plant uptake nutrients [Ca, Fe, Mg, Mn, P, and zinc (Zn)] by blocking entry or binding the ions to the ion carrier (Dong et al., 2009).

EFFECT ON PLANTS

In plants, three molecular mechanisms related to Pb toxicity are established on the basis of chemical and physical plant properties: (a) development of ROS, (b) blocking of essential functional groups in biomolecules, and (c) removal of essential metal ions from biomolecules. Incompletely filled Pb orbital present as cations in various physiological processes and can adversely affect seed germination rate, seedling growth, dry root shoot mass, efficiency of photosynthesis, mineral nutrition, and enzyme-related activity (Munzuroglu and Geckil, 2002). By accelerating the development of hydroxyl radical, Pb toxicity causes oxidative damage to plants (Pirzadah et al., 2020). Cereal crops respond differently to varying Pb toxicity levels and can be classified as metal excluders, metal indicators, and metal accumulators. Excluders avoid the accumulation and translocation of metal

ions in their shoots; metal indicators accumulate metals in the aerial shooting system; metal accumulators absorb, translocate, and accumulate metal ions at levels greater than those found in the soil in various parts of their shoots (Ahmad et al., 2020; Zanganeh et al., 2020). Lead also affects plant growth by interfering with the composition and concentration of nutrients and protein conformation, like transporters and regulatory proteins (Pirzadah et al., 2020).

EFFECT ON PLANT GROWTH AND DEVELOPMENT

It is well known that Pb negatively affects germination, seedling vigor, growth of root and shoot biomass, photosynthetic activity, and enzymatic activity of plants (Munzuroglu and Geckil, 2002). For example, embryo energy generation is a critical germination process; reduction or blockage, along with the normal mitosis process, adversely affects protein, RNA, and DNA synthesis. The effects of Pb toxicity on seed germination are concentration dependent. These effects are more serious under the degree of increased and persistent toxicity (**Figure 2**). Crop germination that is specifically exposed to Pb toxicity in the soil is the first step of plant life. Toxic accumulation of Pb interferes with the formation of spindles and the growth of cell walls, decreasing cell expansion and dividing results in inhibition of root volume (Zulfiqar et al., 2019; Kanwal et al., 2020). During seedling growth and development, roots are more susceptible compared with shoots (Yang et al., 2010) because they are exposed to Pb toxicity. A well-known index of Pb toxicity tolerance is root growth potential. Under a high Pb toxicity level, plant growth is adversely affected due to poor nutrient uptake and transport (Ali et al., 2014b). However, lower concentrations of HMs, like Pb, often promote metabolic activities, and enzymes involved in these processes encourage growth and development.

EFFECTS ON PLANT PHYSIOLOGY

Plants exposed to various environmental contaminants have variable species and genotypic biological responses. Crops, such as cereals, are often exposed to HM toxicity and undergo a drastic reduction in grain yield. HMs can bind within cells with oxygen, nitrogen, and sulfur atoms; thus, HMs inactivate enzymes by binding with cysteine residues. HMs also induce lipid peroxidation, which leads to downregulation of peroxidases, and damages thylakoid membranes (Ali et al., 2014a). Key genes of peroxidase family play a very important role in plant cell enzyme defense by searching for ROS during stress (Gülen et al., 2008). Lead toxicity accelerates development of ROS, including H_2O_2, which in turn causes secondary oxidative stress, leading to inhibition at the early stages of growth (Yang et al., 2010). When plants are facing the extreme levels of environmental stresses, the level of malonaldehyde (MDA) increased (depending upon the nature of stress). Malonaldehyde content represents the level of lipid peroxidation and its increased level acts as stress indicator. No improvement in MDA content under Pb toxicity was noted in germinating wheat seeds (Radić et al., 2010). In conjunction with other metals, Pb forms a complex combination

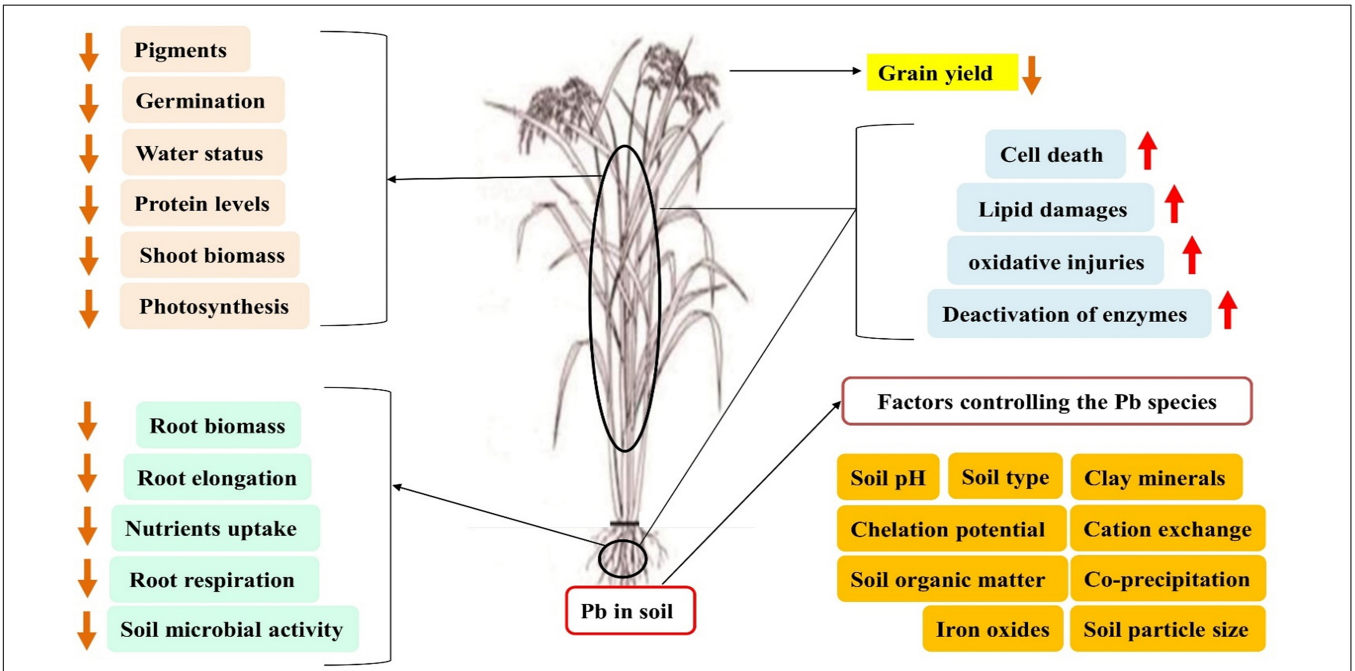

FIGURE 2 | Thematic of Pb stress in plants. Excess quantity of Pb in the soil negatively impact on the soil microbial activity, root respiration, imbalance nutrient uptake, and overall morphology and biomass. Lead in upper plant parts such as stem and leaf deteriorates the photosynthetic machinery and protein level and disturb the water status and shoot and leaf biomass that resulted in the grain yield loss.

to decrease the physiological efficiency of cereals. For example, high Pb and Cd concentrations substantially lower grain yield of rice. As complex in soil, HMs such as Pb, Cd, Cr, and Cu have a complex adverse effect on biochemical and physiological processes at various stages of rice growth and development (Xie et al., 2018; **Figure 3** and **Table 3**).

Plant Growth Regulators

Plant growth regulators (PGRs) are naturally occurring organic compounds that under normal and stressful regimes, play a vital role in plant growth and development (Bajguz and Piotrowska, 2009; Davies, 2010; Piotrowska and Bajguz, 2011; Ahanger et al., 2018; Šimura et al., 2018). These PGRs are auxins, cytokinins, brassinosteroids (BRs), gibberellins, ethylene, abscisic acid, and jasmonic acid (JA). Out of these, BRs belong to a group of phytohormones which controls various biological processes, including HMs and broad range of environmental stresses. They activate the transcription factor coding gene [BRASSINAZOLE RESISTANCE 1 (BZR1)/BRI1-EMS SUPPRESSOR 1 (BES1)], which triggers thousands of BR-responsive genes. In addition, BRs modulate many physiological activities such as photosynthetic functioning (i.e., chlorophyll content and photosynthetic capacity), antioxidant enzyme activities, and metabolism of carbohydrates and mitigate the negative effects of HMs on plants (Anwar et al., 2018). Also, at a very low concentration, BRs function efficiently and alleviate the toxic effects of Pb stress. For example, through exposure to HMs, plant biosynthetic pathways are severely disrupted. One of the main detoxification mechanisms is the upregulation of cytochrome P450s under heavy metal conditions. Many biosynthetic pathways, such as jasmonic acid (JA), isoflavonoids, flavonoids, anthocyanins, coumarins, salicylic acid (SA), phytoalexins, and many others, play an important role in the metabolism of cytochrome P450s.

Other PGRs such as JA and SA (o-hydroxybenzoic acid) also relieve a range of environmental stresses, like HMs, including BRs (Wasternack, 2014; Liu et al., 2016). Jasmonic acid is typically present in higher plants and takes part in essential plant growth and development functions. Its production in plants begins (along with its methyl ester called methyl jasmonate) after exposure to biotic/abiotic stresses (Mohamed and Latif, 2017; Ashry et al., 2018). It also regulates HM toxicity and increases plant growth by modulating gene expression, osmolytes, antioxidant machinery, and carotenoids production (Creelman and Mullet, 1995; Poonam et al., 2013). For example, it improves growth, photosynthetic efficiency, nutrient uptake (i.e., N, P, and K), electrolyte leakage, and antioxidant machinery in Pb-stressed maize plants (Sofy et al., 2020). In comparison, SA is a phenolic acid usually found in plant organisms (Liu et al., 2016). Exposure to Pb is considered to have severely affected maize plants, reducing growth, yield, photosynthetic pigments, and mineral nutrients (nitrogen, phosphorus, and potassium) and increased electrolyte leakage (EL), accumulation of malondialdehyde (MDA), osmolytes, and nonenzymatic and enzymatic antioxidants (Rahmani et al., 2015; Liu et al., 2016; Hafez and Seleiman, 2017). As a hormone-like substance, it modulates physiological processes such as flowering, photosynthetic machinery, seed germination, plant growth, membrane permeability, and plant defense response against biotic and abiotic stresses. A group of researchers recently investigated that SA together in combination of JA effectively reduced the negative effects of Pb stress in maize (Sofy et al., 2020).

Antioxidant System

The lower reactive oxygen species (ROS) level is needed for the functioning of cells and induces oxidative stress in excessive amounts. The excess amount of ROS was deemed harmful to the growth and production of plants. A physiological equilibrium between ROS formation and the defensive antioxidant function of the cell is ensured under normal conditions. Reactive oxygen species attack macromolecules (polyunsaturated chloroplast

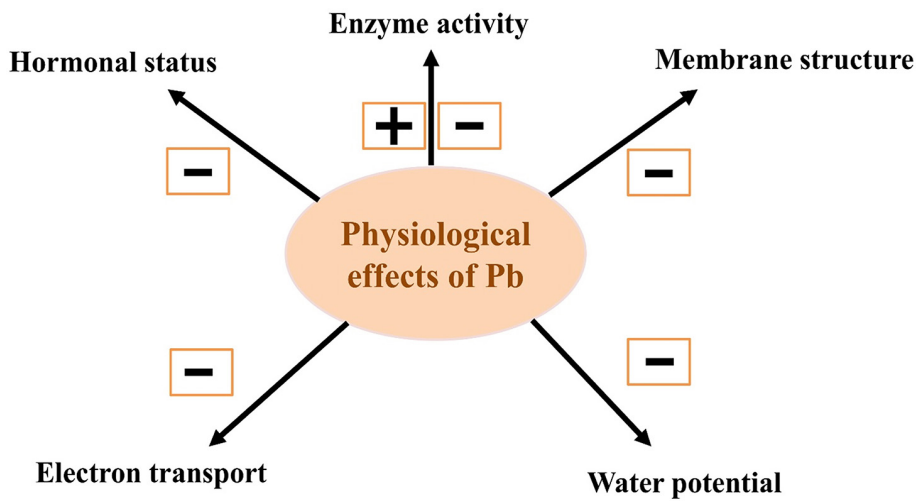

FIGURE 3 | Lead toxicity results in overall disturbance in physiological mechanisms in plants. Here, "+" and "−" signs are positive and negative effects, respectively.

TABLE 3 | Lead induced phytotoxic effects on the morphological and physiological attributes of cereals.

Applied Pb dose	Plant specie	Culture	Exposure hours (h) or days	Alteration in plant parameters	References
250 and 500 mg kg^{-1} $PbNO_3$	Mung bean	Hydroponic	21 days	↓ growth, photosynthetic pigments, protein synthesis, water use efficiency	Arif et al., 2019
100, 200, 300 μM $PbNO_3$	Tartary buckwheat	Hydroponic	15 and 30 days	↓ shoot and root length and biomass, chlorophyll ↑ proline, soluble sugar, protein content	Pirzadah et al., 2020
418.64 mg kg^{-1} Pb	Rice	Hydroponic	23 days	↑ proline, soluble protein content	Rao et al., 2018
0, 50, and 250 μM	Wheat	Hydroponic		↑ radicle and coleoptile length	Kaur et al., 2015b
228 mg L^{-1}	Rice	Hydroponic	8-16 days	↑ protein carbonylation, nonprotein thiols ↓ protein thiols	Srivastava et al., 2014
4,968 mg L^{-1}	Wheat	Hydroponic	30 days	↓ growth traits, nutrients uptake	Lamhamdi et al., 2011
1,656 mg L^{-1}	Rice	Hydroponic	30 days	↑ phosphorylation of PSII core proteins, protein degradation	Romanowska et al., 2012
1 mM	Rice	Hydroponic	4-7 days	↓ shoot or root length, biomass, nutrients uptake	Khan et al., 2018
0 and 100 μM	Rice	Hydroponic	7 days	↓ plant height, shoot, and root dry or fresh weights ↓ photosynthetic pigments, gas exchange attributes	Chen et al., 2017
0.5 and 1 mM	Wheat	Hydroponic	7 days	↓ plant growth, biomass, leaf relative water, chlorophylls ↑ proline	Hasanuzzaman et al., 2018
2 mM	Wheat	Hydroponic	63 days	↓ plant growth traits, biomass, leaf relative water, Rubisco activity, ATP sulfurylase, nutrients level, total chlorophyll	Alamri et al., 2018
1.5 mM	Wheat	Hydroponic	5 days	↓ root elongation and coleoptile growth	Turk et al., 2018
0, 1, 25, 50, 100, 200, and 500 mM	Maize	Hydroponic	14 days	↓ early growth, biomass, seed germination, total protein contents, Pb uptake	Hussain et al., 2013
500 mg kg^{-1}	Wheat	Soil	120 days	↓ growth, biomass, Pb uptake, grain yield, chlorophyll, gas exchange parameters	Rehman et al., 2017
0.1 mM	Maize	Hydroponic	4 days	↓ growth rate of coleoptile segments ↑ membrane hyperpolarization	Kurtyka et al., 2018
0, 200, 400, 800, 1,600, and 3,200 mg kg^{-1}	Sorghum	Soil	21 days	↓ growth, dry matter, photosynthetic rate, transpiration rate, starch, proteins, total soluble sugars	Cândido et al., 2020

membrane fatty acids) which leads to lipid peroxidation acceleration (Ledford and Niyogi, 2005). In foods, lipid peroxidation results from rancidity and unpleasant odors/tastes. Superoxide and hydrogen peroxide (H_2O_2) are the main active oxygen species. Hydrogen peroxide has a long life and the ability to diffuse across membranes, so it is considered the second messenger of signals produced by ROS. In the sense of oxidative stress, there are many environmental stresses involved. One of them is Pb toxicity, which causes many enzymes to be inactivated by binding with their SH group, resulting in overproduction of ROS (Vinocur and Altman, 2005). These mutually interactive processes have a detrimental effect on cell structure and metabolism, resulting in a decreased performance of oxidation-reduction enzymes and electron transport systems. The changes in morphological, physiological, biochemical, and molecular processes are due to secondary (osmotic or oxidative) stresses that disturb membrane protein stability and interfere with cellular homeostasis (Ashraf, 2009).

Several enzymatic antioxidants, including super oxide dismutase (SOD), peroxidase (POD), catalase (CAT), ascorbate peroxidase (APX), and glutathione reductase (GR), as well as nonenzymatic antioxidants such as reduced glutathione (GSH), oxidized glutathione (GSSG), and ascorbic acid (AsA), play a significant function on their own and in combination in different plant growth processes to alleviate the adverse effects of ROS. For example, increased SOD and CAT activity was reported in maize at the germination and seedling stage when subjected to Pb stress (Zhang et al., 2018). In another study, AsA improved photosynthetic machinery and osmolyte activity; it also improved antioxidant protection systems in maize under HM stress (Zhang et al., 2019). Under extreme toxic conditions, plant protection mechanisms cannot be sustained at an acceptable level by endogenous regulators, including antioxidants. So, exogenous application of growth enhancers to mitigate the negative impacts of stresses are becoming widespread in many plants (Zulfiqar et al., 2019). For example, Pb stress improves the ROS in wheat, including the rate of H_2O_2, O_2^-, and lipid peroxidation. Exogenous supplementation of GSH greatly alleviates the redox reservoir of antioxidants and raises

antioxidant activity but reduces the amount of ROS. In addition, exogenous GSH improves the quality of proline, balances the water status, prevents chlorophyll degradation, thus increasing plant growth and production and overall biomass (Hasanuzzaman et al., 2018).

Photosynthesis

Higher Pb concentration interferes with physiological and biochemical processes involved in plant growth and development based on photosynthesis as photosynthesis is one of the processes most affected (Gomes, 2011). The toxicity of Pb induces changes in glycolipids, particularly in monogalactosyldiacylglycerol, which is associated with chloroplast membrane permeability (Rizwan et al., 2018). Lead toxicity causes an increase in stomatal resistance and a reduction in the rate of transpiration and photosynthesis. Stomatal conductance, chlorophyll content, and photosynthetic rate are decreased by increased Pb uptake by plants (Rasool et al., 2020). With the rise in the amount of Pb toxicity, a sharp decrease in chlorophyll content was observed (Ali et al., 2014b). The detrimental effect of Pb on the photosynthetic apparatus, enzymatic activities, and mineral nutrition is due to the strain on the physiological processes under Pb toxicity (Tian et al., 2014). Higher Pb concentration in plant tissues substitutes Mg with Pb which inhibits enzymatic activity and electron transport in Calvin cycle and restrict chlorophyll synthesis. The toxicity of Pb reduces the number of cristae in mitochondria, which have a negative effect on photosynthesis and respiration by reducing oxidative phosphorylation potential (Mroczek-Zdyrska and Wójcik, 2012).

Energy Metabolism

Lead toxicity exerts adverse impacts on respiratory activities and ATP concentrations. There is an evidence that Pb toxicity impairs leaf respiratory activities. Lead toxicity enhances mitochondrial respiration with no effect on photorespiration, resultantly, there is an increase in respiratory process. Increase in respiration rate under Pb stress has association with ATP production in mitochondria; this energy is used for survival under Pb toxicity. Both C_3 and C_4 plants, when exposed to Pb toxicity experience 50% increase in respiration rate and fully oxidized substrates in mitochondria. Electron transport chain reactions are disturbed by Pb stress, as Pb bind with mitochondrial membrane causing decoupling of phosphorylation process (Romanowska et al., 2002; Ashraf and Tang, 2017). High Pb accumulation in plant starts NAD^+-malate dehydrogenase activity, interrupts hill reaction, and interferes with cyclic and noncyclic photophosphorylation (Romanowska et al., 2002). Damage to secondary structures of PSII, blockage of energy transfer pathways among amino acids, and reduction in absorption of visible light are the result of high Pb intake. Under Pb stress environment, swelling of mitochondria, vacuolization of endoplasmic reticulum and dictyosomes, and damage to cristae occur. Lead toxicity significantly inhibits guard cells, cell wall elasticity, chlorophyll development, and leaf development which results in plant growth reduction and abnormal plant functioning (Kurtyka et al., 2018).

EFFECTS ON BIOCHEMICAL PROCESSES

Plant growth and development is adversely affected by Pb toxicity. To overcome oxidative damage caused by Pb toxicity, several reactions have been produced by the plant defense mechanism, and various techniques are used to cope and adapt. This adaptability depends entirely on the difference in the relative protein abundance of stress-responsive protein; this fully changes the levels of proteome, transcriptome, and metabolome (Cho et al., 2008). In addition to the post-translational regulatory mechanism including protein degradation and RNA stability, the strength and length of the imposition of Pb toxicity affect the expression pattern and transcription level of these proteins, which have a further role in making the response of the plant more complex. The recent advances in interactome analysis, transcriptome and metabolome clarify in a better way the plant response to stress (Sharma et al., 2013). Such studies further promote understanding of the physiological and molecular pathways involved in Pb stress responses. The typical response to all stresses is mainly oxidative stress induction and gene expression modulation (Shri et al., 2009). Metals such as Pb play a very important role in plant enzymatic behavior. With the displacement of one metal with another, these activities are badly affected, e.g., divalent cations (CO^{++}, Ni^{++}, Zn^{++}) displace Mg^{++} in ribulose-1,5-bisphosphate-carboxylase/oxygenase causing reduced enzymatic activity (**Table 4**). Lipid peroxidation is a biochemical marker for an injury mediated by free radicals. Rising the toxicity of Pb increases the peroxidation of lipids that causes oxidative stress. A similar response is observed in the case of glutathione reductase activity, with a higher level of Pb concentration decreasing catalase activity in roots and shoots (Ali et al., 2014b).

LEAD IN FOOD CHAIN

Lead acts as a physiological and neuronal toxin and is naturally carcinogenic. In humans, the absorption of Pb is by the ingestion of paint chips, vehicle pollution inhalation, Pb-welded canes, and water intake. Due to the capability of rapid bioaccumulation, lower degradability rate and long biological half-life, Pb is of great concern in the food safety-security (FSS) debate (Ayesha et al., 2019). When Pb is consumed, the half-life of long excretion is considered to be continuous (in order of years). Contamination of HMs in marine areas results in the accumulation of HMs in aquatic body tissues. Subsequently, this bioaccumulation is biomagnified (grazer → primary consumer → secondary consumer → top predator) to various levels. Ultimately, by taking polluted sea food, humans are affected. Pregnant women are more vulnerable to HM toxicity because of the trans-placental metal change in maternal blood. Individuals with chronic exposure to Pb toxicity suffer from memory loss, poor nervous system functioning, decreased understandability, decreased blood pressure, kidney and brain damage, adverse effects on intellectual ability, and

TABLE 4 | Lead-induced phytotoxic effects on the oxidative markers and biochemical and metabolic traits of cereals.

Applied Pb dose	Plant specie	Culture	Exposure hours (h) or days	Alteration in plant parameters	References
0,100, 200, and 300 μM	Tartary buckwheat	Hydroponic	15 and 30 days	↑ H_2O_2, membrane stability index, GSH contents ↑ SOD, POD, CAT, GR, GST activities	Pirzadah et al., 2020
418.64 mg kg^{-1} Pb-contaminated soil	Rice	Hydroponic	23 days	↑ SOD, CAT, APX. Activities ↓ MDA, endogenous Pb contents	Rao et al., 2018
0,10, and 50 μM	Rice	Hydroponic	2 and 4 days	↑ SOD, APX, GR activities, MDA, α-tocopherol content ↓ CAT activity	Thakur et al., 2017
0, 16, 40, and 80 mg L^{-1}	Maize	Hydroponic	8 days	↑ MDA, H_2O_2, $O^{-}{}_{.2}$, SOD, APX, GPX, GR activities ↓ CAT activity,	Kaur et al., 2015a
0, 50, and 250 μM	Wheat	Hydroponic	1 days	↑ MDA, H_2O_2, $O^{-}{}_{.2}$, conjugated diene, membrane damage ↑ SOD, CAT, APX, GPX, GR activities	Kaur et al., 2015b
0, 16, 40, and 80 mg L^{-1}	Maize	Hydroponic	3, 12, and 24 h	↑ MDA, H_2O_2, thiols, APX, DHAR, MDHAR activities ↓ AsA, GSH contents	Kaur et al., 2015c
0, 50, 100, 250, and 500 μM	Wheat	Hydroponic	4 days	↑ SOD, CAT, MDA ↓APX, GPX, GR activities	Kaur et al., 2013
0, 50, 100, and 200 μM	Rice	Hydroponic	16 days	↑ SOD, MDA ↓CAT, POD activities	Li et al., 2020
0, 1, 2, and 4 mM	Wheat	Hydroponic	3 days	↑ SOD, CAT, POD, APX activities, MDA	Yang et al., 2011
0, 0.15, 0.3, 1.5, and 3 mM	Wheat	Hydroponic	6 days	↑ SOD, POD, APX activities, MDA ↓ CAT activities	Lamhamdi et al., 2011
0, 500, 1,000, and 2,500 μM	Wheat	Hydroponic	7 days	↑ SOD, GPX activities, MDA	Kaur et al., 2012
228 mg L^{-1}	Rice	Hydroponic	days	↑ SOD, GPX activities, MDA	Srivastava et al., 2014
0-200 μM	*Sedum alfredii*	Hydroponic	14 days	↑ SOD activities ↓ APX activities	Gupta et al., 2010
1 mM	Rice	Hydroponic	18 days	↑ SOD, POD activities, MDA, H_2O_2, OH^{-}, $O^{-}{}_2$ levels	Khan et al., 2018
0 and 100 μM	Rice	Hydroponic	7 days	↑ SOD, GR, APX activities, AsA, G.S.H., H_2O_2, $O^{-}{}_2$ levels	Chen et al., 2017
0.5 and 1 mM	Wheat	Hydroponic	7 days	↑ MDA, H_2O_2, $O^{-}{}_{.2}$ methylglyoxallevels, SOD, GST activities ↓AsA-GSH content, CAT, GPX, GR, glyoxalase system enzymes	Hasanuzzaman et al., 2018
2 mM	Wheat	Hydroponic	63 days	↑ MDA, H_2O_2, cysteine levels, SOD, CAT, GR activities	Alamri et al., 2018
1.5 mM	Wheat	Hydroponic	5 days	↓ AsA-GSH content, CAT activity ↑ MDA, H_2O_2 content, SOD, GPX, GR, APX. Activities	Turk et al., 2018
0, 200, 400, 800, 1,600, and 3,200 mg kg^{-1}	Sorghum	Soil	21 days	↑ SOD, CAT, APX activities, MDA, H_2O_2 contents	Cândido et al., 2020

sluggish reaction by taking more time to respond. Men's exposure to Pb toxicity cause damage to the responsible organs of sperm production, raises the amount of Pb in the blood, and the risk of death.

It is well known that high soil accumulation of Pb is a possible hazard to all soil-related lives (Zhuang et al., 2009). The soil state is frequently undocumented and thus, exposed to high levels of harmful compounds unintentionally. Individuals who eat food cultivated on polluted soils can be at risk of toxic health effects. Lead toxicity in pregnant women causes newly born babies to have low birth weight and intellectual disability. Central nervous system destruction, neurological disease and cancer of various body organs are most of the recorded effects of Pb toxicity (Uwah et al., 2011). Lead accumulation should not be overlooked in particular organs of living organisms (Zhuang et al., 2009). Two known binding polypeptides responsible for Pb binding in the kidneys are thymosin beta 4 and acyl-CoA. Pb binds with low molecular weight compounds like sulfhydryl groups in the blood serum. Exposure to Pb toxicity suppresses Zn-superoxide dismutase activity in humans under zinc deficiency, resulting in oxidative stress in the kidneys, blood, and liver; this disorder may be treated by normal Zn intake (Chemek et al., 2016). The absorption, translocation, metabolism, and retention of Pb in the body are limited by zinc supplementation. Good practices relating to agriculture should be enforced, taking into account the health issues of humans related to farming on polluted soils. Farmers should be informed about the health risks associated with the imbalance of the use of pesticides, fertilizers, and wastewater as irrigation through various official programs and media broadcasts (Uwah et al., 2011; **Figure 4** and **Table 5**).

PHYTOREMEDIATION

Since they are not chemically degradable, most HMs, like Pb, have the ability to remain in the soil for thousands of years. Lead toxicity poses many health problems directly or through plant transport to higher species. The alternative is to physically extract it or convert it into nontoxic compounds (Tangahu et al., 2011). With regard to phytoremediation, the processes involved in nutrient absorption are of great significance, as the same applies to the uptake of toxic elements. In metal accumulating pathways in plants, phytoremediation technology for complex site decontamination has gained recent attention. With low cost and environmental protection, this approach is very evolving (Antonkiewicz and Para, 2016).

Plant absorption mechanisms associated with phyto-remediation technology can be grouped into organic and inorganic pollutants such as phytovolatilization, rhizo-filtration, phyto-stabilization, phyto-degradation, and rhizo-degradation (Tangahu et al., 2011). The method of rhizo-filtration is effectively carried out by young seedlings in ventilated water. A known remedy that works by reducing mobility and phyto-availability in the soil is HM immobilization by using modifications. In the case of Pb in polluted soils, the immobilization technique works well because of its adsorption capacity and biologically less accessibility compared with other toxic metals such as Cd and Cr (Dong et al., 2009). As a Pb remedy strategy, phytoextraction is known to be a good alternative to traditional techniques based on engineering; this solution is low cost, environmentally sustainable, and easily applicable. Various forms of phyto-remediation are defined as follows:

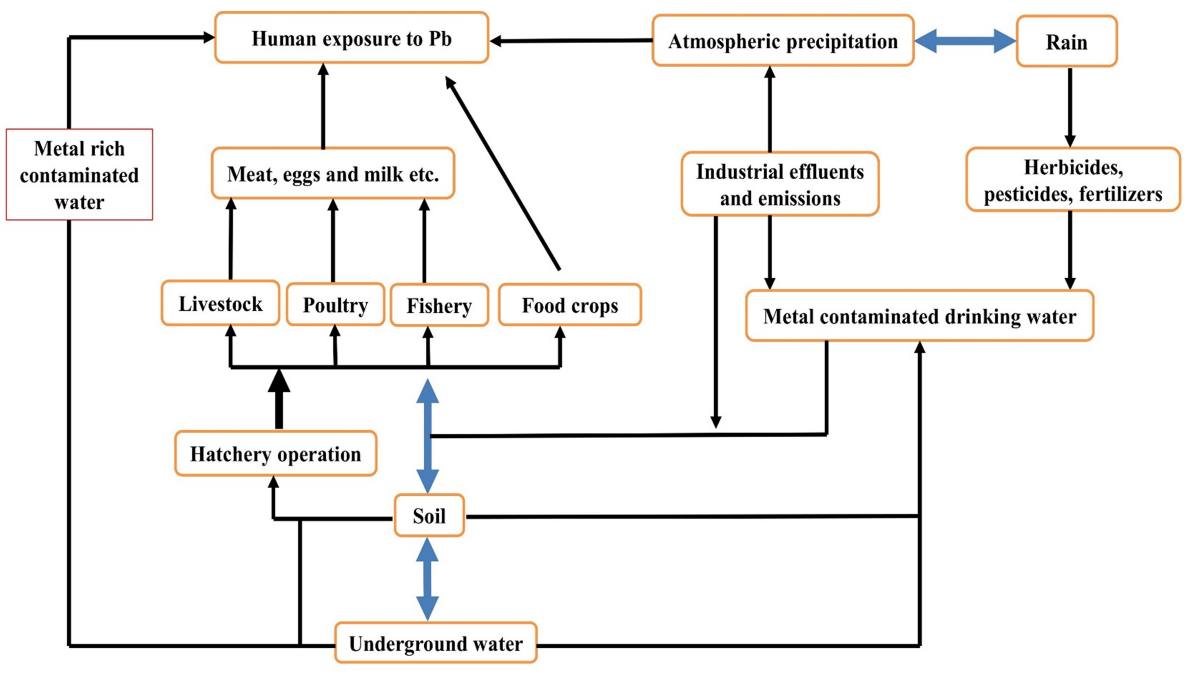

FIGURE 4 | Pathway of terrestrial ecosystem through which humans are exposed to Pb toxicity.

TABLE 5 | Concentration of lead in cereal grains.

Crop	Country	Study/Contamination	Pb contents (mg kg^{-1})	Crop	Country	Study/Contamination	Pb contents (mg kg^{-1})
Barley	Ethiopia	Market survey (Tegegne, 2015)	0.03	Rice	France	Market survey (Leblanc et al., 2005)	0.01
Barley	Ethiopia	Farmer field (Eticha and Hymete, 2015)	0.82–5.64	Rice	Nigeria	Market survey (Akinyele and Shokunbi, 2015)	<0.08
Maize	Nigeria	Contaminated soil (Orisakwe et al., 2012)	1.01	Rice	India	Organic farming (Chandorkar and Vaze, 2013)	0.10
Maize	Nigeria	Market survey (Akinyele and Shokunbi, 2015)	<0.08	Rice	Australia	Market survey (Rahman et al., 2014)	0.02–1.30
Maize	Bangladesh	Field survey (Islam et al., 2014)	0.04–1.30	Rice	India	Peri-urban areas (Tripathi et al., 1997)	0.02
Millet	Finland	Market survey (Ekholm et al., 2007)	0.02	Rice	Bangladesh	Field survey (Islam et al., 2014)	0.07–1.30
Millet	Nigeria	Contaminated field (Orisakwe et al., 2012)	3.54	Sorghum	Ethiopia	Market survey (Tegegne, 2015)	0.08
Oat	Finland	Market survey (Ekholm et al., 2007)	0.05	Sorghum	Bulgaria	Contaminated area (Angelova et al., 2011)	10.30
Rice	Nigeria	Farmer field (Orisakwe et al., 2012)	61	Wheat	India	Peri-urban area (Tripathi et al., 1997)	0.02
Rice	Saudi Arabia	Market survey (Othman, 2010)	0.02–0.03	Wheat	Ethiopia	Market survey (Tegegne, 2015)	0.05
Rice	Saudi Arabia	Market survey (Ali and Al-Qahtani, 2012)	6.16	Wheat	Saudi Arabia	Market survey (Ali and Al-Qahtani, 2012)	2.80
Wheat	Belgium	Organic and conventional farming (Harcz et al., 2007)	0.04–0.10	Wheat	Bangladesh	Field survey (Islam et al., 2014)	0.03–1.30
Wheat	Brazil	Market survey (Santos et al., 2004)	<0.01–0.02	Wheat	Nigeria	Market survey (Akinyele and Shokunbi, 2015)	<0.08
Wheat	Spain	Samples from flour industry (Tejera et al., 2013)	0.04	Wheat	India	Organic farming (Chandorkar and Vaze, 2013)	0.12
Maximum permissible limit			0.20				0.20

Microbial Remediation

There are important economic and ecological benefits from the use of microbes to adjust the concentration of HMs in the soil and to boost the ability of plants to cope with high concentrations of metals (Alamri et al., 2018; Jin et al., 2018). The response of cereals to Pb toxicity can be improved by applying plant-associated microorganisms that promote growth and developmental physiology. The goal of this approach should be to create a plant-mycorrhizal association that is specifically tolerant of HM stress Pb toxicity (Glick, 2010).

Bacteria

Under unfavorable conditions, species that have a strong relationship with plants may be used to enhance plant growth. Inoculation of bacteria increases plant responses to stresses caused by HMs. These microorganisms are capable of fixing atmospheric nitrogen, solubilizing phosphate, and developing growth-promoting compounds, e.g., aminocyclopropane-1-carboxylate deaminase (ACCD), phyto-hormones, or siderophores. ACCD modulates ethylene production at plants (Belimov et al., 2005). Among the plant growth-promoting rhizobacteria (PGPR), some bacterial strains can synthesize auxins to enhance root growth resulted in the improvement in the plant growth and development (Hussain et al., 2013; Ahmed and Hasnain, 2020). Auxin producer bacteria physiologically enhance responses to toxicity of HMs in maize (Cassan et al., 2009). Chelating compounds produced by bacteria acidify the soil, making it possible to reach metals in the soil (Lasat, 2002). The bacterial ACC deaminase degrades ACC (ethylene precursor) and the development of rescue plants under HM stress (Mayak et al., 2004). In the defense of plant cell damage, bacterial catalases and oxidases play a very important role; bacterial catalases are very important for plant pathogenesis (Guo et al., 2012).

Plant growth-promoting rhizobacteria increases HM phytoextraction by promoting plant growth under Pb stress conditions. The trace elements can be immobilized in soils during phyto-extraction, resulting in reduced uptake (Glick, 2010). The main characteristics of phyto-stabilization are high soil-retaining ability and high tolerance to Pb toxicity. Bacterial isolates with good PGP characteristics in cereals help to increase cereal growth not only under normal soil conditions but also under stress conditions of HM. The goal should be to classify and characterize bacterial strains that have a role in improving HM tolerance, including Pb toxicity in cereals.

Fungi

Besides other microorganism's, several strains of fungi are known to date that potentially involve in the phytoremediation of HMs in various plant species. For instance, recently, Manzoor et al. (2019) reported five nonpathogenic fungal strains, i.e., *Trichoderma harzianum*, *Penicillium simplicissimum*, *Aspergillus flavus*, *Aspergillus niger*, and *Mucor* spp. and recorded their ability to modify soil properties including pH and organic matter. They found that these above five strains significantly enhanced the bioavailability of Pb under different concentrations. Biogeochemical cycling of metals is

correlated with microorganisms; their actions finalize the mobilization or immobilization of metals depending on the microenvironment and process involved (Ehrlich et al., 2015). Symbiosis between indigenous and plant microbes (indigenous and plant microbes) reacts to HM toxicity tolerance. The supply of heavy metals and their toxicity to plants depends on rhizospheric reactions and microbial activity. Various plant roots have strong symbiosis with mycorrhiza; this relationship significantly changes plant responses to various types of stresses of HMs (Ehrlich et al., 2015). The access of heavy metals to roots is limited by a fungal sheath around the root surface. In contrast to nonmycorrhizal roots, greater concentrations of soluble phenolics are present in mycorrhizal roots. Mycorrhizal fungi improve protection through the interaction of GSH mycorrhizal roots that act as a strongly armed relationship with physiological defense against Pb toxicity (Tangahu et al., 2011). This is a successful strategy for establishing associations of stress tolerant plant mycorrhizal for phytoremediation and reclamation and enrichment of soils. *Exophialapisciphila* (dark septate endophyte) increases the growth of maize and biomass under polluted metal soils and by regulating root to shoot translocation, it further enhances resistance to HM toxicity (Tangahu et al., 2011).

Plant Engineering

The application of phytoremediation on a large scale, especially in the context of the soil-crop system, is often limited. Other issues exist, such as phytovolatilization, the issue of biomass disposal and the use of various chemicals for remediation. Using gene modification to enhance the resistance of HMs in food crops may overcome these limitations (Ashraf, 2009). This may be useful in enhancing the capacity for plant tolerance and contact between plants and microbes. Plant genetic engineering study to resolve the issue of susceptibility to HMs is a guarantee to increase the phytoremediation ability of polluted HM soils (Vinocur and Altman, 2005).

Advantages and Limitations

Phytoremediation technology looks effective for the purpose, compared with various traditional techniques used to remediate HMs, including Pb-polluted soils. There are various forms of advantages and disadvantages (**Table 6**) associated with the phytoremediation process applied to Pb toxicity (Tangahu et al., 2011).

PHYTO-MANAGEMENT

By following the process of avoidance, tolerance, or both, protection from HM stress can be achieved. In detoxification, tolerance functions better than selective absorption. The most desirable characters in plants involve high Pb accumulation in roots than shoots and strong defense mechanism. Plants with the ability to prevent metals from entering the cytoplasm are known as avoiders, while plants with the ability to detoxify metal ions with the ability to cross plasma/organellar membranes are labeled as tolerant (Ledford and Niyogi, 2005). Mobile and immobilized fractions of HMs need to be separated as they bind to organic and inorganic soil components and to humus. Solubility, availability, and mobility depend entirely on the characteristics of various soil types, such as adsorption, desorption, and complexation (Kaur et al., 2015c). With a priority on food security for a rapidly increasing population, the production of nonfood crops in metal-polluted soils is not feasible. These soils can be used for food crops by adding various modifications to reduce the absorption of metals by plants. Some of the changes are clarified below.

Inorganic Amendments

For enhancing Pb tolerance in cereals, safe and proper nutrition for plants could play an effective role. As a micronutrient, sulfur plays a role in plant protein synthesis and is part of several coenzymes and prosthetic groups as a structural unit. Sulfur (S) improves the accessibility of metals to plants by reducing soil pH (Cui et al., 2004). Zn fertilization increases the yield of grain in cereals by decreasing the negative effect of Pb toxicity due to its antagonistic effect on soil uptake (Dalir et al., 2017). This antagonistic interaction works positively and causes Pb uptake to be decreased, since Pb uses Zn membrane transport proteins for membrane mobility for uptake (Mousavi et al., 2012). Thus, the use of Zn fertilizer acts to compensate for Zn deficiency and mitigate the impact of Pb toxicity. In iron assimilation and eventually chlorosis, excessive Zn concentration induces blockage.

TABLE 6 | Advantages and limitations of phytoremediation mechanism in Pb toxicity.

Advantages	Limitations
Applicable to different contaminants	Requires more root surface area and depth for efficient working
Low cost bearing as compared with traditional processes	Long-term commitment because of less biomass production due to slow root growth in Pb-contaminated soils (time consuming)
Efficiently reduces contaminant	Efficiency effected with the increasing age of plants
Less disruptive as compared with physical removal and chemical treatments	Survival of plants under variable Pb toxicity
Environment friendly	Variable climatic conditions adversely affect the working efficiency of plants
Esthetically pleasing	Variable soil chemistry
Easy monitoring	Pb bioaccumulation in plants and its transportation to plant tissue.
Possibility of recovery of different metals	Availability of contaminant for primary consumer through food chain
Reuse of metals (phyto-mining)	No assurance of complete removal of contaminant from soil

Silicon (Si) application increases plant growth and biomass under HMs. Under HM stress conditions, it improves photosynthetic machinery (chlorophyl concentrations, gas exchange capacity, and fluorescence in cereals) (Rizwan et al., 2019). Silicon deposition increases maize resistance to HM toxicity in root endodermis and pericycle. The application of chelants, EDDS, EDTA, and IDSA could increase the concentration of Pb, Cu, and Cd in hydroponics maize shoots (Zhao et al., 2010). The positive effect of diammonium phosphate (DAP) on root weight and grain yield in cereals is important. This improvement is documented as a result of Pb immobilization and its role in improving Pb toxic effects on plant growth (Park et al., 2012). In case of wheat, diammonium phosphate (DAP) effectively decreased Pb concentrations in roots, straw, and grains; this may be attributed to increased soil pH and decreased Pb mobility (Rehman et al., 2015). Diammonium phosphate decreases soil extractable Pb concentration due to the formation of secondary Pb phosphate precipitates (Miretzky and Fernandez-Cirelli, 2008). Diammonium phosphate increases P concentration in alkaline soils, resulting in the formation of phosphate-induced fluoropyromorphite and other compounds with low soil surface adsorption, solubility, and complexity (Lu et al., 2019). It also improves the photosynthetic rate effectively. Amendments that contain phosphorus and calcium allow stable metal compounds and reduce their mobility and phyto-availability (Rehman et al., 2015). Inorganic nutrients are considered the key ingredient of MS media and the effect on plants is the best variable to study. Magnesium (Mg) and zinc (Zn) improve the efficacy of callus growth and regeneration. For instance, Zn nanoparticles alleviate the negative impacts of abiotic stress in plants and enhance callus regeneration rate, improving the mineral elements (N, P, and K) and enzymatic antioxidants such as SOD and GPX (Alharby et al., 2016). In another study, researchers studied the role of inorganic nutrients such as Mg ($MgSO_4$) and Zn ($ZnSO_4$) to alleviate the toxic levels of HMs (Pb and Ni) for callus induction grown on regeneration medium (MS). They reported the varied response of inorganic nutrients to both HMs and noted that callus induction rate was significantly deteriorated when grown in MS medium containing more than 100 μM concentrations of Pb and Ni. They also concluded that $ZnSO_4$ was best to minimize the Ni stress and $MgSO_4$ was best against Pb toxicity (Krishania and Agarwal, 2012). These above-mentioned studies suggested that regarding phytoremediation, the long-term use of single fertilizer should be discouraged. In combination, different inorganic additions, fertilizers, and agronomic practices could be more beneficial.

Organic Amendments

A selection of farm yard manure can achieve good phytoextraction efficiency in cereals (FYM). Organic matter plays an important role in decreasing metal phyto-availability, providing additional nutrients and changing the physical, chemical, and biological properties of the soil with decomposition (Rizwan et al., 2017). Gypsum-released calcium ions in soil compete with Pb for plant uptake, in addition to $PbSO_4$ since Pb precipitation may be another mechanism of action (Arnich et al., 2003). Application of organic amendments decreases toxicity of HMs and enhances plant growth (Mohamed et al., 2015). Under field conditions, its implementation increases root branching and surface area and fine roots. In maize, the biochar application changes the root architecture and influences the absorption of HMs. The response of cereals varies with the change in organic modification type, growth conditions, and the degree of toxicity of HMs in soil (Al-Wabel et al., 2015). The treatment of metal contaminated soils with dihydrazone facilitates the absorption by maize plants of Zn, Pb, Cu, and Cd (Antonkiewicz and Para, 2016). Organic acids with low molecular weight (LMWOA) play a role in reducing shoot biomass and HM concentration in maize shoots (Sabir et al., 2014).

By minimizing Pb absorption, the application of different modifications improve physiological activity and natural chlorophyll synthesis, all of which help to normalize the transport of electrons and enzymatic activity in the Calvin cycle (Mroczek-Zdyrska and Wójcik, 2012). These amendments release soil nutrients that encourage root growth and development and increase the site's microbial activity. Organic modifications are solar-based, cost-effective, and eco-friendly methods that preserve natural soil properties (using plants and microbes). The use of plants such as *Erigeron canadensis*, *Digitari aciliaris*, and *Solanum nigrum* can mitigate the carcinogenic potential of Pb as bioremediation (Al-Wabel et al., 2015).

Source Reduction

The reduction of HM sources is an important technique for minimizing its dangerous impact. The accumulation of HMs in soil and eventually in food crops could be minimized by an attempt to control air quality. Compared with humans fed food raised under regular irrigation, the content of HMs in humans fed with food raised by irrigation of polluted water is often higher (Blayock, 2000). The major contributor to the accumulation of HMs in the food chain is supply sources. Ultimately, treatment of Pb sources prior to application to plants decreases the content of food crops. Different regions of global cereals and vegetables are irrigated with hazardous metal wastewater that poses serious health concerns. By simply avoiding inadequately treated waste water, pollution of HMs could be decreased by up to 85%. Another technique for reducing Pb content in food crops is land use optimization. Food crops should not be grown within 30 m of the roadside; urban roadside dust serves as a pathway for the accumulation of Pb in food crops (Uwah et al., 2011). Crops produced near the drainage area of acid mining have a high risk of contaminating Pb. Usually, contamination of Pb is from natural sources. Most researchers strongly support the use of pretreated wastewater for irrigation to decrease the content of HMs in food crops, including Pb. In addition, plant breeders and agronomists have to minimize soil crop transfer of Pb (Dong et al., 2009).

Eco-Remediation

The prerequisite for remediation (eco-remediation) is a better understanding of soil-food crop transition mechanisms (Rai et al., 2019). By altering the physiochemical properties of the soil, these techniques minimize the bioavailability of HMs. The use of compost and biochar serves as an ecological solution to minimize the concentration of HMs in soil (as revealed in

the measurement monitor model) by enhancing the ability of cation exchange, humification, and the cycle of soil nutrients. Biochar in combination with *Pseudomonas chenduensis* metal-resistant bacteria greatly decreases the bioavailability of HMs (Li et al., 2020). Detailed information on soil properties, such as biological and physiochemical characteristics and HM concentration, should be available for affective remediation. Here, we have a practical example in wheat plants grown hydroponically under Pb and nitric oxide (NO) supply. Researchers observed that NO significantly reduced the negative impact of Pb toxicity in the form of oxidative stress induced by ROS (malondialdehyde, conjugated dienes, hydroxyl ions and superoxide anion). Furthermore, exogenous NO interferes ROS detoxification mechanism and enhances the antioxidant enzyme activity in wheat roots (Kaur et al., 2015a). Based on the above results, eco-remediation technologies are therefore primarily applicable in the field of wet land agriculture. These approaches are cost-effective and environmentally friendly (Rai et al., 2019).

Chemical and Physiochemical Strategies

Compared with biological strategies, chemical strategies are less preferable but are used to remediate the polluted soil. The complexion of metals in the soil makes it impossible for plants to have access to them. Synthetic zeolites with augmentation of alkaline clay are effectively used to remediate HMs (Lu et al., 2019). To recover soil from HMs, the use of red mud, magnetite, maghemite, silicon calcium fertilizer, hydrous manganese oxide, and hematite zeolite is productive. The soil plant system has the ability to cope with modifications to Pb, chalk, and manure to decrease both soil and H mobile components (Chandra et al., 2018). In the case of wheat, by using triple superphosphate, calcium magnesium phosphate, and single superphosphate in combination with $ZnSO_4$, the phytoavailability of Pb (∼42.14%) in soils was decreased (Chemek et al., 2016). The activity of soil eco-enzymes and the protection of heavy metal concentration in cereal grains sown in chemical-treated industrial soil (acid washing/amendments) was the same as that grown on untreated soils; there were no risks to human health in both cases (Alamri et al., 2018).

Cereals like other plants have protective strategies against environmental contaminants like Pb by manipulating their genetically controlled chemical and physiochemical processes. These strategies operate in layers; firstly, by excluding or linking it to the cell wall, Pb entry into the cell is prevented; secondly, antioxidant production to fight ROS production is prevented (Rossato et al., 2012). The antioxidant protection mechanism was made up of various species such as carotenoids, glutathione, tocopherol, catalase, ascorbate, ascorbate peroxide, and superoxide dismutase found in vacuole (73%), chloroplast (17%), cytosole (5%), apoplast (4%), and 1% in mitochondria (Tangahu et al., 2011). Similarly, various proteins, including Pb, play an important role in counteracting the adverse effect of HMs (Mroczek-Zdyrska and Wójcik, 2012). The uptake of HMs such as Pb by plants is decreased and the uptake of nutritional elements such as Mg, Ca, Cu, and Fe is increased (He et al., 2004). In plants, Pb often initiates a protective mechanism against oxidative stress that relies entirely on the physiological status of plant organs (Rossato et al., 2012).

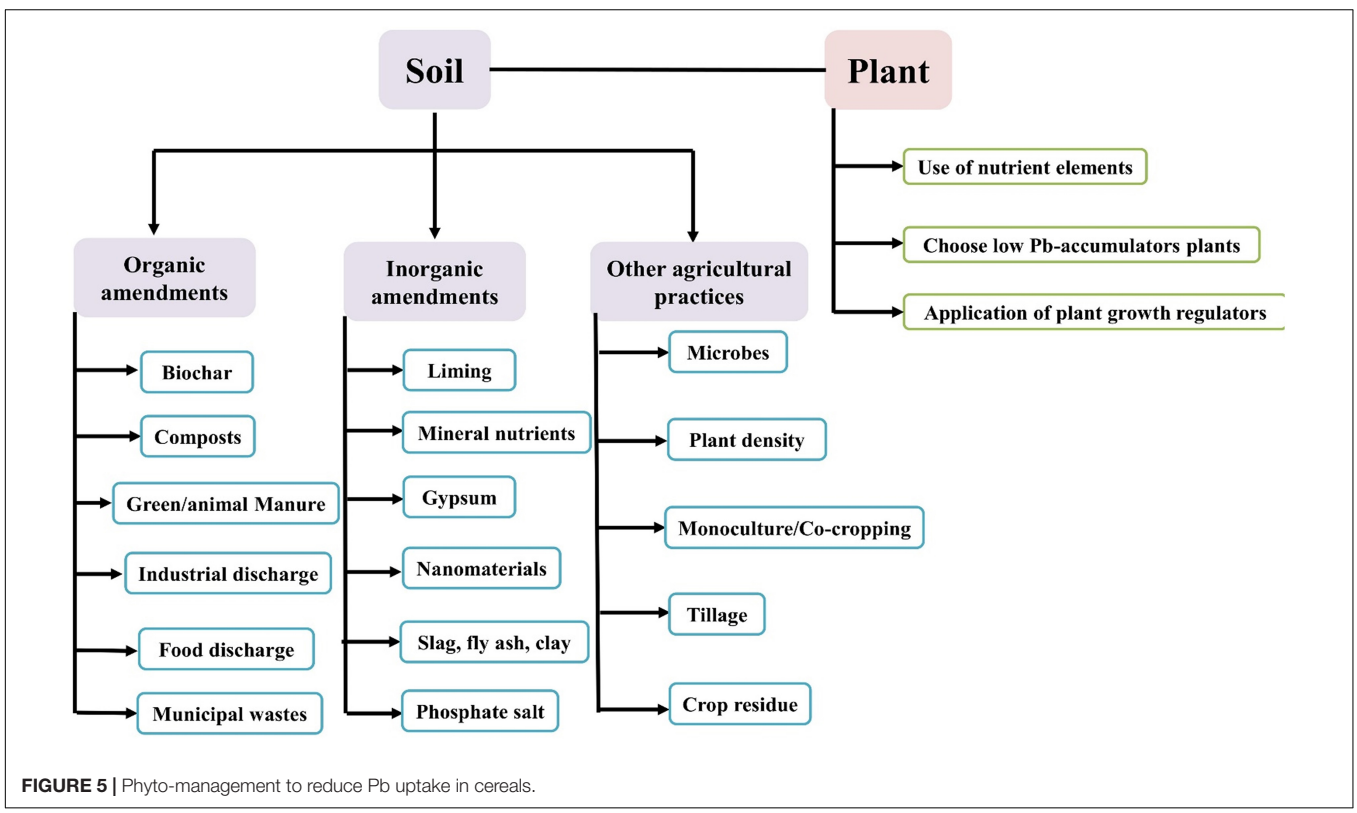

FIGURE 5 | Phyto-management to reduce Pb uptake in cereals.

Nanotechnology

A research hotspot of the present era is agro-nanotechnology; this ensures soil protection by reducing the bioavailability of HMs. The biosynthesis of nanoparticles is verified by advances in plant molecular biology techniques in protein and genetic engineering (Doshi et al., 2008). To detect the level of contamination in food crops, nanosensors are applied for analysis. In order to formulate less toxic biofertilizers and pesticides for the soil, different nanotechnologies may be used. Interaction between nanoparticles, plants, and soil prevails (Karami and Alipour, 2009). Owing to the accumulation of ambient particulate matter on the leaves of plants, there is a major shift in the mechanism of thermal equilibrium, photosynthesis, and transpiration. The suitable catalytic metal nanoparticles are limited to periodic Table Group VIII and IB (platinum, silver, gold, and palladium).

There is a need to know the level of penetration and transport of nanoparticles in plants to understand the role of nanotechnology in plant enhancement in stressful environments. Through its use in plant genomic analysis and gene function, nanotechnology can be used to enhance plant biological response to various types of environmental stresses (Monica and Cremonini, 2009). Nanoparticles are used to enhance germination, root growth, sources of micronutrients, the activities of Rubisco carboxilase and general plant growth in wheat and maize (Doshi et al., 2008).

Electrochemical materials such as electrically conductive adhesives (ECA) exploration for surface mounting technology and flip chip application as Pb free alternatives were studied previously (Jiang et al., 2005; Kano et al., 2009; Karami and Alipour, 2009). Nanotechnological efforts are being carried out to increase plant resistance by improving the ability of plants to remove toxins from soil in order to use plants for soil clean-up (**Figure 5**).

EFFECT ON GENETIC CHARACTERS

A direct measure of susceptibility or tolerance is the monitoring of biological responses of plants in the form of genetic characteristics such as genes, coding transcription factors (TF), and proteins responsive to environmental pollutants. The response of plants, including cereals, to external Pb stress relies on genotypic variation and concentration. Various cellular ingredients such as membrane stability/integrity, lipid peroxidation, redox potential assessment, metabolites (primary and secondary), and enzymatic and nonenzymatic antioxidants can be controlled to assess the oxidative (ROS) pressure caused by excessive Pb (Cassells and Curry, 2001). As biomarkers of Pb toxicity, these above-mentioned biochemicals and their regulated gene(s) expression are used to delineate effects long before symptoms emerge. Zhang et al. (2017) reported 262 differentially expressed TFs (DETFs) that react to Pb stress in maize plants. In addition, they showed that DETFs were divided into four classes. In addition, polymorphism at the level of expression of two bZIP TFs, such as ZmbZIP54 and ZmbZIP107, has been shown to contribute to the Pb tolerance mechanism in different lines of maize. Lead toxicity has significant effects on the pattern of gene expression. Many genes regulating various ingredients of plant metabolism are downregulated because of this form of stress, such as genes related to lipid metabolism, lignin biosynthesis, energy metabolism, xenobiotic biodegradation, metabolism of carbohydrates, metabolism of amino acids, metabolism of phenylalanine, and growth and death of cells. The upregulated genes that control characteristics are mostly linked to secondary metabolite biosynthesis, such as membrane transport, especially multidrug resistance protein, major facilitator superfamily, flavonoid biosynthesis, ascorbate and aldarate metabolism, ABC transporters, mitogen-activated protein kinases (MAPK) signaling pathway, glutathione metabolism, large numbers of GST, and relative water content. These are the key genetic variables to be used as select criteria for tolerance to Pb toxicity in cereals. Lead does not have a clear effect on the synthesis of chlorophyll *b*. Transcription variables play a very important role in plant responses to stresses from HMs, including Pb toxicity, and modulate various genes involved in these stresses. It also describes the variations in HM stresses in the network of pathways.

FUTURE PERSPECTIVES

A detailed study involving antioxidant mechanism, Pb-regulated differential gene expression, and mineral transporters is needed to understand complex plant responses to lead toxicity and other HMs. Different techniques such as flow cytometry (detection of changes in chromosome number and structure), fluorescent in situ hybridization (FISH), microdensitometry, restriction fragment length polymorphism (RFLP), and amplified fragment length polymorphism (AFLP) can be used to assess ROS-induced molecular level injuries. A more in-depth understanding of the stress caused by Pb toxicity in cereals by the use of biological markers would help to understand the mechanisms involved in Pb stress tolerance and improve cereal grain tolerance, which eventually help to increase the production of grain per unit area.

AUTHOR CONTRIBUTIONS

MA, AA, and RG designed and wrote the manuscript. MS, BA, ZU, UN, and WZ revised the manuscript. All authors contributed to the article and approved the submitted version.

FUNDING

This work was supported by the National Key Research and Development Program of China (2018YFD0700701) and National Natural Science Foundation of China (31950410560).

REFERENCES

Ahanger, M. A., Ashraf, M., Bajguz, A., and Ahmad, P. (2018). Brassinosteroids regulate growth in plants under stressful environments and crosstalk with other potential phytohormones. *J. Plant Growth Regul.* 37, 1007–1024. doi: 10.1007/s00344-018-9855-2

Ahmad, I., Tahir, M., Daraz, U., Ditta, A., Hussain, M. B., and Khan, Z. U. H. (2020). "Responses and tolerance of cereal crops to metal and metalloid toxicity," in *Agronomic Crops*, ed. M. Hasanuzzaman (Singapore: Springer), 235–264. doi: 10.1007/978-981-15-0025-1_14

Ahmed, A., and Hasnain, S. (2020). Extraction and evaluation of indole acetic acid from indigenous auxin-producing rhizosphere bacteria. *J. Anim. Plant Sci.* 30, 1024–1036. doi: 10.36899/JAPS.2020.4.0117

Akinyele, I., and Shokunbi, O. (2015). Concentrations of Mn, Fe, Cu, Zn, Cr, Cd, Pb, Ni in selected Nigerian tubers, legumes and cereals and estimates of the adult daily intakes. *Food Chem.* 173, 702–708. doi: 10.1016/j.foodchem.2014.10.098

Alamri, S. A., Siddiqui, M. H., Al-Khaishany, M. Y., Nasir Khan, M., Ali, H. M., Alaraidh, I. A., et al. (2018). Ascorbic acid improves the tolerance of wheat plants to lead toxicity. *J. Plant Interact.* 13, 409–419. doi: 10.1080/17429145.2018.1491067

Alexander, P., Alloway, B., and Dourado, A. (2006). Genotypic variations in the accumulation of Cd, Cu, Pb and Zn exhibited by six commonly grown vegetables. *Environ. Pollut.* 144, 736–745. doi: 10.1016/j.envpol.2006.03.001

Alharby, H. F., Metwali, E. M., Fuller, M. P., and Aldhebiani, A. Y. (2016). Impact of application of zinc oxide nanoparticles on callus induction, plant regeneration, element content and antioxidant enzyme activity in tomato (*Solanum lycopersicum* Mill.) under salt stress. *Arch. Biol. Sci.* 68, 723–735. doi: 10.2298/ABS151105017A

Ali, B., Gill, R. A., Yang, S., Gill, M. B., Farooq, M. A., Liu, D., et al. (2015b). Up-regulation of cadmium-induced proteomic and metabolic changes by 5-aminolevulinic acid in leaves of *Brassica napus* L. *PLoS One* 10:e0123328. doi: 10.1371/journal.pone.0123328

Ali, B., Mwamba, T. M., Gill, R. A., Yang, C., Ali, S., Daud, M. K., et al. (2014b). Improvement of element uptake and antioxidative defense in Brassica napus under lead stress by application of hydrogen sulfide. *Plant Growth Regul.* 74, 261–273. doi: 10.1007/s10725-014-9917-9

Ali, B., Qian, P., Sun, R., Farooq, M. A., Gill, R. A., Wang, J., et al. (2015a). Hydrogen sulfide alleviates the aluminum-induced changes in Brassica napus as revealed by physio-chemical and ultrastructural study of plant. *Environ. Sci. Pollut. Res.* 22, 3068–3081. doi: 10.1007/s11356-014-3551-y

Ali, B., Song, W. J., Hu, W. Z., Luo, X. N., Gill, R. A., Wang, J., et al. (2014a). Hydrogen sulfide alleviates lead-induced photosynthetic and ultrastructural changes in oilseed rape. *Ecotoxicol. Environ. Saf.* 102, 25–33. doi: 10.1016/j.ecoenv.2014.01.013

Ali, M. H. H., and Al-Qahtani, K. M. (2012). Assessment of some heavy metals in vegetables, cereals and fruits in Saudi Arabian markets. *Egypt J. Aquat. Res.* 38, 31–37. doi: 10.1016/j.ejar.2012.08.002

Al-Wabel, M. I., Usman, A. R., El-Naggar, A. H., Aly, A. A., Ibrahim, H. M., Elmaghraby, S., et al. (2015). Conocarpus biochar as a soil amendment for reducing heavy metal availability and uptake by maize plants. *Saudi J. Biolog. Sci.* 22, 503–511. doi: 10.1016/j.sjbs.2014.12.003

Angelova, V., Ivanova, R., Delibaltova, V., and Ivanov, K. (2011). Use of sorghum crops for in situ phytoremediation of polluted soils. *J. Agric. Sci. Technol.* 1, 693–702.

Antonkiewicz, J., and Para, A. (2016). The use of dialdehyde starch derivatives in the phytoremediation of soils contaminated with heavy metals. *Int. J. Phytoremed.* 18, 245–250. doi: 10.1080/15226514.2015.1078771

Anwar, A., Liu, Y., Dong, R., Bai, L., Yu, X., and Li, Y. (2018). The physiological and molecular mechanism of brassinosteroid in response to stress: a review. *Biol. Res.* 51, 46. doi: 10.1186/s40659-018-0195-2

Arif, M. S., Yasmeen, T., Shahzad, S. M., Riaz, M., Rizwan, M., Iqbal, S., et al. (2019). Lead toxicity induced phytotoxic effects on mung bean can be relegated by lead tolerant Bacillus subtilis (PbRB3). *Chemosphere* 234, 70–80. doi: 10.1016/j.chemosphere.2019.06.024

Arnich, N., Lanhers, M. C., Laurensot, F., Podor, R., Montiel, A., and Burnel, D. (2003). In vitro and in vivo studies of lead immobilization by synthetic hydroxyapatite. *Environ. Pollut.* 124, 139–149. doi: 10.1016/S0269-7491(02)00416-5

Ashraf, M. (2009). Biotechnological approach of improving plant salt tolerance using antioxidants as markers. *Biotechnol. Adv.* 27, 84–93. doi: 10.1016/j.biotechadv.2008.09.003

Ashraf, U., and Tang, X. (2017). Yield and quality responses, plant metabolism and metal distribution pattern in aromatic rice under lead (Pb) toxicity. *Chemosphere* 176, 141–155. doi: 10.1016/j.chemosphere.2017.02.103

Ashry, N. A., Ghonaim, M. M., Mohamed, H. I., and Mogazy, A. M. (2018). Physiological and molecular genetic studies on two elicitors for improving the tolerance of six Egyptian soybean cultivars to cotton leaf worm. *Plant Physiol. Biochem.* 130, 224–234. doi: 10.1016/j.plaphy.2018.07.010

Ayesha, I. C., Liu, G., Yousaf, B., Abbas, Q., and Zhou, H. (2019). A comprehensive review of biogeochemical distribution and fractionation of lead isotopes for source tracing in distinct interactive environmental compartments. *Sci. Total Environ.* 719, 135658. doi: 10.1016/j.scitotenv.2019.135658

Bajguz, A., and Piotrowska, A. (2009). Conjugates of auxin and cytokinin. *Phytochemistry* 70, 957–969. doi: 10.1016/j.phytochem.2009.05.006

Belimov, A., Hontzeas, N., Safronova, V., Demchinskaya, S., Piluzza, G., Bullitta, S., et al. (2005). Cadmium-tolerant plant growth-promoting bacteria associated with the roots of Indian mustard (*Brassica juncea* L. Czern.). *Soil Biol. Biochem.* 37, 241–250. doi: 10.1016/j.soilbio.2004.07.033

Blaylock, M. J., and Huang, J. W. (2000). "Phytoextraction of metals," in *Phytoremediation of Toxic Metals: Using Plants to Clean up the Environment*, eds I. Raskin and B. D. Ensley (Hoboken, NJ: John Wiley & Sons, Inc), 314.

Blayock, M. J. (2000). *Phytoremediation of Toxic Metals: Using Plants to Clean Up the Environment*. Hoboken, NJ: John Wiley & Sons, Inc, 53–70.

Cândido, G. S., Lima, F. R., Vasques, I. C., Souza, K. R., Martins, G. C., Pereira, P., et al. (2020). "Lead effects on sorghum and soybean physiology in oxisols," in *Archives of Agronomy and Soil Science*, (Abingdon-on-Thames: Taylor & Francis), 1–15. doi: 10.1080/03650340.2020.1723004

Cassan, F., Perrig, D., Sgroy, V., Masciarelli, O., Penna, C., and Luna, V. (2009). Azospirillumbrasilense Az39 and *Bradyrhizobium japonicum* E109, inoculated singly or in combination, promote seed germination and early seedling growth in corn (*Zea mays* L.) and soybean (*Glycine max* L.). *Europ. J. Soil Biol.* 45, 28–35. doi: 10.1016/j.ejsobi.2008.08.005

Cassells, A. C., and Curry, R. F. (2001). Oxidative stress and physiological, epigenetic and genetic variability in plant tissue culture: implications for micropropagators and genetic engineers. *Plant Cell Tissue Org. Cult.* 64, 145–157. doi: 10.1023/A:1010692104861

Chandorkar, S., and Vaze, N. (2013). Analysis of metal content of organic foods. *J. Environ. Sci. Toxicol. Food Technol.* 3, 44–49. doi: 10.9790/2402-0434449

Chandra, R., Kumar, V., Tripathi, S., and Sharma, P. (2018). Heavy metal phytoextraction potential of native weeds and grasses from endocrine-disrupting chemicals rich complex distillery sludge and their histological observations during in-situ phytoremediation. *Ecol. Eng.* 111, 143–156. doi: 10.1016/j.ecoleng.2017.12.007

Chemek, M., Mimouna, S. B., Boughammoura, S., Delbès, G., and Messaoudi, I. (2016). Protective role of zinc against the toxicity induced by exposure to cadmium during gestation and lactation on testis development. *Reprod. Toxicol.* 63, 151–160. doi: 10.1016/j.reprotox.2016.06.005

Chen, Q., Zhang, X., Liu, Y., Wei, J., Shen, W., Shen, Z., et al. (2017). Hemin-mediated alleviation of zinc, lead and chromium toxicity is associated with elevated photosynthesis, antioxidative capacity; suppressed metal uptake and oxidative stress in rice seedlings. *Plant Growth Regul.* 81, 253–264. doi: 10.1007/s10725-016-0202-y

Cho, K., Shibato, J., Agrawal, G. K., Jung, Y. H., Kubo, A., Jwa, N. S., et al. (2008). Integrated transcriptomics, proteomics, and metabolomics analyses to survey ozone responses in the leaves of rice seedling. *J. Proteom. Res.* 7, 2980–2998. doi: 10.1021/pr800128q

Creelman, R. A., and Mullet, J. E. (1995). Jasmonic acid distribution and action in plants: Regulation during development and response to biotic and abiotic stress. *Proc. Natl. Acad. Sci. U.S.A.* 92, 4114–4119. doi: 10.1073/pnas.92.10.4114

Cui, Y., Dong, Y., Li, H., and Wang, Q. (2004). Effect of elemental sulphur on solubility of soil heavy metals and their uptake by maize. *Environ. Int.* 30, 323–328. doi: 10.1016/S0160-4120(03)00182-X

Dalir, N., Tandy, S., Gramlich, A., Khoshgoftarmanesh, A., and Schulin, R. (2017). Effects of nickel on zinc uptake and translocation in two wheat cultivars differing in zinc efficiency. *Environ. Exp. Bot.* 134, 96–101. doi: 10.1016/j.envexpbot.2016.11.009

Davies, P. J. (2010). *Plant Hormones. Biosynthesis, Signal Transduction, Action*, 3rd Edn. Dordrecht: Springer. doi: 10.1007/978-1-4020-2686-7

Dinh, S. T., Luu, V. T., Hoang, L. H., Nguyen, X. C., and Ho, C. T. (2020). "Biotechnology of Plant-Associated Microbiomes," in *The Plant Microbiome in Sustainable Agriculture*, eds A. K. Srivastava, P. L. Kashyap, and M. Srivastava (Hoboken, NJ: John Wiley & Sons, Inc), doi: 10.1007/s10646-011-0771-5

Dong, D., Zhao, X., Hua, X., Liu, J., and Gao, M. (2009). Investigation of the potential mobility of Pb, Cd and Cr (VI) from moderately contaminated farmland soil to groundwater in Northeast, China. *J. Hazard. Mater.* 162, 1261–1268. doi: 10.1016/j.jhazmat.2008.06.032

Doshi, R., Braida, W., Christodoulatos, C., Wazne, M., and O'connor, G. (2008). Nano-aluminum: transport through sand columns and environmental effects on plants and soil communities. *Environ. Res.* 106, 296–303. doi: 10.1016/j.envres.2007.04.006

Ehrlich, H. L., Newman, D. K., and Kappler, A. (2015). *Ehrlich's Geomicrobiology*. Boca Raton, FL: CRC press. doi: 10.1201/b19121

Ekholm, P., Reinivuo, H., Mattila, P., Pakkala, H., Koponen, J., Happonen, A., et al. (2007). Changes in the mineral and trace element contents of cereals, fruits and vegetables in Finland. *J. Food Compos. Anal.* 20, 487–495. doi: 10.1016/j.jfca.2007.02.007

Eticha, T., and Hymete, A. (2015). Determination of some heavy metals in barley locally grown for brewing and it's malt in Ethiopia. *J. Bioanal. Biomed.* 7, 171.

FAO (2013). *Food Supply Database*. Rome: Food and Agricultural Organization.

Ghani, A., Shah, A. U., and Akhtar, U. (2010). Effect of lead toxicity on growth, chlorophyll and lead (Pb+). *Pak. J. Nutri.* 9, 887–891. doi: 10.3923/pjn.2010.887.891

Glick, B. R. (2010). Using soil bacteria to facilitate phytoremediation. *Biotechnol. Adv.* 28, 367–374. doi: 10.1016/j.biotechadv.2010.02.001

Gomes, E. J. R. (2011). *Genotoxicity and Cytotoxicity of Cr (VI) and Pb2+ in Pisum sativum*. Aveiro: Universidade de Aveiro.

Gülen, H., Çetinkaya, C., Kadıoğlu, M., Kesici, M., Cansev, A., and Eriş, A. (2008). Peroxidase activity and lipid peroxidation in strawberry (Fragaria ananassa) plants under low temperature. *J. Biol. Environ. Sci.* 2, 95–100.

Guo, M., Block, A., Bryan, C. D., Becker, D. F., and Alfano, J. R. (2012). *Pseudomonas* syringae catalases are collectively required for plant pathogenesis. *J. Bacteriol.* 194, 5054–5064. doi: 10.1128/JB.00999-12

Gupta, D., Huang, H., Yang, X., Razafindrabe, B., and Inouhe, M. (2010). The detoxification of lead in Sedum alfredii H. is not related to phytochelatins but the glutathione. *J. Hazard. Mater.* 177, 437–444. doi: 10.1016/j.jhazmat.2009.12.052

Hafez, E. H., and Seleiman, M. F. (2017). Response of barley quality traits, yield and antioxidant enzymes to water-stress and chemical inducers. *Int. J. Plant Prod.* 11, 477–490.

Harcz, P., de Temmerman, L., and de Voghel, S. (2007). Contaminants in organically and conventionally produced winter wheat (*Triticum aestivum*) in Belgium. *Food Addit. Contam.* 24, 713–720. doi: 10.1080/02652030601185071

Hasanuzzaman, M., Nahar, K., Rahman, A., Mahmud, J. A., Alharby, H. F., and Fujita, M. (2018). Exogenous glutathione attenuates lead-induced oxidative stress in wheat by improving antioxidant defense and physiological mechanisms. *J. Plant Inter.* 13, 203–212. doi: 10.1080/17429145.2018.1458913

Hawes, M. C., Bengough, G., Cassab, G., and Ponce, G. (2002). Root caps and rhizosphere. *J. Plant Growth Regul.* 21, 352–367. doi: 10.1007/s00344-002-0035-y

He, P. P., Lv, X. Z., and Wang, G. (2004). Effects of Se and Zn supplementation on the antagonism against Pb and Cd in vegetables. *Environ. Int.* 30, 167–172. doi: 10.1016/S0160-4120(03)00167-3

Hussain, A., Abbas, N., Arshad, F., Akram, M., Khan, Z. I., Ahmad, K., et al. (2013). Effects of diverse doses of lead (Pb) on different growth attributes of Zea-Mays L. *Agric. Sci.* 4, 1–4.

Inoue, H., Fukuoka, D., Tatai, H., Kamachi, M., Hayatsu, M., and Suzuki, S. (2013). Properties of lead deposits in cell walls of radish (*Raphanus sativus*) roots. *J. Plant Res.* 126, 51–61. doi: 10.1007/s10265-012-0494-6

Islam, M. S., Ahmed, M. K., and Habibullah-Al-Mamun, M. (2014). Heavy metals in cereals and pulses: health implications in Bangladesh. *J. Agric. Food Chem.* 62, 10828–10835. doi: 10.1021/jf502486q

Jiang, H., Moon, K. S., and Wong, C. (2005). "Synthesis of Ag-Cu alloy nanoparticles for lead-free interconnect materials," in *Proceedings. International Symposium on Advanced Packaging Materials: Processes, Properties and Interfaces*, (Irvine, CA: IEEE), 173–177.

Jiang, L. W., Wang, Z., Chen, Q., Gao, Q., Xu, Q., and Cao, H. (2017). A role for APX1 gene in lead tolerance in *Arabidopsis thaliana*. *Plant Sci.* 256, 94–102. doi: 10.1016/j.plantsci.2016.11.015

Jin, Y., Luan, Y., Ning, Y., and Wang, L. (2018). Effects and mechanisms of microbial remediation of heavy metals in soil: a critical review. *Appl. Sci.* 8, 1336. doi: 10.3390/app8081336

Jitendra, M., Rachna, S., and Arora, N. K. (2017). Alleviation of heavy metal stress in plants and remediation of soil by rhizosphere microorganisms. *Front. Microbiol.* 8:1706. doi: 10.3389/fmicb.2017.01706

Jones, D. L., Nguyen, C., and Finlay, R. D. (2009). Carbon flow in the rhizosphere: carbon trading at the soil–root interface. *Plant Soil* 321, 5–33. doi: 10.1007/s11104-009-9925-0

Kano, J., Kizuka, T., Shikanai, F., and Kojima, S. (2009). Pure lead nanoparticles with stable metallic surfaces, on perovskite lead strontium titanate particles. *Nanotechnology* 20, 295704. doi: 10.1088/0957-4484/20/29/295704

Kanwal, A., Farhan, M., Sharif, F., Hayyat, M. U., Shahzad, L., and Ghafoor, G. Z. (2020). Effect of industrial wastewater on wheat germination, growth, yield, nutrients and bioaccumulation of lead. *Sci. Rep.* 10, 1–9. doi: 10.1038/s41598-020-68208-7

Karami, H., and Alipour, M. (2009). Synthesis of lead dioxide nanoparticles by the pulsed current electrochemical method. *Int. J. Electrochem. Sci.* 4, 1511–1527.

Kaur, G., Kaur, S., Singh, H. P., Batish, D. R., Kohli, R. K., and Rishi, V. (2015b). Biochemical adaptations in Zea mays roots to short-term Pb2+ exposure: ROS generation and metabolism. *Bull. Environ. Contam. Toxicol.* 95, 246–253. doi: 10.1007/s00128-015-1564-y

Kaur, G., Singh, H. P., Batish, D. R., and Kohli, R. K. (2013). Lead (Pb)-induced biochemical and ultrastructural changes in wheat (*Triticum aestivum*) roots. *Protoplasma* 250, 53–62. doi: 10.1007/s00709-011-0372-4

Kaur, G., Singh, H. P., Batish, D. R., and Kohli, R. K. (2015a). Adaptations to oxidative stress in Zea mays roots under short-term Pb2+ exposure. *Biologia* 70, 190–197. doi: 10.1515/biolog-2015-0023

Kaur, G., Singh, H. P., Batish, D. R., and Kumar, R. K. (2012). Growth, photosynthetic activity and oxidative stress in wheat (*Triticum aestivum*) after exposure of lead to soil. *J. Environ. Biol.* 33, 265–269.

Kaur, G., Singh, H. P., Batish, D. R., Mahajan, P., Kohli, R. K., and Rishi, V. (2015c). Exogenous nitric oxide (NO) interferes with lead (Pb)-induced toxicity by detoxifying reactive oxygen species in hydroponically grown wheat (*Triticum aestivum*) roots. *PLoS One* 10:e0138713. doi: 10.1371/journal.pone.0138713

Khalid, S., Shahid, M., Bibi, I., Sarwar, T., Shah, A. H., and Niazi, N. K. (2018). A review of environmental contamination and health risk assessment of wastewater use for crop irrigation with a focus on low and high-income countries. *Int. J. Environ. Res. Public Health* 15, 895. doi: 10.3390/ijerph15050895

Khan, F., Hussain, S., Tanveer, M., Khan, S., Hussain, H. A., Iqbal, B., et al. (2018). Coordinated effects of lead toxicity and nutrient deprivation on growth, oxidative status, and elemental composition of primed and non-primed rice seedlings. *Environ. Sci. Pollut. Res.* 25, 2185–2194. doi: 10.1007/s11356-018-2262-1

Kiran, B. R., and Prasad, M. N. V. (2017). Responses of *Ricinus communis* L. (castor bean, phytoremediation crop) seedlings to lead (Pb) toxicity in hydroponics. *Selcuk J. Agri. Food Sci.* 31, 73–80. doi: 10.15316/SJAFS.2017.9

Kopyra, M., and Gwóźdź, E. A. (2003). Nitric oxide stimulates seed germination and counteracts the inhibitory effect of heavy metals and salinity on root growth

of *Lupinus luteus*. *Plant Physiol. Biochem.* 41, 1011–1017. doi: 10.1016/j.plaphy.2003.09.003

Krishania, S., and Agarwal, K. (2012). Effects of heavy metals on *Eleusine coracana* (L.) Gaertn. *Res. Plant Biol.* 2, 43–54.

Kumar, A. S., and Bais, H. P. (2012). Wired to the roots: impact of root-beneficial microbe interactions on above-ground plant physiology and protection. *Plant Signal Behav.* 7, 1598–1604. doi: 10.4161/psb.22356

Kurtyka, R., Burdach, Z., Siemieniuk, A., and Karcz, W. (2018). Single and combined effects of Cd and Pb on the growth, medium pH, membrane potential and metal contents in maize (*Zea mays* L.) coleoptile segments. *Ecotoxicol. Environ. Saf.* 161, 8–16. doi: 10.1016/j.ecoenv.2018.05.046

Lamhamdi, M., Bakrim, A., Aarab, A., Lafont, R., and Sayah, F. (2011). Lead phytotoxicity on wheat (*Triticum aestivum* L.) seed germination and seedlings growth. *Comptes Rendus Biolog.* 334, 118–126. doi: 10.1016/j.crvi.2010.12.006

Lasat, M. M. (2002). Phytoextraction of toxic metals: a review of biological mechanisms. *J. Environ. Qual.* 31, 109–120. doi: 10.2134/jeq2002.1090

Leblanc, J., Guerin, T., Noel, L., and Calamassi-Tran, G. (2005). Dietary exposure estimates of 18 elements from the 1st French total diet study. *Food Addit. Contam.* 22, 624–641. doi: 10.1080/02652030500135367

Ledford, H. K., and Niyogi, K. K. (2005). Singlet oxygen and photo−oxidative stress management in plants and algae. *Plant Cell Environ.* 28, 1037–1045. doi: 10.1111/j.1365-3040.2005.01374.x

Li, J., Wang, S. L., Zhang, J., Zheng, L., Chen, D., Wu, Z., et al. (2020). Coconut-fiber biochar reduced the bioavailability of lead but increased its translocation rate in rice plants: elucidation of immobilization mechanisms and significance of iron plaque barrier on roots using spectroscopic techniques. *J. Hazard. Mater.* 389, 122117. doi: 10.1016/j.jhazmat.2020.122117
doi: 10.1016/j.jhazmat.2012.01.052

Liu, Z., Ding, Y., Wang, F., Ye, Y., and Zhu, C. (2016). Role of salicylic acid in resistance to cadmium stress in plants. *Plant. Cell Rep.* 35, 719–731. doi: 10.1007/s00299-015-1925-3

Lu, D., Song, H., Jiang, S., Chen, X., Wang, H., and Zhou, J. (2019). Integrated phosphorus placement and form for improving wheat grain yield. *Agron. J.* 111, 1998–2004.

Manzoor, M., Gul, I., Kallerhoff, J., and Arshad, M. (2019). Fungi-assisted phytoextraction of lead: tolerance, plant growth–promoting activities and phytoavailability. *Environ. Sci. Pollut. Res.* 26, 23788–23797. doi: 10.1007/s11356-019-05656-3

Marschner, H. (2012). *Marschner's Mineral Nutrition of Higher Plants*, 3rd Edn, Vol. 89. Cambridge, MA: Academic press.

Mayak, S., Tirosh, T., and Glick, B. R. (2004). Plant growth-promoting bacteria confer resistance in tomato plants to salt stress. *Plant Physiol. Biochem.* 42, 565–572. doi: 10.1016/j.plaphy.2004.05.009

McNear, D. H. Jr. (2013). The rhizosphere-roots, soil and everything in between. *Nat. Educ. Knowl.* 4, 1.

Meagher, R. B. (2000). Phytoremediation of toxic elemental and organic pollutants. *Curr. Opin. Plant Biol.* 3, 153–162. doi: 10.1016/S1369-5266(99)00054-0

Miretzky, P., and Fernandez-Cirelli, A. (2008). Phosphates for Pb immobilization in soils: a review. *Environ. Chem. Lett.* 6, 121–133. doi: 10.1007/s10311-007-0133-y

Mishra, A. K., Singh, J., and Mishra, P. P. (2020). "Toxic metals in crops: a burgeoning problem," in *Sustainable Solutions for Elemental Deficiency and Excess in Crop Plants*, eds K. Mishra, P. Tandon, and S. Srivastava (Singapore: Springer), 273–301. doi: 10.1007/978-981-15-8636-1_11

Mohamed, H. I., and Latif, H. H. (2017). Improvement of drought tolerance of soybean plants by using methyl jasmonate. *Physiol. Mol. Bio. Plants* 23, 545–556. doi: 10.1007/s12298-017-0451-x

Mohamed, I., Zhang, G. S., Li, Z. G., Liu, Y., Chen, F., and Dai, K. (2015). Ecological restoration of an acidic Cd contaminated soil using bamboo biochar application. *Ecol. Eng.* 84, 67–76. doi: 10.1016/j.ecoleng.2015.07.009

Monica, R. C., and Cremonini, R. (2009). Nanoparticles and higher plants. *Caryologia* 62, 161–165. doi: 10.1080/00087114.2004.10589681

Mousavi, S. R., Galavi, M., and Rezaei, M. (2012). The interaction of zinc with other elements in plants: a review. *Int. J. Agric. Crop Sci.* 4, 1881–1884.

Mroczek-Zdyrska, M., and Wójcik, M. (2012). The influence of selenium on root growth and oxidative stress induced by lead in Vicia faba L. minor plants. *Biolog. Trace Elem. Res.* 147, 320–328. doi: 10.1007/s12011-011-9292-6

Munzuroglu, O., and Geckil, H. (2002). Effects of metals on seed germination, root elongation, and coleoptile and hypocotyl growth in *Triticum aestivum* and *Cucumis sativus*. *Arch Environ. Contamin. Toxicol.* 43, 203–213. doi: 10.1007/s00244-002-1116-4

Najeeb, U., Ahmad, W., Zia, M. H., Zaffar, M., and Zhou, W. (2017). Enhancing the lead phytostabilization in wetland plant Juncus effusus L. through somaclonal manipulation and EDTA enrichment. *Arab. J. Chem.* 10, S3310–S3317. doi: 10.1016/j.arabjc.2014.01.009

Orisakwe, O. E., Nduka, J. K., Amadi, C. N., Dike, D. O., and Bede, O. (2012). Heavy metals health risk assessment for population via consumption of food crops and fruits in Owerri, South Eastern, Nigeria. *Chem. Cent. J.* 6, 77. doi: 10.1186/1752-153X-6-77

Othman, Z. A. A. (2010). Lead contamination in selected foods from Riyadh city market and estimation of the daily intake. *Molecules* 15, 7482–7497. doi: 10.3390/molecules15107482

Park, J. H., Bolan, N., Megharaj, M., and Naidu, R. (2012). Relative value of phosphate compounds in reducing the bioavailability and toxicity of lead in contaminated soils. *Water Air Soil Pollut.* 223, 599–608. doi: 10.1007/s11270-011-0885-7

Peng, J., and Gong, J. (2014). Vacuolar sequestration capacity and long-distance metal transport in plants. *Front. Plant Sci.* 5:19. doi: 10.3389/fpls.2014.00019

Peralta-Videa, J. R., Lopez, M. L., Narayan, M., Saupe, G., and Gardea-Torresdey, J. (2009). The biochemistry of environmental heavy metal uptake by plants: implications for the food chain. *Int. J. Biochem. Cell Biol.* 41, 1665–1677. doi: 10.1016/j.biocel.2009.03.005

Piotrowska, A., and Bajguz, A. (2011). Conjugates of abscisic acid, brassinosteroids, ethylene, gibberellins, and jasmonates. *Phytochemistry* 72, 2097–2112. doi: 10.1016/j.phytochem.2011.08.012

Pirzadah, T. B., Malik, B., Tahir, I., Hakeem, K. R., Alharby, H. F., and Rehman, R. U. (2020). Lead toxicity alters the antioxidant defense machinery and modulate the biomarkers in Tartary buckwheat plants. *Int. Biodeter. Biodegrad.* 151, 104992. doi: 10.1016/j.ibiod.2020.104992

Poonam, S., Kaur, H., and Geetika, S. (2013). Effect of jasmonic acid on photosynthetic pigments and stress markers in *Cajanus cajan* (L.) Millsp. seedlings under copper stress. *Am. J. Plant. Sci.* 4, 817–823. doi: 10.4236/ajps.2013.44100

Radić, S., Babić, M., Škobić, D., Roje, V., and Pevalek-Kozlina, B. (2010). Ecotoxicological effects of aluminum and zinc on growth and antioxidants in *Lemna minor* L. *Ecotoxicol. Environ. Safe* 73, 336–342. doi: 10.1016/j.ecoenv.2009.10.014

Ragaee, S., Abdel-Aal, E. S. M., and Noaman, M. (2006). Antioxidant activity and nutrient composition of selected cereals for food use. *Food Chem.* 98, 32–38. doi: 10.1016/j.foodchem.2005.04.039

Rahman, M. A., Rahman, M. M., Reichman, S. M., Lim, R. P., and Naidu, R. (2014). Heavy metals in Australian grown and imported rice and vegetables on sale in Australia: health hazard. *Ecotoxicol. Environ. Saf.* 100, 53–60. doi: 10.1016/j.ecoenv.2013.11.024

Rahmani, I., Ahmadi, N., Ghanati, F., and Sadeghi, M. (2015). Effects of salicylic acid applied pre-or post-transport on post-harvest characteristics and antioxidant enzyme activity of gladiolus cut flower spikes. *New Zeal. J. Crop. Hortic. Sci.* 43, 294–305. doi: 10.1080/01140671.2015.1096799

Rai, P. K., Lee, S. S., Zhang, M., Tsang, Y. F., and Kim, K. H. (2019). Heavy metals in food crops: Health risks, fate, mechanisms, and management. *Environ. Int.* 125, 365–385. doi: 10.1016/j.envint.2019.01.067

Rao, G., Ashraf, U., Huang, S., Cheng, S., Abrar, M., Mo, Z., et al. (2018). Ultrasonic seed treatment improved physiological and yield traits of rice under lead toxicity. *Environ. Sci. Pollut. Res.* 25, 33637–33644. doi: 10.1007/s11356-018-3303-5

Rasool, M., Anwar-ul-Haq, M., Jan, M., Akhtar, J., Ibrahim, M., and Iqbal, J. (2020). Phytoremedial potential of maize (*Zea mays* L.) hybrids against cadmium (Cd) and lead (Pb) toxicity. *Pure Appl. Biol.* 9, 1932–1945. doi: 10.19045/bspab.2020.90206

Rehman, M. Z., Rizwan, M., Ali, S., Sabir, M., and Sohail, M. I. (2017). Contrasting effects of organic and inorganic amendments on reducing lead toxicity in wheat. *Bull. Environ. Contam. Toxicol.* 99, 642–647. doi: 10.1007/s00128-017-2177-4

Rehman, M. Z. U., Rizwan, M., Ghafoor, A., Naeem, A., Ali, S., Sabir, M., et al. (2015). Effect of inorganic amendments for in situ stabilization of cadmium in contaminated soils and its phyto-availability to wheat and rice under rotation. *Environ. Sci. Pollut. Res.* 22, 16897–16906. doi: 10.1007/s11356-015-4883-y

Rizwan, M., Ali, S., Abbas, F., Adrees, M., Zia-ur-Rehman, M., Farid, M., et al. (2017). Role of organic and inorganic amendments in alleviating heavy metal stress in oil seed crops. *Oil seed crops: yield and adaptations under Environ. stress* 12, 224–235. doi: 10.1002/9781119048800.ch12

Rizwan, M., Ali, S., Rehman, M. Z., Malik, S., Adrees, M., Qayyum, M. F., et al. (2019). Effect of foliar applications of silicon and titanium dioxide nanoparticles on growth, oxidative stress, and cadmium accumulation by rice (*Oryza sativa*). *Acta Physiol. Plant.* 41, 1–12. doi: 10.1007/s11738-019-2863-4

Rizwan, M., Ali, S., ur Rehman, M. Z., Javed, M. R., and Bashir, A. (2018). Lead toxicity in cereals and its management strategies: a critical review. *Water Air Soil Pollut.* 229, 211. doi: 10.1007/s11270-018-3865-3

Roberts, H. (2003). Changing patterns in global lead supply and demand. *J. Power Sourc.* 116, 23–31. doi: 10.1016/S0378-7753(02)00701-2

Romanowska, E., Wasilewska, W., Fristedt, R., Vener, A. V., and Zienkiewicz, M. (2012). Phosphorylation of PSII proteins in maize thylakoids in the presence of Pb ions. *J. Plant Physiol.* 169, 345–352. doi: 10.1016/j.jplph.2011.10.006

Romanowska, E., Wasilewska, W., Fristedt, R., Venerand, A. V., and Zienkiewicz, M. (2002). Phosphorylation of PSII proteins in maize thylakoids in the presence of Pb ions. *J. Plant Physiol.* 169, 345–352. doi: 10.1016/j.jplph.2011.10.006

Rossato, L. V., Nicoloso, F. T., Farias, J. G., Cargnelluti, D., Tabaldi, L. A., Antes, F. G., et al. (2012). Effects of lead on the growth, lead accumulation and physiological responses of *Pluchea sagittalis*. *Ecotoxicology* 21, 111–123. doi: 10.1007/s10646-011-0771-5

Sabir, M., Hanafi, M. M., Zia-Ur-Rehman, M., Saifullah, H. R., Ahmad, K. R., Hakeem, K. R., et al. (2014). Comparison of low-molecular-weight organic acids and ethylene diamine tetraacetic acid to enhance phytoextraction of heavy metals by maize. *Commun. Soil Sci. Plant Anal.* 45, 42–52. doi: 10.1080/00103624.2013.848879

Sahi, S. V., Bryant, N. L., Sharma, N. C., and Singh, S. R. (2002). Characterization of a lead hyperaccumulator shrub, *Sesbania drummondii*. *Environ. Sci. Technol.* 36, 4676–4680. doi: 10.1021/es020675x

Santos, E., Lauria, D., and da Silveira, C. P. (2004). Assessment of daily intake of trace elements due to consumption of foodstuffs by adult inhabitants of Rio de Janeiro city. *Sci. Total Environ.* 327, 69–79. doi: 10.1016/j.scitotenv.2004.01.016

Sen, S., Chakraborty, R., and Kalita, P. (2020). Rice-not just a staple food: a comprehensive review on its phytochemicals and therapeutic potential. *Trends Food Sci. Technol.* 97, 265–285. doi: 10.1016/j.tifs.2020.01.022

Sharma, P., and Dubey, R. S. (2005). Lead toxicity in plants. *Braz. J. Plant Physiol.* 17, 35–52. doi: 10.1590/S1677-04202005000100004

Sharma, R., De Vleesschauwer, D., Sharma, M. K., and Ronald, P. C. (2013). Recent advances in dissecting stress-regulatory crosstalk in rice. *Mol. Plant* 6, 250–260. doi: 10.1093/mp/sss147

Shri, M., Kumar, S., Chakrabarty, D., Trivedi, P. K., Mallick, S., Misra, P., et al. (2009). Effect of arsenic on growth, oxidative stress, and antioxidant system in rice seedlings. *Ecotoxicol. Environ. Saf.* 72, 1102–1110. doi: 10.1016/j.ecoenv.2008.09.022

Šimura, J., Antoniadi, I., Široká, J., Tarkowská, D., Strnad, M., Ljung, K., et al. (2018). Plant hormonomics: multiple phytohormone profiling by targeted metabolomics. *Plant Physiol.* 177, 476–489. doi: 10.1104/pp.18.00293

Sofy, M. R., Seleiman, M. F., Alhammad, B. A., Alharbi, B. M., and Mohamed, H. I. (2020). Minimizing adverse effects of pb on maize plants by combined treatment with jasmonic, salicylic acids and proline. *Agronomy* 10:699. doi: 10.3390/agronomy10050699

Srivastava, R. K., Pandey, P., Rajpoot, R., Rani, A., and Dubey, R. S. (2014). Cadmium and lead interactive effects on oxidative stress and antioxidative responses in rice seedlings. *Protoplasma* 251, 1047–1065. doi: 10.1007/s00709-014-0614-3

Tangahu, B. V., Abdullah, S., Rozaimah, S., Basri, H., Idris, M., Anuar, N., et al. (2011). A review on heavy metals (As, Pb, and Hg) uptake by plants through phytoremediation. *Int. J. Chem. Eng.* 2011, 939161. doi: 10.1155/2011/939161

Tegegne, W. A. (2015). Assessment of some heavy metals concentration in selected cereals collected from local markets of Ambo City, Ethiopia. *J. Cereal. Oilseed.* 6, 8–13. doi: 10.5897/JCO15.0138

Tejera, R. L., Luis, G., González-Weller, D., Caballero, J. M., Gutiérrez, ÁJ., Rubio, C., et al. (2013). Metals in wheat flour; comparative study and safety control. *Nutr. Hosp.* 28, 506–513.

Thakur, S., Singh, L., Zularisam, A. W., Sakinah, M., and Din, M. F. M. (2017). Lead induced oxidative stress and alteration in the activities of antioxidative enzymes in rice shoots. *Biol. Plant* 61, 595–598. doi: 10.1007/s10535-016-0680-9

Tian, T., Ali, B., Qin, Y., Malik, Z., Gill, R. A., Ali, S., et al. (2014). Alleviation of lead toxicity by 5-aminolevulinic acid is related to elevated growth, photosynthesis, and suppressed ultrastructural damages in oilseed rape. *BioMed Res. Int.* 2014, 530642. doi: 10.1155/2014/530642

Tripathi, R., Raghunath, R., and Krishnamoorthy, T. (1997). Dietary intake of heavy metals in Bombay city, India. *Sci. Total Environ.* 208, 149–159. doi: 10.1016/S0048-9697(97)00290-8

Turk, H., Erdal, S., Karayel, U., and Dumlupinar, R. (2018). Attenuation of lead toxicity by promotion of tolerance mechanism in wheat roots by lipoic acid. *Cer. Res. Commun.* 46, 424–435. doi: 10.1556/0806.46.2018.020

Uwah, E., Ndahi, N., Abdulrahman, F., and Ogugbuaja, V. (2011). Heavy metal levels in spinach (*Amaranthus caudatus*) and lettuce (*Lactuca sativa*) grown in Maiduguri, Nigeria. *J. Environ. Chem. Ecotoxicol.* 3, 264–271.

Vinocur, B., and Altman, A. (2005). Recent advances in engineering plant tolerance to abiotic stress: achievements and limitations. *Curr. Opin. Biotech.* 16, 123–132. doi: 10.1016/j.copbio.2005.02.001

Wasternack, C. (2014). Action of jasmonates in plant stress responses and development—Applied aspects. *Biotechnol. Adv.* 32, 31–39. doi: 10.1016/j.biotechadv.2013.09.009

WHO/FAO (2016). *General Standards for Contaminants and Toxins in Food and Feed*. Rome: Food and Agriculture Organization.

Williams, L. E., Pittman, K. J., and Hall, J. (2000). Emerging mechanisms for heavy metal transport in plants. *Biochim. Biophys. Acta Biomembr.* 1465, 104–126. doi: 10.1016/S0005-2736(00)00133-4

Xie, L., Hao, P., Cheng, Y., Ahmed, I. M., and Cao, F. (2018). Effect of combined application of lead, cadmium, chromium and copper on grain, leaf and stem heavy metal contents at different growth stages in rice. *Ecotoxicol. Environ. Saf.* 162, 71–76. doi: 10.1016/j.ecoenv.2018.06.072

Yang, Y., Wei, X., Lu, J., You, J., Wang, W., and Shi, R. (2010). Lead-induced phytotoxicity mechanism involved in seed germination and seedling growth of wheat (*Triticum aestivum* L.). *Ecotoxicol. Environ. Saf.* 73, 1982–1987. doi: 10.1016/j.ecoenv.2010.08.041

Yang, Y., Zhang, Y., Wei, X., You, J., Wang, W., Lu, J., et al. (2011). Comparative antioxidative responses and proline metabolism in two wheat cultivars under short term lead stress. *Ecotoxicol. Environ. Safe.* 74, 733–740. doi: 10.1016/j.ecoenv.2010.10.035

Zanganeh, R., Jamei, R., and Rahmani, F. (2020). Response of maize plant to sodium hydrosulfide pretreatment under lead stress conditions at early stages of growth. *Cereal Res. Commun.* doi: 10.1007/s42976-020-00095-0 [Epub ahead of print].

Zhang, K., Wang, G., Bao, M., Wang, L., and Xie, X. (2019). Exogenous application of ascorbic acid mitigates cadmium toxicity and uptake in Maize (*Zea mays* L.). *Environ. Sci. Pollut. Res.* 26, 19261–19271. doi: 10.1007/s11356-019-05265-0

Zhang, Y., Deng, B., and Li, Z. (2018). Inhibition of NADPH oxidase increases defense enzyme activities and improves maize seed germination under Pb stress. *Ecotoxicol. Environ. Saf.* 158, 187–192. doi: 10.1016/j.ecoenv.2018.04.028

Zhang, Y., Ge, F., Hou, F., Sun, W., Zheng, Q., Zhang, X., et al. (2017). Transcription factors responding to Pb stress in maize. *Genes* 8, 231. doi: 10.3390/genes8090231

Zhao, Z., Xi, M., Jiang, G., Liu, X., Bai, Z., and Huang, Y. (2010). Effects of IDSA, EDDS and EDTA on heavy metals accumulation in hydroponically grown maize (*Zea mays*, L.) *J. Hazard. Mater.* 181, 455–459. doi: 10.1016/j.jhazmat.2010.05.032

Zhu, F. Y., Li, L., Lam, P. Y., Chen, M. X., Chye, M. L., and Lo, C. (2013). Sorghum extra-cellular leucine-rich repeat protein SbLRR2 mediates lead tolerance in transgenic *Arabidopsis*. *Plant Cell Physiol.* 54, 1549–1559. doi: 10.1093/pcp/pct101

Zhuang, P., Huiling, Z., and Wensheng, S. (2009). Biotransfer of heavy metals along a soil-plant-insect-chicken food chain: field study. *J. Environ. Sci.* 21, 849–853. doi: 10.1016/S1001-0742(08)62351-7

Zulfiqar, U., Farooq, M., Hussain, S., Maqsood, M., Hussain, M., Ishfaq, M., et al. (2019). Lead toxicity in plants: Impacts and remediation. *J. Environ. Manag.* 250, 109557. doi: 10.1016/j.jenvman.2019.109557

Conflict of Interest: The authors declare that the research was conducted in the absence of any commercial or financial relationships that could be construed as a potential conflict of interest.

frontiers in Plant Science

ORIGINAL RESEARCH
published: 09 February 2021
doi: 10.3389/fpls.2021.586509

Effect of Engineered Nickel Oxide Nanoparticle on Reactive Oxygen Species–Nitric Oxide Interplay in the Roots of *Allium cepa* L.

*Indrani Manna[1], Saikat Sahoo[2] and Maumita Bandyopadhyay[1]**

[1] Department of Botany, CAS, University of Calcutta, Kolkata, India, [2] Department of Botany, Krishna Chandra College, Hetampur, India

Scientists anxiously follow instances of heavy metals augmenting in the environment and undergoing bioaccumulation and trace their biomagnification across food webs, wary of their potent toxicity on biological entities. Engineered nanoparticles supplement natural pools of respective heavy metals and can mimic their effects, exerting toxicity at higher concentrations. Thus, a thorough understanding of the underlying mechanism of this precarious interaction is mandatory. Most urban and industrial environments contain considerable quantities of nickel oxide nanoparticles. These in excess can cause considerable damage to plant metabolism through a significant increase in cellular reactive oxygen species and perturbation of its cross-talk with the reactive nitrogen species. In the present work, the authors have demonstrated how the intrusion of nickel oxide nanoparticles (NiO-NP) affected the exposed roots of *Allium cepa*: starting with disruption of cell membranes, before being interiorized within cell organelles, effectively disrupting cellular homeostasis and survival. A major shift in the reactive oxygen species (ROS) and nitric oxide (NO) equanimity was also observed, unleashing major altercations in several crucial biochemical profiles. Altered antioxidant contents and upregulation of stress-responsive genes, namely, *Catalase*, *Ascorbate peroxidase*, *Superoxide dismutase*, and *Rubisco activase*, showing on average 50–250% rise across NiO-NP concentrations tested, also entailed increased cellular hydrogen peroxide contents, with tandem rise in cellular NO. Increased NO content was evinced from altered concentrations of nitric oxide synthase and nitrate reductase, along with NADPH oxidase, when compared with the negative control. Though initially showing a dose-dependent concomitant rise, a significant decrease of NO was observed at higher concentrations of NiO-NP, while cellular ROS continued to increase. Modified K/Na ratios, with increased proline concentrations and GABA contents, all hallmarks of cellular stress, correlated with ROS–NO perturbations. Detailed studies showed that NiO-NP concentration had a significant role in inducing toxicity, perturbing the fine balance of ROS–NO, which turned lethal for the cell at higher dosages of the ENP precipitating in the accumulation of stress markers and an inevitable shutdown of cellular mechanisms.

Keywords: nitric oxide, reactive oxygen species, engineered nickel oxide nanoparticle, stress markers, cytotoxicity

OPEN ACCESS

Edited by:
Rafaqat Ali Gill,
Oil Crops Research Institute, Chinese Academy of Agricultural Sciences, China

Reviewed by:
Michael Campbell,
Penn State Erie, The Behrend College, United States
Shafaqat Ali,
Government College University Faisalabad, Pakistan

***Correspondence:**
Maumita Bandyopadhyay
mbbot@caluniv.ac.in

Specialty section:
This article was submitted to Plant Nutrition, a section of the journal Frontiers in Plant Science

Received: *23 July 2020*
Accepted: *06 January 2021*
Published: *09 February 2021*

Citation:
Manna I, Sahoo S and Bandyopadhyay M (2021) Effect of Engineered Nickel Oxide Nanoparticle on Reactive Oxygen Species–Nitric Oxide Interplay in the Roots of Allium cepa L. Front. Plant Sci. 12:586509. doi: 10.3389/fpls.2021.586509

HIGHLIGHTS

- NiO-NP entry into plant cells exhibits dose dependency, and at higher concentrations, NiO-NP display bulk Ni-like characteristics inducing widespread membrane damage before entry into the cytoplasm of exposed cells.
- There is remarkable upregulation of stress-related (APX, CAT, SOD, and RCA) genes in the aftermath of NiO-NP entry into the cells.
- There are significant alterations in cellular hydrogen peroxide and nitric oxide contents, leading to crucial changes in physiological and biochemical parameters of the affected cells due to perturbed ROS–NO homeostasis.

INTRODUCTION

Heavy metals, viz., lead, mercury, arsenic, nickel, chromium, cadmium, and copper, among others, are members of the periodic table with atomic masses of more than 20 and are called as such as their densities are at least five times more than that of water (Tchounwou et al., 2012). Among them, *redox-active metals*, like chromium and copper, can directly affect the reactive oxygen species (ROS) framework of a cell by spontaneously creating an oxidative burst, while *non-redox metals*, like cadmium, nickel, and mercury, induce toxicity either by blocking the functional groups or by replacing cations from essential biomolecules (Schützendübel and Polle, 2002). Though found only in trace amounts on the earth's upper layer (ranging from minute ppb to 10 ppm), anthropogenic activities, compounded by overpopulation, indiscriminate use of fossil fuels, and spillage of domestic as well as industrial wastes into the environment have led to a disproportionate accumulation of these heavy metals in soil, air, and water, aggravating their percolation into the earth's crust. Interestingly, plants, the primary producers of our ecosystem, are resilient to increased concentrations of heavy metals as they have evolved a unique strategy of hyperaccumulating and containing them within vacuoles or attaching them to cell walls and concentrating most of the heavy metal ions into the apoplast of the cell (Vázquez et al., 1992).

In the last few decades, many of these heavy metals have found novel uses as nanoparticles in a range of industrial applications and to increase crop yield and production (Rizwan et al., 2019), bringing in a newer and probably more sinister aspect in the heavy metal pollution spectrum (Mustafa and Komatsu, 2016), leading to the constant exposure of flora to these intruding nanoforms widely distributed in soil, water, and aerosol. Like their bulk forms, heavy metal nanoforms too can enter plants quite easily using endocytosis, *via* pore formation and the plasmodesmata, or by hitchhiking on carrier proteins (Pérez-de-Luque, 2017), helped by absorption in lower pH (Järup, 2003). These augment uptake and cellular sequestration of metallic nanoparticles, which then intrude into food webs *via* the primary consumers, and the prospect for their biomagnification through the food chain constitutes a serious hazard to human health. The role of plants in the uptake and biomagnification of potent toxins in the food chain is a well-accepted fact and, thus, needs detailed investigation (Choudhury, 2019).

Nickel pollution has grave consequences on human health, triggering respiratory troubles and cardiovascular issues, as well as certain types of cancers (Genchi et al., 2020). This has prompted imposition of stringent measures against occupational hazards due to nickel dust exposure[1]. Nickel and nickel compounds are graded in group 2B and 1 among carcinogens[2]. However, nickel oxide nanoparticles (NiO-NP) are increasingly being used in heavy industries and consumer products, especially in smelting, iron and steel, coinage, and electrical goods industry (Danjumma et al., 2019), but escape sanctions of scientific and environmental watchdogs. Unplanned disposal of NiO-NP through industrial or consumer wastes precipitates in their spillage into soil and water systems. An essential trace metal for plants, nickel is taken up easily. Even so, a surfeit of nickel inside plant cells can create an upsurge of ROS, which ultimately compromises their survival *via* extensive physicochemical and genomic damages (Manna and Bandyopadhyay, 2017a; Rastogi et al., 2017; Pinto et al., 2019). Plant systems are, thus, particularly vulnerable to sudden fluxes of NiO-NP in soil, water, or aerosol (Ovais et al., 2020). *Allium cepa* (*A. cepa*), the acclaimed ecotoxicological model plant, not only provides the opportunity to study the toxicological effects of environmental pollutants but also can be used to assess the risk of magnification, as it is cultivated widely to be consumed even in raw and unprocessed forms (Boros and Ostafe, 2020).

The by-products of plant metabolism—nitric oxide (NO), a diatomic free radical gas, and ROS, like superoxide anion (O_2^*) or hydrogen peroxide (H_2O_2)—are integral parts of the central signaling network in plants and act synergistically in the regulation of crucial processes (Černý et al., 2018). ROS are consistently produced in chloroplasts, mitochondria, and peroxisomes and, in excess, are reactive toward DNA, protein, and lipids. NO reacts with superoxide anions to form peroxynitrites that affect posttranslational protein modifications like S-nitrosylation (Lin et al., 2012). NO also regulates superoxide and H_2O_2 production, as well as the function of antioxidant enzymes *via* S-nitrosylation or nitration, thus maintaining an intensive cross-talk with

Abbreviations: ENPs, engineered nanoparticles; NiO-NP, nickel oxide nanoparticles; ROS, reactive oxygen species; RNS, reactive nitrogen species; CAT, catalase; APX, ascorbate peroxidase; SOD, superoxide dismutase; RCA, Rubisco activase; NOS, nitric oxide synthase; NR, nitrate reductase; NOX, NADPH oxidase; NO, nitric oxide; H_2O_2, hydrogen peroxide; K/Na ratio, potassium:sodium ratio; *A. cepa*, *Allium cepa*; EMS, ethyl methanesulfonate; cPTIO, 2-(4-carboxyphenyl)-4,4,5,5-tetramethylimidazoline-1-oxyl-3-oxide potassium salt; Sod. Pyr., sodium pyruvate; FITC, fluorescein isothiocyanate; DMF, dimethylformamide; APTS, aminopropyl triethoxysilane; CLSM, confocal laser scanning microscope; DAF-FM-DA, 4-amino-5-methylamino-2′,7′-difluorofluorescein diacetate; PBS, phosphate-buffered saline; GABA, gamma amino butyric acid; DTT, dithiothreitol; TCA, trichloroacetic acid; KI, potassium iodide; ICP-OES, inductively coupled plasma-optical emission spectroscopy; UNEP, United Nations Environment Programme; USEPA, United States Environmental Protection Agency; OECD, Organization for Economic Co-operation and Development; WHO, World Health Organization; CuO-NP, copper oxide nanoparticle; RBOHs, respiratory burst oxidase homologs; RuBP, Rubisco

[1]https://www.atsdr.cdc.gov/phs/phs.asp?id=243&tid=44

[2]https://monographs.iarc.fr/wp-content/uploads/2018/06/mono100C-10.pdf

ROS (Romero-Puertas and Sandalio, 2016). Their roles in response to environmental stresses have been investigated for quite some time now (Scheler et al., 2013). Interestingly, there are contrasting reports on the ROS–NO interactions in stressed plants, with both beneficial and disadvantageous outcomes (Farnese et al., 2016). NO can help alleviate heavy metal stress, as reported in cases of cadmium, aluminum, arsenic, and copper exposures (Nabi et al., 2019). Similar observations were reported in instances of exposures to silver and zinc oxide nanoparticles (Tripathi et al., 2017a,b). High concentrations of intracellular NO or changes in their distribution on the other hand initiated unfavorable outcomes in the plant (Domingos et al., 2015). Excess of NO compromised photosynthetic efficiency and inhibited electron transport chains, through the formation of chloroplast-damaging peroxynitrites, impairing many downstream processes in the chloroplast (Procházková et al., 2013).

Pathways of NO production *in planta* are complicated and actively debated. Among the two routes of NO production identified so far are the reductive pathway (primarily executed by the peroxisomal and membrane-bound reductases) and the oxidative pathway (including those involving the hydroxylamines and polyamines) (Farnese et al., 2016). Cytosolic nitrate reductase (NR), otherwise involved in nitrogen assimilation, pitches in for the reductive cascades of NO production, especially during developmental programs or stress management. At the same time, the oxidative route of NO formation is mediated by a nitric oxide synthase (NOS)-like protein complex (Astier et al., 2018). Many components of this vital relationship controlling endogenous NO production, especially during heavy metal exposure, remain to be elucidated.

In this manuscript, the authors have hypothesized that ROS and NO play a causal relationship as stress builds up in freshly rooted *A. cepa* bulbs upon treatment with NiO-NP. A thorough study into the internalization mechanism and the general biochemical and physiological parameters confirmed increased generation of ROS and NO in tandem with increasing engineered nanoparticle (ENP) exposure. NO, initially at low levels, played a benign role. However, on a further increase in NiO-NP dosage, it surged with tandem ROS production. At higher concentrations, NO accumulation became detrimental to cell survival, contributing to a total shutdown of cellular activities. Cellular stress markers like proline increased, inducing prominent changes in potassium:sodium (K/Na) ratio and loss in cell viability, as well as an increase in membrane lipid peroxidation, along with a simultaneous increase in antioxidant enzyme activities, all of which portray extensive physiological and biochemical perturbations of the affected tissue under NiO-NP-stressed conditions. The authors have studied both the NR-centric and NOS-like NO pathways in tissues subjected to increasing doses of NiO-NP. The complex interrelationship between ROS and NO and also their interaction with increasing NiO-NP doses were assessed over a range of ENP doses. The addition of compounds like sodium pyruvate, a H_2O_2 blocker, and cPTIO [2-(4-carboxyphenyl)-4,4,5,5-tetramethylimidazoline-1-oxyl-3-oxide potassium salt], a NO blocker, used in combinations or singly, helped to study the dynamics of *in situ* NO on H_2O_2 formation in the NiO-NP-treated tissue.

MATERIALS AND METHODS

Plant Growth Conditions, Treatment Schedule, and Procurement of Nickel Oxide Nanoparticle

Seeds of *A. cepa* were grown according to reported protocols (Manna and Bandyopadhyay, 2017a). In brief, seeds of *A. cepa* (var. Nasik Red), bought from Suttons Seeds Pvt. Ltd., Kolkata, were germinated and seedlings were grown in the Experimental Garden, Department of Botany, University of Calcutta. Fresh, healthy bulbs, grown under controlled conditions, were put on a wet bed made of sand, which was twice sterilized and moistened with double-distilled water and maintained in a growth chamber at 23 ± 2°C in the dark for rooting.

Engineered NiO-NP was obtained from Sigma-Aldrich (St. Louis, United States) as nanopowder (product code 637130, molecular weight: 74.69, EC number: 215-215-7, PubChem Substance ID 24882831, <50 nm particle size (TEM), purity—99.8% trace metal basis). Healthy uniformly rooted bulbs were selected for treatment with various concentrations of NiO-NP suspension (10, 25, 50, 62.5, 125, 250, and 500 mg L^{-1}) for 24 h.

Multiple sets of negative and positive controls were simultaneously maintained under controlled conditions. The negative control set consisted of bulbs treated with double-distilled water only, whereas seven different positive control sets were devised to cross-check experimental parameters: C_1—0.4 mM ethyl methane sulfonate (EMS)/1% Triton X; C_2—10 mM sodium pyruvate (a H_2O_2 scavenger); C_3—100 μM cPTIO (a nitric oxide scavenger); C_4—25 μM H_2O_2; C_5—100 μM cPTIO + 10 mM sodium pyruvate; C_6—125 mg L^{-1} NiO-NP + 100 μM cPTIO + 10 mM sodium pyruvate; C_7—25 μM H_2O_2 + 125 mg L^{-1} NiO-NP + 100 μM cPTIO + 10 mM sodium pyruvate; and C_8—25 μM H_2O_2 + 125 mg L^{-1} NiO-NP + 100 μM cPTIO + 0.4 mM EMS + 10 mM sodium pyruvate (**Supplementary Table 1**).

After the 24-h treatment, bulbs were harvested and the roots used for the subsequent assays.

Internalization of FITC-Tagged Nanoparticles

Uncoated NiO-NP were tagged to fluorescein isothiocyanate (FITC) following the protocol of Xia et al. (2008). NiO-NP were suspended in DMF (dimethylformamide) through sonication, followed by the addition of APTS (aminopropyl triethoxysilane). The suspension was kept under continuous stirring for 24 h, followed by centrifugation at 5,000 × *g*. The supernatant was discarded, while the nanoparticles were further suspended in a DMF and FITC mixture, with continuous stirring for another 12 h. After that, the tagged nanoparticles were thoroughly washed in DMF till the supernatant did not fluoresce any more. The FITC-tagged nanoparticles were resuspended in deionized (DI)

Milli-Q water and used in dose-dependent treatments to study internalization of the ENP.

Rooted bulbs were dipped in FITC-tagged NiO-NP suspensions for the requisite time periods. Root tips of onion bulbs were collected after treatment, thoroughly washed with DI water, hydrolyzed for 60 s in 1 N HCl, and squashed on clean grease-free slides (Manna and Bandyopadhyay, 2017b). The slides were studied and documented under a confocal laser scanning microscope (Olympus, Japan) (1 × CLSM 81) using the software version: FluoView FV1000, 350–470 filter for confirming internalization of FITC-tagged NiO-NP in root cells.

Qualitative and Quantitative Determination of Cell Death and Wall Damage Through Evans Blue Staining

Qualitative estimation of cell death in the NiO-NP-treated root tissues against the control sets was performed using Evans blue dye (0.025% of Evans blue in 1 × PBS). At least 10 root tips from each set were immersed in the dye for 15 min and kept in the dark at room temperature, then washed repeatedly in PBS and observed with a simple microscope under 4 × objective (Zeiss-Primo Star). The Evans blue-stained root tips were immersed in 1 ml of 1% SDS buffer, crushed and centrifuged at room temperature, followed by measurement of color intensity at 600 nm (Vijayaraghavareddy et al., 2017) in a UV–VIS Spectrophotometer (Techcomp). Cell viability percentage was calculated as per the formula used in Manna and Bandyopadhyay (2017b).

Qualitative Estimation of Lipid Peroxidation Through Schiff's Staining

Lipid peroxidation as a result of NiO-NP treatment was determined according to Yin et al. (2010) with slight modifications. Fresh roots of both control and treated samples, at least 10 in number from each set, were treated with Schiff's reagent for 15 min and washed thoroughly with 0.5% sulfite solution, then observed under a simple light microscope (Carl Zeiss-4 × objective) and photographed accordingly. Qualitative determination of color intensity was taken to be indicative of the extent of lipid peroxidation.

Quantitative Determination of Gamma Amino Butyric Acid

Changes in gamma amino butyric acid (GABA) contents in NiO-NP-treated sets were assessed using the protocol of Zhang et al. (2014). One gram of root tissue was homogenized in 5 ml deionized water, vortexed for 30 min, and filtered using Whatman no. 1 filter paper. Then equal volumes of filtrate and 0.2 M borate buffer, along with an equal volume of 6% phenol and half volume of 9% sodium hypochlorite, were added, mixed thoroughly, and boiled for 10 min before immediately cooling in an ice bath. The blue color that developed was measured spectrophotometrically at 645 nm. The absolute value of GABA content was determined through a GABA standard curve (nmol g^{-1} fresh weight).

Estimation of Nitric Oxide in Treated Tissues

Qualitative Detection of Nitric Oxide

NO was measured using the ubiquitous NO detecting fluorescent dye DAF-FM-DA (4-amino-5-methylamino-2′,7′-difluorofluorescein diacetate, Thermo Fisher Scientific) according to the protocol of McInnis et al. (2006) with minor modifications. Root tips were excised from the treated bulbs and immediately immersed in 1 × PBS for 15 min followed by transfer to 2 μM solution of DAF-FM-DA in 1 × PBS and incubation for 15 min. The root tips were then washed in PBS and viewed under the confocal laser scanning microscope (Olympus, Japan) (1 × CLSM 81) at excitation and emission of 495/515 nm. Images of the root tips showing bright green spots of NO localization were captured using the software version FluoView FV1000.

Quantitative Estimation of Nitric Oxide *in situ* (Griess Assay)

Freshly treated root tissues were crushed in phosphate-buffered saline in an ice bath and centrifuged at 4°C for 30 min, and the supernatant was used for further analyses. Since nitrite is the only stable component that can convert into NO, 1 U nitrate reductase (NR, Sigma) was added to the suspension which was then incubated for 30 min; 100 μl of supernatant from each set was then dispensed into a plate reader in triplicate, and an equal volume of Griess reagent [1% sulfanilamide in 5% phosphoric acid; and 0.1% N-(1-naphthyl)ethylenediamine dihydrochloride; Sigma-Aldrich] was added, before incubation for 15 min. The color reaction was assayed using a Bio-Rad iMark^{TM} microplate reader at 550 nm (Saha et al., 2004) and expressed as μg g^{-1} fresh weight.

Quantitative Determination of NOS-like, NOX, and NR

Nitric oxide synthase-like activity was quantified in the root tissues of both treated and control *A. cepa* sets following the protocol of Murphy and Noack (1994) with necessary modifications. Five hundred milligrams of fresh tissue was crushed in a Tris homogenization buffer, containing 0.5 mM EDTA, 1 M leupeptin and pepstatin, 7 mM glutathione, and 0.2 mM PMSF, followed by centrifugation at 10,000 × *g*. The supernatant was recovered and centrifuged again at 80,000 × *g* for 30 min. Part of the supernatant was used to quantify total protein using the Bradford assay (Bradford, 1976) and the rest was mixed with Griess reagent [1% sulfanilamide in 5% phosphoric acid; and 0.1% N-(1-naphthyl)ethylenediamine dihydrochloride]. NR present in the supernatant reacted with available nitrite to give a bright purple azo dye that was measured at 546 nm and expressed as nmol min^{-1} ml^{-1}.

NADPH-oxidase-like enzyme (NOX-like) was quantified in the experimental samples following the protocol of Libik-Konieczny et al. (2015). Fresh root tips were homogenized in protein extraction buffer containing 0.25 M sucrose, 10 mM Tris–HCl, 1 mM EDTA, and 2.5 mM DTT (dithiothreitol). The filtrate was centrifuged at 10,000 × *g* for 15 min at 4°C. The supernatant

was separated and centrifuged at 80,000 × *g* (in ultracentrifuge, Thermo Scientific, Sorvall WX 80) for 30 min at 4°C. The pellet was collected and resuspended in Tris dilution buffer. Protein content was measured through the Bradford assay. A reaction mixture consisting of 1 M Tris buffer, 1 mM XTT, 1 mM NADPH, and membrane protein in the form of the resuspended pellet was prepared and measured at 490 nm. The activity was measured through the extinction coefficient of O_2^- generation expressed as nmol min^{-1} ml^{-1}.

NR was quantified following the protocol of Vega and Kamin (1977) with modifications. Initially, fresh root tips of the treated and untreated samples were homogenized in 50 mM Tris–HCl buffer, and the supernatant was used for further analyses. The reaction mixture consisted of 0.5 M Tris buffer, 2.5 mM sodium nitrite, and 3 mM methyl viologen to which the supernatant was added along with 0.025% of dithionite-sodium carbonate. The mixture was incubated for 15 min at 30°C and shaken well till the blue color disappeared. At this point, Griess reagent was added and absorbance was measured at 550 nm and expressed as nmol min^{-1} ml^{-1}.

Quantitative Determination of Hydrogen Peroxide and Proline

Quantification of H_2O_2 was done following the protocol of Velikova et al. (2000) with minor modifications. In short, 100 mg of fresh root tissue was homogenized in ice-cold 0.1% TCA (trichloroacetic acid) and centrifuged at 14,000 × *g* for 30 min. Following this, 50 μl of the supernatant along with the same volume of phosphate buffer was incubated with double the volume of 1 M potassium iodide (KI) solution. The resultant mix was read at 390 nm in a plate reader (Bio-Rad, iMark^{TM}). The exact amount of H_2O_2 was calculated from a standard curve as nmol g^{-1} fresh weight.

Free proline content in the treated sets of *A. cepa* roots was estimated against the controls and detected following the protocol of Bates et al. (1973) with modifications; 100 mg of root tissue was homogenized in 3% sulfosalicylic acid and centrifuged at 10,000 × *g*. An equal volume of supernatant was reacted with freshly prepared acid–ninhydrin and glacial acetic acid at 100°C. The pinkish-red chromophore that developed was measured at 520 nm in a spectrophotometer (Techcomp). Quantification was done by following a standard curve of proline expressed as nmol g^{-1} fresh weight.

Quantitative Ratio of Intracellular Potassium–Sodium Ions

Potassium:sodium ratio of all the experimental sets of *A. cepa* was determined through inductively coupled plasma-optical emission spectroscopy (ICP-OES) (Manna and Bandyopadhyay, 2017a) (Perkin Elmer Optima 5300 DV, United States) following a wet digestion protocol (Cramer et al., 1990). One gram of fresh root tissue was kept in 80% nitric acid for 10 days, followed by another round of acid digestion in which the partially digested tissue was heat digested in concentrated nitric acid and hydrofluoric acid followed by filtration and dilution.

Quantification of Antioxidant Enzymes Using Biochemical Assays and Detection of mRNA Transcript Using Semiquantitative Reverse Transcriptase PCR

The important antioxidant enzymes, catalase (CAT), superoxide dismutase (SOD), and ascorbate peroxidase (APX), were quantified to understand their activities in both the treated samples and the control sets (negative control sets and the positive control sets). CAT and SOD were measured according to Manna and Bandyopadhyay (2017a), and APX was measured according to the protocol depicted by Das et al. (2018). One hundred milligrams of fresh root tissues were collected from all the sample sets, crushed in liquid nitrogen with 50 mM phosphate buffer (pH 7.4), and centrifuged at 1,000 × *g* for 15 min. The supernatant was collected and total protein was calculated using the Bradford reagent (Bradford, 1976) in a multiwell microplate reader (Bio-Rad, iMark^{TM}) at 600 nm. Enzyme activities were measured using the individual coefficients of the enzymes spectrophotometrically (Technocomp) and each expressed as activity nmol min^{-1} ml^{-1}.

Changes in the expression of transcripts of stress-responsive genes were studied using qRT-PCR. CAT, SOD, APX, and the two subunits of Rubisco activase (RCA) were chosen for the study following Thiruvengadam et al. (2015). Freshly treated roots from *A. cepa* were used to extract RNA following the manufacturers' instructions (NucleoSpin RNA Plant kit, TaKaRa Bio, Cat 740949.50). First-strand cDNA synthesis followed by reverse transcriptase PCR was done using a single reaction by TaKaRa one-step RNA PCR Kit (AMV, Cat RR024B) in a single tube. PCR was carried out in a reaction mixture containing 1× one-step RNA PCR buffer, 5 mM $MgCl_2$, 1 mM dNTP mixture, 0.8 units/μl RNase inhibitor, 0.1 units/μl AMV RTase XL, 0.1 units/μl AMV Optimized Taq, 0.4 μM forward and reverse primers, 1 μg of total RNA, and RNase-free double-distilled water. RT-PCR condition was set as 30 min at 50°C for reverse transcription, 2 min at 94°C for inactivation of RNase, followed by 30 cycles of 94°C for 30 s, annealing temperature for 30 s and 3 min at 72°C for an extension. An equal volume of PCR products was used for electrophoresis on 1.5% (w/v) ethidium bromide-stained gel. Gels were observed under UV light. Actin is used as reference gene for the present study. The gene-specific primers used in this study are listed in **Supplementary Table 2**.

Statistical Analyses

All the experiments were carried out at least thrice to check the authenticity of the data.

Statistical analyses were carried out in the MINITAB environment (MINITAB ver. 18). Data were presented as mean ± standard error. The results were subjected to a one-way analysis of variance (ANOVA). The level of significance was established at $p > 0.05$ at every instance for all the biochemical assays, throughout the study. In case a significant interaction was found among the factors (species × concentrations of NiO-NP or that of various positive

controls), such instances were compared by Tukey's test and Dunnett's test (Manna and Bandyopadhyay, 2017b).

RESULTS

FITC-Tagged NiO-NP Helped Trace the Entry and Mobilization of ENPs Within Exposed Roots

Fluorescein isothiocyanate-tagged ENPs were internalized in *A. cepa* roots within 24 h of treatment with different concentrations of NiO-NP as seen in **Figure 1**. **Figures 1A–G** confirm the transit of NiO-NP into the cytoplasm of the epidermal cells and their entry through the nuclear membranes as well. With increased concentration of NiO-NP, higher fluorescence intensity could be detected in the cytoplasm of root tip cells, indicating toward a dose-dependent increment of tagged ENP entry. This corroborates our earlier findings where ICP-OES data had also shown a dose-dependent increase in NiO-NP content in the treated tissues (Manna and Bandyopadhyay, 2017a).

Figures 1H–L trace the gradual movement of FITC-tagged NiO-NP through root tissues, from epidermal cells to apical meristem cells at the tip, and then moving through the cortex along the zone of elongation, finally reaching the vascular tissues. While both the epidermis and cortical regions of exposed root tips were dotted with specks of FITC-doped NiO-NP in all concentrations (**Figures 1A–G**), it was only at higher concentrations that these were observed in the permanent tissues of the roots, too (**Figures 1H–L**). The presence of FITC-tagged NiO-NP in the vascular bundles alludes to the possibility of transmission of ENP to the aerial parts of exposed plants. Another interesting observation was that at higher doses, NiO-NP agglomerated to form clumps around the membranes of exposed epidermal cells, simulating their bulk counterparts as shown by the SEM images of affected root tips (**Supplementary Figure 1**).

NiO-NP Treatment Caused Substantial Wall Damage, Lipid Peroxidation, and Perturbed K/Na Ratios in the Affected Cells

Evans blue staining of the treated and control sets of root tips showed a dramatic rise in cell wall damage and, thus, cell viability, coinciding with an increase in NiO-NP doses (**Figure 2**). As is known, dead cells with permeable membranes take up the dye which enters the protoplasm and stains it blue. Cumulative accumulation of the dye in damaged cells measured as the color intensity can be directly correlated to cell viability; more color accumulation indicated more membrane damage and, hence, less viable cells (**Supplementary Figure 2**). At the lowest dose of

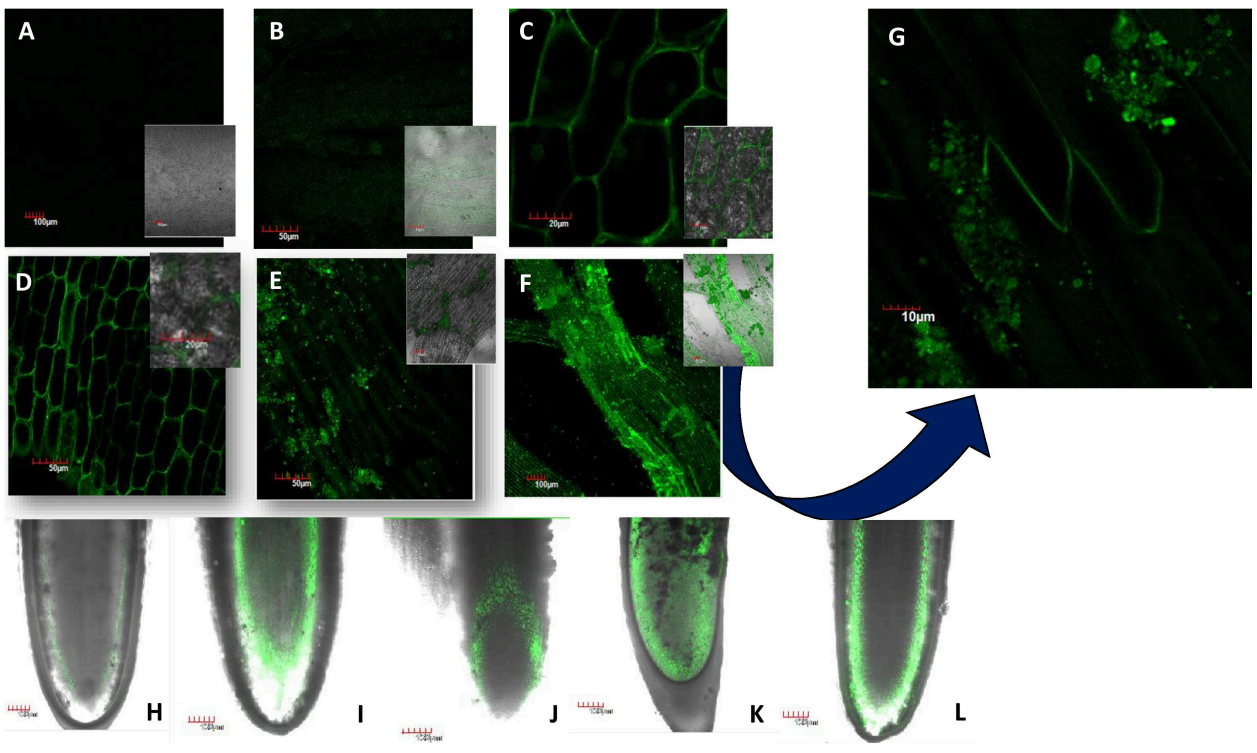

FIGURE 1 | Translocation of FITC-tagged nickel oxide nanoparticles (NiO-NP) entering the tissue and adhering to it in a dose-dependent manner [**(A)** negative control, **(B)** tissue exposed to 10 mg L^{-1}, **(C)** tissue exposed to 50 mg L^{-1}, **(D)** tissue exposed to 125 mg L^{-1}, **(E)** tissue exposed to 250 mg L^{-1}, **(F)** tissue exposed to 500 mg L^{-1}, **(G)** tissue exposed to 250 mg L^{-1}—magnified view showing NiO-NP aggregates on the membrane surface; **(H–L)** vertical translocation of NiO-NP from the meristematic zone to the zone of elongation—**(H)** negative control, **(I)** 25 mg L^{-1}, **(J)** 62.5 mg L^{-1}, **(K)** 125 mg L^{-1}, **(L)** 500 mg L^{-1}].

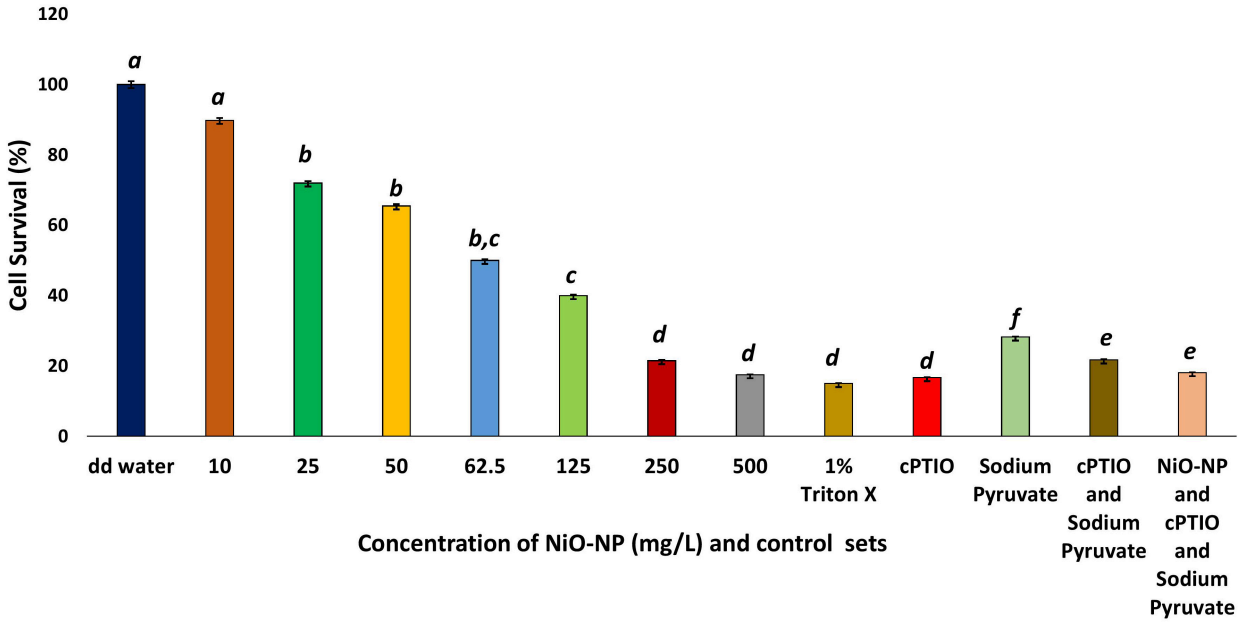

FIGURE 2 | Cell survival percentage calculated through formazan formation. These letters denote statistical grouping after performing One-way ANOVA.

10 mg L^{-1} NiO-NP, about 10% loss of cell viability was noted over the negative control, and at 50 mg L^{-1} NiO-NP, a 35.5% loss of cell viability was registered.

Interestingly, a similar proportion of loss in cell viability (∼82–85% loss over the negative control) was observed in the roots growing in the presence of 1% Triton X, as well as those growing in 100 μM cPTIO, a nitric oxide inhibitor, alone or in combination with 10 mM of the ROS scavenger sodium pyruvate (**Figure 2**) signifying NO plays a pivotal role in maintaining cellular viability.

The primary cause for cell membrane damage is lipid peroxidation that results in the formation of malondialdehyde as an aftermath of ROS-induced damage. Malondialdehyde formation can be macro-documented by Schiff's reagent staining. NiO-NP-treated roots showed a sustained increase in the absorbance of the dye in a dose-dependent manner, indicating an increase in cell membrane damage with increasing NiO-NP doses (**Supplementary Figure 3**). Maximum lipid peroxidation was observed in the roots exposed to 250–500 mg L^{-1} of NiO-NP, in line with the observations from the cell viability assay.

In the present study, a constant decrease in K/Na ratio was noted congruent to increasing NiO-NP dosages used, due to an increase of sodium ions in the cell with a concomitant decrease in the intracellular potassium pool in the affected tissues. In the negative control sets, this ratio was 1.544, while it reduced to 1.27 in the roots exposed to 10 mg L^{-1} NiO-NP and 0.8 upon exposure to 25 mg L^{-1} NiO-NP (**Figure 3A**). Subsequent decrease against the negative control coincided with a general deterioration in cellular well-being of the treated roots with increasing NiO-NP concentrations. All positive control sets also showed a considerable decrease in this ratio when compared with the negative control showing 0.4 mM EMS effectively reduced K/Na ratio and cPTIO blocked NO formation leading to decreased K/Na ratio, and blocking only H_2O_2 is not enough to reduce ROS-induced damages and it has a role in maintaining homeostasis.

A. cepa Roots Show Rise in GABA, Proline, and Hydrogen Peroxide Concentrations on NiO-NP Treatment

Gamma amino butyric acid showed an upsurge in all the NiO-NP-treated tissues and in the positive control sets when compared with the roots growing as a negative control (DD water). In the negative control sets, GABA content was estimated to be 0.168 nmol g^{-1}, and it increased to 0.231 nmol g^{-1} with a percentage increase of 85.7 in the roots exposed to 10 mg L^{-1} NiO-NP. In the roots exposed to median ranges of NiO-NP doses (50–125 mg L^{-1}), GABA content increased by 124–187%. GABA contents in the roots treated with higher concentrations of NiO-NP (250–500 mg L^{-1}) were comparable to the positive control sets. The percentage increase in the case of roots growing in 250 and 500 mg L^{-1} NiO-NP was 234 and 247, respectively, comparable to the roots treated with cPTIO and sodium pyruvate (**Figure 3B**), indicating that the absence of both H_2O_2 and NO is not beneficial for the treated tissue, showing their native roles in the maintenance of cellular metabolic activities.

Proline profiles of the treated and positive control sets were studied against the negative control set. As with GABA, proline content also showed a dose-dependent increase in the roots under NiO-NP treatment, up to a concentration of 125 mg L^{-1}, as was the case in some of the positive control sets, too. While the percentage increase in proline content was 32.8 in the roots growing at 10 mg L^{-1} and 43.7 in those growing

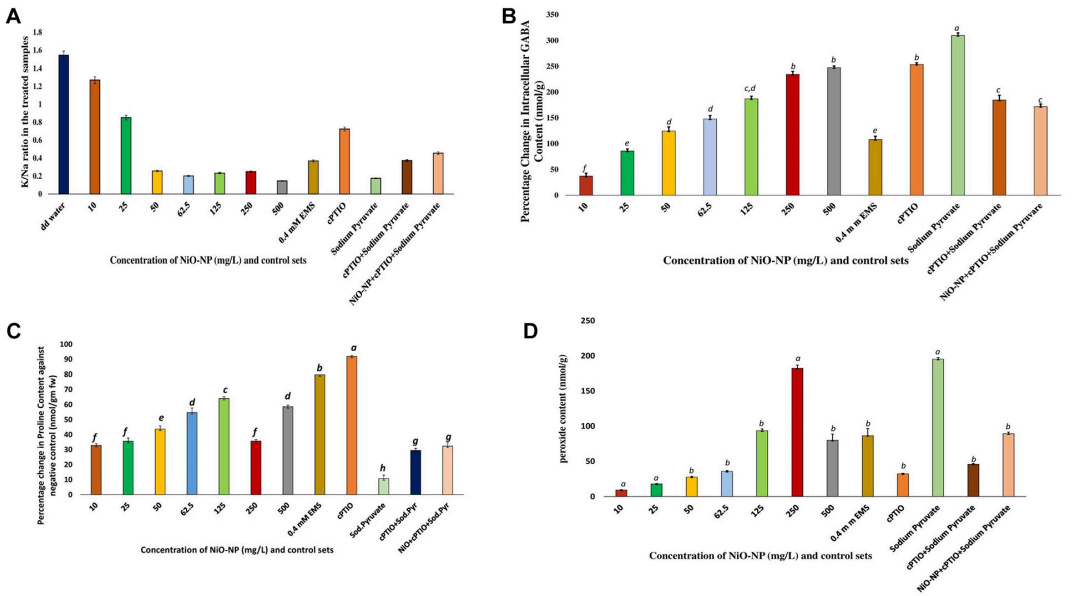

FIGURE 3 | (A) Bar graphs showing the K/Na ratio in the exposed tissue against the negative control; **(B)** Bar graphs showing percentage change in gamma amino butyric acid content in the exposed tissue against the negative control ($p < 0.05$); **(C)** Bar graphs showing intracellular proline content in the exposed tissue against the negative control ($p < 0.05$); **(D)** Bar graphs showing intracellular hydrogen peroxide content in the exposed tissue against the negative control ($p < 0.05$). These letters denote statistical grouping after performing One-way ANOVA.

at 50 mg L^{-1} of NiO-NP treatment, at the median treatment concentration of 125 mg L^{-1} NiO-NP, an increase of 64% proline content over the negative control was noted. However, at higher concentrations of NiO-NP (250–500 mg L^{-1}), proline content decreased substantially (58.58% decrease over the negative control at 500 mg L^{-1} NiO-NP). In the 0.4-mM EMS-treated set, a 91% increase of proline content over the negative control was observed (**Figure 3C**). However, in the other positive control sets, proline content reduced when compared with the negative control.

H_2O_2 content increased drastically, even in the roots exposed to the lowest dose of NiO-NP (10 mg L^{-1}) when compared with the negative control. While the roots of negative control sets contained 0.023 nmol g^{-1} H_2O_2, in the 10 mg L^{-1} NiO-NP-treated roots, the total content rose to 0.045 nmol g^{-1}. A concurrent increase in H_2O_2 content was noted in the subsequent higher concentrations of NiO-NP as well, with an almost 900% increase to that of the negative control observed from 62.5 mg L^{-1} onward. In the case of cPTIO-treated root tissues, H_2O_2 content was almost 1,900% more than the negative control, directly correlating a lack of NO with increased H_2O_2 production. Roots treated with 500 mg L^{-1} NiO-NP showed similar H_2O_2 content with that of the roots exposed to 0.4 mM EMS (**Figure 3D**).

Nitric Oxide Shows Upsurge Upon Exposure of *Allium cepa* Roots to NiO-NP

Griess assay is a sensitive analytical test where gaseous NO is quickly converted to nitrite form, for absolute and easy detection through color formation. In the present study, a concurrent increase in nitrite content was observed which was in tandem to qualitative data generated using DAF-FM-DA staining of experimental sets *via* confocal microscopy (**Figures 4A,B**). A basal level of NO was detected in the roots of the negative control sets, which surged upon the introduction of NiO-NP even at the lowest dose (10 mg L^{-1}), showing an increase of 24.77% in NO content over the negative control. Exposure to 50 mg L^{-1} NiO-NP caused a 63.82% increase in NO content over the negative control, while around 85% increase was noted in the tissues growing at 125 mg L^{-1} NiO-NP. At higher doses (250–500 mg L^{-1}) of NiO-NP, a further spike in NO content was noted (around 115 and 140% increase, respectively, over the negative control), which again was in concert with the confocal microscopic observations (**Figure 4A**).

Allium cepa roots of all the treated and control sets were studied through laser scanning confocal microscopy, after staining with DAF-FM-DA, a NO detector at the cellular level. An increase in color intensity directly dependent on the NiO-NP dose was observed, signifying the trend in increase in cellular NO levels under increasing ENP exposure. While a stable NO content was detected even in the negative control sets (**Figure 4B**), the introduction of a heavy metal nanoparticle was found to instigate a sudden upsurge in NO levels in the exposed tissues. From a slight rise in intracellular NO at the lowest dose of 10 mg L^{-1} NiO-NP (**Figure 4A**), a further increment in NiO-NP dose resulted in increased fluorescence of DAF-FM-DA. At the median concentrations of NiO-NP (50–125 mg L^{-1}), NO content and fluorescence increased prominently, and at higher concentrations (250–500 mg L^{-1}), as well as in the positive control sets,

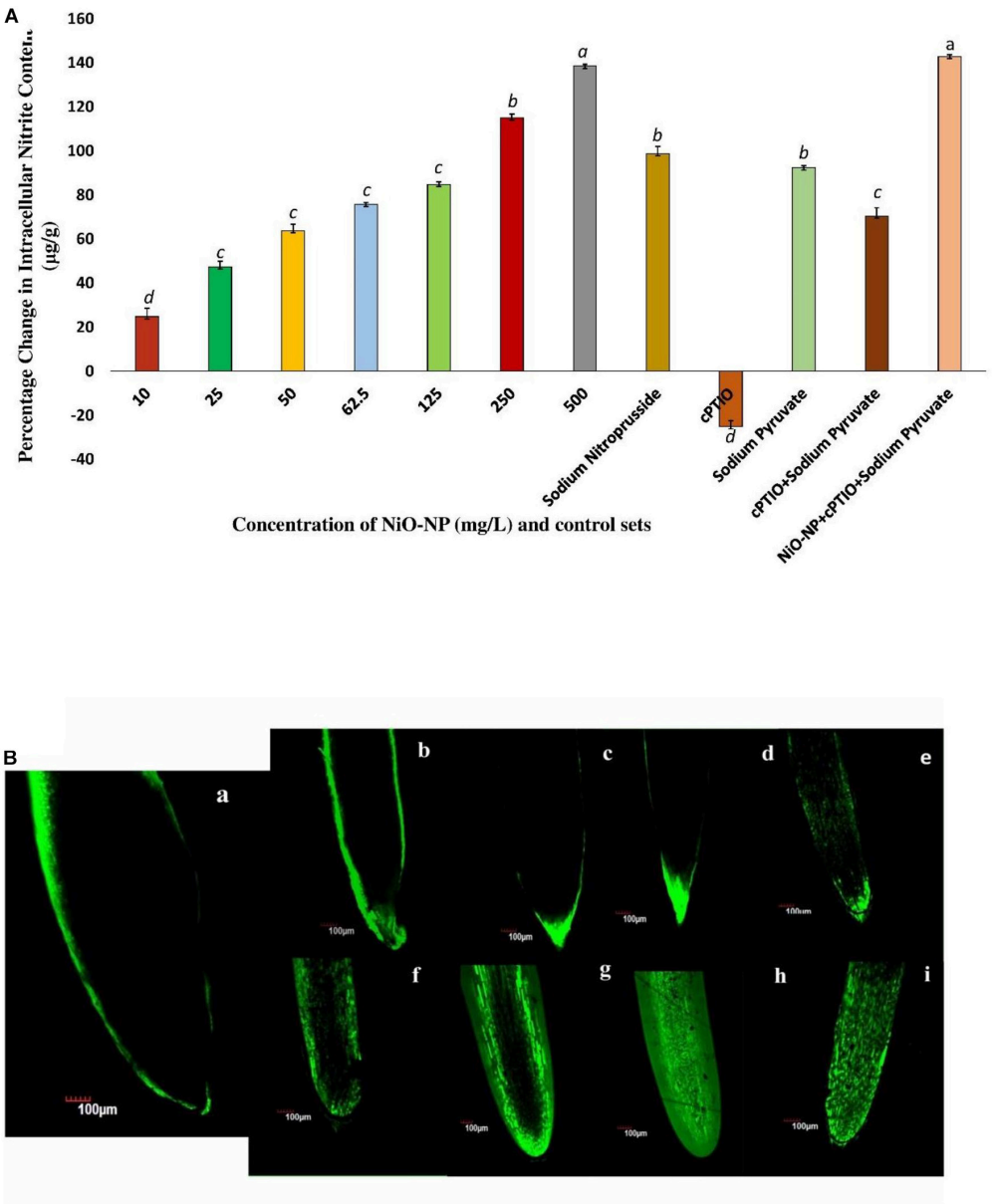

FIGURE 4 | (A) Bar graphs showing intracellular nitric oxide content in the exposed tissue through Griess reagent ($p < 0.05$); **(B)** Root tips stained with DAF-FM-DA showing the extent of nitric oxide formation: **(a)**, negative control; **(b)**, tissue exposed to 10 mg L^{-1} NiO-NP; **(c)**, tissue exposed to 25 mg L^{-1} NiO-NP; **(d)**, tissue exposed to 50 mg L^{-1} NiO-NP; **(e)**, tissue exposed to 62.5 mg L^{-1} NiO-NP; **(f)**, tissue exposed to 125 mg L^{-1} NiO-NP; **(g)**, tissue exposed to 250 mg L^{-1} NiO-NP; **(h)**, tissue exposed to 500 mg L^{-1} NiO-NP; **(i)**, tissue exposed to 100 µM cPTIO + 125 mg L^{-1} NiO-NP + 10 mm sodium pyruvate. These letters denote statistical grouping after performing One-way ANOVA.

characteristically enhanced fluorescence was observed, pointing to the presence of excessive NO in treated tissues (**Figure 4Bi**).

Quantification of NOS-like, NOX, and NR Enzymes Confirm Augmented NO Production in the NiO-NP-Affected Tissue

Nitric oxide synthase-like proteins and NR are among the few known enzymes responsible for NO production in plants, and thus, their activities were quantified to understand fluctuations in NO production. NOX-like activity increased consequent with an increase in cellular ROS in the present study, as was also reported earlier (Yadu et al., 2018). NR and NOS-like activities both showed dose-dependent increase in the treated tissues when compared with the negative control. NR activity showed an upturn in roots exposed to even the lowest dose of 10 mg L^{-1} NiO-NP used (30% increase over the negative control). With subsequent increments in NiO-NP concentrations, there was a

gradual increase in NR activity with a 45–47% increase over the negative control across all the sets (**Figure 5**). In the case of NOS-like activity, however, a decrease was noted in the roots exposed to the lower doses of NiO-NP (10–50 mg L^{-1}), which was around 40% less than that of the negative control. A further increase in NiO-NP doses increased NOS-like activity, with a 40% augmented activity observed at 125 mg L^{-1} NiO-NP (**Figure 5**). NOX showed increased activity in the NiO-NP-treated sets, too, though the increase was not dose-dependent. There was around 30% increase in the roots growing at 10 mg L^{-1} NiO-NP, whereas a 12% increase was noted in the tissues exposed at 50 mg L^{-1} NiO-NP. At higher concentrations, there was only a nominal increase in NOS-like activity (**Figure 5**).

Biochemical Assays and Semiquantitative RT-PCR Confirmed Increased Activity and Upregulation of Important Antioxidant Enzymes and Genes in NiO-NP-Exposed Roots

Nickel oxide nanoparticles can cause perturbation in antioxidant activities as a direct outcome of oxidative stress. CAT, SOD, and APX contents were measured to study the extent of oxidative damage induced by NiO-NP in the treated samples. CAT showed a significant increase of 25% at 10 mg L^{-1} NiO-NP treatment over the untreated samples. As NiO-NP concentration increased further, CAT content increased to 38% over the negative control at 62.5 mg L^{-1} NiO-NP dose and 49% increase over the untreated sets at 250 mg L^{-1} NiO-NP concentration (**Figure 6**). SOD also followed a similar trend, where an initial increase of 28% activity over the negative control was noted at 10 mg L^{-1} followed by a significant increase as the dose of NiO-NP increased, and a 150% increase over the negative control was witnessed at 62.5 mg L^{-1} NiO-NP concentration (**Figure 6**). APX activity increased notably in the treated sets against the negative control at all the concentrations of NiO-NP. There was an increase of 38% APX activity over basal control levels even at the lowest dose of NiO-NP (10 mg L^{-1}). APX activity continued to increase across all the concentrations of NiO-NP. The highest APX activity was seen at 125 mg L^{-1} NiO-NP dose (440% increase) over the untreated control sets (**Figure 6**).

Cytotoxic aspects of NiO-NP have already been speculated using various biochemical assays, but the exact molecular mechanism of antioxidant profile perturbation was investigated using qRT-PCR. The expressions of crucial antioxidant genes, namely, CAT, SOD, and APX, and the RCA (large and small units) were studied in treated and untreated sets, and they showed upregulation in all the treated sets when compared with the negative control. CAT expression showed a maximum of 1.97-fold increase at the highest concentration of NiO-NP (500 mg L^{-1}), while a 1.5-fold increase was seen in the roots exposed to median concentrations (125–250 mg L^{-1}). SOD transcripts also showed an average 2-fold increase in expression at the median and higher concentrations, with the highest 4.22-fold increase observed at 62.5 mg L^{-1} NiO-NP concentration. The APX gene showed the highest expression among all the genes studied upon NiO-NP exposure. An 8.5-fold increase was documented in the tissues growing at 125 mg L^{-1} NiO-NP, while a 5.8-fold increase was seen at 50 mg L^{-1} NiO-NP (**Figure 7**). Both the RCA large and small transcripts showed median upregulation at all the NiO-NP concentrations. While the expression of the small subunit increased by 2–4-folds across all the concentrations of NiO-NP tested, the large subunit showed

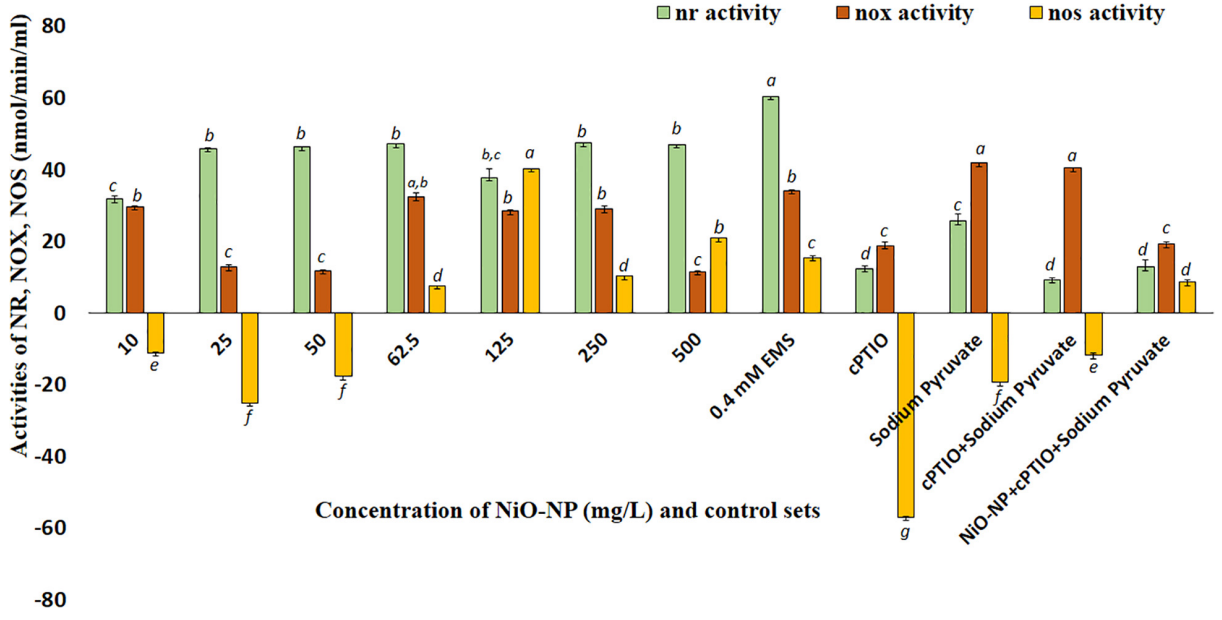

FIGURE 5 | Bar graphs showing nitric reductase, NADPH oxidase, and nitric oxide synthase activity in the exposed tissue against the negative control ($p < 0.05$). These letters denote statistical grouping after performing One-way ANOVA.

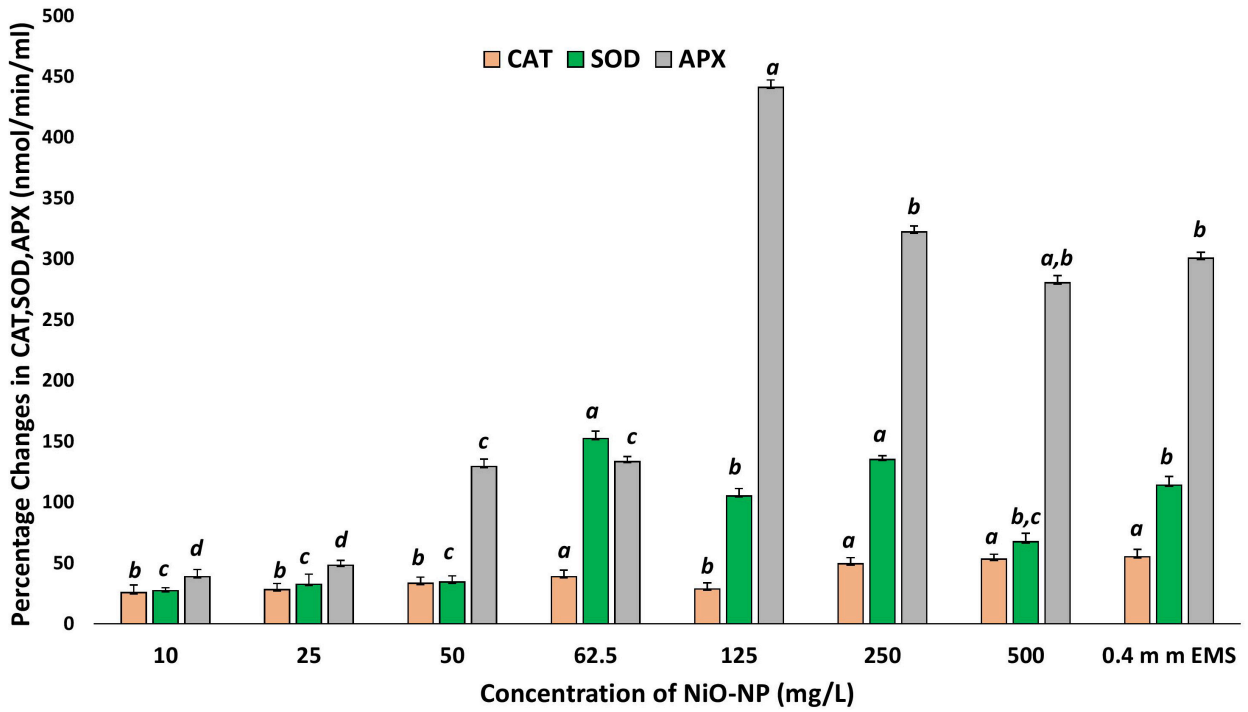

FIGURE 6 | Effect of increasing NiO-NP concentration on catalase and SOD activity and on APX activity, expressed as percentage change ($p < 0.05$). These letters denote statistical grouping after performing One-way ANOVA.

an average 1.5-fold upregulation (**Figure 7**). Actin was used as a reference gene that showed constant expression in all the samples (control sets and treated ones), and the quantitative level of actin is shown in **Supplementary Figure 4**.

DISCUSSION

Increased industrial uses of NiO-NP and its associated introduction into the natural environment in recent decades have drawn scientific attention to the specter of its harmful effects on plants as well as in humans (Chung et al., 2019; Cambre et al., 2020). Nickel is already categorized as a potent carcinogen by the WHO, and when it became known that the NiO-NP can mimic the activities of their bulk counterparts especially at higher concentrations, it became imperative that the exact mechanism of NiO-NP-induced damage to biological systems be studied in detail. Even though there are a few reports of NiO-NP-induced toxicity in plants underlining its dose-dependent toxicity, the whole gamut of physicochemical perturbations is yet not elucidated. One of the huge gaps in information that clouds our understanding is the dynamics of ROS and NO relation. Both ROS and NO are important participants in the normal cellular signal transduction that, at low concentrations, help in preserving cellular homeostasis (Romero-Puertas and Sandalio, 2016). Their integrative role in plants, from development to stress response, has been a topic of active research (Asgher et al., 2017). In this manuscript, the authors have ventured to augment existing information on how ROS and NO act in tandem in case of the advent of an engineered nanoparticle, and how an increase in NO can trigger ROS overproduction inadvertently causing physicochemical upheavals due to rampant oxidative damage. It was during this work that it became obvious that NiO-NP-induced toxicity incremented in a dose-dependent manner, leading to an overproduction of both ROS and NO. These two crucial components of the stress management cascade work initially in tandem, but at higher doses of NiO-NP (250–500 mg L^{-1}), they behave antagonistically, leading to acute cellular damages.

The present experimental parameters accommodated a wide range of NiO-NP concentrations (10–500 mg L^{-1}) keeping in mind their natural distribution and concentrations of Ni encountered in nature, which could go up to 1,600 mg kg^{-1} in coalfields[3]. It was noteworthy that *A. cepa*, the chosen plant model, did not show documentable disruption in cellular functions at lower doses of NiO-NP (below 10 mg L^{-1}) and almost 100% cell death at concentrations higher than 500 mg L^{-1} after an exposure of 24 h. *A. cepa* is a popular choice for the detection of cytotoxicity and genotoxicity of any xenobiotic compound as endorsed by the various international organizations of repute like UNEP, USEPA, and OECD (Boros and Ostafe, 2020)[4]. It is easily available and fast-growing and shows uniform growth and comparable effects that can be extrapolated to mammalian systems. Also, parts of *A. cepa* are

[3]WHO,2000; http://www.euro.who.int/__data/assets/pdf_file/0014/123080/AQG2ndEd_6_10Nickel.pdf

[4]https://www.oecd.org/chemicalsafety/testing/33653757.pdf

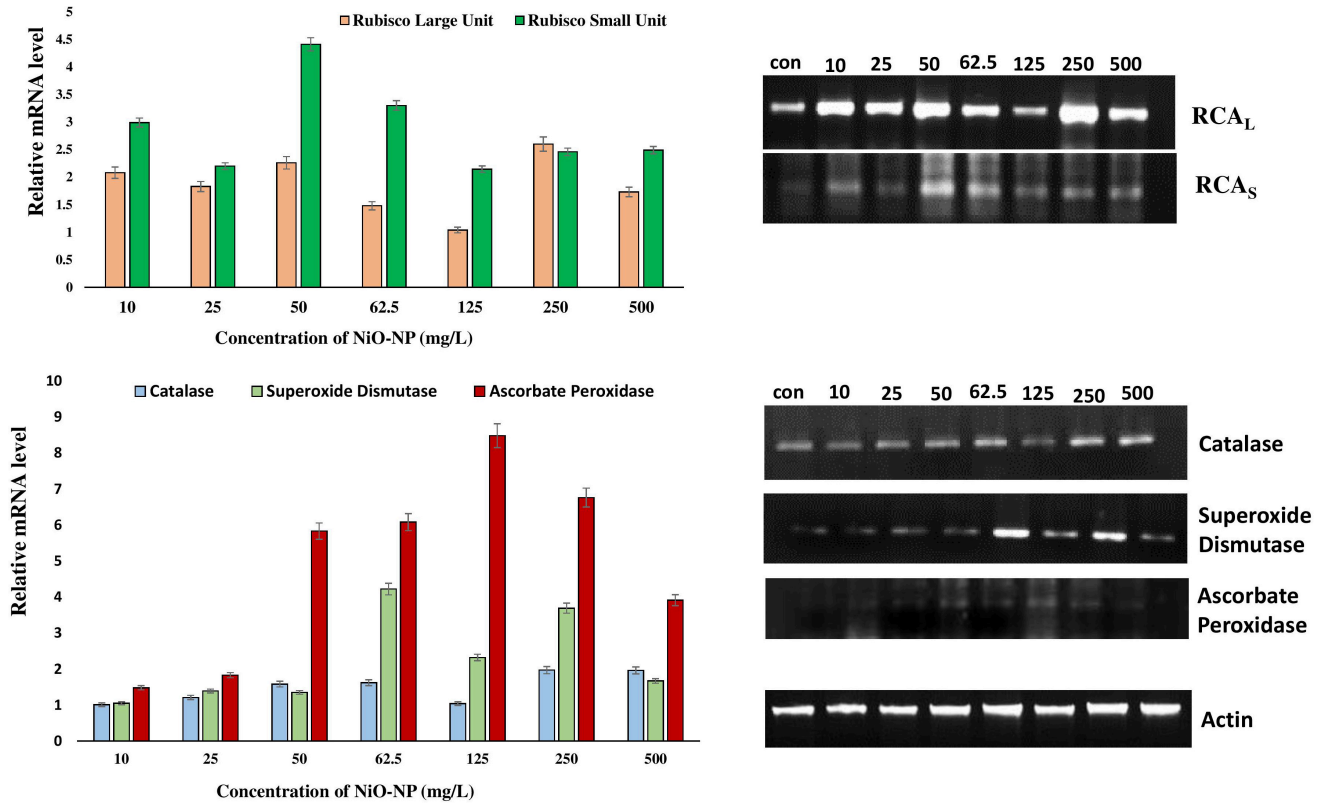

FIGURE 7 | Representative gels showing the activities of different antioxidant genes and RCA subunits in *Allium cepa* control roots and NiO-NP-treated roots with their relative mRNA levels with the reference gene.

consumed raw, opening the possibility of NiO-NP introgression into the food web and its biomagnification. The authors have shown earlier that *A. cepa* roots take up NiO-NP readily, most probably *via* the plasmodesmata, in a dose-dependent manner (Manna and Bandyopadhyay, 2017b).

In the present work, FITC-tagged NiO-NP were utilized to unravel the dynamics of its internalization within tissues and cells of *A. cepa* roots using a confocal laser scanning microscope. FITC, possibly the most widely known fluorescent tracer used in biological sciences, has a reactive isothiocyanate which can be tagged to amine and sulfhydryl groups of different biomolecular moieties. FITC also finds widespread use as a tag for nanoparticles to check and record their entry into biological systems and localize them within cells and tissues, aiding biomedical studies (Veeranarayanan et al., 2012; Huang et al., 2018). In plants, FITC tagging of chitosan (Chandra et al., 2015) and zein nanoparticles (Ristroph et al., 2017) is reported. Other authors have also documented the entry of FITC-tagged zinc and cerium metallic nanoparticles into the cells (Xia et al., 2008). In the present study, it was observed that hydroponically administered FITC-tagged NiO-NP breached the root epidermis and were translocated to the meristematic zone, and then to the zone of elongation and differentiation, in a progressively dose-dependent manner (**Figure 1**). These NP entered individual cells and were seen scattered in the cytoplasm or accumulated around the nuclear membrane (**Figure 1**). From these pieces of evidence, we can deduce that the *modus operandi* of NiO-NP-induced toxicity rests on their ability to gain entry into the cells, causing damage to important organelles like the nucleus, peroxisomes, or mitochondria, which showed hindered functioning, similar to those reported in cases of NiO-NP in tomato seedlings by Faisal et al. (2013) and of CuO-NP on soybean (Yusefi-Tanha et al., 2020) earlier.

An increase in NiO-NP dosage brought about a steady deterioration of cellular membrane integrity, as was reported earlier (Manna and Bandyopadhyay, 2017b). Earlier reports have indicated that capricious numbers of aggregated NiO-NP of various sizes and conformations clustered over the epidermal cell membranes, abrading them, and caused substantial damage to their surfaces, before gaining entry into the cells (Ates et al., 2016). Such damage to the membrane surfaces led to an immediate increase in cellular ROS (Sohaebuddin et al., 2010; Shang et al., 2014). Uncontrolled ROS upsurge induced malfunction of the antioxidant profiles and indirectly compromised integrity and, thus, survival in the treated tissues, as documented by Evans blue staining of root tips in the present study. Evans blue, an azo dye, can penetrate into damaged and ruptured membranes more easily than healthy membranes (Vijayaraghavareddy et al., 2017). Hence, normal cells do not take up the blue color, while those with membrane

damage do. The intensity of the color reaction can be studied spectrophotometrically to ascertain the quantum of membrane damage in the treated tissues. Increasing color intensities in the root tissues treated with NiO-NP showed prominent loss of cell viability with rising concentration of the ENP. Lipid peroxidation, an early sign of membrane damage, occurs when unstable membrane lipids form malondialdehyde that can react with Schiff's reagent on the aldehyde group to produce a colored output (Awasthi et al., 2018). Interestingly, exposure to bulk nickel does not produce significant lipid peroxidation in affected tissue (unpublished data). However, *A. cepa* roots exposed to NiO-NP showed significant lipid peroxidation that was confirmed biochemically by TBARS assay earlier (Manna and Bandyopadhyay, 2017b). In the present work, also color reaction with Schiff's reagent observed in the affected tissues increased with increasing doses of NiO-NP exposure (**Supplementary Figure 3**). It is known that during initial treatment with heavy metals, plants undergo dehydration (Singh et al., 2016), similar to osmotic stress (Osakabe et al., 2013). In a tissue having depleted potassium and augmented sodium ion contents, the ionic homeostasis becomes unhinged leading to cellular shutdown (Osakabe et al., 2013). Hence, the K/Na ratio was studied in a bid to find out possible changes in the ionic balance of the affected tissues. A marked dose-dependent decrease in K/Na ratio was observed in exposed root tissues upon NiO-NP treatment, similar to those seen in plants affected with dehydration and salinity stress confirming this ENP's ability to damage cellular integrity and perturb ionic balance of affected cells. Thus, NiO-NP damages cell integrity leading to a cascade of physicochemical perturbations that induce stress in the exposed root tissues of *A. cepa*.

The increase in ROS content of tissues exposed to NiO-NP in the present experiment, especially H_2O_2, confirmed the trend of a dose-dependent upsurge in reactive species, as seen in earlier reports as well (Manna and Bandyopadhyay, 2017a,b). ROS acts as a double-edged sword that has immense importance in signal transduction and stress management. Exposure of plants to metals induces oxidative challenges through pathways specific to a particular metal (Rizwan et al., 2017), often culminating in a mismatch between production and neutralization of ROS, most notably H_2O_2, hydroxyl ion, and superoxides (Cuypers et al., 2016). H_2O_2 is a selectively reactive, uncharged non-radical, having both oxidizing and reducing properties, making it crucial for energy-efficient stress mitigation (Bienert and Chaumont, 2014; Das and Roychoudhury, 2014). The mitochondria, despite being the primary location of H_2O_2 generation, suffer maximum damage from its excess in the cell. It is noteworthy that nickel, a non-redox active metal, can indirectly lead to an increase in intracellular ROS levels in exposed tissues, either by inhibiting specific enzymes by blocking their binding sites, or by diminishing cellular GSH pool, or affecting NOX, upending the cellular antioxidant profiles, thereby creating a ROS furor as seen in the present experimental system (Valko et al., 2016).

Coincidentally available NO also showed a marked change in the NiO-NP-treated tissue against the control sets. There was a rise in NO, even at the lowest dose of NiO-NP, followed by a marginally stalled increase in the treated tissues observed around the median dose of 125 mg L^{-1} NiO-NP, followed by a burst of NO production at the higher doses (**Figure 4**). The intricate interplay of various NO production mechanisms in the affected tissues, either independently or in conjunction with augmented ROS, can cause a spike in NO accumulation (Romero-Puertas and Sandalio, 2016). As mentioned earlier, NR, an important molybdenum-containing multiredox enzyme, is crucial for both nitrogen assimilation in plants and for the reductive pathway of NO production, thus maintaining NO homeostasis. NR effectuates the transfer of electrons from NAD(P)H to downstream substrates, producing NO in the process, which also makes it a major enzymatic producer of NO in plants (Chamizo-Ampudia et al., 2017). Another important mode of NO production is through the oxidative pathway, where NOS catalyzes the production of NO in animals, though the exact homomers have not yet been found in plants so far. Scientists have long debated about the presence of NOS-like protein in plants (Astier et al., 2018) and have suggested that these are protein complexes working in coordination with subunits of arginine, NADPH, and NOS co-factors. Though orthologous genes of NOS similar to animals were not detected in plants, numerous reports depicting the biochemical presence of L-arginine-dependent NOS-like protein complexes have been documented that perform a similar function (Corpas and Barroso, 2018). Recent reports suggest a lateral rise in NOS-like activity with abiotic stress factors (Asgher et al., 2017), similar to the observations documented by the authors in the present study. Studies have shown that it is NR that produces a bulk of NO in a plant from nitrate reservoirs and controls the first rate-limiting step and even producing NO under high nitrite accumulation or in acidic/anoxic conditions; however, the turnover rate for NO formation following this pathway is quite low. The reactivity of NOS-like enzymes, on the other hand, is affected by many individual co-enzymes and co-factors which constitute its active form. Hence, a consequential increase in NR becomes more prominent than NOS-like for NO production during conditions of stress (Astier et al., 2018). NR activity in exposed roots showed a dose-dependent linear rise in all the concentrations of NiO-NP used, with an initial rise of ∼30% at the lowest dose of 10 mg L^{-1} NiO-NP, followed by ∼47% increase at 250 mg L^{-1} NiO-NP and 80% increase at the highest dose of 500 mg L^{-1} NiO-NP. Thus, it becomes obvious that the NiO-NP-treated tissue implemented the reductive pathway as the major source of intracellular NO generation. There is no evidence of a direct correlation between NR and NOS-like activity in plant systems so far, but *in vivo* S-nitrosylation loop inhibits NO formation by NR, and also, NR is competitively inactivated by higher cellular nitrate concentration. Therefore, the presence of alternate NO-forming mechanisms is evidently present in every plant cell, the most eligible candidate for such being the NOS-like complexes (Fu et al., 2018). In the present study, there was an initial fall (11% depletion) in NOS-like activity in *A. cepa* root tips exposed to the lowest dose of NiO-NP (10 mg L^{-1}) against the negative control, followed by a 17% fall in such activity in the roots treated with 50 mg L^{-1} NiO-NP. Interestingly, the roots exposed to NiO-NP ranging between 62.5 mg L^{-1} and

above showed a steady rise in NOS-like activity with as much as a 40% rise at 125 mg L^{-1} NiO-NP concerning the negative control and 20% increase in activity at the highest dose of NiO-NP (500 mg L^{-1}). Thus, NOS-like activity showed a non-linear correlation with NiO-NP dose among the treated samples, and these values are not significantly different among themselves in many instances. The present dataset corroborates that NOS-like activity is controlled by multiple factors, and perturbations in Ca^{2+} and/or NADPH that is inevitable in NiO-NP-affected tissue can also impact NOS-like activity (Faisal et al., 2013). In fact, detailed work by the present group has found increased cytosolic Ca^{2+} in the treated tissue, consequent to severe damages incurred by the chloroplast and mitochondria at toxic concentrations of NiO-NP (unpublished), alluding to such a possibility. Few reports that document the rise in both NOS-like and NR activity in higher plants subjected to abiotic stressors include the study of maize under dehydration stress that showed a rise in NOS-like activity on exogenous SNP (NO donor) application (Hao et al., 2008). In *Hibiscus*, aluminum treatment inhibited NOS-like activity but did not affect NR activity (Tian et al., 2007), while a rise in NR alleviated Al-induced damages in soybean and wheat (Wang et al., 2017; Sun et al., 2018). Cadmium exposure increased NR activity in alfalfa and barley (Lentini et al., 2018; Yang et al., 2019), which was similar to the observations recorded by the present authors in the case of NiO-NP stress on *A. cepa*. Our findings have indicated a dose-dependent increase in NR activity with rising NiO-NP concentrations and an accompanying increase in NO, thus affirming that NR acts in a linear manner using the cellular nitrate reservoir available to produce NO, which is in contrast to NOS-like activity which depends on various other intrinsic factors as well.

Exposure to increasing concentrations of NiO-NP incited an upsurge in NOX activity, which was concomitant with the higher levels of intracellular NO and was confirmed by the rise of H_2O_2 incidence, as evident even at the lowest ENP concentration used on *A. cepa* in the present study. The most prevalent enzymatic ROS producers in plants, NOX, are deemed as respiratory burst oxidase homologs (RBOHs). Implicated in several aspects of normal plant growth and development, these are also involved in maintaining the cellular balance of ROS and RNS (Chu-Puga et al., 2019). Increment in intracellular NO is known to increase NOX production since inflation of cellular H_2O_2 leads to an active breakdown of NADPH. This in turn augments NOX activity in the plasma membrane, which is primarily responsible for superoxide production in the apoplast of plants (Podgórska et al., 2017). Intrusions of xenobiotic agents are known to trigger NOX activity contributing to an oxidative burst. In the present study, an increase in NOX activity (∼30% more than negative control) was observed in *A. cepa* roots treated with 10 mg L^{-1} NiO-NP. Roots exposed to higher concentrations of NiO-NP showed a steady increase in NOX content, though not linear, with the highest increase documented at the dose of 500 mg L^{-1} NiO-NP (**Figure 5**). Our data corroborated recent reports of a dose-dependent increase in NOX activity in plants due to increased iron exposure (Yadu et al., 2018). A similar increase in NOX activity was observed upon cadmium and copper treatment in *Arabidopsis thaliana* roots (Remans et al., 2010) and Pb stress in the roots of *Medicago truncatula* (Zhang et al., 2019). Selenium-induced phytotoxicity in *Brassica rapa* also showed NOX-dependent ROS induction (Chen et al., 2014). Heyno et al. (2008) reported that treatment with heavy metals like cadmium induced ROS from the plasma membrane and not from the mitochondria. Similarly, the present work also confirmed increased plasma membrane was linked to NOX activity. There are confirmatory reports that, as a response to metal toxicity, cytosolic Ca^{2+} levels increased proportionately, activating and increasing NOX activity as well (Sosan et al., 2016). This in turn regulated cytosolic ROS generation through peroxidases (Heyno et al., 2008). Such concomitant steady increase in cytosolic Ca^{2+} levels with ROS increase was also recorded in the NiO-NP-treated sets of *A. cepa* (unpublished).

Intracellular levels of GABA and proline, both deemed to be universal markers of stress, were escalated with increased NiO-NP exposure in plants. GABA is an important non-protein amino acid useful in plant signaling, much like its role in the neurotransmission of animals (Ramos-Ruiz et al., 2019). It has an undeniable yet complex relationship with the ROS and RNS pools that has implications in increasing plant resilience to stress (Bor and Turkan, 2019). During oxidative stress response when intracellular ROS and related antioxidant levels inflate in a system, there is an impromptu rise in GABA levels as well, though whether as a cause or as its effect is yet debated. As the exogenous application of GABA reportedly induced antioxidant activity (Song et al., 2010), in the present work also, the authors have observed a marked increase in GABA content on NiO-NP exposure (**Figure 3B**), concomitant with a spike in ROS content and augmented antioxidant profiles. An increase of ∼37% GABA activity was observed in the roots exposed to the lowest dose of 10 mg L^{-1} NiO-NP, which increased to ∼190% at 125 mg L^{-1} of NiO-NP. A further dose-dependent increase in GABA activity was registered in the higher NiO-NP concentrations, too. Roots exposed to sodium pyruvate, a H_2O_2 inducer, also showed a significant increment in GABA content (∼110%) over the negative control. Since GABA is primarily synthesized by polyamines, indirectly dependent on the nitrite pool, it was not surprising that roots exposed to cPTIO, a NO blocker, did not show a significant enhancement of GABA content over the negative control. A major portion of the GABA shunt is located in the mitochondria (Bor and Turkan, 2019), which is also the epicenter of abiotic stress mitigation and signaling; as such, any disturbance of this organelle due to metal exposure can cause multiple physicochemical malfunctions. It has already been reported that NiO-NP exposure damages the mitochondria *via* perturbation of antioxidant activities, which could be correlated with possible alterations of the GABA shunt, too. Many groups in recent times have shown increased GABA content in various plants under heavy metal treatments. In *Nicotiana tabacum*, treatment with zinc increased the endogenous GABA levels which in turn augmented the antioxidant enzymatic activities of those plants (Daş et al., 2016). Wheat subjected to arsenic stress also showed higher levels of GABA content in the treated roots and shoots (Sil et al., 2018). Proline, another non-protein amino acid and marker of stress response in plants, is known to increase considerably with any exigencies, including metal-effected stress.

In this work, a marked increase in proline content was recorded even at the lowest dose of NiO-NP against the negative control, with a linear dose-dependent increase in proline content in all the higher concentrations of NiO-NP, as also reported in many other plants exposed to other metallic nanoparticles. Barley plants treated with titanium oxide nanoparticles showed higher proline content than untreated control plants (Doğaroğlu and Köleli, 2017). Another heavy metal nanoparticle, copper oxide nanoparticles, also induced increased proline content in treated rice plants (Da Costa and Sharma, 2016). All these results were in tandem with the observations documented by the authors in the present study.

Antioxidant enzymes like CAT, SOD, and APX form the backbone of the stress mitigation system in a plant cell, responding minutely to any incoming stress signal and often leads to altered activities (Hasanuzzaman et al., 2019). In the present work, CAT, SOD, and APX showed significant increases following dose dependency of NiO-NP. These findings are in tandem to the previous reports available for NiO-NP-induced phytotoxicity. In fact, 24 h of uninterrupted NiO-NP treatment caused permanent damages to the framework of the cell as shown by decreasing cell survivability indices. Uninterrupted ROS generation, as shown by increased H_2O_2 accumulation, followed by excess NO generation led to multiple damages altering the biochemical framework of the cell and an imbalance in the activities of vital antioxidants (enzymes, metabolites), which also caused marked increase in proline and GABA levels along with changes in NO concentrations. A similar sequence of events was also observed when plants combat oxidative burst mechanism by a number of authors (Manna and Bandyopadhyay, 2017a; unpublished, Faisal et al., 2013; Oukarroum et al., 2015, 2017).

Semiquantitative reverse transcriptase polymerase chain reaction is especially convenient for the study of biomarker genes that are crucial for abiotic stress amelioration and survival (Qian et al., 2013). CAT, SOD, and APX, the chief players in the endogenous antioxidant systems of a plant cell, are instrumental in managing excess H_2O_2 and superoxides produced owing to oxidative burst linked to metabolic upheavals. Metallic nanoparticles often act as non-competitive inhibitors for several essential enzymes, like that of –SH groups of cysteine residues, forming covalent bonds and affecting folding during tertiary structure formation. This misfolding alters active site conformation, thus hindering the efficiency of many vital enzymes (Adeyemi and Whiteley, 2013) and affecting the normal metabolism of the affected cells. Enzymatic assay of CAT activity showed an upsurge in NiO-NP-treated roots against untreated sets (Manna and Bandyopadhyay, 2017b), as it participates in breaking down excess H_2O_2. Higher transcript levels of CAT in the present study affirm the previous report, proving evidence for the upregulation of CAT gene with increasing NiO-NP concentrations. APX, which not only helps detoxify excess H_2O_2 but also uses H_2O_2 for signaling and regulating the feedback loop of the GSH cycle (Singh et al., 2016), also showed increased transcript levels when compared with untreated controls. Higher transcript values of APX coincided with the general excess of H_2O_2 in the affected tissue. SOD also showed increased activity in the previous work reported by the authors detected through enzymatic assay, and the present data confirmed that SOD is the primary enzyme for dismantling the highly reactive superoxides. Thus, higher transcript levels maintained in tandem to oxidative burst indicate the intricate role SOD plays among stress-mitigating enzymes. All the concentrations of NiO-NP induced a general increase in activities of these antioxidants, except at 125 mg L^{-1}, where a marked decrease in most of these enzyme activities was observed. This may be because this concentration was probably most toxic under specific biotic interactions for this ENP in this particular study, beyond which the formation of bigger clumps and their dissociation constantly alter the stoichiometry of individual NiO-NP units (Manna and Bandyopadhyay, 2017a,b) and prevent their entry into the tissue as well. Consistent results in many other heavy metals, like lead, cadmium, and arsenic, where antioxidant profiles have shown considerable upregulation in the treated plants (He et al., 2004; Bharwana et al., 2013; Lou et al., 2017), confirmed that antioxidant enzymes helped nullify the aftermath of metallic stress. Hence, it was deduced that NiO-NP caused major oxidative stress in affected plants and upregulation of antioxidant enzymes constituted a major form of defense responses. Rubisco (RuBP) is the primary enzyme required for carbon fixation in plants. It consists of eight subunits each of nucleus-encoded small units and chloroplast-encoded large units and is designated as a potential housekeeping gene, necessary for the well-being of any plant (Siedlecka et al., 1998). RCA is necessary for the formation of RuBP to maintain optimum carbon fixation, but it has been shown that abiotic stress signals necessitate its upregulation (Demirevska-Kepova et al., 2004). RCA activity is known to be adversely affected consequent to heavy metal intrusion (Khairy et al., 2016). Therefore, RCA is an important candidate in studying the extent of damage due to oxidative stress. In the present work, however, we have tried to interpret the effect of a heavy metal nanoparticle on its subunits, trying to understand whether they were being upregulated individually or in tandem. It is known that the two domains of ATP-dependent structures of RCA encode chloroplast proteins, with the large subunit being more sensitive to abiotic stress than the smaller one (Chen et al., 2015). RuBP is affected quite harshly during oxidative stress, marking a lower transcriptomic presence (Cohen et al., 2005). Antioxidants like GSH play an important role in maintaining RuBP levels in case of metabolic inconsistencies (Son et al., 2014), whereas APX is largely responsible for its proper functioning under optimum conditions, exerting an effect over a crucial rate-limiting step (Liu et al., 2008). In the case of oxidative stress in the form of NiO-NP intrusion, GSH levels deplete, while APX is negatively affected (unpublished). The interrelationship of NO and GSH is quite interesting though complex, and they form GSNO which could inhibit NR-related NO synthesis. NO, in turn, can react with the heme group, thus potentially inhibiting APX activity. In fact, NO affected all the enzymes of the Asa–GSH cycle, though report of its inhibition of APX has not been confirmed yet (Romero-Puertas and Sandalio, 2016). This explains the high expression level of APX in the treated tissue observed in the present study. Proline, the ubiquitous marker of ROS imbalance, when found in excess similar to that reported by the authors, is also known

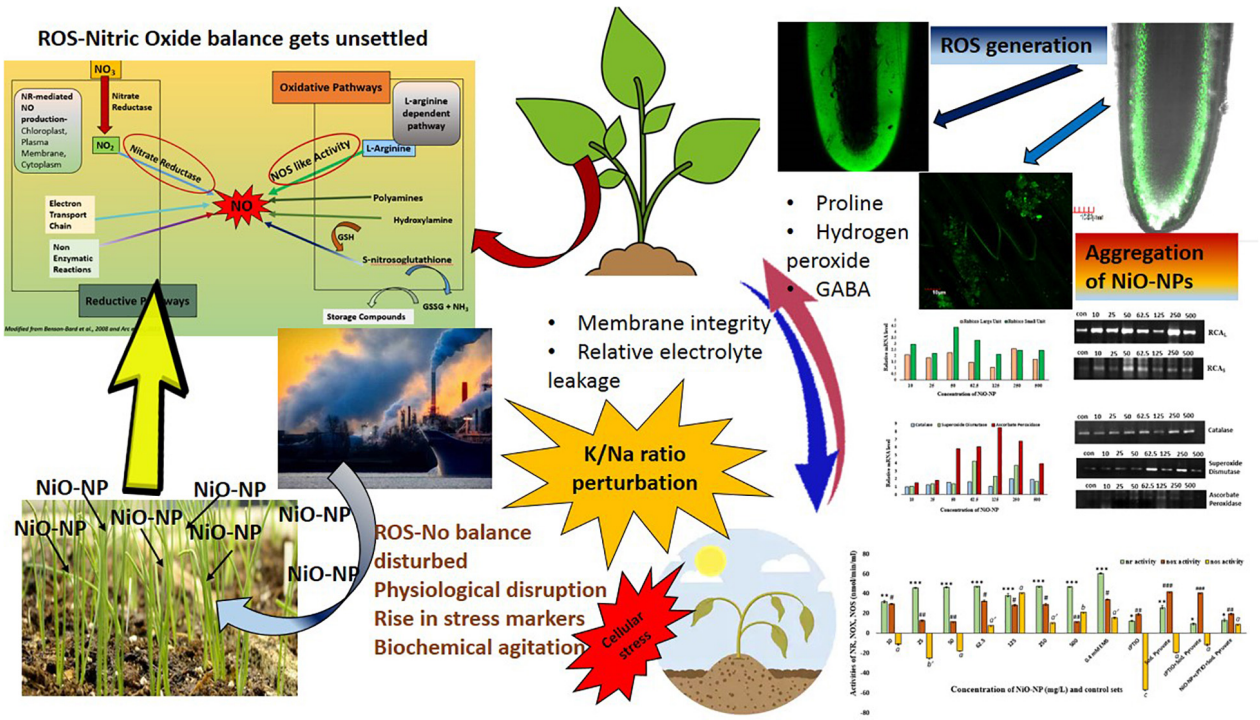

FIGURE 8 | Diagrammatic view of the change in ROS–NO dynamics and the effect on cellular physiology.

to lead to dissociation of RuBP subunits (Sivakumar et al., 2001). Demirevska-Kepova et al. (2004) reported a minor decrease in the activity of subunits of RCA in tomato treated with cadmium. Interestingly, in the present study, activities of both the subunits of RCA increased on NiO-NP exposure (**Figure 7**). According to Chen et al. (2015), such an event can lead to buffering of carbon fixation in a toxic environment. In case of the larger subunit, an increase in its activity in the NiO-NP-treated sets was only marginal and not statistically significant in all the concentrations. However, the activity of the smaller subunits showed a 2-fold increase in all the NiO-NP doses, making the change more relevant and contributing to an overall increase of RCA activity. Such an increase in RCA activity was observed in *Populus nigra* leaves on cadmium stress (Lomaglio et al., 2015). Higher intracellular NO content restored RCA activity in a stressed tissue (Khairy et al., 2016), and a similar trend was observed here where both intracellular NO content and RCA activity showed inflation.

In its entirety, it can be stated that NiO-NP exposure in *A. cepa* roots does indeed lead to oxidative stress, by way of perturbed production and dissociation of various reactive species, especially RNS (NO) and ROS (H_2O_2) (**Figure 8**). The unique properties of NiO-NP initiate a compelling duel between intracellular ROS, NO production, and the ameliorating antioxidant systems present in the plant tissues. This distinctive interaction is unique to this particular nanoparticle and the biotic component and is aided by the surrounding biophysical features like temperature, time of exposure, the dissociation constant, and aggregate formation. Different cellular cascades were individually discomposed and those in turn affected the entire abiotic stress response system of the exposed plant; the most affected are the antioxidant systems headed by CAT. Different mechanisms of NO production cascades were affected as well, which was documented by upregulated transcripts of antioxidants and higher activities of key enzymes. At higher concentrations, this ENP induced overwhelming oxidative stress and superfluous ROS accumulation, with a NO upsurge that was beyond restoration by the existing cellular mechanism, thus eventually leading to suspension of cellular activities and cell death. Further investigations on cellular signal transduction and signal cascades are necessary to understand the exact mechanism of this physiological collapse in cells subjected by NiO-NP. Such studies in a metallic nanoparticle-treated plant are still in preliminary stages and the present body of work could add up to the current bursar of existing knowledge in ROS–NO interaction in plants and help plant biologists to have a better understanding of ROS–NO dynamics in stressed tissue (Xiong et al., 2010). Additionally, further work to detect the gene-level cascades operating in case of NiO-NP-induced stress should be carried out, which will help in understanding the core mechanism of plants' retaliation to heavy metals and engineered nanoparticles.

DATA AVAILABILITY STATEMENT

The raw data supporting the conclusions of this article will be made available by the authors, without undue reservation.

AUTHOR CONTRIBUTIONS

All authors listed have made a substantial, direct and intellectual contribution to the work, and approved it for publication.

FUNDING

The authors would like to acknowledge the facilities provided by the Department of Botany (UGC–CAS phase VII and DST-PURSE and DST-FIST) and DBT-IPLS facility along with CRNN under the University of Calcutta for various instrumentation facilities. IM appreciates CSIR-UGC NET Fellowship scheme under UGC, Government of India, for financial support.

SUPPLEMENTARY MATERIAL

The Supplementary Material for this article can be found online at: https://www.frontiersin.org/articles/10.3389/fpls.2021.586509/full#supplementary-material

REFERENCES

Adeyemi, O. S., and Whiteley, C. G. (2013). Interaction of nanoparticles with arginine kinase from *Trypanosoma brucei*: kinetic and mechanistic evaluation. *Int. J. Biol. Macromol.* 62, 450–456. doi: 10.1016/j.ijbiomac.2013.09.008

Asgher, M., Per, T. S., Masood, A., Fatma, M., Freschi, L., Corpas, F. J., et al. (2017). Nitric oxide signaling and its crosstalk with other plant growth regulators in plant responses to abiotic stress. *Environ. Sci. Pollut. Res.* 24, 2273–2285. doi: 10.1007/s11356-016-7947-8

Astier, J., Gross, I., and Durner, J. (2018). Nitric oxide production in plants: an update. *J. Exp. Bot.* 69, 3401–3411. doi: 10.1093/jxb/erx420

Ates, M., Demir, V., Arslan, Z., Camas, M., and Celik, F. (2016). Toxicity of engineered nickel oxide and cobalt oxide nanoparticles to *Artemia salina* in seawater. *Water Air Soil Pollut.* 227:70.

Awasthi, J. P., Saha, B., Chowardhara, B., Devi, S. S., Borgohain, P., and Panda, S. K. (2018). Qualitative analysis of lipid peroxidation in plants under multiple stress through schiff's reagent: a histochemical approach. *Bio Protoc.* 8:e2807. doi: 10.21769/BioProtoc.2807

Bates, L. S., Waldren, R. P., and Teare, I. D. (1973). Rapid determination of free proline for water-stress studies. *Plant Soil* 39, 205–207.

Bharwana, S. A., Ali, S., Farooq, M. A., Iqbal, N., Abbas, F., and Ahmad, M. S. A. (2013). Alleviation of lead toxicity by silicon is related to elevated photosynthesis, antioxidant enzymes suppressed lead uptake and oxidative stress in cotton. *J. Bioremed. Biodeg.* 4:187. doi: 10.4172/2155-6199.1000187

Bienert, G. P., and Chaumont, F. (2014). Aquaporin-facilitated transmembrane diffusion of hydrogen peroxide. *Biochim. Biophys. Acta* 1840, 1596–1604. doi: 10.1016/j.bbagen.2013.09.017

Bor, M., and Turkan, I. (2019). Is there a room for GABA in ROS and RNS signalling? *Environ. Exp. Bot.* 161, 67–73. doi: 10.1016/j.envexpbot.2019.02.015

Boros, B. V., and Ostafe, V. (2020). Evaluation of ecotoxicology assessment methods of nanomaterials and their effects. *Nanomaterials* 10:610. doi: 10.3390/nano10040610

Bradford, M. M. (1976). A rapid and sensitive method for the quantitation of microgram quantities of protein utilizing the principle of protein-dye binding. *Anal. Biochem.* 72, 248–254. doi: 10.1016/0003-2697(76)90527-3

Cambre, M. H., Holl, N. J., Wang, B., Harper, L., Lee, H. J., Chusuei, C. C., et al. (2020). Cytotoxicity of NiO and Ni (OH) 2 nanoparticles is mediated by oxidative stress-induced cell death and suppression of cell proliferation. *Int. J. Mol. Sci.* 21:2355. doi: 10.3390/ijms21072355

Černý, M., Habánová, H., Berka, M., Luklová, M., and Brzobohatý, B. (2018). Hydrogen peroxide: its role in plant biology and crosstalk with signalling networks. *Int. J. Mol. Sci.* 19:2812. doi: 10.3390/ijms19092812

Chamizo-Ampudia, A., Sanz-Luque, E., Llamas, A., Galvan, A., and Fernandez, E. (2017). Nitrate reductase regulates plant nitric oxide homeostasis. *Trends Plant Sci.* 22, 163–174. doi: 10.1016/j.tplants.2016.12.001

Chandra, S., Chakraborty, N., Dasgupta, A., Sarkar, J., Panda, K., and Acharya, K. (2015). Chitosan nanoparticles: a positive modulator of innate immune responses in plants. *Sci. Rep.* 5:15195.

Chen, Y., Mo, H. Z., Hu, L. B., Li, Y. Q., Chen, J., and Yang, L. F. (2014). The endogenous nitric oxide mediates selenium-induced phytotoxicity by promoting ROS generation in *Brassica rapa*. *PLoS One* 9:e110901. doi: 10.1371/journal.pone.0110901

Chen, Y., Wang, X. M., Zhou, L., He, Y., Wang, D., Qi, Y. H., et al. (2015). Rubisco activase is also a multiple responder to abiotic stresses in rice. *PLoS One* 10:e0140934. doi: 10.1371/journal.pone.0140934

Choudhury, S. R. (2019). "Genome-wide alterations of epigenomic landscape in plants by engineered nanomaterial toxicants," in *Analysis, Fate, and Toxicity of Engineered Nanomaterials in Plants*, Vol. 84, eds S. K. Verma, and A. K. Das (Amsterdam: Elsevier), 199–223.

Chung, I. M., Venkidasamy, B., and Thiruvengadam, M. (2019). Nickel oxide nanoparticles cause substantial physiological, phytochemical, and molecular-level changes in Chinese cabbage seedlings. *Plant Physiol. Biochem.* 139, 92–101. doi: 10.1016/j.plaphy.2019.03.010

Chu-Puga, Á, González-Gordo, S., Rodríguez-Ruiz, M., Palma, J. M., and Corpas, F. J. (2019). NADPH oxidase (Rboh) activity is up regulated during sweet pepper (*Capsicum annuum* L.) fruit ripening. *Antioxidants* 8:9. doi: 10.3390/antiox8010009

Cohen, I., Knopf, J. A., Irihimovitch, V., and Shapira, M. (2005). A proposed mechanism for the inhibitory effects of oxidative stress on Rubisco assembly and its subunit expression. *Plant Physiol.* 137, 738–746. doi: 10.1104/pp.104.056341

Corpas, F. J., and Barroso, J. B. (2018). Peroxisomal plant metabolism–an update on nitric oxide, Ca2+ and the NADPH recycling network. *J. Cell Sci.* 131:jcs202978. doi: 10.1242/jcs.202978

Cramer, G. R., Epstein, E., and Läuchli, A. (1990). Effects of sodium, potassium and calcium on salt-stressed barley. I. growth analysis. *Physiol. Plant.* 80, 83–88.

Cuypers, A., Hendrix, S., Amaral dos Reis, R., De Smet, S., Deckers, J., Gielen, H., et al. (2016). Hydrogen peroxide, signaling in disguise during metal phytotoxicity. *Front. Plant Sci.* 7:470. doi: 10.3389/fpls.2016.00470

Da Costa, M. V. J., and Sharma, P. K. (2016). Effect of copper oxide nanoparticles on growth, morphology, photosynthesis, and antioxidant response in *Oryza sativa*. *Photosynthetica* 54, 110–119. doi: 10.1007/s11099-015-0167-5

Danjumma, S. G., Abubakar, Y., and Suleiman, S. (2019). Nickel oxide (NiO) devices and applications: a review. *Int. J. Eng. Res. Technol.* 8, 461–467. doi: 10.17577/IJERTV8IS040281

Das, K., and Roychoudhury, A. (2014). Reactive oxygen species (ROS) and response of antioxidants as ROS-scavengers during environmental stress in plants. *Front. Environ. Sci.* 2:53. doi: 10.3389/fenvs.2014.00053

Das, P., Manna, I., Biswas, A. K., and Bandyopadhyay, M. (2018). Exogenous silicon alters ascorbate-glutathione cycle in two salt-stressed indica rice cultivars (MTU 1010 and Nonabokra). *Environ. Sci. Pollut. Res.* 25, 26625–26642. doi: 10.1007/s11356-018-2659-x

Daş, Z. A., Dimlioğlu, G., Bor, M., and Özdemir, F. (2016). Zinc induced activation of GABA-shunt in tobacco (*Nicotiana tabaccum* L.). *Environ. Exp. Bot.* 122, 78–84. doi: 10.1016/j.envexpbot.2015.09.006

Demirevska-Kepova, K., Simova-Stoilova, L., Stoyanova, Z., Hölzer, R., and Feller, U. (2004). Biochemical changes in barley plants after excessive supply of copper and manganese. *Environ. Exp. Bot.* 52, 253–266. doi: 10.1016/j.envexpbot.2004.02.004

Doğaroğlu, Z. G., and Köleli, N. (2017). TiO2 and ZnO nanoparticles toxicity in barley (*Hordeum vulgare* L.). *Clean Soil Air Water* 45:1700096. doi: 10.1002/clen.201700096

Domingos, P., Prado, A. M., Wong, A., Gehring, C., and Feijo, J. A. (2015). Nitric oxide: a multitasked signaling gas in plants. *Mol. Plant* 8, 506–520. doi: 10.1016/j.molp.2014.12.010

Faisal, M., Saquib, Q., Alatar, A. A., Al-Khedhairy, A. A., Hegazy, A. K., and Musarrat, J. (2013). Phytotoxic hazards of NiO-nanoparticles in tomato: a study on mechanism of cell death. *J. Hazard. Mater.* 250, 318–332. doi: 10.1016/j.jhazmat.2013.01.063

Farnese, F. S., Menezes-Silva, P. E., Gusman, G. S., and Oliveira, J. A. (2016). When bad guys become good ones: the key role of reactive oxygen species and nitric oxide in the plant responses to abiotic stress. *Front. Plant Sci.* 7:471. doi: 10.3389/fpls.2016.00471

Fu, Y. F., Zhang, Z. W., and Yuan, S. (2018). Putative connections between nitrate reductase S-nitrosylation and NO synthesis under pathogen attacks and abiotic stresses. *Front. Plant Sci.* 9:474. doi: 10.3389/fpls.2018.00474

Genchi, G., Carocci, A., Lauria, G., Sinicropi, M. S., and Catalano, A. (2020). Nickel: human health and environmental toxicology. *Int. J. Environ. Res. Public Health* 17:679. doi: 10.3390/ijerph17030679

Hao, G. P., Xing, Y., and Zhang, J. H. (2008). Role of nitric oxide dependence on nitric oxide synthase-like activity in the water stress signaling of maize seedling. *J. Integr. Plant Biol.* 50, 435–442. doi: 10.1111/j.1744-7909.2008.00637.x

Hasanuzzaman, M., Bhuyan, M. H. M., Anee, T. I., Parvin, K., Nahar, K., Mahmud, J. A., et al. (2019). Regulation of ascorbate-glutathione pathway in mitigating oxidative damage in plants under abiotic stress. *Antioxidants* 8:384. doi: 10.3390/antiox8090384

He, P. P., Lv, X. Z., and Wang, G. Y. (2004). Effects of Se and Zn supplementation on the antagonism against Pb and Cd in vegetables. *Environ. Int.* 30, 167–172. doi: 10.1016/S0160-4120(03)00167-3

Heyno, E., Klose, C., and Krieger-Liszkay, A. (2008). Origin of cadmium-induced reactive oxygen species production: mitochondrial electron transfer versus plasma membrane NADPH oxidase. *New Phytol.* 179, 687–699. doi: 10.1111/j.1469-8137.2008.02512.x

Huang, Q., Wang, F. B., Yuan, C. H., He, Z., Rao, L., Cai, B., et al. (2018). Gelatin nanoparticle-coated silicon beads for density-selective capture and release of heterogeneous circulating tumor cells with high purity. *Theranostics* 8, 1624–1635. doi: 10.7150/thno.23531

Järup, L. (2003). Hazards of heavy metal contamination. *Br. Med. Bull.* 68, 167–182. doi: 10.1093/bmb/ldg032

Khairy, A. I. H., Oh, M. J., Lee, S. M., and Roh, K. S. (2016). Nitric oxide overcomes Cd and Cu toxicity in in vitro-grown tobacco plants through increasing contents and activities of rubisco and rubisco activase. *Biochim. Open* 2, 41–51. doi: 10.1016/j.biopen.2016.02.002

Lentini, M., De Lillo, A., Paradisone, V., Liberti, D., Landi, S., and Esposito, S. (2018). Early responses to cadmium exposure in barley plants: effects on biometric and physiological parameters. *Acta Physiol. Plant.* 40:178. doi: 10.1007/s11738-018-2752-2

Libik-Konieczny, M., Kozieradzka-Kiszkurno, M., Desel, C., Michalec-Warzecha, Ż, Miszalski, Z., and Konieczny, R. (2015). The localization of NADPH oxidase and reactive oxygen species in in vitro-cultured *Mesembryanthemum crystallinum* L. hypocotyls discloses their differing roles in rhizogenesis. *Protoplasma* 252, 477–487. doi: 10.1007/s00709-014-0692-2

Lin, A., Wang, Y., Tang, J., Xue, P., Li, C., Liu, L., et al. (2012). Nitric oxide and protein S-nitrosylation are integral to hydrogen peroxide-induced leaf cell death in rice. *Plant Physiol.* 158, 451–464. doi: 10.1104/pp.111.184531

Liu, K. L., Shen, L., Wang, J. Q., and Sheng, J. P. (2008). Rapid inactivation of chloroplastic ascorbate peroxidase is responsible for oxidative modification to Rubisco in tomato (*Lycopersicon esculentum*) under cadmium stress. *J. Integr. Plant Biol.* 50, 415–426. doi: 10.1111/j.1744-7909.2007.00621.x

Lomaglio, T., Rocco, M., Trupiano, D., De Zio, E., Grosso, A., Marra, M., et al. (2015). Effect of short-term cadmium stress on *Populus nigra* L. detached leaves. *J. Plant Physiol.* 182, 40–48. doi: 10.1016/j.jplph.2015.04.007

Lou, Y., Zhao, P., Wang, D., Amombo, E., Sun, X., Wang, H., et al. (2017). Germination, physiological responses and gene expression of tall fescue (*Festuca arundinacea* Schreb.) growing under Pb and Cd. *PLoS One* 12:e0169495. doi: 10.1371/journal.pone.0169495

Manna, I., and Bandyopadhyay, M. (2017a). Engineered nickel oxide nanoparticles affect genome stability in *Allium cepa* (L.). *Plant Physiol. Biochem.* 121, 206–215. doi: 10.1016/j.plaphy.2017.11.003

Manna, I., and Bandyopadhyay, M. (2017b). Engineered nickel oxide nanoparticle causes substantial physicochemical perturbation in plants. *Front. Chem.* 5:92. doi: 10.3389/fchem.2017.00092

McInnis, S. M., Desikan, R., Hancock, J. T., and Hiscock, S. J. (2006). Production of reactive oxygen species and reactive nitrogen species by angiosperm stigmas and pollen: potential signalling crosstalk? *New Phytol.* 172, 221–228. doi: 10.1111/j.1469-8137.2006.01875.x

Murphy, M. E., and Noack, E. (1994). "[24] Nitric oxide assay using hemoglobin method," in *Methods in Enzymology*, Vol. 233 (Cambridge, MA: Academic Press), 240–250. doi: 10.1016/S0076-6879(94)33027-1

Mustafa, G., and Komatsu, S. (2016). Toxicity of heavy metals and metal-containing nanoparticles on plants. *Biochim. Biophys. Acta* 1864, 932–944. doi: 10.1016/j.bbapap.2016.02.020

Nabi, R. B. S., Tayade, R., Hussain, A., Kulkarni, K. P., Imran, Q. M., Mun, B. G., et al. (2019). Nitric oxide regulates plant responses to drought, salinity, and heavy metal stress. *Environ. Exp. Bot.* 161, 120–133. doi: 10.1016/j.envexpbot.2019.02.003

Osakabe, Y., Arinaga, N., Umezawa, T., Katsura, S., Nagamachi, K., Tanaka, H., et al. (2013). Osmotic stress responses and plant growth controlled by potassium transporters in *Arabidopsis*. *Plant Cell* 25, 609–624. doi: 10.1105/tpc.112.105700

Oukarroum, A., Barhoumi, L., Samadani, M., and Dewez, D. (2015). Toxic effects of nickel oxide bulk and nanoparticles on the aquatic plant *Lemna gibba* L. *Biomed. Res. Int.* 2015:501326. doi: 10.1155/2015/501326

Oukarroum, A., Barhoumi, L., Samadani, M., and Dewez, D. (2017). Toxicity of nickel oxide nanoparticles on a freshwater green algal strain of *Chlorella vulgaris*. *Biomed. Res. Int.* 2017:9528180. doi: 10.1155/2017/9528180

Ovais, M., Khalil, A. T., Ayaz, M., and Ahmad, I. (2020). "Metal oxide nanoparticles and plants," in *Phytonanotechnology: Challenges and Prospects*, eds N. Thajuddin, and S. Mathew (Amsterdam: Elsevier), 123–141. doi: 10.1016/B978-0-12-822348-2.00007-3

Pérez-de-Luque, A. (2017). Interaction of nanomaterials with plants: what do we need for real applications in agriculture? *Front. Environ. Sci.* 5:12. doi: 10.3389/fenvs.2017.00012

Pinto, M., Soares, C., Pinto, A. S., and Fidalgo, F. (2019). Phytotoxic effects of bulk and nano-sized Ni on *Lycium barbarum* L. grown in vitro–oxidative damage and antioxidant response. *Chemosphere* 218, 507–516. doi: 10.1016/j.chemosphere.2018.11.127

Podgórska, A., Burian, M., and Szal, B. (2017). Extra-cellular but extra-ordinarily important for cells: apoplastic reactive oxygen species metabolism. *Front. Plant Sci.* 8:1353. doi: 10.3389/fpls.2017.01353

Procházková, D., Haisel, D., Wilhelmová, N., Pavlíková, D., and Száková, J. (2013). Effects of exogenous nitric oxide on photosynthesis. *Photosynthetica* 51, 483–489. doi: 10.1007/s11099-013-0053-y

Qian, H., Peng, X., Han, X., Ren, J., Sun, L., and Fu, Z. (2013). Comparison of the toxicity of silver nanoparticles and silver ions on the growth of terrestrial plant model *Arabidopsis thaliana*. *J. Environ. Sci.* 25, 1947–1956. doi: 10.1016/S1001-0742(12)60301-5

Ramos-Ruiz, R., Martinez, F., and Knauf-Beiter, G. (2019). The effects of GABA in plants. *Cogent Food Agric.* 5:1670553. doi: 10.1080/23311932.2019.1670553

Rastogi, A., Zivcak, M., Sytar, O., Kalaji, H. M., He, X., Mbarki, S., et al. (2017). Impact of metal and metal oxide nanoparticles on plant: a critical review. *Front. Chem.* 5:78. doi: 10.3389/fchem.2017.00078

Remans, T., Opdenakker, K., Smeets, K., Mathijsen, D., Vangronsveld, J., and Cuypers, A. (2010). Metal-specific and NADPH oxidase dependent changes in lipoxygenase and NADPH oxidase gene expression in *Arabidopsis thaliana* exposed to cadmium or excess copper. *Funct. Plant Biol.* 37, 532–544. doi: 10.1071/FP09194

Ristroph, K. D., Astete, C. E., Bodoki, E., and Sabliov, C. M. (2017). Zein nanoparticles uptake by hydroponically grown soybean plants. *Environ. Sci. Technol.* 51, 14065–14071. doi: 10.1021/acs.est.7b03923

Rizwan, M., Ali, S., Ali, B., Adrees, M., Arshad, M., Hussain, A., et al. (2019). Zinc and iron oxide nanoparticles improved the plant growth and reduced the oxidative stress and cadmium concentration in wheat. *Chemosphere* 214, 269–277. doi: 10.1016/j.jhazmat.2016.05.061

Rizwan, M., Ali, S., Qayyum, M. F., Ok, Y. S., Adrees, M., Ibrahim, M., et al. (2017). Effect of metal and metal oxide nanoparticles on growth and physiology of globally important food crops: a critical review. *J. Hazard. Mater.* 322, 2–16.

Romero-Puertas, M. C., and Sandalio, L. M. (2016). Nitric oxide level is self-regulating and also regulates its ROS partners. *Front. Plant Sci.* 7:316. doi: 10.3389/fpls.2016.00316

Saha, K., Lajis, N. H., Israf, D. A., Hamzah, A. S., Khozirah, S., Khamis, S., et al. (2004). Evaluation of antioxidant and nitric oxide inhibitory activities of selected Malaysian medicinal plants. *J. Ethnopharmacol.* 92, 263–267. doi: 10.1016/j.jep.2004.03.007

Scheler, C., Durner, J., and Astier, J. (2013). Nitric oxide and reactive oxygen species in plant biotic interactions. *Curr. Opin. Plant Biol.* 16, 534–539.

Schützendübel, A., and Polle, A. (2002). Plant responses to abiotic stresses: heavy metal-induced oxidative stress and protection by mycorrhization. *J. Exp. Bot.* 53, 1351–1365. doi: 10.1093/jxb/53.372.1351

Shang, L., Nienhaus, K., and Nienhaus, G. U. (2014). Engineered nanoparticles interacting with cells: size matters. *J. Nanobiotechnol.* 12:5. doi: 10.1186/1477-3155-12-5

Siedlecka, A., Samuelsson, G., Gardeström, P., Kleczkowslci, L. A., and Krupa, Z. (1998). "The "activatory model" of plant response to moderate cadmium stress-relationship between carbonic anhydrase and Rubisco," in *Photosynthesis: Mechanisms and Effects*, ed. G. Garab (Dordrecht: Springer), 2677–2680. doi: 10.1007/978-94-011-3953-3_630

Sil, P., Das, P., and Biswas, A. K. (2018). Silicon induced mitigation of TCA cycle and GABA synthesis in arsenic stressed wheat (*Triticum aestivum* L.) seedlings. *S. Afr. J. Bot.* 119, 340–352. doi: 10.1016/j.sajb.2018.09.035

Singh, S., Parihar, P., Singh, R., Singh, V. P., and Prasad, S. M. (2016). Heavy metal tolerance in plants: role of transcriptomics, proteomics, metabolomics, and ionomics. *Front. Plant Sci.* 6:1143. doi: 10.3389/fpls.2015.01143

Sivakumar, P., Sharmila, P., and Saradhi, P. P. (2001). Proline suppresses rubisco activity by dissociating small subunits from holoenzyme. *Biochem. Biophys. Res. Commun.* 282, 236–241. doi: 10.1006/bbrc.2001.4540

Sohaebuddin, S. K., Thevenot, P. T., Baker, D., Eaton, J. W., and Tang, L. (2010). Nanomaterial cytotoxicity is composition, size, and cell type dependent. *Part. Fibre Toxicol.* 7:22. doi: 10.1186/1743-8977-7-22

Son, J. A., Narayanankutty, D. P., and Roh, K. S. (2014). Influence of exogenous application of glutathione on rubisco and rubisco activase in heavy metal-stressed tobacco plant grown in vitro. *Saudi J. Biol. Sci.* 21, 89–97. doi: 10.1016/j.sjbs.2013.06.002

Song, H., Xu, X., Wang, H., Wang, H., and Tao, Y. (2010). Exogenous γ-aminobutyric acid alleviates oxidative damage caused by aluminium and proton stresses on barley seedlings. *J. Sci. Food Agric.* 90, 1410–1416. doi: 10.1002/jsfa.3951

Sosan, A., Svistunenko, D., Straltsova, D., Tsiurkina, K., Smolich, I., Lawson, T., et al. (2016). Engineered silver nanoparticles are sensed at the plasma membrane and dramatically modify the physiology of *Arabidopsis thaliana* plants. *Plant J.* 85, 245–257. doi: 10.1111/tpj.13105

Sun, C., Liu, L., Lu, L., Jin, C., and Lin, X. (2018). Nitric oxide acts downstream of hydrogen peroxide in regulating aluminum-induced antioxidant defense that enhances aluminum resistance in wheat seedlings. *Environ. Exp. Bot.* 145, 95–103. doi: 10.1016/j.envexpbot.2017.10.020

Tchounwou, P. B., Yedjou, C. G., Patlolla, A. K., and Sutton, D. J. (2012). "Heavy metal toxicity and the environment," in *Molecular, Clinical and Environmental Toxicology*, ed. A. Luch (Basel: Springer), 133–164. doi: 10.1007/978-3-7643-8340-4_6

Thiruvengadam, M., Gurunathan, S., and Chung, I. M. (2015). Physiological, metabolic, and transcriptional effects of biologically-synthesized silver nanoparticles in turnip (*Brassica rapa* ssp. rapa L.). *Protoplasma* 252, 1031–1046. doi: 10.1007/s00709-014-0738-5

Tian, Q. Y., Sun, D. H., Zhao, M. G., and Zhang, W. H. (2007). Inhibition of nitric oxide synthase (NOS) underlies aluminum-induced inhibition of root elongation in *Hibiscus moscheutos*. *New Phytol.* 174, 322–331. doi: 10.1111/j.1469-8137.2007.02005.x

Tripathi, D. K., Mishra, R. K., Singh, S., Singh, S., Singh, V. P., Singh, P. K., et al. (2017a). Nitric oxide ameliorates zinc oxide nanoparticles phytotoxicity in wheat seedlings: implication of the ascorbate-glutathione cycle. *Front. Plant Sci.* 8:1. doi: 10.3389/fpls.2017.00001

Tripathi, D. K., Singh, S., Singh, S., Srivastava, P. K., Singh, V. P., Singh, S., et al. (2017b). Nitric oxide alleviates silver nanoparticles (AgNps)-induced phytotoxicity in *Pisum sativum* seedlings. *Plant Physiol. Biochem.* 110, 167–177. doi: 10.1016/j.plaphy.2016.06.015

Valko, M., Jomova, K., Rhodes, C. J., Kuča, K., and Musílek, K. (2016). Redox-and non-redox-metal-induced formation of free radicals and their role in human disease. *Arch. Toxicol.* 90, 1–37. doi: 10.1007/s00204-015-1579-5

Vázquez, M. D., Barceló, J., Poschenrieder, C. H., Madico, J., Hatton, P., Baker, A. J. M., et al. (1992). Localization of zinc and cadmium in *Thlaspi caerulescens* (Brassicaceae), a metallophyte that can hyperaccumulate both metals. *J. Plant Physiol.* 140, 350–355. doi: 10.1016/S0176-1617(11)81091-6

Veeranarayanan, S., Poulose, A. C., Mohamed, S., Aravind, A., Nagaoka, Y., Yoshida, Y., et al. (2012). FITC labeled silica nanoparticles as efficient cell tags: uptake and photostability study in endothelial cells. *J. Fluoresc.* 22, 537–548. doi: 10.1007/s10895-011-0991-3

Vega, J. M., and Kamin, H. E. N. R. Y. (1977). Spinach nitrite reductase. Purification and properties of a siroheme-containing iron-sulfur enzyme. *J. Biol. Chem.* 252, 896–909.

Velikova, V., Yordanov, I., and Edreva, A. (2000). Oxidative stress and some antioxidant systems in acid rain-treated bean plants: protective role of exogenous polyamines. *Plant Sci.* 151, 59–66. doi: 10.1016/S0168-9452(99)00197-1

Vijayaraghavareddy, P., Adhinarayanreddy, V., Vemanna, R. S., Sreeman, S., and Makarla, U. (2017). Quantification of membrane damage/cell death using evan's blue staining technique. *Bio. Protoc.* 7, e2519. doi: 10.21769/BioProtoc.2519

Wang, H., Hou, J., Li, Y., Zhang, Y., Huang, J., and Liang, W. (2017). Nitric oxide-mediated cytosolic glucose-6-phosphate dehydrogenase is involved in aluminum toxicity of soybean under high aluminum concentration. *Plant Soil* 416, 39–52. doi: 10.1007/s11104-017-3197-x

Xia, T., Kovochich, M., Liong, M., Zink, J. I., and Nel, A. E. (2008). Cationic polystyrene nanosphere toxicity depends on cell-specific endocytic and mitochondrial injury pathways. *ACS Nano* 2, 85–96. doi: 10.1021/nn700256c

Xiong, J., Fu, G., Tao, L., and Zhu, C. (2010). Roles of nitric oxide in alleviating heavy metal toxicity in plants. *Arch. Biochem. Biophys.* 497, 13–20. doi: 10.1016/j.abb.2010.02.014

Yadu, B., Chandrakar, V., Korram, J., Satnami, M. L., Kumar, M., and Keshavkant, S. (2018). Silver nanoparticle modulates gene expressions, glyoxalase system and oxidative stress markers in fluoride stressed *Cajanus cajan* L. *J. Hazard. Mater.* 353, 44–52. doi: 10.1016/j.jhazmat.2018.03.061

Yang, S., Zu, Y., Li, B., Bi, Y., Jia, L., He, Y., et al. (2019). Response and intraspecific differences in nitrogen metabolism of alfalfa (*Medicago sativa* L.) under cadmium stress. *Chemosphere* 220, 69–76. doi: 10.1016/j.chemosphere.2018.12.101

Yin, L., Mano, J. I., Wang, S., Tsuji, W., and Tanaka, K. (2010). The involvement of lipid peroxide-derived aldehydes in aluminum toxicity of tobacco roots. *Plant Physiol.* 152, 1406–1417. doi: 10.1104/pp.109.151449

Yusefi-Tanha, E., Fallah, S., Rostamnejadi, A., and Pokhrel, L. R. (2020). Particle size and concentration dependent toxicity of copper oxide nanoparticles (CuONPs) on seed yield and antioxidant defense system in soil grown soybean (*Glycine max* cv. Kowsar). *Sci. Total Environ.* 715:136994. doi: 10.1016/j.scitotenv.2020.136994

Zhang, Q., Xiang, J., Zhang, L., Zhu, X., Evers, J., van der Werf, W., et al. (2014). Optimizing soaking and germination conditions to improve gamma-aminobutyric acid content in japonica and indica germinated brown rice. *J. Funct. Foods* 10, 283–291. doi: 10.1016/j.jff.2014.06.009

Zhang, X., Zhang, H., Lou, X., and Tang, M. (2019). Mycorrhizal and non-mycorrhizal *Medicago truncatula* roots exhibit differentially regulated NADPH oxidase and antioxidant response under Pb stress. *Environ. Exp. Bot.* 164, 10–19. doi: 10.1016/j.envexpbot.2019.04.015

Conflict of Interest: The authors declare that the research was conducted in the absence of any commercial or financial relationships that could be construed as a potential conflict of interest.

Advantages of publishing in Frontiers

OPEN ACCESS
Articles are free to read for greatest visibility and readership

FAST PUBLICATION
Around 90 days from submission to decision

HIGH QUALITY PEER-REVIEW
Rigorous, collaborative, and constructive peer-review

TRANSPARENT PEER-REVIEW
Editors and reviewers acknowledged by name on published articles

Frontiers
Avenue du Tribunal-Fédéral 34
1005 Lausanne | Switzerland

Visit us: www.frontiersin.org
Contact us: frontiersin.org/about/contact

REPRODUCIBILITY OF RESEARCH
Support open data and methods to enhance research reproducibility

DIGITAL PUBLISHING
Articles designed for optimal readership across devices

FOLLOW US
@frontiersin

IMPACT METRICS
Advanced article metrics track visibility across digital media

EXTENSIVE PROMOTION
Marketing and promotion of impactful research

LOOP RESEARCH NETWORK
Our network increases your article's readership